

NASA Conference Publication 2360

Orbital Debris

Compiled by
Donald J. Kessler
NASA Lyndon B. Johnson Space Center
Houston, Texas

Shin-Yi Su
Lockheed-EMSCO
Houston, Texas

Proceedings of a workshop sponsored by
NASA Lyndon B. Johnson Space Center and
held in Houston, Texas
July 27-29, 1982

NASA
National Aeronautics
and Space Administration
Scientific and Technical
Information Branch

1985

PREFACE

The papers presented at this workshop are the most complete publications to date concerning orbital debris. Since the workshop, several new lines of investigation have begun, each promising to provide new data on the small orbital debris environment.

The most promising new data are expected from the Infrared Astronomical Satellite (IRAS) telescope. Although IRAS stopped gathering data in December, 1983, the existing data are expected to contain information on the debris population larger than a few millimeters and higher than 900km altitude. A proposal to obtain samples of the IRAS data has been approved by NASA Headquarters, pending resolution of proprietary agreements established with the Laboratory's IRAS principal investigators.

The second most promising data are expected from Lincoln Laboratory's Experimental Test Site (ETS), using their two 31-inch telescopes. A contract to detect orbital debris at altitudes below 1000km and sizes larger than 1cm is expected within the next few months.

As a direct result of the workshop, we have tasked the North American Air Defense Command (NORAD) to develop a technique of routinely providing a sampling of objects too small to be in the official catalogue, to maintain and improve their techniques of reporting on satellite breakups, and to search for a "collision signature" in the satellite breakup data. This work is being conducted by Teledyne Brown and will be published every 6 months as a "Sample Catalogue of Small Objects." Most of the small object data will come from NORAD's PARCS radar which routinely collects data on objects too small to be in the official catalogue.

Much of this work will be presented in the Space Debris Workshop as part of COSPAR in Graz, Austria, June 25, 1984 to July 6, 1984. The papers presented there are expected to be published.

Donald J. Kessler
March 1984

PRECEDING PAGE BLANK NOT FILMED

CONTENTS

	Page
PREFACE	111
ATTENDEES	1x
SUMMARY OF WORKSHOP ACTIVITIES	1
SPACE DEBRIS ASSESSMENT - 10-YEAR PROGRAM PLAN, PROGRAM TECHNICAL PLAN	8
SESSION 1. ENVIRONMENT DEFINITION: PARTICLES LARGER THAN 1 MM	
<u>MEASUREMENTS</u>	
NORAD OPERATIONAL SYSTEM David Brach	22 ✓
HISTORY OF SATELLITE BREAK UPS IN SPACE John Gabbard	30 ✓
NORAD'S PARCS SMALL SATELLITE TESTS (1976 AND 1978) Donald J. Kessler	39 ✓
MANMADE ORBITAL DEBRIS STUDIES AT NASA LANGLEY Donald H. Humes, David R. Brocks, Jose M. Alvarez, and T. Dale Bess	45 ✓
<u>MODELING</u>	
NASA/JSC ORBITAL DEBRIS STUDY: DEBRIS MODEL J. Brad Roberds, Donald J. Kessler, and Shin-Yi Su	69 ✓
PROPOSED PRELIMINARY DESIGN CRITERIA - MODEL ENVIRONMENT FOR THE 1990'S Donald J. Kessler	78 ✓
ASSESSMENT OF SATELLITE COLLISION HAZARDS BY SIMULATED SAMPLING IN SPACE V. A. Chobotov	84 ✓
A MODEL FOR THE EVOLUTION OF ON-ORBIT MANMADE DEBRIS ENVIRONMENT Robert C. Reynolds, Norman H. Fischer, and Donald S. Edgecombe ...	102 ✓
GEOSYNCHRONOUS SATELLITE COLLISION AVOIDANCE William Fraser	133 ✓
<u>PROPOSED MEASUREMENTS</u>	
<u>IN SITU ORBITAL DEBRIS EXPERIMENT CONCEPTS</u> Sherman L. Neste	134 ✓

~~PRECEDING PAGE BLANK NOT FILMED~~

PRECEDING PAGE BLANK NOT FILMED



	Page
PRELIMINARY DESIGN OF AN EARTH-BASED DEBRIS DETECTION SYSTEM USING CURRENT TECHNOLOGY AND EXISTING INSTALLATIONS T. H. Morgan	150 ✓
USE OF GROUND RADAR TO DETECT REENTERING DEBRIS Jeanne Lee Crews	164 ✓

**SESSION 2. ENVIRONMENT DEFINITION:
PARTICLES SMALLER THAN 1 MM**

PARTICLE SIZE, NUMBER, COMPOSITION, AND VELOCITY FROM SOLID ROCKET MOTORS Barney B. Roberts	170 ✓
HYPERVELOCITY IMPACTS ON SKYLAB IV/APOLLO WINDOWS Uel S. Clanton, Herbert A. Zook, and Richard A. Schultz	177 ✓
SURVEY OF PROBABLE MICROMETER-SIZED EARTH-ORBITAL DEBRIS FRAGMENTS IN THE NASA/JSC COSMIC DUST SAMPLE COLLECTION U. S. Clanton and J. L. Gooding	190 ✓
IMPACTS ON EXPLORER 46 FROM AN EARTH ORBITING POPULATION Donald J. Kessler	220 ✓
<u>IN SITU</u> DETECTION OF MICKON-SIZED DUST PARTICLES IN NEAR-EARTH SPACE E. Grun and H. A. Zook	233 ✓
PARCS SMALL SATELLITE TEST - 1976 (CLASSIFIED) T. Lennertz (PAPER NOT INCLUDED)	246 ○
POTENTIAL HAZARDS OF DEBRIS CLOUDS (CLASSIFIED) N. L. Johnson (PAPER NOT INCLUDED)	246 ○

**SESSION 3. SPACECRAFT HAZARD
AND SHIELDING REQUIREMENTS**

HYPERVELOCITY IMPACT INVESTIGATIONS AND METEOROID SHIELDING EXPERIENCE RELATED TO APOLLO AND SKYLAB Burton G. Cour-Palais	247 ✓
SOLID PARTICLE ENVIRONMENT AND PROTECTION FOR THE GALILEO ORBITER (VIEWGRAPHS ONLY) Andrew J. Beck and Robert Bamford	276 ✓
SPACE DEBRIS PROTECTION FOR A REUSABLE ORBITAL TRANSFER VEHICLE Eldon E. Davis and Ray Sperber	279 ✓
PARAMETRIC ANALYSIS: SOC METEOROID AND DEBRIS PROTECTION Robert Kowalski	287 ✓

SPACE HEAT REJECTION RADIATORS: METEOROID/DEBRIS CONSIDERATION— J. Gary Rankin	295 ✓
---	-------

SESSION 4. SPACE OBJECT MANAGEMENT

SATELLITE SERVICES AND ORBITAL RETRIEVAL Rudolph J. Adernato	299 ✓
A REMOTELY CONTROLLED ORBITING RETRIEVER Marshall H. Kaplan	316 ✓
THE LONG TERM BEHAVIOUR OF EARTH ORBITS AND THE IMPLICATIONS FOR DEBRIS CONTROL Alan C. Mueller	332 ✓
DEBRIS IN THE GEOSTATIONARY ORBIT RING: "THE ENDLESS SHOOTING GALLERY" - THE NECESSITY FOR A DISPOSAL POLICY David H. Suddeth	349 ✓

SESSION 5. POLICY CONSIDERATIONS

SPACE DEBRIS: AN AIAA POSITION PAPER Malcolm G. Wolfe	365 ✓
THE INTERNATIONAL ENVIRONMENT: UNISPACE 1982 AND THE ITU Dean Olmstead	372 ✓
TRANSMISSION AND ORBITAL CONSTRAINTS IN SPACE-RELATED PROGRAMS: BRIEFING SUMMARY A. L. Hiebert	379 ✓
AIR FORCE ORBITAL POSITION MANAGEMENT POLICY D. Hyland	393
AIR FORCE SATELLITE POSITION MANAGEMENT R. Davis	399 ✓
ORBITAL DEBRIS POLICY ISSUES/BATTELLE INVOLVEMENT AND SOME PERSONAL OBSERVATIONS Donald S. Edgecombe	402 ✓
CONSIDERATIONS FOR POLICY ON MAN-MADE DEBRIS PROPAGATION CONTROL D. Fielder	410



**SESSION 6. SUMMARY REPORT OF WORKING GROUP SESSION
AND DISCUSSIONS**

ENVIRONMENT DEFINITION, LARGE PARTICLES	
Don Kessler	419
MODELING	
Herb Zook	421
MEASUREMENTS	
Andrew E. Potter	424
ENVIRONMENT DEFINITION, SMALL PARTICLES, DIAMETER \leq 1 MM	
Barney Roberts	426
SPACECRAFT HAZARD AND SHIELDING REQUIREMENTS	
Burton Cour-Palais	430
DISPOSITION TECHNIQUES	
J. P. Basu	436
POLICY CONSIDERATIONS	
Dennis Fielder	437



ATTENDEES

Adornato, Rudy; Grumman Aerospace
 Armitage, Pete; NASA/JSC
 Baillie, Richard; NASA/JSC
 Barbieri, Lou; NOAA/NESS
 Basu, J.; NASA/JSC
 Brach, David Capt.; NORAD HQ
 Bristow, R.D.; NASA/JSC
 Brudos, Jim; Lockheed
 Bulgher, Debbie; NASA/JSC
 Cehelsky, Marta Dr.; Nat. Sci. Foundation
 Chen, Ralph; NASA/JPL
 Chobotov, V.A. Dr.; The Aerospace Corp.
 Cintala, Mark J.; NASA/JSC
 Chu, Adam; Lockheed, Sunnyvale
 Clanton, U.; NASA/JSC
 Cour-Palais, B.; NASA/JSC
 Crews, Jeanne; NASA/JSC
 Culbertson, P.E.; NASA Hqs.
 Dalton, M.; NASA/JSC
 Davis, Richard Capt.; Space Division AF
 Davis, Eldon; Boeing Aerospace Corp.
 Duke, Mike; NASA/JSC
 Ebersole, Harvey; Battelle Columbus
 Edgecombe, Donald Dr.; Battelle Columbus
 Fielder, D.; NASA/JSC
 Fraser, William; HQ AFSCF/ROSR
 Gabbard, John; NORAD HQS
 Gabel, Elizabeth; Northrup
 Gooding, James; NASA/JSC
 Grun, Eberhard; Max Planck Institute
 Hall, Alvin; HQ AFSCF/ROSR
 Hartung, Jack; NASA Hqs.
 Hechler, Martin; European Space Agency
 Hiebert, A.L.; The Rand Corp.
 Horz, Fred; NASA/JSC
 Humes, Donald; NASA/LARC
 Hyland, David Capt.; HQ Air Force Pentagon
 Isaacs, Drew; Lockheed
 Jenkins, Lyle; NASA/JSC
 Johnson, Nicholas; Teledyne Brown Eng.
 Jost, Jerry; NASA/JSC
 Kaplan, Marshall H. Dr.; Spacotech, Inc.
 Kessler, Don; NASA/JSC
 Kowalski, R.; NASA/JSC
 Krishen, Kumar; NASA/JSC
 Lamping, Neil Col.; NORAD HQS
 Lennertz, T. Major; SAF/SS, Pentagon
 Livingston, L.E.; NASA/JSC
 Loftus, Joe; NASA/JSC
 Lowe, J.; NASA Hqs.
 Manley, Paul; NASA/JSC
 Martin, John; COMSAT Operations
 MacCuish, Earl; The Aerospace Corp.
 Mackinnon, Ian; Lockheed
 May, Col; NORAD HQS
 McCaskill, Greg; NASA/JSC
 Morgan, Steve; Lockheed
 Morgan, Tom; Southwestern University
 Morrison, Karen; NASA/JSC
 Mueller, Alan; Univ. of Texas
 Neste, Sherm Dr.; General Electric Co.
 Oberg, Jim; NASA/JSC
 Olmstead, Dean; NASA Hqs.
 Plummer, Bob; Teledyne Brown Eng.
 Potter, Andrew; NASA/JSC
 Rand, James L.; Southwest Research Inst.
 Rankin, Gary; NASA/JSC
 Reynolds, Robert Dr.; Battelle Columbus Labs.
 Robbins, Don; NASA/JSC
 Roberts, B.; NASA/JSC
 Ruck, George; Battelle Columbus
 See, Tom; Lockheed
 Simpkins, Gary; Martin Marietta
 Stanley, John; NASA/JSC
 Su, Shin-Yi; Lockheed
 Suddeth, David; NASA/GSFC
 Sanquinet, Joe; Santa Barbara Research
 Thompson, Tommy; Lockheed
 Wells, Curtis; Lockheed
 Warren, Jack; Northrup
 Wesselski, Clarence; NASA/JSC
 Wolfe, Malcolm G. Dr.; The Aerospace Corp.
 Zook, H.; NASA/JSC
 Zrubek, W.; NASA/JSC



SUMMARY OF WORKSHOP ACTIVITIES

On July 27-29, 1982, the Space Science Branch of the Johnson Space Center conducted an Orbital Debris Workshop. The workshop was attended by 90 persons representing NASA, DOD, other government agencies, private companies and universities. A total of 37 papers were presented in the areas of Environment Definition, Spacecraft Hazard and Shielding Requirements, and Space Object Management. After the formal presentations, the attendees divided into six working groups: Environment Definition was sub-divided into three groups; (1) Measurements of Large Particles (those originating from payloads, rocket bodies and the fragmentation of both), (2) Modeling of Large Particles, and (3) Measurements of Small Particles (from solid rocket motor products). The other groups were (4) Spacecraft Hazard and Shielding Requirements, and Space Object Management, which was sub-divided into the two groups (5) Disposition Techniques, and (6) Policy Considerations. The conclusions reached by each group were presented by the group chairman to the workshop for discussion on the final day.

Environment Definition

Capt. Brach discussed how NORAD capabilities have increased in response to the increased use of space. Even though they are charged with the responsibility "to detect, track, and identify all man-made objects in space", it was concluded in the workshop that this capability only exists for objects larger than 1 meter in diameter. John Gabbard, also from NORAD, reviewed the 69 known explosions in space to date, plus 9 events over the last two and one-half years where several large fragments have been observed to separate from older payloads, most in polar orbit. Although there is some evidence that one or more of these explosions or events may be the consequence of collisions, it was concluded that we do not currently have sufficient data to know what a "collision signature" would look like from ground tracking data.

Don Humes from Langley Research Center summarized the work conducted there between 1973 and 1975. They researched existing explosion data, conducted hypervelocity fragmentation tests, and modeled these data, together with the NORAD data. They concluded that the orbits of small untrackable explosion fragments disperse along the orbit very rapidly, and remain in orbit for a significantly long time. They also concluded that an untrackable population even more numerous than the tracked population must exist in orbit.

Modeling results were presented by Don Humes, Val Chobotov from Aerospace Corp., Bob Reynolds from Battelle, Shin-Yi Su from Lockheed, and Don Kessler from JSC. All modelers concluded that the probability of a large structure (approximately 100 meters in diameter) colliding with a currently tracked object in low earth orbit is already significant--approximately 0.1 in a 10 year period. When Lockheed, Battelle, and Langley added their current estimates of the untracked population, this probability grew 3 to 5 times larger. Battelle and JSC studied fragmentation resulting from collisions. This fragmentation process was concluded to be important for 2 reasons: (1) It can quickly produce a population of objects that is orders of magnitude larger than the current tracked population, (2) The frequency of subsequent

collisions could increase exponentially with time. Two secret papers were presented in a classified session, both of which discussed the possible existence of a current untracked population.

Several papers were presented on techniques to improve measurements of smaller particles in space. Sherm Nester from G.E. concluded that an orbiting satellite with either radar, passive optical, or active optical (lidar) could detect and determine orbits and size of particles as small as 1mm. A study by Tom Morgan of Southwestern University concluded that 1cm particles at 1000km could be detected from the ground using passive optical techniques. Evidence was also presented that reentering debris has been observed using the same ground radar techniques that have been used to detect the ion trail produced by small meteors.

The workshop concluded that we have no data on the number of objects in space smaller than approximately 4cm diameter and that obtaining this data should have the highest priority. It was concluded that impacts with 1cm particles would certainly damage most spacecraft and impacts with 1mm particles might damage spacecraft, depending on the system impacted. However, it was pointed out that shielding was added to the Galileo spacecraft to protect it from 0.1mm particles traveling at velocities not much higher than average debris velocities. Better estimates of the small debris population could be made using data from ground experiments on the particle sizes and velocity distribution from hypervelocity impacts. These data could also be used to look for a "collision signature" among the known satellite breakups. Such an analysis could lead to lower and/or upper limits to the current environment. At geosynchronous altitudes, the workshop concluded that neither sufficient data, nor sufficient modeling exists to even compare the environment at geosynchronous altitude to the environment in low earth orbit.

Data were presented illustrating the large number of Al_2O_3 particles which are produced during a solid rocket burn. Although most of these particles are retro-fired during an engine burn in space, a small fraction would be expected to remain in orbit and apparently do measurably affect certain experiments in earth orbit. Herb Zook, Uel Clanton and Don Kessler, all of JSC, presented papers describing experiments which were designed to detect meteoroids, but appear to have also detected an artificial orbiting population which was comparable to, or exceeded, the meteoroid population. Since the impacting sizes ranged from only a few microns to 80 microns, these particles should not seriously damage spacecraft. However, they did seriously compromise the scientific and engineering objectives of these experiments and have raised questions about others, such as the HEOS-2 experiment reported on by Eberhard Grun of the Max-Planck Institute. Thus, it was concluded by the workshop that the environment created by these smaller particles is important. It can degrade engineering and scientific experiments directly as well as indirectly by changing the optical properties of sensitive surfaces. It was also concluded that more testing and modeling is required to properly understand the lifetime and long-term effects of these particles.

Spacecraft Hazard and Shielding Requirements

Several papers were presented describing past efforts to take either a known meteoroid or debris environment, and use it to ensure that a particular spacecraft design achieved a desired reliability. Burt Cour-Palais, of JSC,

described the hypervelocity testing performed during the Apollo Program, and how this was used to shield certain Apollo sub-systems from meteoroids. Ralph Chen from JPL described the procedure used for determining the extra shielding required to protect Galileo against the increased meteoroid environment found around Jupiter. Eldon Davis, from Boeing, and Bob Kowalski and Gary Rankin, both from JSC, described how the meteoroid and debris environment affected Orbital Transfer Vehicle (OTV) and Space Operation Center (SOC) design. They all concluded that extra shielding would be required for protection and thus would affect the design of the systems that they investigated. They pointed out that there were many other systems on SOC to be investigated.

Although a large amount of hypervelocity testing has been conducted in the past, the workshop concluded that a significant amount of new work is required. A literature search is required to pull together all of the existing appropriate data. New system damage criteria will have to be established for the new breed of space vehicles because of reuseability, recycling, and refurbishment planned for the future. "Survivability" classifications, similar to those currently used by the military, were recommended. These classifications would correspond to various levels of mission success, such as "crew alive, but mission terminated", etc. Because many new spacecraft components will have unique construction requirements, or materials, generalization about the consequences of hypervelocity impacts is not always possible and new tests will sometimes be required.

Space Object Management

Several papers described techniques to dispose of satellites in orbit. Satellite retrieval using the Orbiter was discussed by Rudy Adornato of Grumman, and retrieval using a remotely controlled orbiting retriever was discussed by Marshall Kaplan of Spacotech, inc. The major advantages of the remotely controlled retriever are that more than one object per launch could be retrieved, it could go to higher altitudes, and it could collect satellites which were not designed to be retrieved by the Orbiter. Alan Mueller of the University of Texas, discussed how lunar and solar perturbations can be used to remove objects in geosynchronous transfer orbits, and how these perturbations affect objects in geosynchronous orbit. Theoretical studies, confirmed by NORAD tracking data, have shown that by constraining launches to various regions of geosynchronous orbit to certain times of the year, the OTV can be made to reenter within a year. Dave Suddeth from Goddard gave his reasons for recommending that NASA adopt a policy to minimize the number of objects left in geosynchronous orbit. He pointed out that both Intelsat and NOAA already have a written policy to desynchronize unusable spacecraft into higher orbits.

It was concluded by the workshop that while low cost techniques to minimize debris propagation should be encouraged and continued, we do not sufficiently understand the cost or effectiveness of the more expensive techniques (such as satellite retrieval) to recommend their implementation. More studies are required to understand the cost of implementation. These costs should then be compared with the risk of not implementing them. It was also concluded that very different techniques may be required for low earth orbit and geosynchronous orbit.

Under policy considerations, Malcolm Wolfe, Aerospace Corp., discussed

the background and conclusions of the AIAA Position Paper, "Space Debris". The AIAA recognized that the issue of space debris is real and that there is an immediate need for both a national and international space policy and treaty. Dean Olmstead from NASA Headquarters reported that the U.S. does plan to make a "statement of principle" concerning orbital debris in geosynchronous orbit at the UNISPACE Conference next month. Although radio frequency crowding is a much more pressing problem in these orbits, there is a popular perception by the developing countries that physical crowding is important, and therefore orbital debris in geosynchronous orbit will receive an increasing amount of attention. However, there is a connection between collision potential and radio frequency allocation. For example, as Al Hiebert, Rand Corp., pointed out, if a satellite is moved in order to avoid collision, both national (FCC & NTIA) and international (IFRB/ITU) frequency management programs must be consulted.

Two Air Force Orbital Position Management papers described the perception of policy makers, and the current Air Force plans and procedures. Capt. Hyland from Hq, Air Force, noted that the debris problem must first be identified, then stated in layman terms. In identifying the problem, the detection of smaller debris will be required but national defense priorities make it difficult to assign NORAD sensors to detect small debris. Capt. Richard Davis, from Space Division, endorsed NASA's planned research as being essential to understanding the cost effectiveness of any requirement or policy on the space user community. Both Air Force speakers believed the workshop and any follow-on activities would provide an excellent start toward identifying the issues which could later be resolved by policy and international treaties if required.

Don Edgecombe, from Battelle, summarized many unresolved policy issues such as the characterization of risk, need for immediate action, national-international coordination, and military implications. Both Don Edgecombe and Dennis Fielder, JSC, stressed the different aspects of policy which could either be defined in terms of objectives and general guidance and remain fixed, or contain specific recommendations of procedures which may change as new problems arise.

The workshop concluded that it is too early to propose specific national or international policy, although there was a consensus that a policy would eventually be required. More technical information is required, especially in the area of environment definition for objects less than 4 cm in diameter. The spacecraft user community must become involved, especially in the areas of Spacecraft Hazard and Shielding Requirements and Space Object Management. For the immediate future, the workshop concluded that NASA should continue as a lead agency to focus and coordinate debris related investigations, information exchange, general activity planning, and development and formulation of prospective civil policy approaches. The adoption and use of low cost measures that decrease debris propagation, such as reducing the incidence of unplanned explosions, using reentering trajectories for planned explosions, and the adopting of anti-litter design and operations habits should be encouraged. Finally, the participants in the workshop expressed the need to formalize a program structure, through an interagency space debris working group, which would develop a program plan and coordinate research and future activities, including subsequent workshops.

Evaluation of Workshop

This workshop represented the first time that all of the various elements of space debris work have been collected and discussed before a diverse audience. Participation was larger than originally expected, both in the number of papers presented, and in audience participation. The workshop audio was recorded and the viewgraphs have been distributed to participants. Within the next few months, all of the papers and the conclusions of the workshop will be published.

The formal presentations and discussions illustrated a basic conflict within the data available: Based on the population of objects known to be in orbit as a result of NORAD cataloging, there is no problem with debris, except possibly when large structures are built in low earth orbit. Thus, one is tempted to ignore the issue. However, based on limited data and reasonable assumptions, a significant population of uncatalogued objects can be modeled to predict problems for much smaller spacecraft. However, the test of these assumptions requires that one not ignore the issue, and obtain more data. It is clearly possible that the problem for smaller spacecraft can be either better, or worse than predicted by the current models. Therefore, the participants put the highest priority on obtaining new data on objects smaller than 4cm in diameter. Such data are not only important in the current design and operations of spacecraft, but they are important in understanding how soon debris will be a significant problem.

The workshop produced an increased awareness of the consequences of the problems caused by particles ejected by solid rocket motors fired in space. Data were presented which showed that at least one scientific experiment and one engineering experiment have had their conclusions seriously compromised because of the presence of these orbiting solid rocket motor products. The detection of these small particles by orbiting experiments clearly illustrates the ease in which the manmade particle flux in earth orbit can be measurably affected. The flux of artificial debris in low earth orbit has thus been measured in two extreme sizes--the very small particles (by meteoroid impact sensors) and the very large objects (by NORAD). In both cases, this flux was comparable to, or greatly exceeded, the natural meteoroid flux. The flux of the debris sizes which is most likely to affect spacecraft design and reliability has not been measured.

The workshop provided an excellent opportunity for NASA, NORAD and the Air Force to exchange their viewpoints, and bring all participants to a common level of understanding. Once this level was achieved, there seemed to be a consensus on the direction of future research. That is, whether the objective is to determine if there is a problem, or to seek a solution to an obvious problem, the first task is the same in both cases--define the environment better. As new data become available, there is an obvious need to maintain dialogue between all interested parties; however, there is currently no forum to do this.

It appeared obvious from the technical papers presented and the discussions which followed that orbital debris can affect spacecraft designs and operations in the future. The extent to which these designs and operations are affected, and the timing and content of future policy are important.

Recommendations Resulting from Workshop

The results of the Orbital Debris Workshop reaffirm the need for research to better understand the character of orbital debris, its effects on future spacecraft, and the related requirements for policy. A clear charter is required for this research to receive the necessary support, focus, and coordination. It is recommended that NASA assume the role of lead agency. The first task is to develop an overall plan with both DOD and NORAD participation. The immediate emphasis of the plan should be in performing the necessary tests, experiments, and modeling which are appropriate for defining the environment of orbiting objects which are smaller than is currently being detected and catalogued by NORAD. The plan should include research in the major areas of Environment Definition, Spacecraft Hazard, and Space Object Managements. Tasks to be performed in each of these areas are as follows:

Environment Definition

The major emphasis relative to LEO should be placed on defining the environment for sizes smaller than 4cm in diameter. This can be accomplished through a combination of laboratory tests, modeling, and ground-based observations of orbiting debris. Ground-based detection techniques can be developed to see smaller particles in orbit. Laboratory hypervelocity and explosion tests can be performed to determine the effects and "signatures" (size and velocity distributions) of these events, which can be used in modeling and analyzing NORAD break-up events. NORAD's capabilities to track smaller objects should continue to be used to the fullest extent consistent with NORAD's basic national security mission. However, since both NORAD and advanced ground-based sensors are limited in their ability to track small orbiting objects, research should continue toward defining and developing a space based sensor to detect even smaller debris. A low-cost, light-weight sensor capable of being flown piggy-back on a number of different missions appears to be the best approach to covering the wide range of altitudes for which data are needed.

Nothing at all is known about debris below 1 meter in size at GEO, and ground-based techniques are at or near their limits. A small, optical sensor in GEO could provide important new information about this valuable region of space. Conceivably, an existing sensor in GEO could provide this data; if not, a light weight sensor could be constructed to fly piggy-back on a planned payload to GEO. The cost of flight requirements make joint Air Force-NASA efforts desirable for both LEO and GEO.

Spacecraft Hazard

The damage to spacecraft resulting from collisions should be determined by compiling all the available data on hypervelocity and relevant low velocity impact tests. New tests are required for composite materials. Damage criteria should be established to reflect the new generation of spacecraft planned for the future, and to reflect various types of failures.

Space Object Management

A more detailed analysis of the cost and impact to future operation is required of the various techniques to control the environment. In addition,

new concepts should be encouraged and evaluated. Until the effectiveness of active techniques to control the environment is understood, it is recommended that the U.S. study and encourage the use of spacecraft designs and operations which will minimize the generation of debris in orbit, such as:

- 1) reducing the incidence of unplanned explosions,
- 2) use reentering trajectories for planned explosions,
- 3) adopt anti-litter design and operational habits,
- 4) use solar and lunar perturbations to reenter objects in geosynchronous transfer orbits.

Concluding Remarks

All of these tasks have been proposed in some detail by NASA/JSC in the past. However, the recommendations contained here reflect a change in emphasis resulting from the workshop. The major changes are to delay a space experiment, increase emphasis on ground-based observations and laboratory tests, and increase emphasis on compiling the results of past impact tests and damage criteria. Although NASA should continue to be the lead agency in implementing these tasks, Air Force participation is essential and channels of communications should be fully explored and used. A joint plan, detailing the tasks to be performed and the individual responsibilities should be prepared jointly by NASA and DOD. A continuing forum, consisting of representatives from NASA and DOD should be established to update the plan, as appropriate.

SPACE DEBRIS ASSESSMENT

10-YEAR PROGRAM PLAN

PROGRAM TECHNICAL PLAN

1.0 Introduction

Prior to 1970, a significant amount of research was conducted to define the meteoroid environment and to develop techniques for shielding spacecraft against particles impacting at very high velocities. Although shielding was required for some spacecraft, the basic structure provided an acceptable reliability for meteoroid protection for most spacecraft. Thus, with the meteoroid environment defined, with techniques to shield against meteoroids defined, and with any remaining uncertainties in these two areas being of only marginal importance to spacecraft planned within this time interval, research in these areas has been terminated.

In the early 70's, investigators at both the Johnson Space Center and the Marshall Space Flight Center concluded that the collision probability between a large structure (100 meters in diameter) and the tracked population of artificial satellites was significant. In the mid 70's, the Langley Research Center investigations predicted a large untracked population resulting from the numerous explosions in space, but still affecting only large structures. These activities were also terminated.

In the late 70's, investigators at the Johnson Space Center predicted that if past growth trends continue, within the next 10 to 20 years, a large number of particles will be generated as a consequence of collisions between artificial satellites. The number, size and relative velocity of these particles could be sufficient to represent a greater spacecraft damage potential to most spacecraft in low earth orbit than the damage from the natural meteoroid environment. In addition, experiments conducted by NORAD confirmed that a population of orbiting objects too small to be tracked by the operational radar system now exists. Even though these objects are too small to be tracked, they are relatively large when considered in terms of their damage potential. These objects, along with the remaining tracked population, already represent a damage potential much greater than the ambient environment.

Recent results from three meteoroid impact sensors (two flown on Skylab, and one on Explorer 46), indicate that the natural meteoroid environment may also already be exceeded by an artificial environment for very small (less than 0.1 mm) particles. Two of the experiments were returned from Skylab, where composition analysis of the surfaces revealed hypervelocity pits containing mostly aluminum. The Explorer 46 "meteoroid impacts", measured between 1973 and 1975, had a strong time correlation with solid rockets fired in orbit, and also a directionality which could only come from earth orbiting particles. Most of these particles were too small to damage any but the most sensitive spacecraft surfaces.

The trend toward larger and longer duration spacecraft in the 80's increases their sensitivity to possible damage from both meteoroids and space debris. Larger structures and longer times in space will increase the probability of collisions from larger meteoroids and space debris. In addition, the desired light weight of reusable space vehicles and of structures built in space may increase their susceptibility to damage from smaller particles, so that meteoroid shielding may be required on an increasing number of future spacecraft payloads. The prospect that these spacecraft may be exposed to an increasing artificial environment which exceeds the natural environment means that even more shielding would be required. As mission costs increase with the amount of shielding, it is

important to define the debris environment so that no more than the necessary amount of shielding is added.

A more important reason to define the environment may be to evaluate the importance of reducing the population growth. Techniques to reduce the population growth have recently become obvious. Only 5% of the tracked population represents operational payloads, leaving 95% as orbital debris. Most of this debris resulted from either intentional or accidental explosions in space which could either be eliminated or reduced in frequency. The mixture of these explosion fragments and old rocket bodies and payloads represents the primary source of future collisional fragments; hence the retrieval of large objects would eliminate potential fragment sources. Techniques to cause objects to reenter using solar perturbations exist. However, whether any of these or other techniques to control the future environment should be used depends on their cost and effectiveness weighed against either the future spacecraft failure rate or the cost of shielding to minimize the failure rate.

The purpose of this plan is to describe the necessary studies, analysis, and experiments to determine which policies should be pursued.

2.0 Objectives

The objective of this program plan is to develop the decision tools and the management schemes necessary to minimize the hazard to spacecraft from orbital debris in a cost effective manner. In order to obtain this objective, several short term objectives are required:

- (1) Using appropriate modeling, ground experiments, and flight experiments, develop the capability to define the orbital debris environment.
- (2) Using appropriate ground tests and systems analysis, develop the capability to evaluate the effect of this environment on spacecraft.
- (3) Using appropriate studies and the results of tests, develop techniques of either controlling the environment or protecting spacecraft from the environment.
- (4) Develop an algorithm which will evaluate the costs versus savings of either controlling the environment, shielding from the environment, or doing nothing.
- (5) Develop the rationale for establishing policy positions.
- (6) Develop the capability to monitor the effects of any policy position and the mechanism to change that policy when necessary.

3.0 Justification and Rationale

3.1 Debris Environment Definition

3.1.1 Modeling - A mathematical computer model translates applicable experimental measurements into the pertinent information required when that information cannot be measured directly. Experimental measurements are sometimes replaced by "reasonable assumptions," especially when extrapolations are required. The pertinent information required deals with spacecraft failure rates, now and in the future, caused by collisions with orbital debris. Major experimental measurements consist of the ground detection of earth orbiting objects, ground explosion tests, and hypervelocity impact tests. Some of these measurements to date are inadequate, as shall be detailed later. Reasonable assumptions are required to predict future atmospheric densities (solar activity), and future space activities. Also, some of the hypervelocity impact tests are performed at energy levels which are different than those expected in space, so that extrapolations in energy are required.

Equations have already been developed which relate orbital elements to collision probabilities. However, the major problem in developing a computer model is in computer limitations. As a consequence of collisional fragmentation, literally millions of objects must be handled by predicting the collision potential of each through all volumes of space which they may pass, now and in the future. This large amount of data and computations precludes handling each of these objects on an individual basis. Statistical approaches have been developed and must be developed further.

When known, the physical characteristics, launch date, source, or any other characteristics of each satellite should also be maintained. This will allow for the examinations of trends and the discovery of principal sources. The physical size of objects is important in determining collision probability, although a measure of the physical size is obtained from radar cross section. How an object may fragment is also a function of physical characteristics.

Current launch traffic models do not list every object which is placed into orbit during the launch of a particular payload. Usually, a rocket body does remain in orbit for each payload launched, and these objects are usually tracked by NORAD. However, smaller objects, such as attachment fittings, springs, clamps, etc. are not listed in any traffic model, and these objects are not tracked by NORAD.

3.1.2 Ground Experiments

3.1.2.1 Spacecraft Fragmentation Experiments

Although some ground experiments have been performed to determine the probable distribution of space debris fragments resulting from satellite disintegration, more studies are required to accurately model the current and projected environment of small debris. Fragmentation tests in the past have been sufficient to define some issues, but are inadequate to develop a definitive model. Explosion tests have mostly consisted of thin walled cylinders, bombs, shells, or grenades. Data were obtained from the ground explosion of an Atlas missile tank. However, no ground tests have been performed on any object which is known to have exploded in space, such as the Delta 2nd stage, or Agena stage. Only two tests to determine the size distribution due to hypervelocity impact into a spacecraft structure have been performed. These tests used a relatively small (.37 to 1.65 gram) projectile fired at a relatively low velocity (3 to 4.5 km/sec). The tests yielded a size distribution similar to the many similar tests into basalt. However, the

basalt tests revealed a fragment velocity which increased with decreasing size, whereas the analysis of the spacecraft tests was only analyzed sufficiently to determine that the fragment velocities were very low. These velocities are necessary to determine the amount of fragment mass which is ejected into different orbits, or reenters.

3.1.2.2 Ground Observations

The ability of NORAD to detect and track objects in Earth orbit varies with altitude. Below 6000km, radar systems are the principle means of detecting objects. Most objects detected by radar are larger than 10cm in diameter. Above 6000km, radar efficiency is reduced to the point that optical tracking is required. The optical technique currently uses a Baker-Nunn camera, which can detect a 1 meter object in geosynchronous orbit. Within a few years, an electro-optical system will be operational and will improve that capability slightly; however, the principle advantage to this system is its quicker turn-around time of data.

Two radar ground experiments have been performed in order to test NORAD's ability to track small objects in space. These tests, using the PARCS radar, only slightly increased the sensitivity of the operational system, but did reveal an untracked population. However, both the PARCS and operational radar system are limited by the radar wavelength at which they operate. Objects smaller than about 10 cm are small compared to the radar wavelength, and hence become very difficult to find and track. Similar tests could be performed with available shorter wavelength radars enabling the minimum size detected to be reduced. According to a study by General Electric Co., the use of optical tracking in low earth orbit could reduce the minimum size even further to approximately 1 cm. However, the electro-optical system developed for NORAD is currently planned to only track at orbital altitudes above 6000 km. Changes in their software could allow it to be used to track in low earth orbit.

3.1.3 Other Data Sources

Less direct techniques to determine the untracked population may be available. For example, some satellites have obtained abnormal data or shown abnormal behavior which could be interpreted as detection of, or impact by orbital debris. It is expected that a more thorough search for, and examination of, such data may reveal more clues to the current untracked population.

3.1.4 Flight Experiment and Debris Monitoring System

Ground observations of orbital debris are limited in their ability to detect objects of interest to spacecraft. In addition, some events, such as the consequence of USSR anti-satellite tests, cannot be modeled, and unforeseen events may cause an environment significantly different than predicted by a model. Therefore, model predictions must be tested, and the environment monitored so that model assumptions may be tested and updated as appropriate. Such a monitoring system must be able to detect a large range of object sizes in sufficient numbers to be statistically significant, and to be able to discriminate between earth orbiting objects and interplanetary meteoroids. Studies conducted in the 60's for meteoroid applications demonstrated the feasibility of using both radar and optical techniques in order to accomplish these objectives. The optical sensor studied eventually flew on Pioneers' 10 and 11. Later studies concluded that either of these systems could be applied to debris measurements, and that technology advancements have been significant since the original studies. Although sufficient studies have not been performed to identify a preference between

optical and radar techniques, recent studies have demonstrated a preference for a radar technique.

Smaller debris particles, as those which may originate from solid rocket exhaust, can be measured by impact sensors. Since the late 60's, meteoroid impact sensors have been flown on many spacecraft. Below about 0.1 mm, the flux of meteoroids is at least several impacts per sq. meter per year, so that a debris flux which exceeds this level could be measured with a few sq. meters of collecting area.

3.2 Debris Hazard Assessment

The probability of collision is not necessarily the same as the probability of sustaining significant damage. Whether a particular collision causes significant damage or not depends on the size and velocity of the projectile, as well as the physical construction and importance of the area impacted. By combining hypervelocity impact data and spacecraft systems configuration with an environmental flux model, the probability of significant damage to any particular spacecraft can be obtained.

3.2.1 Impact Damage Assessment Studies

Prior to 1970, a large number of impact tests were performed in order to determine the amount of damage which would result from a meteoroid impact on a spacecraft. Projectiles, usually consisting of aluminum or glass, with masses as large as several grams were impacted on targets at velocities of 6 to 8 km/sec. Much smaller projectiles obtained velocities greater than 10 km/sec. These tests more accurately duplicated the size, velocity, and composition of impacts from manmade orbital debris than impacts from meteoroids. Thus, the results of these tests are directly applicable in determining the amount of damage that debris impacts will cause a spacecraft. However, since 1970, some new structures and materials have been developed. Accurate determination of the effects of impacts into these materials would require some additional testing.

3.2.2 System Damage Criteria

Whether the hole, pit, or ejecta which results from an impact is significant or not also depends on the criticality of the system impacted and its susceptibility to damage. For example, previous tests have shown that very minor pits on the surface of spacecraft windows can cause these windows to crack when experiencing the pressures of lift-off. Similarly, highly pressurized containers have been shown to fail when only pitted by an impact. The complete penetration of a structure may or may not produce significant damage. Systems tests may be required to determine if the failed structure causes a critical loss in mission capabilities. Hypervelocity tests may be required to determine if the plasma and particle ejecta associated with the penetration will effect electronic components or other hardware, or crew safety. In most cases, data obtained from previous tests would predict the amount of additional hardware damaged from particle ejecta.

3.2.3 Mission Success Assessment Algorithms

During Apollo, and some other missions, each subsystem was listed, along with its exposed area, and the size meteoroid impact which would cause significant damage. Since the meteoroid environment was not initially well defined, these data were stored and up-dated as new impact tests were performed. In addition, as new data describing the meteoroid environment became known, the probability of mission success from the meteoroid hazard, as well as the need for additional shielding or redundancy, were quickly evaluated. Such algorithms can be generalized to include a variety of spacecraft subsystems exposed to both a meteoroid and orbital debris environment.

3.3 Space Object Management Studies

3.3.1 Control of the Debris Environment

The only natural removal mechanism for earth orbiting objects is caused by orbital decay from atmospheric drag. However, orbital decay acts very slowly and tends to replace objects removed from lower altitudes by objects which have migrated down from higher altitudes. Some recent studies have demonstrated that other options exist, although most may prove to be impractical. The following are some of these possibilities.

3.3.1.1 Minimization of explosions in space

Approximately half of the tracked population is the result of explosions in space. Most of these explosions were of old U.S. rocket stages which blew up for no apparent reason after years in space. For the last 10 years, the Delta 2nd stage has been the major contributor. Actions are being taken to minimize the risk of future Delta explosions.

Although the USSR anti-satellite tests have not contributed as much to the trackable population as the U.S.'s accidental explosions, they could be the major contributor to a population too small to be tracked. High intensity explosions are known to produce many orders of magnitude more small particles than the U.S.'s low intensity explosions. The USSR tests were performed at sufficiently high altitudes and most of the debris will remain in orbit. However, if these tests were performed at lower altitudes, the fragments would reenter at a higher rate and constitute much less of a risk to other spacecraft.

3.2.1.2 Reentry of orbital transfer vehicles

Any object placed in GEO leaves behind a rocket body whose perigee is in low earth orbit, and apogee is at geosynchronous altitude. This rocket body can be made to reenter by a very small velocity change at apogee. The velocity change could be made with small thrusters; however, recent studies have shown that lunar and solar perturbations can accomplish the necessary velocity change over a few years, if the launch is made at an appropriate time. Otherwise, lunar and solar perturbations are just as likely to increase the perigee distance, causing the rocket to remain in orbit for a much longer period. Scheduling launches to cause the rocket body to reenter earlier would place another constraint on launch operations. Whether this constraint is acceptable or not has not been determined.

3.3.1.3 Retrieval of large, non-operational objects

Large, non-operational payloads may be the principle source of debris generated by collisions in the future. Previous studies have concluded that the Orbiter can reach about half of the U.S. non-military payloads. Thus, use of the Orbiter to retrieve many of these objects is feasible, but may prove to be expensive. Another approach may use permanent stations in space where objects are returned to the station and later returned to earth. However, to retrieve a large number of objects, many orbit changes would be required. The use of an efficient low thrust system (e.g. ion propulsion) may be required for the retrieval vehicle.

3.3.1.4 Debris catcher

Every day an object passes within a few tens of km of another tracked object in space. Thus, any spacecraft would only have to maneuver a few tens of kilometers in order to collide with an object each day. If this spacecraft were large enough to survive the collision and capture the ejecta from the collision, then it could reduce the debris population by one per day. However, the feasibility of such a system has not been studied. There are major engineering problems in the tracking of such objects, in surviving the collision, and in containing the ejecta. If the "debris catcher" were a

few tens of kilometers in diameter, it could collect a tracked object each day without maneuvering, plus a significant fraction of the untracked population. Light weight foam might be used to construct such a structure, but again, the feasibility of such a system has not been studied.

3.3.1.5 Collision avoidance maneuvers

Collisions with objects too small to be tracked cannot be avoided. In addition, the current ground system cannot track objects with sufficient accuracy to predict a collision. However, it is conceivable that some improvements in the ground system combined with an on-board tracking and avoidance system may be of some advantage. However, feasibility studies have not been performed.

3.3.1.6 Removal of spacecraft from geosynchronous orbit

Although collisions in GEO are currently not probable, suggestions have been made from several sources to place payloads outside GEO before the payload fuel is exhausted. Since such a maneuver requires only a small amount of fuel, it has already been used once. However, before such a practice becomes commonplace, care must be taken that either geosynchronous space does not become redefined to include the altitude at which these dead satellites are placed, or that the dead satellites do not drift back into geosynchronous space. A study has shown that at inclinations greater than 45° , objects may easily drift into geosynchronous space. However, further studies are required.

3.3.2 Assess Effectiveness of Control Measures

Associated with each control measure is a cost, or "investment." This investment will eventually show a return or "savings" through a reduced future spacecraft failure rate. Whether the return on any or all of the control techniques is worth the original investment has yet to be determined.

3.4 US Policy and International Agreement

Currently, there are no formal US policies or international agreements concerning orbital debris. The US Air Force Space Division has a Commanders Policy 550-11 on the subject. Informal agreements within NASA have led to actions to eliminate objects in geosynchronous orbit, and to minimize the chance of the accidental explosion of the Delta 2nd stage in orbit.

4.0 Technical Approach

In order to meet the objective of this program plan, the following tasks are required.

4.1 Debris Environment Definition

4.1.1 Model Development

A three dimensional, time dependent mathematical model will be developed which translates launch traffic models, debris tracking data, ground fragmentation data, and eventually flight experimental data, into particle flux as a function of impacting size and velocity on any particular spacecraft. Since adequate debris traffic models do not exist, part of this effort must include a detailed accounting of planned objects placed into orbit. A search will be made for existing data which may indicate the nature of the current or future untracked debris population. A significant amount of new data will be required from ground and flight experiments as detailed in the following sections.

The mathematical model will be used to obtain a definition of the consequences of the projected orbital debris population growth rates. The uncertainty in these consequences and the need for additional data will be evaluated as the model is developed. Population growth rates will be varied to determine the effectiveness of various techniques to control growth.

4.1.2 Ground Experiments

A cooperative program will be developed with NORAD as a means of obtaining experimental ground tracking data of smaller objects. Emphasis will be placed on obtaining optical tracking data in low earth orbit. However, should this prove impractical, tests will be planned using their radar systems.

Fragmentation ground tests will consist of chemical explosions and hypervelocity impact tests. A 2nd stage Delta will be exploded under test conditions where both the size and velocity of fragments can be determined. The collision between two orbiting objects will be simulated by using a hypervelocity gun, where the projectile and target structure have been scaled down in size. The fragment size and velocity distribution will also be determined.

4.1.3 Other Data Sources

A search will be made for other data which may give clues to the existing untracked population. Particular attention will be paid to any flight experiment data which may have detected debris. In addition the sudden failure of some payloads, and the unexpected break-up of some objects in space will be examined for a possible collision explanation.

4.1.4 Flight Experiment

A study will be conducted to update the 1960's studies and technology and determine the most desirable instrument for detecting, and obtaining orbits for, orbital debris which is too small to be detected from the ground, but large enough to cause significant damage to spacecraft. This size range is expected to be between approximately 1mm and 10cm in diameter. The experiment should be capable of sampling at least one object every few days, and determining its size and orbit. The experiment is expected to use either optical or radar measurements to detect these objects, and be a free-flying satellite in an elliptical orbit between approximately 400 and 1000 km.

The need for the instrument to also have an impact sensor, capable of detecting orbiting solid rocket exhaust particles .1mm, or smaller, will be evaluated. A reevaluation of the need for, and characteristics of, a flight experiment will be made based on the results of this study, the modeling and hazard analysis, ground experimentation, and other data sources. If this reevaluation still indicates the need for a flight experiment, or debris

monitoring system, then such an instrument will be designed, built, and flown.

4.2 Debris Hazard Assessment

The objective of debris hazard assessment task is to translate debris impact rates into spacecraft failure rates. To accomplish this, three sub-tasks are required.

4.2.1 Impact Damage Assessment Studies

A literature search will be conducted to consolidate the impact data and models generated from previous experiments. The results of this data is expected to describe the amount of damage to most surfaces when impacted with a projectile of known size and velocity. However, gaps in the data are expected, primarily because of some new materials which are currently used on spacecraft. Therefore, some new tests will be conducted.

4.2.2 Systems Damage Assessment Studies

The spacecraft designers and builders will be used to assess the criticality of damage to various spacecraft sub-systems. In most cases, the existing failure analysis can be used. However, tests may be required in some cases to determine the extent of damage required to cause a sub-system to fail.

4.2.3 Mission Success Assessment Algorithms

The object of this task is to combine the results of the debris model, impact damage assessment studies, and systems damage assessment studies into an algorithm, or model, which will be used for both engineering design studies and to determine the overall environmental cost to the spacecraft community. The spacecraft designer will be able to input the nature of a particular sub-system, its size, duration and location in space, and obtain a reliability for that subsystem. If that reliability is not acceptable, he can use the algorithm to determine what design changes are necessary to obtain the desired reliability.

This algorithm will be generalized to evaluate the cost of a given debris environment on the overall spacecraft community. Spacecraft type and debris environment will be inputted into the algorithm. The output will be the expected failure rate or the extra shielding weight required for this type of spacecraft in the given debris environment.

4.3 Space Object Management Studies

4.3.1 Control of the Debris Environment

All of the potential control techniques listed in section 3.3.1 will be evaluated in terms of their feasibility, impact on space operations and their cost to implement. As additional ideas evolve, they will also be evaluated using these criteria. Initial emphasis will be placed on eliminating explosions in space, retrieval of large, non-operational satellites, and removal from geosynchronous orbit.

4.3.2 Assess effectiveness of control measures

An algorithm, or model, will be developed which will compare the "cost investment versus savings" for each control technique. This algorithm will then be used to determine the most cost-effective techniques of obtaining the desired reliability in spacecraft. It will become the basis of formulating a comprehensive NASA Management Instruction (N.M.I.), and will identify those areas where broader policy may be required.

4.4 U.S. Policy and International Agreement

As the results of various studies become known, it may become obvious at any point in time that a U.S. policy or international agreement is required. However, the elements of this plan are designed to determine the most cost effective policies. Therefore, at the completion of the tasks within this plan, any existing policies will be reexamined for their cost effectiveness. When necessary, new U.S. policy will be formulated and

international agreements will be negotiated. The effects of any policies are planned to be monitored by the flight experiment/debris monitoring system. Should the monitored environment change from that expected, policies will again be reexamined.

5.0 Program Schedule and Projected Costs

5.1 Program Schedule by Major Element

Figure 5-1 depicts the schedule for the major elements of the program. Associated costs have been estimated for each of the sub-elements for each major task and are shown in figures 5-2, 5-3, and 5-4. It should be noted that these costs must be critically reviewed in the light of projected inflationary factors.

5.2 Project Program Costs

Figure 5-5 depicts costs by major elements and yearly FY totals, as well as element totals. It should be noted that further analysis will be required of the annual sensor deployment and data analysis costs, as well as the costs for payload processing at the launch site, data pre-processing and processing, establishment of a baseline data base and maintenance there of. It is also recognized that mission profiles and sensor deployment configurations will affect program costs significantly.

6.0 Program Management and Structure

It is considered premature at this time to define the program management responsibilities and interfaces with other agencies because of the many groups and agencies already addressing the space debris problem. However, the NASA JSC program management plan will be included in the Program Implementation Plan (PIP).

Figure 6-1 shows a preliminary logic flow of key program elements and milestones. The program management structure would be tailored to those program requirements. The milestone dates are shown in the flow are tentative, but provide target dates for program planning purposes.

7.0 Bibliography

1. Donahoo, M. E., "Collision Probabilities of Future Manned Missions with Objects in Earth Orbit", MSC Internal Note NO. 70-FM-168, Oct. 20, 1970.
2. Kessler, D. J. and B. G. Cour-Palais, "Collision Frequency of Artificial Satellites: The Creation of a Debris Belt," J. Geophysical Res., Vol. 83, A6, 1 June 1978.
3. Reynolds, Robert C. and Norman H. Fischer, "The Hazard Presented to Shuttle by Other Satellites in its Operating Environment," Proceedings of the March, 1980 JANNAF Safety and Environmental Protection Specialist Session, CPIA Pub. #313, March 1980.
4. AIAA Technical Committee on Space Systems, "Space Debris", An AIAA Position Paper, American Institute of Aeronautics and Astronautics, 1290 Avenue of the Americas, New York, NY 10104, July 1981.
5. Kessler, D. J., "Sources of Orbital Debris and the Projected Environment for Future Spacecraft," Journal of Spacecraft and Rockets, Vol. 18, No. 4, pp. 357-360, July-Aug 1981.
6. Hechler, Martin, and Jozef Van Jer Ha, "Probability of Collisions in the Geostationary Ring", Journal of Spacecrafts and Rockets, Vol. 18, No. 4, pp. 361-366, July-Aug 1981.
7. Chobotov, V. A., "The Collision Hazard in Space," Preprint No. 81-148, AAS/AIAA Astrodynamics Conference, Lake Tahoe, California, 3-5 August 1981.

SCHEDULED ELEMENTS FOR MAJOR ELEMENTS FOR ORBITAL DEBRIS ASSESSMENT

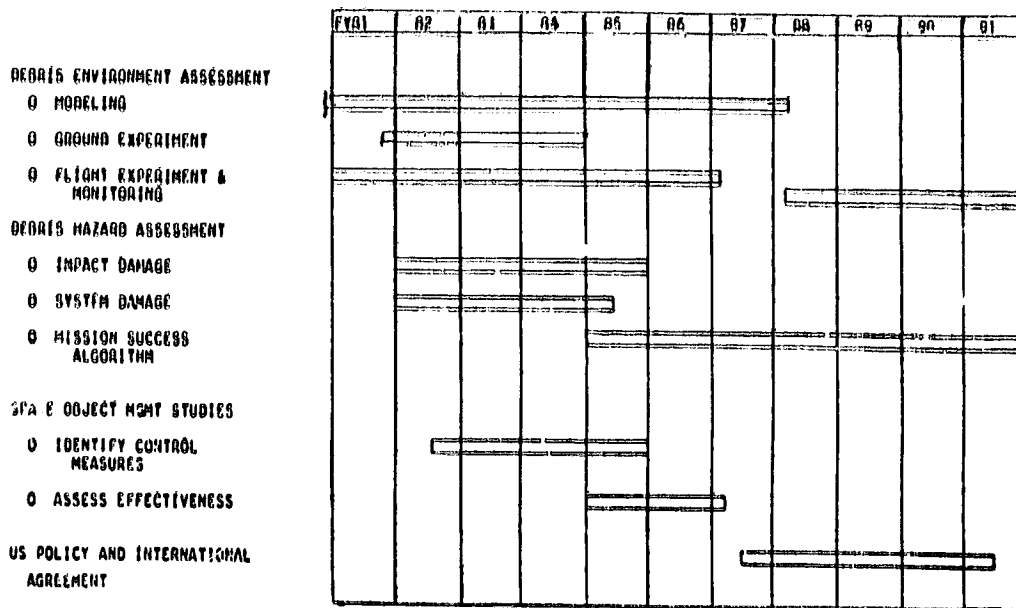


FIGURE 5-1

SCHEDULED ELEMENTS FOR ORBITAL DEBRIS ASSESSMENT

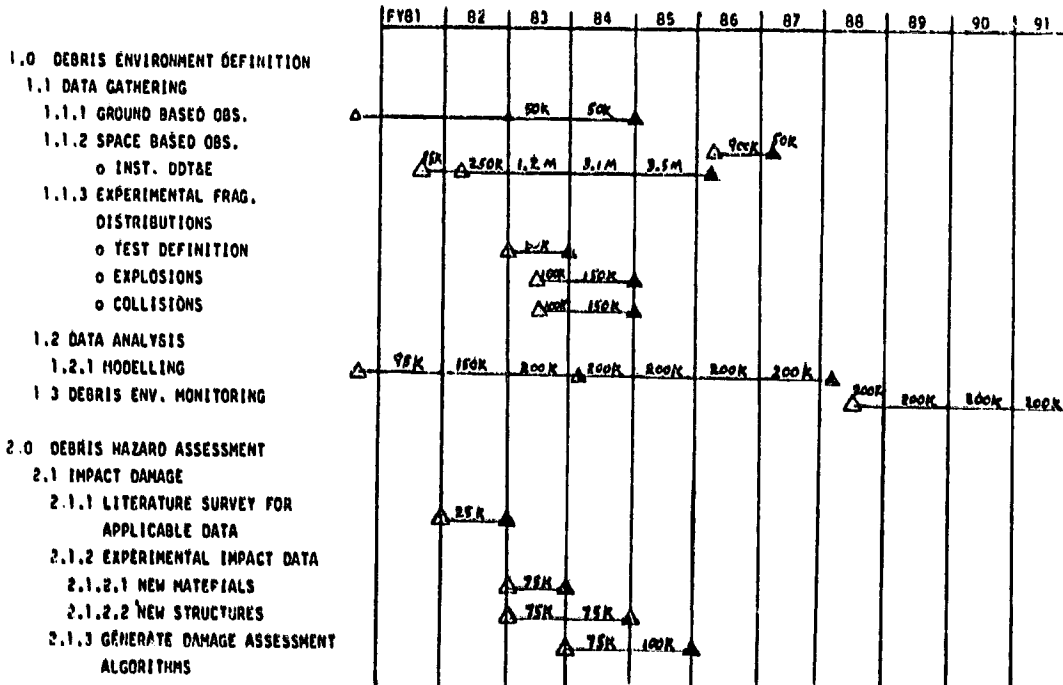


FIGURE 5-2

SCHEDULED ELEMENTS FOR ORBITAL DEBRIS ASSESSMENT

- 2.2 SYSTEM DAMAGE CRITERIA
 - 2.2.1 CRITICAL DAMAGE CRITERIA DEFINITION
 - 2.2.1.1 THERMAL CONTROL SYST.
 - o TILFS
 - o RADIATORS
 - 2.2.1.2 CONTROL SURFACES & LINKAGES
 - 2.2.1.3 NOZZLES
 - 2.2.1.4 TANKS
 - 2.2.1.5 POWER GENERATION SYS.
 - o SOLAR PANELS
 - o FUEL-CELLS
 - o BUSES
 - 2.2.1.6 PRESSURE CABINS
 - 2.2.2 INVESTIGATE REDUNDANT SYSTEMS
 - o COMPLEXITY
 - o FLEXIBILITY
 - o COST-EFFECTIVENESS
- 2.3 MISSION SUCCESS ASSESSMENT ALGORITHMS

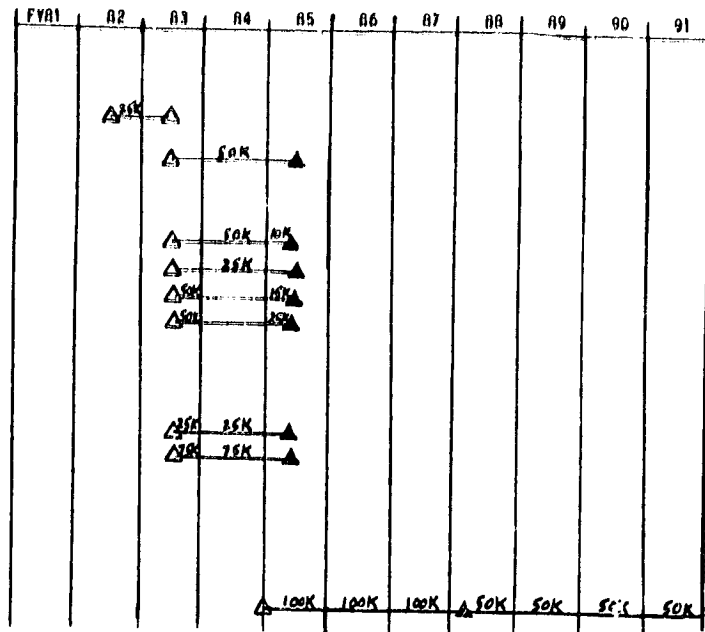


FIGURE 5-3

SCHEDULED ELEMENTS FOR ORBITAL DEBRIS ASSESSMENT

- 3.0 SPACE OBJECT MANAGEMENT STUDIES
 - o IDENTIFY NASA CONTROL MEASURES
 - o PASSIVE TECHNIQUES
 - o ACTIVE TECHNIQUES
 - o ASSESS EFFECTIVENESS OF CONTROL MEASURES
 - o ENVIRONMENT
 - o MISSION CAPABILITY
 - o COST-EFFECTIVITY
 - o NASA MANAGEMENT INSTRUCTION
 - o PROGRAM MANAGEMENT DECISION ALGORITHMS
- 4.0 U.S. POLICY AND INTERNATIONAL AGREEMENT
 - o U.S. POSITION
 - o UN POSITION
 - o INTERNATIONAL AGREEMENT

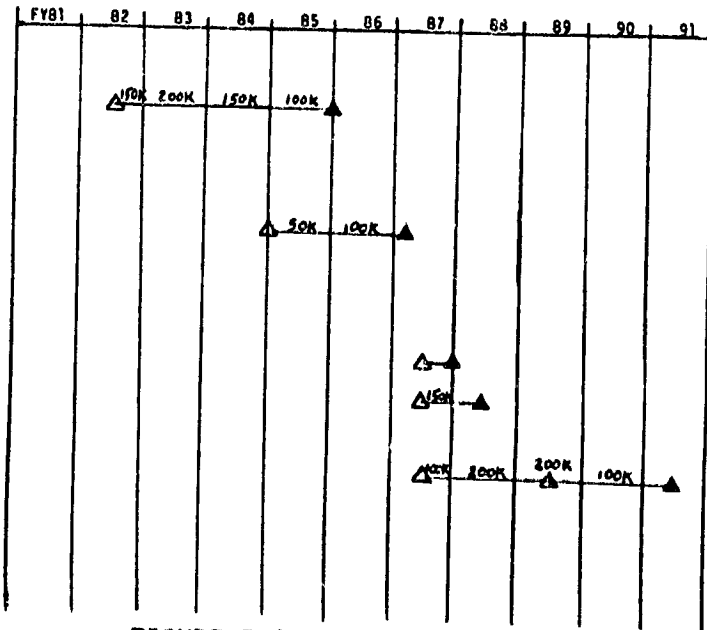


FIGURE 5-4

MAJOR ELEMENT	FY81	82	83	84	85	86	87	88	89	90	91	TOTAL
1.0 DEBRIS ENVIRONMENT DEFINITION	180K	400K	1.7M	3.65M	3.7M	1.1M	250K	200K	200K	200K	200K	11.78M
2.0 DEBRIS HAZARD ASSESSMENT	-	50K	350K	375K	250K	100K	100K	50K	50K	50K	50K	1425K
3.0 SPACE OBJECT MANAGEMENT STUDIES	-	150K	200K	150K	150K	100K	150K	-	-	-	-	900K
4.0 U.S. POLICY AND INTERNATIONAL AGREEMENT	-	-	-	-	-	-	100K	200K	200K	100K	-	600K
TOTAL	180K	600K	2.25M	4.175M	4.1M	1.3M	600K	450K	450K	350K	250K	14.705M

FIGURE 5-5 PROJECTED COSTS FOR ORBITAL DEBRIS ASSESSMENT BY MAJOR ELEMENTS

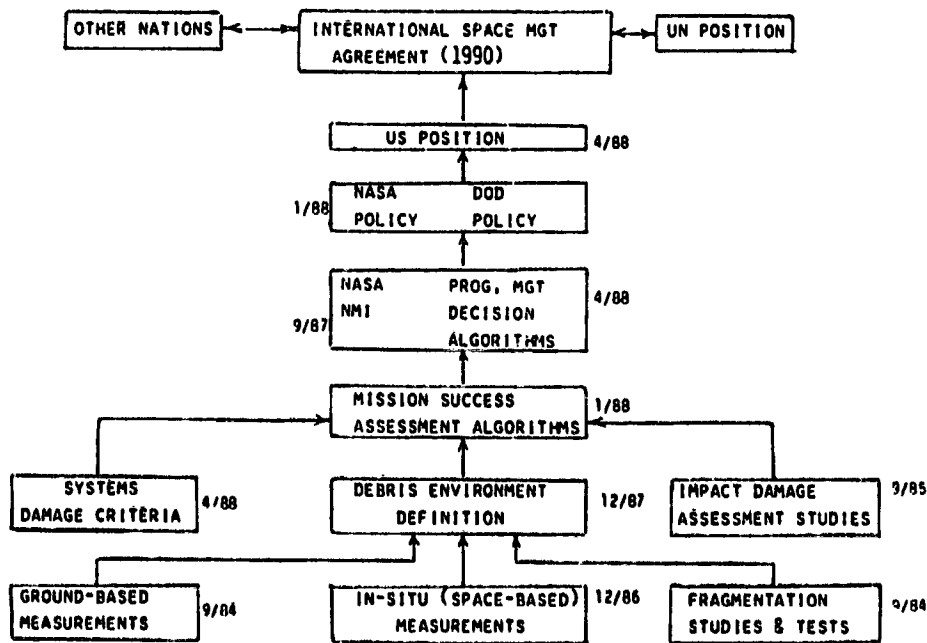


FIGURE 6-1 - PROGRAM ELEMENTS AND MILESTONES

D1-
N 85-21189

NORAD Operational System

Captain David Brach
NORAD Headquarters
Peterson AFB
Colorado 80914

1. SPACE SURVEILLANCE AND DETECTION

Thank you very much. It is both an honor and a pleasure to be able to address this workshop today. We, at NORAD, view space defense as our most dynamic mission area and welcome any opportunity to tell the Command Space story.

2. SPACE DEFENSE TASKS

There are three aspects to the Space Defense Mission -- satellite surveillance, satellite protection and satellite negation. We have been doing the satellite surveillance mission for over two decades and by all measurement, we do it very well. We have had a negation mission in the past, but the protection mission is relatively new. Although I have been asked to speak primarily about the surveillance area, I am sure you will see that space surveillance is the foundation for the protection and negation functions.

On your program the specific subject of my presentation is entitled "NORAD Operational System." I have modified that topic just a bit in recognition that the overall concern of this workshop is orbital debris. I have focused on space surveillance and detection as currently accomplished by both ground and space based assets.

3. OVERVIEW

The following is what we will be talking about today. To understand the space surveillance business, one needs to understand how the current system has grown over the years. We will talk about how the system has matured to the present, then describe the characteristics of the current system. The remaining half of our presentation which deals with the requirements for a future surveillance system will not be presented at this time. However, I would be happy to discuss this subject with anyone interested later in the week.

4. EVOLUTION OF THE SYSTEM

The space surveillance system has evolved over 25 years. This evolution can be divided into three phases. We are currently in phase three. Phase four would be initiated with the fielding of a new generation space borne surveillance system. That initiation date is not established.

4.1 PHASE ONE (1957-1964)

When the Soviet Union launched Sputnik I on 4 October 1957, the U. S. became aware it had almost no capability to detect, track, or identify manmade objects in space. The launch of Sputnik came as a complete surprise to the U. S.

4.1.1 REQUIREMENT

The requirement for a space surveillance system goes back to 1955 when the United States decided under Project Vanguard to orbit a small scientific satellite during the 1957-58 International Geophysical Year. This goal resulted in the establishment by the Naval Research Lab of several mini-track radio stations ranging from Blossom Point, Maryland, to Santiago, Chile (see Figure 1). In addition to these mini-track stations, a network of optical tracking stations was established by the Smithsonian Astrophysical Observatory Headquarters at Cambridge, Massachusetts. These optical sensors were the Baker-Nunn cameras which were specially designed for tracking man-made satellites. Also, the Smithsonian organized a network of amateur astronomers to assist in tracking satellites. This effort was called Operation Moonwatch.

While preparations were being made for tracking Project Vanguard IGY satellites, efforts were also underway to develop a radar to track ballistic missiles. This was being done at Millstone Hill, Massachusetts, where the Lincoln Lab people were working with an 84-foot diameter radar dish.

In response to the requirement to ensure tracking of orbiting satellites over the North American continent, the newly established Advanced Research Projects Agency (ARPA) directed the Naval Research Lab to develop an electronic fence. This facility, which became known as the Naval Space Surveillance Network or NAVSPASUR, became operational in March 1960 with Headquarters and Correlation Center at Dahlgren, Virginia.

NAVSPASUR and the spacetrack sensors were subsequently combined into a national-capability called the Space Detection and Tracking system (SPADATS). On 7 November 1960, the Joint Chiefs of Staff assigned operational control of this SPADATS network to NORAD.

The Baker-Nunn cameras, certain radars, and NAVSPASUR constituted the dedicated system. In the early 1960's, the SPADATS system was augmented by observational data from certain cooperative sensors, such as the Ballistic Missile Early Warning System (BMEWS). BMEWS was primarily designed against the threat of missile attack over the Pole, but had a good spacetrack capability too.

4.1.2 CHARACTERISTICS

In summary, the early system had the following characteristics. The optical systems were the Baker-Nunn cameras and the various optical instruments operated by amateur astronomers under Project Moonwatch. The

radio systems were radio telescopes, and a system of radio and doppler receivers. The radars included the Shemya and Dlyarbakir tracking radars and fans, the Moorestown and Laredo tracking systems, and the three BMEWS sites.

The Command and Control Center which had begun with a very primitive Filter Center at the Cambridge Research Center at Hanscom AFB, had by 1961 moved to a more automated capability next to the NORAD Command Post at ENT AFB Colorado. By 1964, plans were validated for a Space Defense Center to be located in the Cheyenne Mountain Complex which was then under construction.

As a data point, the inventory of objects in space had grown to approximately 400 by the end of 1963.

4.2 PHASE TWO (1964-1971)

4.2.1 REQUIREMENT

Phase Two was basically a period in which computational capability and existing ground based systems were upgraded to respond to more demanding requirements. For example, in May of 1963, the Air Force was directed to deploy an operational anti-satellite system. In May of 1964, the Air Force completed a successful launch of the system using a Thor missile launched from Johnson Island in the Pacific. This program, which was active for the rest of the decade, was dependent upon positional data from the Space and Detection and Tracking network.

The second requirement which placed significant demands on the network was the need to accurately determine the impact points of reentering space objects. Initially, this was a requirement of U. S. spacecraft owners but later was formalized in the 1967 Outer Space Treaty which made States responsible for damages resulting from space objects impacting other countries.

This map (see Figure 2) shows the SPADATS network as it evolved during this period. The network was expanded to include the FPS-85 radar at Eglin AFB. This was the first radar designed expressly for satellite surveillance; just before LOC, it was modified to include a secondary mission for detection of submarine-launched ballistic missiles. The operational date of this phased array radar received a major setback when fire destroyed the transmitter and receiver antenna faces during Category II testing in January 1965. Four years later it began operating as part of the Spacetrack System and the SLBM Detection System. Almost immediately, the FPS-85 was able to identify numerous "Unknown Space Objects" which had earlier been catalogued but never successfully tracked for the Space Defense Center.

The FPS-85 allowed the network to pick up the low inclination satellites and greatly increased the capability of the overall system. For example, the FPS-85 could track 200 known satellites or 20 "unknown" simultaneously where previously we were limited to one "real time" track. Because of the radar's computational capability it was designated the Alternate Space Defense Center.

Two Baker-Nunn cameras were relocated during this period to their current locations. The camera which had been deployed to Chile was relocated at the Mt. John Observatory in New Zealand and became operational in October 1969.

The camera in Norway was relocated to San Vito, Italy, and became operational in December 1970.

The capability of the Baker-Nunn System was also enhanced during this period. The response time to search, find, and produce an accurate observation and report it to the Space Defense Center in Cheyenne Mountain was reduced from 24 hours to 12 hours.

4.2.2 CHARACTERISTICS

During Phase Two, the system computational capability was significantly upgraded. Within the Space Defense Center, more powerful software had been developed that could take many more forces into consideration such as variations in atmospheric drag and gravitational forces as functions of latitude and longitude.

Command, Control and Communications were upgraded between various sensor locations and the Space Defense Center.

The Space Defense Center in Cheyenne Mountain came on line in 1966 as the Command, Control and Communications Center. By the end of 1970, the Space Defense Center had catalogued a total of approximately 4300 objects of which about 1850 objects were still in orbit.

4.3 PHASE THREE (1971-PRESENT)

With the Soviet's development of an operational anti-satellite system, space surveillance information was now needed to provide timely warning of an attack against our space assets. In addition to providing the warning the network had to be capable of verifying that an attack had or had not been successful.

The third requirement developed later in this period with the development of the new U. S. ASAT System. Its very flexibility requires accurate tracking data to ensure a successful intercept.

This is the network essentially as it exists today (see Figure 3). There have been several additions to the system during this period. We mark the beginning of this phase with the operational deployment of a spaceborne infrared system. I'll talk more about this satellite in the next section.

As far as ground-based sensors are concerned, the perimeter acquisition and attack characterization system (PARCS) at Concrete, North Dakota, was added in 1974 to the SPADATS network. This sensor, which had been designed to provide the long range acquisition and tracking of ballistic missiles for the safeguard antiballistic missile system, was already constructed when

the Congress elected not to continue the ABM system. This system provides both missile warning of ICBM and SLBM attack as well as detection and tracking satellites. Since it was designed to track small objects reentering the atmosphere, PARCS is one of our most precise spacetrack sensors. You will be hearing more about the capabilities of this system later in the workshop.

The mechanical tracker and detection fan at Shemya, Alaska, was replaced in 1974 with a new phased array system called Cobra Dane. This provided greatly increased capability in the number of objects which could be tracked simultaneously. Cobra Dane also extends the radar coverage well beyond clear BMEWS coverage for detecting and tracking ICBMs.

On the optical side, the Maui Optical Tracking and Identification Facility (MOTIF) was added to the network in 1978. This capability was an advancement over the existing Baker-Nunn capability by providing near-real time observations on deep space satellites -- those beyond 3000 miles. This near-real time capability is provided by linking an optical telescope to a television camera and computer.

About three years ago, Pave Paws phased array radars at Otis AFB, Massachusetts, and Beale AFB, California, were added to the network as a mission secondary to missile warning. These systems were specifically designated to extend the SLBM coverage and data handling capacity; however, they also provided precise detection and tracking of satellites.

Finally, in the command and control area, the Space Defense Operations Center (SPADOC) was established in Cheyenne Mountain in October 1979. SPADOC replaced the Space Defense Center and was established in recognition of the requirement to provide advisory warning to U. S. satellite owner/operators of any hostile threat to their systems and to provide collision avoidance information. This is the satellite protection role I mentioned at the beginning of the presentation. SPADOC will also play a very key role as NORAD's operational Command and Control Center of the U. S. ASAT system current under development. The F-15 with miniature vehicle, when operational, will be our satellite negation capability.

4.3.2 CHARACTERISTICS

After being totally dependent upon ground based sensors since 1957, a new era was ushered in with the operational deployment of a spaceborne infrared satellite in the early 1970's. While this system was deployed to provide a timely warning of Soviet missile attack, the benefits of this surveillance system in providing data to the spacetrack network soon became obvious. Previously, we had to wait 20-30 minutes to determine whether a launch was a missile test or space launch. With this infrared satellite at synchronous altitude we could now make that determination in a matter of minutes.

In the past ten years, several systems have come on line. This has evolved from rudimentary beginnings adequate for small numbers of satellites and limited tasking beyond space catalogue maintenance, to a system which is adequate for the Terrestrial Surveillance Mission today but has certain shortcomings in supporting the Satellite Protect and Negation Missions.

We have programmed and are funded for several upgrades to our system which will substantially improve our capability in the coming years. I'll briefly touch on these improvements.

5. MISCELLANEOUS SENSORS

5.1 GEODSS

With the increasing use of deep space, we are deploying a ground-based electro-optical deep space sensor (GEODSS). Basically, this is a TV camera mounted on the back of a deep space telescope tied to a computer that will provide tracking data to Cheyenne Mountain.

5.1.1 GEODSS SITING

This system will consist of five sites. The first three, located in White Sands, New Mexico; Taegu, Korea; and Mau, Hawaii, will be operational by the end of the year. Site #4 is programmed for Diego Garcia in the Indian Ocean, and the U.S. Government is currently negotiating for basing rights at a site to cover the eastern Atlantic.

5.2 PACBAR

To improve our capability to detect Soviet space launches early in their flight and to accurately describe their orbits, we are deploying a series of radars termed "Pacific Radar Barrier" or PACBAR in the Philippines and Kwajalein.

Additionally, the radars at Kwajalein and Diyarbakir in Turkey are being upgraded for geosynchronous satellite tracking.

5.3 SPADOC

The SPADOC now has been in operation for two and a half years. This is a picture of the facility. As many of the functions still are performed manually and there is a requirement to correlate very large amounts of intelligence and operational data to meet short timelines, we have a major SPADOC upgrade in work. This effort, known as SPADOC 4, is presently in the definition phase. Two contractors are defining and proposing SPADOC specifications and one will be selected in early 1983 to develop the full-up capability. IOC for SPADOC 4 is programmed for CY 1986.

5.4 SURVEILLANCE PROGRAMS

In addition to the tracking aspects of this mission, there are numerous other programs which are supported by the surveillance function. These include: early orbit determination is used to support domestic launch programs on determining the initial orbit parameters, SATRAN provides notice to subscribers of pass times for satellites, TIP is the program used to track decaying satellites, and SOI is used to find the shape and motion of orbiting satellites.

6. SHUTTLE

NORAD is also deeply involved in the Space Shuttle program.

Our support to this critical national program has been in three areas. Our primary effort is the prediction of conjunctions between the Shuttle and all other objects in orbit. On the last mission you may have heard about a close approach to a USSR rocket body. This information was initiated by the Space Defense Operations Center in CMC. Additionally, we are prepared to support NASA in a variety of contingency conditions. Finally, we support the effort for tracking an external tank during its reentry.

7. SPACE COMMAND

In June 1982, the USAF announced the establishment of the Space Command in September 1982. This new organization was established in order to better meet our present and future challenges and give the United States a better capability to protect and assert its rights in space.

In summation, our space surveillance capability has evolved over the past twenty-five years to a point where we do a fine job in handling the Space Cataloging Mission and nominal launches. We have now cataloged nearly 13,400 satellites and are still tracking in excess of 4700 satellites. Currently this requires 30,000 observations per day to maintain this catalog. In the future, these numbers will continue to grow. The space surveillance task will be substantially more difficult.

1957-1964

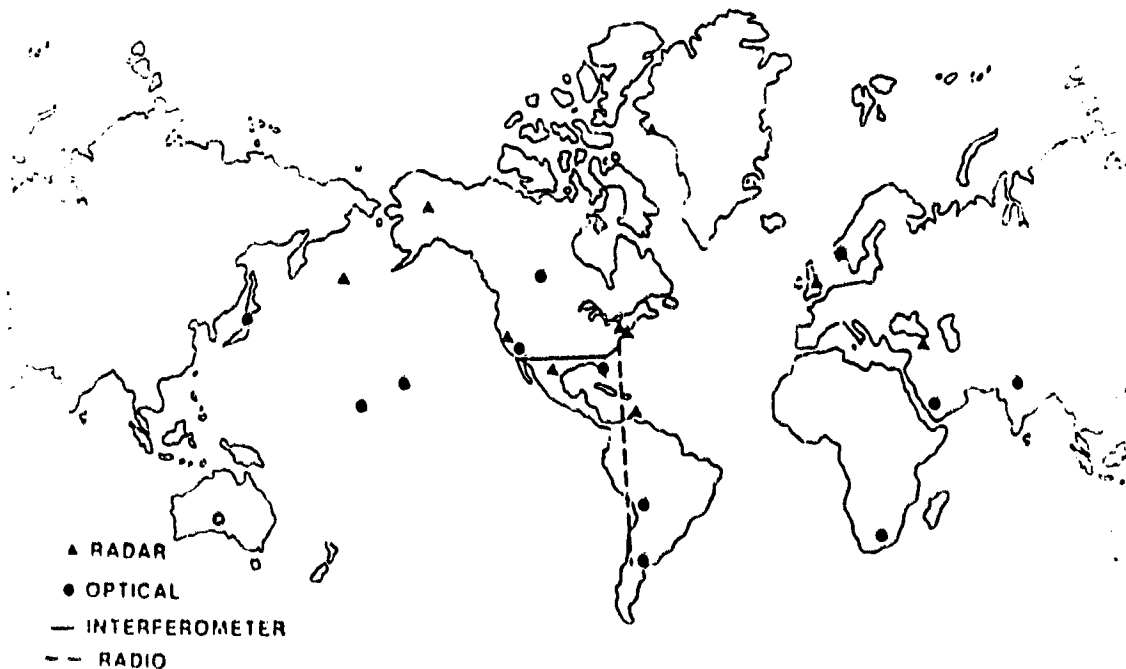


FIGURE 1

1964-1971



FIGURE 2

1971-PRESENT

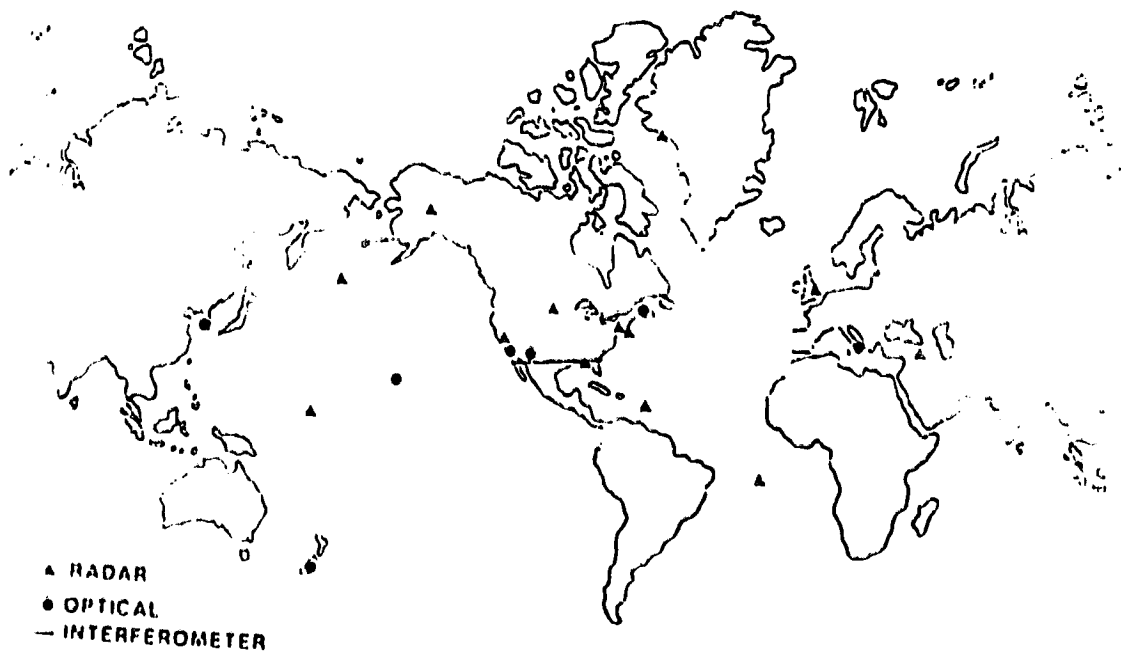


FIGURE 3

Doc-16
N 85-21190

History of Satellite Break-ups in Space

John Gabbard
NORAD Headquarters
Peterson AFB
Colorado 80914

1. History of Satellite Breakups in Space

The SPACETRACK system had its beginning in Hanscom Field, Massachusetts on 30 November 1957 when a data filter center was established at the Cambridge Research Center. The center was moved to Colorado Springs in 1961 and the 1st Aerospace Control Squadron, a USAF organization, was established to operate the center.

By 28 June 1961 the 1st Aerospace Control Squadron had cataloged 115 Earth orbiting satellites from data supplied by a rather diverse collection of radar and optical sensors. On 29 June 1961, the Able Star rocket of the 1961 Omicron launch exploded causing a quantum jump in the number of Earth orbiting objects.

Since that time there have been 69 Earth orbiting satellites break up in space whose debris remained in orbit long enough for orbital elements to be developed. In addition, there have been several low altitude breakups where the debris decayed before orbital elements could be developed.

Shown here in Table 1 is a list of the 69 breakups. As you can see, 256 fragments were eventually cataloged from the 1961 Omicron explosion and 195 are still in orbit 21 years later.

You can also see that the debris from some of the lower altitude breakups has all decayed. Among the 69 breakups, 44 have cataloged debris remaining in orbit.

As of 1 July 1982, the size of the cataloged orbiting population was exactly 4700. Forty-nine percent of these objects are fragments of the forty-four breakups.

For each breakup the various orbits of its debris represent a family of orbits that are related in characteristics due to their common impulse launch. As we page through the remainder of the list of breakups I will show a few examples of how the families are oriented in space.

2. 1961 Omicron Explosion, November 1965

Figure 1 is one way of showing how the orbits of debris in one breakup family are related. The diagram shows dependency between altitude and period and the data points shown are the apogee and perigee altitude of each orbit plotted at the period of the particular orbit. The data plotted were current about 17 years ago or approximately four years after the explosion. As you can see the continuum of orbits populate altitudes between about 400 and 2200 kilometers.

3. 1961 Omicron Explosion, June 1982

To get a general idea of how fast these orbits are decaying, Figure 2 shows the same family of debris as it existed on 29 June of this year which is exactly 21 years after the explosion and about 17 years after the previous plot. Some of the lower altitude debris has decayed and other orbits at the lower altitudes have become more circular.

4. 1961 Omicron Explosion, November 1965 and June 1982

To more graphically display the 17 year change, the two plots are shown simultaneously in Figure 3 and the 1982 data is red. It is obvious the higher period orbits have lowered very little over the 17 years and from this you suspect that these fragments will continue in orbit for a very long time.

5. Satellite Breakup History (Page 2 of Table 1)

This particular page of the breakup history lists the first of the USSR ASAT tests. Eleven of these tests have resulted in fragments that were large enough to be observed by the SPACETRACK sensors. Notice also that the breakup may have been a double. The second ASAT test was about ten days later using an orbit that was essentially a duplicate of the first test.

6. 1968-97 Explosion, November 1, 1968

Shown in Figure 4 is that distribution of debris cataloged from the second test. Because the parent orbit was fairly eccentric the geometric pattern appears somewhat different, however, I think you can see that the distribution is essentially a segment of the geometric distribution shown on the 1961 Omicron slide previously shown.

7. Satellite Breakup History (Page 3 of Table 1)

Continuing on with the breakup catalog shows additional Delta second stage events and more ASAT test events. Notice also that two more possible double events are listed. The Itos F launch using the Delta second stage rocket caused this rocket to be at a relatively high altitude and in a circular orbit. When it exploded, it launched fragments over a very wide range of altitudes and this spread is shown on the next slide.

8. Delta Rocket, 6921, 1973-86

Again a geometric distribution of orbits similar to 1961 Omicron is noted (see Figure 5). We previously commented that a number of the 1961 Omicron fragments would continue in orbit for a very long time. It is obvious that many of these fragments will continue to orbit for a much longer time -- perhaps hundreds of years.

9. Satellite Breakup History (Page 3 of Table 1)

The next page of the catalog shows numerous entries of breakups of USSR payloads in highly eccentric orbits. To date there have been ten of these events. Notice that relatively few objects have been cataloged from these events and this is because our sensors have a problem of observing orbits of this type. It is my opinion that many additional fragments may be in these orbits and when the GEODSS optical system becomes fully operational we may find some of them.

10. Satellite Breakup History (Page 4 of Table 1)

This completes the catalog of breakups and shows the most recent breakups. Note that three breakups have already occurred this year, one in May, one in June, and now, one in July after the data for this presentation had been recorded. The Cosmos 1275 event shown here is very interesting because in my view it represents a case that appears to have a high probability of having been a collision.

11. 12504 Debris

This figure (Figure 6) shows the distribution of debris orbits from the Cosmos 1275 event. Evident in the plot is an asymmetrical distribution of orbits where more fragments were forced forward than rearward. Not evident in the plot is the situation where there is a significant skew in inclinations of those orbits launched forward such that a large percentage of them are at a slightly lower inclination than the parent satellite.

12. Recent Other Known Anomalous Events

Table 2 shows recent anomalous events noted by the sensor system that appear to be of a different class of events than those listed in the breakup catalog. Listed first is a series of events that have involved seven old US payloads. These payloads each spawned one or two small pieces of debris on the dates shown and the debris was separated from the parent at low velocity. The last two entries on the list are judged to be other classes of events. In the case of "Cameo," a Delta second stage rocket, two fragments separated from the rocket, at or near the same time and decayed within two weeks from 900km altitude. No other satellite cataloged by SPACETRACK has decayed as rapidly. The NOAA debris is the only case known where a small piece of debris has fragmented. Six pieces were counted by our sensors shortly after the event but they are very small and hard to keep track of. Therefore, none of these have been cataloged.

Table 1 (Page 1) 1 July 1982

INTERNATIONAL DESIGNATOR	COMMON NAME	SCC CATALOG NUMBER	LAUNCH DATE	DATE OF EVENT	SATELLITES CATALOGED	CATALOGED SATELLITES IN ORBIT	PARENT SATELLITE			REMARKS
							INCL (°)	APOGEE (KM)	PERIGEE (KM)	
1961-040101	TRAMKIT 4A	116	29 Jun	29 Jun	256	195	66.7	292	875	
1962-0101	SPUSNIK-29	443	24 Oct	20 Oct	24	0	65.1	760	202	
1963-47	Atlas Cent.2	694	27 Nov	27 Nov	14	12	10.4	1710	475	More debris cataloged with 65-92
1964-26	Ops 4412	Unknown/009	4 Jun	Jan-Feb 66	11	11	90.5	935	848	809 most likely parent
1964-76	COSMOS 50	919	20 Oct	2 Nov	97	0	51.3	232	190	
1965-12	COSMOS 57	1093	22 Feb	22 Feb	168	0	64.8	708	159	
1965-20	COSMOS 61	1267/70 ?	15 Mar	15 Mar	149	25	56.0	1737	262	Satellite # indefinite
1965-82	Titan IC-4	1640	18 Oct	27 Jul 66	465	105	32.6	791	708	
1965-80	COSMOS 95	1706/07 ?	4 Nov	22 Feb 66	24	0	48.4	521	211	Satellite # indefinite
1966-12	Ops 1194	2012	15 Feb	15 Feb	40	0	96.5	290	142	
1966-46	ATD-Atlas	2186	1 Jun	1 Jun	54	0	28.8	296	292	
1966-56	Pages 1	2253	24 Jun	12 Jul 75	74	7	85.3	5224	1140	
1966-59	AG-203	2289	5 Jul	5 Jul	15	0	31.9	212	183	
1966-88	USSR	2437	17 Sep	17 Sep	53	0	49.6	702	138	
1966-101	USSR	2537	2 Nov	2 Nov	41	0	49.7	651	186	
1966-101	INTELSAT 3-F	2640	11 Jan	Unk(1971-72)	22		24.7	562	244	Delta second stage

Table 1 (Page 2)

SATELLITE BREAKUP HISTORY
1 July 1982
(Continued)

INTERNATIONAL DESIGNATOR	COMMON NAME	SCC CATALOG NUMBER	LAUNCH DATE	DATE OF EVENT	SATELLITES CATALOGED	CATALOGED SATELLITES IN ORBIT	PARENT SATELLITE			REMARKS
							INCL (°)	APOGEE (KM)	PERIGEE (KM)	
1967-24	COSMOS 149	2714	21 Mar	21 Mar	18	0	48.4	284	246	
1967-86	COSMOS 176	2942	12 Sep	12 Sep	12	0	89.1	1555	195	
1968-91	COSMOS 249	3504	20 Oct	20 Oct	82	48	62.3	2134	538	ASAT. Two fragmentations same revolution?
1968-97	COSMOS 252	3530	1 Nov	1 Nov	118	68	62.3	2134	538	ASAT
1968-117	COSMOS 261	3624	19 Dec	22 Dec	24	0	71.2	637	206	
1969-21	COSMOS 269	3775	5 Mar	5 Mar	23	1	74.0	414	412	
1969-29	Hereos 1	3835	26 Mar	28 Mar	38	5	81.1	841	464	
1969-64	INTELSAT 3-F5	4051	26 Jul	26 Jul	22	2	30.3	4988	267	Delta second stage
1969-82	Ops 1807	4111	30 Sep	4 Oct	251	140	69.6	488	482	
1970-25	Nimbus 4	4367	8 Apr	17 Oct	327	284	99.8	1094	1033	
1970-89	COSMOS 374	4594	23 Oct	23 Oct	91	48	62.9	2133	514	ASAT
1970-91	COSMOS 375	4598	30 Oct	30 Oct	39	31	62.8	2103	518	ASAT
1971-15	COSMOS 397	4964	25 Feb	25 Feb	84	69	65.3	2203	572	ASAT
1971-35	COSMOS 407	5174/5	23 Apr	Unk(May/Jun)	13	7	74.0	819	789	Satellite # indefinite
1971-106	COSMOS 462	5646	3 Dec	3 Dec	29	0	65.0	1800	229	ASAT
1972-58	Landat A	6127	23 Jul	22 May 75	216	90	98.3	910	635	Delta second stage

Table 1 (Page 3)

1 July 1982
(Continued)

INTERNATIONAL DESIGNATOR	COMMON NAME	SCC CATALOG NUMBER	LAUNCH DATE	DATE OF EVENT	SATELLITES CATALOGED	CATALOGED SATELLITES IN ORBIT	PARENT SATELLITE			REMARKS
							INCL. (°)	APOGEE (KM)	PERIGEE (KM)	
1973-21	COSMOS 554	6432	19 Apr	6 May	197	0	72.0	931	172	
1973-75	COSMOS 601	6876	16 Oct	16 Oct	14	0	81.5	1536	212	
1973-86	ITOS F	6921	6 Nov	29 Dec	179	167	102.0	1525	1522	Delta second stage
1974-74	COSMOS 686	7447	20 Sep	26 Sep	20	0	70.9	676	279	
1974-89	ITOS G	7532	15 Nov	20 Aug 75	129	127	101.5	1461	1460	Delta second stage
1974-101	COSMOS 699	7587	24 Dec	17 Apr 75	51	0	65.0	444	432	Two fragmentations one revolution apart?
1975-04	Landsat B	7616	22 Jan	9 Feb 76	198	61	97.8	918	745	Delta second stage. Two explosions?
1975-27	GEOS 3	7735	9 Apr	Unk (Mar 78)	5	5	115.0	847	807	Delta second stage
1975-80	COSMOS 758	8191	5 Sep	6 Sep	77	0	67.1	336	105	
1975-102	COSMOS 777	8416	29 Oct	26 Jan 76	63	0	65.0	446	445	
1976-12	COSMOS 801	8658	5 Feb	5 Feb	17	0	71.0	790	268	
1976-63	COSMOS 838	8922	2 Jul	17 May 77	41	0	65.0	444	443	
1976-67	COSMOS 843	9043	8 Jul	29 Sep 77	46	45	65.9	2096	986	ASAT target
1976-72	COSMOS 844	9046	27 Jul	25 Jul	249	0	67.1	358	188	Cataloged but no element.
1976-77	ITOS H	9063	29 Jul	24 Dec 77	120	120	102.0	1517	1510	Delta second stage
1976-105	COSMOS 862	9495	22 Oct	15 Mar 77	14	3	64.4	39214	1103	Observation problem
1976-120	COSMOS 886	9634	9 Dec	27 Nov 78	49	16	65.8	620	533	ASAT Target

Table 1 (Page 4)

INTERNATIONAL DESIGNATOR	COMMON NAME	SCC CATALOG NUMBER	LAUNCH DATE	DATE OF EVENT	SATELLITES CATALOGED	CATALOGED SATELLITES IN ORBIT	PARENT SATELLITE			REMARKS
							INCL. (°)	APOGEE (KM)	PERIGEE (KM)	
1976-126	COSMOS 886	9634	27 Dec	27 Dec	57	49	65.8	2306	496	ASAT
1977-27	COSMOS 903	9911	11 Apr	8 Jun 78	5	2	62.9	39042	1511	Observation problem on debris
1977-67	COSMOS 917	10059	16 Jun	30 Mar 79	2	2	62.8	39495	849	Observation problem on debris
1977-65	GMS	10144	14 Jul	15 Jul	150	103	29.0	1865	498	Delta second stage
1977-68	COSMOS 931	10150	20 Jul	24 Oct	5	4	62.9	39664	669	Observation problem on debris
1977-121	COSMOS 970	10531	21 Dec	21 Dec	47	47	65.8	1139	946	ASAT
1978-26	Landsat 3	10704	5 Mar	27 Jan 81	144	106	98.9	909	899	Delta second stage
1978-83	COSMOS 1030	11015	6 Sep	10 Oct	5	4	63.0	39714	690	Observation problem on debris
1979-33	COSMOS 1094	11333	18 Apr	17 Sep	2	0	65.0	410	387	23 decayed before catalog
1979-58	COSMOS 1109	11417	27 Jun	Unk	7	5	63.3	39427	954	Observation problem on debris
1979-63	COSMOS 1112	11443	6 Jul	6 Jul	26	0	50.6	541	357	
1979-77	COSMOS 1124	11509	28 Aug	9 Sep	6	6	62.9	40258	566	Observation problem on debris
1980-21	COSMOS 1167	11729	14 Mar	15 Jul 81	13	1	65.0	448	355	Fragmented twice
1980-10	COSMOS 1174	11765	18 Apr	18 Apr	14	4	66.1	1652	379	ASAT

Table 1 (Page 5)

1 July 1982
(Continued)

INTERNATIONAL DESIGNATOR	COMMON NAME	SCC CATALOG NUMBER	LAUNCH DATE	DATE OF EVENT	SATELLITES CATALOGED	CATALOGED SATELLITES IN ORBIT	PARENT SATELLITE			REMARKS
							INCL. (°)	APOGEE (KM)	PERIGEE (KM)	
1980-89	COSMOS 1220	12054	4 Nov	20 Jun 82	43 est	-	65.0	878	581	
1981-16	COSMOS 1247	12303	19 Feb	1 Oct	6	4	63.0	39420	934	Observation problems on debris
1981-28	COSMOS 1260	12364	20 Mar	8 May 82	42	38	65.0	748	456	
1981-31	COSMOS 1261	12376	31 Mar	12 May	5	3	63.2	39462	507	Observation problem on debris
1981-53	COSMOS 1275	12504	4 Jun	24 Jul	143	143	82.9	1010	958	Payload
1981-71	COSMOS 1285	12627	4 Aug	21 Nov	4	2	63.0	40169	658	Observation problem on debris
1981-89	COSMOS 1306	12630	19 Sept.	12 Jul 82	Est. 25	Est. 25	64.9	402	377	

TABLE 2 - RECENT OTHER KNOWN ANOMOLOUS EVENTS

<u>Identification</u>	<u>Launched</u>	<u>Spawned Debris</u>	<u>Event Date</u>	<u>Inclination</u>
Ops 1953	1966	2	13 AUG 80 17 SEP 80	89.7
OSCAR-4	1965	2	22 AUG 80 24 AUG 80	89.9
GREB-6	1965	1	26 Nov 80	70.0
SNAPSHOT	1965	3	LATE Nov 79 6 DEC 80 1-15 APR 82	90.2
Ops 4412	1964	2	19 DEC 80 2 JUL 82	90.5
Ops 4947	1967	2	LATE APRIL - MAY 31	103.9
Ops 1117	1966	1	5 JUL 81	89.9
DEBRIS (NOAA)	1974	6	17 SEP 81	101.9
CAMEO (DELTA)	1978	2 13	6 MAY 81 26 DEC 81	99.3

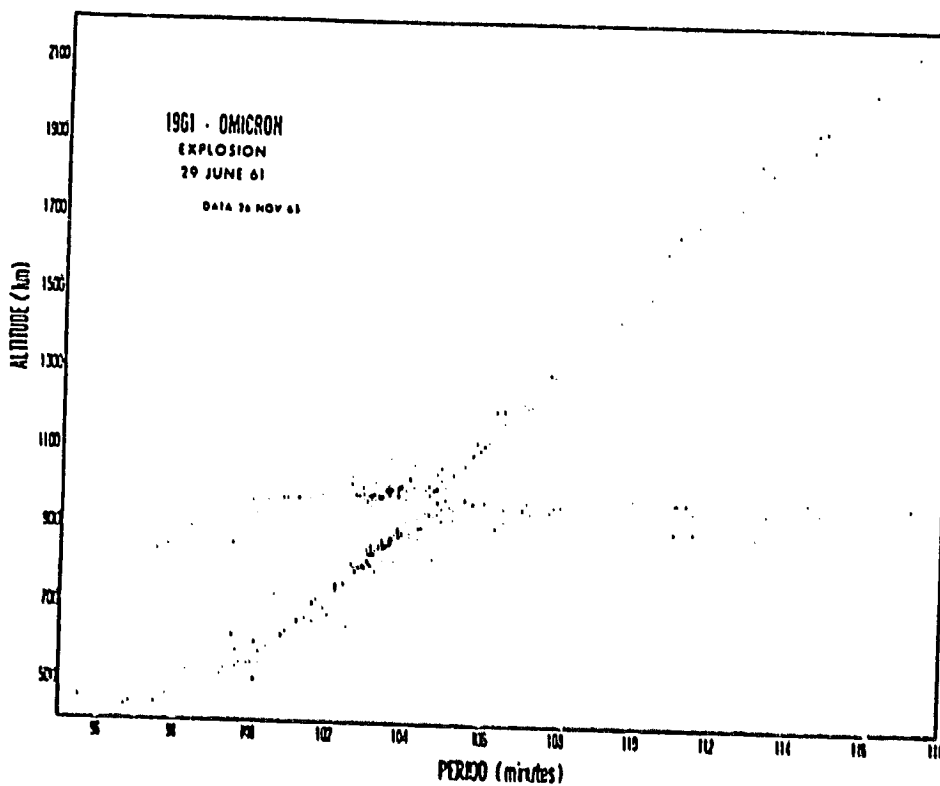


FIGURE 1

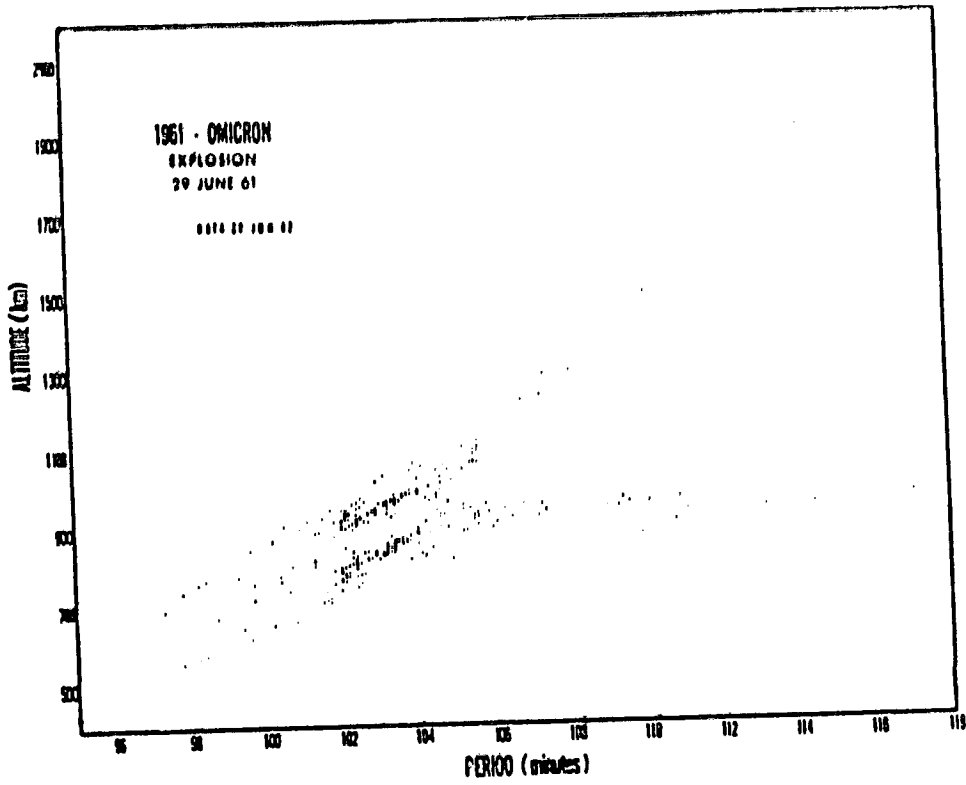


FIGURE 2

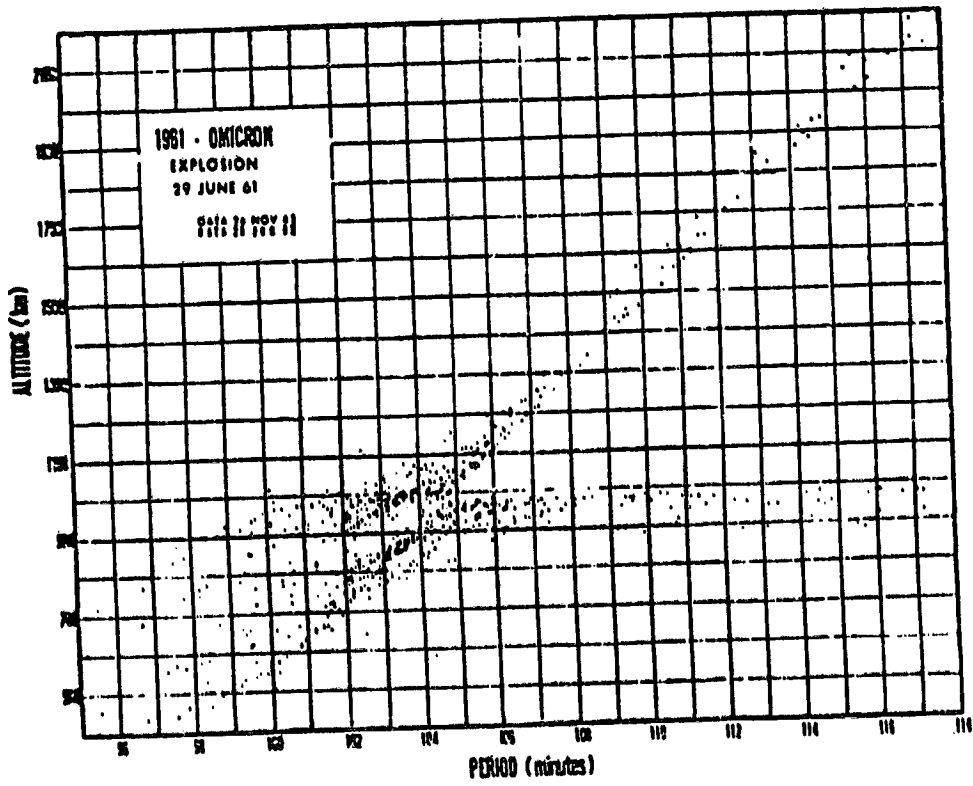


FIGURE 3

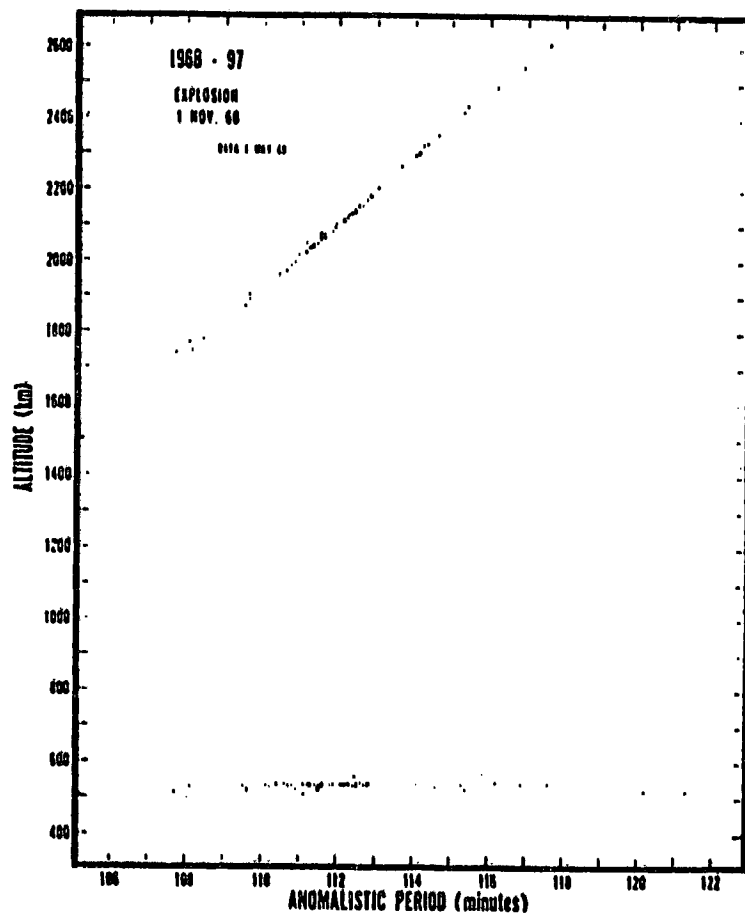


FIGURE 4

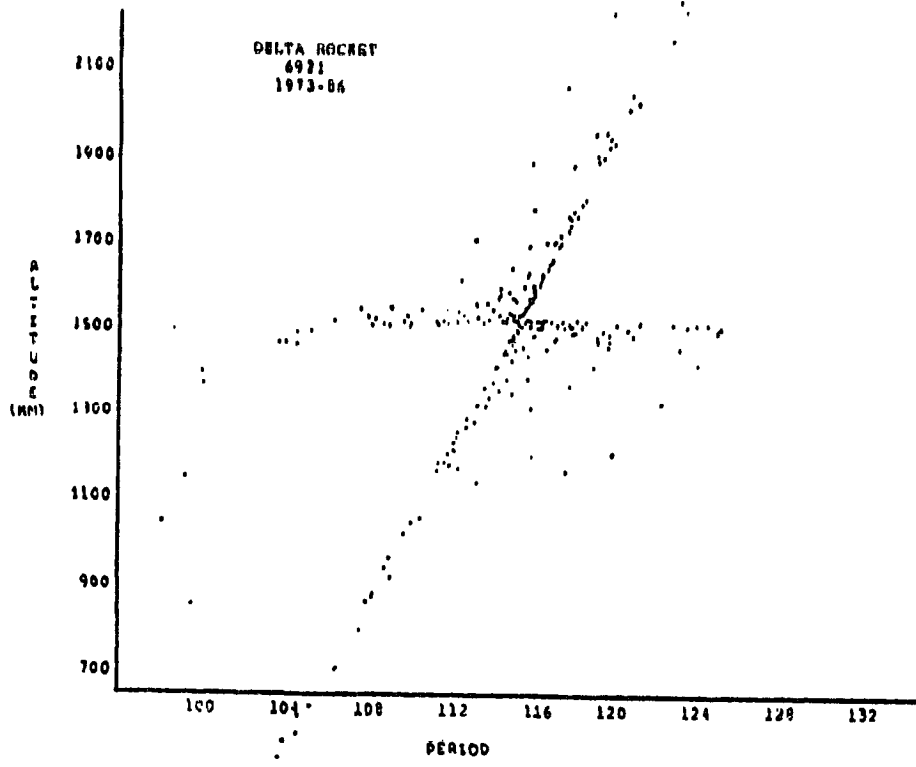


FIGURE 5

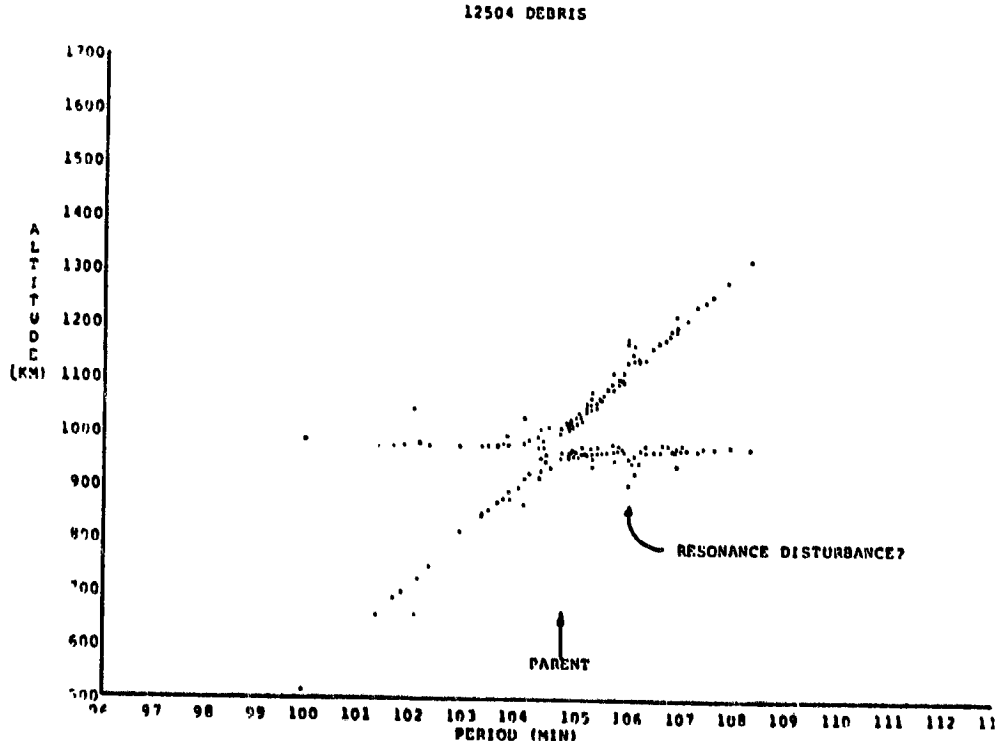


FIGURE 6

NORAD'S PARCS Small Satellite Tests (1976 and 1978)

by
Donald J. Kessler
NASA/Johnson Space Center
Houston, Texas 77058

NORAD sponsored small satellite tests in 1976 and 1978. The purpose of the tests was to use their more sensitive radar to determine the number of Earth orbiting objects which are not part of the official catalogue. Both tests were coordinated by Preston Landry at NORAD Hq., in Colorado Springs, Colorado, and used the PARCS radar. The characteristics of this radar are given in Table 1. Figure 1 estimates the detection capability of NORAD's operational system and compares it to the PARCS's radar sensitivity during these tests. Note that the tests only slightly improved the detection capability, and the largest improvements were at the lowest and highest regions of its sensitivity range.

The 1976 results are summarized in reference 1 and in Table 2. The major conclusion of the test is that 17.7% of the objects detected were uncorrelated (i.e., not in the official catalogue). However, perhaps most significant is that 90% of the objects detected below 400 km were uncorrelated. Some of these uncorrelated objects probably came from the breakup of Cosmos 844, 6 days earlier. Figures 2 and 3 illustrate the altitude and size distribution of detected objects. Notice between RCS of 10^{-3} and 10^{-4} met^2 objects were detected at altitudes below 500 km. However, because their orbital lifetime at this altitude is short (e.g. from 300 km, less than a month, and from 200 km, just a few days), these objects must have a recent source. A source other than the Cosmos breakup is from altitudes above 500 km, where the objects minimum range is too large for the object to be detected. The data could suggest a large reservoir of objects in this size range that slowly "rain-down" through lower altitudes before they are detectable. Reference 2 is a classified report which uses the test results to estimate the number of objects in space by correcting for the decreasing probability of detection with increasing range and decreasing size.

The 1978 results are summarized in reference 3 and in Table 3. This test concluded that at least 7% of the objects detected were not in the official catalogue. Another 6% of the detected objects were not tracked well enough to determine their status (this category was not determined in the previous test). Again, a large percentage of the detected objects at lower altitudes were not in the catalogue. This is illustrated in figures 4 and 5. (The numbers in these figures represent the number of objects found in each altitude and size bin, up to 9, then A = 10, B = 11, etc., and X is greater than 15). A clue that the number of unknown objects is underestimated from this test is from the fact that all of the small objects detected passed nearly directly over the radar sight. Such a trajectory returns the maximum signal, hence allows for the detection of otherwise undetectable objects. However, the volume of space covered by the radar is then much smaller for small objects than it is for larger objects, reducing the probability of detection of small objects.

The large percentage of uncatalogued objects at lower altitudes found during this second test supports the conclusion that a large reservoir of

these objects exist above 500 km since there were no breakups prior to the test. Other interesting observations concerning this test are the orbital inclinations of the unknowns. The unknowns with 60° to 64° inclinations could be uncatalogued fragments from spacecraft breakups in Molaiya-type orbits. These unknowns found between 84° and 88° inclinations have orbits that are consistent with the 1963 "West Ford Space Needle" experiment. However, there are no known breakups with inclinations between 103° and 106° .

Table 4 summarizes the results of both tests. Both tests demonstrated that there are objects in Earth orbit which are not catalogued, and that a much larger number of objects may exist just below the detectable threshold of ground based radar.

References

1. Hendren, J.K., and A. Anderson. "Comparison of the Perimeter Acquisition Radar (PAR) Satellite Track Capability to the Space Defense Center (SDC) Satellite Catalogue - Unknown Satellite Track Experiment", Science Applications, Incorporated, Huntsville, Alabama. Report No. SAI-77-701-HU and SAI-77-724-HV (Vol. I and II), Oct 13 and Oct 15, 1976.
2. Lennertz, Thomas, "The Number of Objects in Space: Modifying the Perimeter Acquisition Radar (PAR) Unknown Track Experiment for Probability of Detection". Tech Memo 81-4 from Office of the Secretary of the Air Force Space Systems (OSAF/SS), Pentagon, Va. Classified Secret by HQ NORAD/ADCOM.
3. Moran, John L.T. "Spacetrack System -PARCS Small Satellite Test - Preliminary Analysis - Case 28758-500" Bell Laboratories Memorandum for file, Oct. 19, 1978.

TABLE 1

PARCS RADAR TESTS CHARACTERISTICS

TYPE: PHASED ARRAY, CAPABLE OF SIMULTANEOUSLY TRACKING A LARGE NUMBER OF OBJECTS

LOCATION: NORTH DAKOTA (48.7° N, 97.9° W)

WAVELENGTH: APPROX. 70cm (1110 MHz)

BORE SITE: 8° E OF NORTH, 25° ELEVATION

MAX RANGE: APPROX. 3200km

DETECTION ANGLES: 1.7° - 43° ELEVATION
 $\pm 54^{\circ}$ AZIMUTH (ABOUT BORE SITE)
 "FAN" REGION:
 56° - 32° ELEVATION
 $\pm 67^{\circ}$ AZIMUTH

TABLE 2
1976 TESTS RESULTS

PERFORMED BY SAI UNDER DIRECTION OF BMDSC-W AT REQUEST OF ADCOM

DATA TIME: 08:39 TO 29:31, JULY 31, 1976 (11 HR, 52 MIN.)

NUMBER DETECTIONS:

8745 CORRELATED PLUS "NEW" TRACKS

1494 UNCORRELATED, OR "NEW" TRACKS

CONCLUSIONS:

17.7% NEW OBJECTS

90% OF OBJECTS BELOW 400KM WERE NEW

TABLE 3
1978 TESTS RESULTS

PERFORMED BY BELL LABS UNDER DIRECTION OF ADCOM AT REQUEST OF NASA

DATA TIME: AUG 21 TO 23, 1978 (8 HR 24 MIN IN SIX 84 MINUTE INTERVALS)

NUMBER DETECTIONS

5586 KNOWN

437 UNKNOWN

379 UNCORRELATED

CONCLUSIONS:

7% OF OBJECTS TRACKED WERE UNKNOWN

6% WERE TRACKED WITH INSUFFICIENT ACCURACY TO MAKE DETERMINATION
PERCENTAGE OF UNKNOWN NEARLY DOUBLES IN MORE SENSITIVE REGIONS
OF RADAR

80% OF OBJECTS BELOW 300KM WERE UNKNOWN

32% OF OBJECTS ABOVE 2000KM WERE UNKNOWN

TABLE 4 - SUMMARY OF BOTH TESTS

- O CONSISTANTLY SHOW BETWEEN 6% AND 18% UNKNOWNNS
- C CONSISTANTLY SHOW MUCH LARGER PERCENTAGE UNKNOWNNS AT LOWER ALTITUDES
- O SOURCE OF MOST SMALLER OBJECTS AT LOWER ALTITUDE MUST BE FROM HIGHER ALTITUDE
 - O ORBITAL LIFE-TIMES VERY SHORT AT LOWER ALTITUDES
 - O LARGE RESERVOIR OF SMALL OBJECTS ABOVE 500KM IS REQUIRED TO EXPLAIN THE NUMBER OF SMALL OBJECTS OBSERVED AT ALTITUDES BELOW 100KM
- O 1976 TEST - SIGNIFICANT NO. NEW OBJECTS FROM EXPLOSION OF COSMOS 844
- O 1978 TEST - SIGNIFICANT NO. UNKNOWNNS BETWEEN INCLINATIONS 62° & 64°, 84° & 88°, 103° - 106°

NORAD'S OPERATIONAL CAPABILITY TO DETECT OBJECTS

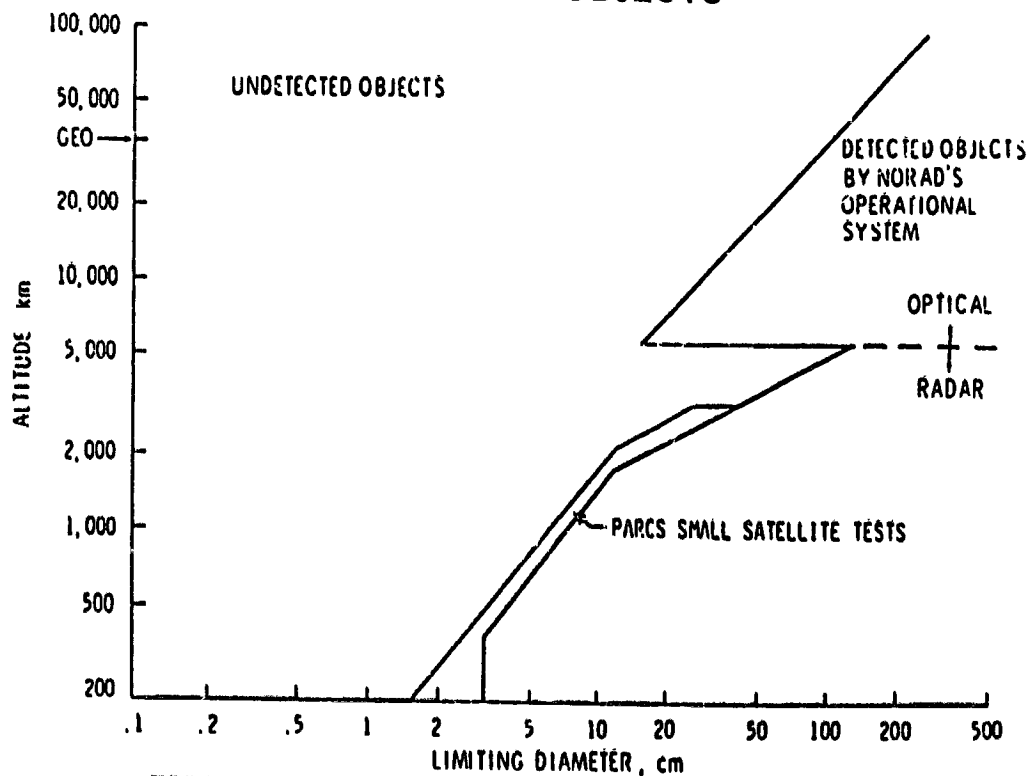


FIGURE 1

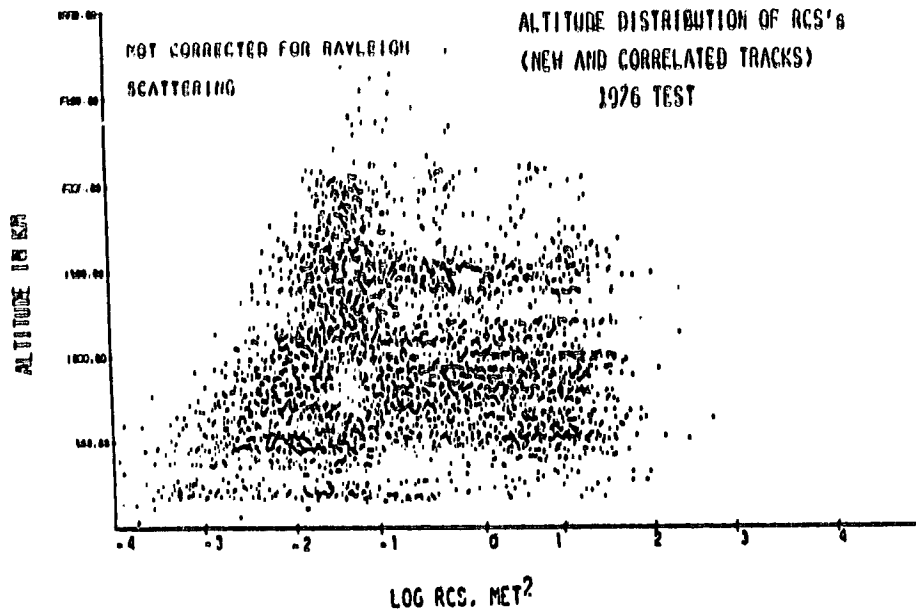


FIGURE 2 - Altitude Distribution of RCS's (New and Correlated Tracks).

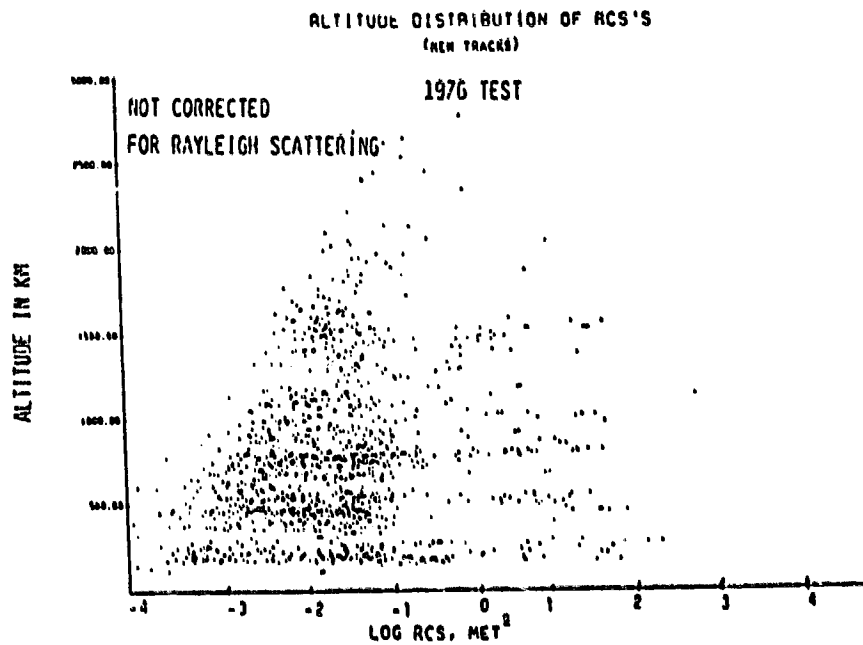


FIGURE 3 - Altitude Distribution of RCS's (New Tracks Only).

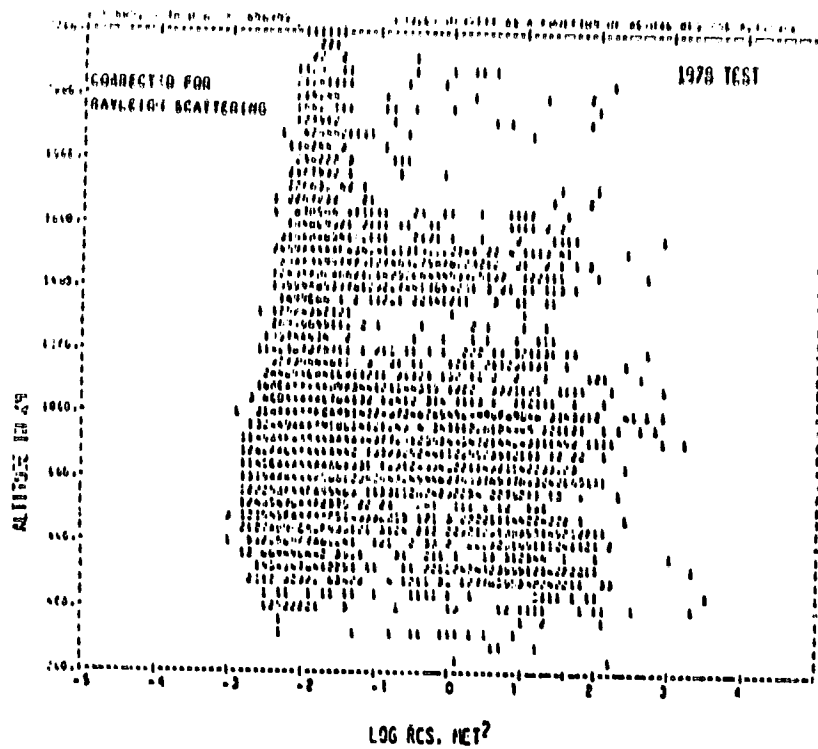


FIGURE 4 - Altitude Distribution of RCS (Unknowns).

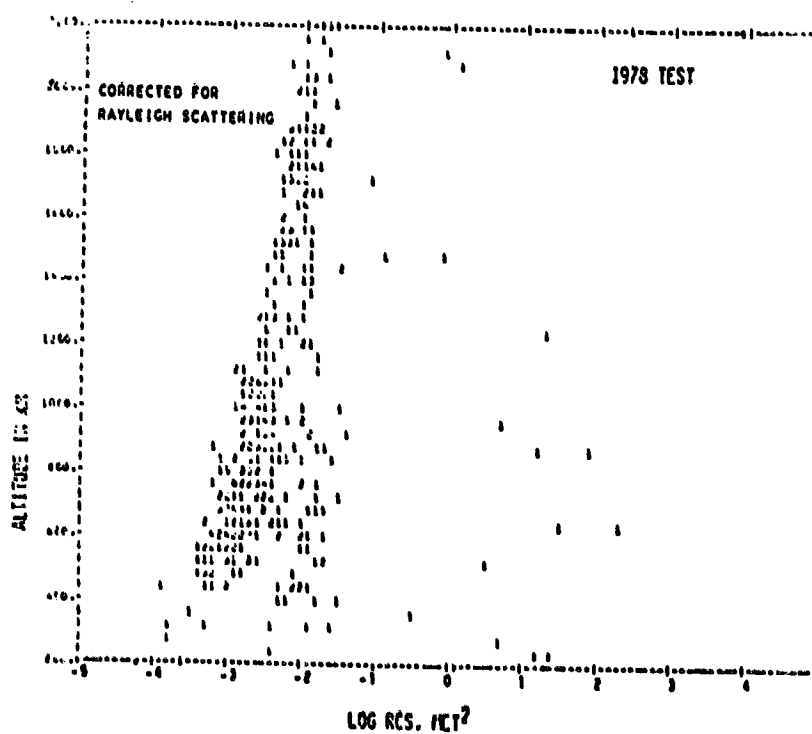


FIGURE 5 - Altitude Distribution of RCS (Unknowns).

Donald H. Mumes
David R. Brooks
Jose M. Alvarez
T. Dale Bess

INTRODUCTION

In 1973 NASA Langley had a very active group conducting meteoroid research, with our focus being on the hazard to spacecraft. We had three flight experiments in progress to define the meteoroid environment near the Earth and in interplanetary space, and to measure the effectiveness of meteoroid bumpers. These flight experiments were aboard Pioneer 10, Pioneer 11, and Explorer 46. We were conducting hypervelocity impact tests in the laboratory to study protective structures, and we were determining the composition of meteoroids from the hundreds of meteor spectra we obtained with our observation station in New Mexico.

During that year we became aware that manmade debris presented a similar hazard to spacecraft near the Earth and decided to make an assessment of that hazard. We worked on the problem for a couple of years, and this paper is a summary of the results we obtained.

The major results of our work were reported in the five publications listed in figure 1.

The work by Brooks, Gibson, and Bess entitled Predicting the Probability that Earth-Orbiting Spacecraft Will Collide with Manmade Objects in Space is the central point of our effort. It is a detailed analysis of the collision probability problem with much attention given to the population of small untrackable fragments created during explosions.

In his 1976 paper, Brooks applied the previous work to calculate actual spacecraft penetrations as opposed to just impacts, and compared the penetration hazard from manmade debris to that from meteoroids. In addition, this paper gives revised collision probability results to correct some numerical errors in the previous work.

The other three papers deal with what was found to be the most important element of the manmade debris problem - the small untrackable fragments created during explosions. The paper by Bess deals with the size distribution of the fragments and is a detailed look at his contribution to the 1974 paper. The papers by Fuss and by Dasenbrock, Kaufman and Heard deal with the orbits of the fragments.

BROOKS, GIBSON, AND BESS [1974]

Brooks, Gibson, and Bess [1974] used the NORAD catalog of observable debris as a basis for a model of the total orbital debris population. The number and size of the objects in the catalog is shown in figure 2. The nonlinearity on the log-log plot of the size distribution of the objects is at least partially due to the limitations of the radar used. Much work was devoted to defining a "reasonable" extrapolation for manmade objects.

Brooks, Gibson, and Bess [1974] noted that it would not be reasonable to simply extrapolate the total population curve because it is composed of objects of different classes; payloads, rocket bodies, debris released during normal performance of a mission (explosive bolts, shrouds, etc.), and fragments created during explosions in space. The total population

should be broken down into its components and an extrapolation of each component should be made.

The relative abundance of the various components of the debris population is given in figure 3. Explosion fragments make up the biggest part of the population and are the result of only ten explosions in space. Payload debris encompasses objects associated with normal performance of a mission - the explosive bolts, shrouds, etc.

Figure 4 shows the size distribution of the various classes of objects, this time on a semilog plot. The payloads and rocket bodies are combined in one curve. Objects in this class are large. No extrapolation to smaller sizes is in order because we know that no smaller payloads or rocket bodies exist. The payload debris class should contain smaller objects and the extrapolation was made by simply extending this line.

Brooks, Gibson, and Bess [1974] noted that a simple extrapolation of the explosion fragments population also would not be reasonable because they were produced by ten different explosions. They extrapolated the size distribution curve of the fragments from each explosion individually.

The extrapolation to smaller sizes was made for each explosion by extending a straight line fit to the observed fragments on a semilog plot, see figure 5.

Small objects will be removed from the population due to drag. Brooks, Gibson, and Bess [1974] calculated the minimum size object that would remain in orbit from each explosion as a function of time. They took

into account, (1) the elapsed time since the explosion took place, (2) the altitude of the perigee of the fragment orbits, (3) the variation in air density during solar cycle, and (4) the shape of fragments to determine drag coefficient.

This detailed examination of losses due to drag resulted in quite different minimum sizes for different explosions at a given time.

Orbital lifetimes were calculated using a modification of the RAND satellite lifetime program.

Brooks, Gibson, and Bess [1974] thus had a method and a computer program to generate a model population at any given time that included the objects in the NORAD catalog plus a large number of smaller untracked objects. The untracked fragments were assumed to be in orbits that varied slightly from the parent object in a random fashion, see figure 6. The equations show the range of orbit parameters assigned to the untrackable fragments.

The method of distributing ω and Ω about explosion fragment "parents" was selected after plots of trackable explosion fragment orbit element distributions showed that these two elements were not yet randomized several years after the explosion.

Having generated a model population of orbital debris, Brooks, Gibson, and Bess [1974] used that model to determine the probability that a spacecraft will be struck by space debris. The probability of a collision is calculated because a deterministic approach to collisions is not

feasible, see figure 7. We do not know the orbital elements of observable debris accurately enough to determine if they will pass through a region of space as small as a spacecraft. We know only with much less accuracy where the unobserved small fragments are.

Brooks, Gibson, and Bess [1974] calculated the probability of a spacecraft being struck by debris by a two-step analysis.

The first step was to locate orbital trace intersection points as a function of time for the spacecraft orbit and each debris object orbit, see figure 8. They considered that the orbital traces were constantly being perturbed due to the Earth's oblateness. The relative motion of the orbital traces, which determined orbital trace intersection locations and durations, was considered an absolutely essential feature of the population.

The second step was to calculate the probability that the debris and spacecraft are in the intersection region at the same time. It was assumed that the location of the debris and spacecraft in their orbits is random. This assumption was made because the uncertainty in actual position of objects in their orbits encompasses the entire orbits in just a matter of weeks.

Brooks, Gibson, and Bess [1974] calculated the number of objects that could potentially strike a spacecraft in circular orbits at various altitudes. The results are shown in figure 9. The hazard is greatest for a spacecraft in a 900 km altitude circular orbit.

Brooks, Gibson, and Bess [1974] calculated the number of debris orbit intersections with a 1000 km circular orbit at various spacecraft orbit inclinations. The results are shown in figure 10. The collision hazard is greatest around an inclination of 120°.

The probability that a 100 m diameter spherical spacecraft in a 1000 km orbit will be struck by space debris during a 1000-day mission is shown in figure 11 as a function of orbit inclination. The probability was found to be nearly 0.08 at an inclination of 120°.

BROOKS [1976]

Brooks in his 1976 paper compares the manmade orbital debris hazard to the meteoroid hazard for a spacecraft, by looking at the penetrations that each would produce if the spacecraft had a double wall structure like that used on Skylab. At an altitude of 500 to 800 km. orbiting debris and meteoroids were found to be equally hazardous, see figure 12. The magnitude of the hazard is a 1 percent to 10 percent probability of a penetration in 1000 days if the spacecraft is 100 m in diameter.

Brooks makes the point that if you find that probability is unacceptable and try to reduce it by increasing the thickness of the material in the wall, you will find you reduce the meteoroid hazard easily, but not the manmade debris hazard. That is because of the difference in the size distribution of the two populations. It takes about a 10^{-3} g to 10^{-5} g particle to penetrate the Skylab wall. In that mass range the

meteoroid size distribution is steep and the manmade debris size distribution is flat, refer to figure 2. Making the spacecraft wall twice as thick reduces the meteoroid penetration hazard by a factor of 12, but does not reduce the manmade debris penetration hazard noticeably.

BESS [1975]

Bess's 1975 paper presents in detail his contribution to the Brooks, Gibson and Bess [1974] paper, which was the data and analysis that led the authors to assume that the size distribution of explosion fragments is exponential.

Bess looked at the three fragmentation processes illustrated in figure 13, namely,

- (1) high intensity explosion of a cylindrical shell by a charge in contact with the inside of the shell (from military weapons testing)
- (2) low intensity explosion of a cylindrical shell by overpressure (Atlas tank fragmentation test for range safety considerations)
- (3) hypervelocity impact of typical spacecraft walls

This paper was mainly an analysis of experimental data with some consideration given to fragmentation theory. The hypervelocity impact data were generated by Bess himself.

Bess found that size distribution of the fragments was exponential for internal explosions of shells (both low intensity and high intensity), see figure 14. It was this result that led Bess [1974] to extrapolate the

observed population of explosion fragments into the unobserved size range along an exponential curve

The 10 mg minimum size high-intensity explosion fragments led to the assumption by Brooks, Gibson, and Bess[1974] that the minimum area for a fragment was 10^{-6} m^2 .

Because no fragment shape data were available from the explosion tests, they used the most common shape of hypervelocity impact fragments to determine the drag coefficient for explosion fragments in space.

The size distribution of the fragments produced by low intensity explosions and high intensity explosions are quite different, see figure 15. The high intensity distribution is quite steep while the low intensity distribution is very flat.

FUSS [1974]

Realizing that the untracked fragments would be more numerous than the observed population and, therefore, could present the greatest hazard we had two contract efforts to study the dynamics of satellite fragmentation. One effort was by Fuss, a student working on his Master's thesis.

Fuss performed computer studies of the spatial and temporal distribution of explosion fragments from simulated explosions. He assumed that fragments scattered in all directions (in three dimensions) when a satellite exploded. One situation he studied is that shown in figure 16.

Looking first at the envelope that would be produced if there were no perturbations, he discovered a deformed and pinched toroidal configuration, like that shown in figure 17. The pinched section is where the explosion took place and 180° from that point. The envelope was biggest when explosion took place at perigee and smallest when explosion took place at apogee. The greater the intensity of the explosion, the bigger the envelope. The fragments are all together at the moment of explosion and they gradually disperse because they are all in different orbits. Fuss was surprised to find that within 8 hours the fragments were uniformly distributed throughout this volume.

When Fuss included the perturbations due to drag and the Earth's oblateness (precession of nodes), he discovered that the envelope became more uniform and more like a torus, see figure 18. The drag caused an inward expansion of the volume. Fuss considered that fragments were a mixture of 1 mm, 10 mm, 30 mm, and 100 mm aluminum spheres. In one computer run, he simulated a violent explosion at the perigee of a 250 x 440 km orbit. Half the fragments struck the Earth during the first orbit; 7 percent more fell during the next 10 hours. He ran the calculation out to 500 hours. At that time 90 percent of the 1 mm particles produced were removed from orbit. Many of the 10 mm particles were lost also. But very few of the 30 mm and 100 mm particles that survived the first orbit were subsequently lost during the first

500 hours. Fuss considered this a significant indication that debris too small to be detected by radar could be orbiting in space, especially since his simulated explosion was at low altitude and violent.

DASENBROCK, KAUFMAN, AND HEARD [1975]

Dasenbrock, Kaufman and Heard of the Naval Research Lab also looked at the dynamics of satellite disintegration under a NASA contract. They looked at two approaches - the one where a large number of individual orbits are followed in time to estimate the hazard at some future time - this is the approach used by Fuss. This approach can also be used in reverse to run the fragments back to a common site, thus determining the time and location of the explosion.

You would think it would be a simple task to backtrack fragments to the time and place of their origin, but it is not, because orbit parameters are not known precisely and drag is difficult to account for. The fragments never come back to a precise point. Dasenbrock et al. determined the accuracy required in the state vectors of fragments 10 days after an explosion in order to track the fragments back to a common origin. They did this by simulating an explosion on the computer. For example, the explosion depicted in figure 19 was simulated on the computer and fragment state vectors determined after 10 days. The fragment state vectors were then modified randomly within various uncertainty limits and the proximity functions applied to the modified data to see if the explosion point could be determined.

Dosenbrock, et al showed that the proximity functions all peaked at the breakup time when the state uncertainty was 0.05 percent. However, when state uncertainties reached 0.16 percent, the breakup time could not be resolved, see figure 20.

At the time of the explosion the fragments are thrown into orbits of different inclinations, but the orbit planes all intersect along the line from the gravitational center of the Earth to the explosion point. Plotting the position vector direction in right ascension and declination coordinate system confirms the calculated explosion time, see figure 21. Even more it provides the explosion location.

They tried to determine the time and position of real spacecraft explosions using the method and were successful. The KOSMOS 699 fragments were tracked back as shown in figure 22.

The ERTS I explosion was more violent which provided a clear indication of the breaking time and a precise location of the explosion location, see figure 23. The more violent the explosion is, the easier it is to find out when and where it occurred.

Another completely different method of modeling spacecraft explosions was explored by the authors. That is the method of statistical mechanics whereby the fragment cloud is treated as a continuum of non-interacting particles. This method implicitly interpolates the unobserved fragments. The structure of the fragment cloud is calculated from its phase space

distribution function. An analytic expression for the spatial density of the fragments can be found.

This method holds the promise of greatly reduced computation time because it is not necessary to track the orbits of individual fragments. Examples of the spatial densities calculated are shown in figure 24.

Figure 1
SPACE DEBRIS REPORTS

1. Brooks, David R. ; Gibson, Gary G. ; and Bess, T. Dale: Predicting the Probability that Earth-Orbiting Spacecraft Will Collide With Man-Made Objects in Space, XXVth International Astronautical Congress, Seventh Annual Space Rescue and Safety Symposium, paper no. A74-34, Amsterdam, 30 September 1974.
2. Brooks, David R. : A Comparison of Spacecraft Penetration Hazards Due to Meteoroids and Manmade Earth-Orbiting Objects. NASA TM X-73978, November 1976.
3. Bess, T. Dale: Mass Distribution of Orbiting Man-Made Space Debris. NASA TN D-8108, December 1975.
4. Fuss, Joseph T. : Dynamics of Explosion Remnants in Earth-Orbits. Master's Thesis, Old Dominion University, July 1974.
5. Dasenbrock, Robert; Kaufman, Bernard; and Heard, William: Dynamics of Satellite Disintegration. Final Report, NASA Langley Contract NASA-L5106A, October 1975.

Brooks, Gibson, and Bess (1974)

SIZE DISTRIBUTION OF ORBITING OBJECTS

(June 1973 NORAD catalog)

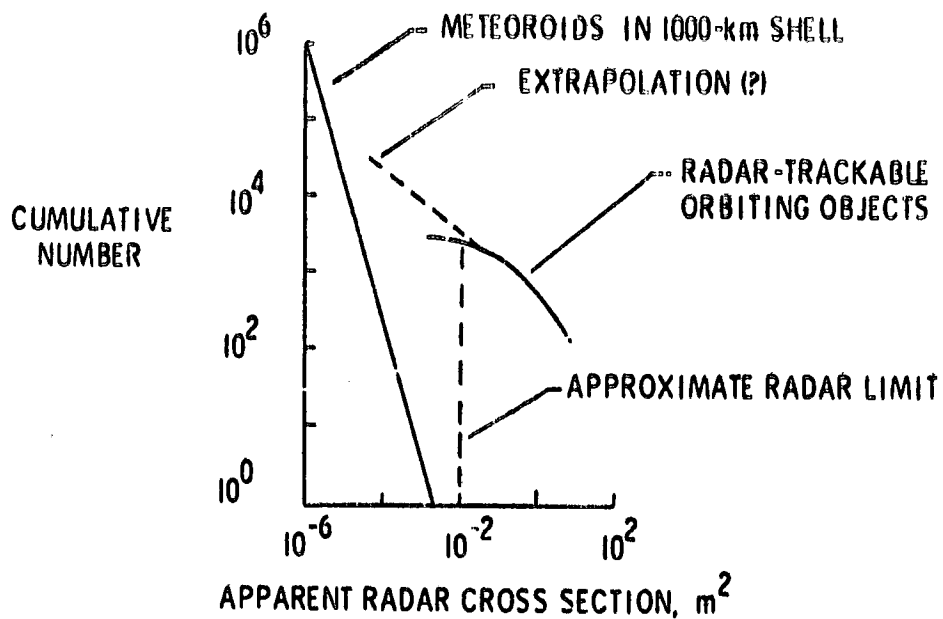


FIGURE 2

Brooks, Gibson, and Bess (1974)

CLASSIFICATION OF ORBITING OBJECTS

Payloads	16.8 %
Rocket bodies	10.1 %
Payload debris	17.3 %
Explosion fragments	55.8 %

FIGURE 3

SIZE DISTRIBUTION BY CLASSIFICATION

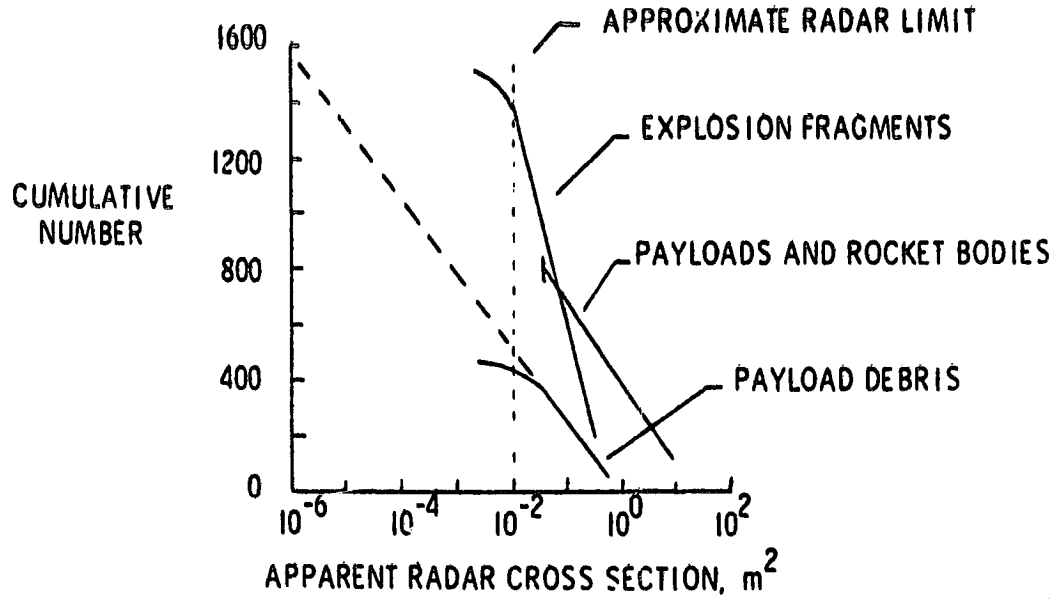


FIGURE 4

SIZE DISTRIBUTION OF EXPLOSION FRAGMENTS

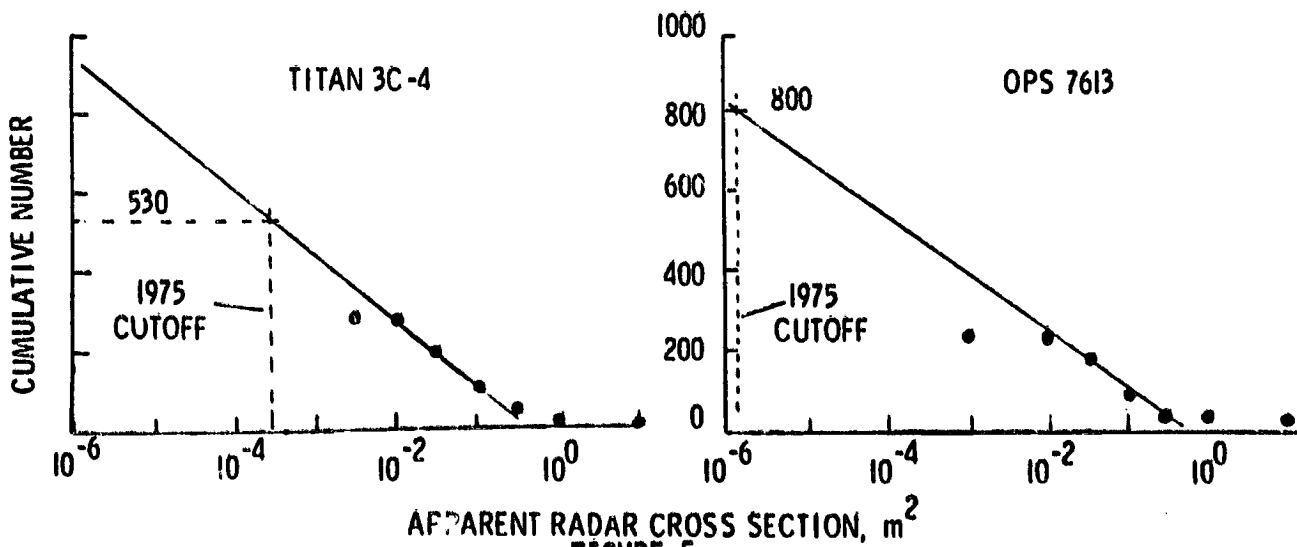


FIGURE 5

Brooks, Gibson, and Bess (1974)

ORBITAL ELEMENTS OF EXPLOSION FRAGMENTS

$$a = a_{\text{Parent}} + (100 \text{ km} \times \text{RU}) \quad a > 6678 \text{ km} \\ \text{perigee} > 250 \text{ km}$$

$$i = i_{\text{Parent}} + (0.5^\circ \times \text{RU})$$

$$e = \left| e_{\text{Parent}} \pm (0.1 \times e_{\text{Parent}}) \right|$$

$$\omega = \omega_{\text{Parent}} + (20^\circ \times \text{RU})$$

$$\Omega = \Omega_{\text{Parent}} + (20^\circ \times \text{RU})$$

RU is a random number between ± 1

FIGURE 6

Brooks, Gibson, and Bess (1974)

REASONS WHY DETERMINISTIC APPROACH TO COLLISIONS NOT FEASIBLE

- insufficient quality of orbital elements
- lack of completeness of information about population

FIGURE 7

Brooks, Gibson, and Bess (1974)

ORBIT INTERSECTIONS

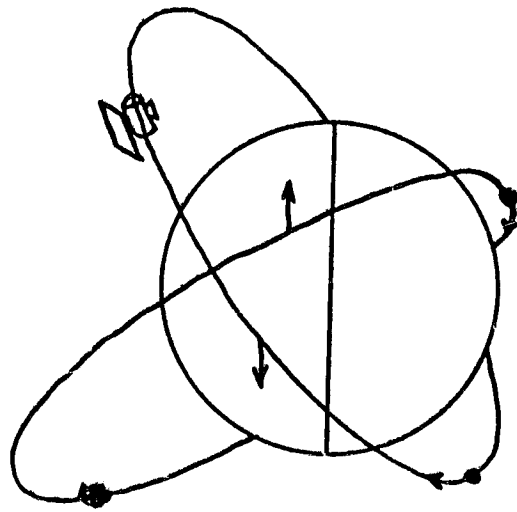


FIGURE 8

Brooks, Gibson, and Bess (1974)

DEBRIS HAZARD AS A FUNCTION OF ALTITUDE

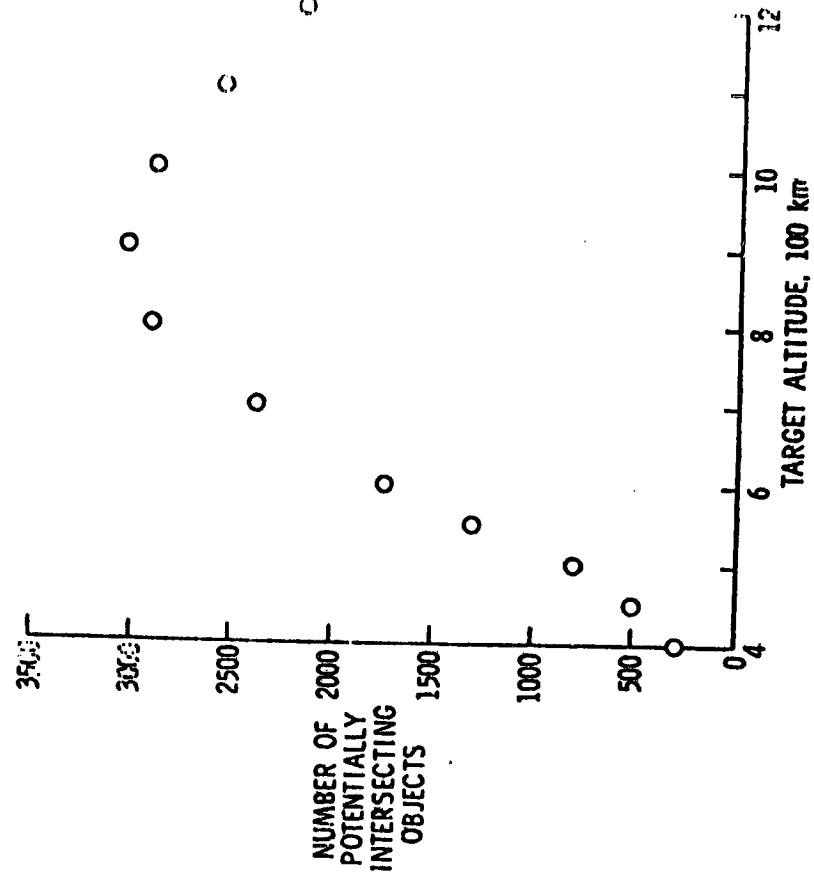


FIGURE 9

DEBRIS HAZARD AS A FUNCTION OF SPACECRAFT INCLINATION

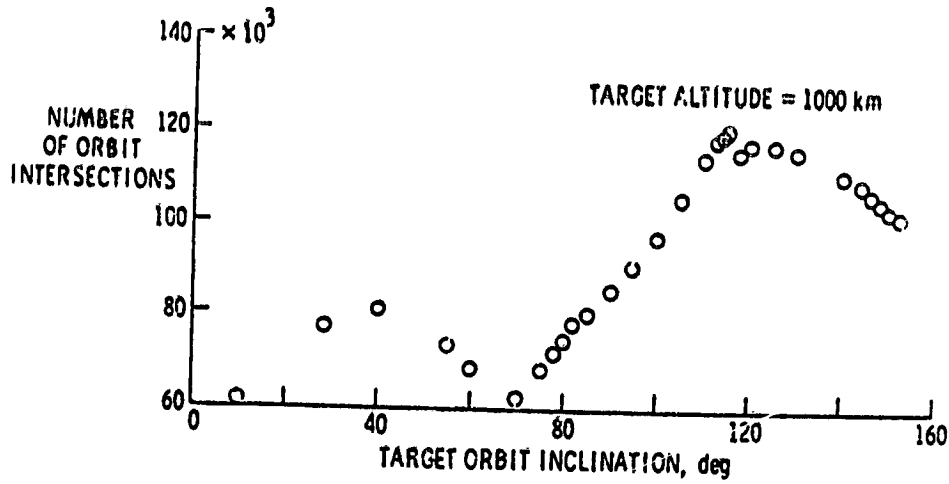


FIGURE 10

COLLISION PROBABILITIES

(100 m diameter, 1000 days)

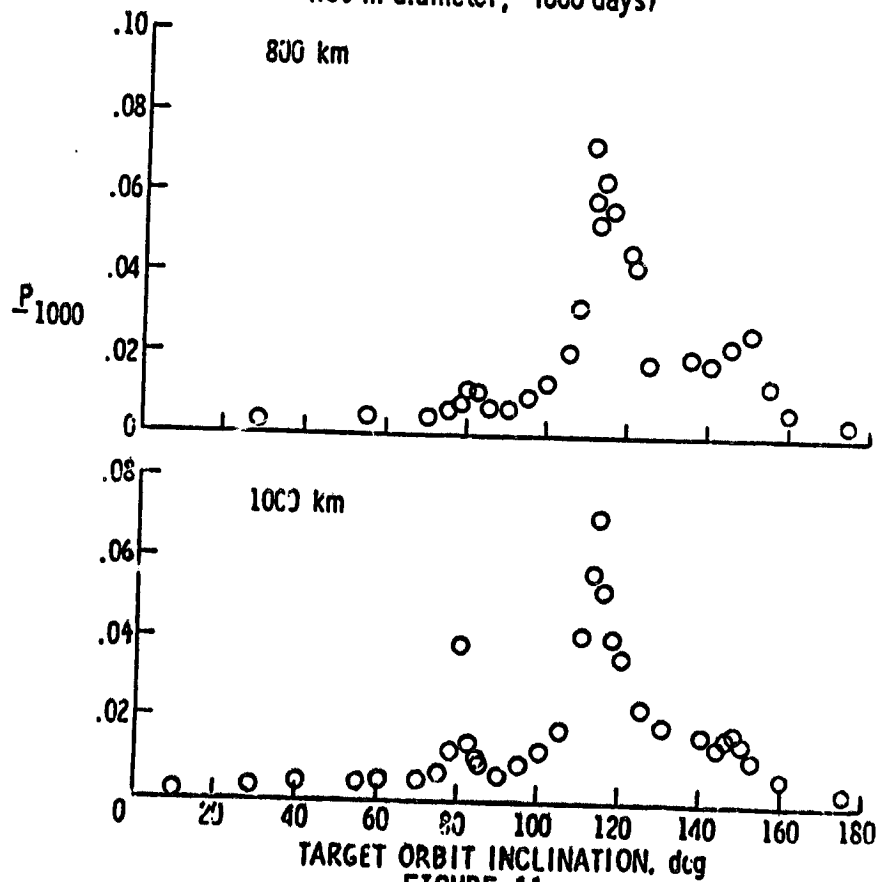
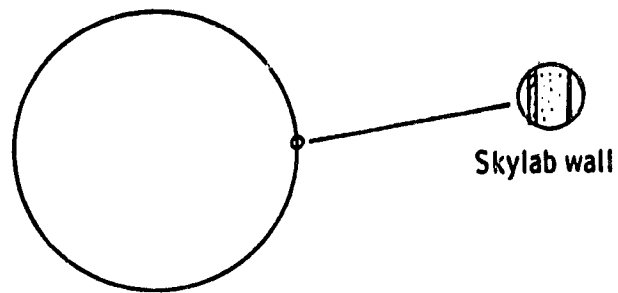


FIGURE 11

Brooks (1976)
PENETRATION HAZARDS

(100 m diameter, 1000 km altitude, 1000 days)



POTENTIAL PENETRATORS

Meteoroids
Man-Made debris

PROBABILITY

1 - 10 %
1 - 10 %

FIGURE 12

Bess (1975)
FRAGMENTATION PROCESSES

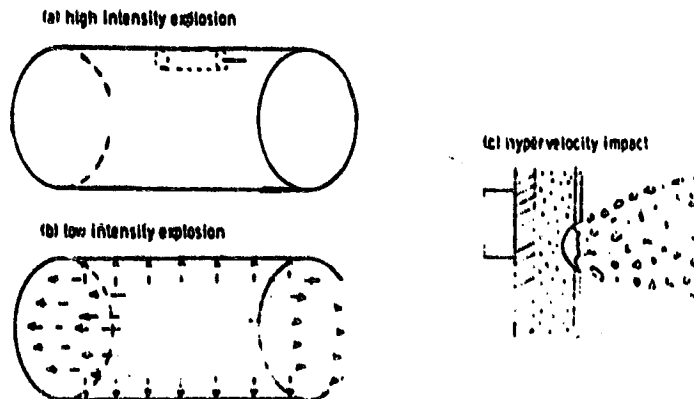


FIGURE 13

**Bess (1975)
FRAGMENT CHARACTERISTICS**

	high intensity explosion	low intensity explosion	impact
Size distribution	$N = N_0 e^{-cm^{1/2}}$	$N = N_0 e^{-cm^{1/2}}$	$N = am^b$
Minimum size	10 mg	-	-
Velocity	≈ 3000 m/s	100 - 600 m/s	10 - 30 m/s
Shape	-	-	1 x 4 x 8

FIGURE 14

**Bess (1975)
SIZE DISTRIBUTION OF EXPLOSION FRAGMENTS**

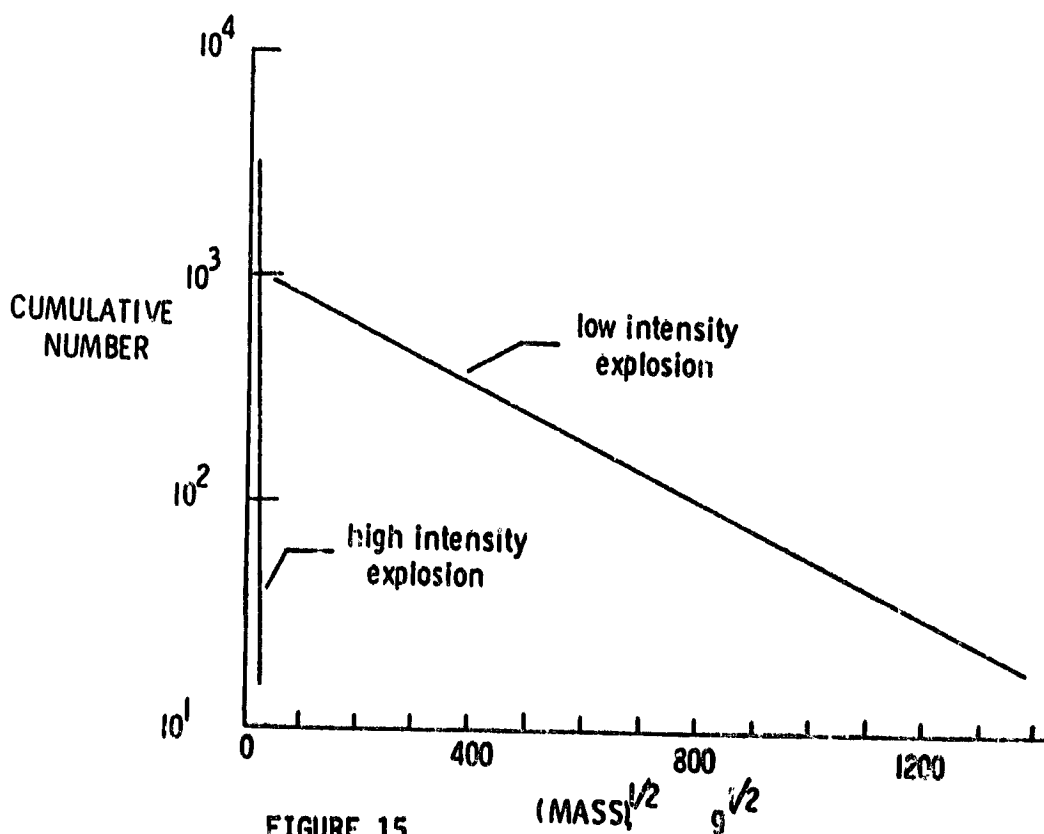
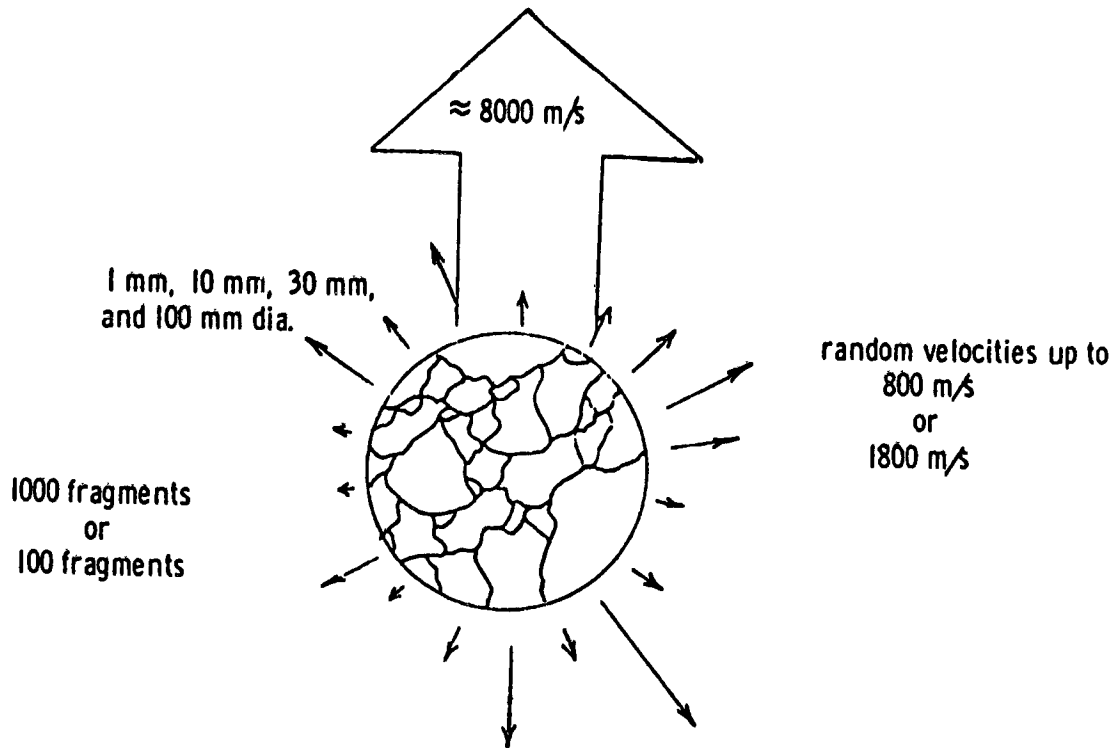


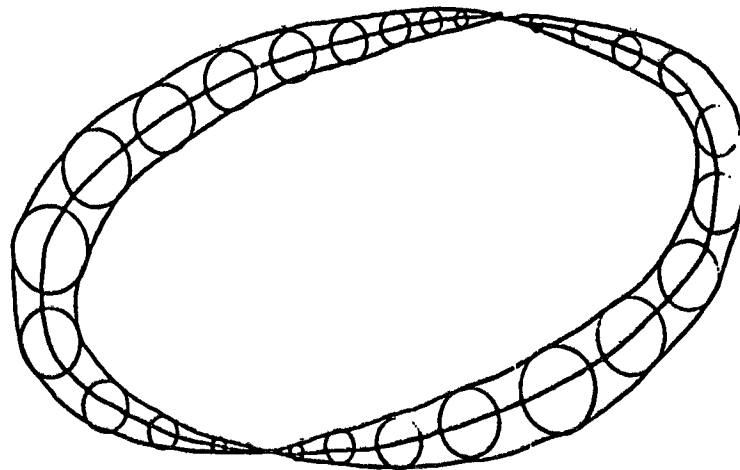
FIGURE 15

Fuss (1974)
SIMULATED EXPLOSION

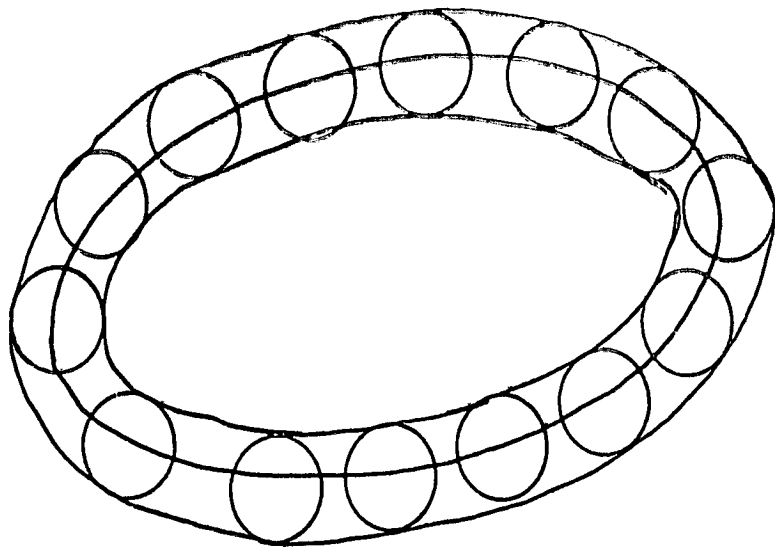


3 dimensions
FIGURE 16

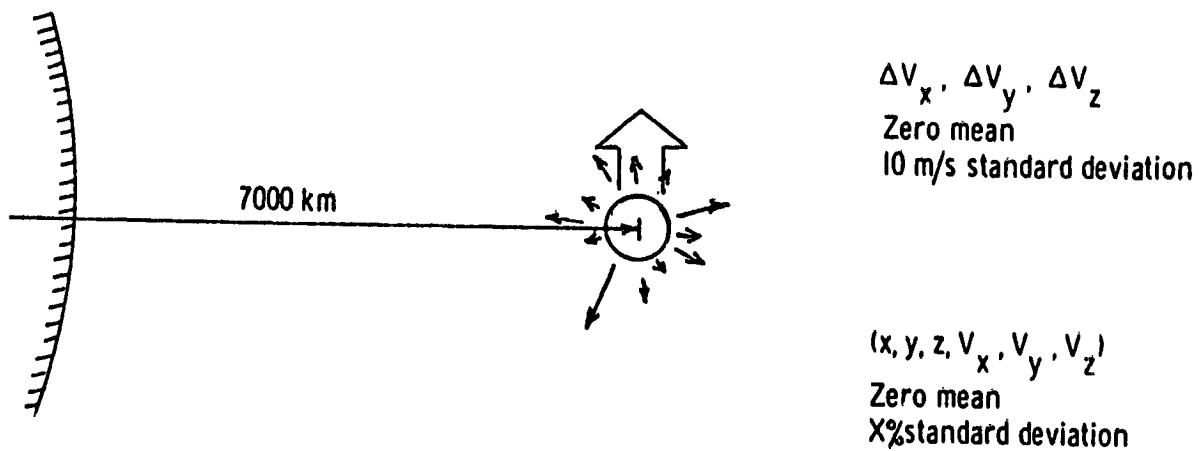
Fuss (1974)
DEBRIS ENVELOPE
(no perturbations)
FIGURE 17



Fuss (1974)
 DEBRIS ENVELOPE
 (with drag and Earth's oblateness)
 FIGURE 18



Dasenbrock, Kaufman, and Heard (1975)
 SIMULATED EXPLOSION



PROXIMITY FUNCTIONS

$$F_1 = \sum_{i \neq j}^n \frac{1}{|\vec{r}_i - \vec{r}_j|^2 + \delta^2}, \quad \delta = 10 \text{ km}$$

$$F_2 = \frac{1}{\sum_{i \neq j}^n |\vec{r}_i - \vec{r}_j|^2}$$

$F_3 =$ no. of pairs such that $|\vec{r}_i - \vec{r}_j| \leq d_1, \quad d_1 \approx 100 \text{ km}$

FIGURE 19

Dasenbrock, Kaufman, and Heard (1975)

PROXIMITY FUNCTIONS FOR SIMULATED EXPLOSION

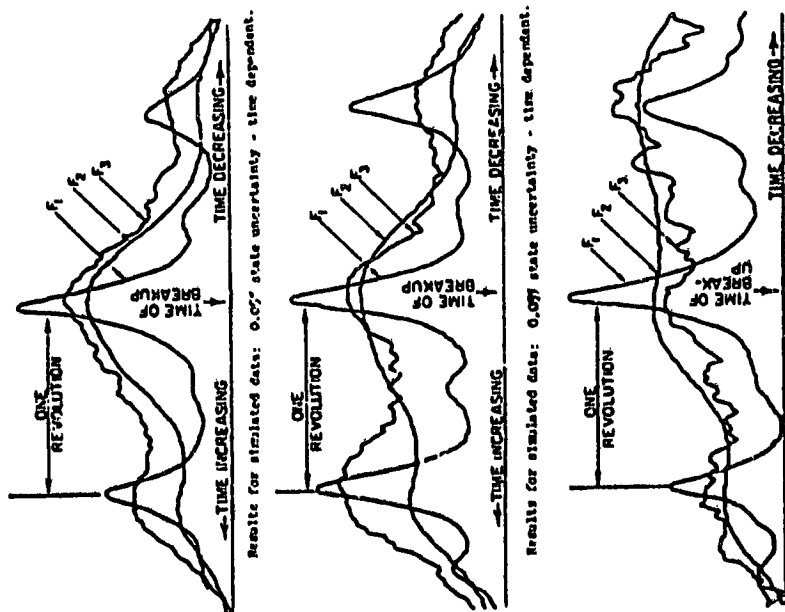


FIGURE 20

Dasenbrock, Kaufman, and Heard (1975)

ORBIT PLANE INTERSECTION LINES FOR FRAGMENTS

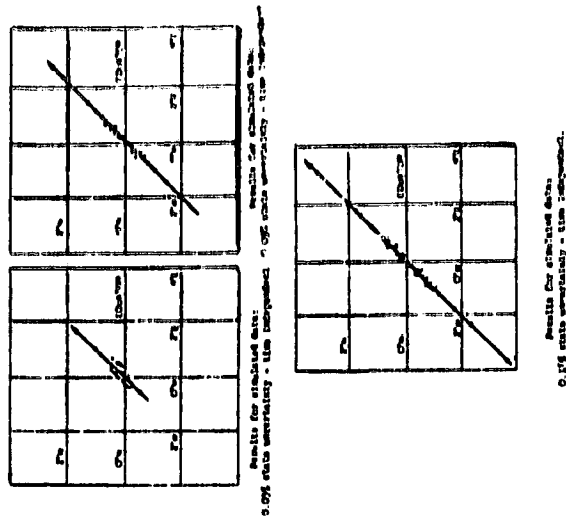
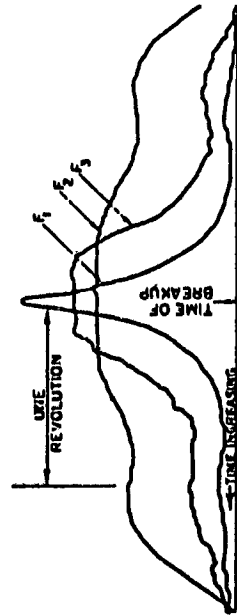


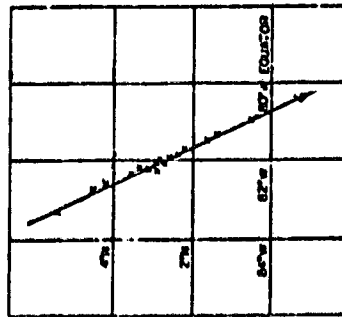
FIGURE 21

Dasenbrock, Kaufman, and Heard (1975)

KOSMOS 699 - EXPLOSION FRAGMENTS



Time dependent analysis of rocket body fragments.

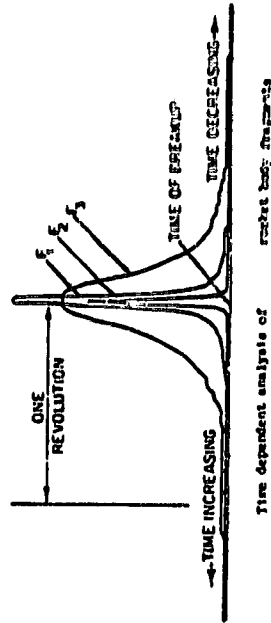


Time independent analysis of KOSMOS 699 fragments.

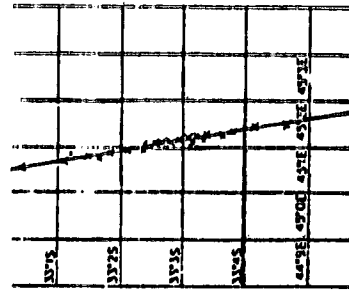
FIGURE 22

Dasenbrock, Kaufman, and Heard (1975)

ERTS - I EXPLOSION FRAGMENTS



Time dependent analysis of rocket body fragments.



Time independent analysis of ERTS-I rocket body fragments.

FIGURE 23

Dasenbrock, Kaufman, and Heard (1975)

SPATIAL DENSITY OF ORBITING OBJECTS

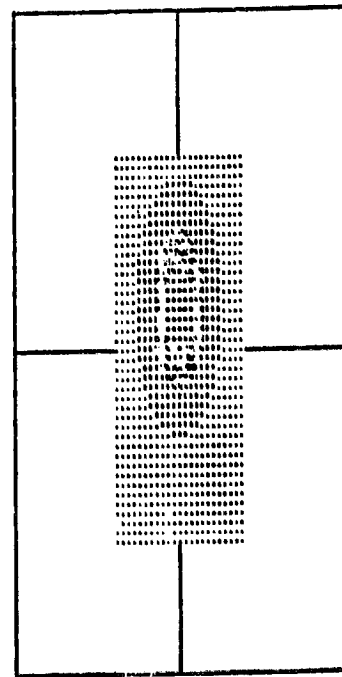
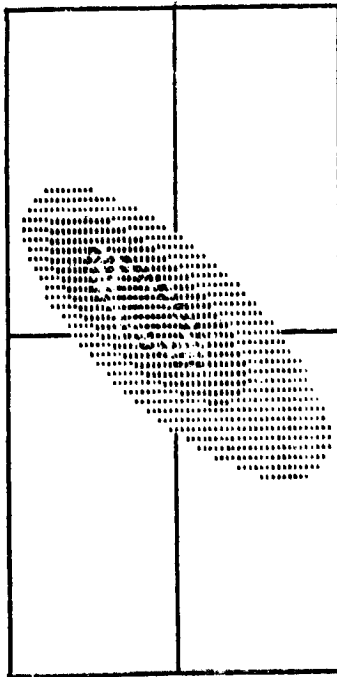
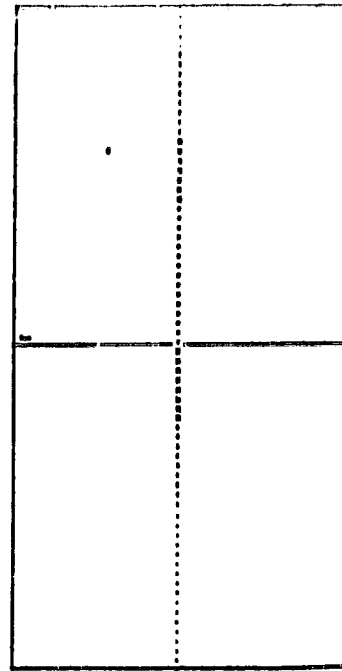
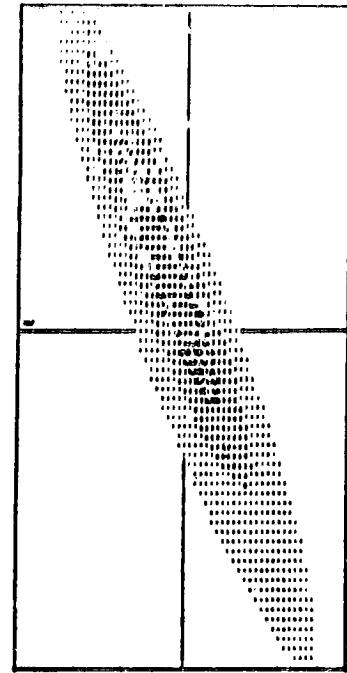


FIGURE 24

NASA/JSC ORBITAL DEBRIS STUDY: Debris Model

J. Brad Roberds
Donald J. Kessler
Shin-Yi Su

With the publication of the paper on the collision frequency of artificial satellites by Kessler and Cour-Palais (1978), the aerospace community became more aware of the possibility of the creation of a debris belt around the Earth and the great hazard the debris belt will impose on any future spacecraft mission. Lockheed Engineering and Management Services Company (Lockheed-EMSCO) at Houston as a support contractor for National Aeronautics and Space Administration at Johnson Space Center (NASA-JSC) has put together a computer model which describes the near-Earth space environment created by the existing spacecraft and fragments from the associated spent launching vehicle attachments and explosions. The present debris model adopts the mathematical formulations published in a paper by Kessler (1981a). Thus, the model uses more rigorous mathematical formulation in calculating the collision rate between two orbiting objects than the one published by Kessler and Cour-Palais (1978). However, it should be noted that although the present model gives more accurate results, the difference in the results between the two methods is considered insignificant.

The present model has been developed with the intent for public use so that the model contains many general but detailed analyses on the debris environment such as manipulating and/or sorting the existing debris objects, describing the physical dimensions of the objects, extrapolating the number density to include the unobservable small objects, the simple orbital decay due to atmospheric drag and so on. A user guide of the model has also been published (Roberds and Kessler, 1982).

Data Sources

The major source for the satellite data base used in the model came from the tape supplied quarterly by North American Air Defense Command (NORAD) containing 3-card satellite element sets plus the radar cross-section. After the data is extracted from the tape and stored as the debris data base, additional information such as launch data, country source, satellite physical dimensions and so on are obtained from TRW Space Log, Launch Summary prepared by National Space Science Data Center (NSSDC) and Royal Aircraft Establishment Table for Earth Satellites 1957-1980. Table 1 lists the items that the data base contains.

Data Base Manipulation

With the data base compiled, one can then sort out and examine any specific data sub-set according to one's interest. For example, one can randomly choose a certain number of satellites, then attach them with some weighting factors to prepare for the calculation of the collision probability for the whole population. This is one of the ways to obtain accurate collision probability among 4000 or more orbital objects cataloged by NORAD because of the enormous computation time involved.

One of most important analyses of the existing data base is to sort out the explosion fragments associated with certain satellites and the international

designation number for the study of the satellite break-up phenomena. By comparing the number and size distribution of the explosion fragments of the satellite family catalogued by NORAD with that of explosion fragments obtained from the ground Atlas explosion experiments, we can obtain additional number-size distributions of the explosion fragments which are unobservable by NORAD detectors. Examples will be shown in the next section.

Debris Environment Analysis

Table 2 lists various debris environmental analyses that can be performed by the present model. Some of the results can be conveniently presented by graphics. We will not show all the results that the model can do because all the figures from the present model are very similar to the ones published by Kessler and Cour-Palais (1978) and Kessler (1981b). For example, we use the April 1982 NORAD data and produce a debris flux versus altitude figure in Figure 1. It is noted, this figure is very similar to Figure 1 of Kessler's (1981b) paper in shape and value. Again the highest flux is centered between 800 and 1000 km altitude where most circular orbiting spacecraft and the associated explosion fragments exist. Another figure which shows the spacecraft area versus the radar cross section (RCS) for the entire population is shown in Figure 2.

As was mentioned in the previous section, the present model can be a valuable tool in analyzing the spacecraft break-up phenomena and predicting the additional explosion fragments not detectable by ground radar. Figure 3 shows a plot devised by John Gabbard to present an explosion of a spacecraft (payload or launching vehicle). This is an explosion of the second stage of the launching vehicle for the NOAA 3 satellite (international designate number 1973 - 86). This is a plot for the altitudes of fragment versus the period for that fragment. There are two points for the altitude, namely the apogee and the perigee. The most striking feature in the figure is the indication of the slanted x-shape for all the points to fall in. By the nature of the orbital mechanics, all fragments should pass through the origin of explosion and the origin should lie between all the apogees and perigees of the fragments. We thus claim that the explosion should have occurred at an altitude of about 1500 km where the center of the x-shape figure is. However, it should be noted that not all explosions display the x-shape figure. Sometimes only one upper or lower branch of the x-shape figure exists. In this case, the explosion origin is still located at the altitude between all apogees and perigees, but no longer at the center of the extrapolated x-shape figure.

Figure 3 shows the plot of the accumulated number of the fragments in logarithmic scale versus the 0.565 power of fragments RCS in the explosion of 1973-86 spacecraft. The reason for choosing $(RCS)^{0.565}$ as the horizontal axis is that the result from the ground Atlas explosion test reported by Bess (1975) indicated that a linear relationship exists between the log of the accumulated fragment number and the square root the fragment mass. When the relationship between the RCS and the mass for the spacecraft is applied, we found that $M^{1/2} (RCS)^{0.565}$. The fitting of the line to the fragments is also shown in Figure 4. The deviation of the

1973-86 explosion from the straight line in the larger RCS region can be attributed to the statistical fluctuation, while the deviation in the smaller RCS region is due to the size limitation of the ground radar detectability. Thus we can extrapolate to obtain the number size distribution of the explosion down to 4mm size fragments. The difference in fragment numbers is then assigned as a weighting factor for the known fragments. Figure 5 shows 2 curves for the spatial density of 1973-86 explosions, the lower curve indicates the contribution from the observable fragments and the upper one is for all the fragments down 4mm size when the weighting factor is included to account for the unobservable portion of fragments. It is seen that the unobservable fragments can contribute several times as much as the observed fragments in the spatial density for each explosion.

When all the significant explosion events were analyzed and the results were then added to the NORAD data base, we show in Figure 6 two different curves of the spatial density versus altitude. The lower curve in Figure 6 is the original spatial density contributed by the observed orbiting objects while the upper one includes all the correction factors for the explosion events. It is seen that the unobserved population of the orbiting objects actually contribute 2 to 3 times more spatial density than the cataloged ones.

Another example is to estimate roughly the total number of collisions that could occur as years pass by from today with the assumption of 400 new satellites input per year and no collision debris is generated and no orbital decay for the existing objects. The result is shown in Figure 7. As expected, the number of collisions increases as the square of the number of the orbiting objects.

Finally, we shall examine the effect of the atmospheric drag on the orbital decay. The mathematical formula used for the model basically derived from the book by King-Hele (1964) plus additional lunar-solar perturbation effects on objects in higher orbits. The sun spot number and the geomagnetic effect are included in the calculation of the exospheric temperature. The result is shown in Figure 8 for the changes in spatial density for 50 years purely due to atmospheric drag effect.

Concluding Remarks

The NASA/JSC Orbital Debris Model is capable of carrying out many debris environmental analyses for a given input satellite population. Although the model gives many excellent results, it can only perform a time-independent analysis. A time-dependent debris model which takes into account the effect of the interaction between the generated collision and explosion fragments with the existing satellite population is now being studied. It is hoped that this new model will become available in the near future.

Table 1: SATELLITE DATA BASE

- International Designation
- NORAD Satellite Number
- Satellite Name
- Source
- Launch Date
- Apogee Height
- Perigee Height
- Inclination
- Mass
- RADAR Cross-Section
- Type
- Physical Geometry
- Physical Length
- Physical Diameter
- Total Surface Area
- B*
- Drag Coefficient
- Argument of Perigee
- Long. of Ascending Node
- Epoch
- Scratch Pad
- Scratch Pad
- Weighting Factor

Table 2

Debris Model Capabilities

- o Satellite Data Base Manipulation
- o Debris Environment Analysis
 - o General Questions
 - o Specific Questions
 - o Plotting Graphic Data
 - Generate Another Data Base Subset
 - Delete Some Satellite Data
 - Combine Two Satellite Data Base
 - Sort Satellite Data in a Specific Order
- o Debris Environment Analyses
 - o General Questions
 - Print Out Satellite Data Base
 - Count Satellite Numbers for a Given Year, Year, Source, Orbital Parameter, Etc.
 - o Specific Questions
 - Debris Flux on a Target Satellite
 - Collision Rate for a Given Satellite Population
- o Plotting Graphic Data
 - Spatial density vs Altitude or Latitude
 - Cumulative Spatial Density vs Satellite Cross-section or Diameter
 - Satellite Number vs Orbital Parameters
 - Satellite Number vs Satellite Mass or Cross-section
 - Total Area vs Cross-section
 - Collisions per Year vs Altitude
 - Collisions to Date vs Year

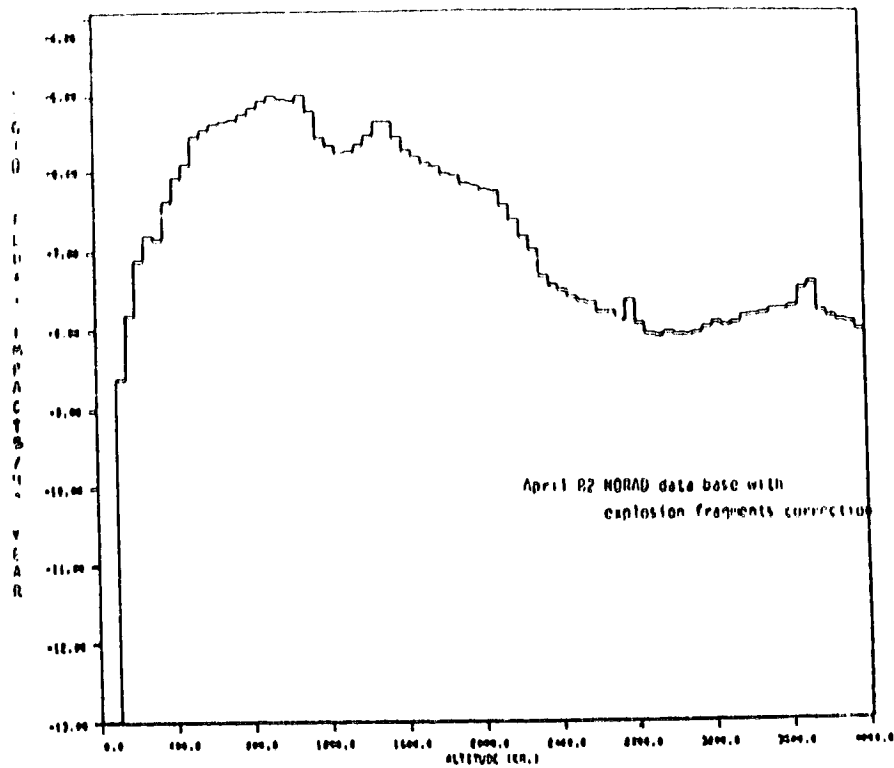


Figure 1: Total fluxes for the earth orbiting debris including the non-radar detectable explosion fragments is plotted as function of altitude.

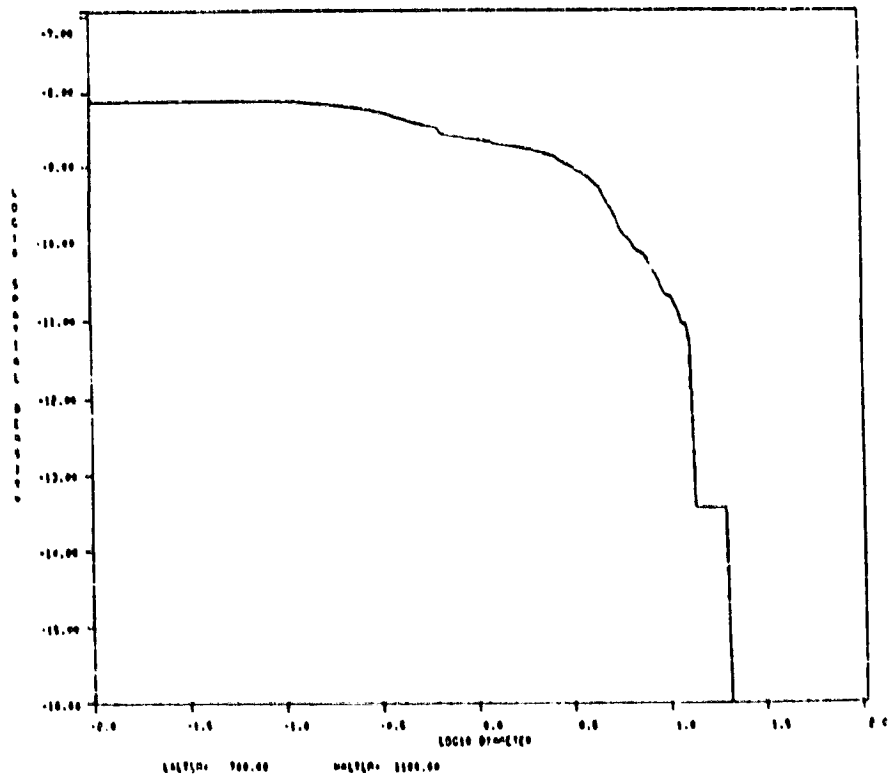
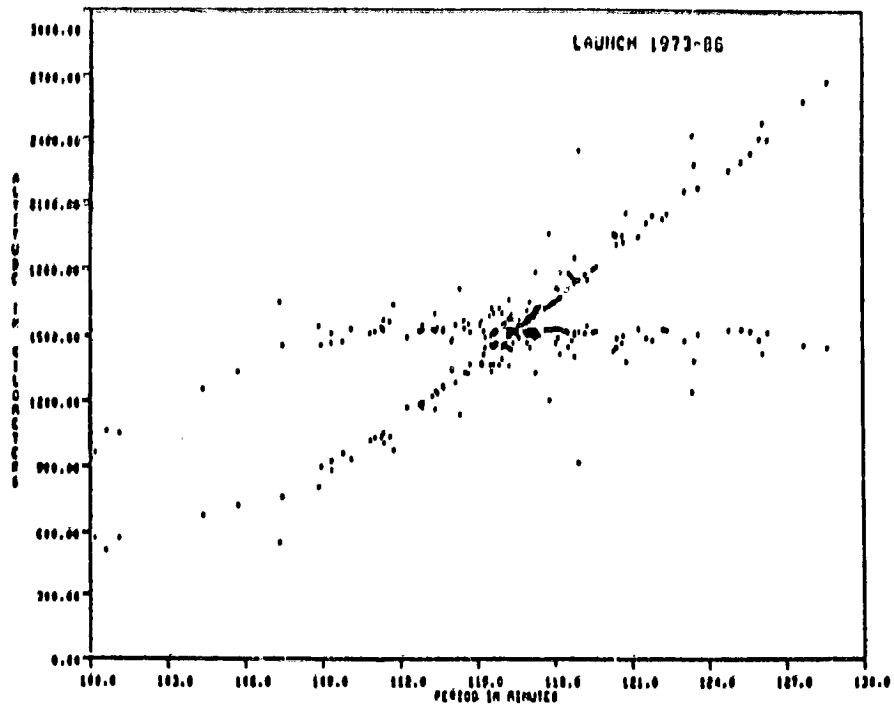


Figure 2: The cumulative spatial density is plotted against the particle sizes between altitude of 700km and 1100km for NORAD April 1982 data base.



LAUNCH 1973-86 DECEMBER 1980 NORAD DATA. BOTH APOGEE AND PERIOD OF EACH ORBIT PLOTTED. (JULY 16, 1981)

Figure 3: Apogee and perigee of an explosion fragment is plotted against the fragment's period.

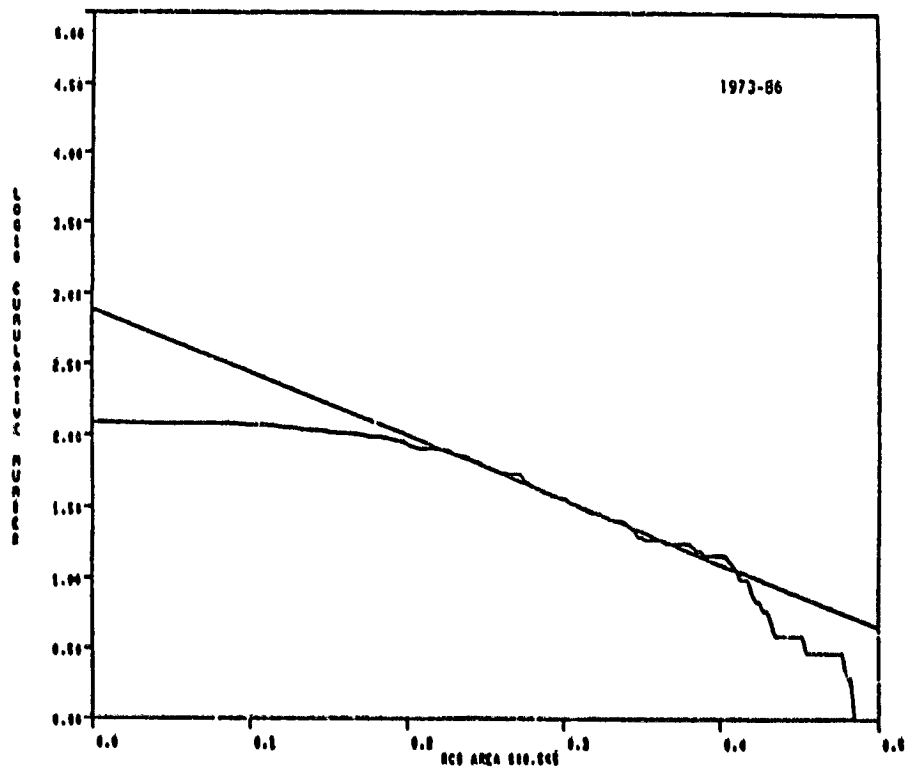


Figure 4: The cumulative particle number is plotted as function of (RCS)^{0.565} for the explosion event of satellite 1973-86. The straight line fit of the observed curve comes from the empirical formula derived from the ground Atlas explosion test.

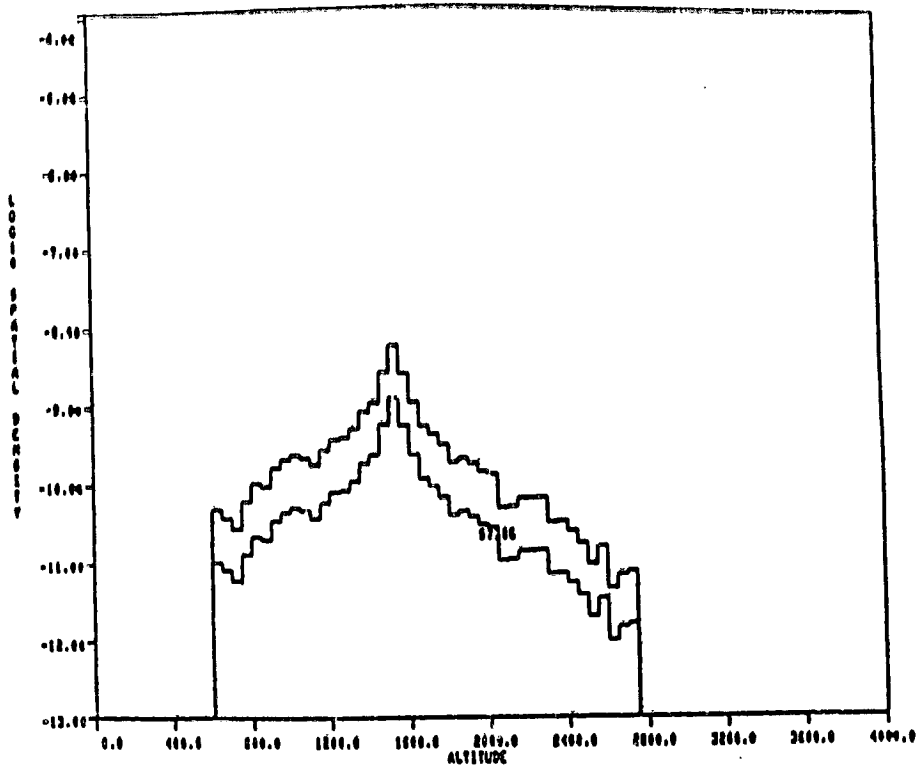


Figure 5: the original and the extrapolated spatial density from satellite 1973-N6 are plotted. The extrapolated data come from small particle sizes that are not observable from NORAD ground radar.

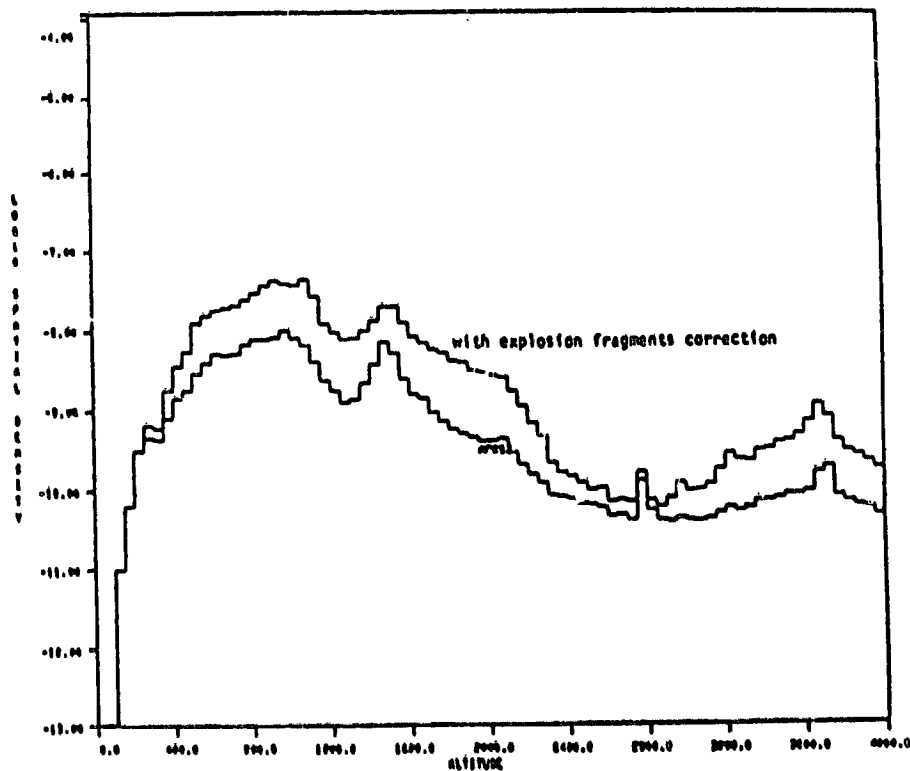


Figure 6: Two curves of spatial density associated with NORAD 1982 April data base are plotted here. The upper curve indicates the inclusion of most explosion events below 2800km altitude.

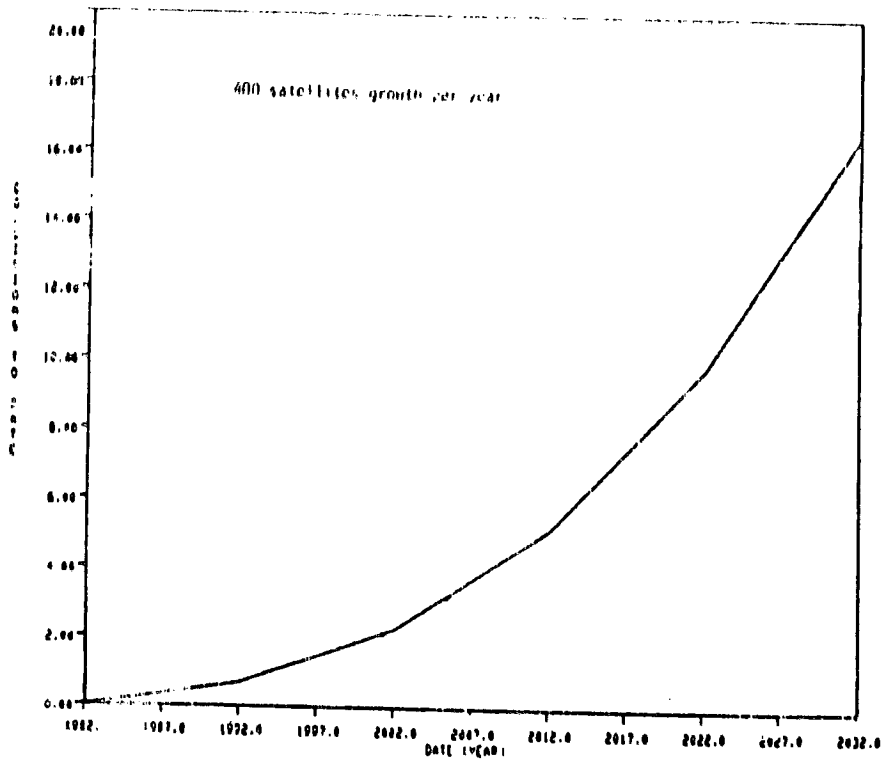


Figure 7: Estimate of number of collisions by the given date with the assumption 400 satellites input per year and no collision fragmentation and no air drag effect.

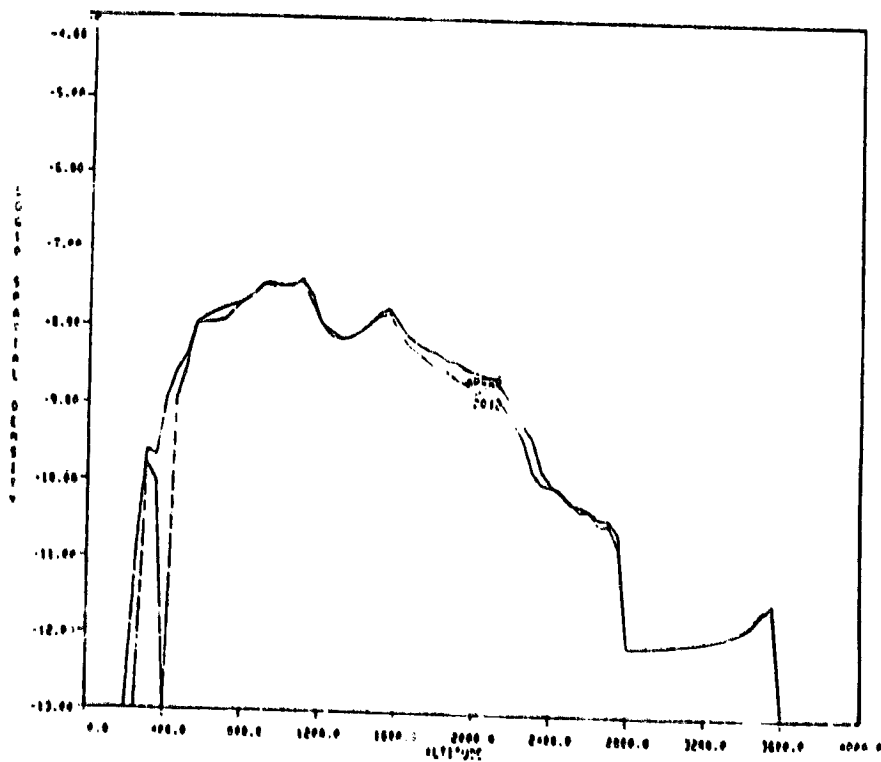


Figure 8: Effect of atmospheric drag in 50 years on the existing spacecraft from year 1982 to 2032.

Acknowledgment

We would like to express our appreciation to Ms. Debra Reed and Ms. Mary Tarlton for their efforts in manually inputting data information to complete the satellite data base, and to Ms. Mary Tarlton for her assistance in extracting all the explosion data from the data base. Also, special thanks to Mr. Alan Mueller for putting together the FORTRAN coding of the atmospheric drag program.

References

- Bess, T. D., Mass Distribution of Orbiting Man-Made Space Debris, NASA Technical Note, NASA TE D-8108, 1975.
- Kessler, D. J. and Cour-Palais, B. G., Collision Frequency of Artificial Satellites: Creation of a Debris Belt, J. Geophys. Research, 83, 2637, 1978.
- Kessler, D. J., Derivation of the Collision Probability between Orbiting Objects: The Lifetimes of Jupiter's Outer Moons, ICARUS, 48, 39, 1981a.
- Kessler, D. J., Sources of orbital Debris and the projected Environment for Future Spacecraft, J. Spacecraft and Rockets, 18, 357. 1981b.
- King-Hele, O., Theory of Satellite Orbits in an Atmosphere, Butterworths, London, 1964.
- Roberds, J. B. and Kessler, D. J., Orbital Debris Study: Debris Model User Guide, Lockheed-EMSCO, 1982.

1980

2119

UNO

1/6-12
N 85-21194

Proposed Preliminary Design Criteria
Model Environment for the 1990's
by Donald J. Kessler
NASA/Johnson Space Center

Introduction

An environment must first be defined before one can begin to evaluate the effects of that environment. The environment may later prove to be either more severe or less severe, and consequently the effects will also become either more severe or less severe. Thus, the original environment can also serve as a reference point for future updates. It is in this spirit that this paper proposes a model environment for orbital debris. It is recognized that much more is unknown about the environment than is known, and any model at best represents an educated guess based on a limited amount of data.

Assumptions and Uncertainties

The major assumptions in the proposed model environment and the uncertainty in those assumptions are as follows:

1. The catalogued population will be 2.5 times its current population. Extrapolations of past growth rates give a tracked population of between 2 and 3 times its current value.

2. The only sources of untracked objects are low intensity explosion fragments and collision fragments. Other sources, such as the probable high intensity explosions by anti-satellite testing, or paint flaking would increase the number of untracked objects. However, since we do not have any data on these sources, they were not included in the model.

3. Past major satellite break-ups were low intensity explosions and the size distribution can be represented by the Atlas missile ground explosion data given in reference 2. This assumption could significantly underestimate the population between 1mm and 1 cm if any of these break-ups were either high intensity, or the result of a collision.

4. Three collisions will have occurred over a 9-year period just prior to the mid-1990's between objects larger than 4 cm and the fragments are evenly distributed in the region between 600 and 1000 km altitude. This assumption may represent the largest uncertainty. While modeling in reference 3 indicates that an average of 3 collisions can be expected, the actual number, location, and size of the collision depends totally upon chance, and could produce very different results.

5. The size distribution of collision fragments is given by the impact tests in reference 2, scaled to the energy levels of the expected collisions in orbit. This assumption represents the 2nd greatest uncertainty. The impact tests which were performed were at relatively low impact mass and velocities, and the structures impacted represented only one type of spacecraft structure. Thus, scaling these tests to larger energy levels, and generalizing them to all types of spacecraft structures may produce results which could either be too large or too small.

6. Atmospheric drag is the only mechanism to transport fragments to altitudes below 600 km. If objects are ejected into this altitude region, the flux would be higher.

7. The meteoroid environment is given in reference 4. It was adjusted for Earth shielding (x0.7) and the units were changed from impacts per unit surface area to impacts per unit cross-sectional area (x4).

A_c = cross-sectional area exposed to flux, sq. meters

A_s = surface area, sq. meters

t = time exposed to the environment, years

N = average number of impacts /yr.

P_0 = probability of no impacts

$$A_c = A_s/4$$

for any randomly oriented solid with only convex surfaces

$$N = FA_c t$$

$$P_0 = e^{-N}$$

Mass density:

Meteoroids: $\rho = 0.5 \text{ gm/cm}^3$

Debris, less than 1 cm: $\rho = 2.8 \text{ gm/cm}^3$

larger than 1cm: $\rho = 2.8/d^{.74}$ (d = ave. dia., cm)

Velocity (Average):

Meteoroid: 20 km/sec

Debris: 10 km/sec (inclination dependent)

Directionality:

Meteoroids: assumed omni directional (except when Earth shielded)

Debris: Mostly in plane parallel to Earth's surface

Environment

Current Environment:

The current debris flux is given in reference 3 and shown on figures 1 and 2.

Predicted Environment:

The predicted debris flux for the 1990's is shown on figure 3. This flux is average over all spacecraft inclinations and have an average relative velocity of 10 km/sec.

The flux on a spacecraft having a specific inclination may have a slightly lower, or higher flux and relative velocity. The ratio of this flux to the average flux is given in figure 4, and the average velocity is given in figure 5. Velocity distributions for 4 specific inclinations is given in figure 6.

Definition and General equations

F = flux, impacts/cross-sectional sq. meter-year

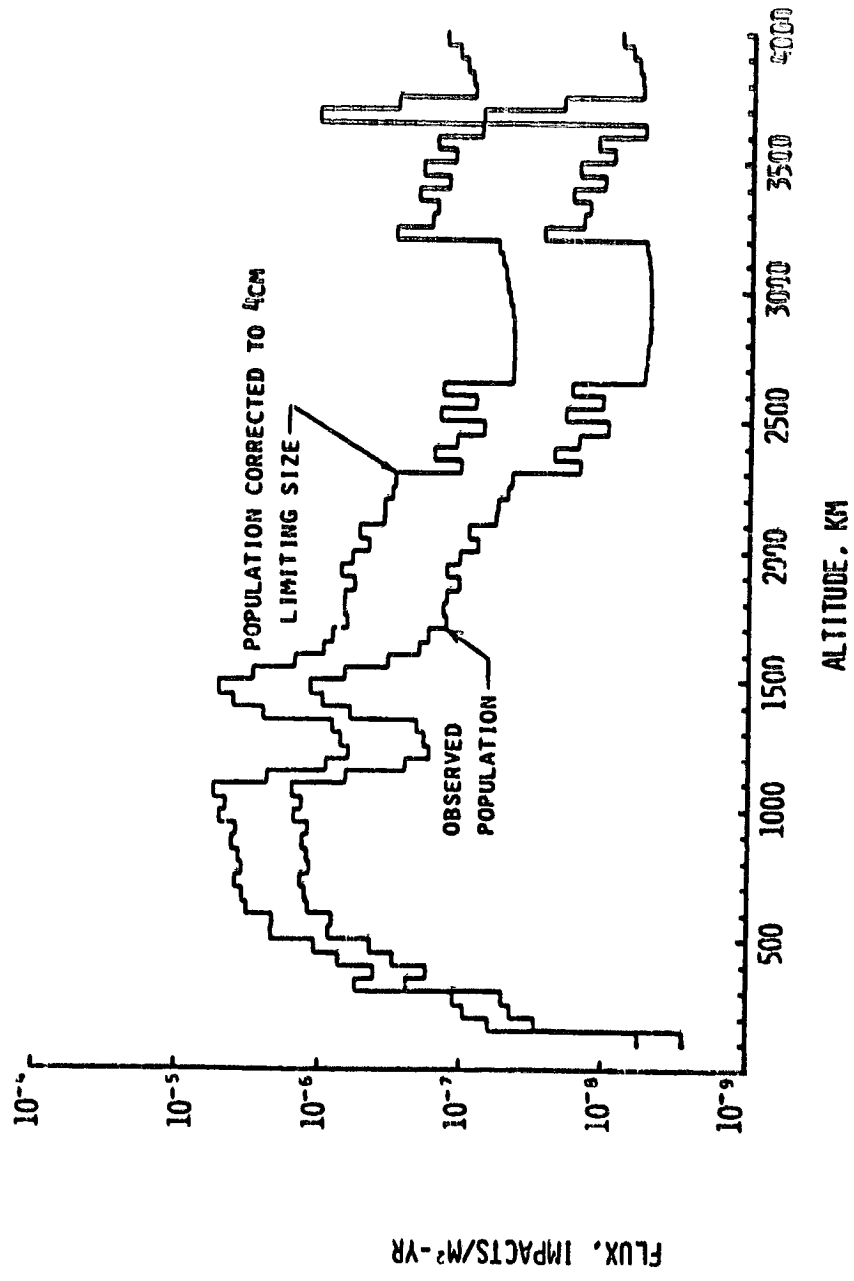


FIGURE 1 OBSERVED AND CORRECTED TO 4 CM LIMITING SIZE

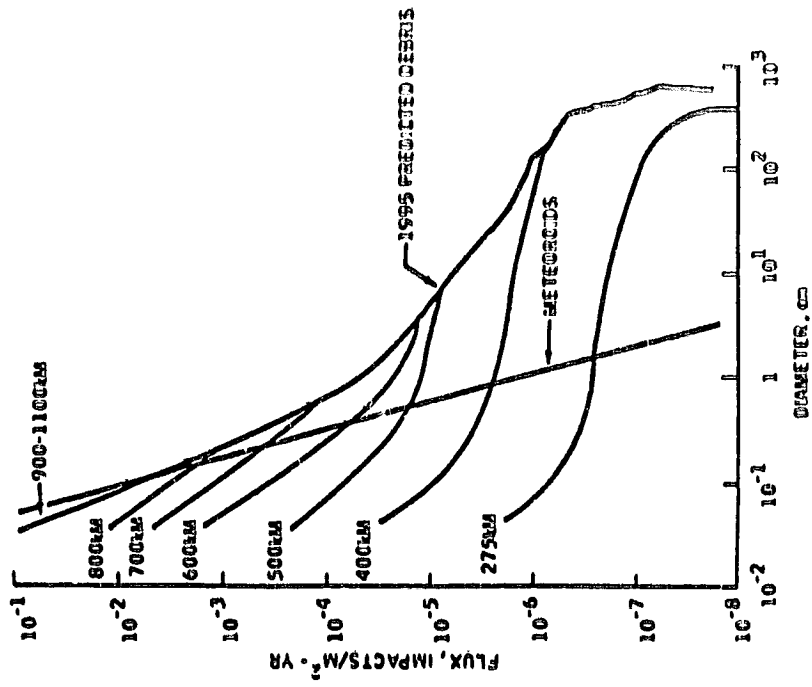


FIGURE 3. PREDICTED 1995 CUMULATIVE AVERAGE ORBITAL DEBRIS FLUX

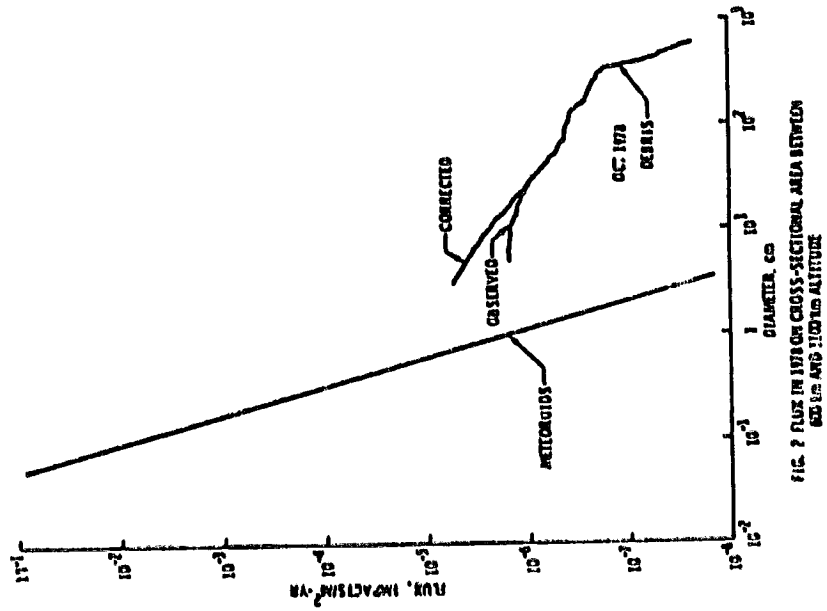


FIG. 2 FLUX IN 1978 ON CROSS-SECTIONAL AREA BETWEEN 600 KM AND 1100 KM ALTITUDE

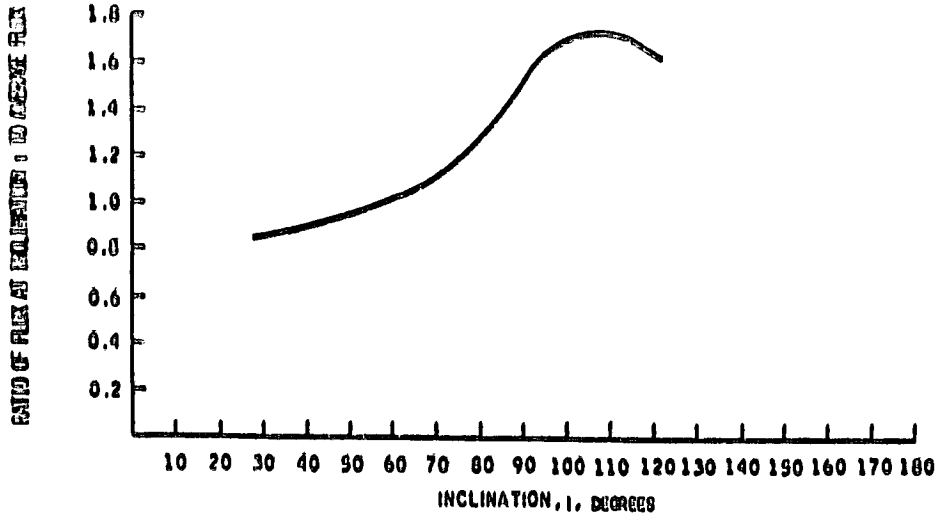


FIGURE 4. FLUX RATIO VARIATION WITH INCLINATION FOR ORBITAL ALTITUDES BELOW 1100 KM.

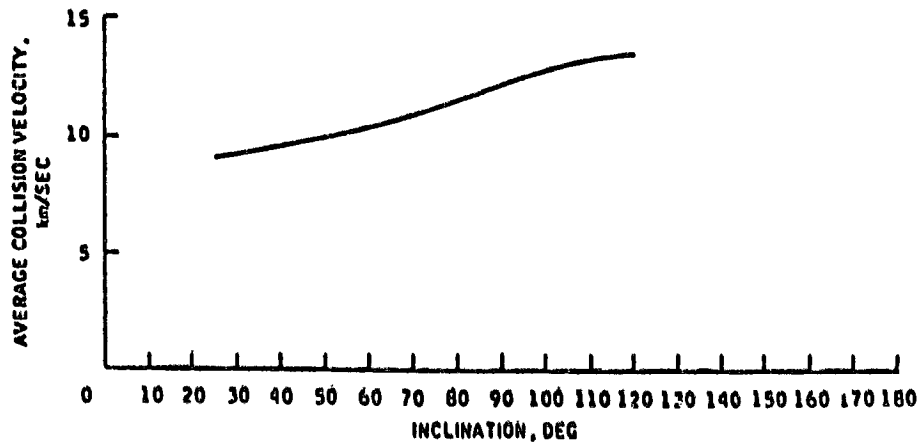


FIGURE 5. AVERAGE RELATIVE COLLISION VELOCITY VARIATION WITH INCLINATION

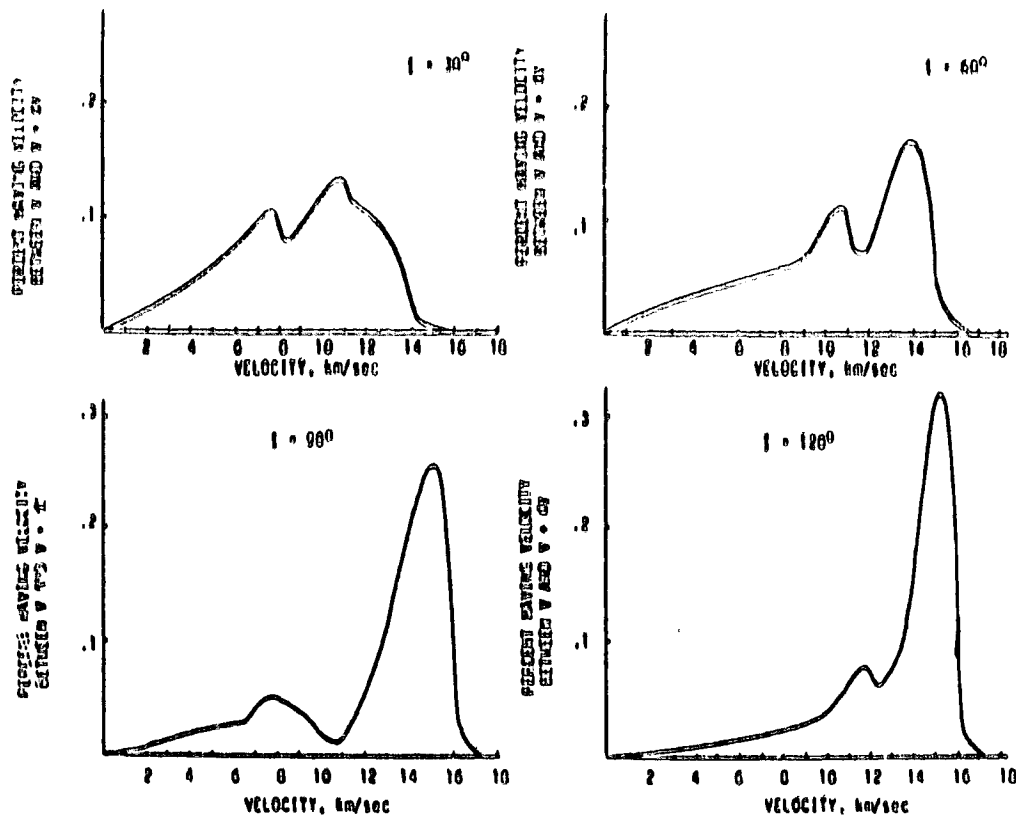


FIGURE 6. VELOCITY DISTRIBUTION RELATIVE TO A SPACECRAFT HAVING VARIOUS ORBITAL INCLINATIONS, i

References

1. Kessler, D.J. and Cour-Palais, B.G. "Collision Frequency of Artificial Satellites: The Creation of a Debris Belt," Journal of Geophysical Research, vol. 83, June 1, 1978, pp. 2637-2646.
2. Bess, T.D. "Mass Distribution of Orbiting Manmade Space Debris," NASA Technical Note TND-8108, 1975.
3. Kessler, D.J. "Sources of Orbital Debris and the Projected Environment for Future Spacecraft." Journal of Spacecraft and Rockets, Vol. 18, July-Aug. 1981, pp. 357-360.
4. Cour-Palais, B.G., "Meteoroid Environment Model - 1969 (Near Earth to Lunar surface). NASA SP-8013, 1969.

27-12
N 85-21195

I. Introduction

The presence of manmade debris in space presents a collision hazard to spacecraft which is proportional to the density of debris, relative velocity at encounter, projected area of the spacecraft and mission duration. The principal hazard is due to large objects which can be tracked by radar that are in the vicinity of the operational orbits. The objects consist of spent spacecraft, rocket stages, payload separation devices and some explosion fragments. Objects larger than 4 cm in diameter fall into this category. A secondary hazard is due to the presumed existence of a much larger population of smaller objects which are the products of more than 60 spacecraft explosions to date. The existence of this population can be inferred from terrestrial tests in which the particle distributions from high and low intensity explosions have been measured. The number of such particles may be in the tens of thousands or even in the millions. Several studies (Ref. 1 to 5) have examined the origin and distribution of the tracked population of objects and implications for future missions. This study considers the distribution of the tracked population of objects as a function of altitude and orbital inclination. Representative encounter parameters such as the number, relative velocity, and miss distance are determined for circular mission orbits and are used to classify regions of space according to the degree of collision hazard presented. Implications for Space Shuttle and geosynchronous orbits are examined.

II. Low Altitude Orbits

A. Encounter Parameters

Consider the encounter geometry of a satellite in a circular orbit of radius R illustrated in Fig. 1. A space object encounters the satellite at a distance of closest approach R_{MIN} (miss distance) with an "encounter sphere" of radius R_{MAX} . The relative velocity V_R , measured in an inertial frame, and the relative aspect angle θ between the velocity vectors of the satellite and of the space object are indicative of the severity of each encounter. The total number of encounters per revolution of the satellite is proportional to the density of space objects in the vicinity of the mission orbit.

A numerical simulation was used to examine the encounters for satellites in circular orbits with space objects listed in the March 1981 NORAD catalog. The rate of encounters, mean relative velocities, relative aspect angle and distributions in range were obtained as functions of altitude and orbit plane inclination. The results are given in Figs. 2-5. Data in Fig. 2 reveal that the greatest rates of encounters generally occur in the 600 to 1200 km altitude range. The results in Fig. 3 indicate that the relative velocities at encounter are in the 8 to 12 km/sec range depending on altitude and inclination of the mission orbit. Figure 4 shows that the mean aspect angle $\bar{\theta}$ is generally low for equatorial orbits ($i = 0^\circ$) and high for polar orbits. The standard deviation of $\bar{\theta}$ is listed in Table 1.

A sample of distributions of encounters for a 1000 km circular orbit in Fig. 5 shows the relative frequency of encounters for the 0° , 45° , 90° and 135° circular mission orbits.

The number of encounters per revolution of the satellite within a sphere of radius \bar{R}_{MIN} yields an "average" density ρ_T of space objects in the vicinity of the mission orbit. The "average" density ρ_T may be used to define a hazard index I_h for all orbits of interest. Thus, for example, the probability of collision for a satellite with a projected area A moving with a mean relative velocity \bar{V}_R in a time period Δt may in general be expressed as

$$p(\text{col}) = \rho_T \bar{V}_R A \Delta t \quad (1)$$

where

$$\rho_T = \frac{N}{V_{TOR}} \quad (2)$$

N = the number of encounters per revolution of the satellite

$$V_{TOR} = 2\pi^2 R (\bar{R}_{MIN})^2$$

= "mean" volume of torus centered about the mission orbit

(3)

Table 1. Mean Relative Angle and Standard Deviation at Encounter

Altitude (km)	i (deg)	N_T	Mean Angle $\bar{\theta}$ (deg)	Standard Deviation σ (deg)
500	0	20	64.7	25.5
500	45	57	122.5	46.2
500	90	22	92.7	27.1
500	135	55	129.5	28.4
750	0	75	76.6	21.2
750	45	79	88.8	31.7
750	90	102	121.7	45.8
750	135	103	113.8	37.5
1000	0	68	84.9	15.9
1000	45	55	101.3	30.7
1000	90	95	110.9	50.6
1000	135	105	100.6	37.4
1250	0	28	92.5	18.2
1250	45	39	100.9	31.7
1250	90	36	109.9	44.6
1250	135	32	106.4	32.8
1500	0	32	81.2	20.2
1500	45	45	106.0	27.2
1500	90	53	122.2	42.7
1500	135	53	110.6	32.2
2000	0	6	90.9	17.6
2000	45	8	97.3	34.1
2000	90	6	126.8	46.2
2000	135	10	127.0	27.6



From Eq. (1)

$$\begin{aligned}\frac{p(\text{col})}{A \Delta t} &= \frac{N\bar{V}_R}{V_{\text{TOR}}} \\ &= N\bar{V}_R / 2\pi^2 R(\bar{R}_{\text{MIN}})^2 \\ &= I_h / 2\pi^2\end{aligned}$$

where the "collision hazard index"

$$I_h = N\bar{V}_R / R(\bar{R}_{\text{MIN}})^2 \quad (4)$$

is plotted in Fig. 6 as a function of altitude and inclination of the mission orbit.

B. Collision Hazards

As an example of the collision hazards in low altitude orbits, the collision hazard for typical Shuttle missions has been examined via the on-orbit sampling method. A 278 km altitude circular orbit was assumed at 28.5°, 57° and 98° inclinations.

A set of NORAD catalog objects whose perigee and apogees bracket the Shuttle orbit was selected to determine the number and distribution of close approaches for a typical mission. The results are summarized in Table 2 for three different inclinations of the Shuttle orbit. The results reveal that the total number of encounters N_T within 200 km range increases as the inclination increases, the average miss distance \bar{R}_{MIN} is of the order of 145 km, and the average relative velocity is about 11 km/sec. It can be seen that there are generally more encounters than objects (element sets) indicating that some objects are encountered more than once during the mission.

The normalized relative frequency distribution of encounters for the 28.5 deg inclined orbit is shown in Fig. 7. It can be seen that the relative frequency distribution $f(r)$ can be approximated by a straight line.



Table 2. Shuttle Encounters Within 200 km of NORAD
Catalog Objects at 278 km Altitude

Shuttle inclination i (deg)	Two Days			Four Days		
	28.5°	57°	98°	28.5°	57°	98°
N_T	35	44	56	67	79	108
\bar{R}_{MIN} (km)	138	150	145	142	146	147
\bar{V}_{REL} (km/sec)	9.37	10.7	12.5	9.45	10.8	12.4
EL Sets Used	33	35	37	46	47	50

Based on geometric considerations, the probability that the shuttle with an effective collision radius R_S will be hit at an encounter is

$$p(\text{col}) = \int_0^{R_S} f(r) dr. \quad (5)$$

Since

$$\int_0^{R_{MAX}} f(r) dr = 1 \quad (6)$$

and from Fig. 7 the probability density function is

$$f(r) = CR_{MIN} \quad (7)$$

where $r = R_{MIN}$, it follows from Eq. (6) and (7) that

$$C = \frac{2}{R_{MAX}^2} \quad (8)$$

Therefore the probability of collision per encounter is

$$p(\text{col}) = 2 \int_0^{R_S} \frac{R_{MIN}}{R_{MAX}^2} dR_{MIN} \\ = \left(\frac{R_S}{R_{MAX}} \right)^2 \quad (9)$$

The probability of collision for the mission is

$$p(\text{col/mission}) = N_T \left(\frac{R_S}{R_{\text{MAX}}} \right)^2 \quad (10)$$

which is equivalent to the probability of impacting a circular area πR_S^2 within a larger circular area πR_{MAX}^2 N_T times during a mission assuming that the probability of impacting the larger area is 1.

For $i = 28.5$ deg, $R_S = 10$ m, $R_{\text{MAX}} = 200$ km, $p(\text{col}/4 \text{ days}) = 0.168 \times 10^{-6}$ or 15.3×10^{-6} per year. The collision hazards for the 57 and 98 deg inclination orbits are increased by the ratio of the number of encounters for these orbits. They are 18.0×10^{-6} and 24.7×10^{-6} per year respectively.

III. Geosynchronous Orbits

A. Population

One of the fastest growing satellite groups is at or in the vicinity of the geosynchronous altitude. At these altitudes active satellites maintain fixed longitudinal positions (within a fraction to several degrees) while inactive spacecraft and debris generally drift around the globe or oscillate about geopotential stable points. A portion of the total geosynchronous population is being tracked by ground stations, while a significant number of smaller objects cannot be seen by radar or optical sensors. A "snapshot" of the geostationary population (those which remained within ± 2 deg of the nominal longitude between 20 September 1981 and 21 January 1982) is illustrated in Fig. 8 and the objects are listed in Table 3. The locations of all other tracked geosynchronous objects on 20 September 1981 whose drift rates varied from 0.1 to 5 deg per day are given in Fig. 9 and the objects listed in Table 4.

B. Distribution of Encounters

Because of the possibility of electromagnetic or physical saturation the geosynchronous orbit (GEO) is a limited resource. For example, nominal position and frequency allocations are governed by the provisions of Radio Regulations of the International Telecommunication Union (ITU) for commu-

Table 3. Geostationary Satellites - NIRAN Catalog for Sept. 1981 to Jan. 1982 (±2° of Nominal Longitude)

1. INTELSAT 7	16. OPS 966	69. NATO 10 OPS 936A
2. INTELSAT 4F2	17. OPS 2112	70. ARDJI
3. OTS-2	40. 12100	71. NATO 10 OPS 936B
4. 1201A	41. WESTAR	72. Marleat A
5. Raduga 6	42. ECA B	73. Gorizont 4
7. RISSO1	43. Elektron 7	74. OPS 9444
8. Gorizont 3	44. Anik 3 (Telesat C)	75. Symphonie A
9. R1019	46. Anik 4	
11. OPS 9436	48. GOES B	
17. Intelsat 4AFO	49. LES 6	
18. OPS 9442	50. ATB 2	
19. OPS 3151	51. 03335	6. GOES 2 ^a
16. Marleat B	52. Anik 1 (Telesat)	10. OPS Elektron 1 ^a
17. OPS 0392	53. NATO 1 OPS 9361	14. Intelsat 3 F3 ^a
18. OPS 3011	54. 12065	20. Raduga 4 ^a
19. 03010	55. OPS 0101	23. Elektron 6 ^a
21. Intelsat 4AF3	56. Westar A	33. SMS C (GOES A) ^a
22. Elektron 5	57. Comstar 1 D2	38. OPS 7404 ^a
24. UNK	58. Comstar 1 D1	39. RCA A ^a
25. 12066 Flotcom-D	59. Westar C	43. NATO 2 OPS ^a
26. OPS 9438	60. Comstar 1 D3	47. LES 6 ^a
27. Intelsat 4FB	61. GOES E	
28. Marleat C	62. 03301	
29. Intelsat 4FA	63. ATB 5	
30. Intelsat 4F2	64. Intelsat 4F3	
31. ATB 1	65. Intelsat 4AF4	
32. OPS 3151 R/B	66. Intelsat V F1	
33. OPS 9441	67. OPS 0393	
34. GOES D	68. Intelsat 4A F2	

^a±1.5° of Nominal Longitude

Table 4. Listing of Drifting Geosynchronous Satellites (Sept 1981 to Jan 1982)

D° < 0.1	0.1 < D ≤ 1.0	1 < D ≤ 3	3 < D
1. Meteorat	2. OTS 2	1. 03306	8. Symphonie B
14. Cosmos 775	7. Raduga 1 R/B	4. Elektron 2 R/B	10. Elektron 4 R/B
	9. Molniya 15		
40. Raduga 5	10. Palapa B	5. 03015	26. Elektron 4
44. BEE	20. UNK	6. 03306	28. OPS 9431-2 R/B
46. CS	23. Gorizont	11. Elektron 6 R/B	29. OPS 9431 9432 R/B
54. GMS	24. Elektron 4	12. 03030	31. 11200 ECS 6 RR
57. OPS 9437	27. Raduga 7	13. Gorizont 3 R/B	34. 03599
60. 12077	30. UNK	15. OPS 0157 R/B	35. OPS 9441-2 R/B
69. 03530	31. 00313	17. ECS B	36. 03292
91. OPS 9431	32. UNK	18. 12097	39. 10CSP 20-27 R/B
93. 03502	36. Elektron 3	19. Cosmos 037	43. UNK
97. 03586	45. 12345	21. Raduga 8	49. UNK
101. UNK	47. UNK	22. OPS 2112 R/B	52. LES 0,9/SOL 11A, R R/B
106. 03017	48. Palapa A	25. 03125	59. OPS 5900
111. 03595	50. Gorizont 2	37. ATB V R/B	61. 03571
113. Raduga 1	51. 03372	41. Translage	62. SMS A
114. 12130	53. Skytel 20 OPS 9350	42. LES A R/B	63. Raduga 6 RB
122. Intelsat 1F1	56. ETS 2	34. Elektron	64. O-B 9367 (10CSP 20)
125. NATO 10 OPS 9365	60. OPS 3105 R/B	55. UNK Lost	66. OPS 9326 (10CSP 13)
131. Intelsat 4A F1	72. Intelsat 4F5	65. 12055	67. Gorizont 4 R/B
139. Intelsat 4 F1	75. UNK	69. COSMOS 037 R/B	73. 04470
	77. Raduga 2	73. OPS 1570	76. OPS 9443/9444 R/B
	81. OPS 9433	71. 04277	82. OPS 9433/9434 R/B
	84. UNK	74. Elektron 1 R/B	83. 04976
	85. OPS 9432	76. Elektron 2	104. 03574
	87. GOES C	79. Gorizont 1 R/B	110. 03503
	88. RISSO1	80. OPS 3011 R/B	116. Raduga 3 RB
	93. LES 6	86. OPS 7404 R/B	115. OPS 9437/9438 R/B
	100. UNK	91. 042-5	117. 03222
	102. Strela	92. UNK Lost	118. 10CSP 1-7 R/B
	103. UNK	94. OPS 1570 OPS	119. 03509
	105. Cosmos 775 R/B	96. OPS 1570 R/B	121. ECS
	107. Anik 7	98. 12171	126. OPS 5901 R/B
	108. 12035	99. 03053	128. Elektron 1-2 R/B
	109. OTS A	112. Skytel A	129. Intelsat 3 FA
	116. SMS B	127. 00133	130. Elektron 2
	123. 116	131. Seatho	132. OPS 2
	140. 03011	131. OPS 0157	134. 0360A
	142. 12009	136. 03107	135. 10CSP 14-19 R/B
			137. Raduga 4 R/B
			138. Raduga 4 R/B
			141. Raduga 7 R/B
			143. ATB 1

D = drift rate (deg/day)

nication satellites. The actual longitudinal positions of such satellites are generally maintained within ± 1 deg of the nominal position. Several different satellites may, however, share the same general longitudinal location which can result in periodic encounters between spacecraft or between spacecraft and various debris objects. A procedure recently developed by a U.S. government agency (AFSCF) monitors all close approaches between a set of primary communication satellites and all other objects that may come within 300 km of these satellites. A prediction is made for all close approaches every seven days based on numerical integration of appropriate orbits. Appropriate user agencies are alerted at 50 km separation and increased tracking is initiated at 20 km separation. A collision avoidance maneuver is considered at 5 to 8 km separation and is implemented if near simultaneous tracking of both objects one to two days before encounter (closest approach) verifies that the predicted positions of the satellites are accurate. However, a major uncertainty in this procedure is the orbit determination error resulting from inadequate tracking opportunities or other causes. For certain objects the position error can be equal to or greater than the predicted miss distance.

A sample of geosynchronous orbit encounters for 21 satellites, for example, over a period of six months (from July through December 1981) showed that there were 120 predicted encounters within a range of 50 km. The mean distance of closest approach was 20.68 km with a standard deviation of 13 km. Several close approach predictions were in the 1-5 km range which have caused a number of collision avoidance maneuvers to be made.

Table 5, for example, shows a distribution of closest approaches for the four geosynchronous satellites with the largest number of encounters over a period of six months. It can be seen that several encounters can occur repeatedly if the satellites remain in close proximity to each other over a period of time. The distribution of the encounters for the four satellites is shown in Fig. 10. A sample of predicted geosynchronous orbit encounters for a satellite located at 240°E longitude is illustrated in Fig. 11. Typical mean relative velocities at encounter are shown in Fig. 12 for satellites at 0° and 240° east longitude as a function of orbital inclination.

Table 5. Predicted Worst Case Encounters for Four Geosynchronous Satellites

Sat. #1	Sat. #2	MIN (km)	Date	Satellite Time (GMT)
10669/ 6391 (100°W)	12065/SBS-A	2.6	23 Jul 81	2305
	12065/SBS-A	4.2	29 Jul 81	2220
	12065/SBS-A	5.6	02 Aug 81	0952
	12065/SBS-A	4.0	03 Aug 81	0943
	3431/LES 6	45	31 Aug 81	1032
	10953/GOES-C	31	16 Nov 81	0501
	8585/CTS-A	48	23 Nov 81	1849
	4353/NATO 1	28	13 Dec 81	0413
	12065/SBS-A	6	19 Dec 81	2341
	12065/SBS-A	17.9	22 Dec 81	2257
	12065/SBS-A	14	25 Dec 81	2302
	12065/SBS-A	8.5	27 Dec 81	2306
	4353/NATO 1	5.2	04 Jan 82	0248
	10001/ 9438 (175°E)	1940/RB	36	11 Jul 81
7544/INTELSAT 4-F8		15	14 Sep 81	0911
80277/UNKNOWN		14	22 Sep 82	1508
11436/RB		36	14 Oct 81	0629
11684/RB		26	21 Oct 81	0512
9478/MARISAT-C		2.9	02 Nov 81	2346
9478/MARISAT-C		10.3	03 Nov 81	2346
8978/MARISAT-C		5.8	07 Nov 81	2326
9478/MARISAT-C		3.7	07 Nov 81	2346
6796/INTELSAT 4-F7		4.0	18 Dec 81	1350
7544/INTELSAT 4-F8		2.0	09 Jan 82	0029
8916/ 2112 (130°W)	9885/RB	30	06 Jul 81	1717
	12309/COMSTAR	6.9	31 Jul 81	1648
	12309/COMSTAR	6.4	01 Aug 81	1611
	11621/9443	13.5	23 Aug 81	1532
	8476/RCA-SATCOM-1	19	05 Sep 81	1437
	8476/RCA-SATCOM	46	02 Sep 81	1452
	11621/9443	14	17 Sep 81	0158
	11621/9443	14	18 Sep 81	0153
	8366/GOES-A	2.8	19 Dec 81	0843
	8366/GOES-A	13	20 Nov 81	0844
	9785/ 9364 (20°W)	12089/INTELSAT	7.7	30 Jul 81
12089/INTELSAT		6.3	30 Jul 81	1929
12089/INTELSAT-VF-2		3.7	22 Aug 81	1822
12089/INTELSAT-VF-2		8	24 Aug 81	0618
11669/6393		36	20 Sep 81	2113
11669/6393		33	26 Sep 81	2101
11669/6393		26	06 Oct 81	2073
5854/RB		41	13 Nov 81	1333

C. Collision Hazard

Frequency of encounters was computed for a number of geosynchronous orbit communication satellites (comsats) as shown in Table 6. - The results were obtained by numerical simulation of predicted encounters within 500 km of each satellite for a period of 30 days. The total number of such occurrences varied from 160 to 1. The mean miss distance and relative velocity for all encounters was also calculated. The encounter frequency, N_T , differs by about two orders of magnitude depending on the longitudinal location of the primary satellite. Least hazardous orbits may thus be determined by evaluating N_T as a function of the orbital parameters of interest.

The worst case probability of collision for satellites in Table 5 was computed using the formula

$$p(\text{col})_{\text{max}} = \frac{4N_T}{\pi e} \left(\frac{R_S}{\bar{R}_{\text{MIN}}} \right)^2$$

where N_T is the number of encounters within a given mean miss distance \bar{R}_{MIN} , and R_S is the effective collision radius (Ref. 5). Thus, for $R_S = 6.1 \text{ m}$ (20 ft) $p(\text{col})_{\text{max}}$ per 1000 days is on the order of 10^{-5} to 3.5×10^{-5} for the satellites in Table 4 based on the encounters within 10 km of the primary object. This represents an increase of about two orders of magnitude over those for "typical" geosynchronous satellites based on object density averaged over all longitudes as given in Ref. 5. The effects of longitudinal bunching of satellites are thus very significant and should be fully evaluated in assessing the collision hazards for geosynchronous satellites.

IV. Summary and Conclusion

A method of analysis has been described which can be used to determine the collision hazard to satellites from space objects listed in the NORAD catalog. A collision hazard index has been derived which indicates the degree of hazard presented for satellites in low altitude circular orbits at various inclinations to the equator. The results, obtained by simulation, reveal that

Table 6. Frequency of Encounters for Selected Geosynchronous Satellites

Rank	Satellite Number	Satellite Name	(ΔT = 30 Days R _{HAK} = 500 km)		
			N _E	R _{MIN} (km)	V _R (km/sec)
1	6391	FLTSATCOM	100	203.28	0.06
2	9443	DSCS II	102	359.47	0.12
3	6392	FLTSATCOM	77	178.87	0.08
4	6393	FLTSATCOM	76	332.18	0.10
5	9442	DSCS II	74	289.98	0.18
6	9441	DSCS II	28	291.15	0.10
7	9438	DSCS II	27	302.21	0.12
8	6394	FLTSATCOM D	29	313.53	0.13
9	9434	DSCS II	24	279.17	0.09
10	9444	DSCS II	21	351.29	0.10
11	9363	NATO III-A	20	329.42	0.15
12	9364	NATO III-B	16	315.06	0.13
13	9365	NATO III-C	12	347.59	0.24
14	6395	FLTSATCOM V	1	488.69	0.32

the collision hazard increases as the orbit plane inclination increases and is maximum in the 700 to 1300 km altitude range. Relative velocities at encounter are in the 8 to 12 km/sec range.

Collision probabilities with tracked debris for typical four-day Space Shuttle missions were found to be of the order of 10^{-5} per year. Worst case collision probabilities for four geosynchronous satellites were also found to be of the same order of magnitude varying somewhat with the longitudinal location of the satellites. However, concentration (bunching) of satellites at different longitudes was found to affect the collision hazard by as much as two orders of magnitude for other satellites. The results of the study show that the described method of on-orbit sampling can be used effectively to evaluate satellite collision hazards as a function of the orbital parameters and of the longitudinal location for "fixed" or station-kept geosynchronous satellites.

REFERENCES

1. Kessler, P. J., "Sources of Orbital Debris and Projected Environment for Future Spacecraft," J. Spacecraft and Rockets, Vol. 18, No. 4, July-August 1981, p. 397.
2. Hochler, M. and VanderHa, J. C., "Probability of Collisions in the Geostationary Ring," J. Spacecraft and Rockets, Vol. 18, No. 4, July-August 1981, p. 361.
3. Schnal, L. and Pospisilova, L., "Collisions of Artificial Earth Orbiting Bodies," Bull. Astron. Inst. Czechosl., Vol. 32 (1981), pp. 310-315.
4. Chobotov, V. A., "Collision Hazard in Space," Astronautics and Aeronautics Journal, Sept. 1980.
5. Chobotov, V. A., "The Probability of Collision in Space," Paper No. 81-148 presented at the AAS/AIAA Astrodynamics Specialist Conference, Lake Tahoe, Nevada, August 3, 1981.

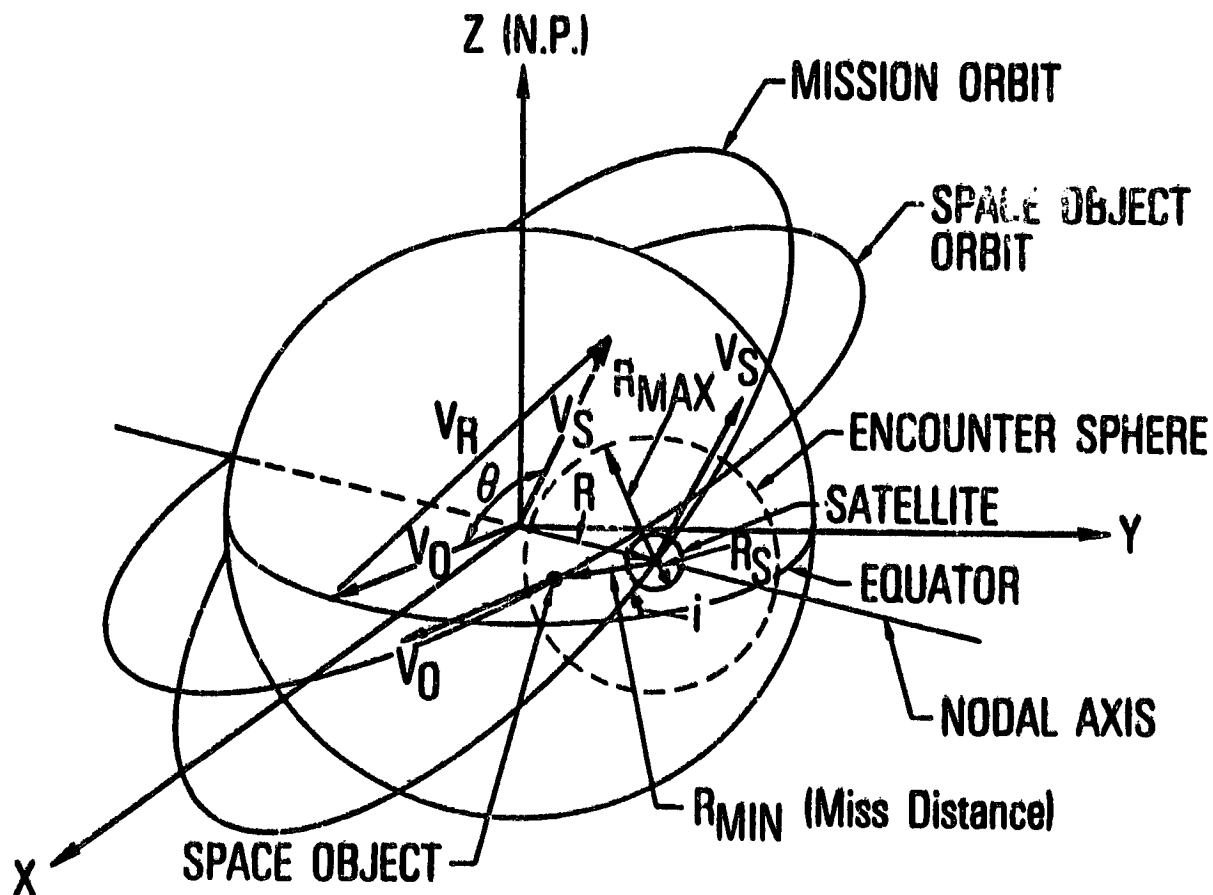


Figure 1. Satellite Encounter Geometry

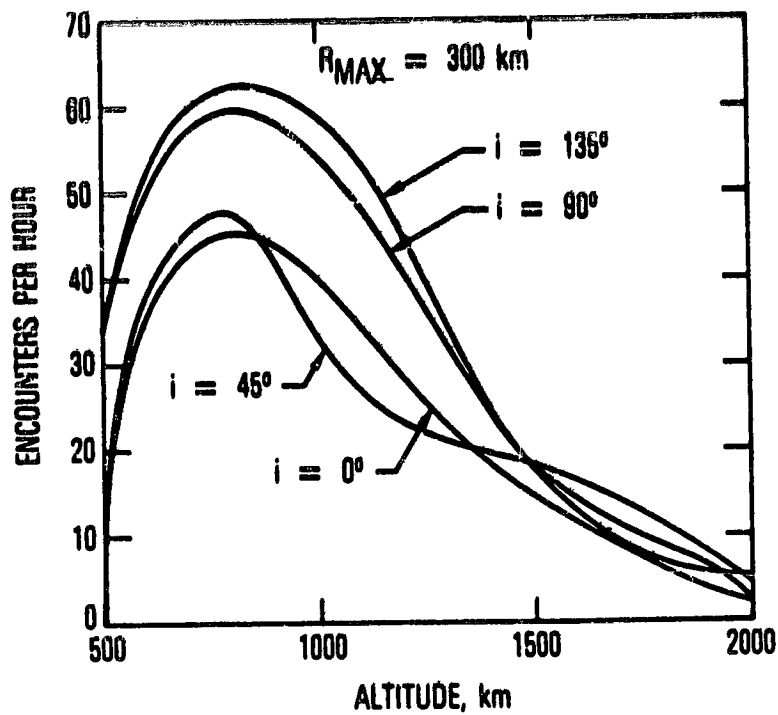


Figure 2. Satellite Encounter Rates

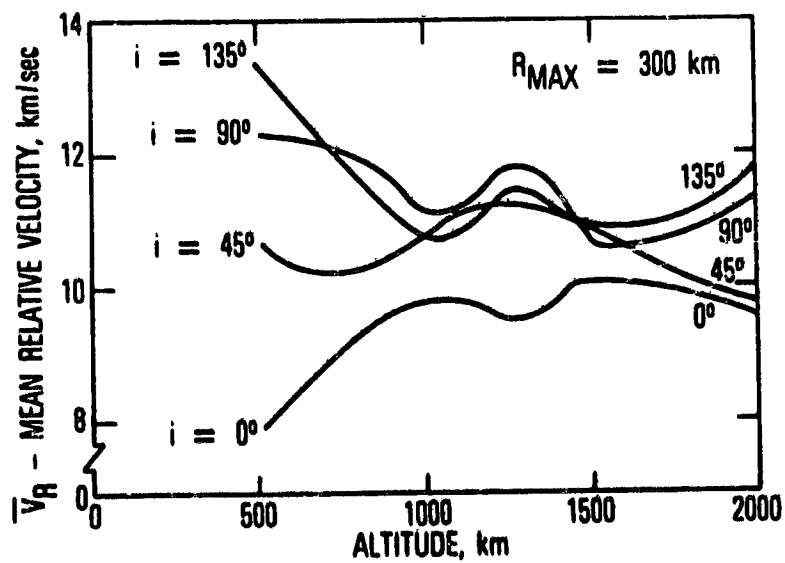


Figure 3. Mean Relative Velocity at Encounter

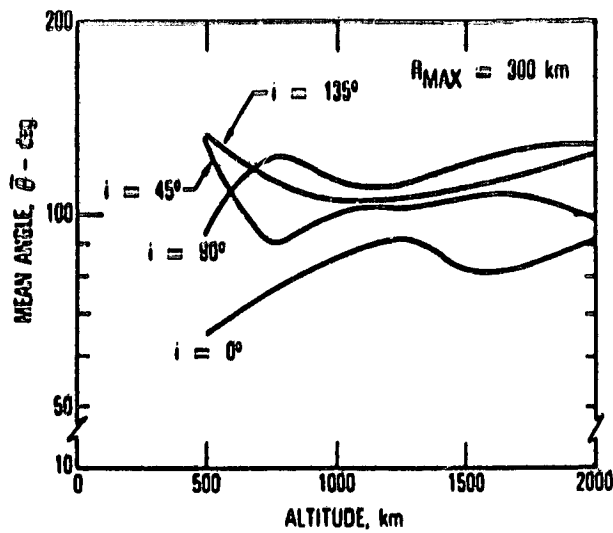


Figure 4. Mean Relative Angle at Encounter For Low Altitude Circular Orbits

N - NUMBER OF CLOSE ENCOUNTERS ($R_{MIN} \leq 300 \text{ km}$) PER REVOLUTION (105.1 min) IN ΔR_{MIN} ALTITUDE BAND
 N_T - TOTAL NUMBER OF CLOSE ENCOUNTERS PER REVOLUTION (3/8) NORAD catalog)

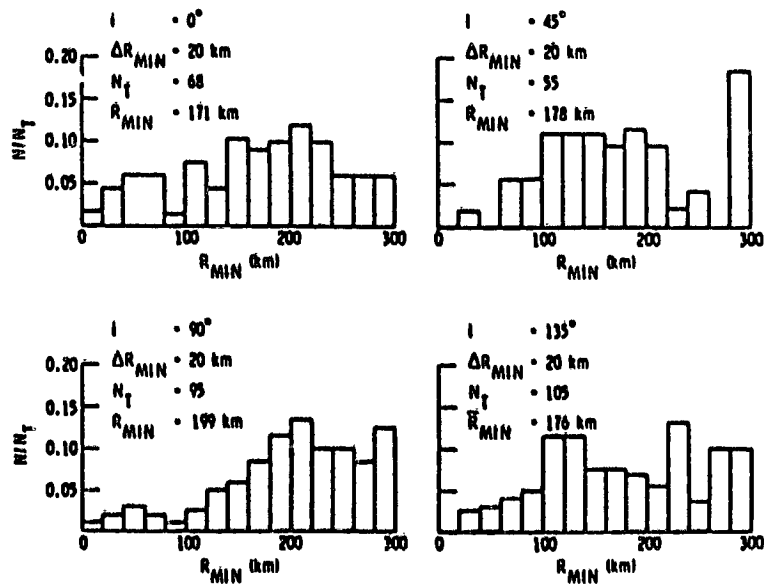


Figure 5. Miss Distance Frequency Distribution for an Object in a 1000 km Circular Orbit

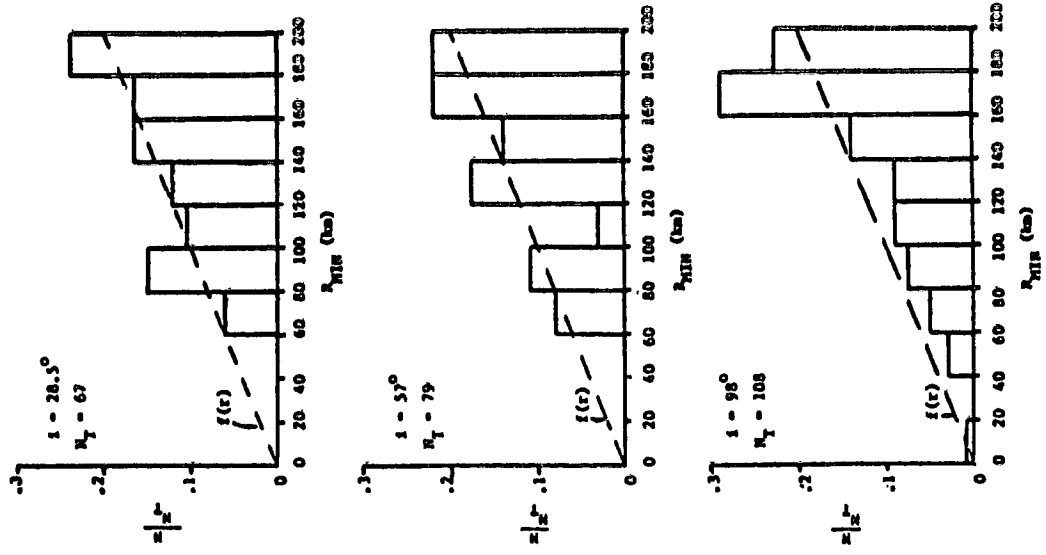


Figure 7. Normalized Frequency Distribution of Encounters for a 4 Day Shuttle Mission

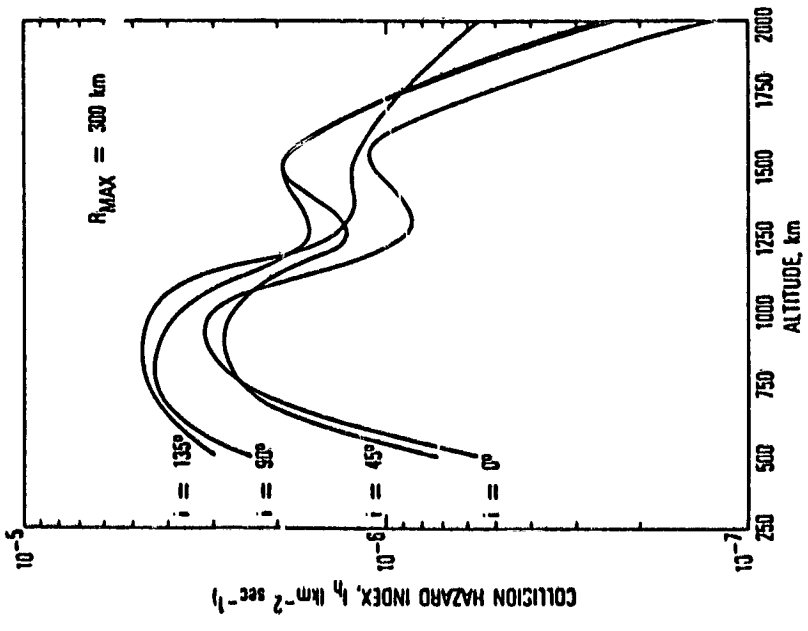


Figure 6. Collision Hazard Index vs Altitude

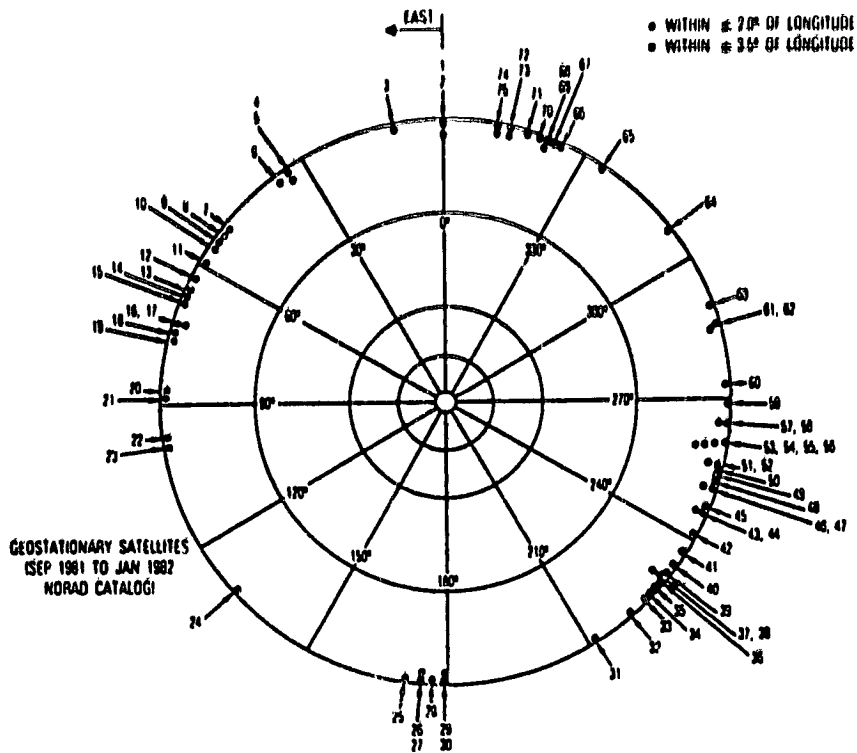


Figure 8. Geostationary Satellites (Sep 1981 to Jan 1982 NORAD Catalog)

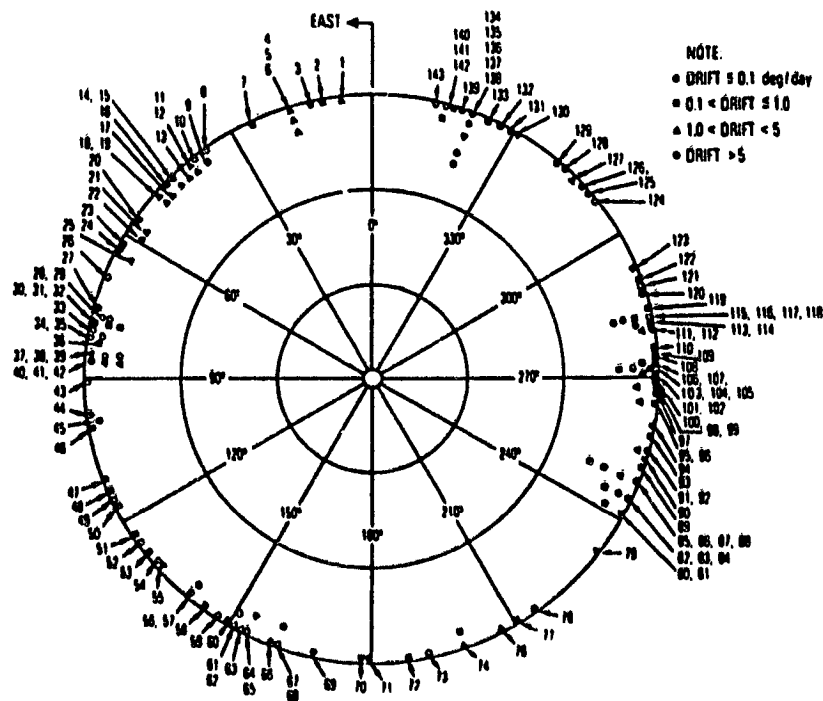
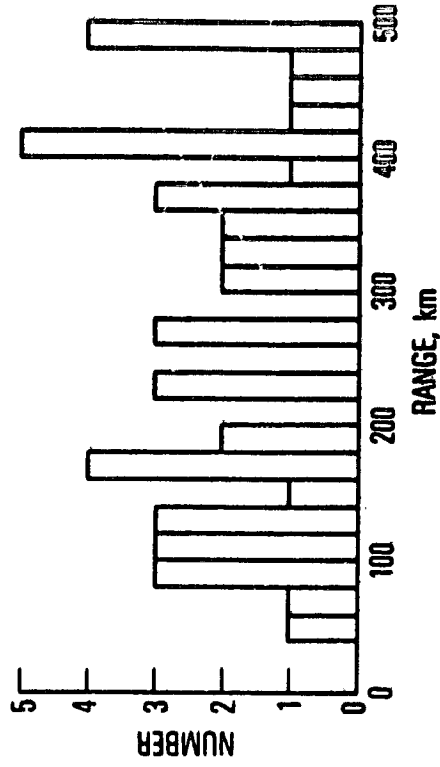


Figure 9. Nonstationary Geosynchronous Satellites (Sep 1981 to Jan 1982 NORAD Catalog)

INCLINATION, $i = 1^\circ$
 TOTAL ENCOUNTERS $N_T = 47$
 MEAN MISS DISTANCE, $\bar{R}_M = 273.17$ km
 MEAN RELATIVE VELOCITY, $\bar{V}_R = 0.15$ km/sec



NOTE:
 $R_{MAX} = 500$ km

$\lambda = 240^\circ$ E

Figure 11. Sample Geosynchronous Frequency Encounter Distribution for 30 Days

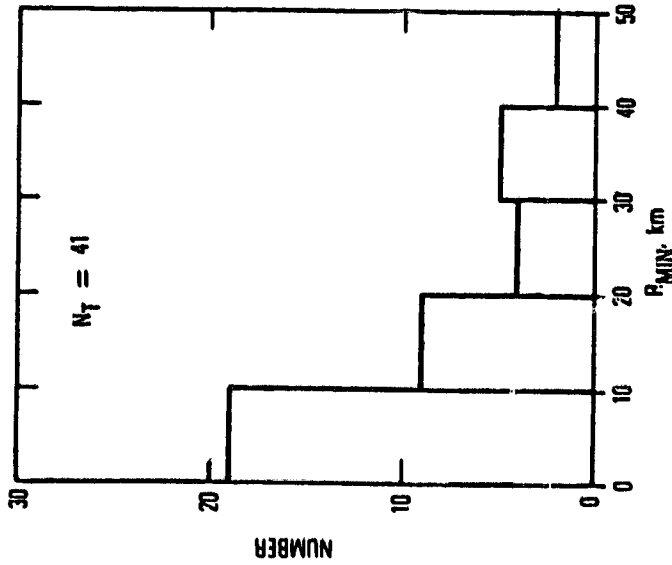


Figure 10. Four Satellite Worst Case Geosynchronous Encounter Frequency Distribution for Six Months (July 1982 to January 1982 NORAD Catalog)

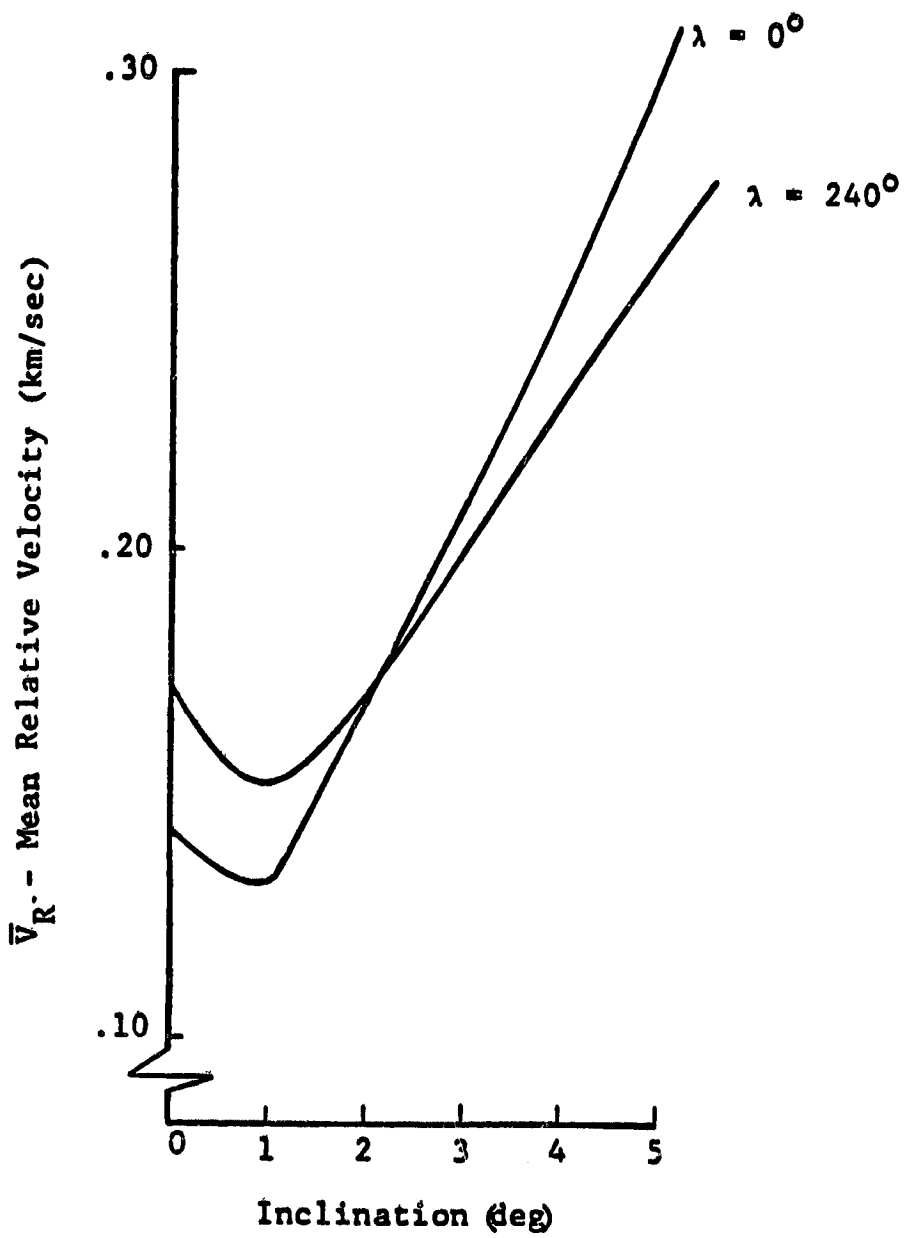


Figure 12. Geosynchronous Relative Velocity

3/12
N 85-21196

A MODEL FOR THE EVOLUTION OF ON-ORBIT
MANMADE DEBRIS ENVIRONMENT

BY

Robert C. Reynolds
Norman H. Fischer
Donald S. Edgcombe

NOMENCLATURE

a	Semi-major axis (cm)
β	Intersection angle between orbital planes
$\langle \beta \rangle$	Expected angle between orbital planes
$\langle \beta_0 \rangle$	Expected angle between velocity vectors of colliding objects
C_D	Drag Coefficient
E	Specific energy of orbit (ergs/gm)
$g(\beta)$	Distribution function for angle of orbital plane intersections
$H(\beta)$	Cumulative distribution function for orbital plane intersections
h	Specific angular momentum (cm ² /sec)
M_E	Mass of Earth (gm)
μ	GM_E
n	Particle number density (cm ⁻³)
r_a	Radius of apogee (cm)
r_p	Radius of perigee (cm)
r_e	Radius of perigee for short lived orbits (re-entry) (cm)
ρ_A	Atmospheric density (gm/cm ³)
S	Particle source term (cm ⁻³ sec ⁻¹)
u	Particle flow velocity (cm/sec)
u_{\perp}	Radial component of flow velocity (cm/sec)
v_r	Radial velocity in Earth-centered coordinates (cm/sec)
v_t	Transverse velocity in Earth-centered coordinates (cm/sec)
v_x	In-plane component of transverse velocity (cm/sec)
v_y	Out of plane component of transverse velocity (cm/sec) ($\hat{e}_{v_y} = \hat{e}_{v_r} \times \hat{e}_{v_x}$)
v_0	Circular velocity ($= \sqrt{\mu/r}$) (cm/sec)
\bar{v}	Center-of-mass velocity (cm/sec)
v_a	Velocity at apogee (cm/sec)
v_p	Velocity at perigee (cm/sec)
V_i	Volume (cm ³)

INTRODUCTION

As is becoming increasingly apparent, there should be serious concern for man-made debris in Low-Earth Orbit (LEO) and the conduct of operations/procedures which leave debris in orbit. Debris deposition is an essentially irreversible act which, under many circumstances, leaves the debris in the environment for many years. Continued deposition therefore increases the population and, with the larger vehicles and longer times on orbit being discussed for LEO operations, the probability of collisions between such vehicles and some member of the debris population becomes large. Because the collisions will occur at very large relative speeds, on the order of 8-12 km/sec,¹ a small object which would not normally be considered a hazard might in fact pose a lethal threat to an operating spacecraft.

One of the factors which has impeded the growth in concern for the problem has been an inability to provide definitive predictions of future population states, a fact which has arisen because future debris deposition events are expected to be significant and the occurrence of such events cannot be predicted with certainty either in time or spatial location. Consequently, future debris states must be deduced from an evaluation of many models using a Monte Carlo model for future deposition events.

In this paper a model for the population evolution will be presented and results of model calculations discussed. Contributions to the population which may be expected to arise from on-orbit collisions and explosions are examined in some detail. Results are presented as models for future space usage as an extrapolation of usage in the past, for an era of enhanced space usage, and for an era in which anti-satellite tests provide a debris contribution.

DISCUSSION

The future state of the man-made debris population must be discussed in probabilistic terms. This arises from two factors: (1) collision occurrences are by necessity probabilistic events, and (2) other future debris deposition events, which include normal operations, intentional debris deposition, anti-satellite tests/operations, and accidental explosions, will also happen in a probabilistic manner. In the latter case, general characteristics of future deposition events can be postulated, based on a knowledge of mission models, perceived trends in antisatellite test programs and the like, but particular information concerning the time, location, and deposition properties of such events cannot be determined before-hand.

Because of this probabilistic character in future debris states, it is essential that an evolution model be conceived which allows a rapid computation of specific future population states, so that appropriate ensemble averages of many of these states can be calculated to produce future population characteristics with a known statistical reliability and attendant statistical uncertainty. A complete evolutionary model will consist of the mathematical formalism required to propagate the required population properties, the definition of the population properties which will be taken to characterize the future state, and the means of evaluating these properties and their uncertainty.

The evolution model presented here provides a satisfactory conceptual basis for producing such an evolutionary model. In its current form, it propagates the number density and a set of debris distribution characteristics sufficient to

account for collision processes. Debris population properties are defined on an Earth-centered spherical Eulerian mesh. Within each cell, collisions are treated as random events whose probability of occurrence is determined by the locally defined collision rate. At each time step the change in the number of particles and the population composition is updated, as required by the debris source and sinks to provide new local conditions and to define the updated collision rates.

A Monte Carlo model for neutron diffusion through a reactor core is a familiar problem. Given that only a single type of neutron encounter interaction is allowed, the debris evolution model is logically equivalent to studying the propagation of an ensemble of N^2 (the number of cells) neutrons whose behavior is coupled and which are moving through a material with properties changing in time. Cell coupling in this problem arises from debris orbit decay from atmospheric drag and from scattering of debris into neighboring cells as a result of collisions and explosions.

Model Characteristics

The debris population is taken to consist of K statistically independent population subsets. The distinguishing characteristic between subsets could be any number of attributes--characteristic size, mean density, or objects from specific interactions. In the current model, characteristic size is the distinguishing feature, and three population subsets are used.

Population subset 1, the largest objects, consist initially of the large objects deposited in orbit during normal operations--spacecraft, spent stages, and separation components, roughly objects of size 1 kg and larger. As the population evolves, large fragments from catastrophic collisions involving these large objects will also fall into this group.

Population subset 2 contains the medium sized objects, those in the 1 gm to 1 kg range. Initially, these objects are identified with the explosion fragments from observed accidental explosions, but as the population evolves, both collision and explosions will contribute to this subset.

Population subset 3 contains the smallest of the objects presenting a significant hazard to spacecraft--those in the mass range of 10^{-3} gm to 1 gm. These objects are too small to be tracked from the ground and this subset is taken to be empty initially.

All debris is taken to be of spherical objects. Collision and explosion fragments conserve volume and the fragments populating a given subset are taken to be of the same size. In each cell, the number of objects and their mean radius, \bar{r} , mean square radius \bar{r}^2 , and mean inverse radius, \bar{r}^{-1} , are explicitly transported and therefore conserved. The rationale for selecting \bar{r} , \bar{r}^2 , and \bar{r}^{-1} will emerge in the following discussion.

Particle Transport

The conservation equation being considered in the present model is conservation of particle number, which is expressed as:

$$\frac{\partial n}{\partial t} + \nabla \cdot n\vec{u} = \beta \quad (1)$$

For the one dimensional spherical problem

$$\nabla \cdot n\vec{u} = \frac{1}{r^2} \frac{\partial}{\partial r} (r^2 n u_r) = \frac{\partial}{\partial V} (Anu_r) \quad (2)$$

where

$$V = 4\pi r^2 \partial r = \text{the volume differential}$$

$$A = 4\pi r^2 = \text{cell interface area}$$

Equation 1 with the form of the divergence in Eq. 2 can be translated into a difference equation for number of objects in the cell

$$\frac{\Delta_t n}{\Delta t} + \frac{\Delta_s (Anu_r)}{\Delta V} = \beta \quad (3)$$

where

$$\Delta_t = \text{time difference}$$

$$\Delta_s = \text{space difference}$$

$$(\Delta_t n)\Delta V + (\Delta_s (Anu_r)) \Delta t = \beta \Delta V \Delta t = \beta \quad (4)$$

For an Eulerian coordinate system

$$(\Delta_t n)\Delta V = \Delta_t N$$

where

$$N = n\Delta V = \text{number of objects in volume } \Delta V$$

The divergence term differences to

$$\Delta_s (Anu_r) \Delta t = (A_{j+1} u_{j+1}^{j+1} n_{j+1} - A_j u_j^j n_j) \Delta t \quad (5)$$

where

j refers to the lower boundary of the cell

j + 1 refers to the upper boundary of the cell

The expression $\beta = \beta \Delta V \Delta t$ is the number of objects deposited in (or removed from) the cell during the time interval Δt .

The divergence expression was defined to make the differencing explicit so that Eq. 1 finally differenced to

$$N_{t_k} = N_{t_{k-1}} + \left(A_{j+1} u_{\perp}^{j+1}, t_{k-1/2} n_{t_{k-1}}^{j+1} - A_j u_{\perp}^j, t_{k-1/2} n_{t_{k-1}}^j \right) \Delta t + \delta_{t_{k-1}} \quad (6)$$

where

$$\Delta t = t_k - t_{k-1}$$

To avoid having time step limitations imposed by debris infall rates, a pseudo-Lagrangian updating scheme is used to allow transport across more than a single cell in a single time step.

The distribution means are updated in a manner which is most easily expressed by viewing Eq. 6 as an operator equation of form.

$$N_{t_k} = \mathcal{O} \quad (7)$$

so that for transporting a quantity

$$N_{t_k} \xi_j = \mathcal{O}(\xi_j, \xi_{j+1}) \quad (8)$$

where

$\xi = r, r^2,$ and $1/r$ to update $\bar{r}, \bar{r}^2,$ and \bar{r}^{-1} , respectively. That is

$$\bar{\xi}_j = \mathcal{O}(\xi_j, \xi_{j+1}) / N_{t_k} \quad (9)$$

Particle Infall via Atmospheric Drag (\bar{r}^{-1})

The rate at which an object in circular orbit experiences a loss of altitude as a result of energy loss from atmospheric drag is given by

$$u_{\perp} = \frac{1}{4} \mu^{1/2} (R_E + h)^{1/2} \rho_A \frac{C_D A}{M} \quad (10)$$

where

A = particle area
M = particle mass

For spherical particles of uniform density, ρ_p , and radius r,

$$\frac{A}{M} = \frac{3}{\rho_p r} \quad (11)$$

Each of the population subsets is characterized by a ρ_i ; in each cell the quantity of $r^{=1}$ is updated and the proper inflall velocity for each population subset in each cell is defined to be

$$\bar{A} = \frac{\int r^{=1}}{\rho_p} \quad (12)$$

The atmospheric density, ρ_A , has both an altitude and a time dependence. The standard NASA atmosphere model² is used. Time dependence in the atmosphere is modelled as an exoatmospheric temperature range which varies sinusoidally with the sunset cycle. The minimum and maximum temperature and the phase in the cycle at the beginning of the model calculation are input quantities.

The drag coefficient, C_D , is taken to be 2 throughout the altitude range.

The Collision Model (\bar{V} , r^2)

The probability that a collision occurs in cell i in a time τ is given by

$$P_c(\tau) = 1 - e^{-C_R^i \tau} \quad (13)$$

where C_R^i , the collision rate in cell i , is taken to be constant during the time interval. There are two types of collisions that can occur--collisions between members of the same population subset (self-interactions) and collisions involving objects from different population subsets (coupling interactions). The expression for C_R for self-interactions is

$$C_{R, KK}^i = \frac{1}{2} n_K^2 v_{R, KK} \sigma_{KK} v_i \quad (14)$$

where K is the identifier for the subgroup. For coupling interactions

$$C_{R, KK'}^i = n_K n_{K'} v_{R, KK'} \sigma_{KK'} v_i \quad (15)$$

where

K and K' are population identifiers for the subgroups involved.

The expressions for the collision cross-section are easily derived. For self interactions in a population of N_K spherical objects, the mean collision cross-section is given exactly by

$$\begin{aligned} N_K (N_K - 1) \sigma_{KK} &= \sum_{i=1}^{N_K} \sum_{j \neq i}^{N_K} \pi (r_i + r_j)^2 \\ &= \pi \left\{ (N_K - 1) \sum_i r_i^2 + 2 \sum_i r_i \sum_{j \neq i} r_j \right. \\ &\quad \left. N_K \sum_{j \neq i} r_j^2 \right\} \\ &= \pi N_K (N_K - 1) \left\{ \overline{r_K^2} + 2 \overline{r_K}^2 + \overline{r_K^2} \right\} \end{aligned} \quad (16)$$

or

$$a_{KK} = 2\pi \left(\overline{r_K^2} + \overline{r_K}^2 \right) \quad (17)$$

For coupled interactions with populations of size N_K and $N_{K'}$

$$\begin{aligned} N_K N_{K'} a_{KK'} &= \sum_{i=1}^{N_K} \sum_{j=1}^{N_{K'}} \pi (r_i + r_j)^2 \\ &= \pi \left\{ N_K N_{K'} \overline{r_K^2} + 2N_K N_{K'} \overline{r_K} \overline{r_{K'}} + N_K N_{K'} \overline{r_{K'}}^2 \right\} \end{aligned} \quad (18)$$

or

$$a_{KK'} = \pi \left\{ \overline{r_K^2} + \overline{r_{K'}}^2 + 2 \overline{r_K} \overline{r_{K'}} \right\} \quad (19)$$

Collision Rules

The rules used to describe the consequences of a collision are provided to the model as described in the discussion of debris sources. An improvement in the rules or a definition of different rules can be made with minimal impact on the existing software.

Debris Sources

Future LEO debris states may be critically dependent on future debris deposition events. There are several reasons for this. First, the large intersection speeds of objects populating these orbits makes even very small objects present a serious threat and the debris hazard therefore becomes driven by the number of objects in orbit, rather than the mass of debris in orbit. Second, collisions and explosions are events which might generate order of magnitude more objects in a single event than is believed to presently reside in orbit, so that the occurrence of a few events could dramatically alter the severity of the problem. Third, once the debris is in the environment it is virtually impossible to remove; hence uncontrollable sources such as collisions may make the problem unmanageable once they begin occurring.

To place the discussion of debris sources in perspective, NORAD is currently tracking about 5000 objects, some of which are at low altitude, some at geosynchronous altitudes. Roughly 40 percent of these are spacecraft, spent stages, and other objects; about 60 percent are fragments resulting from explosions.

Normal Operations

Normal operations will leave operating satellites in orbit along with separation components associated with staging operations and spent stages. Uncertainties in the future rate of deposition by this source revolve around uncertainties in launch times and launch rates, lack of information on mission models for Soviet and U.S. DoD space operations, and uncertainty in the debris items released during staging. Viewed on an individual basis, normal operations do not appear to be a significant source, but the combined effect of many launches/deployments may contribute significantly to the population of large objects.

NASA pre-launch reports of objects being injected into orbit during launch of expendable vehicles generally indicate 6 or fewer objects large enough to be seen by NORAD should be released. Although there is some scatter in the number of objects seen versus the number of objects predicted, it will be seen that in an era of heavy space usage control of debris released during normal operations may prove to be necessary.

Intentional Deposition on Orbit

Intentional deposition and dispersal of debris, as well as explosive ejection of debris, has occurred in the littering of space by the Soviet Soyuz program³, the dispersal of bundles of copper dipole rods by the U.S., and the conduct of the Soviet ASAT test program. The number of objects dispersed by these sources varies, but the occurrence of a single ASAT test injecting debris into long-lived orbits would dramatically increase the hazard to all spacecraft in LEO; certainly this is the most serious of the controllable debris sources.

Clearly, the conduct of operations involving intentional debris deposition without a clear understanding of the long-term consequences is extremely ill-advised. The debris will not only present an immediate hazard to other spacecraft, but the fragments produced by collisions involving this debris will present a threat which may, in fact, be considerably greater.

Collisions

Collisions between objects on orbit represent an uncontrollable debris source which might prove extremely important for future debris population states, as single collision event will produce millions of debris objects.⁴ Although most of these objects will be too small to pose a collision threat to other spacecraft, several thousand to several tens of thousands might be sufficiently large to pose such a threat.

In his discussion of collisions, Kessler⁵ divides collision events into catastrophic events, those leading to breakup of the larger object involved in the collision, and non-catastrophic events, those not resulting in breakup of the larger object. The mass ratio of the colliding objects determines the types of collision for hypervelocity impact and Kessler finds a minimum mass ratio of 1:115 to lead to non-catastrophic collisions. In this work we identified coupling collision events as non-catastrophic and self-interaction collisions as catastrophic.

Non-catastrophic collisions have been mentioned previously as coupling collisions, that is collisions between different population subsets. For this type of collision there is some experimental data⁴ and the dynamics of the debris

presents minimal problems--the center-of-mass velocity is essentially the velocity of the larger object. The debris velocities relative to the center of mass will be small (<100 m/sec) so that the debris will have essentially the same orbital properties as the larger craft.

In terms of the model parameters, there will be three types of non-catastrophic collisions, those involving class 1 with class 2 objects (type (2,1)), those involving class 1 with class 3 objects (type (3,1)), and those involving class 2 with class 3 objects (type (3,2)). From the data in Bess,⁴ the largest fragments fall into the size class of the smaller impacting object, with the mass distribution of smaller objects following a power law relationship into the microgram region.

A partitioning of fragments consistent with the two experiments discussed in Bess would place 50 fragments in the class of the smaller impacting particle and 2000 fragments into the class of next smaller particles, a distribution shown in Table 1. The larger impacting object remains intact. The size distribution of fragments were modelled as the mean radius size for the larger class and one-tenth that size for the smaller class.

Since the debris velocities relative to the velocity of the larger colliding object are small, all collision fragments were taken to remain in the altitude band in which the collision occurred.

TABLE 1. FRAGMENT SIZE DISTRIBUTION FOR COUPLING COLLISIONS

Type of Collision	Number of Class 2 Fragments	Number of Class 3 Fragments
(2,1)	50	2000
(3,1)	--	50
(3,2)	--	50

Catastrophic collisions, discussed previously as self-interaction collisions, are much more problematic. In part this is because there is no experimental data for hypervelocity collisions between comparably sized objects so existent data must be extrapolated. Moreover, the motion of the center of mass is not that of the larger object and the geometry of the interaction becomes important in determining the types of orbits populated by the fragments. A formalism to analyze this problem is presented in the appendix. One similarity with the non-catastrophic collisions is that the debris fragments should have a sufficiently small velocity relative to the center-of-mass to remain in orbit only if the center-of-mass velocity is orbital, and whether this occurs depends on the angle of impact, altitude of collision, and mass ratio, as shown in Table A-1 of the appendix.

One important requirement in modeling catastrophic collisions is obviously whether the center of mass is orbital or suborbital for a particular event. This is determined in part by the angle of impact of the colliding objects. Chobotov¹ has studied this problem for the objects in the NORAD catalog and finds a typical collision angle of 100° for 3 non-zero inclination orbits. His analysis is presented in his Figure 4. In the analysis in the appendix, a similar conclusion

is reached for debris populating random orbital planes with 70° inclination. If the assumption is made that the distribution of collision angles can be deduced from this same 70° population, then a mechanism for calculating the collision angle of a particular event, using a Monte Carlo approach, is available.

As shown in the appendix, the distribution function, $g(\beta)$, is

$$g(\beta) = \frac{1}{\pi} \frac{\sin \beta}{\sqrt{\sin^4 70^\circ - (\cos \beta - \cos^2 70^\circ)^2}} \quad 0 \leq \beta \leq 140^\circ \quad (20)$$

for inclination 70° . Although $g(0)$ is undefined, it has a well-defined limit of $1/(\pi \sin 70^\circ)$; g also has a pole at $\beta = 140^\circ$.

The cumulative distribution function for collision angle is

$$H(\beta_c) = \frac{\int_0^{\beta_c} \sin(\beta/2) g(\beta) d\beta}{\int_0^{140^\circ} \sin(\beta/2) g(\beta) d\beta} \quad 0 \leq \beta_c \leq 140^\circ \quad (21)$$

The integral is analytic and the form for H is

$$H(\beta_c) = 1 - \sqrt{1 - \left(\frac{\sin(\beta_c/2)}{\sin 70^\circ}\right)^2} \quad 0 \leq \beta_c \leq 140^\circ \quad (22)$$

A Monte Carlo determination of β_c is made by treating H as a probability density function and, picking a random variable p on the interval $(0,1)$, solving

$$p = H(\beta_c) \quad (23)$$

for β_c . This becomes

$$\beta_c = 2 \sin^{-1} \left(\sin 70^\circ \sqrt{1 - (1 - p)^2} \right) \quad (24)$$

With β_c determined by Eq. 24, the decision on re-entry depends upon the mass ratio of the colliding objects. For a mass distribution in the debris population of $\psi(m)$, an expression for the expected value of the mass ratio, $\left\langle \frac{m_1}{m_2} \right\rangle$, is

$$\left\langle \frac{m_1}{m_2} \right\rangle = \frac{\int_{M_a}^{M_b} \psi(m) dm \int_0^{M_b} \psi(m') \left(\frac{m}{m'} \right) dm'}{\int_{M_a}^{M_b} \psi(m) dm \int_0^{M_b} \psi(m') dm'} \quad (25)$$

where

M_b = upper limit on the mass interval
 M_a = lower limit on the mass interval.

Having carried the discussion to this point, there are now 2 reasons for discussing type (1,1) collisions as distinct from types (2,2) and (3,3) collisions. First, the mass distribution of objects in class 1, objects primarily associated with normal operations, would be expected to be considerably different from that in classes 2 and 3. Second, the fragmentation process in a type (1,1) collision might be expected to be significantly different than in the other 2 cases.

For the class 1 population, a distribution function which is a constant does not seem unreasonable. For this case, the expectation value for the mass ratio takes on a particularly simple form

$$\left\langle \frac{m_1}{m_2} \right\rangle = \frac{M_b^2 \left[\frac{1}{2} - \frac{M_a^2}{M_b^2} \left(\frac{1}{2} - \ln \frac{M_a}{M_b} \right) \right]}{(M_b - M_a)^2} \quad (26)$$

which for $M_b \gg M_a$ simplifies to

$$\left\langle \frac{m_1}{m_2} \right\rangle = \frac{1}{2} \quad (27)$$

For this mass ratio, the impact angle which separates the orbital debris generation events from the non-orbital can be determined. Using the formalism developed in the appendix, the critical angle is presented in Table 2 as $\beta_{MAX}^{0.5}$, $H(\beta_{MAX}^{0.5})$, is also given.

For the class 2 and class 3 self-interactions, a power law form for ψ is more appropriate than the constant function of the class 1 objects. For the power law mass spectrum, the form for the expectation value of the mass ratio is

$$\left\langle \frac{m_1}{m_2} \right\rangle = \frac{\frac{M_b^{2\alpha+2}}{(\alpha+1)(\alpha+2)} + \frac{M_a^{2\alpha+2}}{\alpha(\alpha+1)} - \frac{2M_b M_a^{\alpha+2}}{\alpha(\alpha+2)}}{\left(\frac{M_b^{\alpha+1} - M_a^{\alpha+1}}{\alpha+1} \right)^2} \quad (28)$$

with the special cases $\alpha = 0, -1, -2$ introducing logarithmic forms. For $\alpha < -1$ and $M_D \gg M_A$

$$\left\langle \frac{m_1}{m_2} \right\rangle = \frac{M_D^{2\alpha+2}}{a(a+1)} \cdot \frac{(n+1)^2}{M_A^{2\alpha+2}} = \frac{a+1}{a} \quad (29)$$

If the distribution of class 2 and 3 objects follows that for collisions fragments, $\alpha = -1.8^{4,5}$, and

$$\left\langle \frac{m_1}{m_2} \right\rangle = 0.44 \quad (30)$$

Using the formalism presented in the appendix, the critical angles for this mass ratio are presented in Table 2 as $\beta_{MAX}^{0.44}$, $H(\beta_{MAX}^{0.44})$, is also presented.

TABLE 2. MAXIMUM COLLISION ANGLE FOR WHICH DEBRIS WILL REMAIN IN ORBIT AND THE PROBABILITY THAT THIS ANGLE WILL NOT BE EXCEEDED, FOR MASS RATIOS 0.44 and 0.5 (RE-ENTRY PERIGEE ALTITUDE = 100 KM)

Collision Altitude (km)	$\beta_{MAX}^{0.44}$	$H(\beta_{MAX}^{0.44})$	$\beta_{MAX}^{0.50}$	$H(\beta_{MAX}^{0.50})$
100	0.0	0.0	0.0	0.0
300	15.4	.010	15.0	.010
500	21.7	.020	21.1	.019
700	26.4	.030	25.8	.029
800	28.5	.035	27.8	.033
900	30.3	.040	29.6	.038
1000	32.1	.044	31.4	.042
1100	33.8	.049	33.0	.047
1200	35.4	.054	34.5	.051
1300	36.8	.058	36.0	.056
1500	39.6	.067	38.7	.064
2000	45.7	.089	44.6	.085
2500	50.8	.110	49.6	.105
3000	55.3	.130	54.0	.124
3500	59.3	.150	57.8	.143
4000	62.9	.169	61.4	.160

The remaining issue is the number and distribution of collision fragments. There is an important distinction between the type (1,1) collisions and these of type (2,2) or (3,3). The class 1 objects are generally complex, multicomponent structures which might be expected to break up into many relatively large fragments as a result of the severe shock propagated through the structure on impact, as well as a very large number of objects created at the impact site. On the other hand, class 2 and 3 objects will be simple, single component fragments so that the

fragments from a (2,2) collision might be similar to that of a (2,1) collision and a (3,3) collision similar to that of a (3,2) collision.

The distribution of fragments coming out of a type (1,1) collision has not, of course, been experimentally tested. However, such a collision will doubtlessly generate debris falling into classes 1, 2, and 3. A distribution which would appear plausible in extrapolation of the Bess data would place 100 fragments in class 1, 4000 fragments in class 2, and 40,000 fragments in class 3. The distribution of type (2,2) has twice as many class 3 fragments as for a type (2,1) collision; the distribution for the type (3,3) collision is the same as for the (3,1) or (3,2) collisions.

A summary of fragment distributions used in the modeling for self-interactions is presented in Table 3.

TABLE 3. FRAGMENT SIZE DISTRIBUTION FOR SELF-INTERACTION COLLISIONS

Type of Collision	Class 1 Fragments	Class 2 Fragments	Class 3 Fragments
(1,1)	100	4000	40,000
(2,2)	---	50	4,000
(3,3)	---	---	50

For collisions in which the fragments remained orbital, the assumption was made that the fragments populated only the cell in which the collision occurred (50 percent went into this cell) and the adjacent cells (25 percent went into each).

MODELING RESULTS

Initial Debris Population

The objects contained in the October 1976 Satellite Situation Report constitutes the initial debris population. The density of objects as a function of altitude is shown in Figure 1. The reduction of data to yield this density profile is described in Reynolds and Fischer.⁶

The collision hazard which this population presents to various types of spacecraft is shown in Figure 2. As can be seen in this figure, the hazard the population presents to a spacecraft varies considerably over the range of sizes of currently operating spacecraft or projected new space systems.

To provide a comparison of results from the models calculated, a projection of the population with a uniform annual growth rate of 5 percent for 20 years is also presented in Figure 2.

Model Calculations

The model calculations were designed to show the effect of normal operations and accidental explosions on future debris states. The first two cases had normal operations and collisions as debris sources, the first using a 5 percent annual increase in the number of large objects, modeling an extension of future space activity as in the past, and the second a 10 percent annual increase in the large objects, modeling an era of enhanced space activity. The third case combined a contribution from accidental explosions with a 5 percent annual increase in large objects.

Two hundred solutions were averaged for each of the cases. The information that was extracted from the calculations was the population densities as a function altitude, population size and composition, and time, location, and type of collisions.

Case I. Five Percent Annual Growth Rate in Large Objects

This case served as the reference model, providing a prediction of the state to which the debris population will evolve if there is a continuation of past practices and activities and assuming explosions do not play a role.

A comparison of the initial population with the population evolved for 30 years in this model is presented in Figure 3. Of more interest in terms of a hazard analysis is the translation of these debris densities into expected collision frequencies, which are shown for the same altitudes as in Figure 2 and presented for the 10, 20, and 30-year population state in Figures 4, 5, and 6.

The total population size as a function of time is presented in Figure 7. If collisions had not occurred, the size of the population would have been about 8700 at the 30 year point.

In the course of calculating the 200 solutions, 496 collisions occurred. In some solutions, no collisions occurred; one solution had 14 collisions and several had more than 10. Of the 496 collisions, 323 were type (1,1) events, of which 16 left debris in orbit. The first collision occurred in the 16-17 year time frame.

Case II. Ten Percent Annual Growth in Large Objects

This case was designed to present the debris situation in an era of enhanced space activity in which no effort was made to restrict the debris deposited by normal operations. The result differs considerably from Case I, as the increase in density brings collisions in as a dominant source.

The initial and final populations are compared by their altitude distribution in Figure 8, with the same collision hazard charts as Figure 4, 5, and 6 being presented in Figures 9, 10, and 11 for this model. Figure 12 presents the growth in population size as a function of time.

A sample of 100 of the solutions yielded a total of 2,356 collisions, or an expectation of 24 collisions over a 30 year period. The time to first collision was reduced from Case I to about 11 years and by the time 30 years was reached, several collisions per year were often found to occur.

Case III. Five Percent Annual Growth Rate in Large Objects and Accidental Explosions

The final case was run to determine the effect of accidental explosions on the debris population. These events have been observed to happen on a number of occasions, the Delta second stage being one type of space vehicle for which it has occurred several times.

The number of objects associated with an explosion event was taken to be 500, of which 150 were large (class 1) objects and 350 were class 2 objects. These numbers are consistent with the number of observed fragments from the Delta explosions.⁶ The fragments were distributed as half into the cell of the explosion and one-fourth into each of the adjacent cells.

The rate of explosions was arbitrarily set to be 1 explosion per 5000 large objects per year. This led to an average of 18 explosion events over a 30 year time period, a number conservative when compared with observed explosion frequencies.

Over the first 5 years of the calculation, this case had a larger population than either I or II. However, at the 5 year point, the increased deposition of large objects in Case II began to have more effect and with the onset of collisions after the 11 year time, the size of the Case II population began to get much larger.

CONCLUSIONS

A model for the evolution of the manmade debris environment has been developed. Future debris sources will deposit objects on orbit in a non-deterministic manner, so that averages of many solutions for a given case must be taken to provide solutions with significant statistical reliability.

Besides providing a capability for predicting future debris states, the model introduces two important analysis capabilities into the debris problem. First, the sensitivity of future debris states to future deposition events must be determined, and the model will facilitate this process. Second, the effectiveness of practices and procedures to reduce the risk to future systems can be tested and evaluated using the model. Both of these activities will promote the understanding of the debris problem as well as providing insight into the possibilities for keeping it under control.

A method for discriminating between debris injected into short- or long-life orbits has been presented and applied to the problem of collisions. For a plausible set of assumptions on the distribution of debris encounter angles, a probability distribution for debris being left in orbit has been derived for low Earth orbit collisions; about 5 percent of the collisions between large objects will leave debris in long-life orbits.

Three cases were run with the model. Conservative assumptions were made in the debris population (only tracked objects were used) and in the explosion source rate. Hence, the results represent a minimum threat to future space systems. Nevertheless, in all of the cases a severe hazard to large space systems was found in the altitude regime below 1200 km. For the low growth rate model, a 5 percent annual increase in large objects and collisions did not begin until the 16-17 year time frame; a 10 percent annual growth rate reduced this to an 11 year time frame.

APPENDIX

For the purposes of studying debris sources in the debris evolution model, it is important to be able to identify those debris objects which are placed in rapid-decay orbits. To do this, it is useful to study the mapping of orbits of specified radius at perigee (r_p) into local velocity space.

The expression for specific energy of an orbit is

$$2E = v_t^2 + v_r^2 - \frac{2\mu}{r} = -\frac{\mu}{a} \quad (A-1)$$

while the expression for specific angular momentum is

$$h = |\vec{v}_t| r = |\vec{v}_a| r_a = |\vec{v}_p| r_p = \sqrt{\frac{\mu r_a r_p}{a}} \quad (A-2)$$

Therefore

$$v_t^2 r^2 = \frac{\mu r_p (2a - r_p)}{a}$$

so that

$$v_t^2 = \frac{2\mu r_p}{r^2} + \frac{r_p^2}{r^2} \left(v_t^2 + v_r^2 - \frac{2\mu}{r} \right) \quad (A-3)$$

Letting $\alpha = r_p/r$, so that $\alpha \leq 1$, Equation (A-3) takes the form

$$\frac{v_t^2}{A^2} - \frac{v_r^2}{B^2} = 1 \quad (A-4)$$

where

$$K_o^2 = \frac{2\mu\alpha}{r} (1 - \alpha) = 2 v_\oplus^2 \alpha (1 - \alpha)$$

$$A^2 = \frac{K_o^2}{1 - \alpha^2} = 2 v_\oplus^2 \frac{\alpha}{1 + \alpha}$$

$$B^2 = \frac{K_o^2}{\alpha^2} = 2 v_\oplus^2 \frac{(1 - \alpha)}{\alpha}$$

This is the equation for a hyperbola with properties shown in Figure A-1. At a given radius r , the orbits having perigee radius r_p fall on the hyperbola. Orbits with perigee radius less than r_p fall in the shaded area. If r_p is taken to be the radius of the Earth, R_E , the shaded area would contain all orbits which would impact the Earth's surface. In fact, orbits with perigee radii somewhat larger than R_E decay rapidly.

The discussion of orbital properties of deposited debris requires the three-dimensional form of Equation (A-4), which is

$$\frac{v_x^2 + v_y^2}{A^2} - \frac{v_z^2}{B^2} = 1 \quad (A-5)$$

which is the expression for a hyperboloid of revolution about the v_z axis and yields Figure A-2.

At the instant of debris deposition, a debris cloud is created in velocity space. This cloud is characterized by a "centroid velocity", which is the center of mass velocity at the instant of debris deposition, and a distribution of points in velocity space relative to the centroid velocity, which are referred to as peculiar velocities.

The particles in the cloud which lie inside the hyperboloid will have short orbital lifetimes and can be ignored for debris evolution calculations. Those outside the hyperboloid will be long lived and must be accounted for in the evolution model.

Debris deposition might involve a single source object, as in the case of explosions or debris released during staging, in which case the centroid velocity is the velocity of the source vehicle. If this vehicle is in a long-life orbit, the debris will also populate long-life orbits unless sufficient peculiar velocity is imparted to the debris to significantly lower perigee. The large peculiar velocities will not occur for debris deposited during normal operations and do not appear to have occurred for most of the peculiar explosive events observed on orbit. The high intensity explosions associated with anti-satellite tests will impart significant peculiar velocities to alter perigee but, while possibly injecting some debris into rapid decay orbits, these tests may also raise apogee in some debris and place it in longer life orbits.

The picture is considerably different for collision processes. When collisions occur, the centroid velocity is the center-of-mass velocity and, in some cases, will be suborbital. The fragment peculiar velocities are expected to be small (on the order of a few 100's of feet per second) relative to the orbital speed, so that only collisions having a center-of-mass velocity characteristic of a long-life orbit will contribute significant debris.

For collisions between objects in circular orbits, the collision angle required to produce a specified radius of perigee can be easily computed as a function of collision altitude and mass ratio. Let \bar{v} refer to the center-of-mass speed and $v = \sqrt{\mu/r}$ the circular orbit speed. Then the collision angle, β , is related to the colliding particle properties by

$$\cos \beta = \frac{M^2 \bar{v}^2 - v^2 (m_1^2 + m_2^2)}{2m_1 m_2 v^2} \quad (\text{A-6})$$

where

$$\begin{aligned} m_1, m_2 &= \text{impacting object masses} \\ M &= m_1 + m_2 \end{aligned}$$

Translating to dimensionless notation

$$\cos \beta = \frac{(\xi + 1)^2 \bar{v}^2 - v^2 (\xi^2 + 1)}{2\xi v^2} \quad (\text{A-7})$$

where

$$\xi = m_1/m_2 \leq 1$$

However, relating to the development of the hyperbolic surface in velocity space, clearly the requirement for the orbital/suborbital boundary is that $\bar{v} = A$, or

$$\bar{v}^2 = A^2 = \frac{2v^2 a}{a+1} \quad (\text{A-8})$$

so that

$$\cos \beta = \frac{2(\xi + 1)^2 a - (\xi^2 + 1)}{a + 1} \quad (\text{A-9})$$

The values for β determined for a range of mass ratios and collision altitudes is presented in Table A-1. For the special case that the reentry perigee altitude is taken to be 100 km, the collision altitudes are provided explicitly. By choosing such a low altitude for reentry, the resulting collision angles may be regarded as conservative; that is, angles which are somewhat smaller will cause the very small debris (i.e., that debris having a characteristically larger area to mass ratio) to reentry rapidly.

To understand the importance of the angles presented in Table A-1, the expected angle of collisions in a debris population must be determined. If this angle is large compared to an entry in the table, then an encounter described by the table parameters would very likely produce no long lived orbital debris; if the angle is small, then the encounter would probably produce long-lived orbital debris.

TABLE A-1. ANGLE AT WHICH TWO OBJECTS IN CIRCULAR ORBIT WILL COLLIDE AND HAVE A CENTER-OF-MASS VELOCITY WITH PERIGEE AT RE-ENTRY ALTITUDE (r_0) AS A FUNCTION OF IMPACT ALTITUDE AND MASS RATIO

r_0/r_1	1.0	0.98	0.96	0.94	0.92	0.90	0.80	0.60	0.40	0.20	0.00
m_1/m_2											
1.0	0.0	11.5	16.4	20.3	23.6	26.5	29.3	31.8	34.3	36.7	38.9
0.9	0.0	11.6	16.4	20.3	23.6	26.6	29.3	31.9	34.4	36.7	39.0
0.8	0.0	11.6	16.5	20.4	23.7	26.7	29.5	32.1	34.9	36.9	39.2
0.7	0.0	11.7	16.7	20.6	23.9	27.0	29.7	32.4	34.9	37.3	39.6
0.6	0.0	11.9	17.0	20.9	24.3	27.4	30.3	32.9	35.5	37.9	40.3
0.5	0.0	12.2	17.4	21.5	25.0	28.2	31.1	33.8	36.5	39.0	41.4
0.4	0.0	12.8	18.2	22.4	26.1	29.4	32.5	35.4	38.1	40.7	43.3
0.3	0.0	13.7	19.5	24.1	28.0	31.6	34.9	38.0	41.0	43.8	46.6
0.2	0.0	15.5	22.1	27.3	31.8	35.9	39.6	43.2	46.6	49.9	53.1
0.1	0.0	20.1	28.8	35.6	41.6	47.0	52.1	57.0	61.7	66.3	70.9
0.05	0.0	27.3	39.2	48.8	57.3	65.2	72.8	80.2	87.6	95.2	103.0
0.02	0.0	42.5	62.0	78.7	94.8	111.7	131.3	163.3	--	--	--
0.01	0.0	61.0	92.3	125.3	--	--	--	--	--	--	--
0.001	0.0	--	--	--	--	--	--	--	--	--	--
Impact altitude (km)	100	232	370	513	663	820	983	1155	1334	1522	1720

In this paper, we present results for debris occupying randomly distributed orbital planes having a specified inclination. The distribution function for the intersection angle, β , between orbital planes is given by

$$g(\beta) = \frac{1}{\pi} \frac{\sin \beta}{\sqrt{\sin^4 i - (\cos \beta - \cos^2 i)^2}} \quad 0 \leq \beta \leq 2i \quad (A-10)$$

The expected angle between orbital planes, $\langle \beta \rangle$, is given by

$$\langle \beta \rangle = \int_0^{2i} \beta g(\beta) d\beta \quad (A-11)$$

However, the expected angle of collision must be calculated by taking into account the fact that the relative speed must be included as a weighting function. For 2 objects in circular orbit with velocity v and encountering at angle β , the relative speed, v_R , is given by

$$v_R = 2v \sin \beta/2 \quad (A-12)$$

Since the collision probability depends linearly on the relative speed, the expected collision angle, $\langle \beta_c \rangle$, is given by

$$\langle \beta_c \rangle = \frac{\int_0^{2\pi} \beta \sin(\theta/2) g(\theta) d\theta}{\int_0^{2\pi} \sin(\theta/2) g(\theta) d\theta} \quad (A-13)$$

Values for $\langle \beta \rangle$ and $\langle \beta_c \rangle$ as a function of inclination are provided in Table A-2.

TABLE A-2. VALUES FOR $\langle \beta \rangle$ AND $\langle \beta_c \rangle$ AS A FUNCTION OF INCLINATION (DEGREES)

i	$\langle \beta \rangle$	$\langle \beta_c \rangle$
10	12.7	15.7
20	25.3	31.2
28.5	35.8	44.3
30	37.6	46.5
40	49.4	61.4
50	60.7	75.7
60	70.9	88.9
70	79.9	100.7
80	86.8	110.0

The results from Table A-2 should be used with care in examining Table A-1. The fact that objects are distributed in inclination as well as in orbital plane orientation will increase the expected angle for low inclination and decrease the angles for high inclination. The β distribution will be given by

$$g(\beta, i_1, i_2) = \frac{1}{\pi} \frac{\sin \beta}{\sqrt{\sin^2 i_1 \sin^2 i_2 - (\cos \beta - \cos i_1 \cos i_2)^2}} \quad |i_1 - i_2| \leq \beta \leq i_1 + i_2 \quad (A-14)$$

However, since the inclination distribution varies with altitude, the expectation values on β require a more complex model than has been incorporated at this time.

REFERENCES

1. Chobotov, V. A., "Assessment of Satellite Collision Hazards by Simulated Sampling in Space", presented at the NASA/Johnson Space Center Orbital Debris Workshop, July, 1982.

2. Anen., "Models of the Earth's Atmosphere (90 to 2500 km)", NASA SP-8021, March, 1973.
3. Anen., "Litterbugs in Space", Spaceflight, Vol. 23, January, 1981.
4. Bess, T. D., "Mass Distribution of Orbiting Manmade Space Debris", NASA Technical Note (TN D-8100), 1975.
5. Kosler, D. J. and Gour-Painis, D. G., "Collision Frequency of Artificial Satellites: The Creation of a Debris Belt," Journal of Geophysical Research, Vol. 83, June 1, 1978, pp. 2637-2646.
6. Reynolds, R. C. and Fischer, N. H., "The Hazard Presented to the Shuttle by Other Satellites in Its Operating Environment", Proceedings of the 1980 JANNAF Safety and Environmental Protection Session, March, 1980, CPIA Publication 313.

PARTICLE NUMBER DENSITY AS A FUNCTION OF ALTITUDE

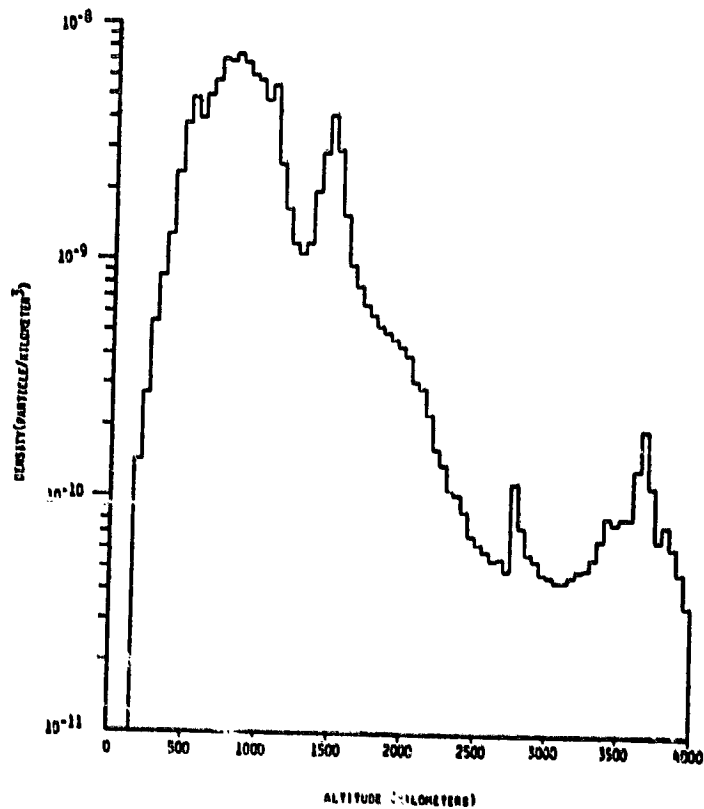


FIGURE 1. DENSITY OF TRACKED DEBRIS AS A FUNCTION OF ALTITUDE (OCTOBER, 1976, SATELLITE SITUATION REPORT, THE "ZERO TIME" POPULATION)

TIME BETWEEN COLLISIONS AS A FUNCTION OF COLLISION CROSS-SECTION AND ALTITUDE FOR THE CURRENT AND PROJECTED POPULATION OF TRACKED DEBRIS

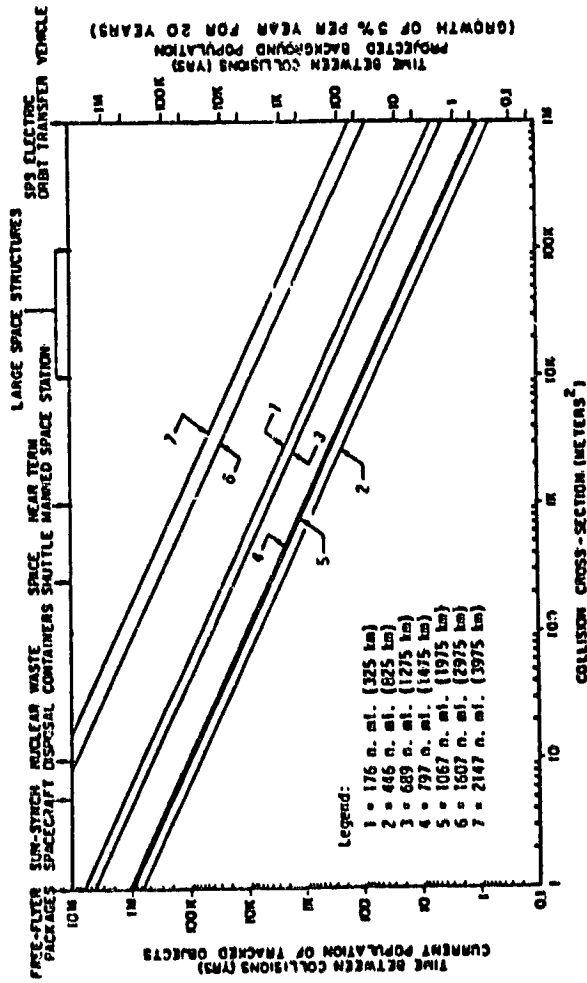


FIGURE 2. EXPECTED TIME BETWEEN COLLISIONS AS A FUNCTION OF COLLISION CROSS-SECTION FOR THE ZERO-TIME AND PROJECTED POPULATION OF TRACKED DEBRIS

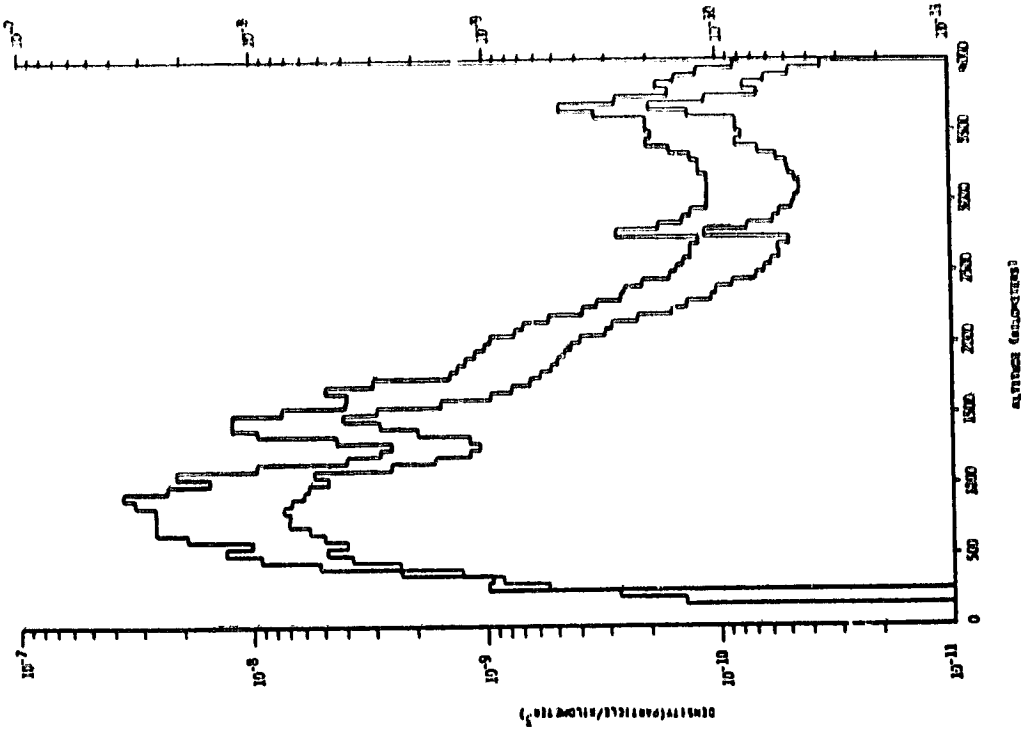


FIGURE 3. DENSITY OF MANMADE DEBRIS AS A FUNCTION OF ALTITUDE FOR THE ZERO TIME AND 30 YEAR POPULATIONS

DEBRIS SOURCES: COLLISIONS • 5 PERCENT ANNUAL GROWTH RATE IN LARGE OBJECT POPULATION

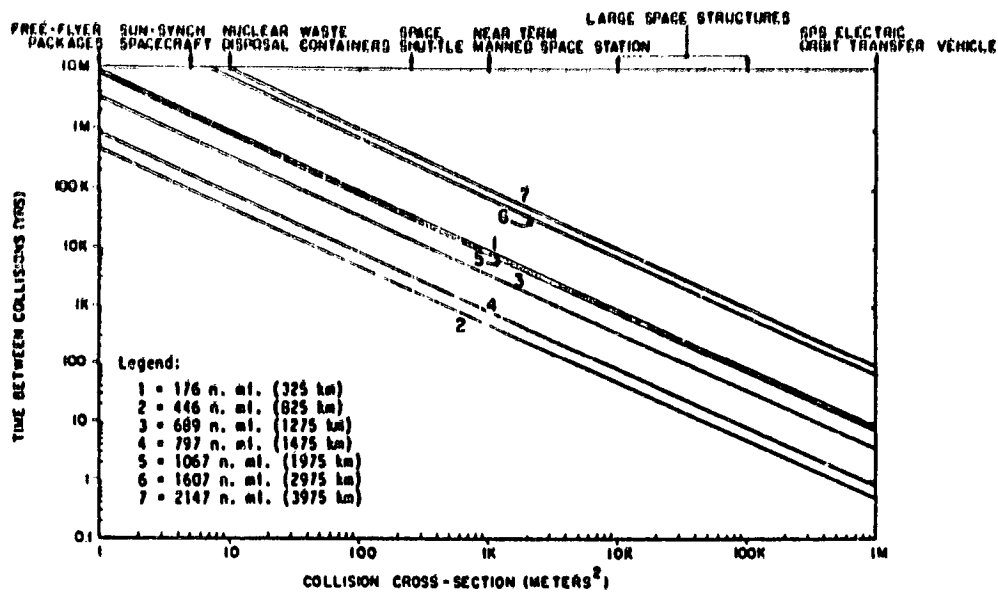


FIGURE 4. EXPECTED TIMES BETWEEN COLLISIONS AFTER 10 YEARS, AS A FUNCTION OF COLLISION CROSS-SECTION

DEBRIS SOURCES: COLLISIONS + 5 PERCENT ANNUAL GROWTH RATE IN LARGE OBJECT POPULATION

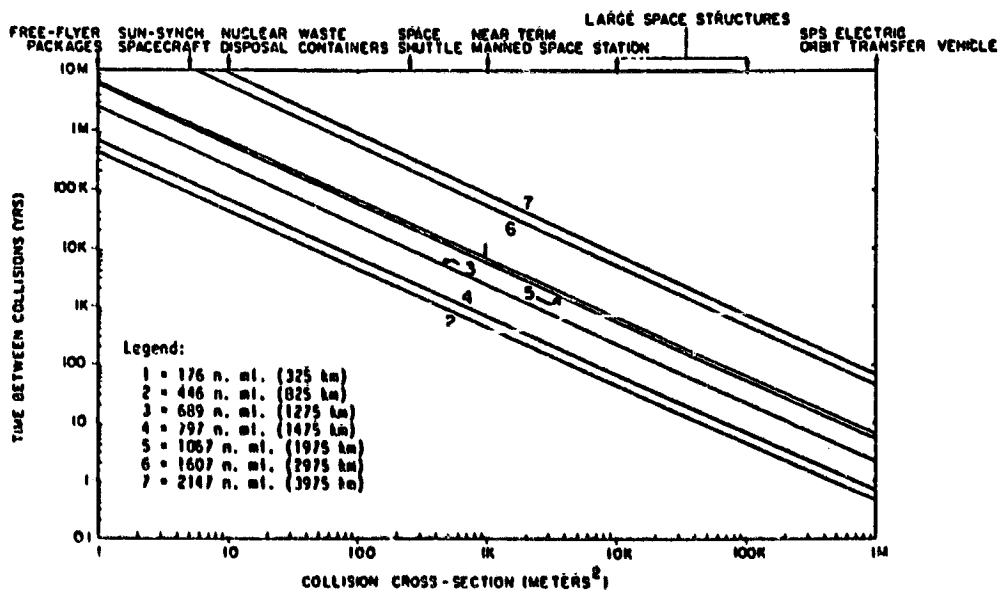


FIGURE 5. EXPECTED TIMES BETWEEN COLLISIONS AFTER 20 YEARS, AS A FUNCTION OF COLLISION CROSS-SECTION

DEBRIS SOURCES: COLLISIONS + 5 PERCENT ANNUAL GROWTH RATE IN LARGE OBJECT POPULATION

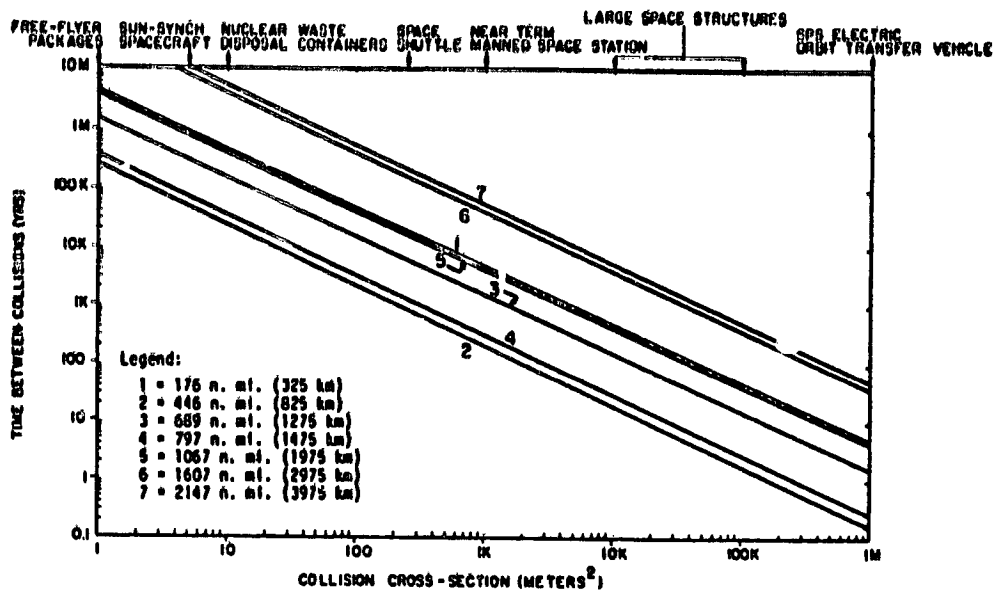


FIGURE 6. EXPECTED TIMES BETWEEN COLLISIONS AFTER 30 YEARS, AS A FUNCTION OF COLLISION CROSS-SECTION

DEBRIS SOURCES: COLLISIONS + 5 PERCENT ANNUAL GROWTH RATE IN LARGE OBJECT POPULATION

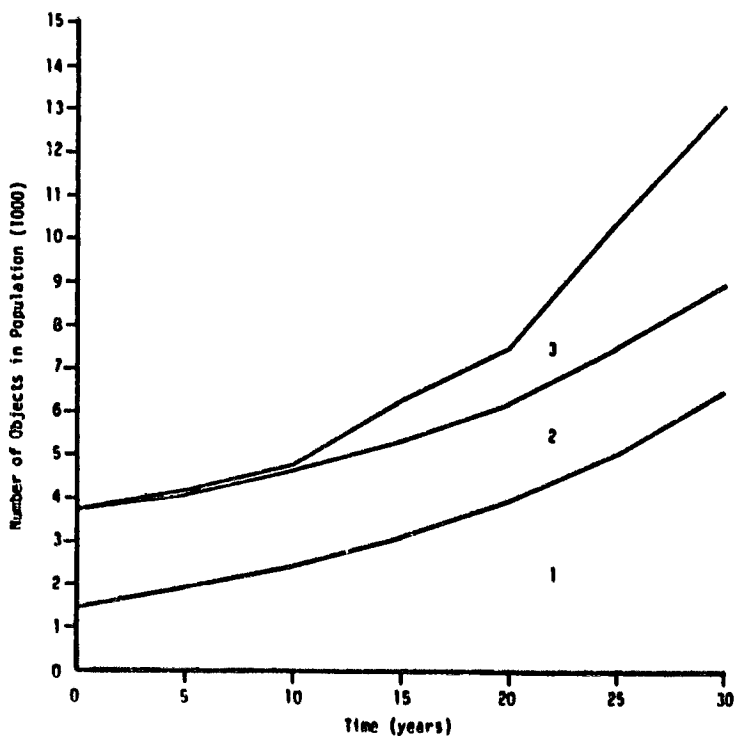


FIGURE 7. NUMBER OF OBJECTS IN DEBRIS POPULATION AS A FUNCTION OF TIME

DEBRIS SOURCES: COLLISIONS + 5 PERCENT ANNUAL GROWTH RATE IN LARGE OBJECT POPULATION

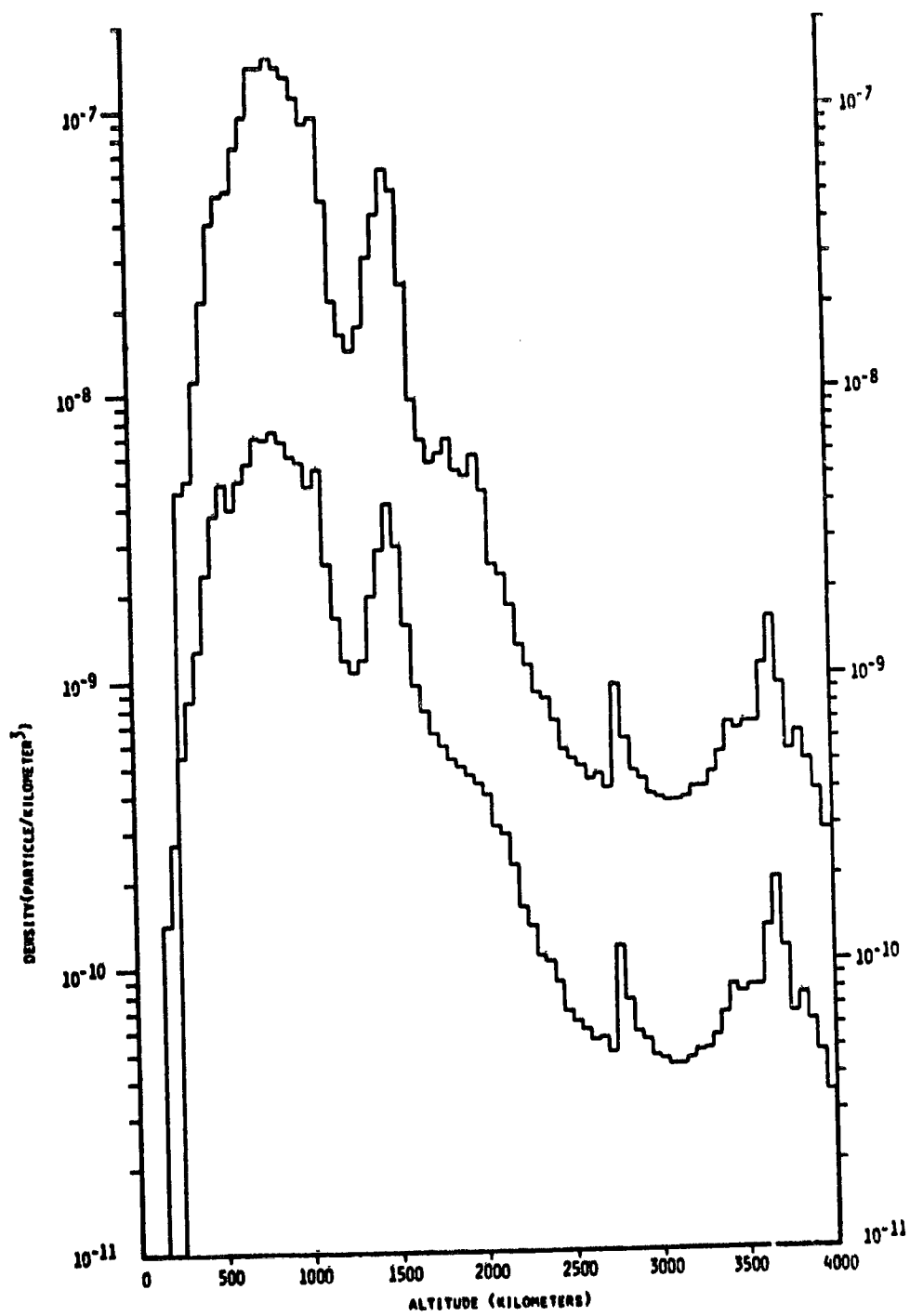


FIGURE 8. DENSITY OF MANMADE DEBRIS AS A FUNCTION OF ALTITUDE FOR THE ZERO TIME AND 30 YEAR POPULATIONS

DEBRIS SOURCES: COLLISIONS + 10 PERCENT ANNUAL GROWTH RATE IN LARGE OBJECT POPULATION

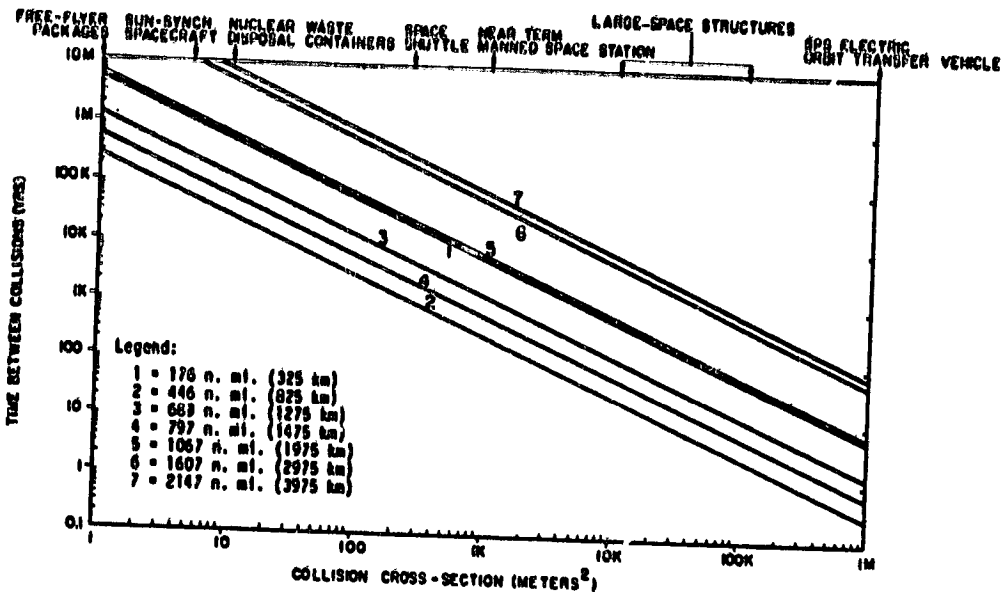


FIGURE 9. EXPECTED TIMES BETWEEN COLLISIONS AFTER 10 YEARS, AS A FUNCTION OF COLLISION CROSS-SECTION
 DEBRIS SOURCES: COLLISIONS + 10 PERCENT ANNUAL GROWTH RATE IN LARGE OBJECT POPULATION

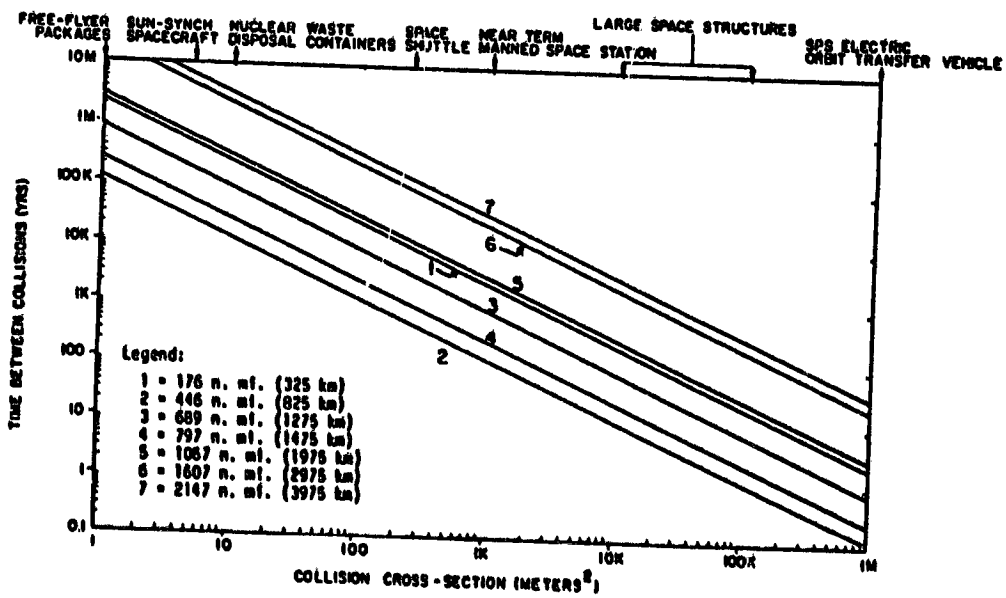


FIGURE 10. EXPECTED TIMES BETWEEN COLLISIONS AFTER 20 YEARS, AS A FUNCTION OF COLLISION CROSS-SECTION
 DEBRIS SOURCES: COLLISIONS + 10 PERCENT ANNUAL GROWTH RATE IN LARGE OBJECT POPULATION

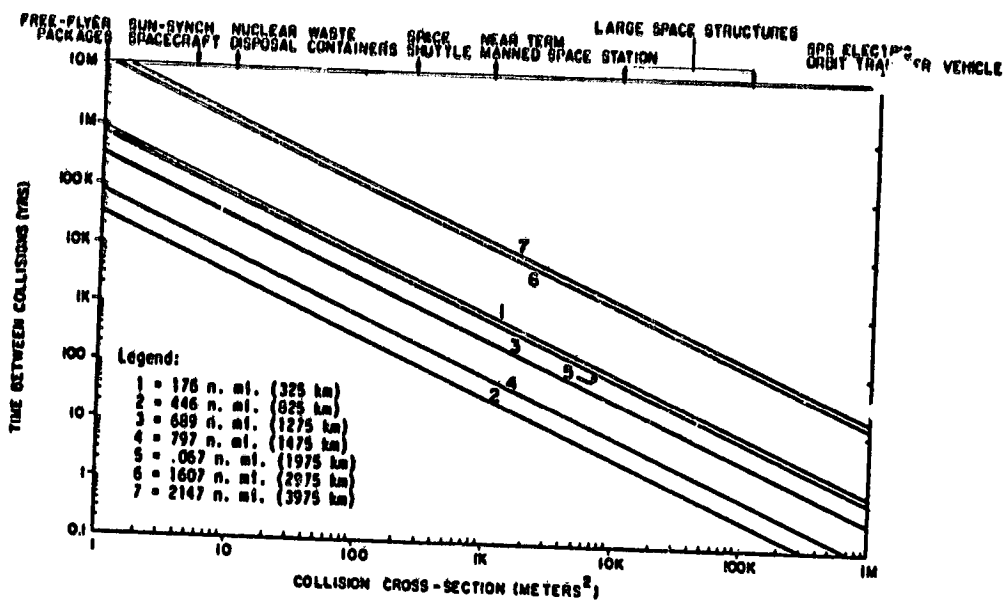


FIGURE 11. EXPECTED TIMES BETWEEN COLLISIONS AFTER 30 YEARS, AS A FUNCTION OF COLLISION CROSS-SECTION
 DEBRIS SOURCES: COLLISIONS + 10 PERCENT ANNUAL GROWTH RATE IN LARGE OBJECT POPULATION

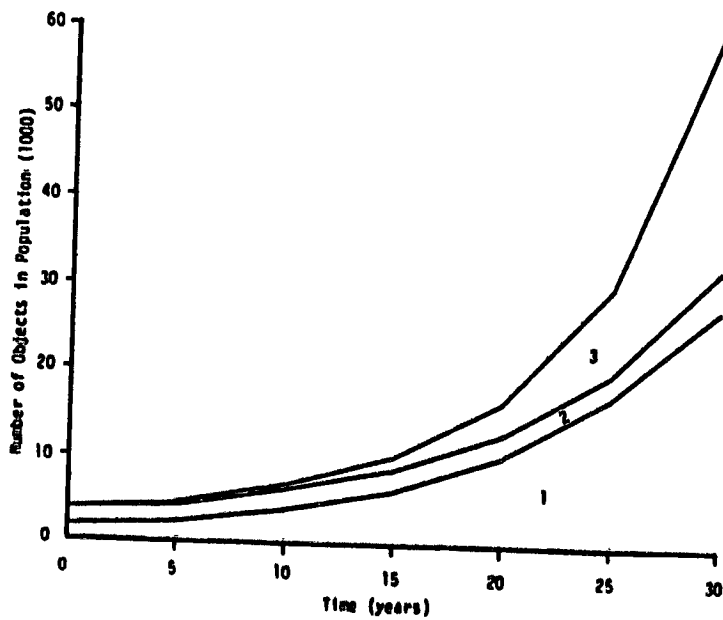


FIGURE 12. NUMBER OF OBJECTS IN DEBRIS POPULATION AS A FUNCTION OF TIME
 DEBRIS SOURCES: COLLISIONS + 10 PERCENT ANNUAL GROWTH RATE IN LARGE OBJECT POPULATION

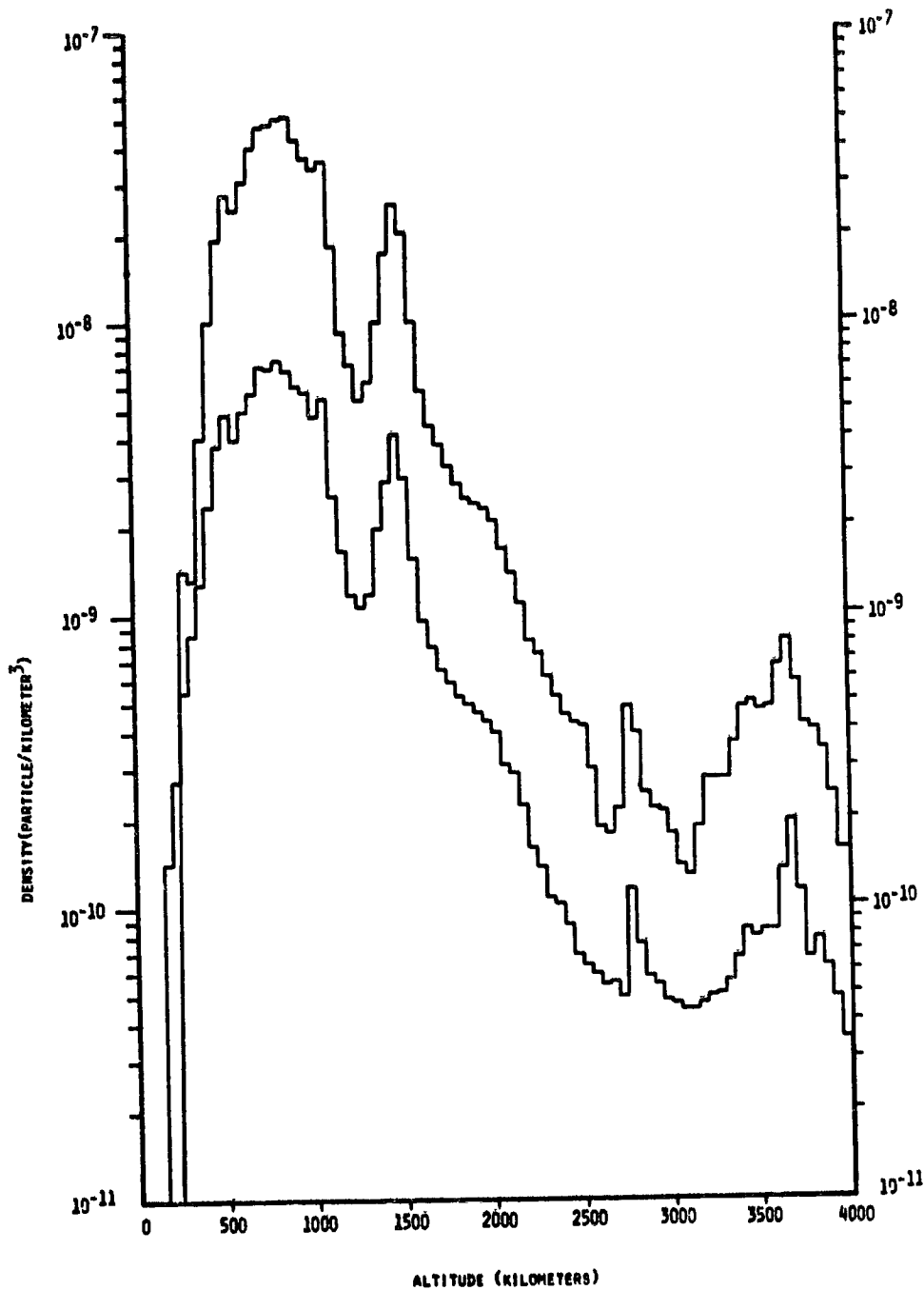


FIGURE 13. DENSITY OF MANMADE DEBRIS AS A FUNCTION OF ALTITUDE FOR THE ZERO TIME AND 30 YEAR POPULATIONS

DEBRIS SOURCES: COLLISIONS + 5 PERCENT ANNUAL GROWTH RATE IN LARGE OBJECT POPULATION + ACCIDENTAL EXPLOSIONS

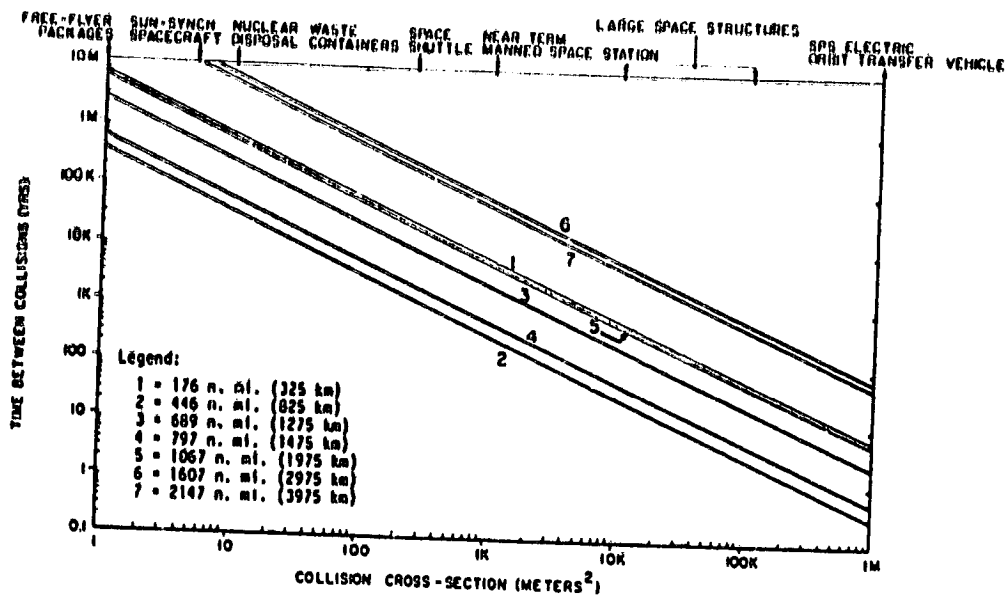


FIGURE 14. EXPECTED TIMES BETWEEN COLLISIONS AFTER 10 YEARS, AS A FUNCTION OF COLLISION CROSS-SECTION

DEBRIS SOURCES: COLLISIONS + 5 PERCENT ANNUAL GROWTH RATE IN LARGE OBJECT POPULATION + ACCIDENTAL EXPLOSIONS

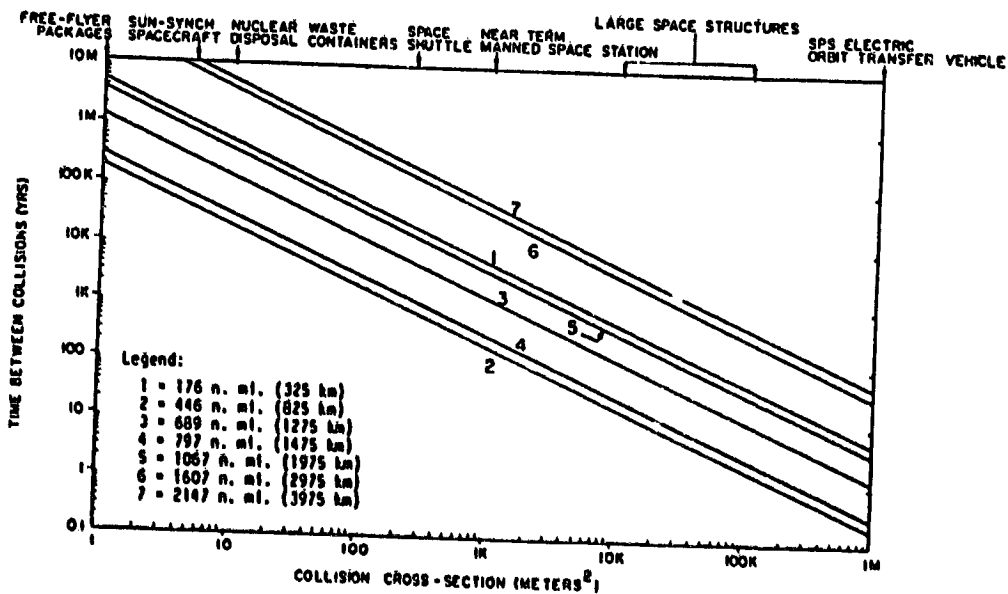


FIGURE 15. EXPECTED TIMES BETWEEN COLLISIONS AFTER 20 YEARS, AS A FUNCTION OF COLLISION CROSS-SECTION

DEBRIS SOURCES: COLLISIONS + 5 PERCENT ANNUAL GROWTH RATE IN LARGE OBJECT POPULATION + ACCIDENTAL EXPLOSIONS

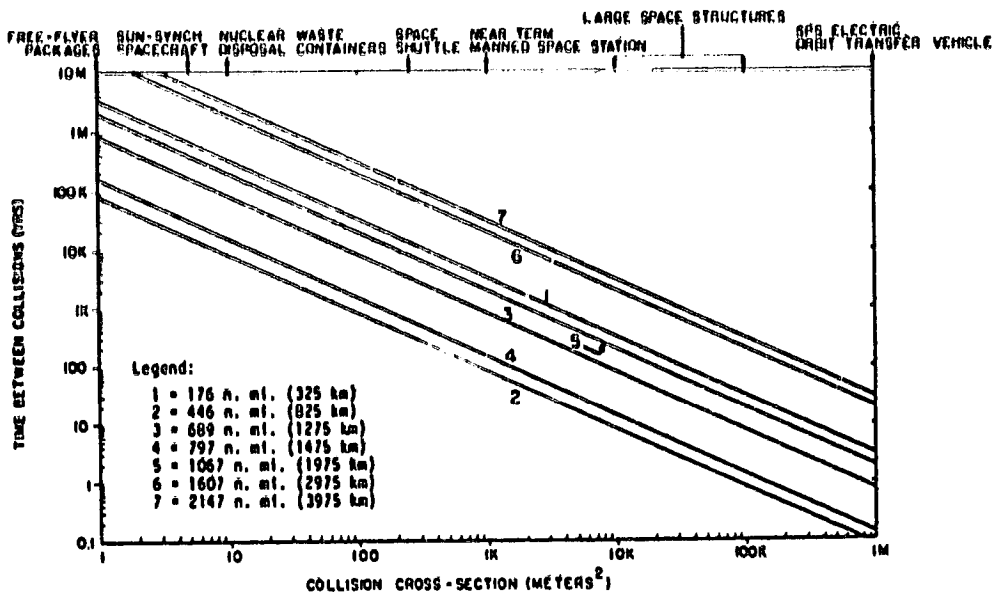


FIGURE 16. EXPECTED TIMES BETWEEN COLLISIONS AFTER 30 YEARS, AS A FUNCTION OF COLLISION CROSS-SECTION

DEBRIS SOURCES: COLLISIONS + 5 PERCENT ANNUAL GROWTH RATE IN LARGE OBJECT POPULATION + ACCIDENTAL EXPLOSIONS

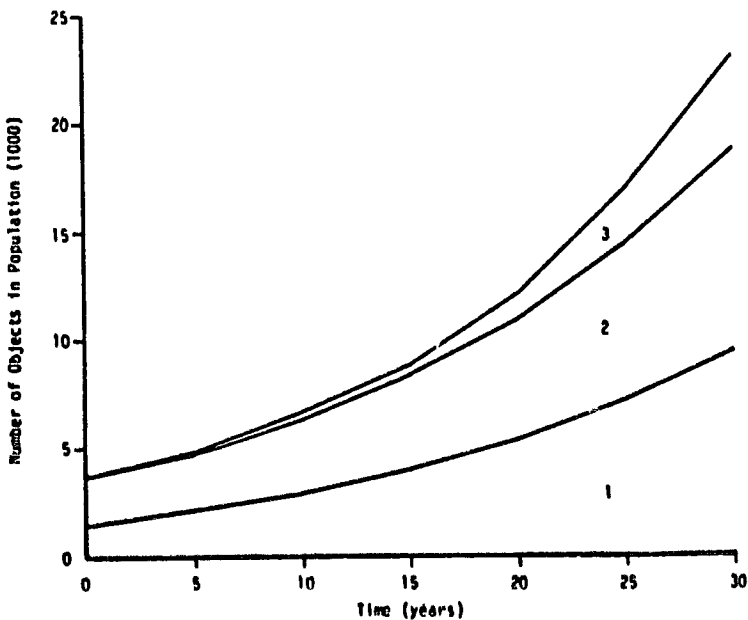


FIGURE 17. NUMBER OF OBJECTS IN DEBRIS POPULATION AS A FUNCTION OF TIME

DEBRIS SOURCES: COLLISIONS + 5 PERCENT ANNUAL GROWTH RATE IN LARGE OBJECT POPULATION + ACCIDENTAL EXPLOSIONS

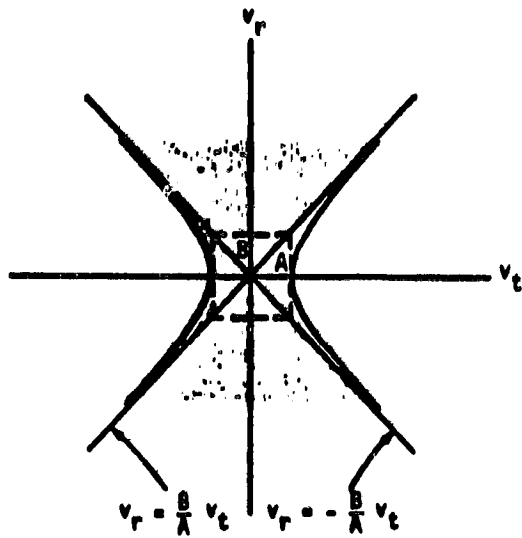


FIGURE A-1. HYPERBOLA IN VELOCITY SPACE SEPARATING SHORT-LIFE (SHADED) ORBITS FROM LONG-LIFE ORBITS

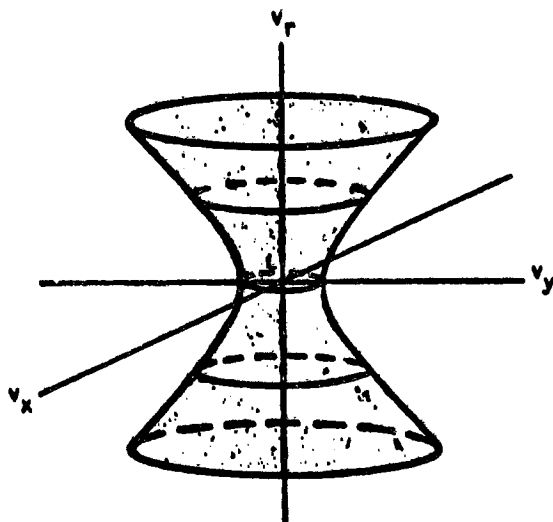


FIGURE A-2. HYPERBOLOID IN 3-DIMENSIONAL VELOCITY SPACE

Dy 12
11/15/67

Geosynchronous Satellite Collision
Avoidance

N 85-21197

Lt. Wm. Fraser
HQ AFSCF
Sunnyvale, AFS, CA

Satellites are a resource vital to the support of U. S. civil and military operations. Maintaining acceptable distance between satellites is necessary to reduce the probability of physical damage resulting from collisions with another satellite, active or inactive, and space debris. Satellite "bunching", the concentration of satellites in a particular orbital region, is an immediate concern at geosynchronous altitudes where many satellite programs tend to favor the same regions of space for maximizing mission data acquisition and ground station access.

The satellite population is constantly increasing due to the rapid growth of space systems which support communications, weather forecasting, attack warning and other civilian and military needs on an international scale. The rapid increases in the number of satellite systems, the growing dependency on these systems, and the potentially hazardous conjunctions in space, dictates careful management of satellite positions.

The potential for satellite collision increases as more objects are placed in orbit. One of the fastest growing satellite groups is near geosynchronous altitudes. At these altitudes, active satellites maintain fixed longitudinal station-keeping control while inactive satellites and debris generally drift around the globe or oscillate about two geopotential stable points. Some portion of the total objects in geosynchronous orbit are currently being tracked by ground stations while a significant number of additional pieces of space debris are believed to regularly pass through geosynchronous orbit altitudes. Although the probability of an operational satellite colliding with another satellite or a piece of space debris is apparently small at present, it will increase with the increase in the number of space objects, their sizes, and on-orbit lifetimes.

It is the responsibility of Inter-range Operations (ROSR) at the Air Force Satellite Control Facility (AFSCF) to determine potential space collisions in the geosynchronous belt and subsequently notify the involved parties. Presently ROSR runs 22 primary DOD vehicles against over 200 known satellites or pieces of debris tracked by the North American Aerospace Defense Command (NORAD). Two line mean element sets received by NORAD are run twice a week on the DCOLA program to predict future satellite positions and relative distances between vehicles for a three week period. Further analysis can be performed on vehicles converging within 100 NM of each other with the DODGE program. Predictions are dependent upon the currency and accuracy of the NORAD two line mean element sets. As our tracking technology improves, our collision avoidance predictions will increase in accuracy, thus increasing our chances of surviving in a potentially crowded environment.

410 12
N 85-21198

ABSTRACT

IN SITU ORBITAL DEBRIS EXPERIMENT CONCEPTS

by
Dr. Sherman L. Noste

The feasibility of implementing the radar, lidar and passive optical remote sensing concepts for measuring space debris from an earth orbiting platform was investigated. Each system was defined in sufficient detail to permit a comparison of their requirements on the host platform, their performance relative to the objectives of NASA's space debris measurement program and the estimated cost of developing each concept into a flight instrument.

The three systems can all be designed to provide the desired measurements within the weight and power budgets of typical spacecraft payloads, but each technique has unique capabilities and disadvantages arising from these basic conceptual differences. The radar and lidar systems offer the greatest versatility and accuracy since they control the direction, intensity and duration of the energy incident on the target object. The penalty paid for this capability is increased weight, power, cost and complexity. The performance of the passive optical system is determined primarily by the capability of the detector and to a lesser extent by the baseline separation of the telescopes, which requires the use of an on-orbit deployment mechanism. The passive optical concept provides the largest total event rate, and includes significant detections of particle sizes greater than 10 cm to allow correlation with ground based observations of the larger particles. The event rate for the radar system is relatively constant with particle size while the lidar system is slightly biased toward the smaller sizes. These event rate differences result from a combination of the debris flux size distribution and the variation of sensitive detection area with particle size for the three concepts.

Final selection of the flight concept will most probably result from a comparison between program priorities and available resources. If a dedicated mission is not possible, and the spacecraft resources must be shared with other instruments, the passive optical concept offers the most flexibility for fitting into a "piggy-back" scenario. If a dedicated spacecraft is available, then the concept which most closely fits the objectives of the space debris detection program should be optimized.

BACKGROUND AND ASSUMPTIONS

Unrestricted utilization of the near-earth space environment by manned and unmanned spacecraft during the past twenty-five years has resulted in a space debris environment which is approaching the hazard threshold for future long duration missions. Since the advent of Sputnik in 1957, there has been an increasing number of satellites orbiting the Earth. The largest are primary payloads and spent rockets. However, many of these have generated debris which have also become Earth satellites. In addition, several of the larger satellites have exploded in orbit, generating large numbers of small (<10 cm) debris particles. Although the North American Aerospace Defense Command (NORAD) tracks and categorizes a large number of earth orbiting debris objects, the NORAD system does not track objects less than about 10 cm at 1000 km (4 cm at 400 km), so that the vast majority of particles remain undetected.

Although the current population of small debris resulted from explosions, Kessler (Refs. 1 and 2) has shown that the major future source of debris may be fragmentation caused by collision of larger objects. Based on current projected launch rates, associated collision probabilities and collision statistics, a debris flux model for the 1995 era, as predicted by Kessler, is shown in Figure 1.

The present limits on detection of debris coupled with the increasing hazard as discussed above, point out the need for improving the small particle detection capability. An obvious solution which merits consideration is to use an Earth orbiting sensor system to eliminate the interfering and obscuring effects of the Earth's atmosphere. The objective of this study was to identify potential sensor systems and to evaluate the feasibility, performance and requirements of each, so that an optimum concept could be selected.

The relative performance of the detection concepts was evaluated in terms of the particle detection rate obtained by assuming the debris flux model for the 1995 era shown in Figure 1. Assumptions regarding the debris characteristics and measurement goals are specified in Table 1.

CANDIDATE DEBRIS DETECTION SYSTEMS

Three remote measurement concepts were identified as candidates for use in a debris measurement system: radar, lidar and passive optical. All three concepts provide object detection and measurement by observing and analyzing radiation reflected from the objects. The first two concepts are active in that they transmit energy pulses and "listen" for a return signal during the interpulse period. The passive optical system is constantly in the receive or "listen" mode and detects sunlight reflected from the object as it passes through the system's field-of-view.

The radar technique has been considered previously (Ref. 3) and shown to be a viable concept provided a spacecraft platform existed to provide the required power, and support the large mass. However, until recently, launches of spacecraft carrying instruments of several hundred pounds were not feasible. In the near future such launches will be routine with the limiting factor now becoming the system cost.

Previous consideration of a lidar system for this application has been limited for two reasons: (1) the large weight and power requirements, and (2) the unavailability of a space-qualified laser. The second limitation still exists, technically, but it is not unreasonable to assume that space-qualified lasers will be available in the near future in view of their increasing importance for such applications as Satellite-Submarine Communications, atmospheric probes, cross-link satellite communication, etc.

A passive optical system (Ref. 4) has flown on two spacecraft (Pioneers 10 and 11) and proven the feasibility of the concept. The severe weight and power limitations (6.5 lbs., 2 W) imposed on that system together with the available technology limited the quality of data and the accuracy of the results. Recent advances in detector technology combined with greater weight and power allowances should markedly increase the performance of the passive optical system.

Although each of the above systems makes the same basic measurements, i.e., detection of reflected radiation, the implementation, performance and cost consideration of each concept may indicate a preferred concept for use in monitoring the space debris population.

Design of any system for measuring space debris requires consideration of two major areas: functional operation and hardware implementation. While the system functions will be driven by the measurement objectives, the implementation of those functions may be limited by hardware availability and associated costs. A feasible system requires compatibility between function, hardware and cost.

The conceptual design of the candidate debris detection systems emphasized the desire to maximize detection probability, and hence event rate, for objects in the size range of 0.1 to 10 cm. As a result, no restrictions were placed on the weight and power required other than being reasonable for typical spacecraft instrument payloads.

RADAR DETECTION SYSTEM

Radar detection of debris particles will be accomplished by transmitting a pulse of energy and detecting energy reflected from a particle within the transmitted pencil beamwidth. The objective of maximizing event rate, and hence effective detection area requires that the transmitted pencil beam direction be sequentially scanned through a volume of space consistent with the velocity characteristics of the objects to be detected. Specifically, the angular width of the sectorial fan coverage is established from the time required to repeat the coverage without missing the detection of high velocity debris.

In the normal search mode the radar system will continuously operate in a step/pulse mode until a particle is detected. The stepping function will then temporarily stop and a verification pulse will be transmitted. If a second signal return is detected, the system will continue to transmit at this beam position until a return signal is not observed and the step/pulse sequence will then resume. The system threshold should be adjustable via ground command to control false alarm rate and/or event rate.

When a legitimate event is verified (two successive signals), an on-board micro-processor/controller can be used to optimize (decrease) the interpulse period, consistent with the indicated range of the detected object, to maximize the number of "hits" and improve measurement accuracy. Due to the predicted sparsity of detectable objects, more than one particle is not expected in the beam at one time.

The amplitude comparison monopulse tracking approach is recommended for the space debris radar system for the advantages listed below:

- 1) The angle-offset signal can be extracted from one pulse. This is important when observing objects whose reflection characteristics may change from pulse to pulse as in the case of irregularly shaped, rotating debris particles.
- 2) The direction of particle motion can be tracked with the minimum number of pulses, since each pulse updates the angle-offset signal.

The rapid scan required to effectively search an appreciable volume of space dictates the use of an electrically scanned phased array antenna. The narrow beamwidth needed for accurate angle measurements requires a relatively large antenna aperture. A 2 m x 2 m size is physically realistic and provides acceptable range detection capability, and was used as the baseline size for subsequent performance calculations and for estimating weight, power and cost. A slotted waveguide type of construction using a ferrite circulator to allow one antenna to be used with both the transmitter and receiver results in a relatively lightweight system.

The baseline radar space debris detection system is characterized by the following parameters:

Antenna Size:	2 m x 2 m
Nominal PRF:	20 kHz
Pulse Power:	2000 watts
Transmitter Frequency:	15 GHz
Maximum Scan Range:	$\pm 45^\circ$
Pulse Width:	20 ns

The estimated particle detection rate for this system using the 800 km orbit flux shown in Figure 1 is:

130/year for particle diameter <1 cm
and 260/year for particle diameter <10 cm

The instrument weight and bus power requirements are estimated at 380 lbs. and 155 watts, respectively.

LIDAR DETECTION SYSTEM

The lidar detection of debris particles will be accomplished by transmitting a very short pulse of optical energy and detecting the energy reflected from the particle on a mosaic detector. The lidar transmitter will use a fixed, wide beam transmitter to illuminate the detection volume. The lidar will operate in the 10 micro-meter spectral region with a pulsed CO₂ laser transmitter. The implementation of the system is dictated by the ready availability of laser and detector technology. At the present time, the state of these technologies will allow a simple photon detection system to be built and flown in space. The growth of these technologies, however, is very rapid, and shortly, in a matter of months, or at most a year or two, the state-of-the-art will have advanced to the point where a heterodyning system with a mosaic detector will be possible.

The basic lidar system consists of an optical system of the Schmidt reflecting type with a primary mirror diameter of 1.25 meters. The transmitter and receiver share the same optics with field separation by polarization differences between the outgoing and the reflected signals. The outgoing pulse is spread by the optical system to cover a 5° cone. The optical signals are reflected by the debris particles on the basis of their area. This is because the wavelength is small compared with the diameter of the smallest particle and it is expected that the particles will be rough and irregular and not polished spheres.

The data processor contains the electronics required to process the signals from the detector array and the laser and to compute the time taken by the pulse to go from the laser, out to the particle and back to the detector. This is accomplished by first detecting the outgoing pulse with a photodetector in the laser and using it to generate a range count start pulse for the range computer. When the signal return pulse is detected by the detector array, it is amplified and the position information of the signal on the array is extracted. The signals from the array are then combined and after appropriate blanking to reduce interference from residual scattering from the transmit pulse, a range count stop pulse is generated. Pulse differentiation is used with zero crossing detectors in both start and stop channels. If no range stop pulse is received for a transmitted pulse within the range gate interval, the telemetry simply ignores that pulse. Range and position data are stored and transmitted only when a particle is detected and a range count stop pulse is generated. Velocity data is generated by differentiating the range to obtain range rate.

The baseline lidar space debris detection system is characterized by the following parameters:

Telescope Area	-	1.0 meter ²
Telescope Field-of-View	-	5°
Nominal PRF	-	2 kHz
Laser Wavelength	-	10.6 μm
Transmitted Pulse Power	-	~10 watts

The estimated particle detection rate for this system using the 800 km orbit flux shown in Figure 1 is:

65/year for particle diameter <1 cm
75/year for particle diameter <10 cm

The instrument weight and bus power requirements are estimated at 510 lbs. and 200 watts, respectively.

PASSIVE OPTICAL DETECTION SYSTEM

The passive optical debris detection system will perform the following functions:

- 1) optically view a fixed volume of space,
- 2) detect sunlit particles as they transit the field-of-view,
- 3) track the particles against a relatively fixed star background,
- 4) process the information to provide spatial and temporal data regarding the particle track through the field-of-view.

The baseline system utilizes a minimum of two optical imaging cameras employing large area detector arrays in the focal plane. Two imaging optical systems that can record the path of a particle against a reference star field background are all that is required to determine the six orbital parameters. The mathematics and accuracies were analyzed for the Harvard Meteor Project which used two Baker Super Schmidt cameras to determine orbits of meteors in a similar fashion.

The two imaging cameras can be independently mounted. Only approximate parallelism of the optic axes is required. The exact pointing of each camera will be determined from the star field which is periodically transmitted. The mounting to the spacecraft should be sufficiently rigid to keep individual stars within an element or pixel. For redundancy a third camera is recommended. An alternative may be to provide one redundant camera at each of the two mounting positions on the spacecraft rather than provide one additional camera with an independent mount.

The optic axis of each camera is pointed away from the sun ($>30^\circ$) and aimed at the sky. Information is collected at approximately the inverse of the framing rate ($\sim 1/30$ sec.) and then read into storage. Each frame is subtracted element by element from the previous frame. If stability is maintained or the starfield motion rate is slow compared to the exposure time, this should result in a null signal (except for optical and electronic noise). However, if a sunlighted particle has traversed the field-of-view, there will be a streak across the frame that will not cancel. This streak can be examined by a logic algorithm to distinguish it from random pixel noise (e.g., does it form a straight line, appear in both cameras, etc.). Assuming the logic criteria are met, the data from both cameras would be recorded or transmitted. The next frames from each camera would also be transmitted or recorded in their entirety (without subtraction) so that the reference starfield would be available for camera orientation and parallax measurements.

Selection of the proper type of array detector system for use in the optical system is governed to some extent by the requirements imposed on the system in terms of angular resolution and timing accuracy. Maximizing the number of pixels at the focal plane was a key design parameter since, in general, increasing the number of detection elements will improve measurement accuracy.

Over the past decade solid state detector arrays known as charge coupled devices (CCD's) and charge injection devices (CID's) have been developed in array formats compatible with broadcast television. In addition, silicon detector arrays responsive in the 300 to 1100 nm spectral range with pixel formats as large as 800 x 800 have been specifically developed for astronomical imaging applications. Larger arrays have not been developed because they are not needed for commercial applications and there are few astronomical imaging applications which would justify the effort.

Another type of high gain photon counting array detector available in a 1024 x 1024 pixel format is the Multi-Anode Microchannel Array (MAMA) which has been developed for use in instruments on both ground-based and space-borne telescopes (Ref. 5). The detector system consists of a tube assembly (sealed or open), containing an anode array and a single curved channel microchannel plate (MCP) with the appropriate spectral response photocathode material deposited on the front-face. The spatial location of an event (i.e., an incident photon) is determined by the simultaneous detection of a charge pulse from the MCP by sets of two or more of the electrodes in the anode array, which is mounted in proximity focus with the output face of the MCP. The detector resolution elements are defined by the dimensions of the anode electrodes, and the spectral range of the detector is defined by the photocathode material deposited on the MCP. The MCP provides the high gain (10^6) and narrow pulse-height distribution required for photon statistics noise limited operation. The MAMA detector appears to offer significant advantages over the other detector system and was, therefore, used for purposes of evaluating the capabilities and requirements of a passive optical detection system.

The telescope system which appears most appropriate for the passive optical concept is the Schmidt design since it exhibits uniform image quality over the field-of-view ($\sim 5^\circ$), can be easily shielded from stray light and is lightweight, compact and inexpensive.

A lightweight boom structure which has been developed for spacecraft application by Astro Research Corporation is suggested as one method of deploying the telescope systems. The structure is a lattice structure of fiberglass rods, shear stiffened by diagonal cables, which is retracted into its canister by forcibly twisting it about its axis. The strains induced are elastic so that the structure can be deployed and retracted in a repeatable manner. The structure deploys by means of a motor driven lanyard using the elastic strain energy stored in the system in its stowed configuration. The lattice structure can be designed to provide the required mechanical strength and rigidity.

The baseline passive optical space debris detection system is characterized by the following parameters:

- Optical System - 3 Schmidt telescopes, 30 cm apertures
- Detectors - 3 Multi-anode microchannel arrays,
1024 x 1024 pixel format
- Deployment - 2 Astromast, lightweight booms to provide up to
10 m telescope separation.

The estimated particle detection rate for this system using the 800 km orbit flux shown in Figure 1 is:

- 2370/year for particle diameters <1 cm
- and 3530/year for particle diameters <10 cm.

The instrument weight and bus power requirements are estimated at 130 lbs. and 130 watts, respectively.

COMPARISON OF CANDIDATE DETECTION SYSTEMS

A greatly expanded and more thorough discussion of these three space debris detection concepts, their requirements on the host spacecraft and their performance is given in the final report for this study (Ref. 6). However, the key capabilities and characteristics of each are summarized in Table 2. Also, in order to more easily fix the instruments' size relative to an existing, operational space platform, Figures 2, 3 and 4 depict each concept as it would appear on the Multimission Modular Spacecraft (MMS) recently used for the Landsat-4 Mission.

REFERENCES

1. Kessler, D.J., "Sources of Orbital Debris and the Projected Environment for Future Spacecraft", AIAA Paper 80-0855 presented at AIAA International Meeting & Technical Display, Baltimore, MD, May 6-8, 1980.
2. Kessler, D.J., Landry, P.M., Cour-Palais, B.G., and Taylor, R.E., "Collision Avoidance in Space", IEEE Spectrum, Vol. 17, No. 6, June 1980.
3. Final Technical Report for Feasibility Study of a Spacecraft Mounted Meteoroid Radar System, Volume I - Results of the Analytical Study; Volume II - System Implementation, Technical Report No. U1-943500-1, December 1968.
4. Soberman, R.K., Neste, S.L., and Lichtenfeld, K., "Optical Measurement of Interplanetary Particulates from Pioneer 10", J. Geophys. Res., Vol. 79, No. 25, September 1, 1974.
5. Bybee, R.L. and Timothy, J.G., "Multi-Anode Microchannel Array Detectors for Space Shuttle Imaging Applications", in SPIE Vol. 262, Shuttle Pointing of Electro-Optical Experiments, 1981.
6. Neste, S.L., et al., Final Report on Feasibility Study for Space Debris Detection Concepts, 23 September 1982.

ACKNOWLEDGEMENT

This work was supported by the National Aeronautics and Space Administration/Lyndon B. Johnson Space Center under Contract No. NAS9-16459.

TABLE 1. DEBRIS CHARACTERISTICS AND MEASUREMENT GOALS

- Encounter Velocity of Debris:
 - Velocity range 0 to 17 km/sec
 - Average velocity ~7 km/sec

- Debris Size of Interest:
 - 0.1 to 10 cm diameter size range
 - Emphasis on smaller sizes within this range

- Characteristics of Debris Material
 - Spherical shape for calculation purposes
 - Metallic
 - Totally reflecting (for radar)
 - 0.5 reflection coefficient (for optical)

- Measurement Accuracy Goals
 - Velocity magnitude to 1 percent
 - Velocity component radial to earth to 5 percent
 - Ratio of North-South to East-West velocity to 1 percent (i.e., direction to 1°)
 - Position to 1 percent
 - Size to ~10 percent

- Hardware and technology
 - Available in mid to late 1980's
 - Space qualified
 - High probability of 5 year lifetime

TABLE 2. COMPARATIVE MATRIX OF CANDIDATE SPACE DEBRIS DETECTION SYSTEMS

EVALUATION CRITERIA	RADAR	LIDAR	PASSIVE OPTICAL	COMMENTS
EXPECTED EVENT RATE	130/YEAR; $d \leq 1$ cm 260/YEAR; $d \leq 10$ cm	65/YEAR; $d \leq 1$ cm 75/YEAR; $d \leq 10$ cm	2370/YEAR; $d \leq 1$ cm 3530/YEAR; $d \leq 10$ cm	SENSORS IN 800 KM CIRCULAR ORBITS; OBSERVATION TIME ASSUMED TO BE 100%.
POWER (+30%)	155 WATTS	200 WATTS	130 WATTS	RADAR AND LIDAR SYSTEMS CAN INCREASE DETECTION RANGE BY INCREASING POWER.
TELEMETRY (+30%)	80 BITS/EVENT	3000 BITS/EVENT	95000 BITS/EVENT	TELEMETRY REQUIREMENT IS A STRONG FUNCTION OF ON-BOARD PROCESSING CAPABILITY.
COST TO BUILD	\$15-20 M	\$15-20 M	\$10-15 M	COSTS ARE ESTIMATED FROM VENDOR DATA AND PRELIMINARY RCA PRICE MODEL RESULTS.
HARDWARE RELIABILITY	MOST COMPONENTS HAVE PREVIOUS SPACE HERITAGE	LASERS HAVE NOT BEEN USED IN SPACE	MOST COMPONENTS HAVE PREVIOUS SPACE HERITAGE	REDUNDANT COMPONENTS REQUIRED FOR RADAR AND LIDAR, REQUIRED FOR PASSIVE OPTICAL.
ACCURACY OF VELOCITY	+ 1 %	RANGE RATE + 0.1 % CROSS RANGE + 3 %	+ 1 %	MEASUREMENT ACCURACY DEPENDS ON MAGNITUDE OF RANGE AND VELOCITY.
ACCURACY OF SIZE	RANGE AND SIZE DEPENDENT; (LEAST ACCURATE)	RANGE DEPENDENT; (MOST ACCURATE)	RANGE DEPENDENT	SIZE ACCURACY DEPENDS ON PARTICLE CHARACTERISTICS AND RANGE ACCURACY.
FALSE ALARM RATE	1/10 DAYS	NIL DUE TO ON-BOARD LOGIC	NIL DUE TO ON-BOARD LOGIC	FALSE ALARM RATES MINIMIZED BY ON-BOARD COINCIDENCE TESTS AND DATA PROCESSING.
SIZE AND HEIGHT (+30%)	2 m x 2 m (AREA) 380 lbs.	1.5 m DIA x 1 m L 510 lbs.	0.3 m DIA x .6 m L 130 lbs.	SIZE DETERMINED PRIMARILY BY ANTENNA OR TELESCOPES.
OPERATIONAL EXPENSE	ESSENTIALLY THE SAME FOR ALL SYSTEMS; GROUND STATION SUPPORT, TRANSMIT COMMANDS, ETC.			OPERATIONAL EXPENSE DEPENDS ON COMPLEXITY/VERSATILITY AND DATA RATE OF INSPIRENT.

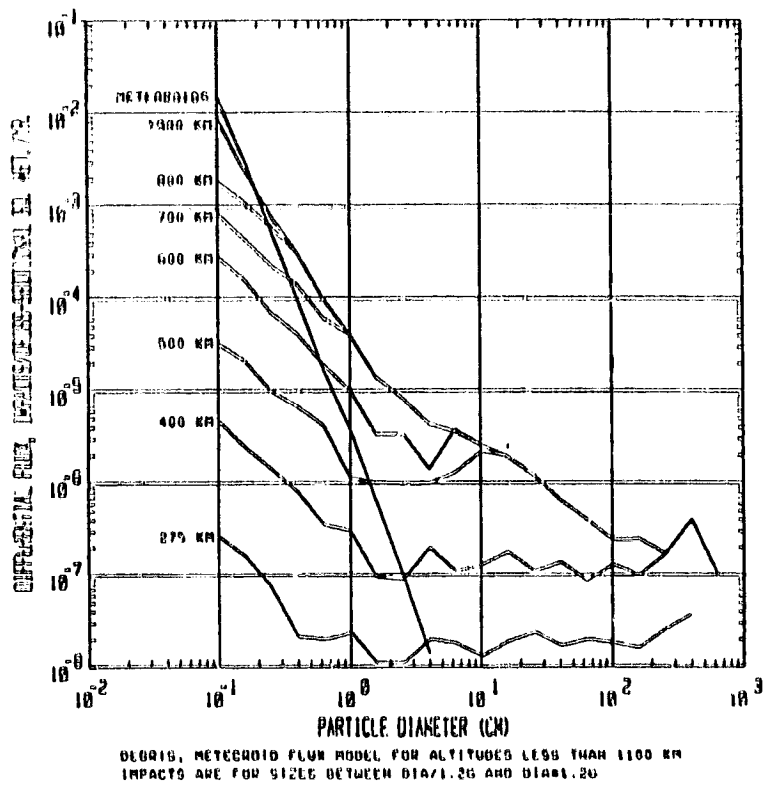


Figure 1

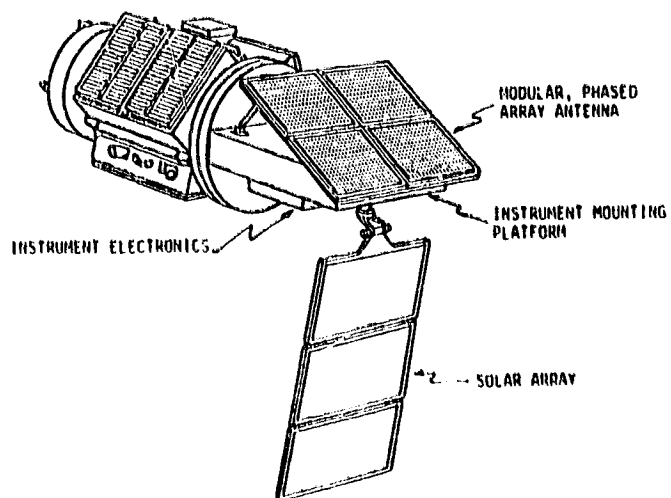


FIGURE 2. RADAR DEBRIS DETECTION SYSTEM SHOWN ON AN IRLS BASED SPACECRAFT.

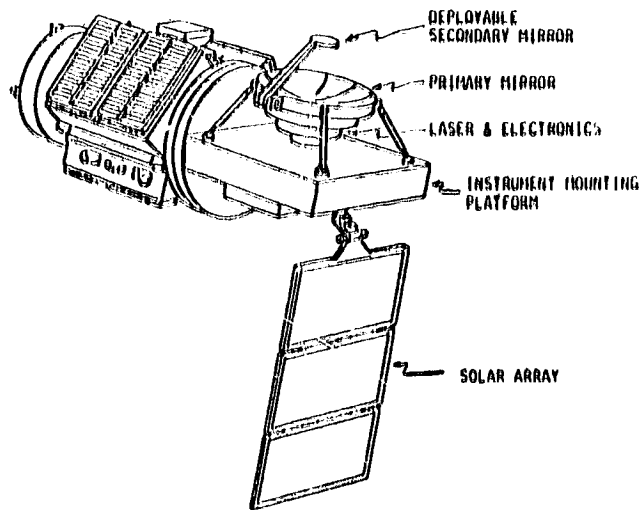


FIGURE 3. LIDAR DEBRIS DETECTION SYSTEM SHOWN ON AN MMS BASED SPACECRAFT.

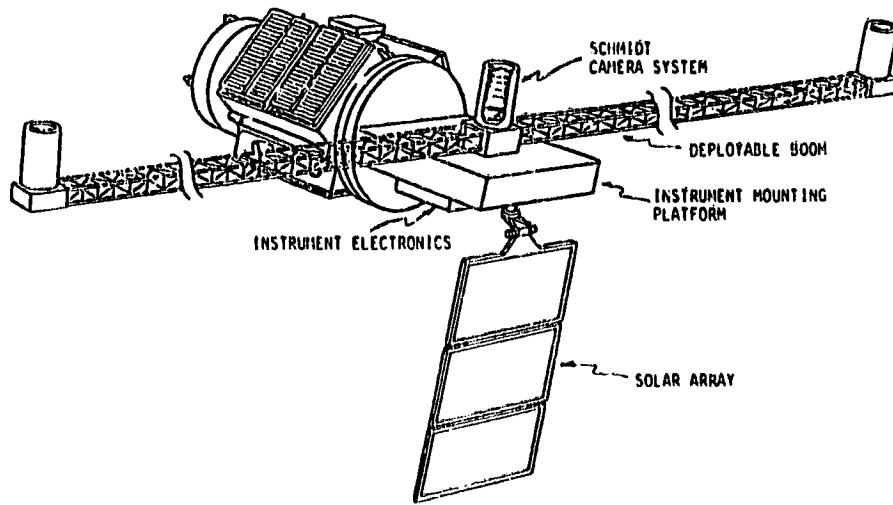


FIGURE 4. PASSIVE OPTICAL DEBRIS DETECTION SYSTEM SHOWN ON AN MMS BASED SPACECRAFT.

D11-12
N 85-21199

Preliminary Design of an Earth - based
Debris Detection System Using Current
Technology and Existing Installations
T. H. Morgan

Since 1958 there has been a slow, but steady, increase of the population of manmade debris. Some of this increase represents break up into many parts of older payloads and rocket bodies which may be in the future somewhat alleviated by better payload design and construction as well as operational management. An overall increase in the use of space by all countries will still lead to a non-negligible debris hazard. Assessment of this hazard requires at least that the population of debris down to mm sizes be determined (both for near-Earth orbits and near-stationary points). It may also be necessary to obtain reasonable orbits for a statistically significant sample of the debris population.

Several ground-based techniques for detection are available. Radar detection has been used to obtain our existing debris population information. Another technique which has been discussed in the past is optical detection. A present epoch (1983) discussion of this technique was needed and what follows is a study of the possibilities for optical detection with state-of-the-art instrumentation.

APPROACH

The considerable period of time between sunset at the surface of the earth and sunset at the altitudes characteristic of orbiting debris provides a period of several hours both after sunset and before sunrise each night in which debris can be observed in reflected light. These objects have significant velocities (6 to 7 km/s) relative to terrestrial observers, so fast that these objects are not normally detected by astronomical instruments. Tracking at appropriate rates (0.6-0.8°/sec) and observing repeatedly with short exposures will reveal these objects.

In what follows, a simple instrument based on present-epoch technology for optical detection of orbital debris which we plan to deploy in the near future is described. The limits of detectability at various altitudes and under different operating conditions for this system are assessed. The kinds of information which can be deduced from this data are examined. Optimal systems for debris detection are next discussed. Alternatives and possible improvements from new technologies are also considered.

BASE SYSTEM DESCRIPTION

Detection of faint objects moving rapidly relative to the fixed stars requires an efficient area detector and a large-aperture, fast optical system. The acceptable optical bandwidth should include at least the 0.4 nm to 0.7 nm spectral region which contains the bulk of the solar flux. In practice, the large quantity of data which must be examined per detectable event requires that equal emphasis be placed on data reduction. This includes highly efficient automated modes of data analysis and high density storage capability.

The heart of the system is the detector. The unit chosen is a 25mm square faceplate ISIT camera. This low light level video camera was originally developed by the QUANTEX corporation and is now available from the SCANCO company. This system, already in use at civilian and military observatories, is a low noise and high quantum efficiency area detector with electronic readout. The optical system chosen is a standard night aerial reconnaissance camera with short focal length, large collecting area, and large field of view. Optics with slightly different characteristics may be scaled from the data below. The characteristics of both the optical system and the detector are given in Table I.

TABLE I

FOV: 2.4°	Aperture: 33.5 cm (coll. area = 698 cm ²)
F/#: 1.8	Arc sec/ pixel: 16.8 (2.16x10 ⁻⁵ sq deg.)
Bandpass: 400-800 nm	
Photocathode: S-20	Ave QE: 10%
Transmission: 80%	Background: 330 10th magnitude stars

The video data stream will be fed into both a video tape recorder and a video data processor. The processor will perform a number of functions both in real-time, and away from the observing period. In essence, this system provides image-to-image addition and subtraction and single image enhancement.

LIMITS OF DETECTION

Ideally one should choose the exposure time in order to maximize system performance in a single frame. However, there are many practical reasons to set the exposure time so that the video data conforms to commercial synchronization rates. Here we have chosen the European PAL system which gives us a frame rate of 25 per second. Now the irradiance due to one 10th magnitude star through a 0.4 to 0.7 m passband is 1.31x10⁻¹⁶ w/cm². Thus the total sky background is 4.32x10⁻¹⁴ w/(cm² square degrees). Projecting a single pixel back into the sky gives an irradiance of 2.60 photons/cm².s. Assuming 90% sky transparency, we find for the numbers given in Table I that there 130.5 photoelectrons/pixel and second and 5.22 photoelectrons/pixel and frame. If we assume that the minimum detectable signal S is given by

$$\frac{S}{\sqrt{S + 2B}} = 1$$

Then S is 3.80 photoelectrons/pixel and frame or 6.76×10^{-19} w/cm² outside atmosphere irradiance. Assuming that the image of the object observed falls equally in 4 pixels,

$$\text{flux} = 2.704 \times 10^{-18} \text{ w/cm}^2$$

which roughly corresponds to a 14th magnitude star.

RAPID SLEWING MODE

Slewing rapidly along an arc of a great circle passing through the zenith at a rate matching the apparent angular motion relative to the observer of objects in circular orbit at a given altitude effectively freezes the location of the images of these objects within any frame and from frame to frame. For simplicity, suppose both that one is observing from a near-equatorial site and that the slew direction is directly west to east. Suppose the angular velocity of the slew is $0.813^\circ/\text{sec}$ which corresponds to the relative angular velocity of an object in a circular orbit at an altitude of 500 km above the earth (6870 km from the center of the earth) and with approximately 0° inclination.

An object at 500 km and having an inclination within approximately 30° of the preferred inclination will fall into at most 4 pixels and most of these will fall into only 1 in one frame. Particles at 375 km will move three pixels forward during one frame, and particles at 850 km with appropriate inclinations will move backward three pixels in one frame. These two are limiting cases, for all altitudes in between experience less than three pixels per frame relative motion. Our limiting cases will illuminate at most 18 pixels (5×2) and generally only 4 pixels (4×1). A star will illuminate at most 18 pixels (9×2). It should be noted that star centers will move by almost 7 pixels from frame to frame, and stars are thus easily

separated from the debris images using simple frame to frame subtraction and background subtraction techniques. One should note here that these differences would be difficult to detect with an emulsion based data storage system.

The limiting flux detectable in a single frame for a given altitude can be determined by multiplying the minimum detectable signal by the number of pixels illuminated. Thus, for an object at 850 km with an acceptable inclination, one finds that the worst case flux is

$$6.76 \times 10^{-18} \text{ W/cm}^2;$$

and the best case flux is

$$2.70 \times 10^{-18} \text{ W/cm}^2.$$

The debris particles will be modeled by assuming them to be Lambertian spheres of albedo 0.5. For convenience the sun-debris-observer angle will be 90° . If I_0 is the solar irradiance over the bandwidth, X is the geometrical cross section, and R is altitude of the debris, then the flux is

$$I_x = \frac{0.034XI_0}{R^2}$$

The bandpass chosen includes 0.59 of the total solar irradiance (0.14 watts per cm^2), thus

$$I_x = 2.81 \cdot 10^{-3} \frac{X}{R^2}$$

Using the limiting flux value $6.76 \times 10^{-19} \text{ w/cm}^2$, we find on solving for X/R^2 that

$$\frac{X}{R^2} = 2.4 \cdot 10^{-2}$$

where X is in cm^2 , for convenience, R is in units of 100 kms (thus R would be 5 for an object 500 km above the Earth). The resulting cross sections and diameters for various altitudes are given in Table II.

TABLE II

Altitude	Pixels Illuminated	Cross Section cm^2	Dia.
800 km	10	6.14	4.43 Cm
800	4	2.40	2.8
500	4	0.60	1.75
500	1	3.84	0.875
400	10	1.536	2.20
400	4		1.41

Assuming a 4 arc second image width, the relative number of images filling 1 pixel to all images (the case 500 km altitude) can be determined--it is 0.3. The same considerations for the "worst case" altitudes give for the ratio objects illuminating two pixels to all objects 0.3 also. As each object should appear in many frames, any particle debris with the limiting cross section will in a few frames illuminate the minimum number of pixels and, thus, be detectable. Such particles will appear to "blink" in and out through the slew. The available volume from the region 375 to 850 km is $3.15 \times 10^5 \text{ km}^3$. The span of inclinations available depends on the criteria for detection. In one frame the available number of inclinations comes from asking what portion of the population has a velocity along the scan direction sufficiently large to maintain a motion of .544 pixels. This is a 10% for

500 kms and rises to 0.16 for particles at a 375 kms. The number decreases slowly from 500 to 850 km. For an average value one might take 10%. Thus the number of events per scan assuming 10^{-7} particles per km^3 ($d \geq 1$ cm) average over the 375 to 850 km range is

$$3.15 \times 10^5 \times 0.1 \times 10^{-7} = 3.15 \times 10^{-3} \text{ Acquisition field}$$

The continued observation along the slew direction does little to alter this probability; to improve the acquisition rate one must slew many times (observe many fields). A continued observation along a slew direction does provide three advantages. First, the limiting signal to noise for objects at the design altitude and inclination can be markedly improved by addition of frames (by the square root of N, with N the number of frames); second, the identification for any faint object is more certain by virtue of observation over many frames; third, the inclination of the object can be determined. In theory data based on very long slews (90°) could be used to completely determine the orbital parameters of the debris. However, the determination would be based on only 2.2% of the orbit.

Assume that the system slews for periods of 13 seconds at a time at a rate of $0.813^\circ/\text{second}$ producing an effective arc of 10.4° length centered on the zenith. Assume 2 seconds reverse time and the next slew in the opposite direction. There are then 4 slews a minute. Thus for a 45 minute observing period, the total probability of detection with N equal to 10^{-7} particles/ km^3 is

$$4 \times 45 \times 3.15 \times 10^{-2} = 0.55 \text{ acquisitions/evening,}$$

The 45 minute period is based on observations at an equatorial site beginning when the sun is 6° below the local horizon. By simply adjusting

the rate the system could be used there after maximized for successively larger altitudes. An observing plan so designed might expect to double the number of acquisitions. One should therefore expect

1.1 acquisition/Evening

One can of course, repeat these observations in the early morning hours using successively larger slew rates as morning comes.

One should note here that the capabilities of the video data system enter into the discussion above only for particle identification and determination of approximate orbital characteristics. The considerable gains possible in threshold detection from summation of frames have not been considered in the threshold calculation or in the acquisition rate determination.

STATIC OPERATIONS

Suppose that the instrument is pointed upward toward the local zenith and fixed. In one 0.04 sec exposure the image of an object at 400 km moves 9 pixels but the image of one at 1600 km moves only 3 pixels--the stars are effectively frozen moving only 1 pixel after 28/frames. The simplest criterion possible may be used for detection (one easily accomplished with modern video image processors); namely, whether an image "moves" from frame to frame. In addition, the debris images will be elongated. An object in a circular orbit at 400km altitude will cover at most 22 pixels (11x2), and in some frames, only 9; at 500km, this becomes 18, and in some frames 7; at 1600km, one finds 8, and in some frames 2. All possible inclinations are included.

The volume of space accessed in one exposure has the figure of a truncated pyramid whose bases are areas on the surface of a sphere bounded

by four arcs of great circles with each arc of equal length. The spheres are centered on the observer and the radii are the limiting altitudes given above. A simple differential volume element of the observing volume is a section of a spherical shell of radius z and thickness dz bounded by 4 arcs of great circles each $\alpha_0 z$ kms in length where α_0 is the field of view in radians. The number of particles per unit time passing through the small volume element of thickness dz and length on a side of z is:

$$nV(\alpha_0 z)dz$$

where V is the "circular" velocity of the debris, r_0 the radius of the earth, the FOV in radians, z the height above the earth, and n the particle density per $(\text{km})^3$.

In a time t the number of particles which enter the slab element is

$$nV t (\alpha_0 z)dz$$

Note that V is just

$$V = V_0 \sqrt{\frac{r_0}{r_0+z}}$$

where V_0 is 7.91 km/s.

For all the particles observed then one has

$$N = n V_0 \alpha_0 T \sqrt{r_0} \int_{z_1}^{z_2} \frac{zdz}{r_0+z}$$

Where T is the total observing time (taken to be 3600 seconds) with a change of variable to the distance from the center of the Earth to the region of integration (simply $r_0 + z$), one finds

$$N = n V_0 \alpha_0 T \sqrt{r_0} \left[\frac{2}{3} (h_u^{\frac{3}{2}} - h_1^{\frac{3}{2}}) + \frac{r_0}{2} (h_u^{\frac{1}{2}} - h_1^{\frac{1}{2}}) \right]$$

Over a region stretching from 6770 km to 7970 km this gives

$$N = 2.89 \times 10^{+9} n$$

For n equal to $10^{-9}/\text{km}^3$ this is

2.89

detections.

While the minimum detectable diameters in a single frame has been increased by a factor of 2.6 at 500km to 2.31 cm, it has not increased appreciably for larger altitudes. Further, more sophisticated multi-frame analysis techniques can be expected to recover much of the lost sensitivity. On the average, a particle in a circular orbit at 500 km will be imaged 56 times. Thus 4 or 5 marginal detections along a straight line may be sufficient for a positive identification.

One should note that meteor trails will be clearly unlike debris. A 20km/s meteor at 100 km would produce a 135 pixel trail on a single frame.

LIMITS OF OPTICAL DETECTION

An ideal optical system must:

1. Have sufficient collecting area and transmission to allow detection of the desired limit in one frame (here taken to be 0.04 seconds).
2. Be sufficiently fast to optimize the conflicting requirements of large field of view and effective pixel size when projected onto the sky.

3. Have a flat field over the field of view.

We shall for this discussion assume a detector which provides 20 pixels per mm and an average quantum efficiency of 10 percent. We shall further assume Lambertian scattering from a spherical particle of diameter d with albedo 0.5, distant R from the Earth's surface with a sun-object-observation angle of 90° . The sky background as before is 330 10th magnitude stars per square degree. The first condition above controls telescope diameter; the second, the f-number.

Under the assumptions above one finds that

$$I_{\text{obs}} + 2.171 \times 10^{-17} \left(\frac{d}{R}\right)^2 \text{ in } \frac{W}{\text{cm}^2}$$

where as before d is the diameter of the debris and R is altitude in units of 100 km. If one assumes that the product of collecting area as a percent of the geometrical collecting area, the instrument transmission, the sky transmission, and the quantum efficiency to be 0.0576, one has

$$\text{Flux producing photoelectrons} = 0.0452D^2 I_{\text{obs}}$$

where D is the telescope diameter. Thus,

$$\frac{\text{Number of photoelectrons}}{\text{pixel and frame}} = \frac{0.1098 d^2 D^2}{R^2}$$

For $d = 1$ cm and $R = 10$ (1000 km)

$$\frac{\text{Number of photoelectrons}}{\text{pixel and frame}} = 1.098 \times 10^{-3} D^2$$

One must now determine the minimum detectable signal in photoelectrons per pixel and frame. For purposes of argument let us set this number as 5 which should be valid for any detector system under consideration. Then,

$$D = 67.5 \text{ cm}$$

This result may be used as a scale factor for comparison to other systems. The practical limit to telescopic detection from the ground is about 2mm at 1000km altitude. To go to 1mm would require a collecting area slightly more than 6 meters in diameter. Two caveats are necessary. First, image processing of multiframe data could push down the detection limit by lowering the single frame signal required. Second, multimirror designs for large telescopes which give large effective collecting areas are under investigation by at least three groups in this country.

The background present in an individual detector element is controlled by the focal length. If we require that

$$\frac{S}{\sqrt{S + 2B}} = 1$$

where S is the signal, then B can be as large as 10 photoelectrons/pixel and frame. Using 4.32×10^{-14} watts per cm^2 per square degree and remembering that the sky subtended by one pixel is $8.208 \times 10^{-2}/(f\text{-number} \times D)^2$, we find that the minimum value is

$$f\text{-number} = 1.30$$

One should remember that a larger f-number improves the noise per pixel at the expense of field of view.

Instruments of half-meter diameter with f-number as small as 1.3 and

acceptable curvature of field have been constructed. Astronomical instruments with 1 meter aperture are generally no faster than 1.8. For diameters beyond 1 meter an optical system with f-numbers as small as 1.8 and flat-focal plane of 40cm presents a significant technical problem. If the f-number requirement is relaxed to 2.5 to 3.5, however, a number of optical approaches are possible--Richey Chretien systems, Schmitt optics with a curved focal plane of sufficient radius to be negligible over 40mn, and standard parabolic systems at Newtonian or prime focus with field correctors. Systems using parabolic primaries and field correction should be examined in more detail.

POSSIBLE OBSERVING SITES

Maximum utilization of rapid slewing instruments over any one night requires that measurements continue as long as a portion of the observable sky volume is in sunlight. In short, one needs a site which has dark sky to horizons. Remarkably few developed observing sites in the continental United States meet this requirement. For example, the Kitt Peak and University of Arizona observatories both suffer from the growing problem of the Tucson light dome. Nor do there appear to be any developed sites in California which are dark to the horizon. There are developed sites in West Texas, New Mexico, and Wyoming with very dark skies, however all three suffer from the Western U.S. weather patterns which limit the number of usable nights per year. The best sites for this work available to U.S. observers are the observatories on Maui (USAF & UH) and on Hawaii (IRTF, UH).

FUTURE IMPROVEMENTS IN DETECTORS

The low light level television system is a mature technology. It would appear to be difficult to push these cameras to larger effective areas. Two developing detectors which could provide larger effective areas are charge coupled devices (CCD) and multi-anode microchannel arrays (MAMA). The largest commercially available CCD is an 800x800 array. However, there are ongoing efforts at GSFL to construct "mosaics" of the arrays to give very large detector areas. These devices have already been used both for astronomical and military observations. The MAMA systems are now approaching 1024x1024 in the laboratory, and smaller arrays have been used in both astronomical, and military applications. At present these systems have approximately the same number of pixels per cm as the low light level cameras. Thus they offer the advantage of larger effective fields of view. The present indications are that the MAMA technology will produce the greatest sensitivity.

V12-22

Use of Ground Radar to Detect Reentering Debris
Jeanne Lee Crews
NASA/Johnson Space Center

N 85-21200

During STS-3, a VHF phased array radar was set up at JSC. The radar was operated in conjunction with the electron beam experiment onboard STS-3. The dimensions of the radar antenna array are shown in Figure 1.

The radiation patterns for the radar are shown in Figure 2 and Figure 3. The 30° elevation angle was chosen to optimize the ionospheric measurements.

The wavelength of this radar is 6 meters, which makes it very sensitive to ionization trails produced by high speed particles entering the atmosphere. These trails show up clearly on the radar display scope.

During the observations of the Shuttle, it was noted that the frequency of these ionization trails (events) increased near the time the Shuttle crossed the radar beam. A representative example is shown in Figure 4. The arrow represents the actual time the Shuttle was acquired by the radar.

Figure 4 shows an increase of event frequency approximately 4 minutes after acquisition of Shuttle (AOS). Some of the data runs have the peak event frequency occurring prior to AOS but in all cases it occurred within $\sim \pm 5$ minutes of AOS.

To identify the type of particles producing the ionization trails (meteoroid or orbital), the velocity of the particle is required. Meteor science has developed a method of approximating the velocity of a meteor from radar data. This method requires the time between the spacings of the Fresnel interference fringes, the range to the ionization trail, and the wavelength of the radar system. Figure 5 shows a plot of the radar echo versus time from which an approximate velocity of 7km/sec was calculated. This velocity is indicative of an orbiting particle reentering the atmosphere.

Since the frequency of events increases near AOS, are the particles in some way associated with the Shuttle? A partial answer to this question involves evaluating the orbital mechanics of the problem; that is, if the particles originate with the Shuttle, will orbital mechanics substantiate the relative position of the particles (as they reenter the atmosphere) with the position of the Shuttle (in orbit)?

A program for determining spacecraft orbital decay due to perturbations (primarily drag) was utilized for a preliminary evaluation of the orbital mechanics of the problem.

Many assumptions concerning the size, shape, density, etc. of the particles were necessary for the preliminary evaluation. These assumptions are shown in Figure 6. The particles were each started at a position in the Shuttle orbit and allowed to decay to an altitude of 100km (this altitude was chosen as a representative reentry altitude; a lower value may be more realistic and will be evaluated).

The results of this program are shown in Figure 7. The orbital lifetime of the three particles is short enough that they essentially remain in the Shuttle orbital plane.

The difference in argument of latitude (ΔU) shows the angular (or time) difference (in the orbital plane) between the particles at reentry (t_0) and the Shuttle's orbital position at t_0 .

These results, although preliminary, do not negate the possibility that the events being observed by the radar may be reentering particles originating from the Shuttle.

A dedicated radar will be built to further investigate the reentering debris problem. It will have a more powerful transmitter and a higher pulse rate than the present radar. This radar will be operated during the upcoming Shuttle missions and the data will be correlated with onboard events to try to identify the origin of the particles.

A rigorous orbital decay analysis will be made for very small particles with various sizes, shapes, and densities to provide a theoretical model with which to assess the radar data.

Comparison of the Shuttle debris data will be made by observing other spacecraft with the radar.

The results of this study will be incorporated into the orbital debris math model.

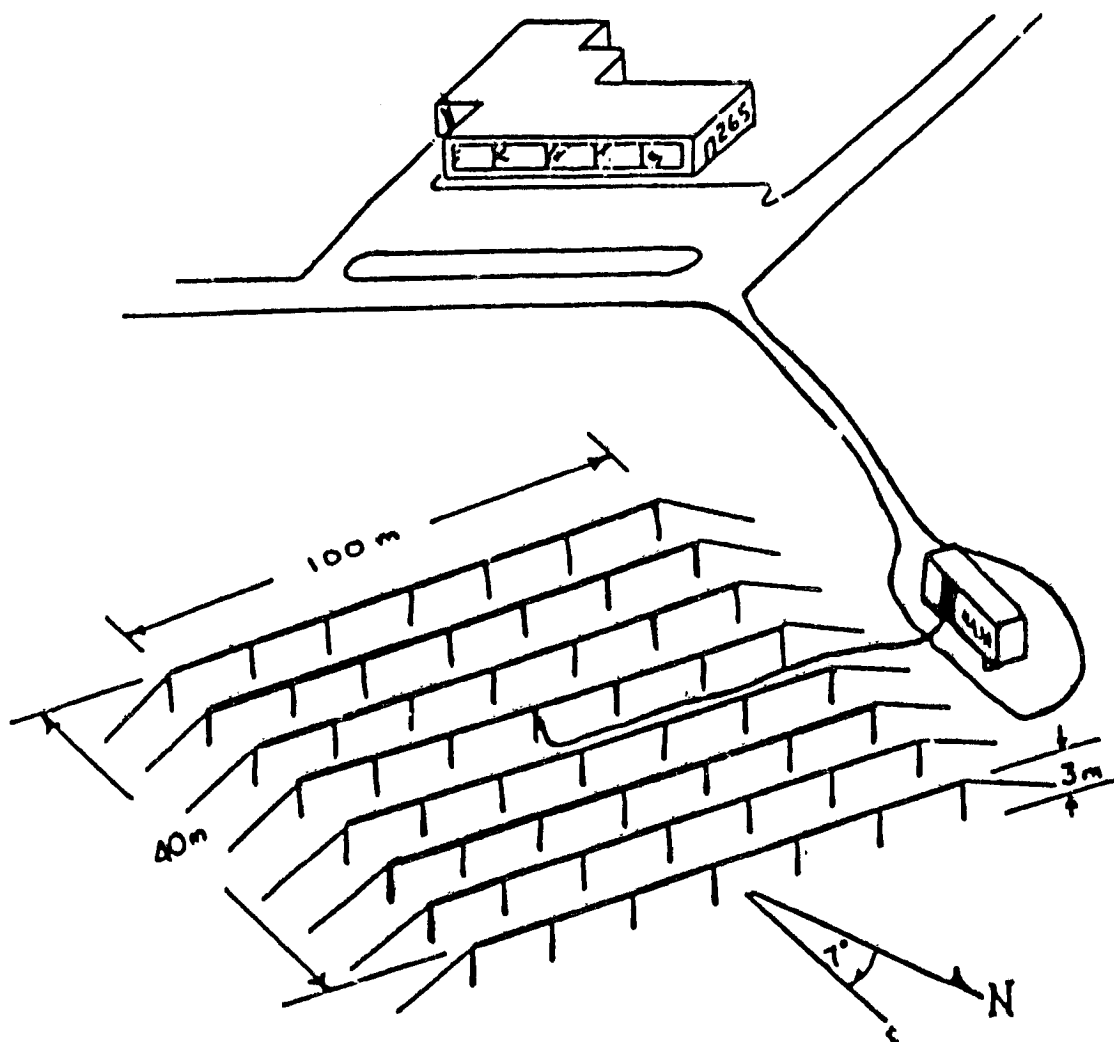


FIGURE 1

NASA/JSC 50 MHz ANTENNA ARRAY FOR STS-3

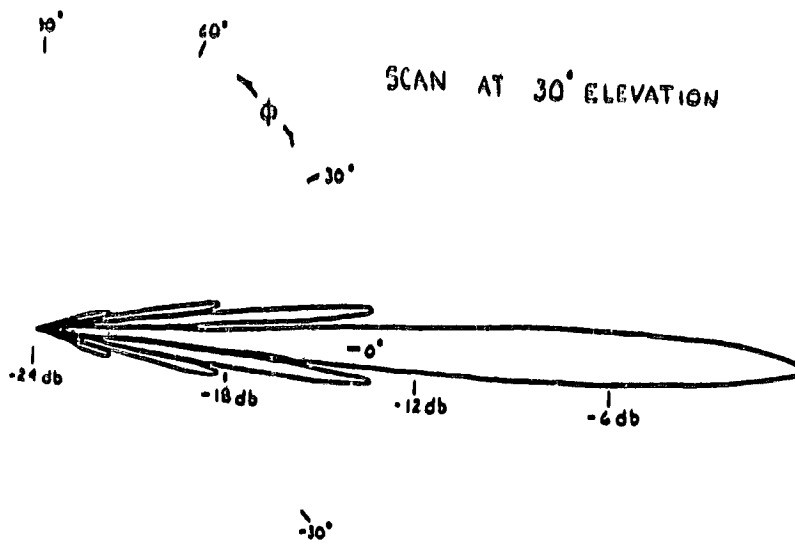


FIGURE 2

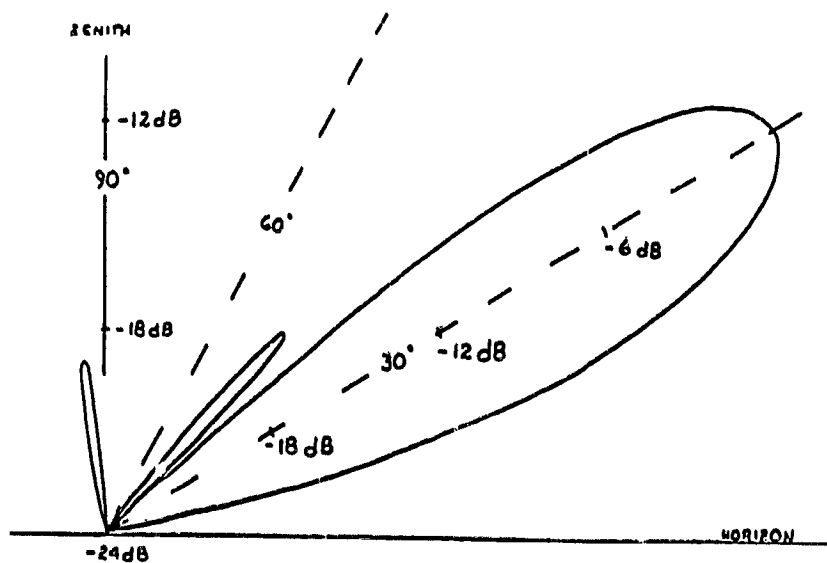


FIGURE 3

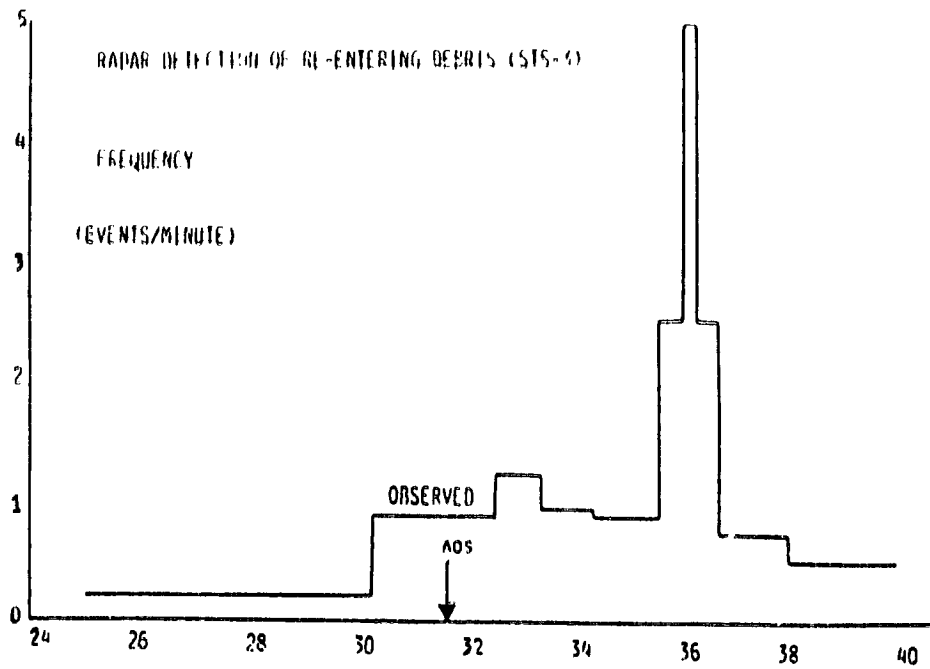
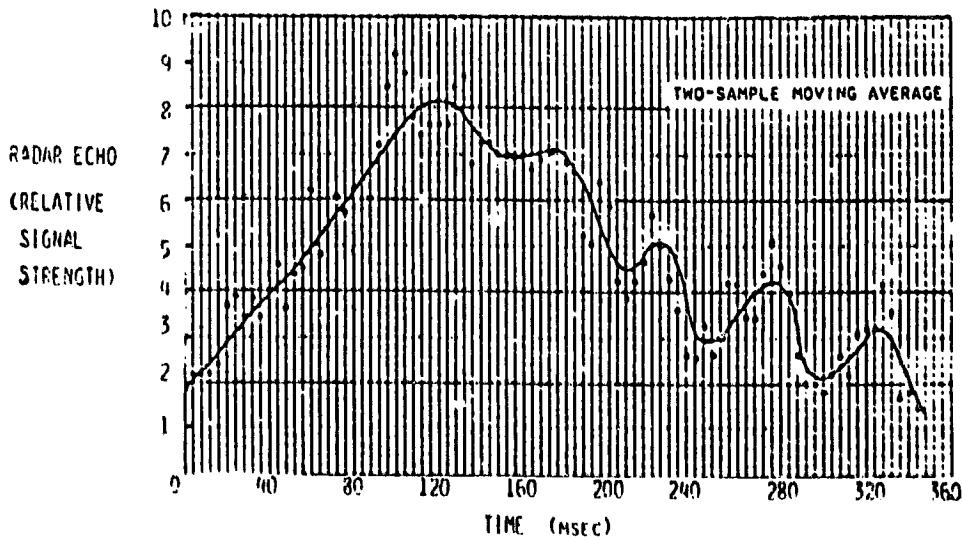


FIGURE 4 - TIME (MINUTES).

STS-3 EVENT 1 (GMT 07:13:30:16)

RANGE ~150 KM

VELOCITY ~7 KM/SEC*



* VELOCITY CALCULATED FROM SPACING OF FRESNEL INTERFERENCE FRINGES IN RETURN
RADAR SIGNAL (50 MHz)

FIGURE 5

0 LIFETIME OF PARTICLE - FROM SHUTTLE ORBIT TO 100KM

0 RELATIVE POSITION OF SHUTTLE AND PARTICLE (WHEN PARTICLE AT 100KM)

ASSUMPTIONS

0 SPHERICAL PARTICLES

0 $C_D = 2.2$

0 $\rho = 1 \text{ G/CM}^3$

0 $R_1 = .1\text{MM} ; M_1 = 4.2 \times 10^{-6} \text{ G}$

0 $R_2 = 1\text{MM} ; M_2 = 4.2 \times 10^{-3} \text{ G}$

0 $R_3 = 1\text{CM} ; M_3 = 4.2 \text{ G}$

0 INITIAL VECTOR SAME AS STS-3

FIGURE 6

<u>PARTICLE RADIUS</u>	<u>LIFETIME (τ_0)</u>	<u>ΔU_0 AT τ_0</u>
.1MM	34 ^M 50 ^S	-0.053 ^O (.03 ^S)
1MM	1 ^M 56 ^M 16 ^S	3.4910 ^O (52 ^S)
1CM	13 ^M 30 ^M	23.0444 ^O (5 ^M 43 ^S)

ΔU_0 = DIFFERENCE IN ARGUMENT OF LATITUDE OF STS-3 AND PARTICLE AT τ_0

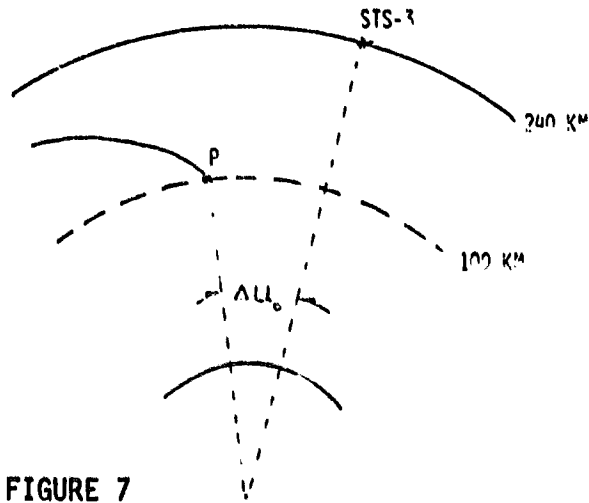


FIGURE 7

PLANNED ACTIVITIES

- 0 BUILD NEW RADAR
 - INCREASED TRANSMITTER POWER
 - INCREASED PULSE RATE

- 0 OPERATE RADAR DURING SHUTTLE FLIGHTS
 - CORRELATE DATA WITH ONBOARD EVENTS TO TRY TO IDENTIFY PARTICLE ORIGIN

- 0 DEVELOP COMPUTER MODEL FOR ORBITAL DECAY OF SMALL PARTICLES OF VARYING SHAPE, DENSITY, ETC.
 - COMPARE WITH RADAR DATA
 - DETERMINE LIFETIMES

- 0 OPERATE RADAR DURING OTHER SPACECRAFT CROSSINGS
 - COMPARE WITH SHUTTLE RESULTS

- 0 INCORPORATE RESULTS INTO DEBRIS MODEL

FIGURE 8

PARTICLE SIZE, NUMBER, COMPOSITION AND VELOCITY FROM SOLID ROCKET MOTORS

By

Barney B. Roberts

NASA Johnson Space Center

Houston, Texas

N 85-21201

BACKGROUND

NASA/JSC became involved in this issue because of the damage potential to the Space Shuttle Orbiter caused by the high velocity particles contained in the exhaust plume of an upper stage. Initial estimates of the damage resulted in Orbiter upper stage separation distances of 80 nautical miles (worst case). To achieve this separation required a ΔV of 80 ft/sec which could represent a payload penalty of 3,500 lbs. Figures 2 through 5 illustrate the analysis and impact of these particles on the separation maneuver. This information is furnished as background. The items of interest to this report are, more specifically, the particle size distribution and composition, the velocity of the particles and the expected contribution from Shuttle launched upper stages.

PARTICLE SIZE DISTRIBUTION

The original estimates were based on historical data for the Al_2O_3 particles and conservative estimates for the carbon particles (i.e., all carbon in each of eight large size "slots") (see figure 6). Subsequent to the original estimates, test measurements were made in the plume of actual upper stage motors during performance testing at the Arnold Engineering and Development Center (AEDC). The test results were different than the original assumptions. The carbon particles were very small $\sim .5\mu$ in diameter and the Al_2O_3 was more sharply peaked (see figure 7). All test measurement techniques are size selective, therefore, it is risky to say that the AEDC test results are an accurate representation of the actual particle distribution. JSC's best judgment is that the actual distribution is somewhere between figure 6 and figure 7 except for the carbon particles. Since the equipment demonstrated its ability to collect larger particles (i.e., Al_2O_3), it is very unlikely that there are carbon particles larger than $.5\mu$.

PARTICLE VELOCITY

Figure 8 shows the particle velocities as determined by the best available plume computational technique. The figure demonstrates the difference between the original distribution and the AEDC distribution. This figure and figure 7 show that most of the particles have a velocity of 10,000-12,000 ft/sec with respect to the upper-stage. To determine absolute velocities, refer to figure 10 where it is noted that upper-stages will be launched from 160 n.mi. circular orbits. This gives an initial upper-stage velocity of 25,300 ft/sec and the upper-stage burn will be postgrade with the particles being retrograde. The upper-stage ΔV will be 8,000 ft/sec for a burn to geosync, and figure 9 shows the angular distribution of the particles. In summary, all this adds up to the fact that many particles will reenter; however, a substantial number will remain in orbit and contribute to a growing population.

EXPECTED CONTRIBUTION

The Shuttle is scheduled to launch approximately 135 upper-stages over its lifetime. Looking at the currently scheduled flights and averaging over a yearly basis yields the contribution of particulates from the upper-stages. Figure 10 shows that, on the average, 91,045 lbs of Al_2O_3 will be ejected on each launch. The analysis to determine how much of this 91,045 lbs will remain in orbit or the decay rate is yet to be accomplished.

PARTICLES SMALLER THAN 1 MM

OUTLINE

- 1. PLUME-PARTICULATE DAMAGE ANALYSIS**
- 2. PLUME-PARTICULATE PROPERTIES**
- 3. PROJECTION FOR FUTURE**
- 4. PROPOSED EXPERIMENT**

Figure 1. Outline.

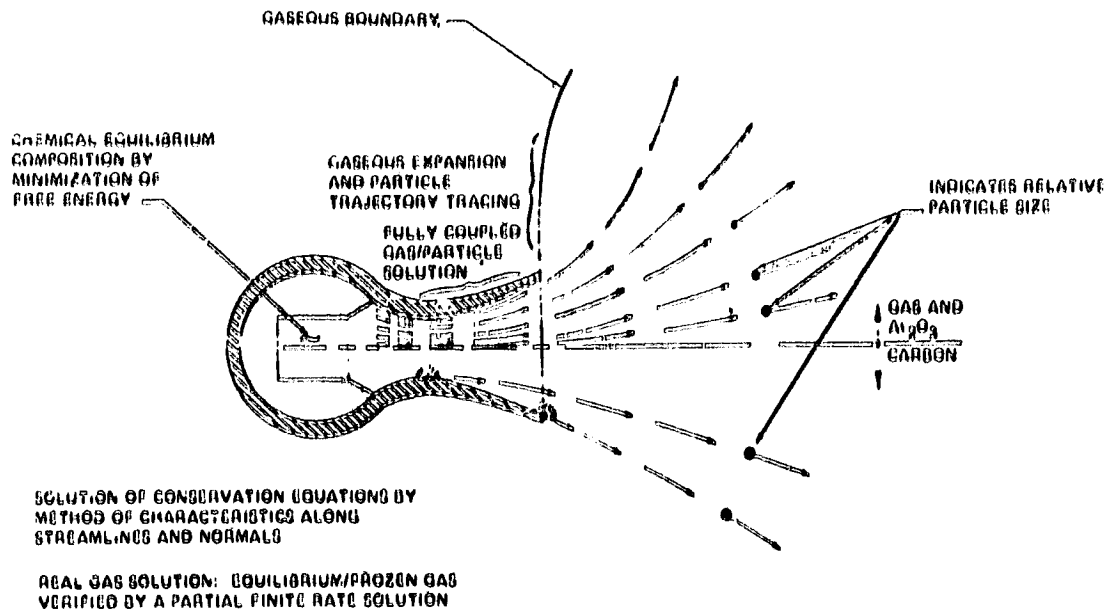


Figure 2. State-of-the-art in plume analysis: solid.

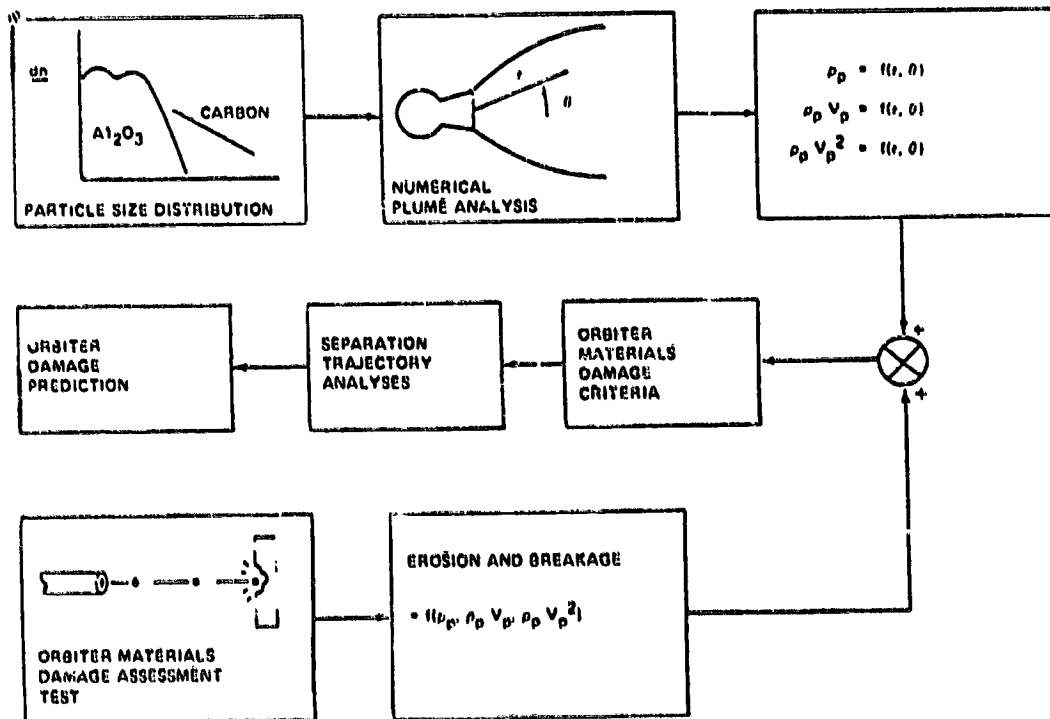


Figure 3. IUS/Orbiter damage prediction.

ORIGINAL PAGE IS
OF POOR QUALITY

IUS IGNITION CONDITIONS

PROPELLANT LOAD = 21400 LB
GRABER WEIGHT = 24025 LB
PITCH = 4.2 DEG, YAW = 0

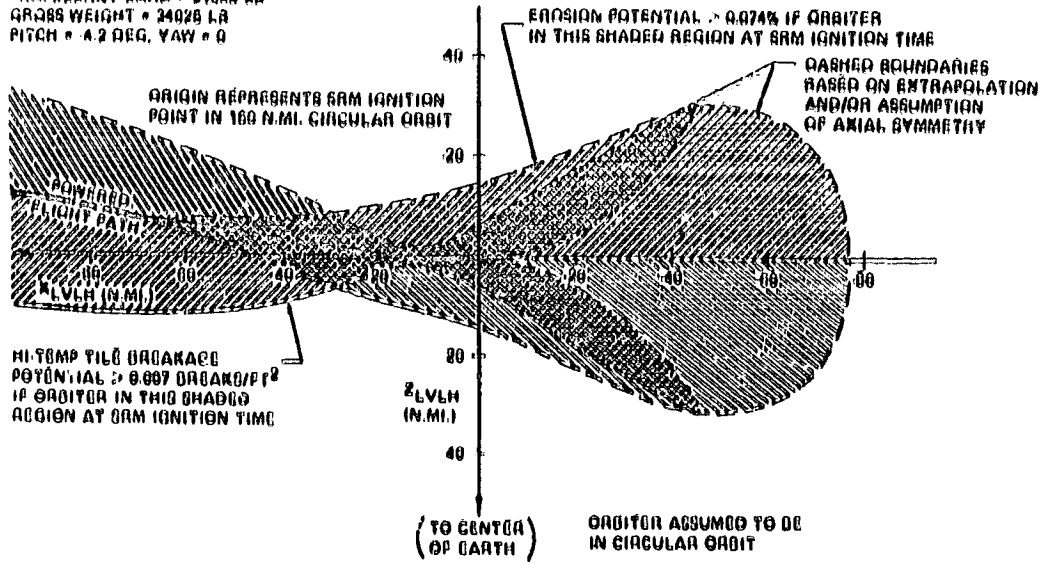


Figure 4. Region of excessive hi-temp tile damage potential in IUS deployment orbit plane.

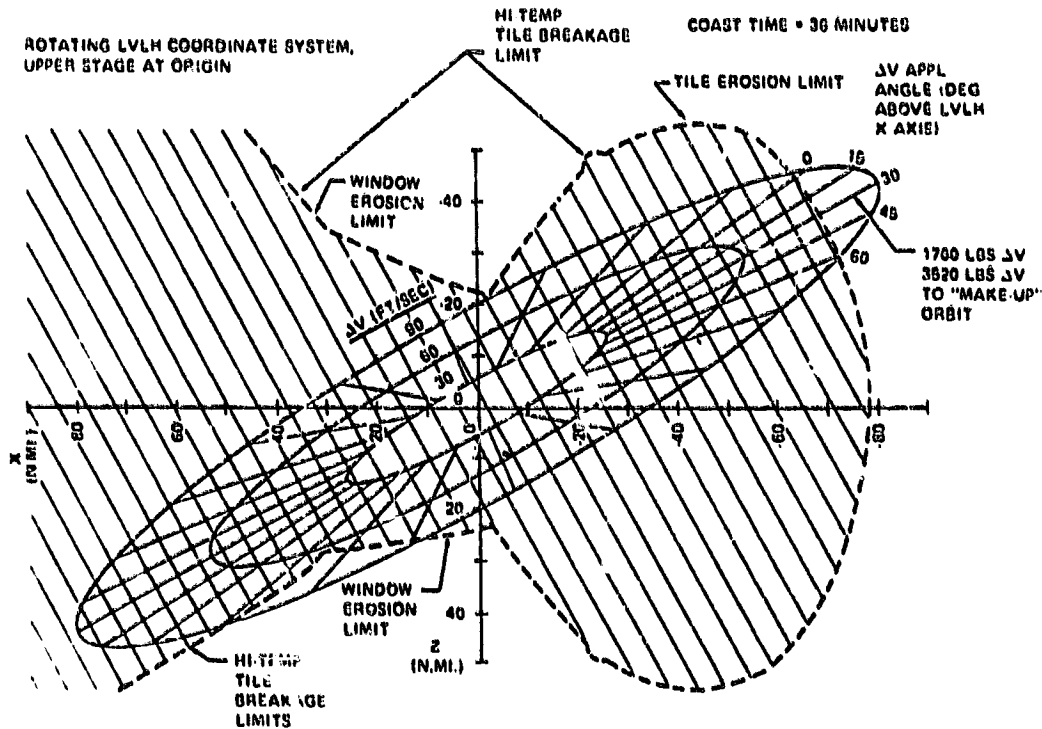


Figure 5. IUS Excessive damage region (with ± 30 degrees pitch variation) superimposed on orbiter accessibility contours

ORIGINAL PAGE IS
OF POOR QUALITY

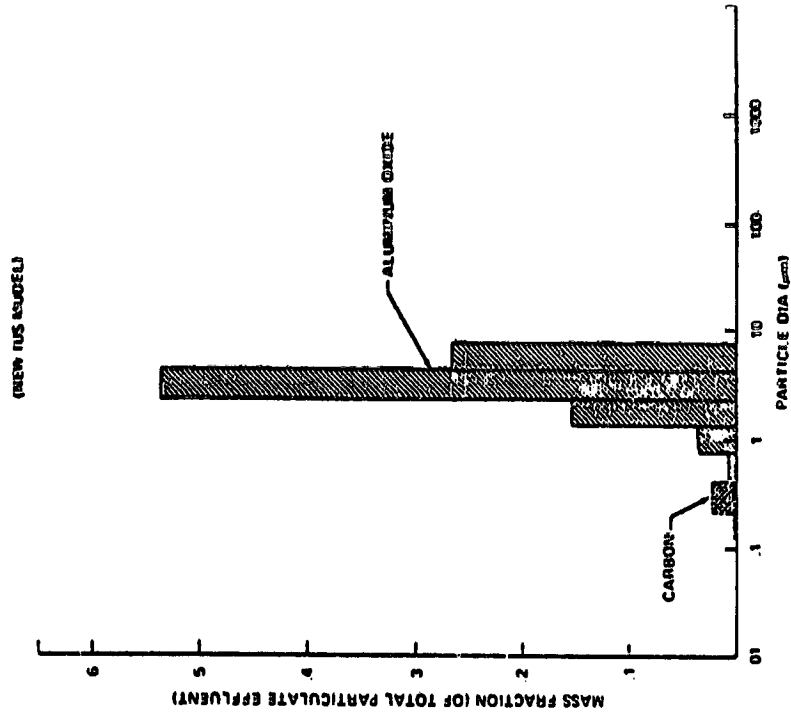


Figure 7 - Particle Mass Fraction vs particle diameter, New IUS Model

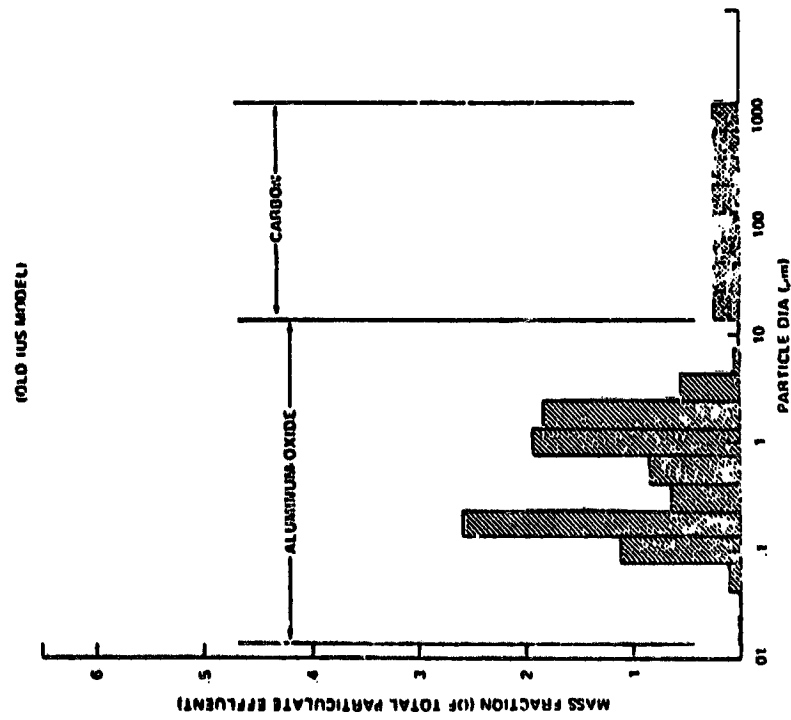


Figure 6 - Particle Mass Fraction vs particle diameter, Old IUS Model.

C-3

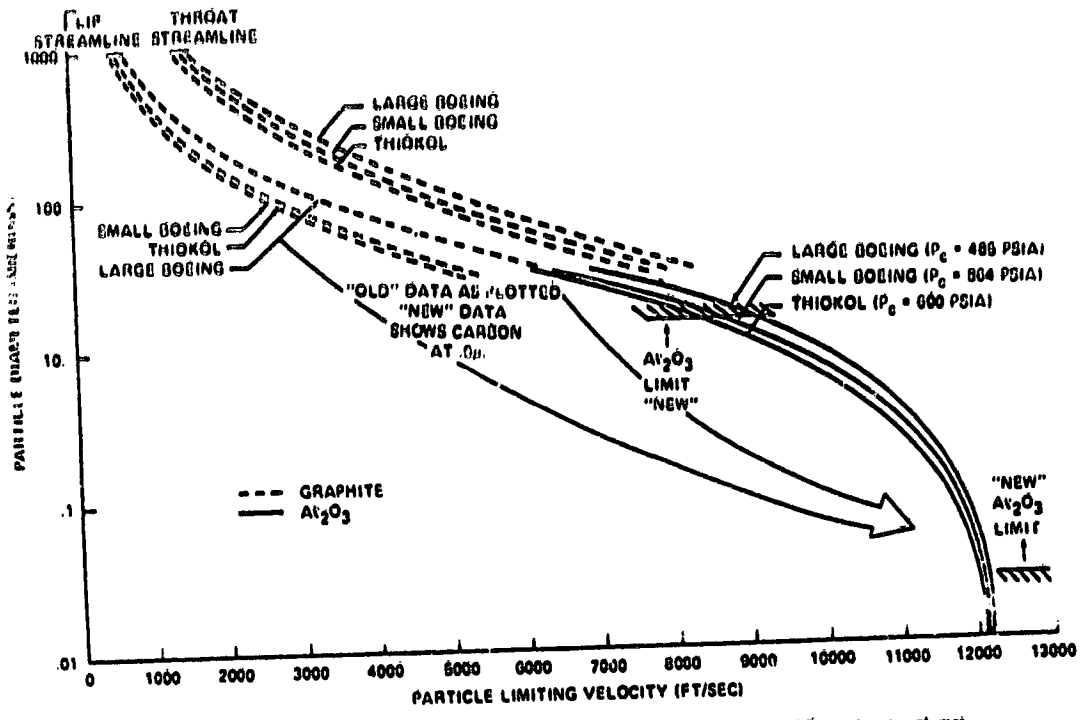


Figure 8. Particle limiting velocity vs. particle radius for large Boeing, small Boeing and Thiokol motor plumes.

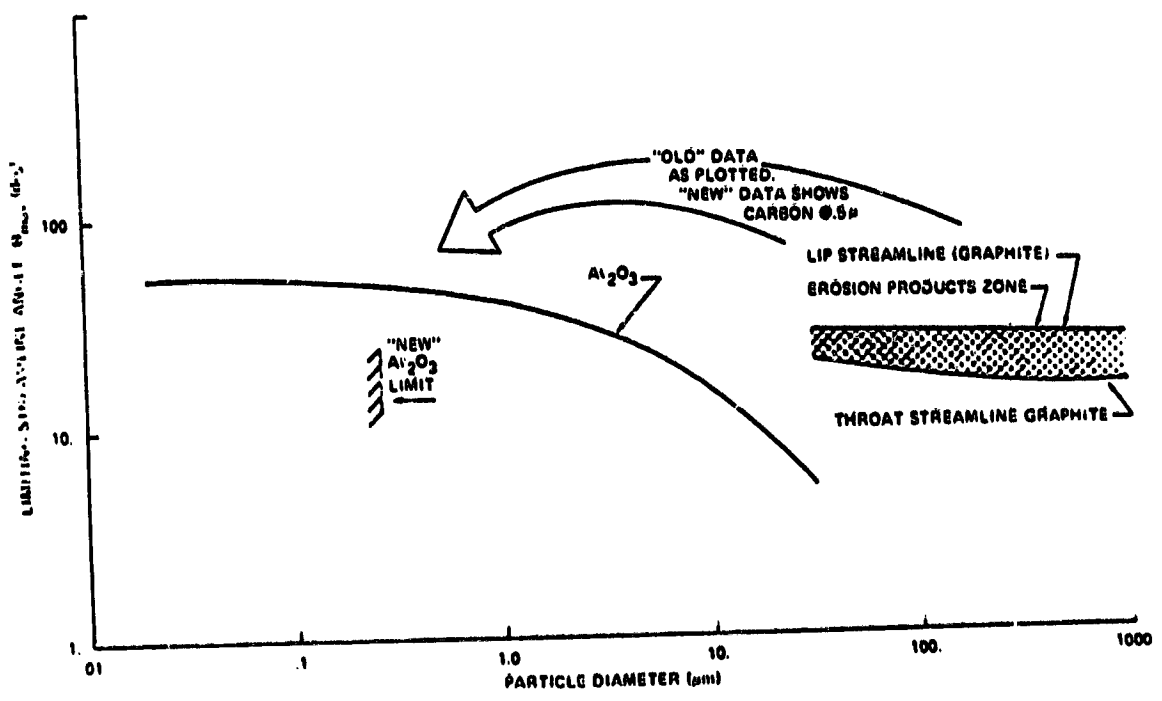


Figure 9. Particle limiting streamline angle vs. particle size for large Boeing motor.



• PROJECTED AVERAGE LAUNCH RATE AND EJECTED $A_{12}O_3$ LBS

MISSION MODEL	SUSS-A	SUSS-D	IUS	TOTAL
LO - 24 FLTS/YR	9,560	20,735	24,708	55,002
NOM - 40 FLTS/YR	15,934	34,558	41,153	91,645
HI - 60 FLTS/YR	23,901	51,836	61,770	137,507

• TOTAL YEARLY CONTRIBUTION

- 137 KLBS $A_{12}O_3$
- INCLINATION 28.5°
- ORBITAL ALTITUDE 160 NM

Figure 10.-Projection for future.

• NASA/JSC IS PURSUING A 2 PHASE EXPERIMENT TO MEASURE UPPER STAGE PARTICULATES

- PHASE I - PASSIVE
 - EXPOSE 4 SQ-FT OF WITNESS SAMPLES TO UPPER STAGE PLUME
 - EVALUATE WITH SEM
 - YIELD ~ PARTICLE ENERGY
- PHASE II - ACTIVE
 - COOPERATIVE EXPERIMENT WITH MAX PLANCK INSTITUTE, HEIDELBERG, FRG
 - MEASURE
 - ENERGY
 - VELOCITY
 - DEDUCE MASS AND SIZE

• STATUS:

- PRELIMINARY PLANNING
- SOME FUNDS MAY BE AVAILABLE IN FY 83
- LETTER OF COOPERATIVE AGREEMENT ON WAY TO NASA HEADQUARTERS

Figure 11.-Proposed experiment.



Hypervelocity impacts on Skylab IV/Apollo windows

Uel S. Clanton,¹ Herbert A. Zook,¹ and Richard A. Schultz²

¹Geology Branch, NASA-Johnson Space Center, Houston, Texas 77058

²Lunar and Planetary Institute, Houston, Texas 77058

Abstract—The three largest Skylab IV Command Module windows that were exposed for 84 days to space were optically scanned for impact features as small as 30 μm in diameter. This scanning effort, which was carried out at an optical magnification of 35 \times , detected features approximately three times smaller than were found in the original 5 \times scanning effort over the entire window surface by Cour-Palais (1979). Some 289 features were recorded from the 35 \times scan for later detailed analyses. Sixty of the largest and most promising features were cored from the windows for SEM and EDS analysis. Twenty-six of the cores contained craters with glassy pits, and of these, fourteen were found to contain strikingly obvious liners coating the interior of the glassy pit. The six largest features cored from the windows do not have a central glassy pit which leaves their previously reported hypervelocity origin in some doubt.

The remaining twenty-eight features that were cored from the windows show no clear evidence for a hypervelocity origin and evidence available at this time is insufficient to identify an origin in earth orbit or as ground damage. EDS analysis of six of the seven liners that have been examined show detectable aluminum in the liner or lip of the glassy pit. The source of aluminum is most probably an earth orbiting population of aluminum oxide spherules, exhaust effluent from solid rocket motors.

INTRODUCTION

The role of microparticle impacts in space and on planetary bodies without an atmosphere has been the focus of considerable research in support of the space program. Laboratory studies and analysis of lunar samples provide the bulk of reference data. This research outlines some new and unique observations of crater morphology on the Skylab IV/Apollo windows, features that have not been observed previously. These unusual data have renewed interest and resurrected certain questions about the nature and origin of some of the impacting materials in space. Our preliminary results are presented in support of this renewed interest.

The Command Module (CM) windows of the Skylab III and IV missions recorded the near-earth impacting meteoroid flux for periods of 59-1/2 and 84 days, respectively. Cour-Palais (1979) examined these windows for meteoroid impact craters and obtained an impact flux in very satisfactory agreement with his previous analyses of windows from the earlier Apollo missions.

These data have several important applications including: (1) obtaining absolute lunar regolith evolution rates; (2) establishing the current absolute erosion rates of lunar rocks; (3) establishing the surface exposure duration for certain lunar rocks still in crater production (if the cratering rate is assumed constant in time); (4) providing a foundation for deducing the space survival time of meteoroids against the collisional destruction of other meteoroids. However, questions had arisen about the origin of the impacting flux. These questions were derived largely from the investigations of Hallgren and Hemenway (1976) and Nagel *et al.* (1976) who detected abundant aluminum in some of the impact craters analyzed from Skylab experiment (S-149). Hallgren and Hemenway showed from field-of-view considerations that some of the craters with aluminum were produced by hypervelocity impacts and were not derived from secondary ejecta from the adjacent orbital workshop. As there are no expectations of meteoroids with only aluminum and no other elements (with $Z > 11$ and thereby detectable by energy dispersive X-ray analysis), these results gave rise to a suspicion of an earth-orbiting cloud of debris.

The above considerations, in part, prompted us to undertake a careful reexamination of the Skylab IV CM windows for meteoroid impacts. We rescanned these windows optically at a magnification of $35\times$. This compares with the original $5\times$ scan of the entire window surface and a $20\times$ scan of 224 cm^2 of surface area (Cour-Palais, 1979). With our detection threshold set for a $30\text{ }\mu\text{m}$ impact spall diameter which corresponds to a pit diameter of about $7\text{ }\mu\text{m}$, we had hoped to detect the inflection point (where the graph curvature changes from convex to concave) in the cumulative pit diameter distribution seen by Morrison and Zinner (1977) in lunar data. With the increase in meteoroid impact velocity largely due to the gravitational field of the earth, we anticipated that this inflection point should move to about $10\text{ }\mu\text{m}$ assuming the fused silica windows reacted similarly to lunar materials. We should, therefore, have had some chance of detecting this inflection point with our improved optical resolution.

WINDOW EXAMINATION AND CORING

The spacecraft windows are held in place by a gasket and a frame that restricts the area of exposure. The exposed area of each window was determined by cutting out sheets of paper to fit snugly into the recessed area of the window frame and then measuring the areas of these paper sheets with a planimeter. We measured areas of 940 cm^2 each for the right and left windows and 685 cm^2 for the hatch window. The last number differs somewhat from Cour-Palais' (1979) determination of 740 cm^2 for the hatch window. We believe our procedure yielded a more precise result ($\pm 1\%$ error) than did his approximate procedure. We then scribed the outline of these exposed areas on the Skylab IV CM windows with a diamond point pen in order to minimize the amount of area we needed to search for hypervelocity impact craters.

After cleaning the surfaces with a detergent (Alconox), the windows were



optically scanned for candidate impact craters at a magnification of $35\times$. A small area of about 30 cm^2 was scanned at $50\times$. We feel that we were able, at $35\times$, to detect and examine essentially all craters with a spall diameter larger than $40\text{ }\mu\text{m}$. Our threshold was set at $30\text{ }\mu\text{m}$ but it is probable that we failed to detect something like 10% of the crater population at that threshold. For the $50\times$ scan we set a threshold of $15\text{ }\mu\text{m}$.

To do the optical scanning we used a System C-7200 COSCAN optical comparator made by Optronics International (Chelmsford, Mass.). This system has an optically transparent table riding on an air bearing with 25 cm of travel in both x and y directions. We used it with transmitted light so that the craters would show up as shadows in an otherwise clear view. The table was motor driven with a logarithmic x-y controller and proved to be very satisfactory for our purposes.

Each window was scribed into four quadrants which were then scanned separately. When a crater was found, we searched it for features (such as a glassy pit) that would indicate a possible hypervelocity impact origin for it. The optical comparator had a $2\times$ zoom capability that was useful for more detailed viewing. All those craters that were considered to be of possible hypervelocity impact origin were then recorded by a penciled dot on a sheet of white paper precisely positioned by retaining tabs glued on the sides of the window. Each such dot was numbered for later reference. We recorded 25 craters on the hatch window, 140 on the right window and 124 on the left window for a total of 289 craters. Approximately two hundred other features were dismissed during the optical scanning as pits clearly resulting from glass polishing processes or from some other non-hypervelocity impact origin.

The sixty craters that were optically judged to be the best candidates for a hypervelocity origin were then cored from the three windows, 25 from the right window, 22 from the left window and 13 from the hatch window. Four other craters were accidentally destroyed during the coring process. A one millimeter thick wafer containing the crater was then sawed from each core and ultrasonically cleaned in acetone, methonal, liquid freon, and occasionally, triply distilled water. Samples were then sputter coated with about 25 \AA of Au40:Pd60 alloy to produce an artifact free surface using the technique of Morrison and Clanton (1979). The coated samples were examined with a JEOL SEM-100CX TEM-SCAN which is capable of better than 30 \AA resolution point-to-point at $100,000\times$ in the SEM mode. Chemical analysis data were obtained with a Princeton Gamma-Tech 1000 EDS.

CRATER MORPHOLOGY AND CHEMISTRY

Although all of the cores contained features whose origin was suspected to be from hypervelocity impacts, the magnification, resolution and depth of field of the optical microscope was inadequate to characterize or classify the features. Based on SEM studies, the impact features can be grouped into three major types: (1) Glassy pit craters, microcraters with a central glass lined pit surrounded



by a raised lip of impact-fluidized glassy material, (2) pitless craters, microcraters without a central glass-lined pit and raised lip but with well developed zones of radial and concentric fracture, (3) damage craters, shallow features without fluidized glass but with poorly developed radial and concentric fracture.

Glassy pit craters

Twenty-six examples of hypervelocity impacts that produced impact-fluidized glassy pits and raised rims have been documented. The morphology in general is similar to features observed on lunar samples but the spall zones often appear to be more shallow (Fig. 1). However, twelve of the glassy pit craters, unlike

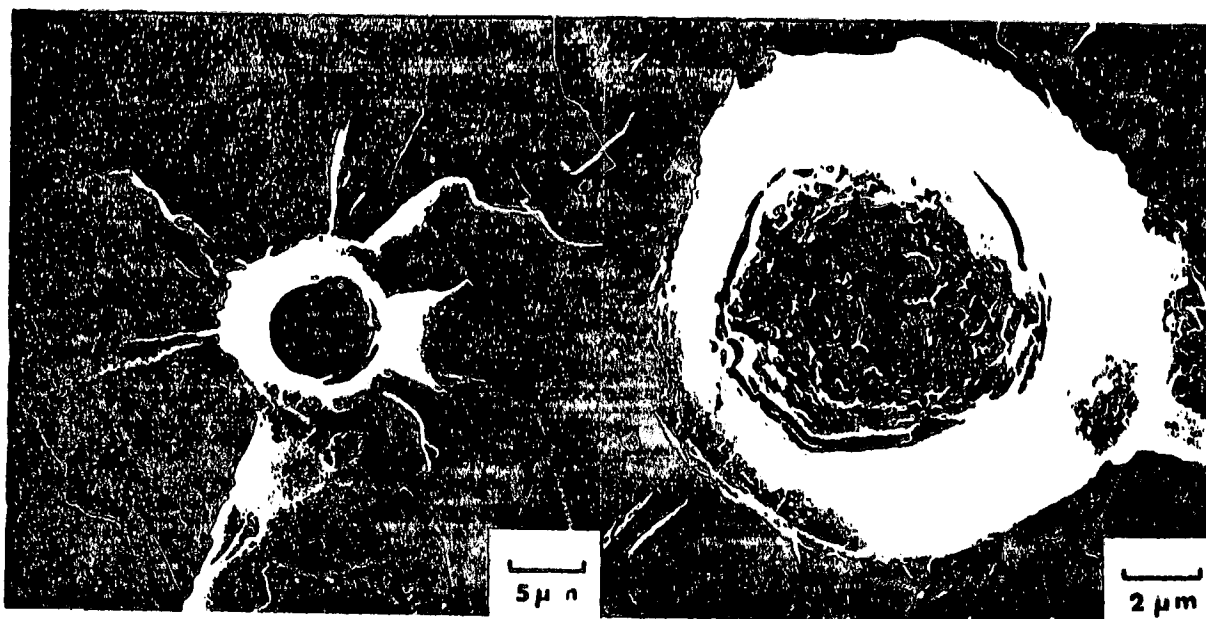


Fig. 1. SEM micrograph of a hypervelocity impact pit of probable micrometeorite origin. Fractures radiate from the glassy rim that surrounds the deep central pit. Most of the original surface near the point of impact has spalled away leaving conchoidal fracture scars. Four of the radial fractures extend beyond the conchoidal spall zone. A small portion of the original surface extends out over the glassy rim and serves to illustrate how the impact feature forms below the original surface. Surrounding the spall area is a thin white line that marks the edge of the magnesium flouride antireflection coating on the window that has been torn away by the impact event.

Fig. 2. SEM micrograph of a liner coating the interior of a hypervelocity impact pit. Based on the morphological relationships of the liner and the pit, a scenario during formation can be outlined. Some rather restricted conditions for the impact event are indicated and in particular, low impact velocities (<10 km/sec) are required because of the large amount of projectile material that survives the impact.

Initially, sufficient impact energy is available to form the classic glassy pit which chills rapidly. The projectile which is shock melted is sufficiently plastic to deform to the shape of the host pit yet not so fluid as to mix with and become an integral part of the glassy pit wall. The liner cools and contracts forming a cast of the pit wall. The separation of liner from the pit wall suggests materials with differing physical and chemical properties.



Fig. 3. SEM micrograph of a hypervelocity impact crater with two liners coating the interior of the glassy pit. Both the liners, although now incomplete and broken, appear to conform to the irregular interior of the pit yet are clearly separate from the wall and each other. The outer liner is crossed by several tension cracks; droplets and debris partially cover the exposed surface. The inner liner, exposed where the outer liner has broken away, is generally smooth with a surface that is almost totally free of debris.

Fig. 4. A higher magnification view of the broken edges of the double liner shown in Fig. 3. Some of the clues of the dynamics of crater and liner formation are illustrated in this SEM micrograph. The two layers were sufficiently plastic during emplacement to deform and coat the interior of the pit but because of physical or chemical differences, the layers do not mix with and become an integral part of the glassy wall. Further cooling and contraction tends to accentuate the separation of the liners from the host pit. The liners appear to have a fairly uniform thickness; the top liner is about 2000Å and the bottom liner is about 3000Å thick.

lunar samples, show clear evidence of a glassy liner in the pit (Fig. 2). Additionally, two other examples have been found that have a double liner (Figs. 3 and 4). Six elongate craters have also been documented and two of these have partially developed liners (Fig. 5). One crater which has a pit within a pit was also found (Fig. 6).

Pitless craters

This group contains the six largest features of possible hypervelocity impact origin observed on the windows (Fig. 7). One has a spall dimension of over 1 mm. The crater morphology is characterized by four distinct and concentric zones, (1) a large outer shallow spall, (2) a deeper spall with well developed radial fractures, (3) a depressed shatter zone of radial and concentric fractures and (4) a deep central shatter pit with well developed radial and concentric fractures. There is, however, no clear evidence impact-fluidized melt and no central pit of melted glass.



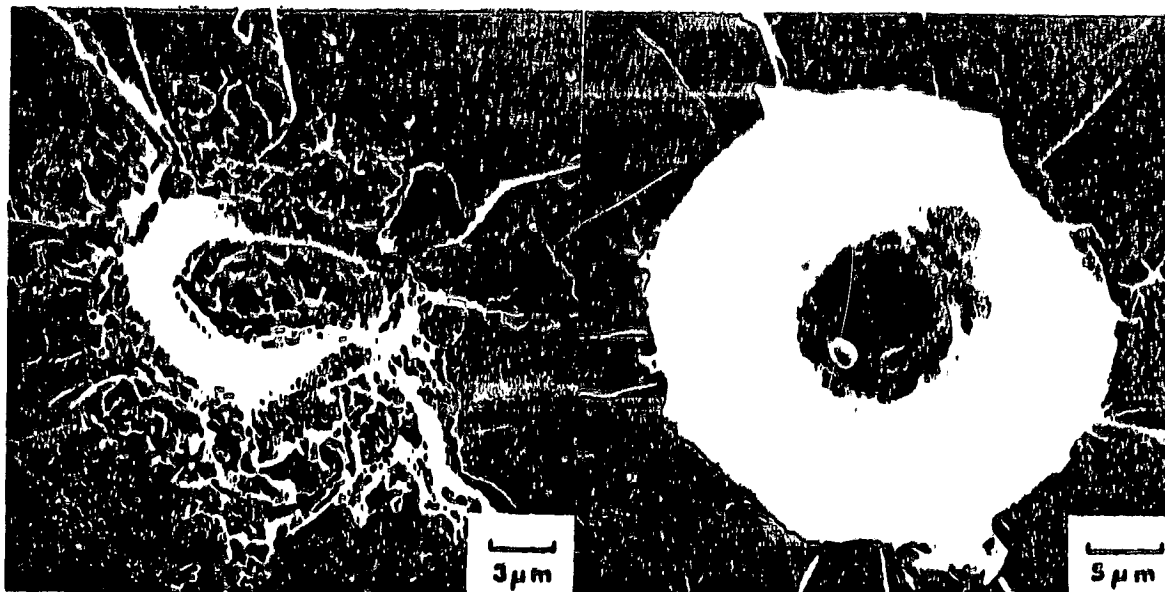


Fig. 5. Elongate hypervelocity impact craters on lunar samples are rare. This crater on the SL-4 window is not only elongate but also has a liner that is partially developed in the central pit. Although EDX analysis of the chemistry of the impact products is incomplete, Si and a small amount of Ti are the only elements detected in the rim materials of this crater.

Fig. 6. The SEM micrograph illustrates a hypervelocity impact pit of possible micro-meteorite origin. Although the general morphology resembles what has now come to be expected from a hypervelocity impact on the lunar surface, the interior morphology of the glassy pit is unusual. The normally concave floor is penetrated by a deeper and nearly concentric pit. An irregularly shaped projectile may explain the origin of the double pit.

Damage craters

These features have some morphological feature that suggest a hypervelocity impact origin when viewed under a binocular microscope. Further study with the SEM, however, dictates a low-velocity impact origin. The variety of fracture, shatter and spall morphology indicates that a wide range of particle sizes, densities and velocities contributed to the window damage. Figure 8 illustrates the damage from a low-velocity directional impact.

A higher energy origin for some of the damage craters may be argued on the basis of deep conchoidal spalls and well developed radial fractures. Some of these craters have what appears to be a fused aggregate of particles a few hundred angstroms in diameter that partially cover selected areas within the spall zone. These "popcorn" like features (Fig. 9) may represent incipient melting of projectile or target material, or perhaps some form of contamination that was not removed during the cleaning processes. Studies to date have not yet clearly identified an origin for these features.

Only a limited amount of chemistry has been attempted on the samples at this

time. The data are limited to some qualitative EDS analysis and WDS analysis of some of the glassy pit craters with liners. The Skylab IV/Apollo window material is an optical grade of fused quartz and impurities do not exceed a few parts per thousand. The surface of the window is coated with about 200 angstroms of magnesium fluoride, an antireflection coating. EDS analysis of areas on the undamaged window easily detects the Mg-rich surface. In the spall areas, Si is typically the only element that can be detected. Six of the seven lined glassy pit craters that have been analyzed by EDS show detectable aluminum in the liner or rim material (Fig. 10). Additionally Ti has been detected in the rim of one of the elongate and lined glassy pit craters (Fig. 5).

Because much of the EDS analysis must be done on submicron thick features, considerable effort will be required to obtain more quantitative data. The glassy pit crater shown in Fig. 2 was also subjected to extensive analysis on a Cambridge

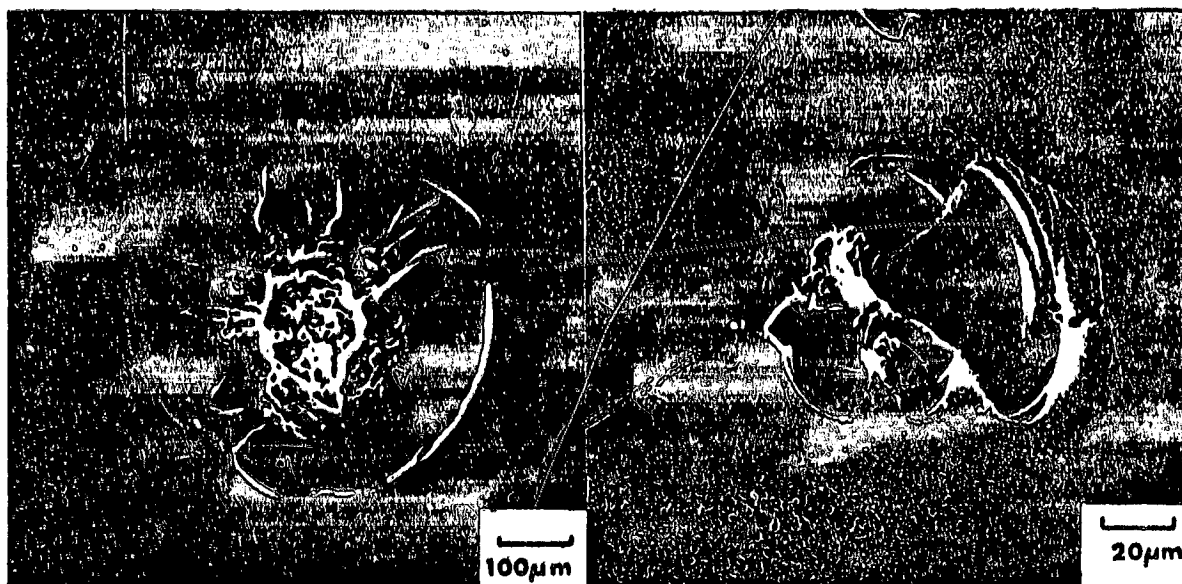


Fig. 7. The pitless craters are the largest damage features on the SL-4 windows and do not have a clear hypervelocity origin—no glassy central pit remains. There is evidence based on some laboratory tests, however, that the glassy pit may be dislodged by the violence of the impact event.

The damage typically forms four distinct zones (1) an outer very shallow spall about 1 mm in diameter, (2) a deeper spall about 500 μm in diameter that is characterized by large well developed radial fractures, (3) a depressed shatter zone about 230 μm in diameter of smaller radial and concentric fractures, and (4) a deep shatter pit about 150 μm in diameter with well developed radial and concentric fractures.

Fig. 8. A number of features too small to be clearly characterized with an optical microscope proved under SEM analysis not to have a hypervelocity impact origin; no central glassy pit had been developed. The variety of fracture, spall and shatter forms indicate a range in particle sizes or densities or velocities may have contributed to the window damage.

A zone of shatter marks the impact point of the projectile. The conchoidal spalls are unequally developed and asymmetrically arranged. An origin from a low-velocity directional impact is indicated.

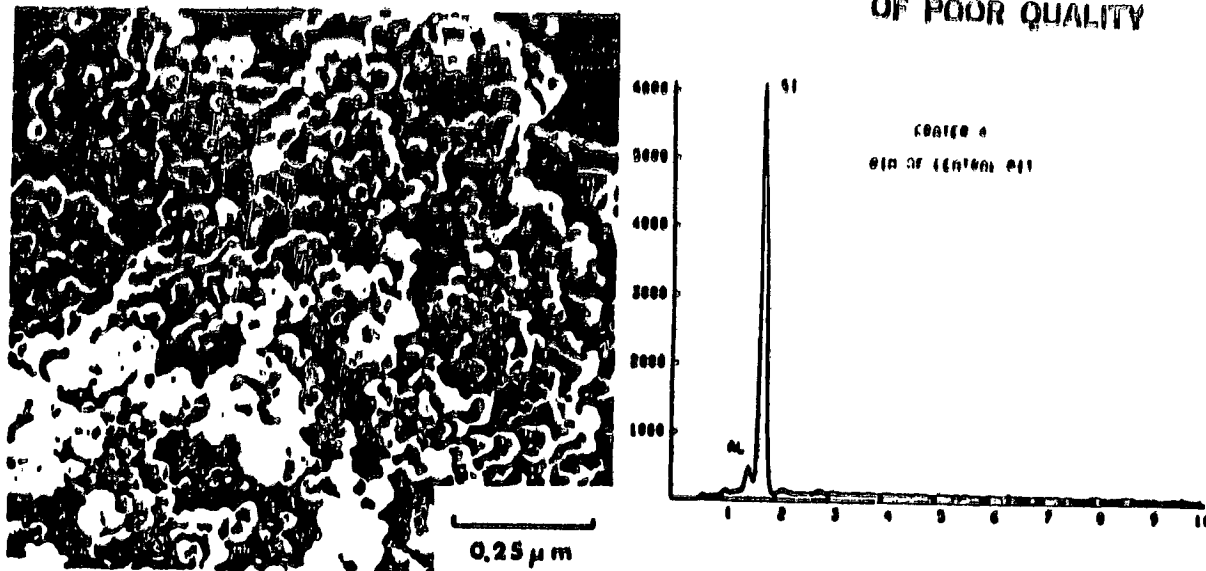


Fig. 9. Some of the craters in the Skylab IV/Apollo windows have patches of what appear to be individual particles, some 400 to 600Å in diameter, that appear to have been fused together to form a "popcorn" morphology. This material may represent target material that has been partially sintered or may represent some form of contamination that was not removed during the cleaning process. EDS analysis of submicron particles is difficult and a definite composition has not yet been obtained.

Fig. 10. EDS spectra from the rim of a glassy pit crater. The vertical axis is count rate, the horizontal is energy (KeV). The dominant peak is silicon from the fused quartz window. The aluminum occurs only in the glassy rim material. The source of the aluminum is thought to be from aluminum oxide spherules, exhaust effluent from solid fuel rocket motors.

SEM equipped with wave length dispersive spectrometers (WDS). This WDS study confirmed the earlier EDS analysis; Al was the only foreign element that could be detected in the glassy pit/liner.

Crater morphology from hypervelocity impacts on lunar samples has been extensively documented since the return of the Apollo 11 samples (e.g., Carter and McGregor, 1970; Frondel *et al.*, 1970; Goldstein *et al.*, 1970; McKay *et al.*, 1970). Later, several research groups (e.g., Hörz *et al.*, 1971, and Fechtig *et al.*, 1976) carried out exhaustive surveys of microcratering on lunar rock surfaces. An extensive bibliography and review of the cratering literature is given by Ashworth (1978). Additionally, the work of Morrison and Clanton (1979) documents details of craters less than 1000Å in diameter on lunar samples.

Experimental studies of hypervelocity impacts under controlled laboratory conditions (e.g., Roy *et al.*, 1972; Roy and Slattery, 1973; Mandeville and Vedder, 1971; Vedder, 1971, 1976) provides an additional insight into such variables as projectile velocity, density, angle of incidence and the role of different target materials. A review of the equipment and the various techniques that have been used to produce hypervelocity impacts under laboratory conditions is given by Fechtig *et al.* (1978). Additionally, a brief description of the micrometeoroid

detectors that have been flown in space is provided along with some of the problems associated with cross calibration of equipment/experiments.

The literature on lunar samples and laboratory simulations fails to document previous observations of liner morphology similar to those occurring on the Skylab IV/Apollo windows. The literature does, however, provide a precedent for hypervelocity craters with high aluminum. Hallgren and Hemenway (1976) analyzed 18 craters found on the S-149 Skylab experiment using a SEM with EDS capability and observed that most of the craters had high aluminum contents. The high aluminum contents are inconsistent with the observations of Anders *et al.* (1973) for the composition of meteorites in lunar soils. Although Nagel *et al.* (1976) and Hallgren and Hemenway (1976) could relate most of the hypervelocity pits to primary or secondary impacts from space debris, some craters appeared to have a true micrometeorite origin.

Our detection of high aluminum in six of the seven glassy pit craters with liners supports the findings of Hallgren and Hemenway (1976) and Nagel *et al.* (1976). A source for the aluminum may be inferred from indirect evidence; Brownlee *et al.* (1976) comment that 90 percent of the collected stratospheric particles in the 3 to 8 μm range are aluminum oxide spherules. Sampling flights through the exhaust plumes of Titan III rockets identified the source of these particles as exhaust effluent of solid rocket motors (Ferry and Lem, 1974). The review by Brownlee (1978) of stratospheric microparticle collection and analysis discusses the basis for identifying cosmic dust particles in this background of rocket exhaust effluent, terrestrial contamination and other man-induced space debris (titanium based paint flakes).

Our original goal was to determine the micrometeorite flux in near earth orbit. Our study has presented us with a much more complex problem than was first anticipated. We now find that we must separate a natural flux from a man-induced flux. At this time, the origin for two of the crater morphologies is not totally clear. The literature fails to provide a previous example of glassy liners in glassy pit craters in glass targets. However, Cour-Palais (pers. comm.) has observed an example of aluminum from a metallic projectile lining a hypervelocity pit in a copper target.

Additionally, the largest craters on the window do not have a clear hypervelocity origin. The radial and concentric fracture pattern of these features is characteristically associated with hypervelocity craters with glassy pits, yet no clear trace of a glassy pit remains. Some basis for arguing that the glassy central pit may have spalled from the surface can be developed. Cour-Palais (pers. comm.) has carried out a number of hypervelocity impact experiments that resulted in the ejection of the glass-lined pits from the fused silicate targets. These experiments were done with a light gas gun with projectile velocities in the range of 7 to 8 km/s. Also Carter and McKay (1971) noted an example of a pit that had nearly left its parent crater in a heated (750°C) fused silica target. The impact velocity in this case was 7.2 km/s. Notwithstanding these observations, however, we cannot yet be sure that the six largest craters did not result from processes occurring during manufacture, checkout or recovery of the Apollo spacecraft.



CRATER SIZE DISTRIBUTION

Cumulative crater size distribution based on SEM studies obtained from 32 of the 60 Skylab IV/Apollo window cores are shown in Fig. 11. The six largest features, the pitless craters, are plotted as closed symbols; the 26 glassy pit craters comprise the remaining plot of data. The 28 damage craters are not included. The 14 craters that have a liner which coats the central glassy pit are, in addition, replotted separately to the lower left in Fig. 11. In each case the total

CUMULATIVE CRATER SIZE DISTRIBUTIONS ON THE SKYLAB IV CM WINDOWS

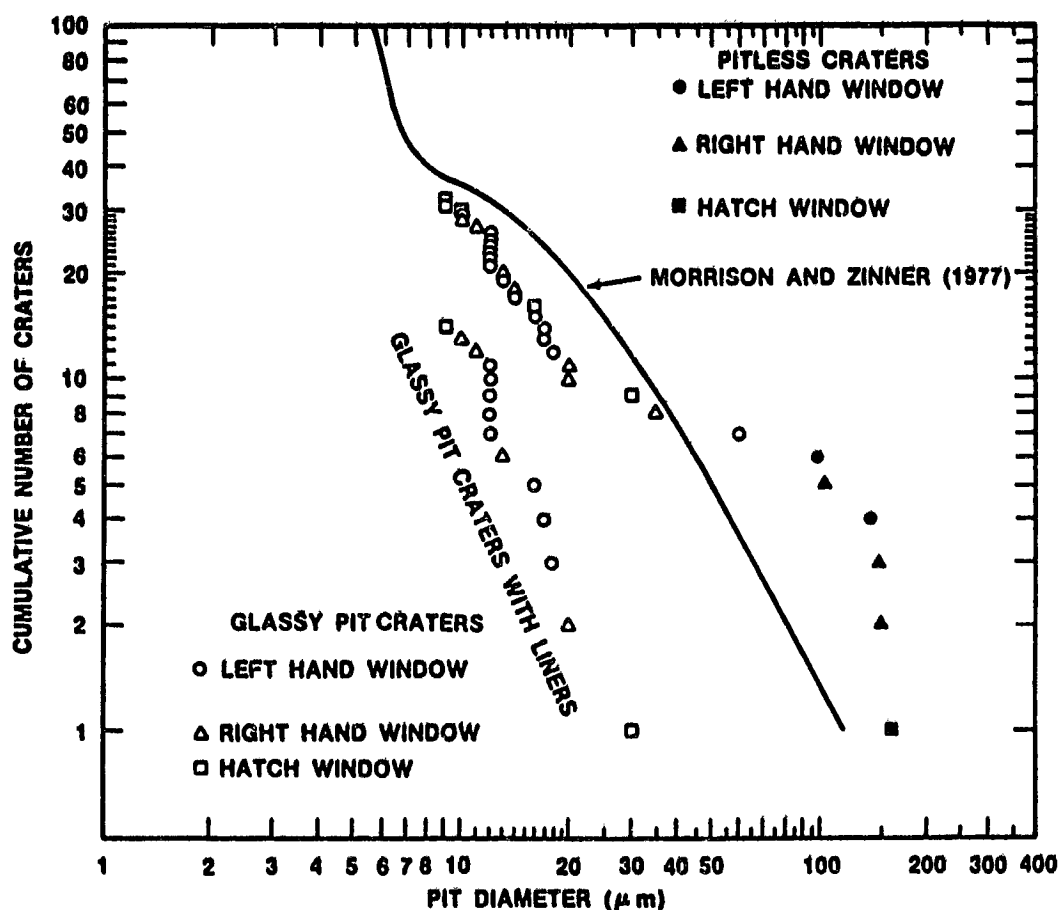


Fig. 11. Cumulative crater number versus crater pit diameter in micrometers for the three Apollo Command Module windows from the 84-day Skylab IV mission. Except for the six largest craters shown as filled symbols, only those craters were chosen that have a remelted glass-lined pit strongly indicative of hypervelocity impact. The data points to the upper right constitute a plot of all the larger candidate hypervelocity craters from the three windows, while the data points to the lower left are a subset in which the glass-lined pit has a separate inner liner of apparently foreign material. Morrison and Zinner's (1977) plot (renormalized to equal 7.5 at a 40 μm pit diameter) of impact pits on lunar rock 12054 is shown for comparison.

number of craters with a pit diameter larger than some chosen diameter are plotted versus that diameter. Both axes are scaled logarithmically.

Pit diameter was measured on SEM micrographs from rim center to rim center as presented by Morrison and Zinner (1977) but unlike Cour-Palais (1979) who measured the diameter of the interior of the rim. This difference in measurement becomes increasingly important in the smaller craters where the rim width is comparable to the rim diameter.

The shape of the cumulative curve formed by the 32 Skylab IV/Apollo datum points does not resemble the lunar impact pit size distribution curve obtained by Morrison and Zinner (1977) on lunar rock 12054, shown as a solid line on Fig. 11 (renormalized for easier comparison). These observations raise questions as to the origin of either the lunar impact pit data or the window impact pit data. One possible solution could be that neither the pitless craters nor the glassy pit craters with liners are due to meteoroid impact. A curve excluding both the pitless craters and the glassy pit craters with liners does give rise to a curve nearly parallel to the Morrison and Zinner (1977) lunar rock data. Another possible solution is to presume that many of the smaller lunar impact craters are formed by hypervelocity secondary ejecta. This latter solution seems less probable, however, because one would then also expect to see numerous low velocity impact features; but lunar samples are dominated by the glassy pit craters.

Because of our uncertainty as to the actual fraction of the impact craters that were due to meteoroid impacts, a flux vs. size curve is not now presented. However, to make a flux calculation in numbers of impacts per cm^2 per year, one merely divides the observed number of craters down to some chosen limiting diameter by 215. The number 215 is derived by reducing the window area (2565 cm^2) to an effective area that sees 2π steradians of space after accounting for Skylab and ATM shielding, window inset shielding and earth shielding (see Cour-Palais, 1979 for details) and then multiplying that effective area by the exposure duration in years (84 days = 0.23 years) of the windows. If one subtracts both the pitless craters and the glassy pit craters with liners from the data, a flux approximately 2.5 times lower than that given by Cour-Palais (1979) is obtained.

SUMMARY

Although more work clearly needs to be done to fully understand the origin and distribution of the microcraters on the Skylab IV/Apollo windows, the following observations seem pertinent:

1. Aluminum is detected as the only foreign component in six of the seven lined glassy pit craters so far examined by EDS analysis. The most probable source is from aluminum oxide spherules, exhaust effluent of solid fuel rocket motors. The seventh crater contains titanium which may have been derived from an impact of a chip of thermal paint.

2. The size distribution of the lined glassy pit craters appears to be compatible with an origin by hypervelocity impacts of aluminum oxide spherules. If the

aluminum oxide spherules are in earth orbit, impact velocities largely in the range of 7 to 10 km/s should be expected. Thus, the impact velocities are well below those expected for most impacts by micrometeorites and these lower velocities may be significant in the development of the lined glassy pit craters.

3. The documentation of hypervelocity impacts on Skylab IV/Apollo windows that contain aluminum support the observations of Hallgren and Hemenway (1976) and Nagle *et al.* (1976) and strongly indicate that there is a significant population of man-induced micro-debris in earth orbit.

4. The six largest craters observed on the windows are pitless craters. No impact fluidized glass is in evidence and an origin has not been clearly established. However, the conchoidal and radial fracture pattern of the pitless craters more closely resembles that observed with hypervelocity impacts than damage caused during polishing, window installation, ground operations, recovery, etc.

5. The shape of the curve of the Skylab IV/Apollo cumulative number versus pit diameter plot compares favorably with the Morrison and Zinner (1977) lunar curve only when the pitless craters and the lined glassy pit craters are excluded. We have not yet seen the inflection point expected at $\sim 10 \mu\text{m}$ pit diameter.

Acknowledgments—We are deeply indebted to Fred Pearce of the Flight Equipment Section of NASA-JSC for the use of his laboratory facilities. His patience and understanding during the three month period while we used the optical comparator is sincerely appreciated.

A portion of this research was done while R. Schultz was an undergraduate Summer Intern at the Lunar and Planetary Institute, which is operated by the Universities Space Research Association under Contract No. NAS 9-3310 with the National Aeronautics and Space Administration. This paper constitutes Lunar and Planetary Institute Contribution No. 419.

REFERENCES

- Anders E., Granapathy R., Krähenbühl U. R. S., and Morgan J. W. (1973). Meteoritic material on the Moon. *The Moon* 8, 3-24.
- Ashworth D. G. (1978) Lunar and planetary impact erosion. In *Cosmic Dust* (J. A. M. McDonnell, ed.), p. 427-526. Wiley, N.Y.
- Brownlee D. E. (1978) Microparticle studies by sampling techniques. In *Cosmic Dust* (J. A. M. McDonnell, ed.), p. 295-336. Wiley, N.Y.
- Brownlee D. E., Ferry G. V., and Tomandl D. (1976) Stratospheric aluminum oxide. *Science* 191, 1270-1271.
- Carter J. L. and MacGregor I. D. (1970) Mineralogy, petrology and surface features of some Apollo samples. *Proc. Apollo 11 Lunar Sci. Conf.*, p. 247-265.
- Carter J. L. and McKay D. S. (1971) Influence of target temperature on crater morphology and implications on the origin of craters on lunar glass spherules. *Proc. Lunar Sci. Conf. 2nd*, p. 2653-2670.
- Cour-Palais B. G. (1979) Results of the examination of the Skylab/Apollo windows for micrometeoroid impacts. *Proc. Lunar Planet. Sci. Conf. 10th*, p. 1665-1672.

- Fechtig H., Gentner W., Hartung J. B., Nagel K., Neukum G., Schneider E., and Storzer D. (1976) Microcraters on lunar samples. In *The Soviet-American Conference on Cosmochemistry of the Moon and Planets* (J. H. Pomeroy and N. J. Hubbard, eds.), p. 585-604. NASA SP-370, Washington, D.C.
- Fechtig H., Grün E., and Kissel J. (1978) Laboratory simulations. In *Cosmic Dust* (J. A. M. McDonnell, ed.), p. 607-669. Wiley, N.Y.
- Ferry G. V. and Lem H. Y. (1974) Particulates in solid fuel rocket exhaust. *EOS (Trans. Amer. Geophys. Union)* 56, 1123.
- Fronzel C., Klein C. Jr., Ito J., and Drake J. C. (1970) Mineralogical and chemical studies of Apollo 11 lunar fines and selected rocks. *Proc. Apollo 11 Lunar Sci. Conf.*, p. 445-474.
- Goldstein J. I., Henderson E. P., and Yakowitz H. (1970) Investigation of lunar metal particles. *Proc. Apollo 11 Lunar Sci. Conf.*, p. 499-512.
- Hallgren D. S. and Hemenway C. J. (1976) Analysis of impact craters from the S-149 Skylab experiment. In *Interplanetary Dust and Zodiacal Light, Lecture Notes in Physics*, 48 (H. Elsässer and H. Fechtig, eds.), p. 270-274. Springer-Verlag, N.Y.
- Hörz F., Hartung J. B., and Gault D. E. (1971) Micrometeorite craters and lunar rock surfaces. *J. Geophys. Res.* 76, 5770-5798.
- Mandeville J.-C. and Vedder J. F. (1971) Microcraters formed in glass by low density projectiles. *Earth Planet. Sci. Lett.* 11, 297-306.
- McKay D. S., Greenwood W. R., and Morrison D. A. (1970) Origin of small lunar particles and breccia from the Apollo 11 site. *Proc. Apollo 11 Lunar Sci. Conf.*, p. 673-694.
- Morrison D. A. and Clanton U. S. (1979) Properties of microcraters and cosmic dust of less than 1000Å dimensions. *Proc. Lunar Planet. Sci. Conf. 10th*, p. 1649-1663.
- Morrison D. A. and Zinner E. (1977) 12054 and 76215: New measurements of interplanetary dust and solar flare fluxes. *Proc. Lunar Sci. Conf. 8th*, p. 841-863.
- Nagle K., Fechtig H., Schneider E., and Neukum G. (1976) Micrometeorite impact craters on Skylab S-149. In *Interplanetary Dust and Zodiacal Light, Lecture Notes in Physics*, 48 (H. Elsässer and H. Fechtig, eds.), p. 275-278. Springer-Verlag, N.Y.
- Roy N. L. and Slattery J. C. (1973) Study of impact cratering in lunar-like materials. TRW Final Report 17433-6002-RO-00 prepared under NASA contract No. NASW-2311. 95 pp.
- Roy N. L., Slattery J. C., and Frichteniot J. F. (1972) Study for Apollo Window Meteoroid Experiment (S-176). TRW Final Report 209021-6001-RO-00 prepared under NASA contract No. NAS 9-12072. 95 pp.
- Vedder J. F. (1971) Microcraters in glass and minerals. *Earth Planet. Sci. Lett.* 11, 291-296.
- Vedder J. F. (1976) Hollow lunar spherules and microcratering. *Meteoritics* 11, 149-161.

215-12

Survey of Probable Micrometer-Sized Earth-Orbital Debris Fragments in the

NASA-JSC Cosmic Dust Sample Collection

N 85-21203

U.S. CLANTON and J.L. GOODING

NASA - Johnson Space Center, Houston TX 77058

Introduction

A limited effort to collect extraterrestrial dust samples from the stratosphere using impactors mounted on NASA U-2 aircraft was initiated at NASA-Ames Research Center in 1974 (1). In order to provide a greater availability of these samples to the scientific community, NASA-Johnson Space Center (JSC) began in May of 1981 a program dedicated to the systematic collection and curation of cosmic dust for scientific investigation. Collections are made at altitudes of 18 to 20 km by means of collectors mounted under the wings of a WB-57F aircraft. When the aircraft reaches operating altitude, the collection plates are deployed into the laminar airstream. Collection surfaces are coated with a thin film of high-viscosity silicone oil to prevent particles from bouncing free. The impactors are retracted and sealed in clean canisters to minimize contamination when not collecting.

An ultra-clean (Class-100) facility at JSC is used for pre- and post-flight handling of the collectors and the curation of collected particles. Individual particles in the size range of 3 to 35 micrometers are removed from the silicone oil on the impactors and placed on a Nucleopore substrate that is bonded to a graphite mount. Complete mounts of 16 particles each are washed with hexane to remove the silicone oil. The particles are not stuck to the substrate and can be removed from the mount for further analysis at any later date.

Preliminary examination of the particles indicates that they represent not only extraterrestrial material, but some fraction of terrestrial contamination from both natural and manmade sources. This examination involves a combination of optical microscopy, scanning electron microscopy (SEM) and qualitative bulk elemental analysis using an energy-dispersive x-ray spectrometer (EDS) to characterize each particle.

The preliminary examination data from our research are compiled into loose-leaf catalogs with all of the information for one particle on a single page. Each page has a SEM micrograph "mug-shot" that documents particle morphology. In addition, optical observations (500X) and an qualitative EDS elemental analysis are included. The catalogs are intended only to inform investigators as to the types of particles available for research and should not be considered as anything more than preliminary data which are subject to revision and update. The prime data are expected to come from the investigators who request the particles for research.

Studies (e.g., 1-9) have clearly established an extraterrestrial origin for some of the material. However, the collection surfaces also contain some particles of natural terrestrial origin (terrestrial contamination natural, TCN) and some exotic materials. The exotic particles include aluminum oxide spheres (AOS), metallic spherules or irregular fragments rich in titanium or copper, and spheres (most commonly) of a high-iron alloy containing lesser amounts of chromium, nickel, magnesium, vanadium,

aluminum and silicon. The non-AOS exotic particles are provisionally classified as man-made contaminants (terrestrial contamination artificial, TCA). The "contamination" term is used primarily to indicate a non-cosmic origin.

Natural contaminants (TCN particles) include fragments of quartz, feldspar, clay, carbonate minerals and volcanic ash. Prior to flight, both wing and pylon surfaces are wet-wiped to remove adhering particles. However, a few particles from the runway or from the lower atmosphere may temporarily cling to wing or pylon surfaces. Some of these particles may blow free when the collectors are deployed in the stratosphere and be caught by the collectors. In contrast, volcanic ash can be collected directly from the stratosphere after major eruptions. For example, the March/April 1982 eruptions of El Chichon in Mexico injected a large volume of ash into the stratosphere, some of which was collected during two separate missions flown in April/May and July/August of 1982.

The aluminum oxide spheres (AOS) are rocket exhaust effluent produced by the oxidation of aluminum powder that is used as a fuel additive in solid-fuel boosters. Collections (10) made with a U-2 aircraft flown through the exhaust plume of a Titan launch documented two of the eight sphere morphologies that we see in the present collection (11-12). The reasons for the different sphere morphologies and the slight chemical variations revealed by our studies are not well understood and present an opportunity for additional research.

Because the primary purpose of our program is to collect and curate cosmic dust, very little effort has been devoted to the exotic spherules and metal fragments. Some of these particles may come from the operations of the aircraft but the alloy spheres are most probably ablation products created by orbital debris re-entering the Earth's atmosphere.

Survey of Possible Orbital Debris Samples

It is beyond the scope of this paper to discuss the full implications of the various particle types in the JSC Cosmic Dust Collection. However, a brief review of some of the particles in the collection will illustrate the types of micrometer-sized material that might damage a spacecraft. Accordingly, we have compiled data pages for particles representing the natural "cosmic" and man-made populations, respectively. Each data page includes an SEM secondary-electron image and a whole-particle, raster-scanned EDS spectrum. In addition, other observable properties are summarized as follows:

- Size (micrometers): two principal dimensions as seen in SEM image.
- Shape: E (equidimensional), I (irregular), S (spherical).
- Transparency: O (opaque), T (transparent), TL (translucent).
- Color: self-explanatory; Dk (dark), Lt(light).
- Luster: D (dull), M (metallic), SM (submetallic), SV (subvitreous), V (vitreous).
- Type: AOS (aluminum oxide sphere), C (cosmic dust), TCA (terrestrial contamination, artificial), TCN (terrestrial contamination, natural).

It should be noted that in some of the EDS spectra, the peak labeled "CU" may include contributions from both sample and instrument. During analysis, stray electrons induce copper x-radiation from some SEM internal parts to produce a "CU" artifact peak. However, some TCA particles yield EDS spectra with such intense "CU" peaks that copper indigenous to the sample particles is strongly indicated.

Figures 1 through 4 provide examples of four different types of cosmic dust particles. Figures 5 through 11 illustrate some of the shapes and surfaces observed on aluminum oxide spheres collected from the atmosphere. Figure 12 is a size-frequency histogram of the AOS. The 5 micrometer data is biased toward low abundances both by aircraft collector efficiency and by the analyst selectively picking larger particles from the collection surface for analysis. Considering this bias, the plots of catalog data indicate that some 17 percent of the AOS collection is twice the diameter, hence eight times the mass, as previously reported for aluminum oxide spheres (10).

Figures 13 through 25 illustrate some of the particles we consider to be Terrestrial Contamination Artificial (TCA) particles. These particles have elemental compositions that are different from cosmic dust and "natural contaminants". They most likely represent aircraft or spacecraft debris; some of the spheres probably represent explosion debris or ablation products from larger masses reentering the atmosphere. Additionally, the elemental compositions of some of the TCA particles may provide clues to the compositions of hardware or alloys used in some spacecraft. Figure 26 is a size frequency histogram of the TCA particles. The greatest abundance of particles is, again, in the 5 to 15 micrometer size range, but it is significant to note that individual particles up to 35 micrometers have been collected in the stratosphere and may be expected to occur in Earth orbit.

Conclusions

The JSC cosmic dust collection contains samples of at least three classes of material that may present some hazard to extended spacecraft operations in near-Earth orbit: (1) micrometeorites/cosmic dust, (2) aluminum oxide spheres (AOS), and (3) alloy spherules and fragments (TCA).

A more complete analysis of the types and sizes of cosmic dust particles may provide a better understanding of the natural particulate environment. In addition, further analyses of AOS and TCA samples may provide additional information on the manmade Earth-orbital debris population.

ORIGINAL PAGE IS
OF POOR QUALITY

W7017B3



<u>SIZE</u>	<u>SHAPE</u>	<u>TRANS.</u>
5x6	I	TL
<u>COLOR</u>	<u>LUSTER</u>	
Lt. Yellow	D/SV	
<u>TYPE</u>	<u>COMMENTS</u>	
C		

S-81-39959

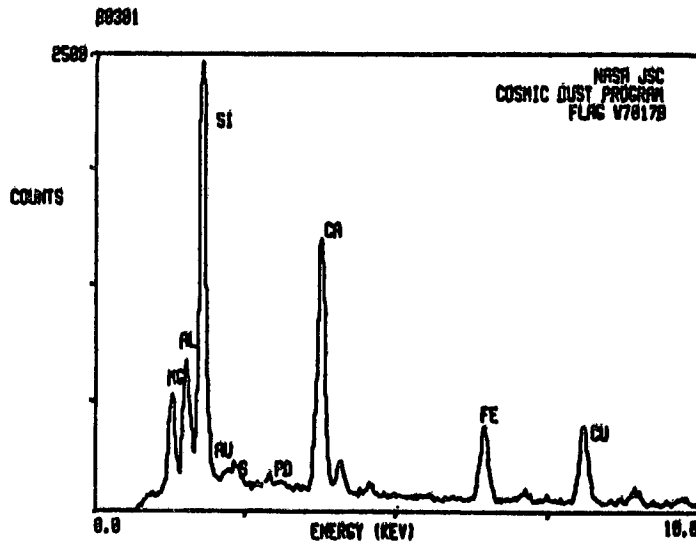
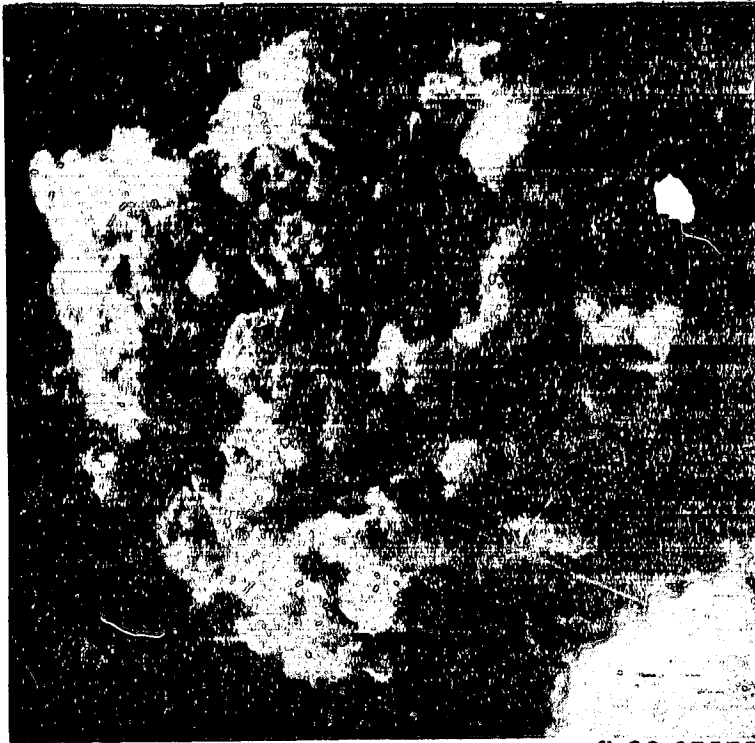


Figure 1 - Sample W7017B3. Type: Cosmic

This particle is classified as cosmic because of its morphology and elemental composition. The particle is composed of a fragile aggregate of rounded grains ranging in size from a few hundred angstroms to several micrometers in diameter that are combined to form an open and porous mass. EDS analysis of selected areas indicate that the larger grains are pyroxenes. The "AU" and "PD" peaks in the EDS spectrum are artifacts of the gold-palladium coating applied to the particle prior to SEM analysis.

W7029B13



S-82-27576

SIZE SHAPE TRANS.
13x14 I 0

COLOR LUSTER
Black D/SV

TYPE COMMENTS
C Fragment of
large (60
micron)
friable
particle

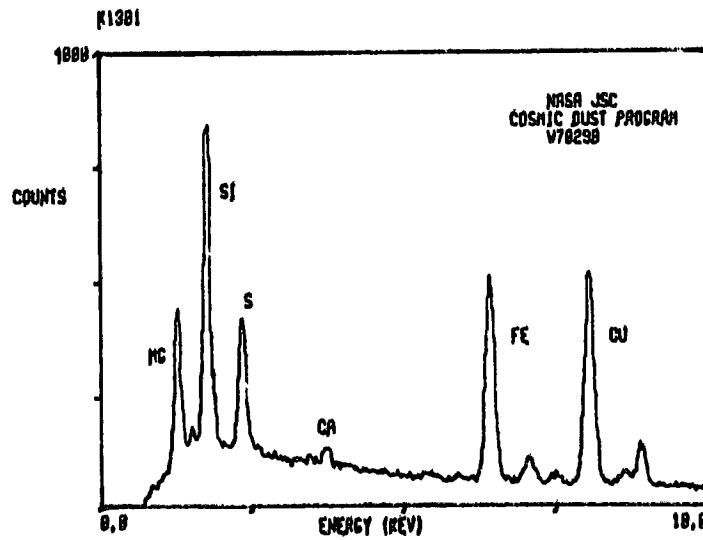
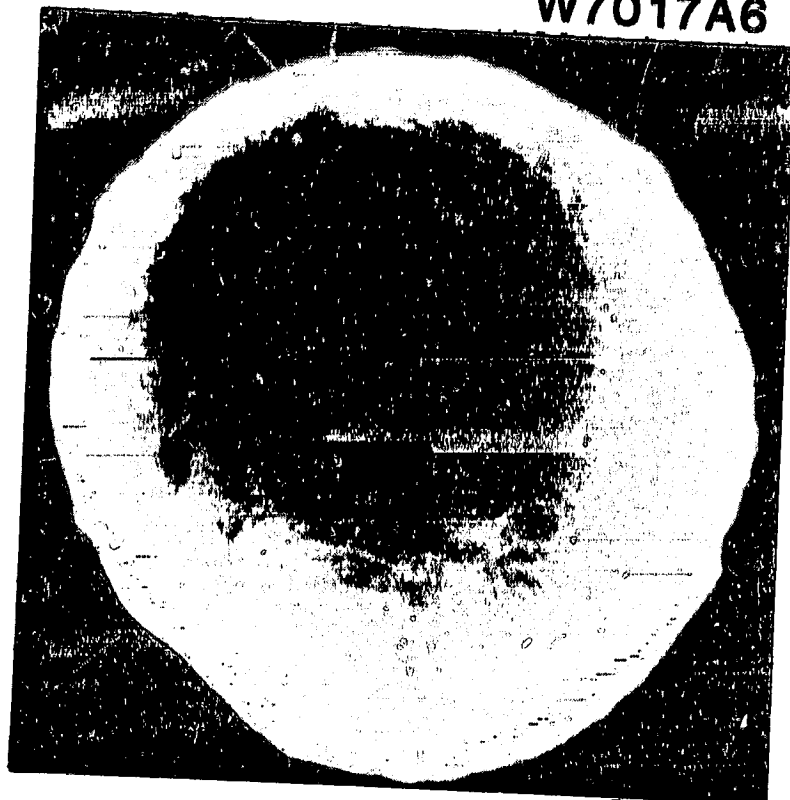


Figure 2 - Sample W7029B13. Type: Cosmic

This particle is classified as cosmic because of its morphology and elemental composition. It is composed of large and somewhat angular micrometer-sized grains set in a matrix of smaller, more rounded grains. Qualitative bulk analysis by EDS indicates the presence of at least two mineral phases, a pyroxene and an iron-sulfur compound.

W7017A6

ORIGINAL PAGE IS
OF POOR QUALITY



S-81-40134

<u>SIZE</u>	<u>SHAPE</u>	<u>TRANS.</u>
17	S	0
<u>COLOR</u>	<u>LUSTER</u>	
Black	M	
<u>TYPE</u>	<u>COMMENTS</u>	
C		

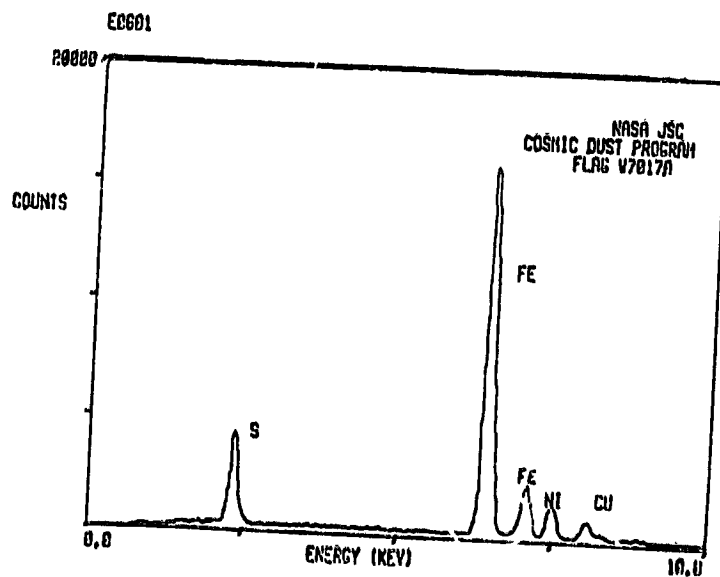
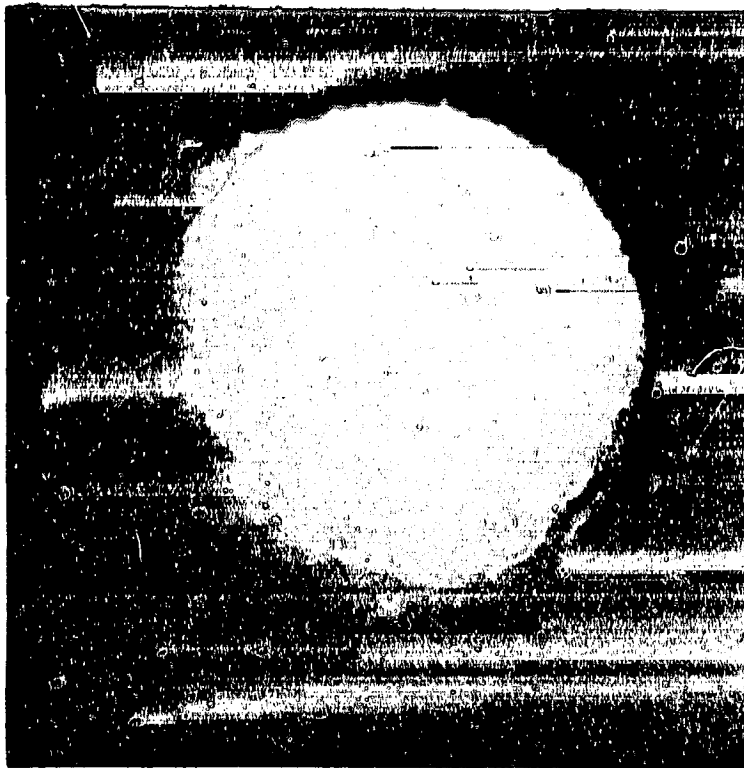


Figure 3 - Sample W7017A6. Type: Cosmic

This particle is classified as cosmic based on its content of Fe, Ni, and S. Its morphology is attributable to fragmentation from a larger mass. More detailed analysis of similar particles indicates that the surface of the sphere should be magnetite (Fe_3O_4) which mantles an iron-sulfur-rich core.

W7017C2

ORIGIN OF PARTICLE



SIZE SHAPE TRANS.
10 S T

COLOR LUSTER
CL/Pale V
Yellow

TYPE COMMENTS
C

s-82-40485

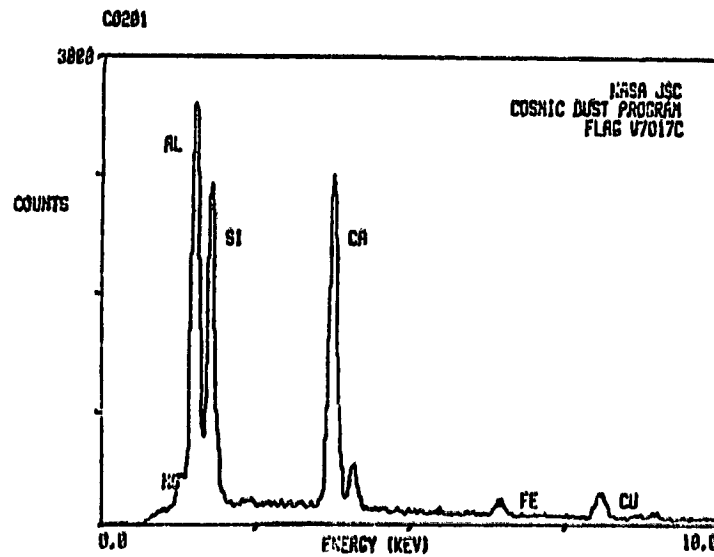
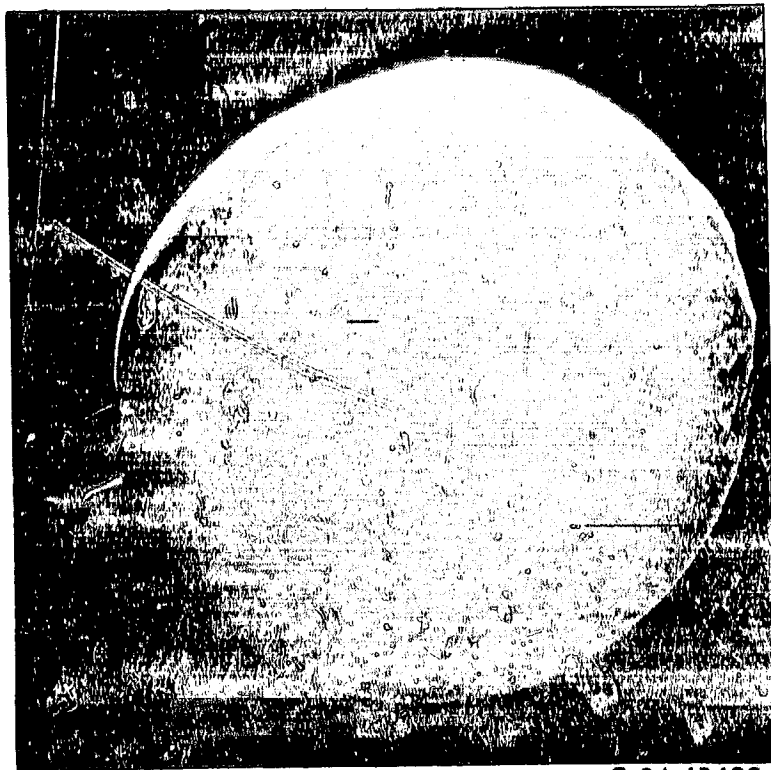


Figure 4 - Sample W7017C2. Type: Cosmic

This particle is classified as cosmic based on the EDS elemental analysis, and to a lesser degree, morphology. Although the elemental composition is not a good match to our usual mineral standards, a high-calcium pyroxene is the most probable source material. The spherical shape indicates a previous molten state, perhaps as an ablation droplet from a larger mass.

ORIGINAL PAGE IS
OF POOR QUALITY

W7017C9



S-81-40493

<u>SIZE</u>	<u>SHAPE</u>	<u>TRANS.</u>
8	S	T
<u>COLOR</u>		<u>LUSTER</u>
CL/Pale Yellow		SV
<u>TYPE</u>	<u>COMMENTS</u>	
AOS		

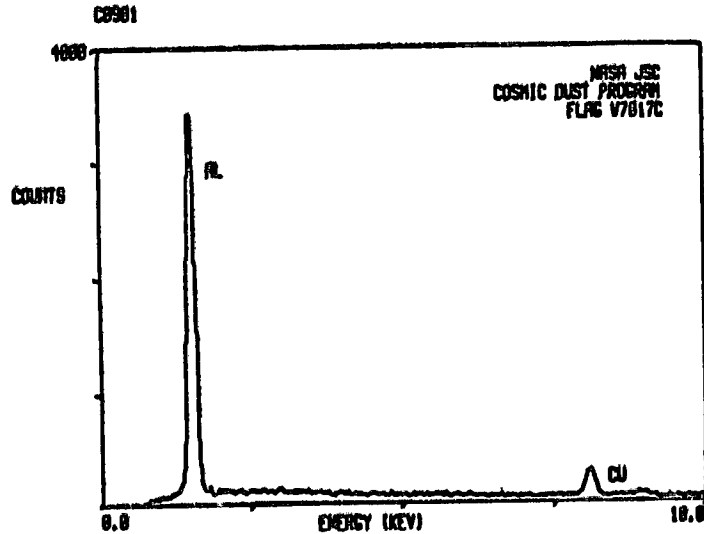
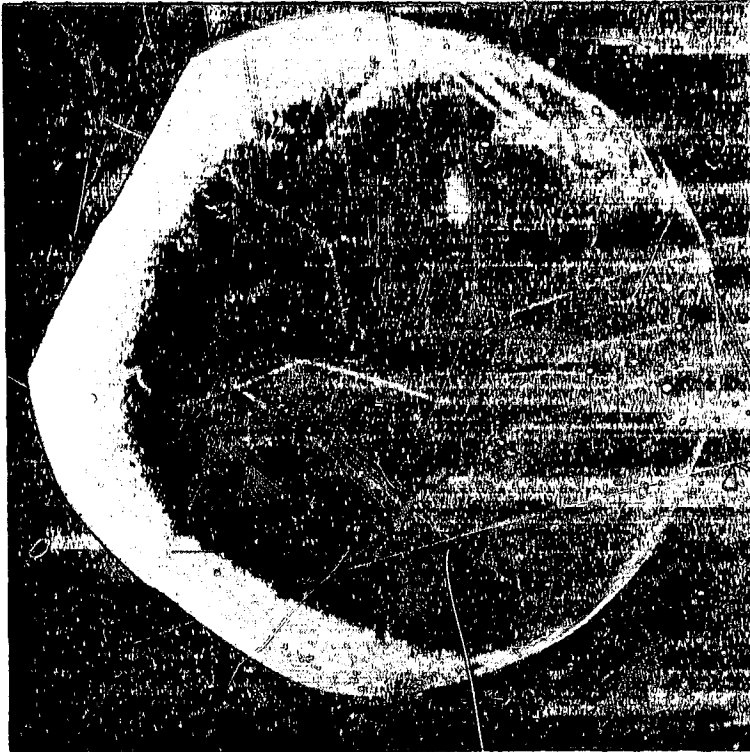


Figure 5 - Sample W7017C9. Type: Aluminum Oxide Sphere (AOS)

The classification as an AOS is based on morphology and the dominant aluminum peak in the EDS spectrum. The EDS technique does not identify elements lighter than sodium so the composition as an oxide, carbide, nitride, etc., is incompletely known from the preliminary examination data. Some 14 percent of the AOS analyzed to date have the concentric-circular ("target") morphology exhibited here. The feature is probably formed by bunched growth lines or "growth steps" on the surface of the sphere during crystallization. The conditions necessary to form this surface morphology are not well understood at this time.

W7017C12



S-81-40496

<u>SIZE</u>	<u>SHAPE</u>	<u>TRANS.</u>
15	S	T
<u>COLOR</u>	<u>LUSTER</u>	
CL(?)	V	
<u>TYPE</u>	<u>COMMENTS</u>	
AOS		

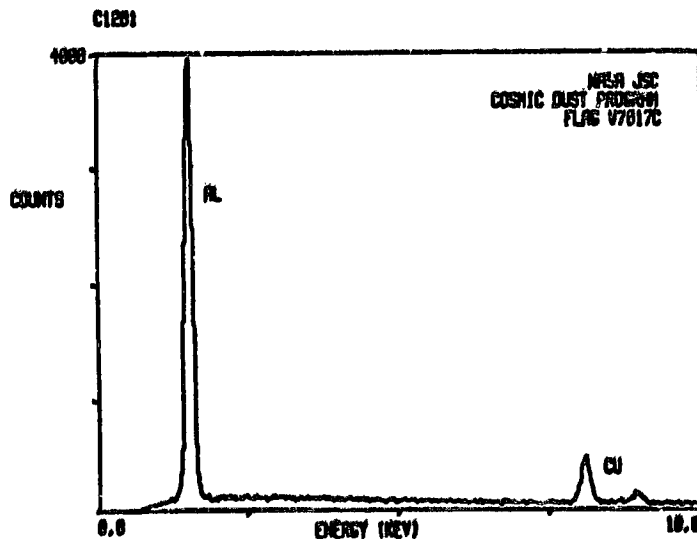


Figure 6 - Sample W7017C12. Type: Aluminum Oxide Sphere (AOS)

This classification is based on the sphere morphology and the intense aluminum peak in the EDS spectrum. As shown here, not all AOS particles have perfect spherical shapes; some have been quenched with some distortion of shape. This specimen appears to be two particles that stuck together while both were still plastic; the groove marks the collision boundary. The "target" patterns (see Fig. 5) terminate at the groove boundary; the flat area may represent the partial development of a crystal face. About 14 percent of the AOS collection appears to consist of such multiple-component particles.

W7017D5



S-82-25175

SIZE SHAPE TRANS.
7 S TL

COLOR LUSTER
CL/Pale V
Yellow-
Gray

TYPE COMMENTS
AOS Al x-ray emis-
 sion may include
 artifacts from
 Al grid on SEM
 mount.

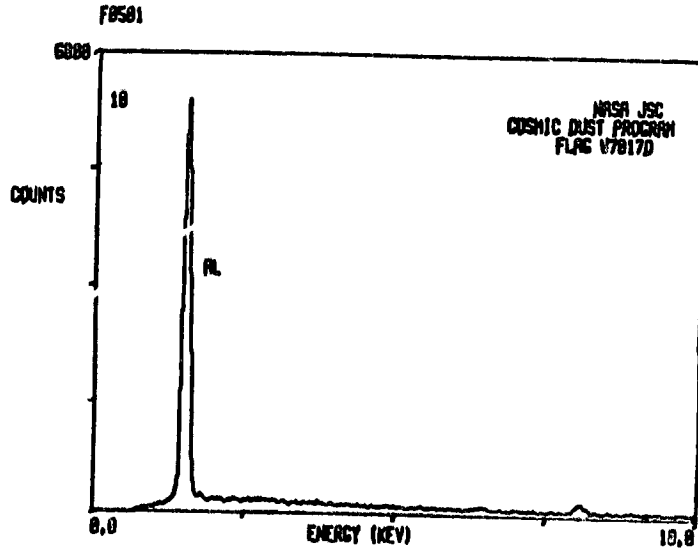
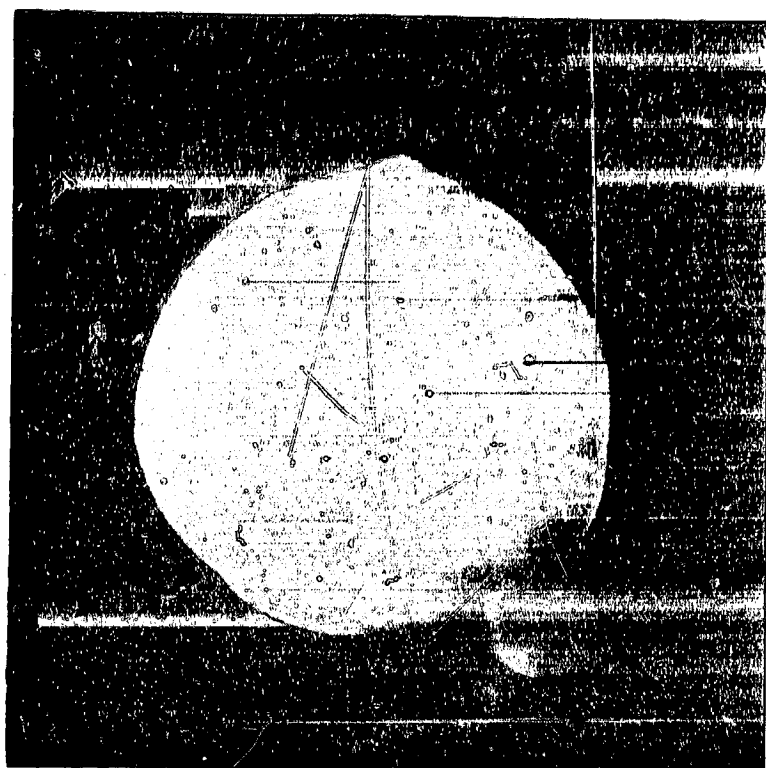


Figure 7 - Sample W7017D5. Type: Aluminum Oxide Sphere (AOS)

This classification is based on the particle morphology and the intense aluminum peak in the EDS spectrum. Approximately 25 percent of the AOS particles analyzed to date have a variation of the "brain" texture exhibited here. Approximately 17 percent of the collection has the coarse "brain" texture pictured here whereas some 8 percent of the collection has a much finer "brain" texture. The origin and conditions necessary for this formation are not understood at this time. The "brain" texture is suggestive of multicrystalline interiors.

W7017F1

ORIGINAL PAGE IS
OF POOR QUALITY



SIZE SHAPE TRANS.
6 S T

COLOR LUSTER
CL/Pale SV
Yellow

TYPE COMMENTS
AOS Compound
 sphere

S-82-25731

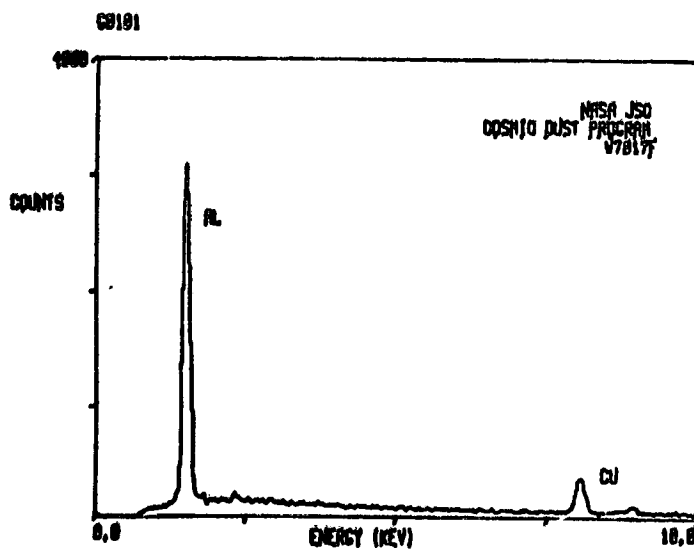


Figure 8 - Sample W7017F1. Type: Aluminum Oxide Sphere (AOS)

The AOS classification is based on the spherical shape and elemental composition of the particle. Smooth spheres represent the most common morphology among the AOS's, comprising some 29 percent of the collection analyzed to date. An additional 26 percent of the AOS's have a slight surface roughness. This particle is unique in the collection examined to date and provides an indication of the lower end of the AOS size range. The protuberance is formed by a sphere about 1.5 micrometers in diameter that stuck on the side of the larger sphere. Both particles were sufficiently plastic to fuse together but rigid enough to mostly retain their spherical shapes.

ORIGINAL PART OF
OF POOR QUALITY.

W7029E3



<u>SIZE</u>	<u>SHAPE</u>	<u>TRANS.</u>
8x14	I	TL
<u>COLOR</u>	<u>LUSTER</u>	
CL/Pale Yellow	V	
<u>TYPE</u>	<u>COMMENTS</u>	
AOS		

S-82-28021

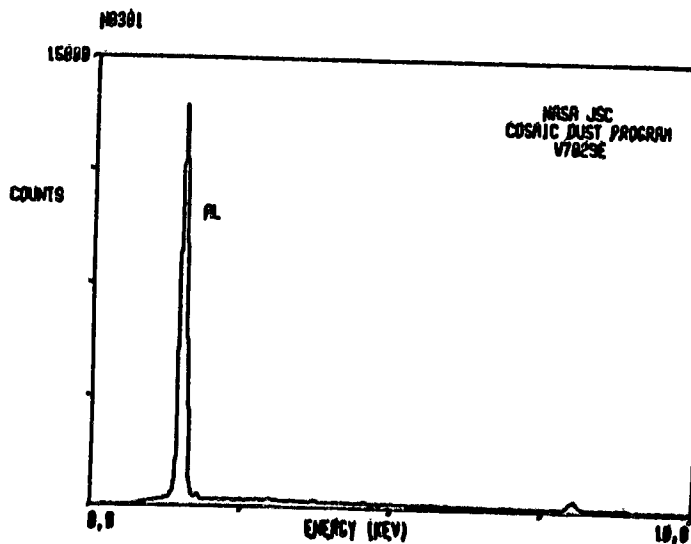
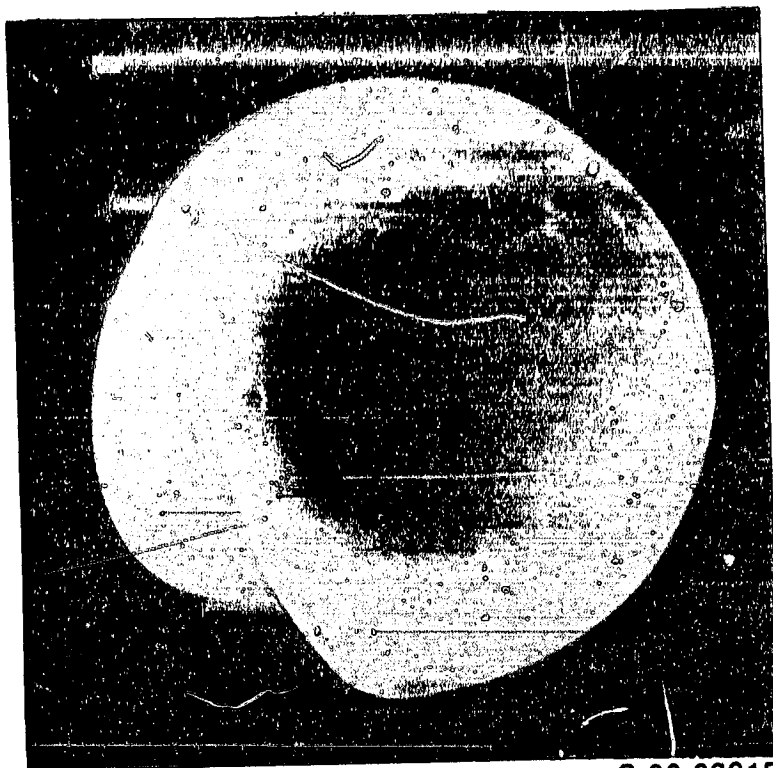


Figure 9 - Sample W7029E3. Type: Aluminum Oxide Sphere (AOS)

Identification is based on morphology and the dominant aluminum peak in the EDS spectrum. The most common AOS shape is the sphere but 5 percent of the AOS collection is composed of prolate ellipsoids. When this shape is observed the most common attendant surface morphology is the coarse "brain" texture shown in Figure 7.

W7029G12

ORIGINAL PARTIAL
OF POOR QUALITY



S-82-29615

<u>SIZE</u>	<u>SHAPE</u>	<u>TRANS.</u>
13	S	T
<u>COLOR</u>	<u>LUSTER</u>	
CL/Pale Yellow	V	
<u>TYPE</u>	<u>COMMENTS</u>	
AOS		

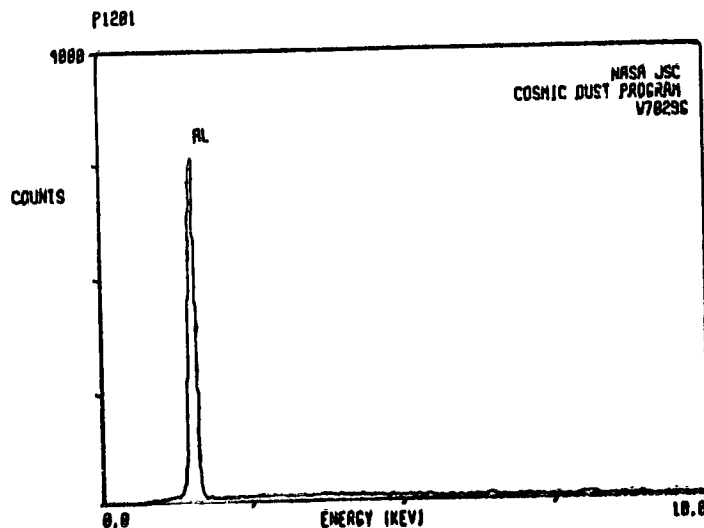


Figure 10 - Sample W7029G12. Type: Aluminum Oxide Sphere (AOS)

Classification is based on morphology and the dominant aluminum peak in the EDS spectrum. The most common AOS shape is the sphere, which is consistent with the oxidative melting of aluminum particles in the exhaust of the solid fuel rockets. This AOS is the only particle found to date that is neither a basic sphere nor a rare prolate ellipsoid. This particle may represent two particles that partially fused together or a sphere that was chipped and then partially remelted.

W7029J15

ORIGINAL, PARTIAL
OF POOR QUALITY



S-82-29234

<u>SIZE</u>	<u>SHAPE</u>	<u>TRANS.</u>
10	S	T/TL
<u>COLOR</u>	<u>LUSTER</u>	
CL/Pale Yellow	V	
<u>TYPE</u>	<u>COMMENTS</u>	
AOS		

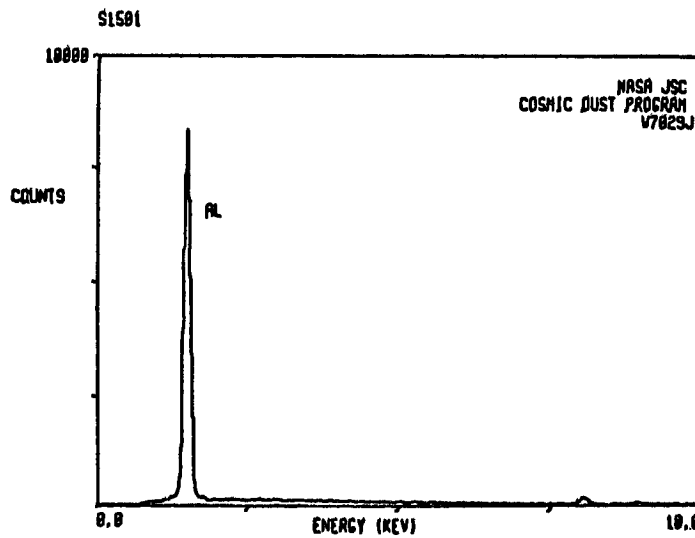


Figure 11 - Sample W7029J15. Type: Aluminum Oxide Sphere (AOS)

The classification is based on the generally spherical shape and dominant aluminum peak in the EDS analysis. This particle morphology is rare in the collection. Only 3 percent of the AOS samples have somewhat angular facets on the surface as shown here. The sample probably represents a more complete development of the bunched growth lines postulated to explain the "target" patterns shown in Figure 5.

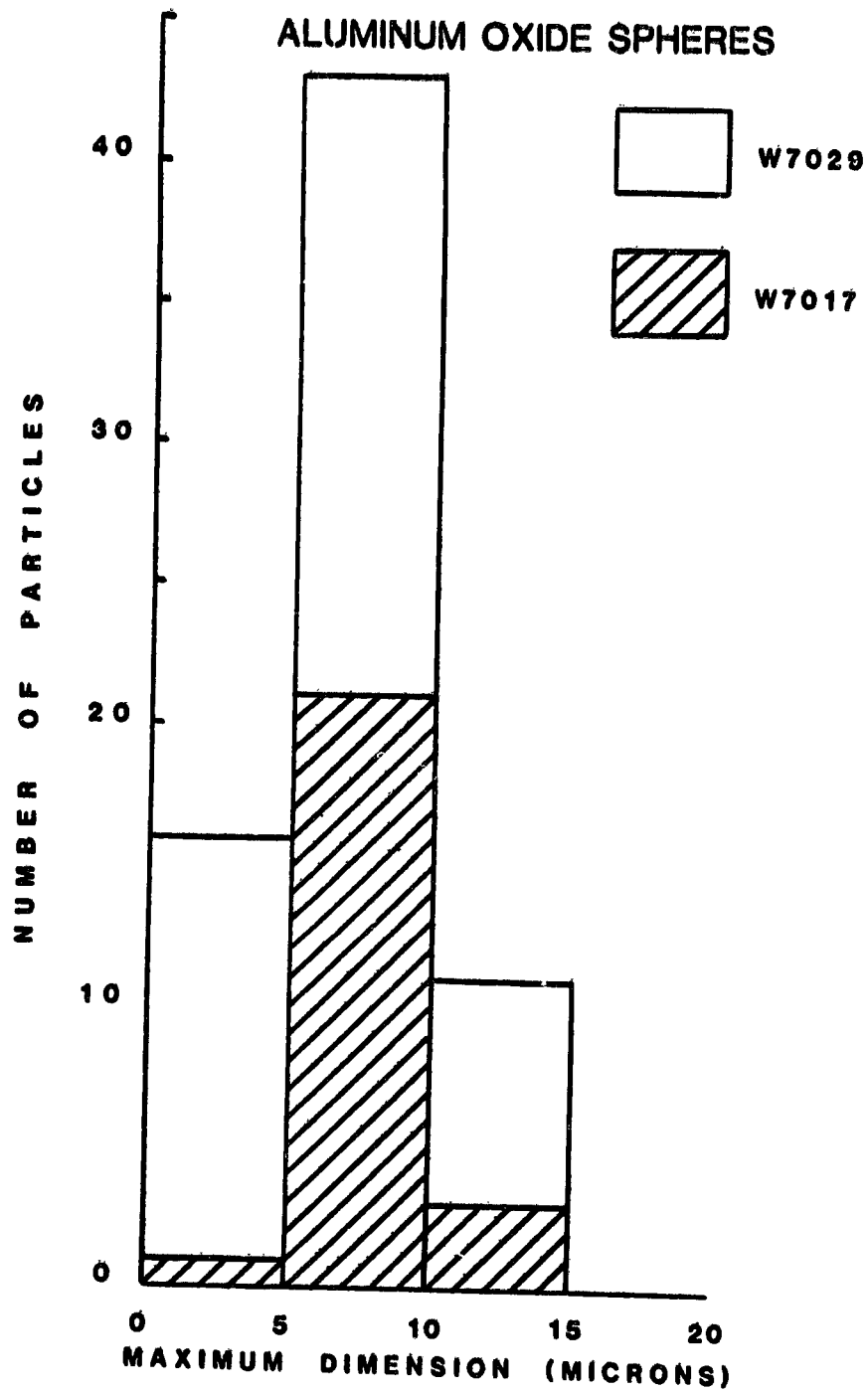
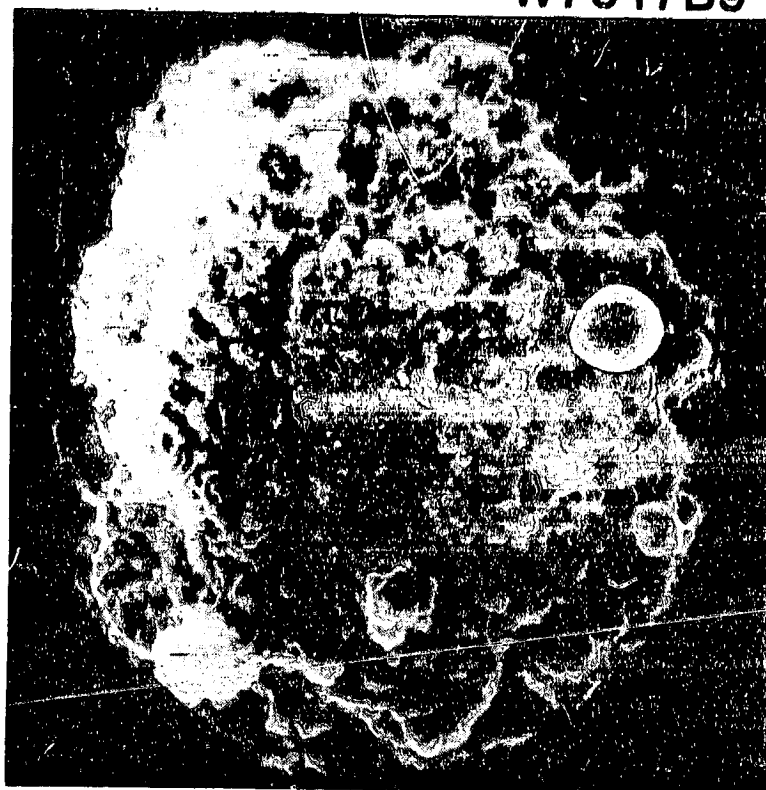


Figure 12

Size distribution of aluminum oxide spheres removed from cosmic dust collection flags W7017 and W7029. Each flag contains several times the number of spheres represented here. The flags were flown on separate WB-57F missions over Central and North America at an altitude of 60,000 feet. W7017 accumulated 45 hours exposure from July 7 to September 15, 1981 whereas W7029 accumulated 35 hours from September 15 to December 2, 1981.

W7017B9

ORIGINAL PHOTOGRAPH
OF POOR QUALITY



<u>SIZE</u>	<u>SHAPE</u>	<u>TRANS.</u>
8	E	0

<u>COLOR</u>	<u>LUSTER</u>
Dk. Brown to Black	D

<u>TYPE</u>	<u>COMMENTS</u>
TCA	

S-81-39951

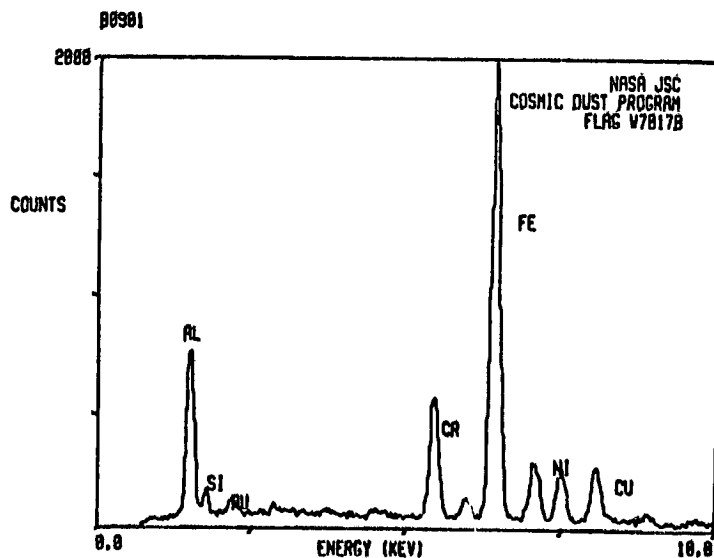
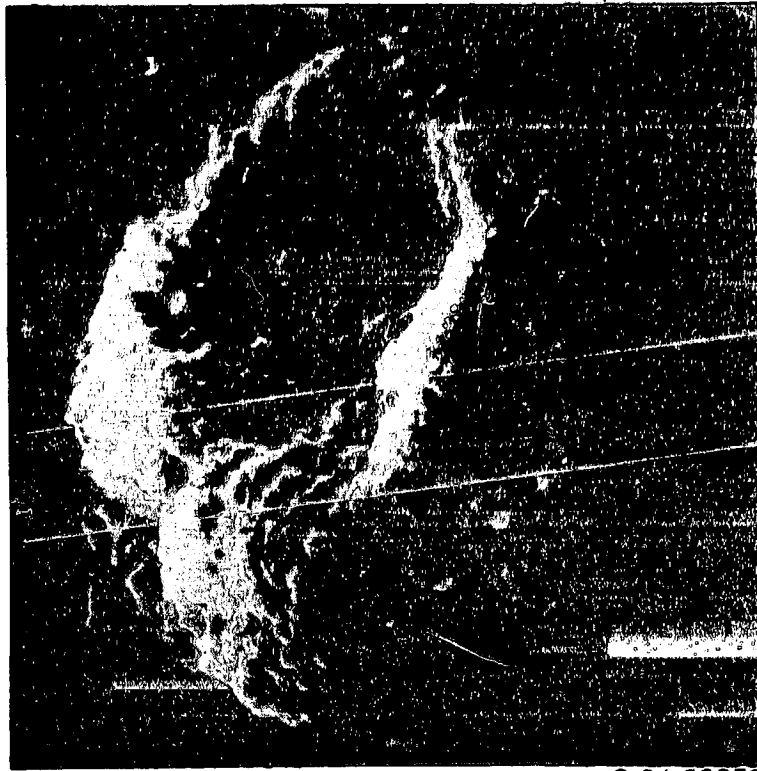


Figure 13 - Sample W7017B9. Type: Terrestrial Contamination Artificial (TCA)

The TCA classification is based on the non-cosmic (and unlikely mineralogical) elemental composition of the particle. The copper peak is probably stray x-radiation from the instrument, the gold peak is from the Au-Pd coating that was sputtered onto the SEM mount to prevent charging. The particle has a rough, somewhat porous surface made up of smaller rounded particles. The dark color and dull luster could be used to argue for its identification as a corrosion or rust fragment.

W7017B11



S-81-39952

SIZE SHAPE TRANS.
9 E T

COLOR LUSTER
Lt. Yellow ?

TYPE COMMENTS
AOS Al' Grain

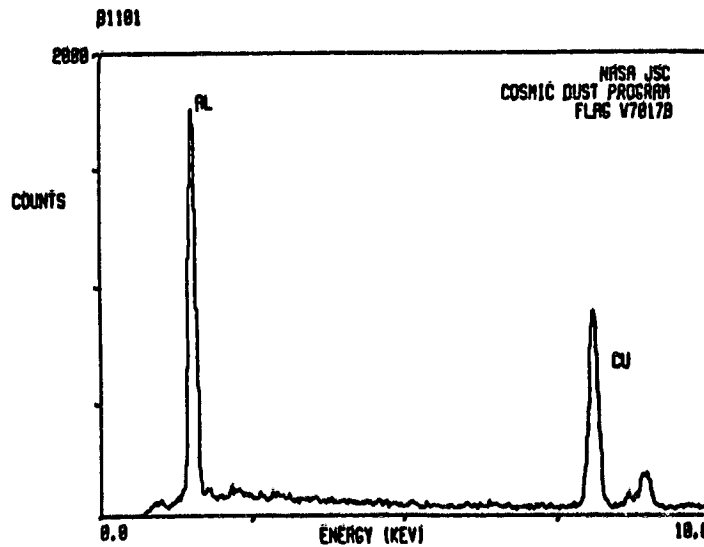


Figure 14 - Sample W7017B11. Type: TCA/AOS/Al'/?

The classification as TCA/AOS is suggested by the elemental composition but the combined morphology/composition does not fit either class well. Some particles rich in aluminum have minor amounts of other elements present (e.g., Mg, Si, S, Ca, Ti, Fe, Ni and Cu). Such particles have been called Al-prime (Al') particles by some investigators to differentiate them from aluminum oxide spheres. Controversy still exists as to the cosmic or contamination origin of these particles. The height of the copper peak cannot be totally attributed to stray x-radiation so that some copper is probably indigenous to the particle. The rough grainy surface does not appear to be porous.

W7017D8

CLASSIFIED
OF POOR QUALITY



S-82-25172

SIZE SHAPE TRANS.
7x11 I 0

COLOR LUSTER
Black SM/M

TYPE COMMENTS
TCA?

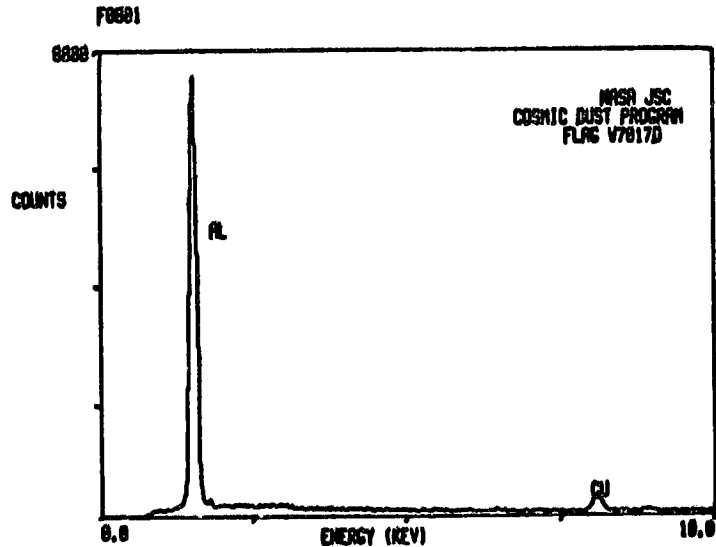
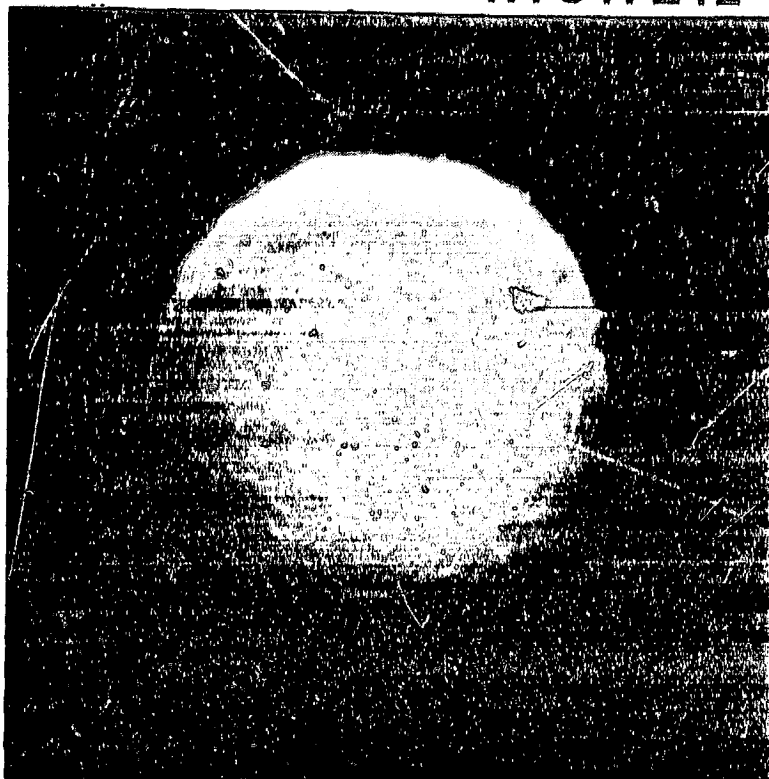


Figure 15 - Sample W7017D8. Type: Terrestrial Contamination Artificial (TCA)

The TCA classification is based on particle morphology and composition. The rough surface, irregular shape, and opacity prohibit an AOS classification even though the composition is correct. The black color and submetallic to metallic luster of the particle would indicate a fragment of aluminum metal, perhaps debris from an aircraft or a particle of unburned rocket solid-fuel additive.

W7017E12

ORIGINAL PAGE IS
OF POOR QUALITY



<u>SIZE</u>	<u>SHAPE</u>	<u>TRANS.</u>
7	S	TL

<u>COLOR</u>	<u>LUSTER</u>
Gray-Brown	SV

<u>TYPE</u>	<u>COMMENTS</u>
TCA/TCN?	A1'?

S-82-25161

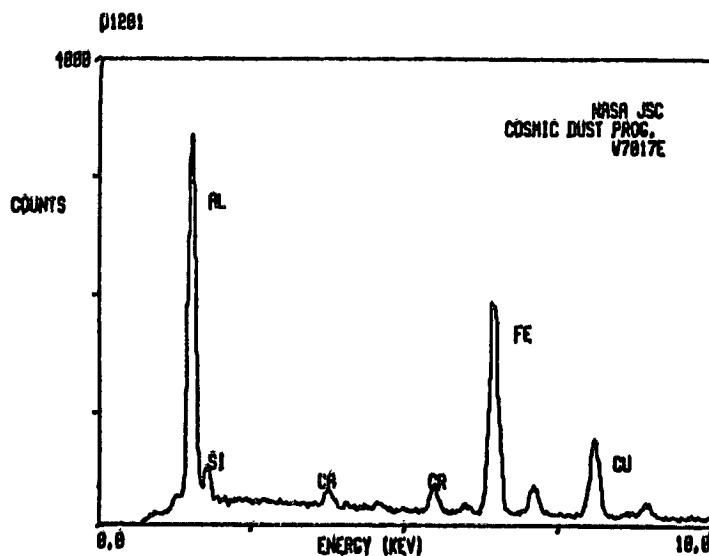


Figure 16 - Sample W7017E12. Type: TCA/TCN/A1'/?

The ambiguous classification is caused by the unusual composition and color. The high aluminum abundance and the spherical shape would argue for an AOS classification but the presence of Si, Ca, Cr, Mn, Fe and perhaps Cu make this category unacceptable. The combination of Al, Si, and Ca would suggest perhaps a TCN origin but the Cr, Mn, Fe, and Ti abundances more favorably match those of a metal alloy. Although the spherical shape is most easily explained by an ablation origin, the rough surface could be used to argue for an abrasion origin.

ORIGINAL PAGE IS
OF POOR QUALITY

W7017G8



S-82-25719

SIZE SHAPE TRANS.
4 S 0

COLOR LUSTER
Black D/SM

TYPE COMMENTS
? Perhaps TCA,
spherical?

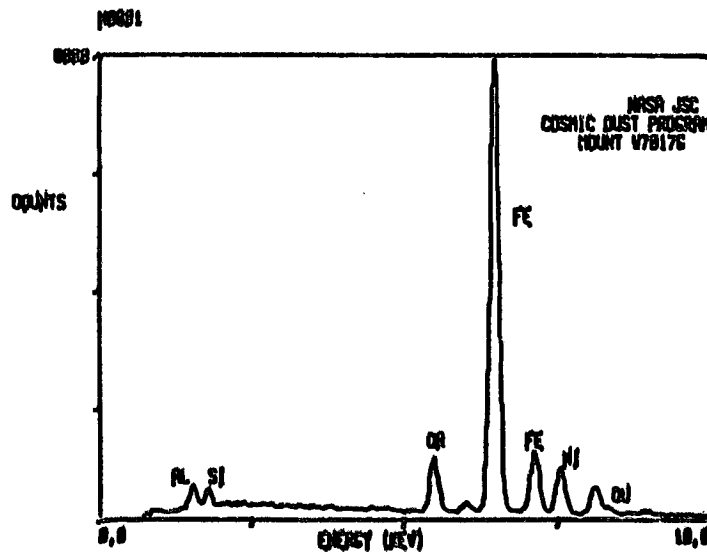


Figure 17 - Sample W7017G8. Type: Terrestrial Contamination Artifact (TCA)?

The spherical shape can be explained as an ablation product although the composition is best explained as an altered or oxidized stainless steel. The surface of the sphere is rough but the individual particles on the surface appear to be rounded. Although the surface is rough the particle does not appear to be porous.

W7017G10

ORIGINAL PAGE IS
OF POOR QUALITY



S-82-25724

<u>SIZE</u>	<u>SHAPE</u>	<u>TRANS.</u>
5x6	S/E	0
<u>COLOR</u>	<u>LUSTER</u>	
Black	SV/SM	
<u>TYPE</u>	<u>COMMENTS</u>	
TCA?		

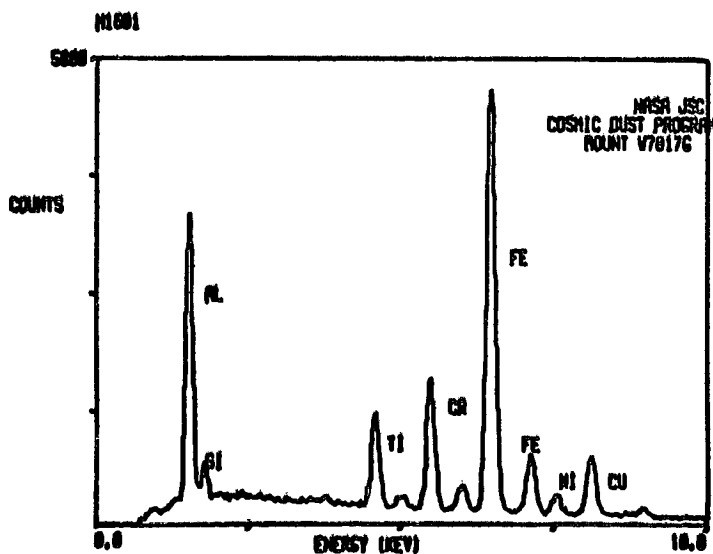
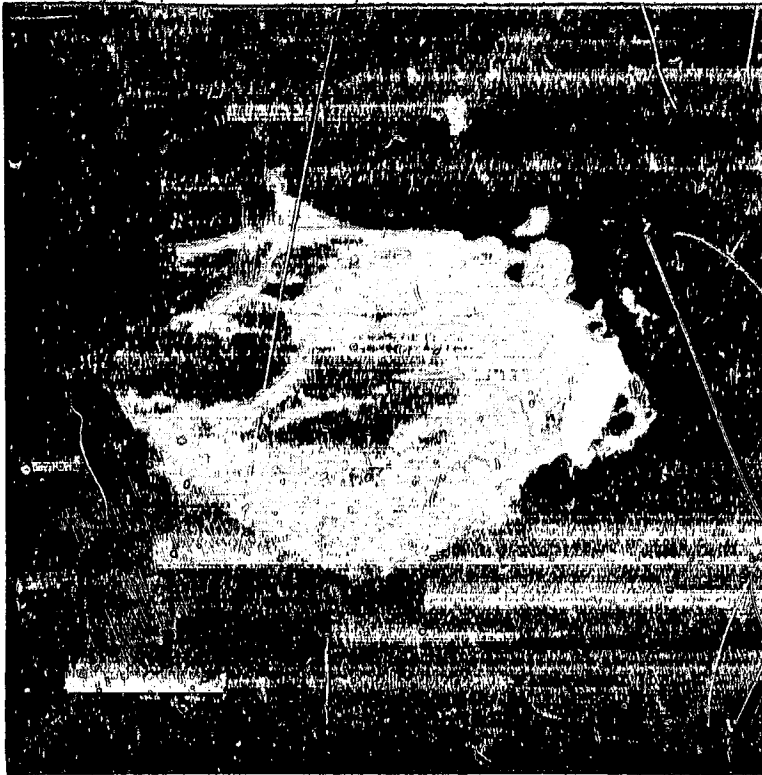


Figure 10 - Sample W7017G10. Type: Terrestrial Contamination Artificial (TCA)?

The composition is best explained as an alteration or ablation product of stainless steel mixed with aluminum. The particle morphology could be interpreted as a small sphere fused to a larger sphere. The surface is rough and pitted but porosity does not appear to extend to any significant depth.

W7029A15

ORIGINAL PAGE IS
OF POOR QUALITY



S-82-27545

SIZE
2x4

SHAPE
I

TRANS.
0

COLOR
Black

LUSTER
SM

TYPE
TCA?

COMMENTS

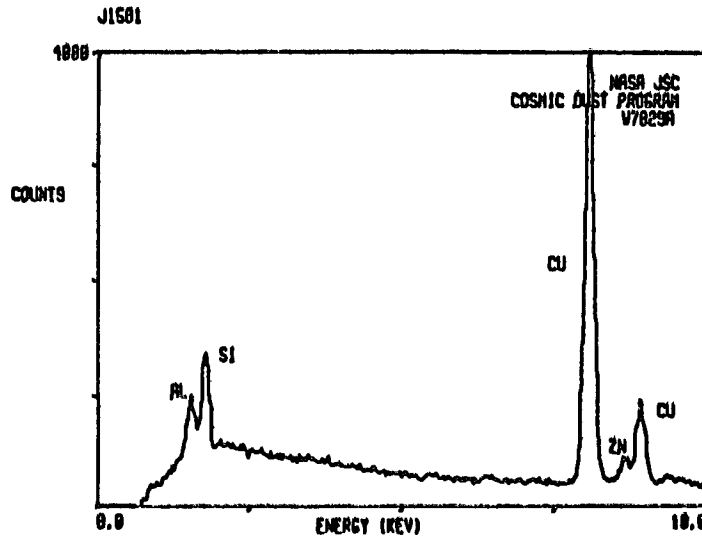


Figure 19 - Sample W7029A15. Type: Terrestrial Contamination Artificial (TCA)

The composition of the particle is best understood as that of an aircraft component. The particle is mainly copper with minor amounts of Zn, Si, and Al. The black color and submetallic luster argues for a metal fragment and not an oxide. Additionally, the particle appears to be sheared or pulled but without evidence of melting.

W7029B7

ORIGINAL PHOTO
OF POOR QUALITY



<u>SIZE</u>	<u>SHAPE</u>	<u>TRANS.</u>
11	S	0

<u>COLOR</u>	<u>LUSTER</u>
Black	M

<u>TYPE</u>	<u>COMMENTS</u>
?	

S-82-27569

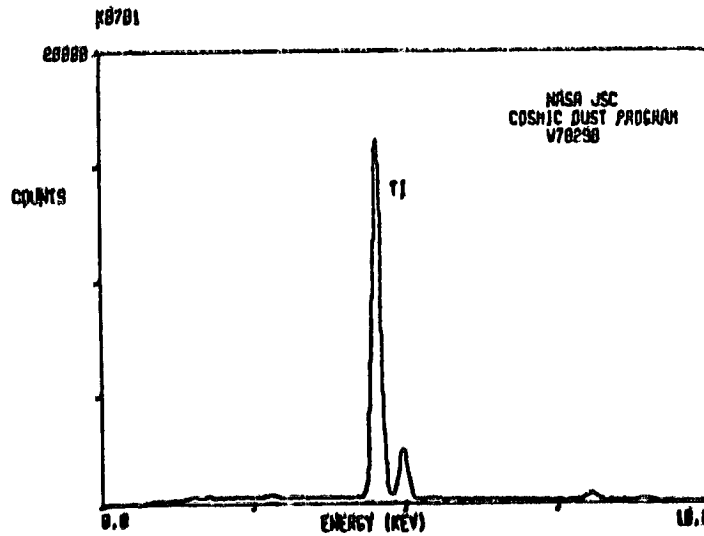


Figure 20 - Sample W7029B7. Type: Terrestrial Contamination Artificial (TCA)?

The unusual composition indicates a man-made origin although it might also be explained as rutile (TiO_2), a rare accessory mineral in some meteorites. The spherical shape suggests an earlier molten state, perhaps formed by ablation. The shape combined with the titanium composition can be interpreted as material eroded from a solid rocket fuel liner or as ablation material from a re-entering spacecraft.

W7029B8

ORIGINAL PAGE IS
OF POOR QUALITY



S-82-27570

<u>SIZE</u>	<u>SHAPE</u>	<u>TRANS.</u>
7x11	I	0
<u>COLOR</u>	<u>LUSTER</u>	
Dk. Red- Brown	SM	
<u>TYPE</u>	<u>COMMENTS</u>	
?		

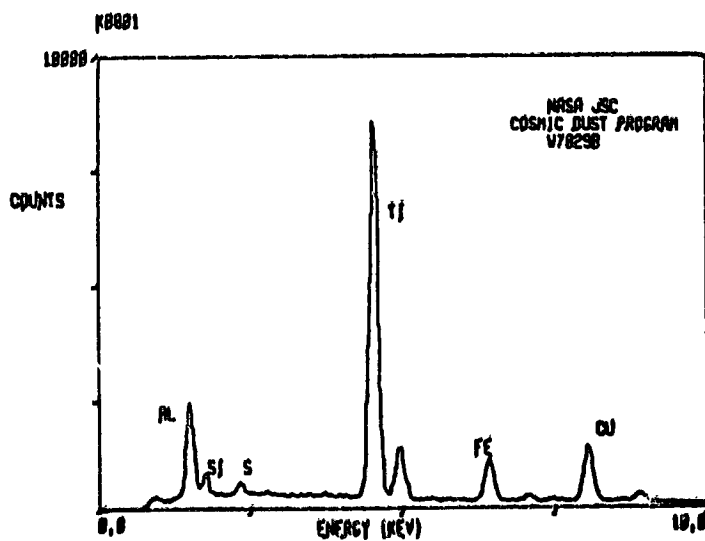
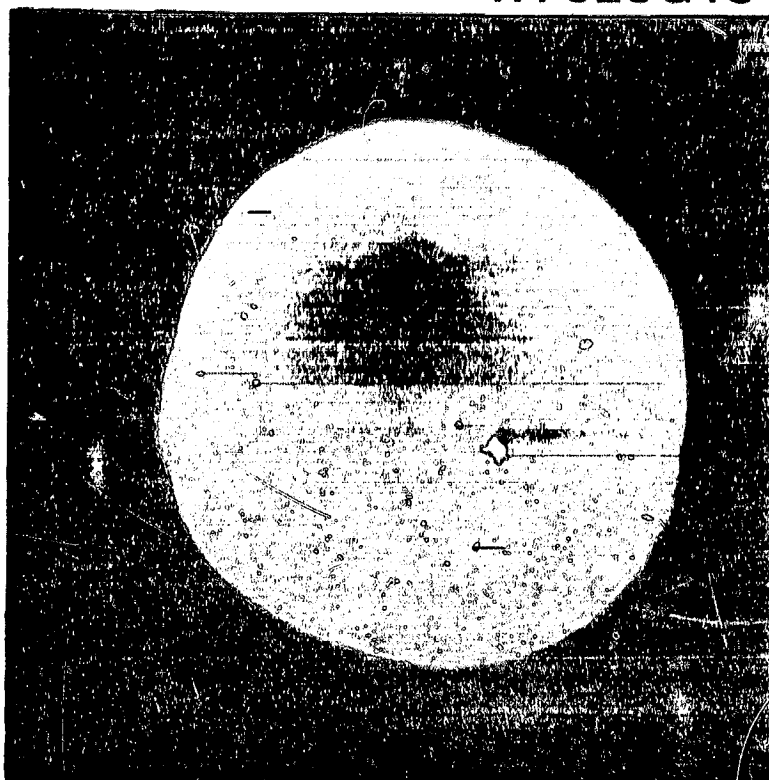


Figure 21 - Sample W7029B8. Type: Terrestrial Contamination Artificial (TCA)?

This classification is chosen because of the high titanium content of the particle. The EDS composition is for the whole particle although spot analyses of different areas on the grain might isolate the sources of some of the minor peaks, (e.g., Al, Si, S). However, the dark color and submetallic luster indicates the presence of a metallic phase.

W7029G13

ORIGINALLY
OF POOR QUALITY



S-82-29616

SIZE SHAPE TRANS.
6 S 0

COLOR LUSTER
Black M

TYPE COMMENTS
TCA?

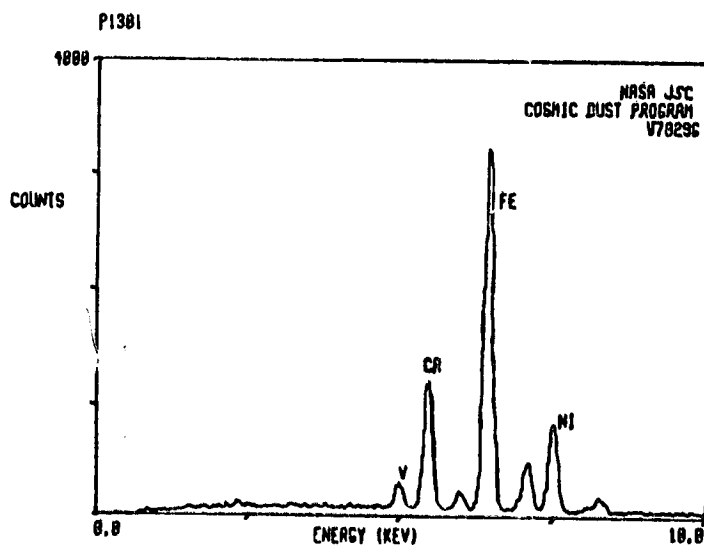
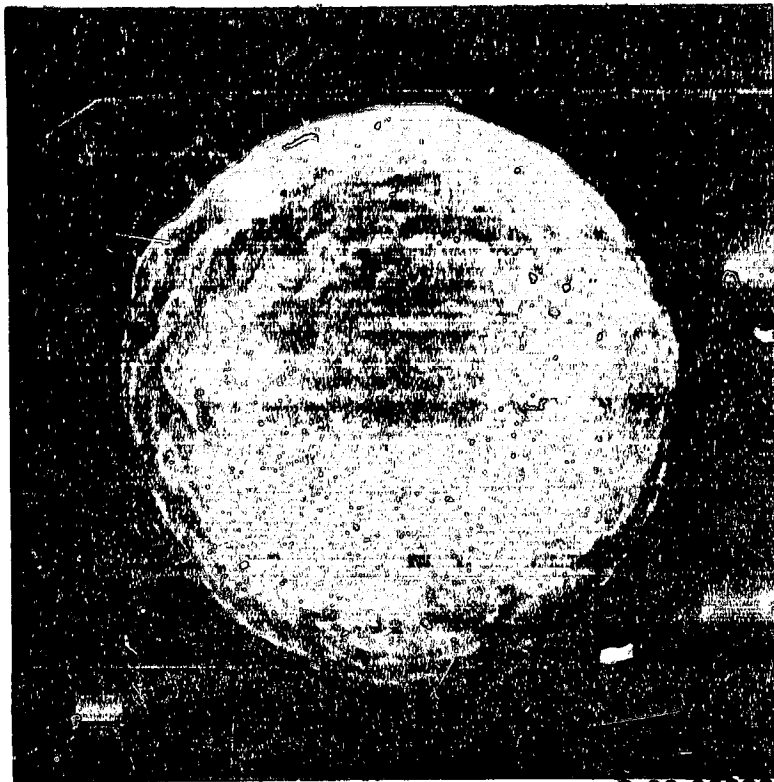


Figure 22 - Sample W7029G13. Type: Terrestrial Contamination Artificial (TCA)

The composition of the particle suggests a man-made alloy. The spherical shape is perhaps best explained as an ablation product. The surface is cracked and it appears that a bubble has broken through to the surface of the sphere in one area.

W7029H6

VERY POOR QUALITY
OF POOR QUALITY



S-82-30202

SIZE SHAPE TRANS.
7 S 0

COLOR LUSTER
Black M

TYPE COMMENTS
TCA?

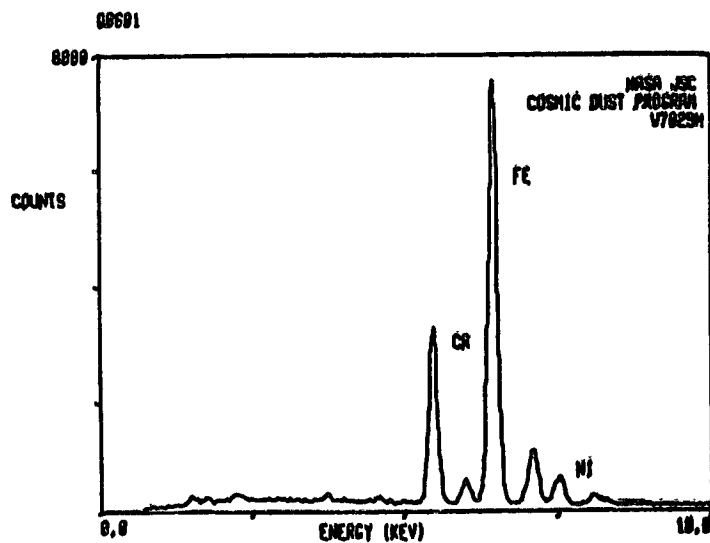
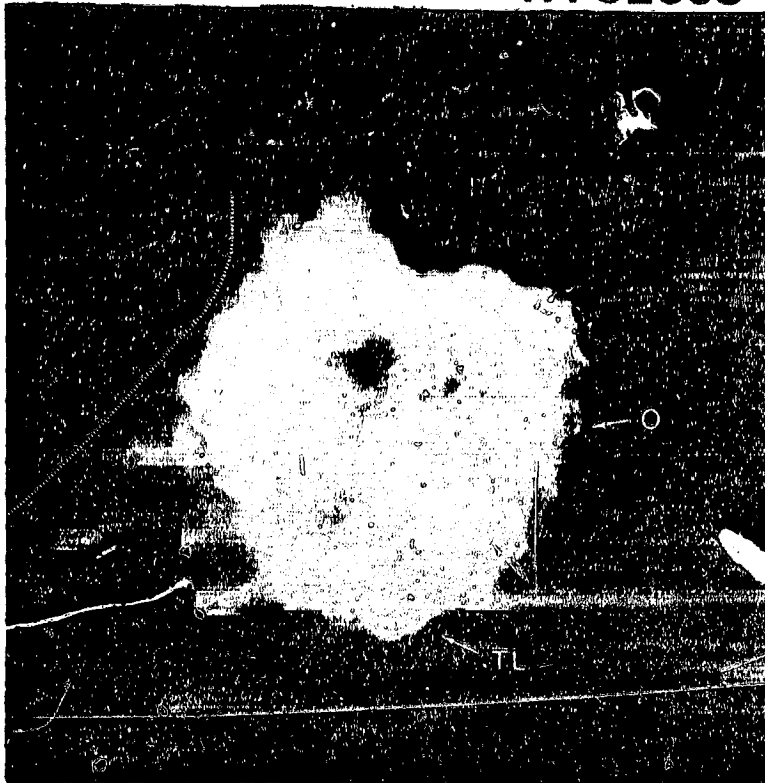


Figure 23 - Sample W7029H6 Type: Terrestrial Contamination Artificial (TCA)

This classification is chosen because of the composition, which is similar to some stainless steels, and because of the lack of common meteorite minerals with this composition. The spherical shape indicates an initially molten phase. The black color, metallic luster and rough surface are consistent with an ablation origin.

W7029J3

ORIGINAL PAGE IS
OF POOR QUALITY



S-82-29225

SIZE SHAPE TRANS.
20x21 E/I O/TL

COLOR LUSTER
Dk. Red- D/V
Brown to
Black

TYPE COMMENTS
TCA?

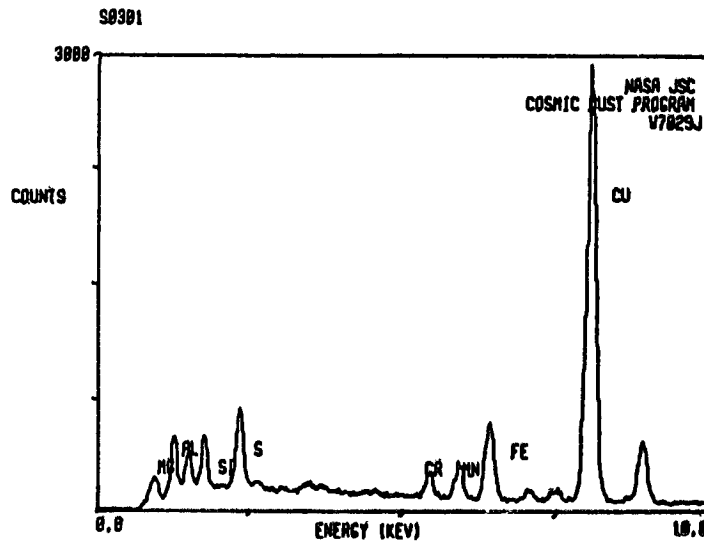


Figure 24 - Sample W7029J3. Type: Terrestrial Contamination Artificial (TCA)?

The TCA classification is selected because of the unusual copper-rich composition and large size of the particle. One could select some of the lower intensity peaks from the EDS spectrum and argue for a partial cosmic component; the presence of both a translucent and an opaque phase would support such a argument. However, the high copper content forces the TCA classification at the present level of characterization.

W7028A5

ORIGINALLY CLASSIFIED
AS UNCLASSIFIED
DATE 08-12-2011 BY 60322 UCBAW



S-82-31348

<u>SIZE</u>	<u>SHAPE</u>	<u>TRANS.</u>
6	S	TL
<u>COLOR</u>	<u>LUSTER</u>	
Brownish Yellow	V	
<u>TYPE</u>	<u>COMMENTS</u>	
?		

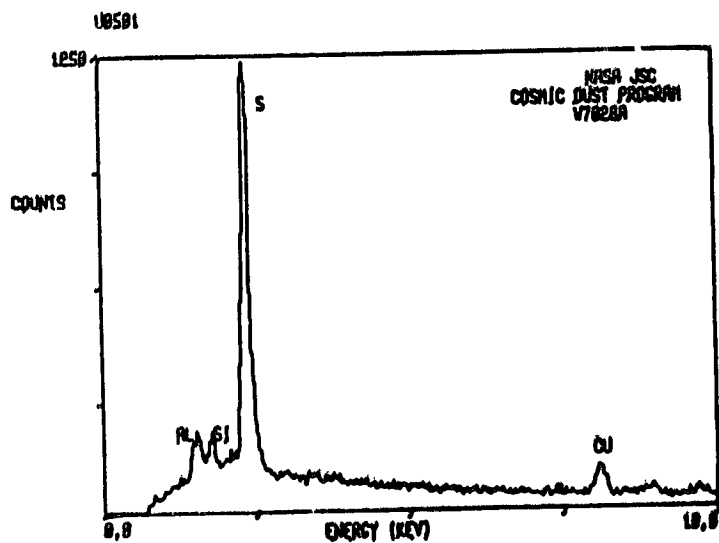


Figure 25 - Sample W7028A5. Type: Terrestrial Contamination Artificial (TCA)?

The TCA classification was chosen because of the unusual sulfur-rich composition of the particle. The full significance of the particle cannot be evaluated until some additional work has been completed. This particle was broken from a larger curved, opaque and metallic particle that remains on the collection surface unanalyzed at this time. However, the origin of a metal particle with beads of sulfur on its surface is difficult to explain.

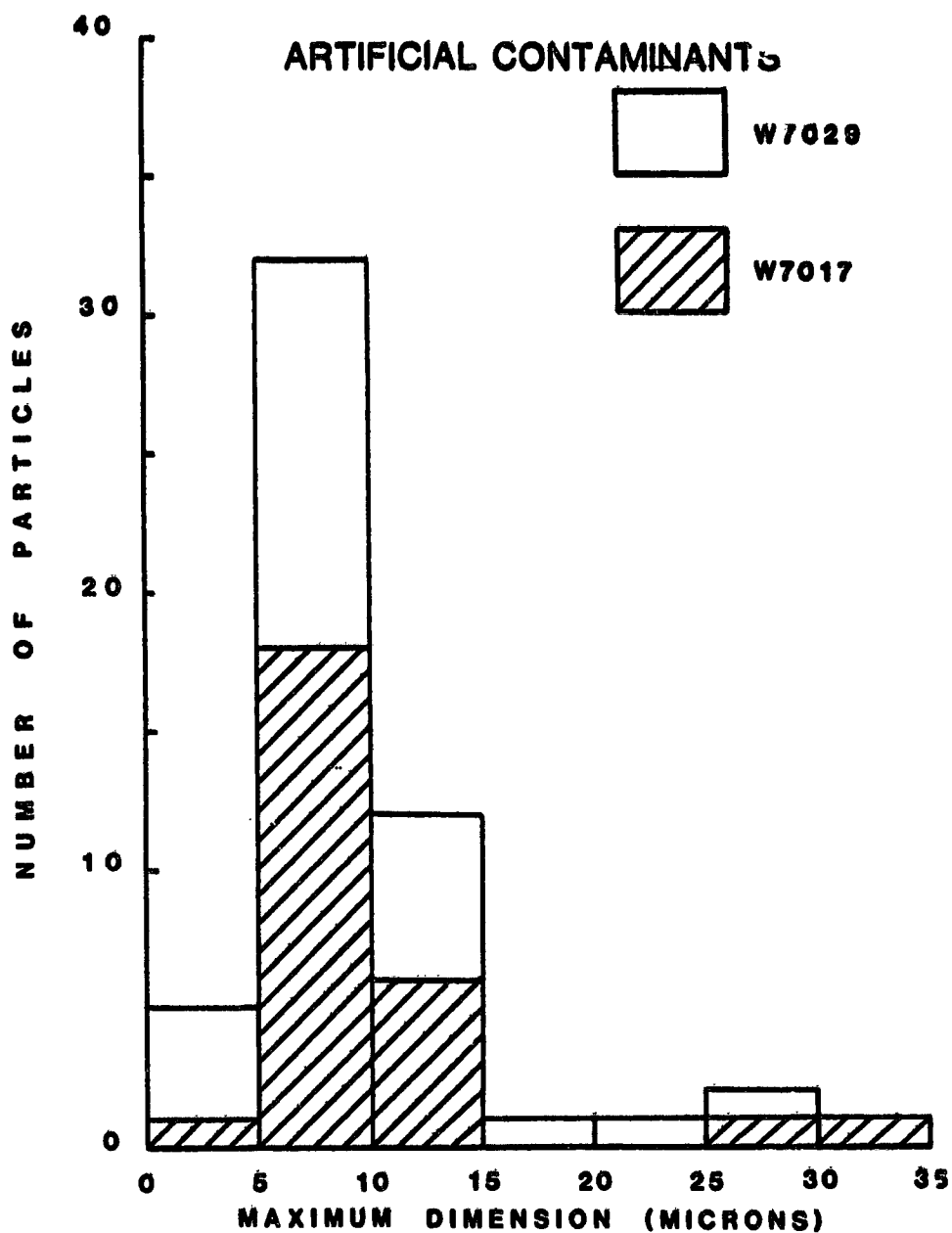


Figure 26

Size distribution of tentatively identified man-made contaminant (TCA) particles (excluding aluminum oxide spheres) removed from cosmic dust collection flags W7017 and W7029. The flags were flown on separate WB-57F missions over Central and North America at an altitude of 60,000 feet. W7017 accumulated 45 hours exposure from July 7 to September 15, 1982 whereas W7029 accumulated 35 hours from September 15 to December 2, 1981.

REFERENCES

1. Brownlee, D.E., Tomandl, D., Blanchard, M.B., Ferry, G.V., and Kyte, F. (1976). An atlas of extraterrestrial particles collected with NASA U-2 aircraft - 1974-1976. NASA TMX 73, 152, National Technical Information Service, Springfield, Virginia, 47 pp.
2. Brownlee, D.E. (1978). Interplanetary Dust: Possible implications for comets and presolar interstellar grains. In Protostars and Planets, (T. Gehrels, ed.) 134-150, Univ. of Arizona Press, Tucson, Arizona.
3. Brownlee, D.E. (1978). Microparticle studies by sampling techniques. In Cosmic Dust (J.A.M. McDonnell, ed.), 295-335. Wiley, NY.
4. Esat, T.M., Brownlee, D.E., Papanastassiou, D.A., and Wasserburg, G.J. (1979). Magnesium isotopic composition of interplanetary dust particles. Science 206, 190-197.
5. Flynn, G.J., Fraundorf, P., Shirck, J., and Walker, R.M. (1978). Chemical and structural studies of "Brownlee" particles. Proc. Lunar Planet Sci. Conf. 9th, 1187-1208.
6. Fraundorf, P. and Shirck, J. (1979). Microcharacterization of "Brownlee" particles: features which distinguish interplanetary dust from meteorites? Proc. Lunar Planet Sci. Conf. 10th, 951-976.
7. Ganapathy, R. and Brownlee, D.E. (1979). Interplanetary dust: Trace element analysis of individual particles by neutron activation. Science 206, 1075-1077.
8. Hudson, B., Flynn, G.J., Fraundorf, P., Hohenberg, C.M., and Shirck, J. (1981). Noble gases in stratospheric dust particles: confirmation of extraterrestrial origin. Science 211, 383-386.
9. Rajan, R.S., Brownlee, D.E., Tomandl, D., Hodge, P.W., Farrar, H., and Britten, R.A. (1977). Detection of ^4He in stratospheric particles gives evidence of extraterrestrial origin. Nature 267, 133-134.
10. Brownlee, D.E., Ferry, G.V., and Tomandl, D. (1976). Stratospheric aluminum oxide. Science 191, 1270-1271.
11. Clanton, U.S., Dardano, C.B., Gabel, E.M., Gooding, J.L., and Isaacs, A.M., Mackinnon, I.D.R., McKay, D.S., Nace, G.A., and Warren, J.L. (1982). Cosmic Dust Catalog Vol. 1, Nos. 1 and 2, Curatorial Publication No. 59, NASA Johnson Space Center, 17903.
12. Clanton, U.S., Dardano, C.B., Gabel, E.M., Gooding, J.L., Isaacs, A.M., Mackinnon, I.D.R., McKay, D.S., Nace, G.A., and Warren, J.L. (1982). Cosmic Dust Catalog Vol. 2, Nos. 1 and 2, Curatorial Publication No. 62, NASA Johnson Space Center, 18221.

1/12
N 85-21204

Impacts on Explorer 46 from an Earth Orbiting Population

by

Donald J. Kessler

NASA/Johnson Space Center

Abstract

Explorer 46 was launched into Earth orbit in August 1972 to evaluate the effectiveness of using double-wall structures to protect against meteoroids. This paper reexamines the data from the Meteoroid Bumper Experiment on Explorer 46 and concludes that most of the impacts originated from an Earth orbiting population. The probable source of this orbiting population is solid rocket motors fired in Earth orbit.

Introduction

It has long been known that meteoroid damage to spacecraft could be reduced by using a double-wall structure instead of a single-wall. However, because of the difficulty of reproducing the high meteoroid velocities in the laboratory, the exact efficiency of the double-wall structure was not known. The Meteoroid Bumper Experiment, flown on Explorer 46, was designed to determine this efficiency by comparing the penetration rate on its double-wall structure to the penetration rate on earlier, single-wall spacecraft sensors.

This paper will reexamine the data obtained from the Meteoroid Bumper Experiment. It will show that the distribution of sensors which were penetrated is totally consistent with an Earth orbiting population, whereas the probability of interplanetary meteoroids causing this distribution is extremely small. In addition, many of the impacts occurred just after a solid rocket motor was fired in space, suggesting this may be the primary source of these impacts.

Description of Experiment

An excellent description of the Meteoroid Bumper Experiment and the data it obtained is given by Humes (1981). The description is sufficiently detailed to allow an independent evaluation of the data. For convenience, some of that description will be reproduced here. Explorer 46 was launched on August 13, 1972 into an orbit of 490 km by 815 km with an inclination of 38° . Figure 1 shows the satellite as it was deployed in orbit. The bumper experiment consisted of 96 pressurized cells. Once a cell was penetrated, the pressure loss was recorded and it was no longer sensitive to penetration. Each cell had a wall thickness of $50 \mu\text{m}$, and was "protected" by a $25 \mu\text{m}$ thick bumper, as shown in figure 2. Figure 3 shows the rate that these cells were penetrated after launch. Humes compares the resulting average flux in figure 4 with the rate obtained by previous single wall satellite experiments. He concludes that the meteoroid bumper provides as much protection as a single-wall structure which is 6.9 times thicker than the total thickness of the double-wall.

Description of a Solid Rocket Motor Exhaust Product

Solid rocket motors have been studied by NASA for the purpose of improving engine performance, determining the effects on the stratosphere, and determining the safe ignition distance from the Space Shuttle. However, no detailed analysis has ever been performed on the effects of these rockets on near-Earth orbital space. It is known that 34% of the rocket's exhaust products are Al_2O_3 particulates. Most of these particulates are between 0.1 and $10 \mu\text{m}$ in diameter. However, particles larger than $100 \mu\text{m}$ have been observed from some rockets. It is likely that particles of this size and larger only originate from older, cooler burning engines, where Al_2O_3 slag has been observed to condense on the rocket motor nozzle. Late in the burn this slag could chip off, producing the larger particles.

Solid rocket motors fired in space and used in the early 1970's consisted of the Delta 3rd stage and the Scout 4th stage. The Delta 3rd stage produces 350 kgm of Al_2O_3 , and the Scout 4th stage produces 93 kgm. Sometimes smaller solid rocket motors were attached to payloads and used to place that payload

in its final orbit. Larger solid rocket motors are now being released by the Space Shuttle and used to place Shuttle payloads into higher orbits.

A first approximation would lead one to conclude that most, if not all, of the Al_2O_3 would have non-orbital trajectories since it is ejected from the rocket in the opposite direction as the rocket moves. However, there are frequently conditions where much, if not most, of the Al_2O_3 would remain in orbit. This is especially true for the larger particulates, which are ejected at lower velocities and are less effected by atmospheric drag. conditions which would leave a larger percentage of particulates in orbit are: (1) the rocket is required to dissipate energy by an out-of-plane burn. Since solid rocket motors cannot be shut down until the fuel is exhausted, such a burn is frequently required in order to place the payload in the correct orbit. (2) The rocket is required to perform a plane change. (3) The rocket fails. The most common failure causes the rocket to tumble. (4) The payload is placed in a high orbit. Toward the end of such a burn, the ejected particles will go into Earth orbit.

Possible Interaction of Solid Rocket Motor Particulates to Explorer 46 Data

The Meteoroid Bumper Experiment was calibrated in the laboratory by Humes (1981) at velocities between 2 km/sec and 7 km/sec. Between velocities 4 km/sec and 7 km/sec, the projectile mass, which just penetrated the structure was about 9×10^{-7} gm, or a 75 μm diameter Al_2O_3 particle. Kessler (1978) calculated an average collision velocity for orbiting objects of 10 km/sec. However, relative to a spacecraft with a 38° inclination, the average velocity would be closer to 7 km/sec, so that the laboratory calibrations have a direct application to orbiting objects.

Since little is known about the number of particles of this size produced by the rockets used during this period, it is impossible to model with precision the effect of solid rockets on the experiment. The possibility that there may be an effect is suggested by the following: (1) Only 5 kgm of Al_2O_3 particles, 75 μm in diameter and distributed between 490 and 815 km altitude is required to account for the average surface area flux of 5×10^{-6} / m^2 -sec measured by the experiment. (See Kessler, 1981 for calculational technique). This represents between 1% and 6% of the Al_2O_3 produced by a single rocket firing. (2) During the 900-day data period, 20 solid rocket motors were fired in low Earth orbit. (3) The orbital lifetime of particles which pass through the altitude range of Explorer 46 is a function of various particle orbital parameters, solar activity conditions, and geomagnetic conditions. However, the lifetime of 75 μm particles in circular orbit during average conditions range from about a week (at 490 km) to a year (at 815 km).

There is evidence to suggest that other experiments, designed to detect meteoroids, also sampled particulates from solid rocket motors. A meteoroid impact experiment, deployed out of the anti-solar air lock and on the Apollo telescope mount on Skylab, was returned to Earth for examination (See Hallgren et al., 1976). In addition, the Apollo windows from Skylab 4 were removed and examined for meteoroid impacts. (See Clanton, et al, 1980). In both cases, the hypervelocity pits were examined under a scanning electron microscope, and discovered to contain a large amount of aluminum. While aluminum is a common element, it has never been found to be the only detectable element in meteoroids as was observed in these pits. In addition, the pits on the

windows showed the unusual character of containing an "aluminum liner". Such a liner has not been observed in meteoroid pits found on returned lunar rocks.

Reexamination of Meteoroid Bumper Experiment Data

The first hint that the experiment may have measured something other than meteoroids is seen in figure 3, where several large increases in flux can be observed around 25, 45, 240, and 560 days after launch. Table 1 contains a list of solid rocket motors fired during this period. Three of the flux increases immediately follow solid rocket firings. However, if there is a cause and effect relationship, then the average flux measured for some arbitrary time after each solid rocket motor firing should be higher than the average flux when there has been no solid rocket firing. To test this possibility, the number of penetrations occurring 20 days after a solid rocket firing were counted and this flux was then compared to the flux resulting from penetrations which occurred more than 20 days after a solid rocket firing. The 20-day period was arbitrarily chosen to satisfy the following criteria: (1) The interval is long enough to allow for orbit plane processions to give some chance of impact and atmospheric drag to begin removal of some orbits. (2) The interval is short enough that there are sufficient periods of remaining time of "no solid rocket firings".

During the 900 days of Explorer 46 data taking, there were 331 days which were within 20 days after a solid rocket motor firing in space. During these 331 days, 24 penetrations were recorded, for an event rate of 0.073/day. The 95% confidence interval event rate would lie between 0.047/day and 0.106/day. The remaining 569 days represent a period which should be less affected by solid rocket motor firings. There were 27 penetrations during this period, leading to an event rate of 0.047/day, with 95% confidence between 0.031/day and 0.069/day. Since the event rate just after solid rocket firings is higher, and since the measured rate of one group is at, or just outside of, the 95% confidence rate of the other group, one can conclude that there is a 95% probability that the larger event rate was due to solid rocket motor firings. While this probability may not be impressive, it is highly suggestive of a solid rocket motor origin for these impacts.

If this is true, then why are there no large flux increases after day 600 into the mission—especially when nearly half of the solid rocket motor firings take place during this period? One possibility is that either new operating procedures or new rocket motor designs ejected fewer large particulates into the altitude range of Explorer 46. While this may be a contributing possibility, a closer examination of the data not only reveals another cause, it also reveals a stronger argument that the Explorer 46 penetrations were mostly Earth orbiting objects. The additional cause, as will be discussed below, is that nearly 70% of the penetration cells which were sensitive to an orbiting population were penetrated by day 600 of the mission.

Direction of Impacts

Explorer 46 was placed into orbit with no preferred orientation, nor with any sensors to determine its orientation. If the spacecraft were randomly tumbling, then any sensor on the spacecraft would have the same probability

per unit area of penetration. The flux on any set of identical sensors should then be the same, regardless of the direction of the impacting particles.

Another possibility is that any initial tumbling was sufficiently small that it was quickly damped out. The only stable orientation of the spacecraft would be with respect to the Earth, becoming gravity-gradient stabilized and not the more massive, central axis of the spacecraft pointing toward the center of Earth. The velocity vector of any objects orbiting at this altitude must be in a plane which is nearly parallel to the Earth's surface, or else they would run into the Earth. Therefore, Earth orbiting objects would most likely impact surfaces perpendicular to the Earth's surface, and not impact surfaces parallel to the Earth's surface. Meteoroids, on the other hand, as part of the interplanetary environment, impact the surface of the Earth at all angles. Even a highly directional meteoroid stream, when averaged over the entire surface of the Earth, shows random impact angles. Therefore, any sensor moving above the Earth's surface and keeping the same orientation with respect to the Earth, will also experience a near random directionality from meteoroids. The only direction from which meteoroids cannot originate is from the Earth. The effect of this Earth shielding is to reduce the number of impacts by about 1/2 for both parallel and perpendicular surfaces to the Earth's surface.

A look at the detailed data given by Hume reveals that certain sets of sensors experienced a much higher flux than others, making it highly unlikely that the spacecraft was randomly tumbling. In fact, of the 51 impacts, 43 of them were on surfaces most sensitive to orbiting objects on a gravity-gradient stabilized spacecraft. A reason that there is not as strong a time correlation with solid rocket motor firing after 600 days then becomes clear - the spacecraft sensor area for orbiting particles had been significantly reduced from 13.3 square meters at the beginning of the data taking to only 4.7 square meters at the end. The corresponding area loss on the sensors perpendicular to these sensors was from 5.9 sq. meters to 4.1 sq. meters.

The significantly higher flux measured by the sensors perpendicular to the Earth's surface compared to those in parallel orientation is clearly shown in figure 5. To obtain figure 5, the flux was calculated from 3 consecutive impacts (i.e. 2 consecutive time intervals) on the two sets of sensors. Thus, the flux for penetration point "n" is $F_n = 2/A_n (t_{n+1} - t_{n-1})$ where A_n is the area exposed at time t_n , and $t_{n-1} - t_{n+1}$ is the time interval between penetration point n-1 and n+1. This flux was plotted as a function of time in figure 5. Notice that during the first 50 days of the mission, both sets of sensors measured a flux in excess of 1×10^{-2} impacts/m²-day. However, for the next 850 days, the flux levels are dramatically different. The flux on the perpendicular surfaces are always larger than the flux on the parallel surfaces, averaging about 5×10^{-3} impacts/m²-day, compared to 1×10^{-3} impacts/m² day for the parallel surfaces. While the large increases in flux do appear to have some time correlation with the solid rocket firing also shown in figure 5, random variations can be expected to cause similar flux increases based on only 3 data points. Therefore, the differences in the average flux is much more significant than the large flux increases.

An additional directionality feature for the flux measured by Explorer 46 was pointed out by Humes (1981) and is shown in figure 6. Humes noted that "for long periods of time during the experiment, ...penetrations occurred

almost exclusively in either the fully deployed wings or the partially deployed wings. ... However, attempts to discover the orbit distribution of the meteoroids that would have produced the observed results have been unsuccessful." If Explorer 46 were gravity-gradient stabilized and not spinning or spinning very slowly, around the axis pointing toward the Earth, an Earth orbiting population flux could will be directional around this axis. This directionality is mostly a function of the impacting particles' orbital inclination and the point of intersection of its orbit with Explorer 46. Most of the expected impact directions would be nearly perpendicular to the Explorer 46 velocity vector. Thus, regardless of whether the detected particles were from a single rocket firing a few days earlier (i.e. acting like a meteor stream), or were from several firings months earlier (i.e., part of an Earth orbiting background flux), the resulting flux would also be highly directional around the axis pointed toward Earth as Humes observed.

Probability that Measurements Resulted from Random Variation

It is useful to explore the possibility that Explorer 46 detected only a natural meteoroid environment, and that all of the observed variations from the "average meteoroid flux" were the result of random variations from that average. If so, then one can ask what is the probability that the observed variation would randomly occur. Or, to state it another way, given some average meteoroid flux, how many Explorer 46 satellites would one have to fly before one of them would show both a time correlation and a directionality at least as great as that measured by Explorer 46. Although an accurate answer is very difficult, a few conservative assumptions leads to the conclusion that this probability is very low, and that the observed variations are not the result of random variations.

To compute this probability, let P_1 be the probability that meteoroid random flux increases would occur just after solid rocket motor firings, P_2 be the probability that the sensors believed to be perpendicular to the Earth's surface would be penetrated more often than the sensors parallel to the Earth's surface, and P_3 be the probability that penetrations would occur almost exclusively in either the fully deployed or partially deployed wings for long periods to time. Then the probability of all three of these events occurring is $P = P_1 P_2 P_3$.

An accurate calculation of P_1 would include a determination of which rocket firings were most likely to cause a flux increase, and take into account the very large flux observed after some firings. However, one can conservatively assume that all are equally likely, and compare the flux just after a firing to the flux when there were no firings, as was done earlier in this paper. The result of this analysis is that $P_1 = 0.05$.

P_2 is essentially the probability of measuring 43 or more penetrations on the perpendicular surfaces, and 8 or less penetrations on the parallel surfaces. Assuming a poisson distribution gives this probability, if the average flux is known. Since the average flux is unknown, the conservative assumption is made that this flux is such to give the maximum probability for P_2 . A small computer program was written to calculate P_2 under various assumed values for the average flux. It was found that a flux rate of 3.8 penetrations/m²-900 days gave a maximum $P_2 = 3.2 \times 10^{-4}$. Any other average flux gives even smaller values of P_2 .

The value of P_3 is difficult to calculate correctly. However, by making conservative assumptions, a maximum value can be obtained. A look at figure 6 shows that there are 5 periods of time when either the partially deployed or fully deployed wings were impacted at least 6 consecutive times. A Monte-Carlo model was constructed to look for similar patterns in a data set of 51 impacts. Out of 104 runs, none came close to having this pattern. However, it was concluded that there is a 0.03 probability of having 3 periods of at least 6 consecutive impacts or a 0.15 probability of having 2 periods of at least 6 consecutive impacts. Thus, the probability of 5 periods must be below 0.0045. The value of P_3 would be far below 0.0045 if it were required that the periods of consecutive impacts be periodic and alternate between the partially deployed and fully deployed wings as they do in figure 6. However, to be conservative, I will adopt $P_3 = 4.5 \times 10^{-9}$.

The value of P is the product of P_1 , P_2 and P_3 , or then 7×10^{-8} ; that is one would have to fly at least 14×10^6 Explorer 46 spacecraft before random variations of meteoroid impacts would produce the time and directional distributions that one would expect to see on an average spacecraft which was sensitive to particulates from solid rocket motors fired in space.

Implications to Explorer 46 Objective: Effectiveness of using Double-Wall Structures against Meteoroids

If only a few of the penetrations measured by Explorer 46 were due to meteoroids, then its double-wall structure must have been much more effective in protecting against meteoroids than Humes concluded. Figure 4 illustrates the technique used by Humes to obtain the "effective thickness" of his experiment. However, from the analysis presented here, the actual meteoroid flux is most accurately represented by the 4 impacts on the surfaces parallel to the Earth's surface between 50 and 900 days after launch. This measured flux is about $1.2 \times 10^{-8} / \text{m}^2\text{-sec}$. Consequently, the effective single sheet thickness is about doubled from Hume's analysis, or about 13 times the combined thickness of the double-walled structure. These results clearly only apply to the high meteoroid velocities. At the lower velocities of Earth orbiting objects (approx. 7 km/sec) laboratory tests have shown double-walls to be much less effective.

Comparison of Explorer 46 Debris Data with Proposed Design Criteria

It is instructive to compare this measured debris flux with debris predictions. The number of impacts on the perpendicular surfaces is 43. The surface average area on these surfaces was 9 m^2 , and exposure was 900 days, leading to an average surface area flux of 1.9 impacts per $\text{m}^2\text{-yr}$. If these surface areas were oriented in directions most sensitive to orbiting debris, their cross-sectional and surface areas are about the same. However, as is concluded from figure 6, about 1/2 of the time a particular set of sensors is not oriented in the most sensitive direction. Consequently, the average flux on a cross-sectional area is about double this, or 3.8 impacts per cross-section $\text{m}^2\text{-yr}$. This compares to the predicted flux of 0.0075 cm debris particles in 1995 of only 0.1 per cross-sectional $\text{m}^2\text{-yr}$ at 800 km, as presented in the earlier paper "Proposed Design Criteria". Obviously unmodelled sources can be very important.

TABLE 1

SOLID ROCKET MOTORS FIRED IN SPACE DURING THE EXPLORER 46 MISSION

Time from Launch	International Designation	Rocket	Final Orbit of Rocket		
			perigee, km	apogee, km	incl. deg.
0	1972-61B	Scout*	490	815	38
20	1972-69B	Scout	738	843	90.1
41	1972-73C	Delta	246	247125	28.8
94	1972-91B	Scout	430	594	1.9
101	1972-92B	Scout	244	1168	91.1
125	1972-100B	Scout	224	859	96.9
251	1973-23C	Delta	215	36508	29.5
302	1973-39B	Delta	182	390244	29.1
439	1973-78D	Delta	197	228809	28.8
555	1974-9B	Scout	233	889	2.9
574	1974-13B	Scout	713	917	97.8
609	1974-22C	Delta	202	36143	24.7
638	1974-33D	Delta	182	32950	24.5
660	1974-40B	Scout	337	794	89.7
703	1974-55B	Scout	220	872	97.4
748	1974-70B	Scout	259	1171	98.0
789	1974-75C	Delta	227	36313	24.8
794	1974-77B	Scout	504	550	2.9
833	1974-94E	Delta	176	36854	24.5
859	1974-101G	Delta	409	38204	12.8

* Used to put Explorer 46 into orbit.

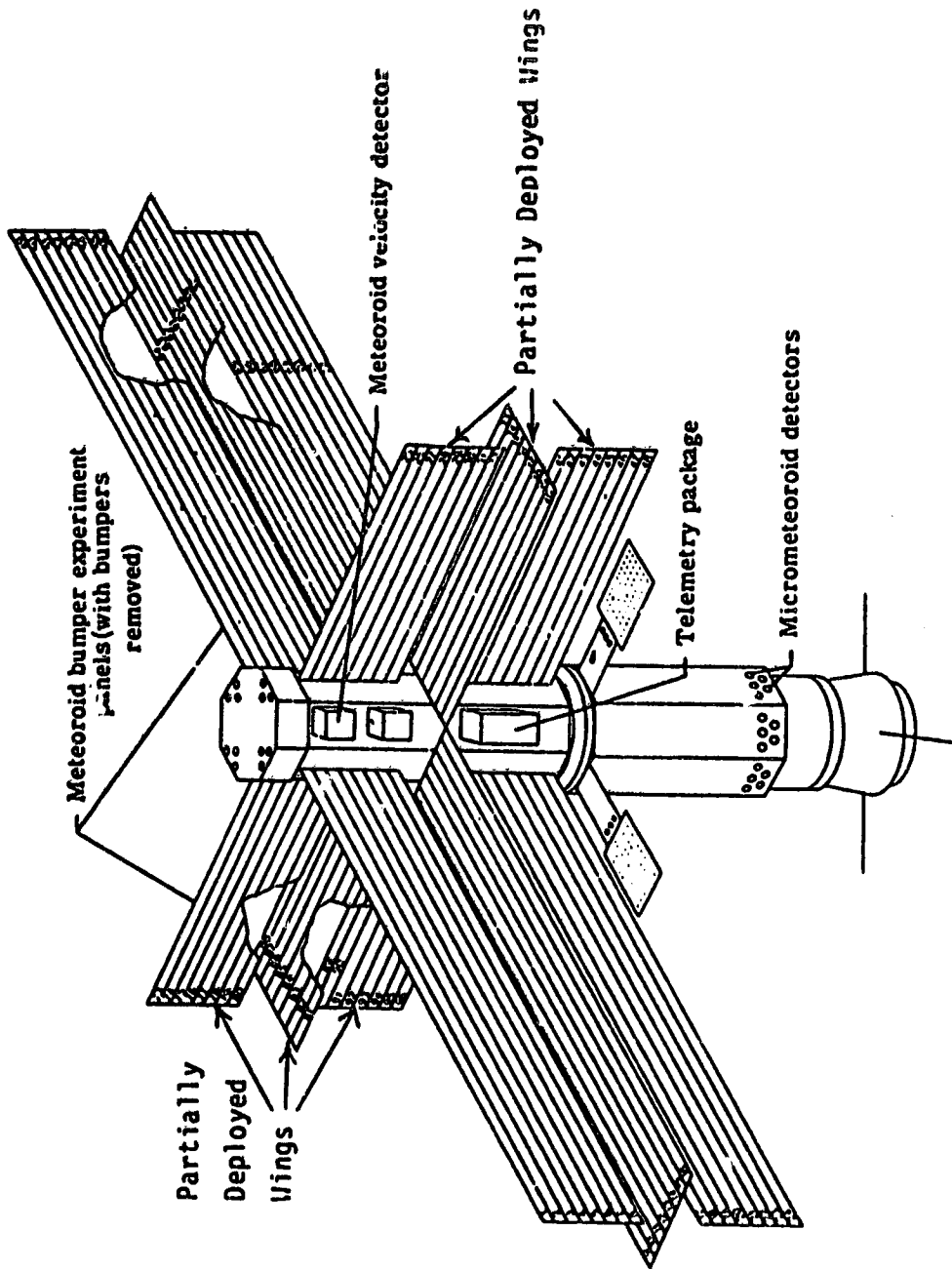


Figure 1.- Drawing of Explorer 46 spacecraft (with bumpers removed) showing numbering system used to identify pressurized cells for meteoroid bumper experiment.

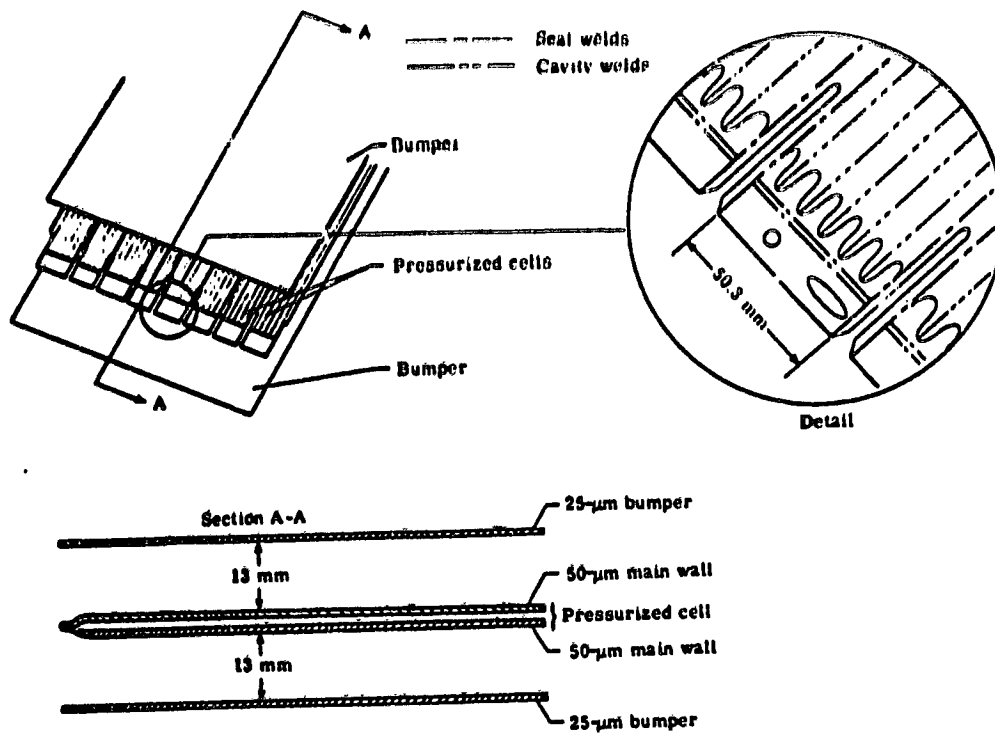


Figure 2.- Drawing of panel with bumpers showing double-wall structure tested on Explorer 46. All material was 21-6-9 stainless steel.

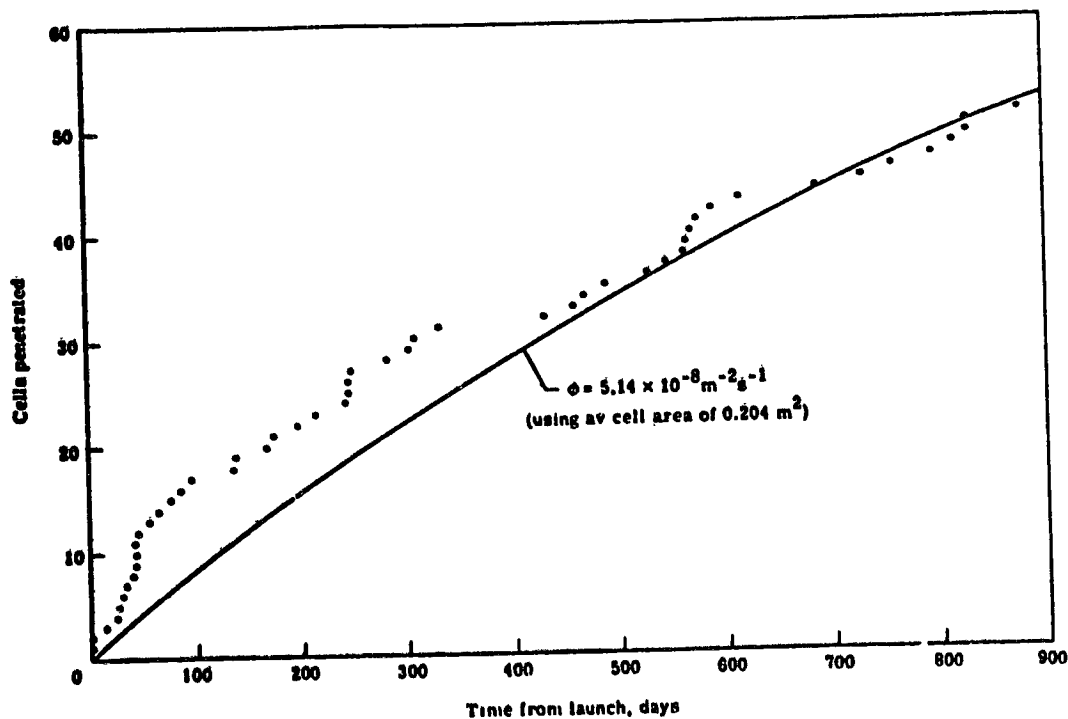


Figure 3.- Time history of penetration of cells on Explorer 46 meteoroid bumper experiment.

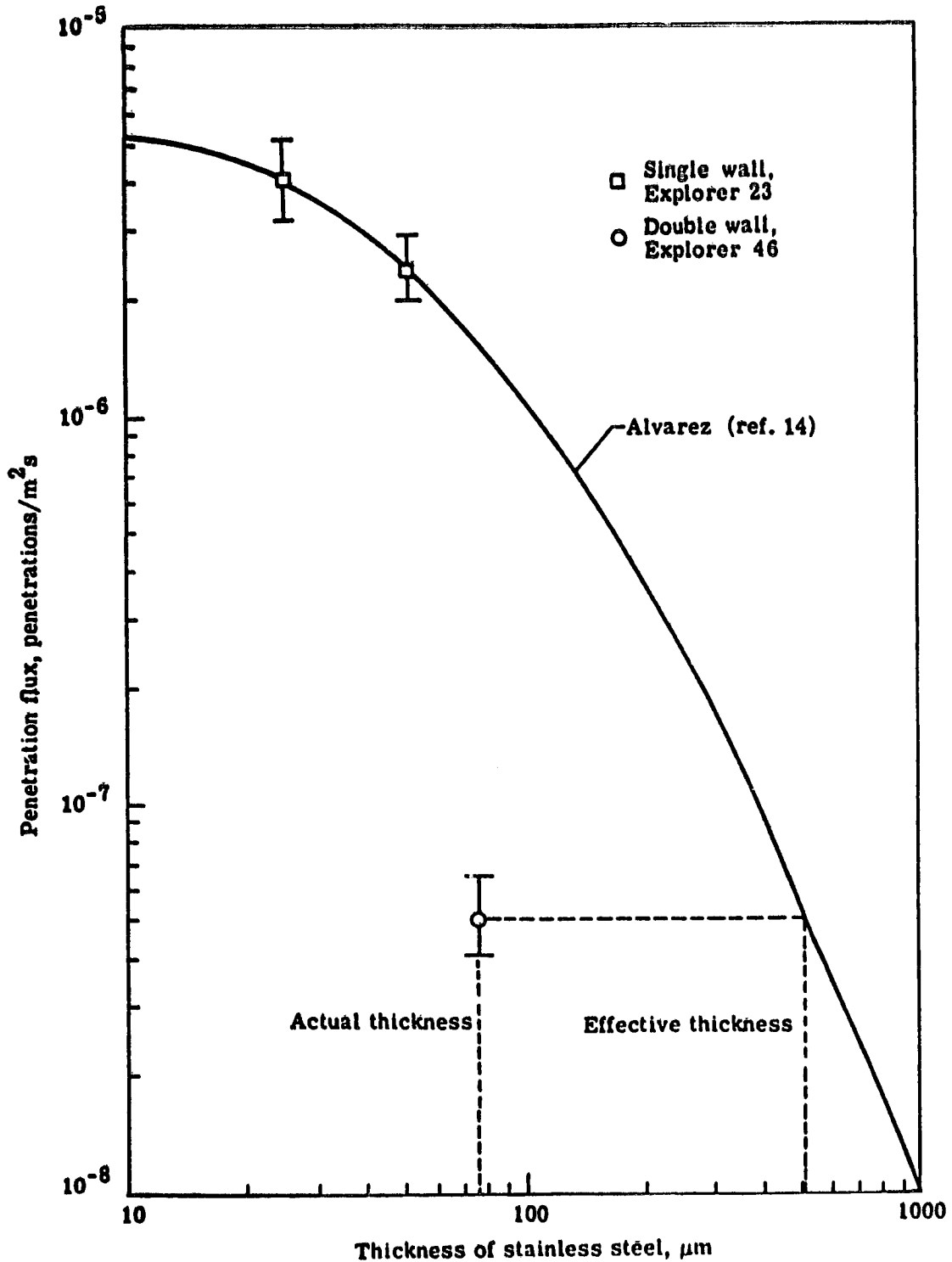


Figure 4.- Penetration flux for single stainless-steel walls and Explorer 46 double-wall stainless-steel structure, with 90-percent confidence limits.

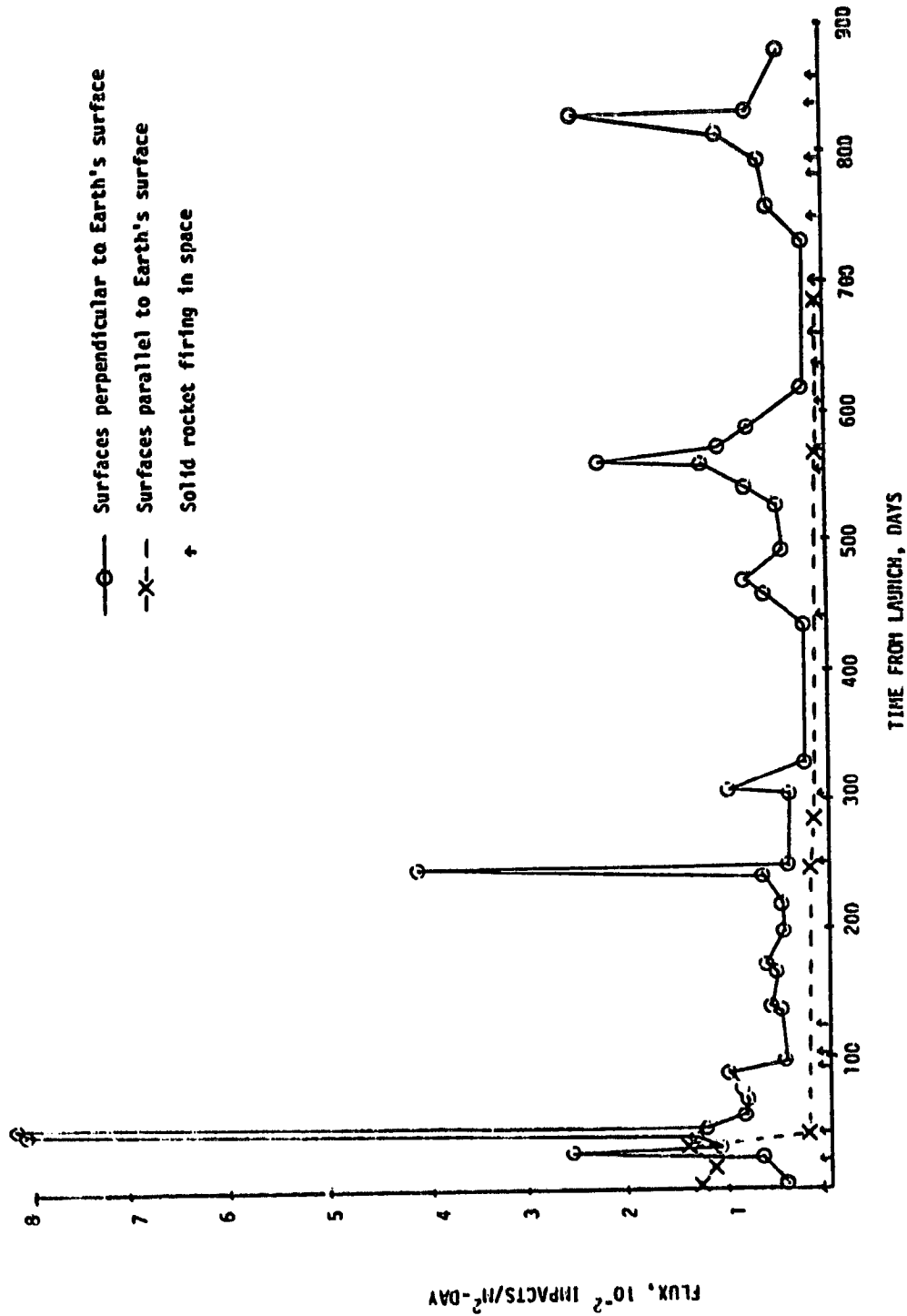


FIGURE 5. THREE IMPACT RUNNING AVERAGE FLUX FOR PERPENDICULAR AND PARALLEL SURFACES

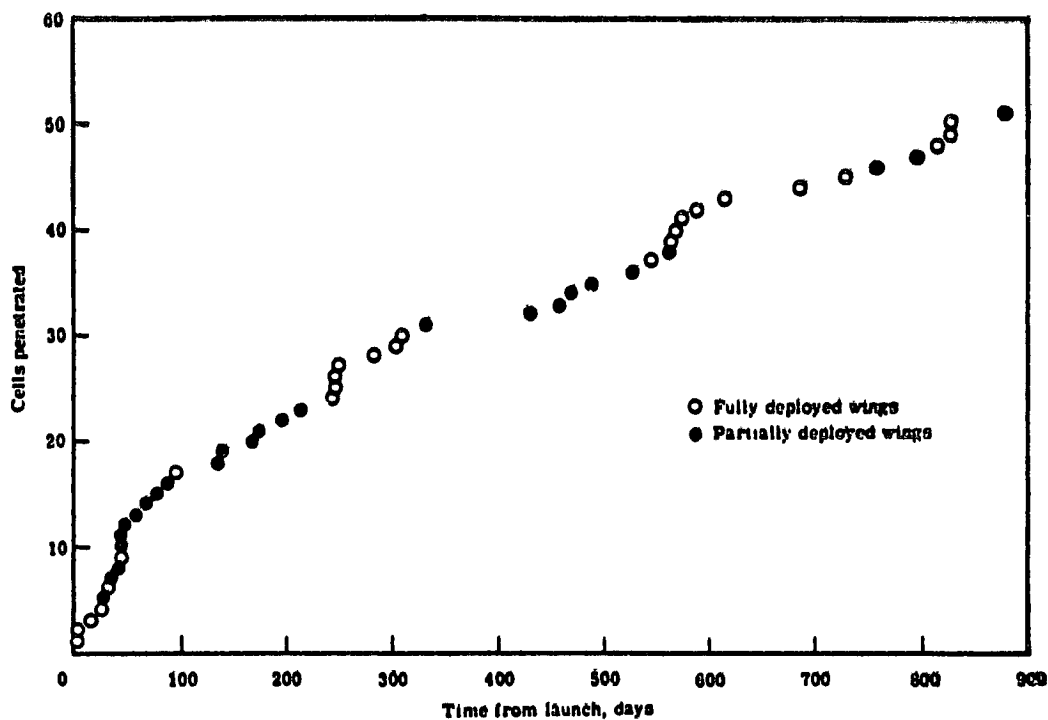


Figure 6 - Time history of cell penetration on Explorer 46 meteoroid bumper experiment showing tendency for penetrations to occur in either partially deployed wings or fully deployed wings for extended periods.

References

- Humes, Donald H. "Meteoroid Bumper Experiment on Explorer 46", NASA Technical Paper 1879, July, 1981.
- Kessler, Donald J., "Derivation of the Collision Probability between Orbiting Objects: The Lifetime of Jupiter's Outer Moons," *Icarus*, vol. 48, p. 39-48, 1981.
- Hallgren, D.S. and C.L. Hemenway, "Analysis of Impact Craters from the S-149 Skylab Experiment," *Lecture Notes in Physics*, published by Springer-Verlag, Berlin, Heidelberg & New York. pp. 270-274. (1976).
- Clanton, Uel S., Herbert A. Zook, and Richard A. Schultz, "Hypervelocity Impacts on Skylab IV/Apollo Windows", Proc. Lunar Science Conf. 11th (1980) p 2261-2273.

N 85 - 21205

D 17-12

In-Situ Detection of Micron-Sized Dust Particles in Near-Earth Space

E. GRÜN

Max-Planck-Institut für Kernphysik, 6900 Heidelberg, F.R.G.

and H.A. ZOOK

NASA Johnson Space Center, Houston, TX 77058, U.S.A.

Abstract:

In-situ detectors for micron-sized dust particles based on the measurement of impact ionization have been flown on several space missions (Pioneer 8/9, HEOS-2 and Helios 1/2). Previous measurements of small dust particles in Near-Earth space are reviewed. An instrument is proposed for the measurement of micron-sized meteoroids and space debris such as solid rocket exhaust particles from on board an Earth orbiting satellite. The instrument will measure the mass, speed, flight direction and electrical charge of individually impacting debris and meteoritic particles. It is a multi-coincidence detector of 1000 cm² sensitive area and measures particle masses in the range from 10⁻¹⁴ g to 10⁻⁸ g at an impact speed of 10 km/s. The instrument is lightweight (5 kg), consumes little power (4 watts), and requires a data sampling rate of about 100 bits per second.

I. Introduction

In the 1960's space experiments were performed to study the particulate environment of the Earth and to explore space hazard due to meteoroids. Penetration detectors like pressurized cells and capacitor-type detectors determined reliably the near-Earth flux of micrometeoroids with masses $m \gtrsim 10^{-9}$ g (cf. Nauman 1966). Early measurements of micron-sized particles with simple microphone detectors were not reliable because of a high noise background. Only recently more sophisticated instruments produced reliable measurements on the small particle population in the Earth's neighbourhood. Most successful were detectors which used the effect of impact ionization to observe micron-sized particles. In the next section we will review previous measurements of small dust particles in near-Earth space and in the final section we describe a system which could be used to measure micron-sized meteoroids and space debris from on board an Earth orbiting satellite.

II. Near-Earth dust measurements

The most extensive measurements of the near-Earth dust environment have been done by the dust experiment on board the HEOS 2 satellite. The experiment was a dual coincidence impact plasma sensor of about 100 cm² sensitive area (for detailed description of the experiment see Dietzel et al. 1973 and Hoffmann et al. 1975). The experiment was active during the period between February 7, 1972 and August 2, 1974. The satellite had a highly eccentric orbit with a perigee between 350 and 3 000 km altitude and an apogee of about 244 000 km. The instrument was mounted in the spin axis of the satellite and could be pointed to four principal directions: ecliptic north (EN), Earth's apex (A), ecliptic south (ES) and Earth's anti-

apex (AA). During its life-time the dust experiment recorded impacts of 431 particles and determined their mass and speed. Two main effects relevant to this paper have been found: 1. The count rate was strongly enhanced close to the Earth (i.e. inside about 60 000 km altitude) and 2. the impact rate showed peaks which were up to 4 orders of magnitude higher than average.

The time-averaged fluxes observed by the HEOS-2 dust experiment both in interplanetary space (i.e. altitude > 60 000 km) and in the "perigee region" (altitude < 60 000 km) are shown in Table 1. It can be seen that the fluxes in the perigee region are a factor 10 to 80 higher than in interplanetary space (for a more complete description of the results see Fechtig et al., 1979).

Table 1: Average cumulative fluxes measured by the HEOS-2 dust experiment

threshold mass (g)	interplanetary space (altitude > 60 000 km) (m ⁻² s ⁻¹)	perigee region (altitude < 60 000 km) (m ⁻² s ⁻¹)
10 ⁻¹⁴	1.8 x 10 ⁻⁴	3.1 x 10 ⁻³
10 ⁻¹³	5.4 x 10 ⁻⁵	2.5 x 10 ⁻³
10 ⁻¹²	3.0 x 10 ⁻⁵	2.3 x 10 ⁻³
10 ⁻¹¹	1.1 x 10 ⁻⁵	4.1 x 10 ⁻⁴
10 ⁻¹⁰	6.8 x 10 ⁻⁶	6.1 x 10 ⁻⁵

Most of the flux in the perigee region is constituted out of bursts of particles which correspond to fluxes significantly higher than the average flux. In interplanetary space, only the flux of the smallest particles (10^{-14} g) is made half part out of burst related particles. Tab. 2 shows the measured parameters of the recorded bursts. The duration of these bursts lasts from a few minutes to several hours during which the fluxes are several orders of magnitude higher than the time-averaged fluxes. Most of the high flux bursts have been observed in the perigee region below an altitude of 60 000 km.

Fechtig et al. (1979) interpret these data as due to the following effects. Gravitational enhancement can account only for a factor of 2 higher flux of interplanetary meteoroids in the perigee region. Therefore an extra source for the observed particles is required there. Also the observed bursts of particle impacts cannot be explained by a random occurrence of meteoroid impacts but a local source is required. During the time intervals of several low-flux bursts occurring in interplanetary space, the Moon was in the field-of-view of the sensor (cf. Tab. 2). Therefore, at least, during these times direct trajectories from the Moon to the sensor are possible. Fechtig et al. (1979) suggest that these bursts and some other recorded in the perigee region are caused by ejecta particles which originate from impacts on the Moon.

The high-flux bursts observed in the perigee region are interpreted by the same authors as being due to fragmentation of larger meteoroids (10 to 10^6 g mass) in the Earth's magnetosphere. The fragmentation process proposed is that of electrostatic disruption of meteoroids of low structural strength in the dense high energy plasma regions of the magnetosphere. However, an additional source like solid rocket motor exhaust plumes is not excluded by their analysis.

Tab. 2: Particle bursts recorded by the HROA-2 dust experiment

date	duration (min)	average particle flux ($m^{-2}s^{-1}$)	typical particle mass (g)	typical impact speed (km/s)	mean altitude ($\times 10^3$ km)	sensor viewing direction*
Mar. 4 1972	340	1.0×10^{-2}	10^{-13}	0	224	A -M
Apr. 7	20	7.6×10^{-1}	10^{-12}	0	63	A
Apr. 10	49	7.1×10^{-2}	10^{-12}	11	239	A -M
Jun. 16	744	7.0×10^{-3}	10^{-14}	13	222	EO -M
Jul. 9	101	3.0×10^{-2}	10^{-13}	10	13	EO
Jul. 12	151	2.3×10^{-2}	10^{-14}	0	209	EO -M
Aug. 6	254	3.4×10^{-2}	10^{-14}	0	166	A
Sep. 13	43	2.1	10^{-14}	0	235	AA -M
Sep. 14	60	0.7×10^{-2}	10^{-14}	0	216	AA -M
Nov. 27	13	4.0	10^{-12}	12	20	EO
Mar. 21 1973	90	1.3	10^{-13}	0	42	A
Mar. 26	29	3.6×10^{-1}	10^{-14}	0	62	A
Apr. 24	77	6.0×10^{-2}	10^{-14}	0	235	A -M
Apr. 27	34	2.6×10^{-1}	10^{-14}	0	20	A
May 23	11	3.0	10^{-11}	7	32	A
Jun. 12	24	1.3	10^{-12}	0	42	A
Jun. 24	96	5.8×10^{-1}	10^{-14}	0	203	A -M

* A : Earth's apex ES: ecliptic south M: moon in sensor field of view
 AA: Earth's antiapex EN: ecliptic north

Tab. 2: (cont.)

date	duration (min)	average particle flux ($m^{-2}s^{-1}$)	typical particle mass (g)	typical impact speed (km/s)	mean altitude ($\times 10^3$ km)	sensor viewing direction*
Jun. 28 1973	6	5.0×10^{-1}	10^{-12}	6	34	A
Jul. 5	139	2.5×10^{-2}	10^{-12}	10	203	A
Jul. 29	6	1.7	10^{-11}	8	41	A
Oct. 20	20	4.4×10^{-1}	10^{-12}	7	27	EN
Nov. 10	4	0.7×10^{-1}	10^{-13}	7	25	EN
Nov. 15	11	1.3	10^{-12}	8	26	EN
Jan. 17 1974	100	3.5×10^{-2}	10^{-14}	0	04	EN
Feb. 26	26	1.3×10^{-1}	10^{-14}	0	180	EN
Mar. 27	332	1.6×10^{-2}	10^{-14}	0	229	EN
Mar. 30	26	9.4×10^{-1}	10^{-13}	0	30	EN
Apr. 10	19	2.3×10^{-1}	10^{-13}	0	27	EN
Apr. 25	15	2.3×10^{-1}	10^{-13}	0	22	EN
May 6	13	2.7×10^{-1}	10^{-11}	7	34	EN
May 11	11	3.2×10^{-1}	10^{-13}	0	21	EN
May 16	2	1.7	10^{-12}	11	20	EN
May 16	2	1.7	10^{-13}	0	57	A
Jul. 11	26	1.3×10^{-1}	10^{-13}	13	187	A -M

* A : Earth's apex ES: ecliptic south M: moon in sensor field of view
 AA: Earth's antiapex EN: ecliptic north

Another observation of a variable dust flux in the Earth's neighbourhood has been reported by Singer and Stanley (1980). They refer to the MTS (Meteoroid Technology Satellite) - Explorer 46 which carried among other experiments solid state capacitor detectors for dust particles. The capacitor detectors had thicknesses of the dielectric of 0.4 μm and 1 μm which corresponds to a threshold sensitivity at 15 km/s of 10^{-17} g and 10^{-15} g, respectively. The satellite orbited the Earth at an altitude of 660 km. The times of enhanced fluxes during the nearly 6 months of detector operation (August 1974 through January 1975) are indicated in Table 3. Singer and Stanley (1980) interpret these enhanced fluxes as due to meteor stream particles although, again, a contribution of man-made debris particles to the observed fluxes is not excluded. This latter possibility is supported by Alvarez (1976) who reported that the flux of 10^{-17} g particles was much greater at the beginning of the mission and he suggests the spacecraft itself as a source of orbital debris in rapidly decaying orbits.

Tab. 3: Enhanced impact fluxes observed by the MTS-Explorer 46 solid-state capacitor detector over 6 days centered on the indicated date (only fluxes in excess of the background flux are shown).

sensor dielectric thickness 0.4 μm		1.0 μm
date	flux ($\text{m}^{-2}\text{s}^{-1}$)	
Oct. 21, 1974	7.8×10^{-4}	-
Nov. 4, 1974	2.7×10^{-3}	5.7×10^{-4}
Nov. 17, 1974	1.0×10^{-3}	7.1×10^{-4}
Dec. 14, 1974	-	5.6×10^{-4}
Dec. 22, 1974	1.0×10^{-3}	2.2×10^{-4}
background	4.6×10^{-4}	2.0×10^{-4}

III. Detection system for micron-sized particles

The most versatile and reliable detectors for micron-and sub-micron particles are impact plasma detectors. They have been used on a number of space missions like Pioneer 8 and 9 (Berg and Richardson, 1969; Grün et al., 1973), HEOS-2 (Dietzel et al.; Hoffmann et al., 1975) and Helios (Dietzel et al; 1973; Grün et al., 1980) and are in preparation for the Galileo, ISPM and Giotto missions.

It is proposed to use a detector similar to those which are in preparation for the Galileo mission and ISPM for the measurement of small meteoroids and space debris from on board an Earth orbiting satellite. In the following such an instrument is described.

The experiment will detect individual particles impacting on the sensor and will measure their mass, impact speed, electric charge and determine the impact direction. The instrument consists of an impact plasma sensor and the appropriate electronics. The modifications to the previous HEOS-2 experiment are: 1. increase of the sensitive area from $\sim 10^{-2} \text{ m}^2$ to 10^{-1} m^2 ; 2. introduction of a measurement channel for the electrical charge of dust particles and 3. installation of an electron multiplier in order to obtain an additional independent signal of dust particle impacts. In Fig. 1 the basic sensor is shown. Positively or negatively charged particles entering the sensor are first detected by the charge which they induce when flying through the entrance grid. The grids adjacent to the charge pick-up grid are kept at the same potential in order to minimize the susceptibility of the charge measurement to mechanical noise. This charge signal will only be evaluated if there is a subsequent impact recorded by the impact plasma detector. Dust particles - charged or uncharged - are detected by the plasma produced during

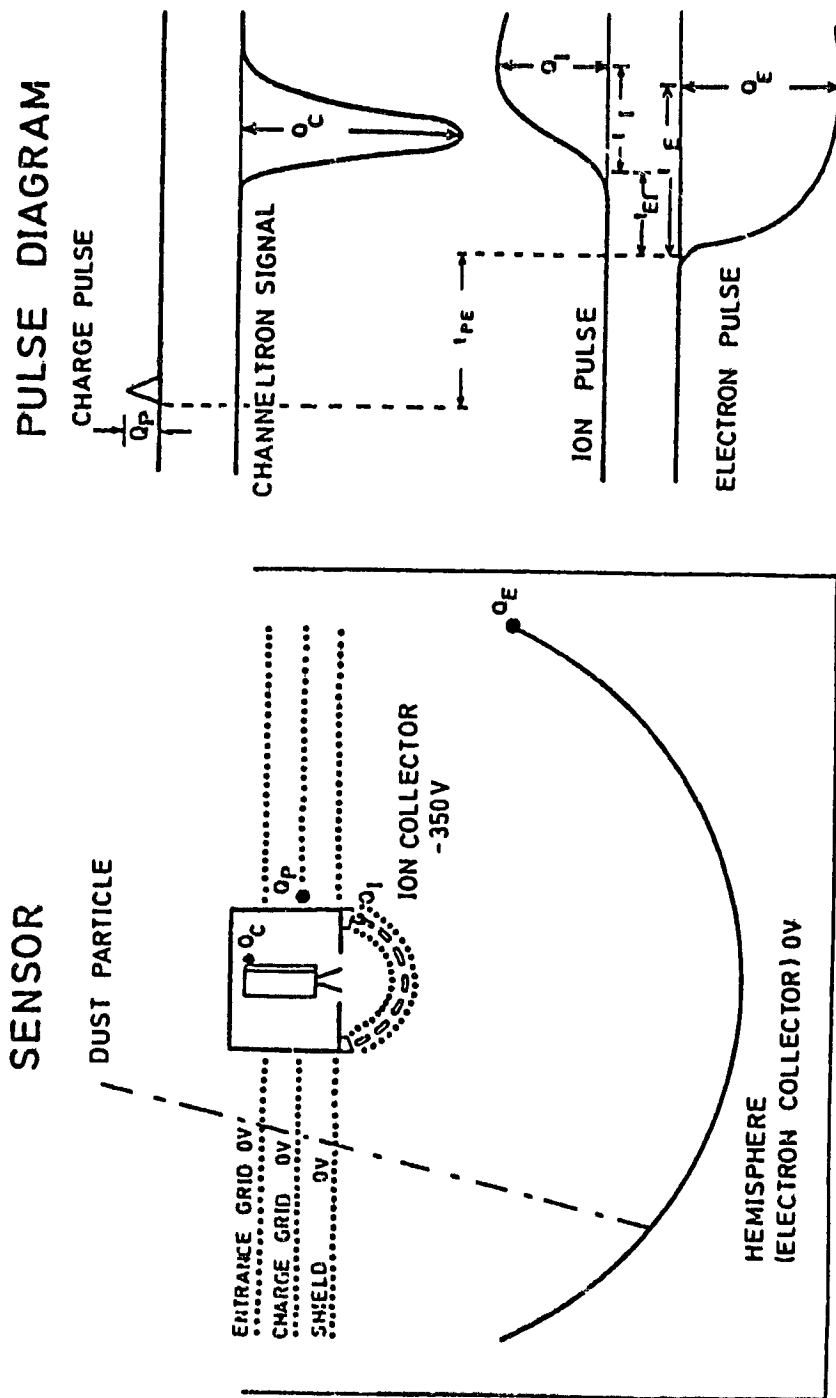


Fig. 1: Sensor configuration (schematic) and measured signals upon impact of a positively charged dust particle

the impact on the hemispherical impact sensor. After separation by an electric field, the ions and electrons of the plasma are accumulated by charge sensitive amplifiers, thus delivering two coinciding pulses of opposite polarity. The heights and rise-times of these two pulses depend on the mass and speed of the impacting particle. The rise-time, which is independent of the particle mass, decreases with increasing particle speed. From both the pulse heights and rise-times, the mass (m) and impact speed (v) of the dust particle are derived, using empirical correlations between these four quantities.

Preliminary calibration of such an instrument has been performed using the Heidelberg 2MV electrostatic dust accelerator. For this preliminary calibration iron particles have been used in the mass range 10^{-14} g to 10^{-9} g and speed range 1 km/s to 50 km/s. The positive charge yield $Q_I/m^{0.9}$ and the rise-time of the negative charge pulse t_E versus the impact speed are shown in Fig. 2 and 3, respectively. The impact charge Q can be described by the empirical law

$$Q = C m^\alpha v^\beta$$

where m is given in g, v in km/s and Q in Coulombs with the following constants for the positive charge Q_I : $C = 1.0 \times 10^{-5}$, $\alpha = 0.9$, $\beta = 3.0$ and for the negative charge Q_E : $C = 5.0 \times 10^{-5}$, $\alpha = 0.94$, $\beta = 3.1$.

The preliminary mass sensitivity threshold of the impact charge measurement is shown in Table 4.

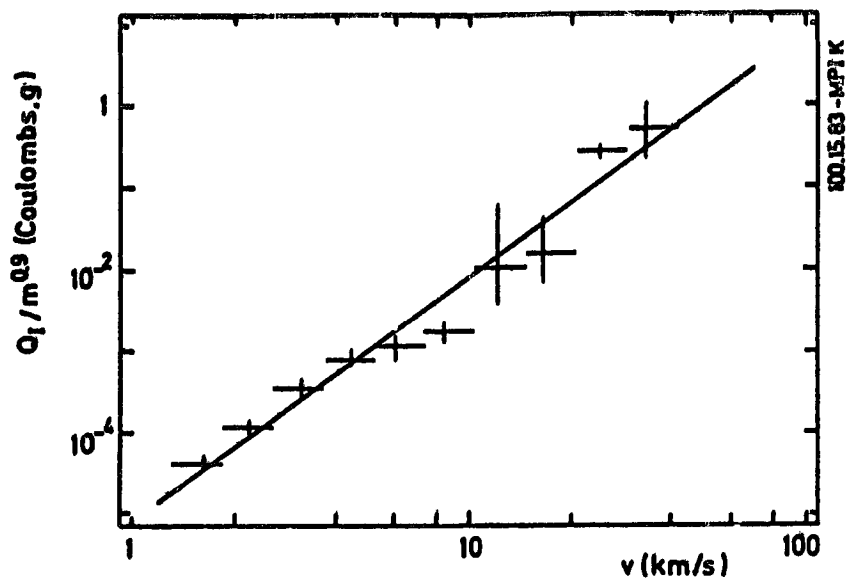


Fig. 2: Positive impact charge Q_I normalized to $m^{0.9}$ versus impact speed v for iron projectiles.

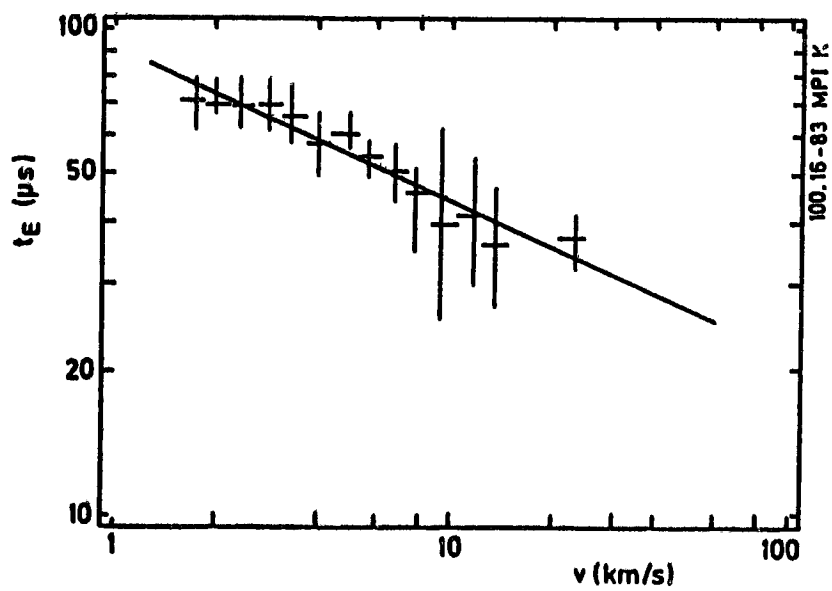


Fig. 3: Rise-time t_E of the negative charge pulse versus impact speed.

Table 4: Mass sensitivity of the impact plasma dust experiment

Speed (km/s)	2	5	10
Threshold (g)	1.0×10^{-11}	4.7×10^{-13}	4.7×10^{-14}
Speed (km/s)	20	40	
Threshold (g)	4.6×10^{-15}	4.6×10^{-16}	

The measurement range for particle masses is 6 decades above the threshold values.

A further independent signal of a particle impact originates from part of the positive impact charge which is detected and amplified (approx. $\times 100$) by an electron multiplier (channeltron). This signal serves as a control for the identification of dust impacts. Because this multiplier has a low dark current at the required amplification even during peak radiation fluxes in the Earth's radiation belts, its threshold will correspond to less than 10^{-15} C impact charge. The output signal will be measured within a dynamic range of a factor of 10^4 . By measuring the output signal of the channeltron and deriving coincidence signals between both charge signals and the channeltron signal one has an unambiguous method to distinguish noise from impact events. Gain loss of the channeltron will be counteracted by commanded changes of the channeltron voltage. The amplitude of the positive and negative charge pulses, the channeltron signal, and the corresponding rise-times are redundant measures of the mass and impact speed of the dust particle. This redundancy gives a further check on the identification of an impact event and increases the accuracy of the measurement considerably.

The experiment parameters and performance criteria are:

weight: 5 kg

power consumption: 4 Watts

volume: Sensor: cylindrical 442 mm diam., 301 mm length
 Electronics box: 283 x 100 x 100 mm

data rate: about 100 bits/s

field-of-view: 140° cone

thermal requirements: -10 °C to +40 °C operating

impact rate: 10^{-6} s^{-1} to 10^2 s^{-1}

particle mass: $5 \times 10^{-16} \text{ g} < m < 5 \times 10^{-10} \text{ g}$ at 40 km/s
 $5 \times 10^{-13} \text{ g} < m < 5 \times 10^{-7} \text{ g}$ at 5 km/s

impact speed: $1 \text{ km/s} < v \lesssim 50 \text{ km/s}$

particle charge: 10^{-14} C to 10^{-10} C negative
 10^{-14} C to 10^{-12} C positive

References

- Alvarez, J.M. (1976) in 'Interplanetary Dust and Zodiacal Light' (H. Elsässer, and H. Fechtig, Eds.) Lecture Notes in Physics, Springer Verlag Heidelberg, 48, 181.
- Berg, O.E., and Richardson, F.F. (1969) Rev.Sci.Instrum., 40, 1333.
- Dietzel, H., Eichhorn, G., Fechtig, H., Grün, E., Hoffmann, H.J., and Kissel, J. (1973) J.Phys. E: Scientific Instrum., 6, 209.
- Fechtig, H., Grün, E., and Morfill, G. (1979) Planet. Space Sci., 27, 511.
- Grün, E., Berg, O.E., and Dohnanyi, J. (1973) Space Research XIII (M.J. Rycroft, and S.K. Runcorn, Eds.) Akademieverlag Berlin, 1057.
- Grün, E., Pailer, N., Fechtig, H., and Kissel, J. (1980) Planet. Space Sci., 28, 333.
- Hoffmann, H.J., Fechtig, H., Grün, E., and Kissel, J. (1975), Planet. Space Sci. 23, 985.
- Nauman, R.J. (1966) "The near earth meteoroid environment", NASA TN D-3717.
- Singer, S.F., and Stanley, J.E. (1980) in 'Solid Particles in the Solar System' (I. Halliday and B.A. McIntosh, Eds.) D. Reidel Publishing Co. Dordrecht, 329.

BT-12
0001

PARCS SMALL SATELLITE TEST - 1976 *
T. LENNERTZ ✓

POTENTIAL HAZARDS OF DEBRIS CLOUDS *
N. L. JOHNSON ✓

*CLASSIFIED PAPERS
NOT INCLUDED IN WORKSHOP PROCEEDINGS

HYPERVELOCITY IMPACT INVESTIGATIONS AND METEOROID
SHIELDING EXPERIENCE RELATED TO APOLLO AND SKYLAB

Burton G. Cour-Palais

1.0 INTRODUCTION

It seems that man must inevitably rediscover the wheel. That technological progress tends to be a spiral; a lot of linear movement, but with periodic returns to some principle or invention left on the shelf. This is what is happening today in the need for protecting a new generation of spacecraft against uncontrollable, unavoidable, very energetic impacts. Some twenty years after the Apollo designers had to contend with the then unknown consequences of meteoroid impact damage, there are similar concerns. A sense of complacency seemed to have pervaded those who planned new space operations, after Skylab survived so well for so long in the near Earth meteoroid environment. Now, however, the specter of man-made orbiting debris has been raised and a whole new ball game has begun. The observed debris population and the associated predictable unseen objects, pose an additional threat to future large area, long duration missions in near Earth space. Depending upon orbital characteristics, either meteoroids or debris can be the predominant shielding design driver or they can complement each other. The average dynamic impact properties of meteoroids ($\rho = 0.5$ g/cc; $V = 20$ km/sec) and orbital debris ($\rho = 2.78$ g/cc; $V = 10$ km/sec), are similar in their effect upon spacecraft components.

This paper has been included in the Orbital Debris Workshop to shed some light on what is available to the spacecraft designer in the basic principles of hypervelocity impact protection. It is primarily focussed on what was done during the Apollo era because it was a forcing program. A considerable amount of time and money was spent in in-house and contracted research effort during the sixties and early seventies. Most of it is relevant today, and it is hoped that the material presented in this paper, and the references cited will be helpful. It is also recognized that similar work was and is being performed by DOD for their purposes, and may also be available to some of you. A bibliography of some of the relevant reports is included for those who would like to pursue this subject in greater detail.

This paper is divided into two sections; generic hypervelocity impact related topics, and specific Apollo/Skylab related investigations. Impacts at the low speed end of the spectrum are possible for orbital debris, but not for meteoroids, and should be considered. Although the Apollo program had to contend with low speed lunar ejecta, and hence did some research in this area, it is not discussed in this paper.

2.0 GENERIC HYPERVELOCITY IMPACT RELATED TOPICS

The three classic cratering regions associated with impacts into thick targets are well illustrated in figure 1 from reference 1, and this particular combination of lead targets and tungsten-carbide projectiles was chosen to emphasize the damage effects. The ordinate in the figure represents the deepest penetration (p) in particle diameters (d) and the abscissa is a parameter involving the impact velocity (V), the sound speed (c) in the target material, and the mass densities of the projectile (ρ_p) and target (ρ_t) materials. By combining the data trends with cross-sections of the craters one has a graphic illustration of three distinctive cratering mechanisms and

physical relationships. It is also very obvious that any extrapolation across the boundaries in either direction could lead to serious errors. The related phenomena illustrated in figure 1 may be explained as follows. At low velocities, the strength of the projectile material is greater than the dynamic pressure at impact and the sphere penetrates the target as an underformed projectile. The cavity is deep and narrow and the penetration depth is proportional to the $4/3$ power of the velocity. With increasing velocity, the impact pressure eventually becomes sufficient to cause the projectile to break into a number of large pieces. This is the beginning of the transition region of impact. As the velocity increases, the fragmentation of the projectile becomes more pronounced and the total penetration decreases for a while before it rises again. The decrease for other combinations is not always as pronounced as it is for the lead data. Eventually a velocity is reached at which the dynamic impact pressure is greater than the target material strength. At this stage, a typical fluid impact crater is formed which is characterized by a near hemispherical shape and a lipped ring if the target material is ductile. If the material is brittle, the lip is missing but is replaced by an annular fracture zone. The depth of penetration in the transition region is unpredictable, and no clear relationship with velocity can be established until the fluid impact boundary is crossed. Once in the fluid region, the penetration depth varies as the $2/3$ power of velocity but tends to reach an equilibrium velocity index of 0.58 at about twice the target sound speed. This is discussed more fully later.

The boundaries between the regions shown in figure 1 are only applicable to the specific combination of projectile and target materials given. Their location for other combinations, depends upon the projectile and target material physical and mechanical properties, as well as the impact velocity. This paper deals with the effects of impacts at hypervelocity, i.e. only those that fall within the fluid dynamic region of figure 1.

The need to simulate the size and energy level of the meteoroids most likely to be encountered during the Apollo missions led to the capability of launching sub-millimeter particles at hypervelocities. It was soon discovered that the parameter p/d as a function of velocity was not constant over the projectile size range available. Figure 2 is a plot of this parameter as a function of velocity for aluminum into aluminum impacts, for spheres ranging from 50 μm to 1.37 cm diameter. If it were not for the 50 μm particles, one could have said that the variation was within experimental limits. However, figure 3 shows what happens if a moderate diameter dependence is incorporated into the expression for the p/d to velocity relationship. The 50 μm diameter result has been brought into line with the rest of the data, which in themselves, are a lot closer together. The size scaling factor of $1/18$ was experimentally determined at the Johnson Space Center and the Ames Research Center almost simultaneously. It was later shown to be related to the rupture stress and mean deformation strength of the target material by Gault and Moore, reference 2. The exponent of d varies between 0.2 for very brittle materials (rock and glass) to nearly zero for a very ductile material such as the aluminum alloy 1100-0. A subsequent analytical study by Rosenblatt, reference 3, showed that this non-linear scaling phenomenon was accounted for by the inclusion of material strain rate effects, and incipient melting, in his numerical code description of the impact process. Diameter scaling

remains an important discovery, because it permits the extrapolation of laboratory test results over a significant size range.

The strength and ductility of the target material also influences the final dimension of the crater in a semi-infinite target. In figure 4, the penetration to diameter ratio with size scaling is plotted as a function of velocity for a very soft (1100-0; $H = 27$) and a hard (2024-T3; $H = 145$) aluminum alloy, where H is the Brinell hardness number. The data was obtained from two different laboratories and the empirical equation to the curves through the data includes a material hardness term. The difference in the penetration depth to projectile diameter ratio for the two alloys is quite pronounced and the reason is well understood, (References 4,5). As mentioned previously, during the initial phase of the impact process, the shock pressure is high enough to cause the target material to behave as a fluid. Crater growth during this phase is identical for the hard and soft aluminum alloys, because their material strength properties are not in control. As the shock pressure decays, and the material properties dominate again, the crater dimensions are eventually "frozen" at different times for the two alloys. To illustrate this, the 1100-0 alloy has a yield strength of 6.4 million psi and an ultimate strength of 13 million psi, whereas the comparable values for the 2024-T3 alloy are 36 million psi and 48 million psi respectively. For a given initial impact shock pressure and similar decay characteristics, the 2024-T3 crater will stop growing before the 1100-0 crater. According to reference 5, the 2024-T3 crater growth limitation begins at 21 μsec after impact, whereas the 1100-0 crater continues to grow for another 16 μsec . The same reference also states that the final crater dimensions for the 1100-0 case can be as much as 15% less than the maximum achieved during the impact process. This rebound effect is probably more noticeable for the ductile metals, and is a transient event that can only be detected by x-radiography.

Several empirical hypervelocity impact equations, describing crater formation in semi-infinite metallic targets, were derived during the Apollo program. They are applicable only when the target is thick enough to prevent spallation from the free surfaces surrounding the crater. Also, they are valid only up to a few kilometers per second beyond the limits of the hypervelocity test facilities. Extrapolation to meteoroid or orbital debris impact velocities, (2 to 3 times test speeds), depended on the results obtained from mathematical models of the impact process such as reference 6. There was an initial disagreement between the analysts as to whether the crater depth would be proportional to the cube-root of impact momentum or energy. However, there was an eventual consensus that the velocity exponent approached a value of 0.58 above an impact speed of 30 km/sec. The relationship between test data and the principal analytical impact relationships is illustrated by Figure 5. Experimental results, even at the highest speeds attained in laboratory tests, (10 km/sec for 0.32 cm and 12 to 15 km/sec for 50 μm glass projectiles), favored a velocity exponent of 2/3. It was decided that the penetration equations specified for Apollo would maintain the 2/3 dependence up to the 20 km/sec average meteoroid impact velocity prescribed, and that the exponent gradually decrease until it reached 0.58 at 30 km/sec. The specific penetration equations for impact into metallic targets used by JSC and the contractor (Rockwell) for their Apollo meteoroid hazard assessments are given in Figure 6. As previously stated,

both retained the velocity exponent of $2/3$, which gave a slight margin of safety when used with the average meteoroid impact velocity of 20 km/sec. Although the two equations differ somewhat in the target material factors considered, as well as the coefficient of proportionality, the resulting crater depth for a specific material is within 10%.

We have been dealing with crater formation in semi-infinite metallic targets up to this point. If the target is made progressively thinner, and the projectile and velocity are kept constant, a piece of the rear surface in line with the impact will eventually be thrown off as spall. The size and cohesiveness of the spallation depends upon the material properties as well as the strength of the shock when it reaches the free surface of the block. Upon further reduction in thickness, the crater and spallation eventually meet and the target is perforated. The basic penetration equations, such as those given in Figure 6, define the depth of a crater in a metallic target that is much thicker than the spallation limit. As it is often necessary to assess the penetration resistance of thin targets, such as might form the outer shell of a space vehicle, finite thickness equations were derived. Most often, they are defined in terms of a multiple of the penetration depth equation, i.e., $t = k \cdot p$ where t is the finite sheet thickness required, k is the factor depending upon the failure criteria considered, and p is the depth of the crater in a semi-infinite target. In a series of tests conducted by GMDRL (reference 8), targets made from aluminum 2024-T3 alloy were impacted by 1/8 inch diameter aluminum at a constant velocity of approximately 7.4 km/sec. As the targets were reduced in thickness, the value of the factor k was determined for several important failure modes as follows:

- (a) The onset of spallation, or semi-infinite limit; $k = 3.0$
- (b) Spall break away; $k = 2.2$
- (c) Perforation; $k = 1.8$

Although these factors have been determined for a specific alloy, they were used interchangeably for any of the other structural aluminum alloys. The JSC and Rockwell preferred values for the finite thickness factor are given in Figure 6. Both are intended to prevent perforation, and to allow some measure of spallation, for weight saving reasons.

Although there are many instances in which space structures can be adequately protected by a single thickness of material against hypervelocity impact, weight considerations usually mitigate against it. The principal of placing another sheet of material some distance ahead of the main structural shell of a spacecraft was first advocated by Dr. Fred Whipple, the well known astro-physicist. He foresaw that an outer sheet was required to fragment or vaporize the meteoroid or debris particle, which would allow the spacecraft wall to deal with the debris fairly easily. The resulting combination of a double wall would be lighter than a single one. When tested in a hypervelocity impact laboratory, the principle was verified and the "Whipple bumper" has become more or less standard procedure for space applications. Initially, the thickness of a double sheet combination was compared with the equivalent single thickness using a "ballistic limit" criterion. This usually meant that for the double sheet configuration there were no perforation holes in the second sheet which would allow any loss of pressure, and for the single

sheet, no spallation off the rear surface. Various double sheet combinations were tested, and empirical standard factors determined for use with single thickness equations. The calculated total shielding thickness would then be equally divided between the "bumper" and the structure wall, i.e., $2t_1 = K t$, where:

- t = finite single thickness to prevent spallation
- t_1 = individual elements of double sheet protection to prevent perforation
- K = empirically derived factors

Examples of some of these double sheet factors are as follows:

a) Double sheet; empty space in between:

$K = 0.5$ for 1" spacing,

$K = 0.2$ for 2" spacing

b) Double sheet; low density, porous foam in between

$K = 0.33$ for 1" spacing,

$K = 0.14$ for 2" spacing

c) Double sheet; honeycomb core in between:

$K = 0.67$ for 2" spacing,

$K = 0.25$ for 2" spacing.

This technique for sizing the elements of a multi-element meteoroid shield on a gross basis was later replaced by a phenomenological approach, which dealt separately with the elements involved. As the "bumper" or outer wall of the protective structure is the key to the success of the succeeding elements, let us take a look at the impact process that takes place. Figure 7 depicts the classical interaction between a projectile and a "bumper" at two instances after initial contact, with the shock or compression waves (S_1, S_2), and the release or tensile waves (R_1 to R_4) moving through the projectile and target. As previously mentioned, when a metallic target subjected to hypervelocity impact is made progressively thinner to the point at which complete penetration occurs, an expanding cloud of projectile and shield fragments is generated. This cloud can consist of solid, liquid or vaporized material or a combination of all three, depending upon the initial impact pressure. The initial pressure for a 10 km/sec aluminum to aluminum impact is of the order of 1.4 megabars, which is about 20 million psi. A debris cloud resulting from a glass sphere impacting an aluminum bumper at about 7 km/sec is shown in Figure 8. The upper photograph is a side view of a disc-shaped grouping of projectile and bumper hole particulate material in flight, some time after penetration. The front view of this same debris cloud, taken through the transparent second sheet of the target, shows that there is a distinct annular region without any material. This is the separation between the projectile

and "hole" debris, and the purely bumper material from the edge of the hole. This view also shows some filamentary material in the debris indicating that some degree of melting has taken place. In the third photograph in Figure 8, which shows the damage pattern on the second sheet, there is an evident correspondence with the incoming debris cloud. Thus there is intense damage in the central zone, consistent with the mainly projectile debris, and a more widely dispersed damage structure outside this zone caused by the predominantly bumper material. Figures 9 and 10 (reference 9) are reproductions of computer generated mass particle plots representing projectile-bumper interactions at two instances after impact. At 0.158 μ secs after impact, the debris cloud has started to expand out from the bumper and the projectile is nearly consumed. Note the ejecta leaving the front surface of the plate against the direction of motion. In the later stage of development shown in Figure 9, the hole material has expanded and is running ahead of the projectile debris. The annular separation between the two sources shown in the photograph discussed earlier is evident. In this case however, there is considerable development of late, slower bumper material in the cloud. The value of these numerical techniques in studying bumper-projectile interactions is apparent, and they were used extensively as a complement to laboratory hypervelocity testing.

The impact of the debris cloud on the second sheet of the protective structure can result in various forms of damage. This is apparent from the photographs in Figure 8 and some of these damage patterns are shown in the views collected in Figures 11 and 12. The physical and material properties that control the resistance to hypervelocity penetration for dual sheet structures are as follows:

- a) Bumper thickness to projectile length ratio
- b) Bumper to projectile mass density ratio
- c) Impact velocity
- d) Spacing between the bumper and second sheet
- e) The presence or absence of material in the space
- f) Thickness of the second sheet
- g) Material properties of the second sheet, e.g. Brinell hardness, yield strength, etc.

Figure 13 shows the parametric variation of the total thickness required to prevent penetration as a function of shield thickness. The ratio of the sum of shield (bumper) thickness, t_s , and back-up or second sheet thickness, t_b to particle length, d , is plotted against t_s over d for 7075-T6 aluminum alloy, 7.4 km/sec velocity and a 5.08 cm (2 in) spacing. The point at t_s over d equal to zero represents a back-up sheet and no shield. Hence, the value of the total thickness parameter is equal to the thickness of a finite sheet at the spallation threshold. As t_s over d increases, the total thickness to projectile length ratio decreases until a minimum is reached. Further increase in the ratio of shield thickness to particle length is accompanied by an increase in total thickness. The large values of t_s to d of 1.0 through 4.0 are characterized by cratering and spall detachment from the rear surface of the shield. A point is reached when the shield by itself is thick enough to prevent spall detachment from its rear surface. Now we are back to single sheet protection and the back-up sheet is redundant. In

practice, optimum dual sheet protection design necessitates working in the region between t_s to d values of 0.1 to 0.25.

The back-up sheet thickness is determined by the particulate debris and the impulsive loading associated with the debris cloud off the shield. The equation used by JSC for the Apollo-Skylab hazard assessments (reference 10), was as follows:

$$t_b = 0.075m^{0.333}V.S^{-0.5} \left(\frac{70,000}{\sigma_y} \right)^{0.5} ; \text{ cm,}$$

where m is the mass (gm) of the impacting particle, V (km/sec) is its velocity, S (cm) is the spacing and σ_y (psi) is the allowable yield strength of the material. The constant in the equation is applicable to a 2024-T3 or similar aluminum alloy. The family of curves in Figure 14 represents the variation of t_b with the ratio t_s to d for a number of t_s values in the optimum range previously mentioned.

The investigation into dual wall shielding was extended to include several variations of the basic principles outlined above. This research included the use of multiple thin sheets in place of the single back-up, multi-layer super insulation in front of and also behind the backup, the use of honeycomb cores bonded to the shield and back-up sheet, oblique impacts, and the effect on non-spherical projectiles, especially thin rods of $L/D \geq 3$ and flat plates, (reference 10).

3.0 SPECIFIC APOLLO & SKYLAB STRUCTURAL COMPONENT INVESTIGATIONS

The hazard analyses performed for the Apollo and Skylab missions necessitated knowledge of the penetration resistance and failure mode of each component exposed to the meteoroid environment. Figure 15 shows four of the elements for which the "ballistic limit" or failure mode limit was obtained; the Service Module honeycomb structure; the Command Module heat-shield; the Command Module outer windows; and the Extra-vehicular (EVA) suit. Some of the results obtained are shown on the next few figures.

The penetration equations derived for the Apollo windows, made from 99% pure fused silica (Corning 7940), are given in Figure 16. In addition to a crater depth equation, criteria to prevent spallation, energy induced cracking, and combined thermal-meteoroid impact induced fracture is included. The Apollo Command Module heat shield was a nylon phenolic honeycomb core impregnated with an ablative material (Avcoat 5026), bonded to a stainless steel honeycomb shell. The failure mode for this component was no penetration into the stainless steel surface which is well illustrated in Figure 15. Figure 17 shows the results of hypervelocity impact tests in the ablative material reinforced with the nylon honeycomb, using several different projectiles of varying mass densities. It is evident that the volume of the craters formed in tests up to 8 km/sec correlate well with impact energy. The resulting crater depth equations are compared with the data in Figure 18. It is noticeable that the fit to the nylon data requires modification of the coefficient, i.e., the density term in the equation is not sufficient to generalize it for widely varying projectile materials. The equation relating

to the copper projectiles ($\rho = 8.9 \text{ g/cc}$) was excluded from Figure 18 because it was not relevant to the meteoroid case, ($\rho = 1.0 \text{ g/cc}$). However, the copper tests established the ballistic limit of the ablator and stainless steel combination. The equivalent meteoroid kinetic energy level required to penetrate it, a catastrophic failure, was beyond the possibility of encounter for either the Apollo or Skylab missions.

The criterion for failure of the EVA suit was a leak rate in the pressurized bladder layer greater than the capability of the portable life support system. The lay up of the EVA suit was such that the bladder was nearest the astronaut's body, and the layer that functioned as the "bumper" was the woven beta cloth outer garment pictured in Figure 15. Hypervelocity impact tests established the ballistic limit as the particle kinetic energy per unit cross-sectional area to just cause the prescribed leak rate in the bladder layer.

Other Apollo spacecraft components required experimentally determined ballistic limits based on prescribed failure modes. These included the fuel and oxydizer tanks inside the Service Module shell, the dual-loop radiator system, the Service Module engine nozzle, Lunar Module windows and thermal-meteoroid shield, astronaut's visor, gloves, boots and the Portable Life Support System. Figure 19 shows the front face of a scaled titanium Service Module tank which was hypervelocity impact tested while under internal pressure. A bumper, simulating the effect of the Service Module shell was placed in front of the test tank. The inside surface of the tank wall, shown in Figure 20, has spalled, a condition which was not permissible for the real case. Tests such as this set the allowable impact criteria for the pressurized Apollo tanks. In the case of the Service Module engine nozzle, the failure mode was a maximum hole size to prevent a burn through from the inside. Hypervelocity impact tests established an equation to predict the diameter of a hole as a function of projectile diameter, velocity and mass density for the specific nozzle material.

The hazard analyses for the Apollo and Skylab missions consisted of calculating the critical damage probability for each structural component, based on the limiting meteoroid diameter for the specific failure mode considered. The individual component probability numbers were combined into an overall "mission success" figure. In the case of the Apollo lunar landing missions, there was the added risk of low speed impacts from secondary ejecta. As mentioned earlier in this paper, and illustrated in Figure 1, this is a very different impact region. Shielding designed by the hypervelocity impact regime, relying as it does on projectile break-up by a thin outer shield, is easily penetrated by a slow moving particle. This was especially true for lunar surface ejecta material of mass density between 2 and 3 g/cc. The Lunar Module and EVA components had to be hardened against low speed in addition to meeting the basic meteoroid impact case. Empirical design curves were derived for the particular combinations of materials and exposure times involved. These low speed curves will not be covered in this report.

4.0 CONCLUSIONS

Where are we with regards to the knowledge required to design long

duration, large area space structures that will be safe for manned operations in space?

Most of the basic knowledge relating to hypervelocity impacts and the equations necessary to perform hazard analyses of existing structures or design appropriate shielding is in existence. What is required is knowing what is available, confidence that 15 to 20 year old information is still valid, and an effort to present it in a logical manner to the current generation of potential users. This paper marks the beginning of such an effort. However, it should be pointed out that there will be a need for more hypervelocity impact research activity, but it will not be on the scale prevalent during the Apollo era. There are new combinations of materials and structural applications, different attitudes towards failure modes, and larger, longer duration space structures. These will need some additional investigative effort no doubt. One such area, involving a hypervelocity test program for the composite materials currently being considered for space applications, has been initiated by the Johnson Space Center. By and large, the information generated during the design phase of the Apollo, provides a solid background for any foreseeable future requirements for hypervelocity impact protection. It is hoped that the bibliography will be of use to those who may need to pursue this subject in greater depth.

Reference List

1. Summers, J.L.: Investigations of High-Speed Impact: Regions of Impact and Impact at Oblique Angles. NASA TN D-94, Oct 1959.
2. Gault, D.E., and Moore, H.J.: Scaling Relationships for Microscale to Megascale Impact Craters. Proc. of 7th Hypervelocity Impact Symposium, Vol. VI, Tampa, Florida, Nov. 1964, pp. 341-351.
3. Rosenblatt, M.: Analytical Study of Strain Rate Effects in Hypervelocity Impacts, Final Report, (Contract NAS 8-20235, NASA, Huntsville, Alabama). Shock Hydrodynamics, Inc., California, Jan 1970.
4. Prater, R.F. Mjr., USAF.: Hypervelocity Impact-Material Strength Effects on Crater Formation and Shock Propagation in Three Aluminum Alloys. AFML-TR-70-295, Air Force Systems Command, Wright-Patterson AFB, Ohio, Dec 1970.
5. Meyers, C.L. et al.: Summary Report of Research on the Properties of Optimum Meteoroid Shields, TR64-48, (Contract NAS 8-11118, NASA, Huntsville, Alabama). AC Electronics Defense Research Laboratories*, Santa Barbara, California, Sept 1964.
6. Rosenblatt, M.: Numerical Calculations of Hypervelocity Impact Crater Formation in Hard and Soft Aluminum Alloys. AFML-TR-70-254, Air Force Systems Command, Wright-Patterson AFB, Ohio, Feb 1971.
7. Halperson, S.M.: Comparisons Between Hydrodynamic Theory and Impact Experiments. Proc. of 7th Hypervelocity Impact Symposium, Vol. V, Tampa, Florida, Nov. 1964, pp. 235-252.
8. Christman, D.R., et al.: Study of the Phenomena of Hypervelocity Impact, Summary Report, TR63-216. (Contract NAS 8-5067, NASA, Huntsville, Alabama). AC Electronics Defense Research Laboratories*, Santa Barbara, California, June 1963.
9. Woodall, S.R.: A Numerical Method for Analyzing Meteoroid Two-Sheet Structural Configuration Impact Problems. Mechanics Section TM No. 067-04, General Electric, Space Sciences Laboratory, Aug 1967.
10. Cour-Palais, B.G.: Space Vehicle Meteoroid Shielding Design. ESA SP-153, Proc. of International Workshop Sponsored by the European Space Agency, Noordwijk, The Netherlands, April 1979, pp. 85-92.
11. Maiden, C.J.: Thin Sheet Impact. Proc. of 7th Hypervelocity Impact Symposium, Vol. IV, Tampa, Florida. Nov. 1964, pp. 63-124. (Also AC Electronics Defense Research Laboratories*, TR64-61, Nov. 1964).

* Formerly, GM Defense Research Laboratories, Santa Barbara, CA.

BIBLIOGRAPHY

- 1.0 ANALYTICAL TOPICS
- 1.1 THEORY OF HIGH SPEED IMPACT (Summary Report 3 November 1960 - 2 November, 1961), Belek, A.G., Technical Report APGC-TDR-62-20, March 1962. Air Proving Ground Center, Air Force Systems Command, Elgin AFB, Florida.
- 1.2 REVIEW OF PHYSICAL PROCESSES IN HYPERVELOCITY IMPACT AND PENETRATION, Bjork, R.L., Memorandum RM-3529-PR, July 1963, The Rand Corporation, Santa Monica, California.
- 1.3 HYDRODYNAMICS OF HYPERVELOCITY IMPACT, Walsh, J.M., and Tillotson, J.J., Technical Report GA-3827, January, 1963. General Atomic, Division of General Dynamics, San Diego, California.
- 1.4 HYPERVELOCITY IMPACT CALCULATIONS AND THEIR CORRELATION WITH EXPERIMENT, Riney, T.D., and Heyda, J.F. Technical Report R64SD64, September 1964. Space Sciences Laboratory, Missile & Space Division, General Electric Company, Philadelphia, Pennsylvania.
- 1.5 SUMMARY REPORT ON THE THEORY OF HYPERVELOCITY IMPACT, Walsh, J.M., Johnson, W.E., et al., Technical Report GA-5119, March 1964, General Atomic, Division of General Dynamics, San Diego, California.
- 1.6 ENERGY PARTITIONING IN HIGH-VELOCITY-IMPACT CRATERING IN LEAD, Turner, G.H., and Palmer, E.P., Part I; INTERNAL ENERGY AND DEFORMATION IN ROD-TO-ROD IMPACT, Palmer, E.P., and Pratt, D.W., Part II; RESPONSE OF A THERMOCOUPLE JUNCTION TO SHOCK WAVES IN COPPER, Palmer, E.P., Turner, G.H., and Christmas, H.W., Part III, Technical Report BSD# TDR-64-95, May 1964, Ballistic Systems Division, Air Force Systems Command, Norton AFB, California.
- 1.7 MEASUREMENT OF THE VERY-HIGH-PRESSURE PROPERTIES OF MATERIALS USING A LIGHT GAS GUN, Jones, A.H., Isbell, W.M., and Maiden, C.J., Technical Report TR65-84, November 1965. AC Electronics Defense Research Laboratories*, Santa Barbara, California.
- 1.8 ANALYTICAL STUDY OF IMPACT EFFECTS AS APPLIED TO THE METEOROID HAZARD, Bjork, R.L., Kreyenhagen, K.N., and Wagner, M.H., Contract Report NAS2-805, September 1966. Shock Hydrodynamics, Inc. Sherman Oaks, California.
- 1.9 THEORETICAL STUDY OF SIZE SCALING IN CRATERING RESULTING FROM HYPERVELOCITY IMPACT, Sedgewick, R.T., Contract Report NAS8-20239, September 1966. Space Sciences Laboratory, Missile and Space Division, General Electric Company, Philadelphia, Pennsylvania.
- 1.10 ANALYTICAL STUDY OF DEBRIS CLOUDS FORMED BY HYPERVELOCITY IMPACTS ON THIN PLATES, Rosenblatt, M., Kreyenhagen, K.N., and Romine, W.E., Technical Report AFML-TR-68-266, December 1968. Air Force Materials Laboratory, Air Force Systems Command, Wright-Patterson AFB, Ohio.

- 1.11 ANALYTICAL STUDY OF STRAIN RATE EFFECTS IN HYPERVELOCITY IMPACTS, FINAL REPORT, Rosenblatt, M., Contract Report NAS8-20235, January 1970, Shock Hydrodynamics, Inc. Sherman Oaks, California.
- 1.12 NUMERICAL CALCULATIONS OF HYPERVELOCITY IMPACT CRATER FORMATION IN HARD AND SOFT ALLOYS. Rosenblatt, M., Technical Report AFML-TR-70-254, February 1971. Air Force Materials Laboratory, Air Force Systems Command, Wright-Patterson AFB, Ohio.
- 1.13 MULTIVARIABLE ANALYSIS OF THE MECHANICS OF PENETRATION OF HIGH SPEED PARTICLES, FINAL REPORT, Bouma, D.D., and Burkitt, W.C., Martin-CR-66-26, July 1966. Martin Marietta Corporation, Denver, Colorado.
- 1.14 THE PARTICLE DYNAMICS OF TARGET PENETRATION, Dehn, J., Technical Report ARBRL-TR-02188, September 1979. U.S. Army Armament Research and Development Command, Ballistic Research Laboratory, Aberdeen Proving Ground, Maryland.

2.0 GENERAL EXPERIMENTAL TOPICS

- 2.1 INVESTIGATION OF HIGH-SPEED IMPACT, Summers, J.L., Technical Note TND-94, October 1959. NASA, Ames Research Center, California.
- 2.2 STUDY OF THE PHENOMENA OF HYPERVELOCITY IMPACT, SUMMARY REPORT, Christman, D.R., Gehring, J.W., et al., Technical Report TR63-216, June 1963. AC Electronics Defense Research Laboratories*, Santa Barbara, California.
- 2.3 RESEARCH ON THE PROPERTIES OF OPTIMUM METEOROID SHIELDS, Meyers, C.L., and Charest, J.A., Technical Report TR64-48, September 1964. AC Electronics Defense Laboratories*, Santa Barbara, California.
- 2.4 THIN SHEET IMPACT, Maiden, C.J. McMillan, A.R., and Sennett, R.E., Technical Report TR64-61, November 1964. AC Electronics Defense Laboratories*, Santa Barbara, California.
- 2.5 EXPERIMENTAL INVESTIGATIONS OF SIMULATED METEOROID DAMAGE TO VARIOUS SPACECRAFT STRUCTURES, Maiden, C.J., McMillan, A.R., et al., Technical Report 65-48, July 1965. AC Electronics Defense Research Laboratories*, Santa Barbara, California.
- 2.6 IMPACT OF ROD PROJECTILES AGAINST MULTIPLE-SHEET TARGETS, Christman, D.R., and McMillan, A.R., Technical Report TR65-61, July 1965. AC Electronics Defense Research Laboratories*, Santa Barbara, California.
- 2.7 HYPERVELOCITY IMPACT STUDIES AGAINST APOLLO-TYPE STRUCTURES UP TO 16.5 KM/SEC, Gehring, J.W., Wenzel, A.B. et al., Technical Report TR65-56, July 1965, AC Electronics Defense Research Laboratories*, Santa Barbara, California.
- 2.8 EXPERIMENTAL INVESTIGATIONS OF SIMULATED METEOROID DAMAGE TO VARIOUS SPACECRAFT STRUCTURES, Gehring, J.W., McMillan, A.R., et al., Technical Report TR66-67, November 1966. AC Electronics Defense Research

Laboratories*, Santa Barbara, California.

- 2.9 HYPERVELOCITY IMPACT DATA FOR CRATERING STUDIES, Howell, W.G. and Wittrock, E.P., Report No. 6611-494-F, October 1966, Denver Research Institute, Denver, Colorado.
 - 2.10 HYPERVELOCITY IMPACT DAMAGE IN ALUMINUM TARGETS, FINAL REPORT, Teng, R.N., Report No. DAC-59816, March 1968. Douglas Aircraft Company, Missile and Space Systems Division, Santa Monica, California.
 - 2.11 THE EFFECTS OF HYPERVELOCITY IMPACT ON STRUCTURES REPRESENTATIVE OF THE APOLLO SERVICE MODULE, Gehring, J.W., Lathrop, B.L. and Sennett, R.E., Technical Report TR68-04, December 1967. AC Electronics Defense Research Laboratories, Santa Barbara, California.
 - 2.12 HYPERVELOCITY PERFORATION MECHANICS OF THIN METAL PLATES, Turpin, W.C. Technical Report AFML-TR-69-203, July 1969. Air Force Materials Laboratory, Air Force Systems Command, Wright-Patterson AFB, Ohio.
 - 2.13 HYPERVELOCITY IMPACT - MATERIAL STRENGTH EFFECTS ON CRATER FORMATION AND SHOCK PROPAGATION IN THREE ALUMINUM ALLOYS, Prater, R.R., Technical Report AFML-TR-70-295, December 1970. Air Force Materials Laboratory, Air Force Systems Command, Wright-Patterson AFB, Ohio.
- 3.0 HYPERVELOCITY IMPACT SHIELDING TOPICS
- 3.1 METEOROID PROTECTION FOR SPACECRAFT STRUCTURES, Lundeborg, J.F., Stern, P.H. and Bristow, R.J., NASA Contract Report CR-54201 or D2-24056, October 1965. Aerospace Group, The Boeing Company, Seattle, Washington.
 - 3.2 A NUMERICAL METHOD FOR ANALYZING METEOROID TWO-SHEET STRUCTURAL CONFIGURATION IMPACT PROBLEMS. Woodall, S.R., Mechanic's Section Technical Memo No. 067-04, August 1967. Space Sciences Laboratory, General Electric Company, Philadelphia, Pennsylvania.
 - 3.3 A PENETRATION CRITERION FOR DOUBLE-WALLED STRUCTURES SUBJECT TO METEOROID IMPACT, Wilkinson, J.P.D., Technical Report 68SD275, June 1968. Missile and Space Division, General Electric Company, Philadelphia, Pennsylvania.
 - 3.4 EQUATIONS FOR THE COMPARISON OF THE BALLISTIC LIMIT OF SINGLE AND DOUBLE WALL STRUCTURES, Madden, R., AIAA Paper No. 69-370, Vol. of Tech Papers. AIAA Hypervelocity Impact Conference, Cincinnati, Ohio, April-May, 1969.
 - 3.5 THEORETICAL PENETRATION MECHANICS OF MULTISHEET STRUCTURES BASED ON DISCRETE DEBRIS PARTICLE MODELLING, Richardson, A.J., AIAA Paper No. 69-371, Vol. of Tech. Paper. AIAA Hypervelocity Impact Conference, Cincinnati, Ohio, April-May 1969.
 - 3.6 METEOROID PROTECTION BY MULTIWALL STRUCTURES. Cour-Palais, B.G., AIAA Paper No. 69-372, Vol. of Tech. Papers. AIAA Hypervelocity Impact Symposium, Cincinnati, Ohio, April-May 1969.

- 3.7 AN EXPERIMENTAL IMPACT INVESTIGATION OF ALUMINUM DOUBLE-SHEET STRUCTURES, Nysmith, C.R., AIAA Paper No. 69-375, Vol. of Tech. Papers, AIAA Hypervelocity Impact Symposium, Cincinnati, Ohio, April-May 1969.
- 3.8 INFLUENCE OF HYPERVELOCITY PROJECTILE SIZE AND DENSITY ON THE BALLISTIC LIMIT OF DUAL-SHEET STRUCTURES, Arenz, R.J., AIAA Paper No. 69-376, Vol. of Tech. Papers. AIAA Hypervelocity Impact Symposium, Cincinnati, Ohio, April-May 1969.
- 3.9 DEVELOPMENT OF THE MARINER MARS 1971 METEOROID SHIELD, Howard, J.R., AIAA Paper No. 69-377, Vol. of Tech. Papers. AIAA Hypervelocity Impact Symposium, Cincinnati, Ohio, April-May 1969.
- 3.10 THE EFFECTS OF BUMPER MATERIAL PROPERTIES ON THE OPERATION OF SPACED HYPERVELOCITY PARTICLE SHIELDS, Swift, H.F., and Hopkins, A.K., AIAA Paper No. 69-379, Vol. of Tech. Papers. AIAA Hypervelocity Impact Symposium, Cincinnati, Ohio, April-May 1969.
- 3.11 CHARACTERIZATION OF DEBRIS CLOUDS BEHIND IMPACTED METEOROID BUMPER PLATES, Swift, H.F., Preonas, D.D., Turpin, W.C., and Cunningham, J.H., AIAA Paper No. 69-380, Vol. of Tech. Papers, AIAA Hypervelocity Impact Symposium, Cincinnati, Ohio, April-May 1969.
- 3.12 SPACE VEHICLE METEOROID SHIELDING DESIGN, Cour-Palais, B.G., ESA SP-153, October 1979. Proc. of International Workshop sponsored by the European Space Agency, Noordwijk, The Netherlands, April, 1979.
- 3.13 DESIGNING DUAL-PLATE METEOROID SHIELDS - A NEW ANALYSIS, Swift, H.F., Bamford, R., and Chen, R., JPL Publication 82-39, March 1982. Jet Propulsion Laboratory, California Institute of Technology, Pasadena, California.

4.0 SPECIFIC HYPERVELOCITY IMPACT TOPICS

4.1 TANKS

4.1.1 PRELIMINARY INVESTIGATION OF CATASTROPHIC FRACTURE OF LIQUID-FILLED TANKS IMPACTED BY HIGH-VELOCITY PARTICLES, Stepka, F.S., and Morse, C.R., NASA Technical Note TN D-1537, May 1963, NASA Lewis Research Center, Cleveland, Ohio.

4.1.2 INVESTIGATION OF CATASTROPHIC FRACTURING AND CHEMICAL REACTIVITY OF LIQUID-FILLED TANKS WHEN IMPACTED BY PROJECTILES OF HIGH VELOCITY, Stepka, F.S., Dengler, R.P., and Morse, C.R., NASA Technical Memorandum TMX-52063, November 1964. NASA Lewis Research Center, Cleveland, Ohio.

4.1.3 HYPERVELOCITY IMPACT EFFECTS ON LIQUID HYDROGEN TANKS, Ferguson, C.W., NASA Contract Report CR-54852 or SM-52027, March 1966. Douglas Aircraft Company, Inc. Missile and Space Systems Division. Santa Monica, California.

4.1.4 ANALYTICAL STUDY OF THE FRACTURE OF LIQUID-FILLED TANKS IMPACTED BY HYPERVELOCITY PARTICLES, Chou, P.C., Schaller, R., and Hoburg, J.,

NASA Contract Report CR-72169 or DIT Report 160-9, March 1967. Drexel Institute of Technology, Philadelphia, Pennsylvania.

4.1.5 HYPERVELOCITY IMPACT OF BUMPER-PROTECTED FUEL TANKS, Chou, P.C., and Gordon, P., AIAA Paper No. 69-369, Vol. of Tech. Papers, AIAA Hypervelocity Impact Symposium, Cincinnati, Ohio, April-May 1969.

4.2 SPACECRAFT CABINS

4.2.1 AN INVESTIGATION OF EXPLOSIVE OXIDATIONS INITIATED BY HYPERVELOCITY IMPACTS, Friend, W.H., Caron, A.P. et al., Technical Report AFFDL-TR-67-92, May 1967. Air Force Flight Dynamics Laboratory, Air Force Systems Command, Wright-Patterson AFB, Ohio.

4.2.2 METEOROID PERFORATION EFFECTS ON SPACE CABIN DESIGN, Long, L.L., and Hammitt, R.L., AIAA Paper No. 69-365, Vol. of Tech. Papers, AIAA Hypervelocity Impact Symposium, Cincinnati, Ohio, April-May 1969.

4.3 SPECIAL APPLICATIONS

4.3.1 PRELIMINARY RESULTS OF EFFECTS OF HYPERVELOCITY IMPACTS ON SPACE RADIATOR TUBES, Gehring, J.W., and Lieblein, S., A.R.S. Paper No. 2544-62, American Rocket Society Space Power Systems Conference, Santa Monica, California, September 1962.

4.3.2 AN INVESTIGATION OF THE PENETRATION OF HYPERVELOCITY PROJECTILES INTO COMPOSITE LAMINATES, McMillan, A.R., Vol. III, Proc. of 6th Symposium on Hypervelocity Impact, Cleveland, Ohio, April-May 1963, pp. 309-356. (This paper covers radiator type impact results extensively).

4.3.3 THE CHARACTERISTICS OF PENETRATION FOR A DOUBLE-SHEET STRUCTURE WITH HONEYCOMB, Jex, D.W., NASA Technical Memorandum TM X-53974, January 1970. NASA Marshall Space Flight Center, Alabama.

4.3.4 IMPACT CHARACTERISTICS IN FUSED SILICA, Flaherty, R.E., AIAA Paper No. 69-367, Vol. of Tech. Papers, AIAA Hypervelocity Impact Symposium, Cincinnati, Ohio, April-May 1969.

4.3.5 EFFECTS OF HYPERVELOCITY PARTICLE IMPACT ON COMPOSITE MATERIALS FOR EXPANDABLE STRUCTURES APPLICATIONS, Reynolds, B.W., Engineering Report GER 10663, August 1962. Goodyear Aircraft Corporation, Akron, Ohio.

4.3.6 EXPERIMENTAL INVESTIGATION OF HYPERVELOCITY IMPACT DAMAGE TO ABLATIVE MATERIAL, Davis, J.A., NRL Report 6370, December 1965. U.S. Naval Research Laboratory, Washington, DC.

4.3.7 DEVELOPMENT OF METEOROID PROTECTION FOR EXTRA VEHICULAR-ACTIVITY SPACE SUITS, McAllum, W.E., AIAA Paper No. 69-366, Vol. of Tech. Papers, AIAA Hypervelocity Impact Symposium, Cincinnati, Ohio, April-May 1969.

5.0 OTHER SOURCES

5.1 PROCEEDINGS OF 6TH SYMPOSIUM OF HYPERVELOCITY IMPACT, Cincinnati, Ohio,

April-May 1963, Contract No. DA-32-124-ARD (D)-16, sponsored by Army Ballistic Research Laboratory (BRL); Air Force, Det 4, ASD; and U.S. Naval Research Laboratory (NRL). Vol I: Projection Techniques; Vol II - Part 1: Thick Target Cratering and Ionization; Vol II - Part 2: Thick Target Cratering and Ionization; Vol. III: Thin Target Perforations and Protection.

- 5.2 PROCEEDINGS OF THE 7TH HYPERVELOCITY IMPACT SYMPOSIUM, Tampa, Florida, November 1964. Sponsored by: Air Force, Det 4, RTD; Army BRL; and U.S. Naval Research Laboratory (NRL). Vol. I: Techniques; Vol. II: Theory; Vol III: Theory; Vol IV: Theory; Vol. V: Experiments; Vol. VI: Experiments.
- 5.3 VOLUME OF TECHNICAL PAPERS. AIAA HYPERVELOCITY IMPACT CONFERENCE, Cincinnati, Ohio, April-May 1969. Published by American Institute of Aeronautics and Astronautics, New York, NY. 25 Papers on Theory and Experiments.
- 5.4 HIGH-VELOCITY IMPACT PHENOMENA. Ed. Ray Kinslow. Academic Press, 1970. New York.

* Formerly GM Defense Research Laboratories, Santa Barbara, CA

THE BASIC REGIONS OF IMPACT FOR
TUNGSTEN-CARBIDE SPHERES IMPACTING LEAD TARGETS.

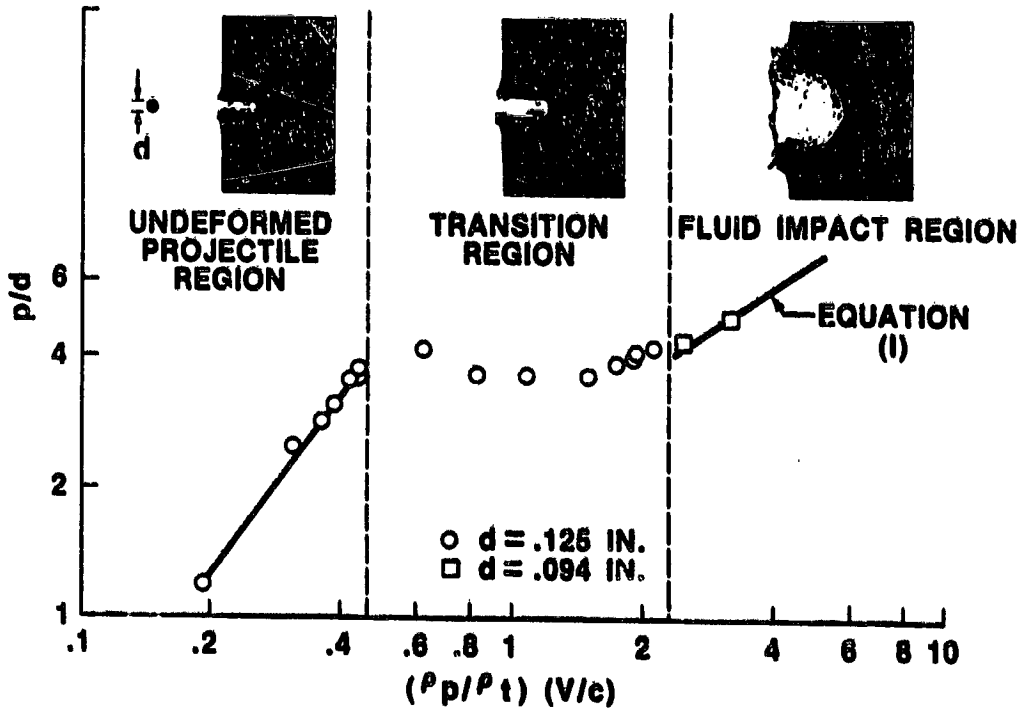


FIGURE 1

p/d VS V FOR A RANGE OF PROJECTILE DIAMETERS

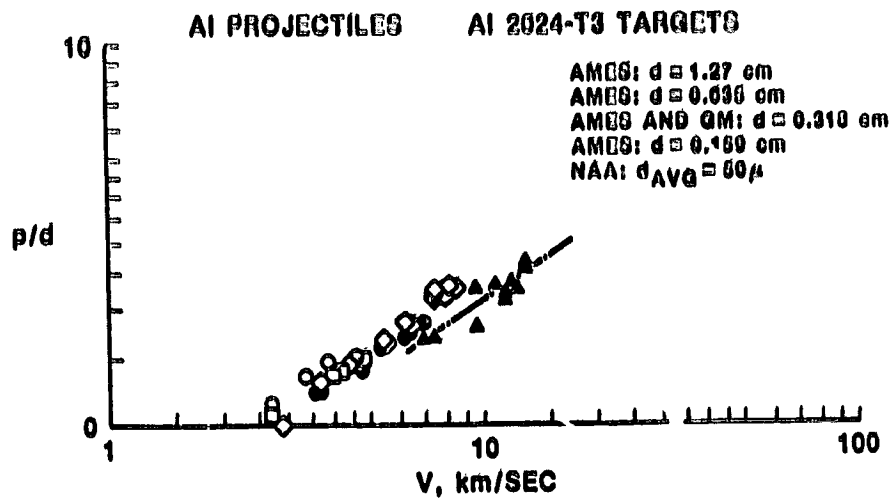


FIGURE 2

p/d 1.056 VS V FOR A RANGE OF PROJECTILE DIAMETERS

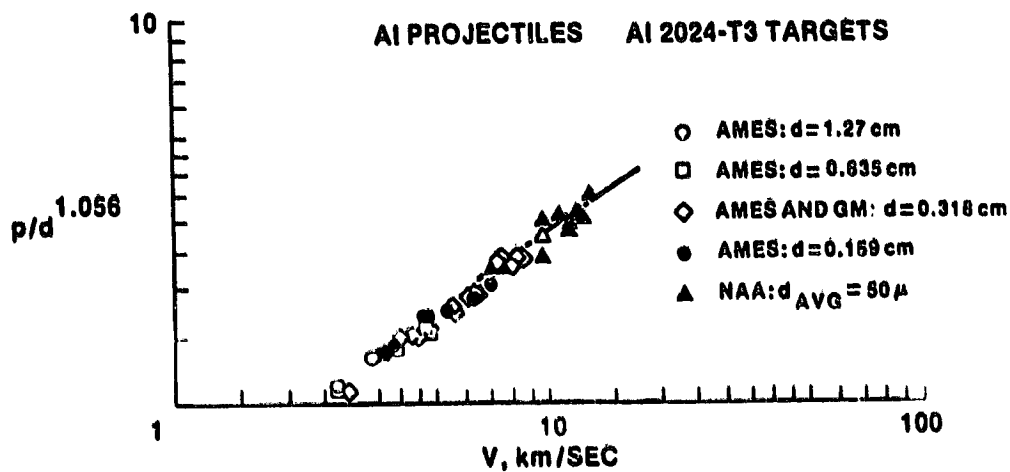


FIGURE 3

APOLLO PENETRATION EQUATION COMPARED WITH EXPERIMENTAL EVIDENCE

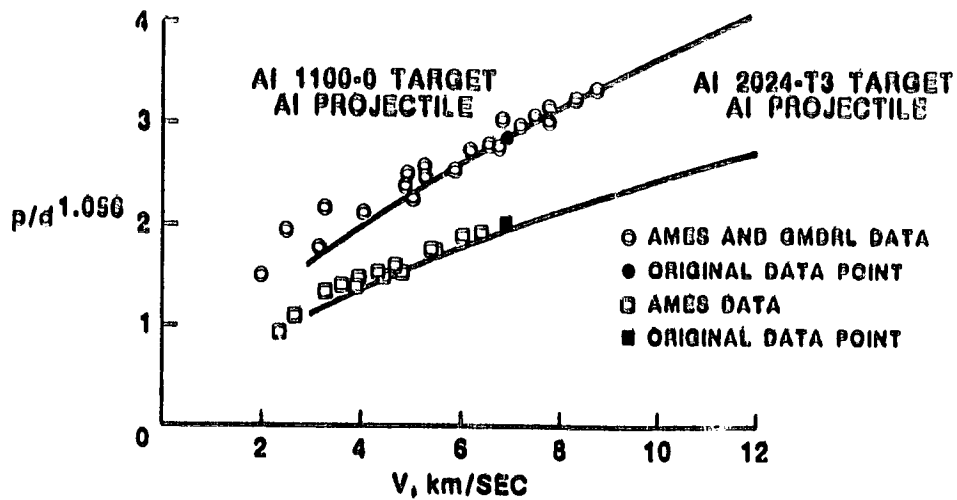


FIGURE 4

COMPARISON OF
NUMERICAL &
EXPERIMENTAL
VELOCITY
DEPENDENCE OF
DIMENSIONLESS
PENETRATION
RATIO FOR
ALUMINUM -
ALUMINUM
IMPACTS

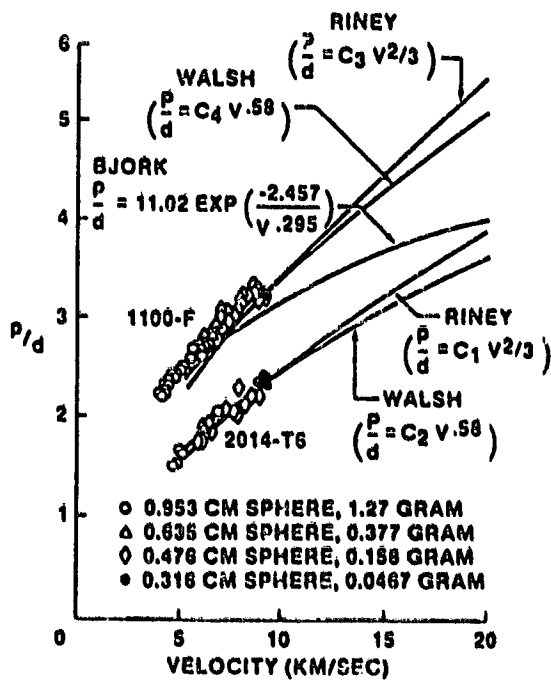


FIGURE 5

APOLLO PENETRATION EQUATIONS (SINGLE THICKNESS METALLIC TARGETS)

- ROCKWELL EQUATIONS

- CRATER DEPTH, $p = 1.38 d_m^{1.1} \cdot H_t^{0.25} \cdot \rho_m^{0.9} \cdot \rho_t^{0.167} \cdot V_m^{0.67}$; cm

- THICKNESS TO PREVENT PERFORATION, $\bar{t} = 1.6 p$

- JSC EQUATIONS

- CRATER DEPTH $p = 9.24 d_m^{1.056} \cdot H_t^{0.20} \cdot \rho_m^{0.5} \cdot \rho_t^{0.107} \cdot C_t^{0.33} \cdot V_m^{0.67}$; cm

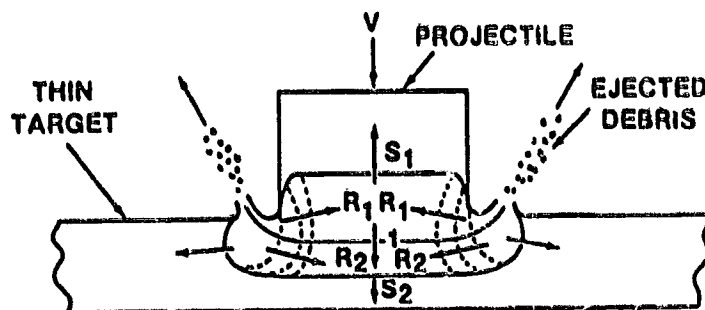
- THICKNESS TO PREVENT PERFORATION, $\bar{t} = 2.0 p$

- MINIMUM THICKNESS FOR NO SPALL EFFECT, $t = 3p$

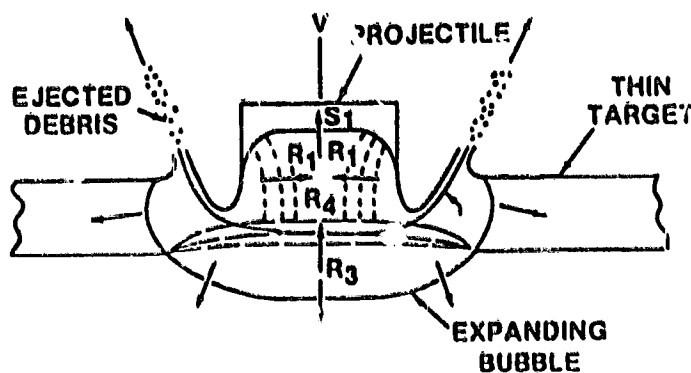
- ROCKWELL AND JSC EQUATIONS WERE INDEPENDENTLY DERIVED

FIGURE 6

THIN TARGET IMPACT MECHANISM



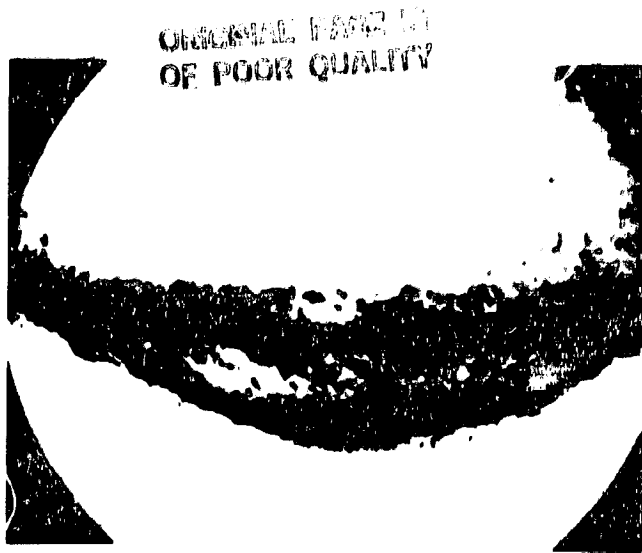
WAVE PATTERN IMMEDIATELY AFTER IMPACT



WAVE PATTERN AFTER FIRST
REFLECTION FROM FREE SURFACE

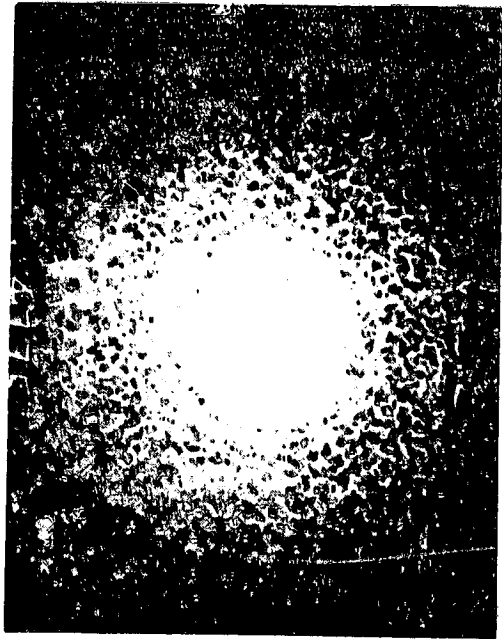
FIGURE 7

**DEBRIS FROM A 0.32 cm
GLASS SPHERE IMPACT
ON A 0.046 cm 2024-T4
ALUMINUM SHIELD
AT > 7 km/SEC**

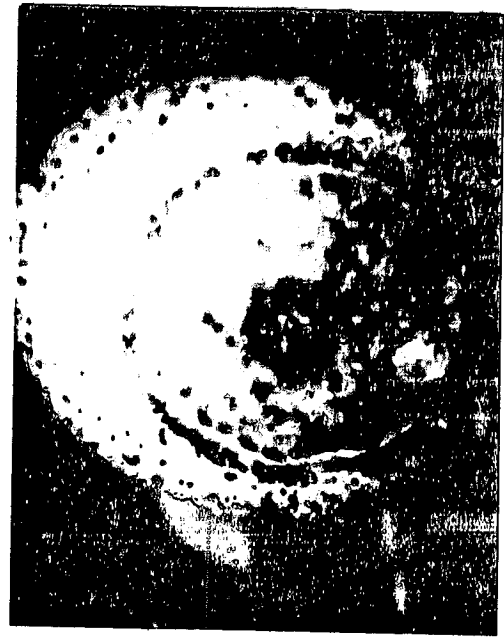


ORIGINAL PAPER IS
OF POOR QUALITY

SIDE VIEW



TARGET DAMAGE



FRONT VIEW

FIGURE 8

C-4

ORIGINAL PAGE IS
OF POOR QUALITY

MASS PARTICLE PLOT OF PROJECTILE-SHIELD CONFIGURATION
AT 0.158 μ SEC AFTER INITIAL IMPACT

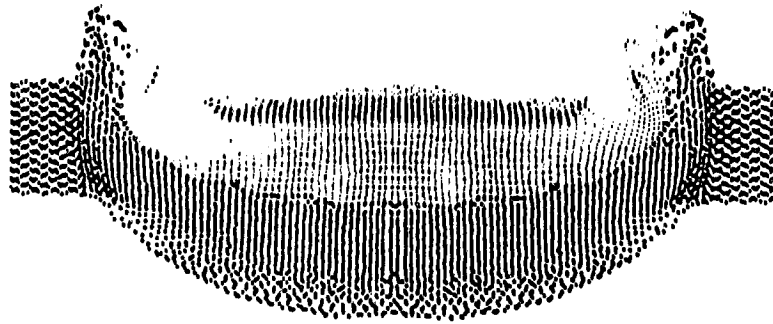


FIGURE 9

MASS PARTICLE PLOT OF PROJECTILE-SHIELD CONFIGURATION
AT 0.570 μ SEC AFTER INITIAL IMPACT

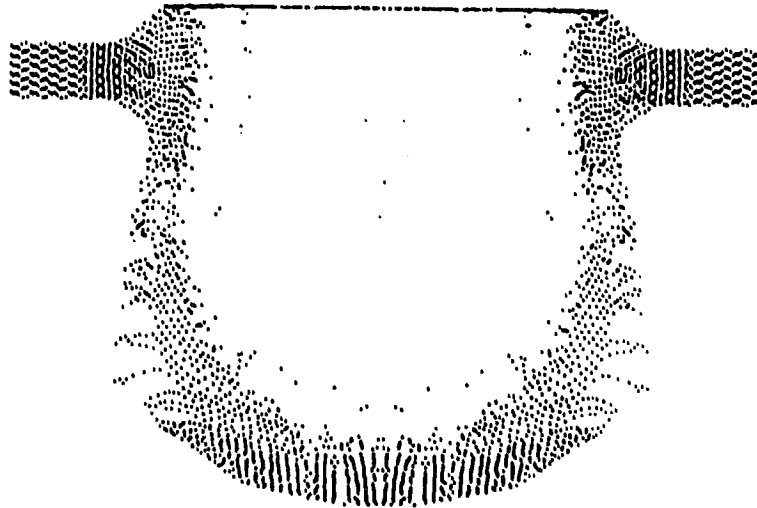


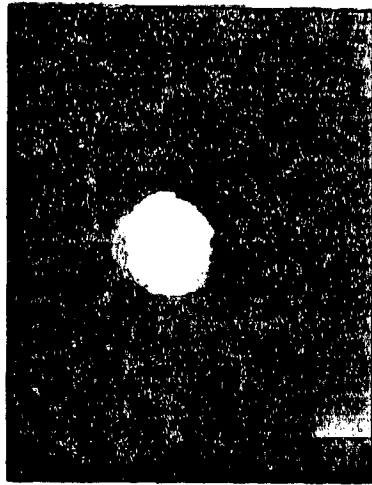
FIGURE 10

TYPICAL BACKUP SHEET DAMAGE

(1.6 mm SOLID GLASS SPHERES INTO
2024-T3 ALUMINUM AT APPROXIMATELY 7 km/SEC)



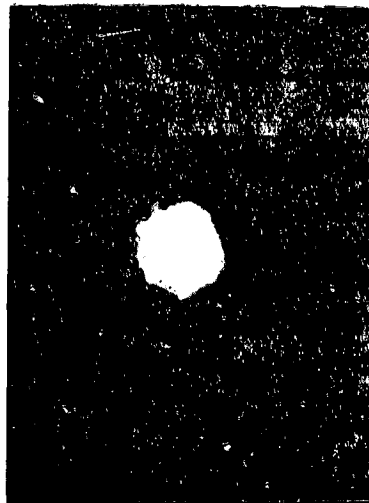
$ts = 0.15$ mm; $S = 2.54$ cm
 $ts/d = 0.094$



$ts = 0.25$ mm; $S = 2.54$ cm
 $ts/d = 0.156$



$ts = 0.51$ mm; $S = 2.54$ cm
 $ts/d = 0.32$



$ts = 0.15$ mm; $S = 5.08$ cm
 $ts/d = 0.094$



$ts = 0.25$ mm; $S = 5.08$ cm
 $ts/d = 0.156$



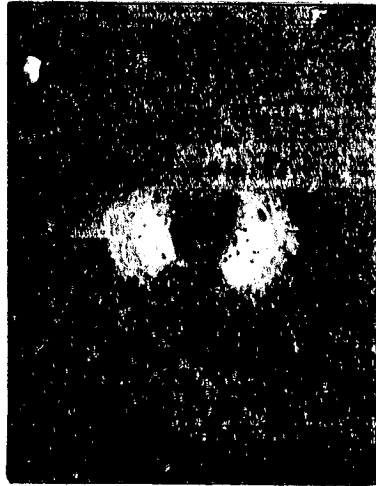
$ts = 0.51$ mm; $S = 5.08$ cm
 $ts/d = 0.32$

FIGURE 11

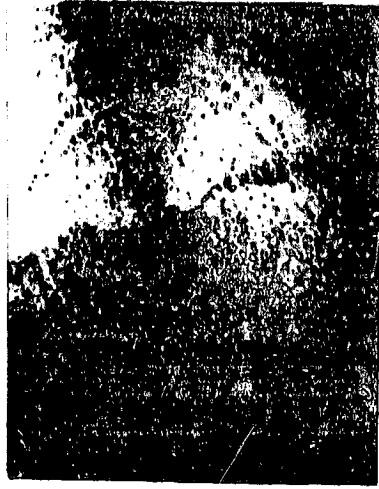


TYPICAL BACKUP SHEET DAMAGE

(SOLID GLASS AND ALUMINUM SPHERES INTO
2024-T3 ALUMINUM AT APPROXIMATELY 7 km/SEC)



GLASS: $d = 1.6$ mm
 $ts = 0.51$ mm; $S = 2.54$ cm



GLASS: $d = 1.6$ mm
 $ts = 0.25$ mm; $S = 7.62$ cm



ALUM: $d = 3.2$ mm
 $ts = 0.51$ mm; $S = 7.62$ cm



ALUM: $d = 1.6$ mm
 $ts = 0.51$ mm; $S = 2.54$ cm



ALUM: $d = 1.6$ mm
 $ts = 0.15$ mm; $S = 5.08$ cm



ALUM: $d = 3.2$ mm
 $ts = 0.71$ mm; $S = 7.62$ cm

FIGURE 12

CLIP: 0001, 000001
OF POOR QUALITY

HYPERVELOCITY SHIELDING SPECTRUM FOR ALUMINUM 7075-T6 AT V=7.4 km/SEC

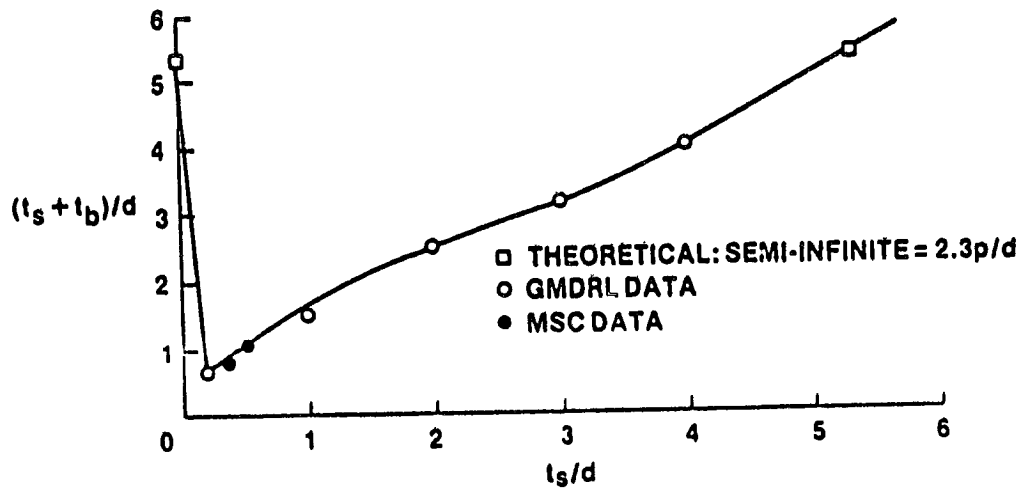


FIGURE 13

FINITE THICKNESS MULTISHEET DESIGN CURVE FOR V > 10 km/SEC

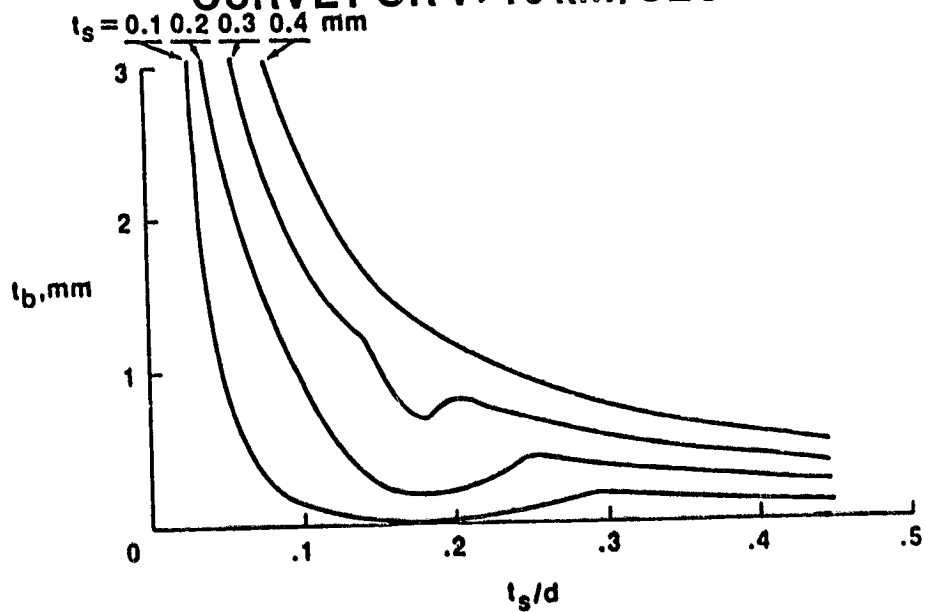
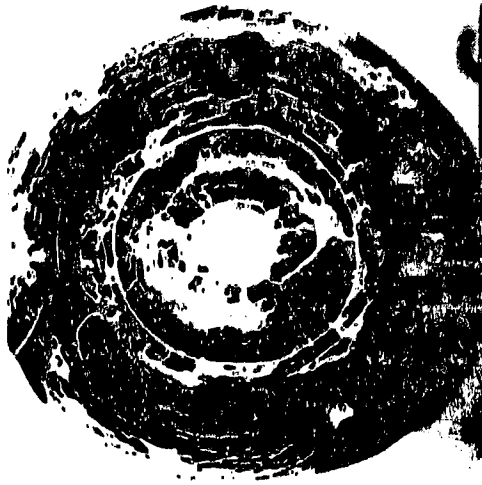


FIGURE 14

APOLLO SUPPORT

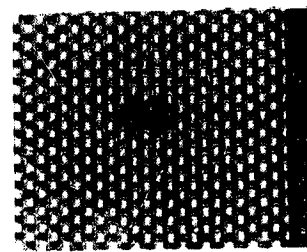


HONEYCOMB



WINDOWS

1 cm



SPACESUITS



ABLATORS

FIGURE 15

APOLLO WINDOW EQUATIONS

CRATERING: $p = 0.53 \rho_m^{0.5} d_m^{1.06} v_m^{0.67}$

NO SPALL: $t_s = 7p$

NO CRACKING: $t_c = p(1.4 \times 10^{-1} v^{1.28})$

COMBINED THERMAL-METEOROID CRITERION:

$d_{\text{FLAW}} = 2p$

FIGURE 16

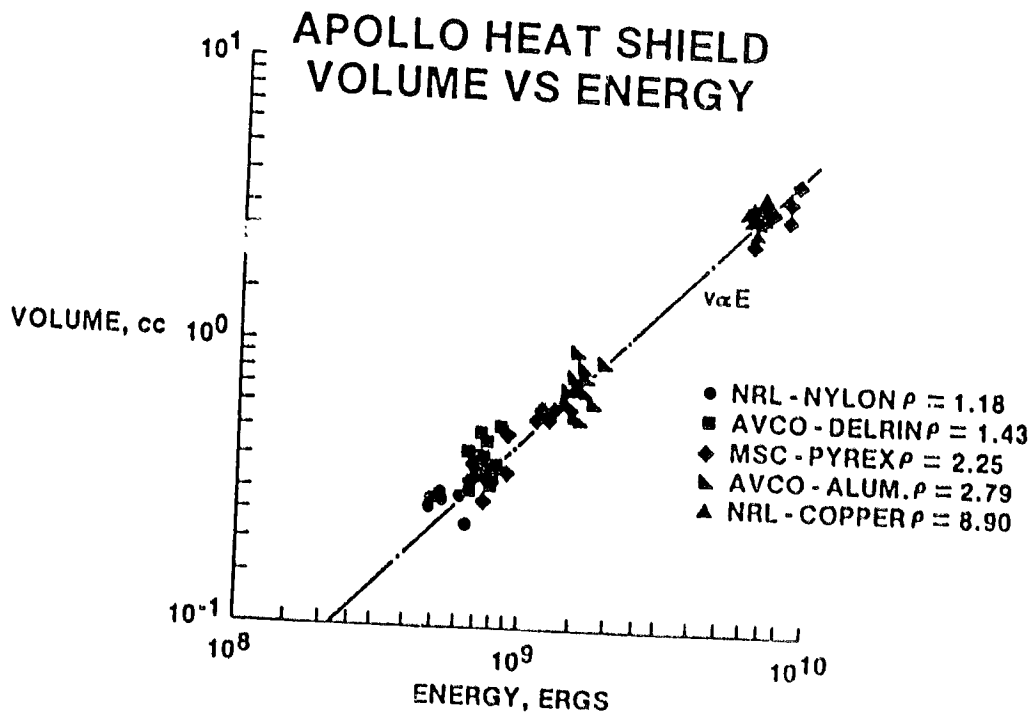


FIGURE 17

APOLLO HEAT SHIELD PENETRATION VS VELOCITY

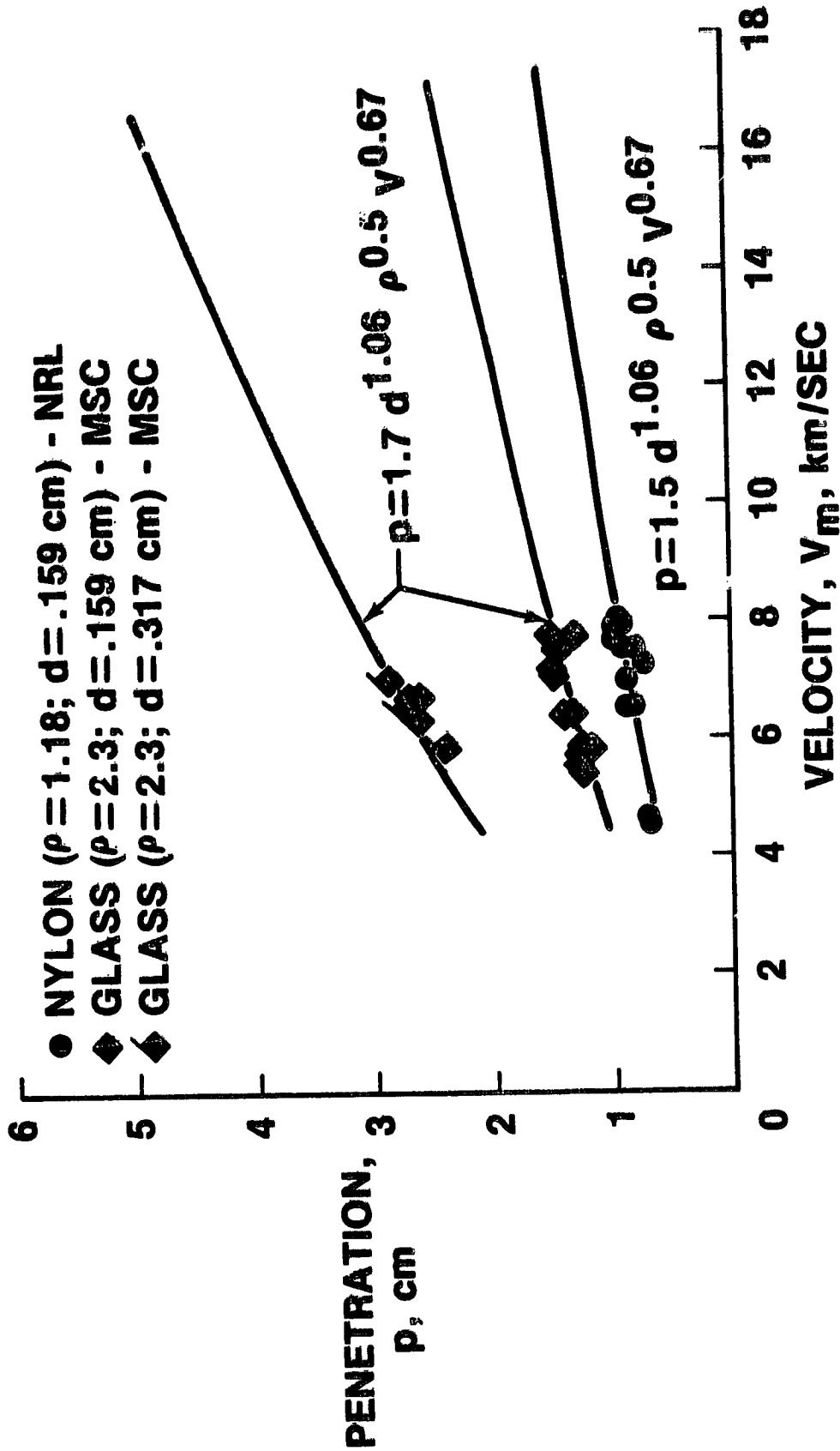
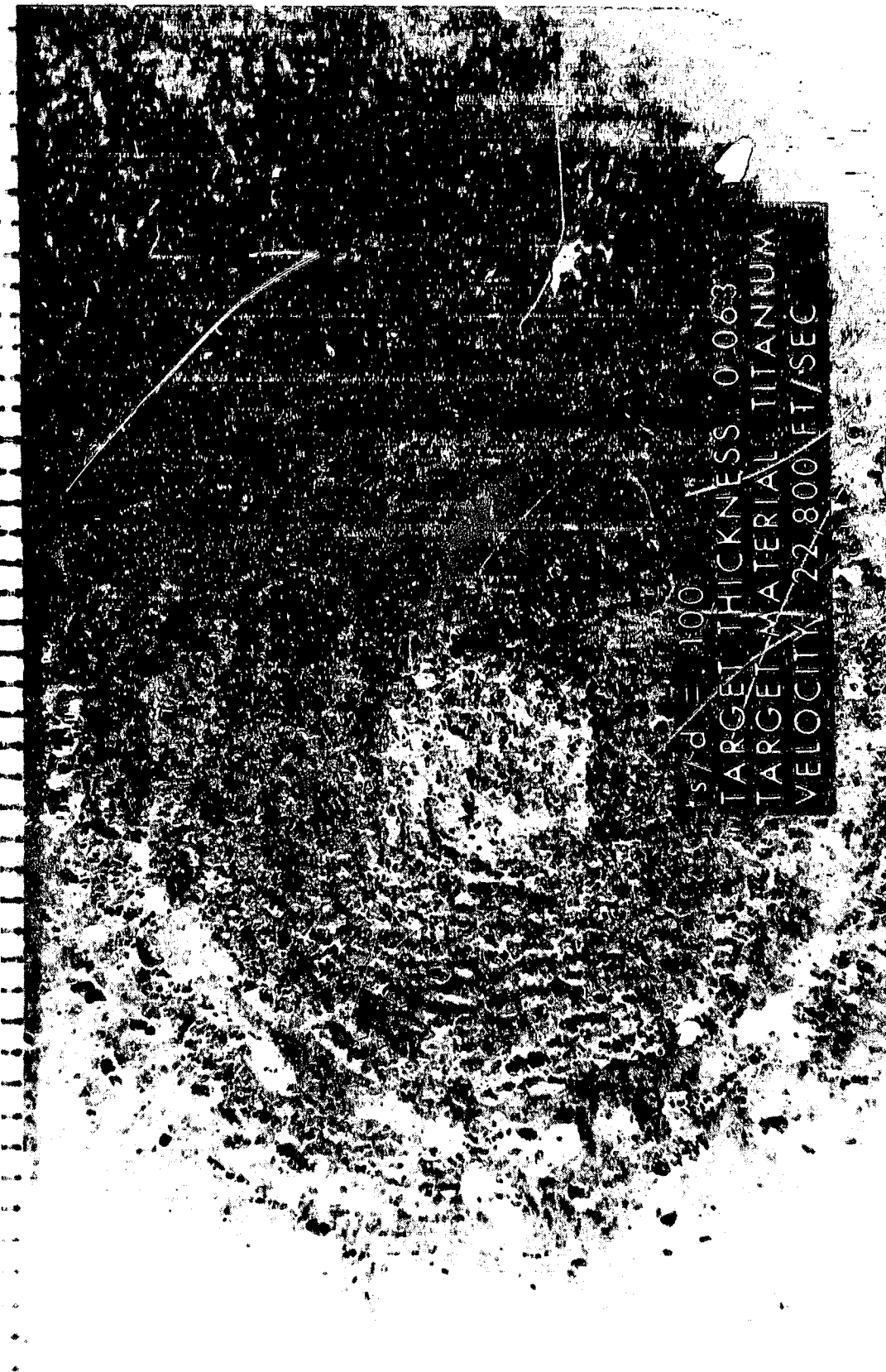


FIGURE 18



TARGET DAMAGE - SPALLATION FRONT FACE

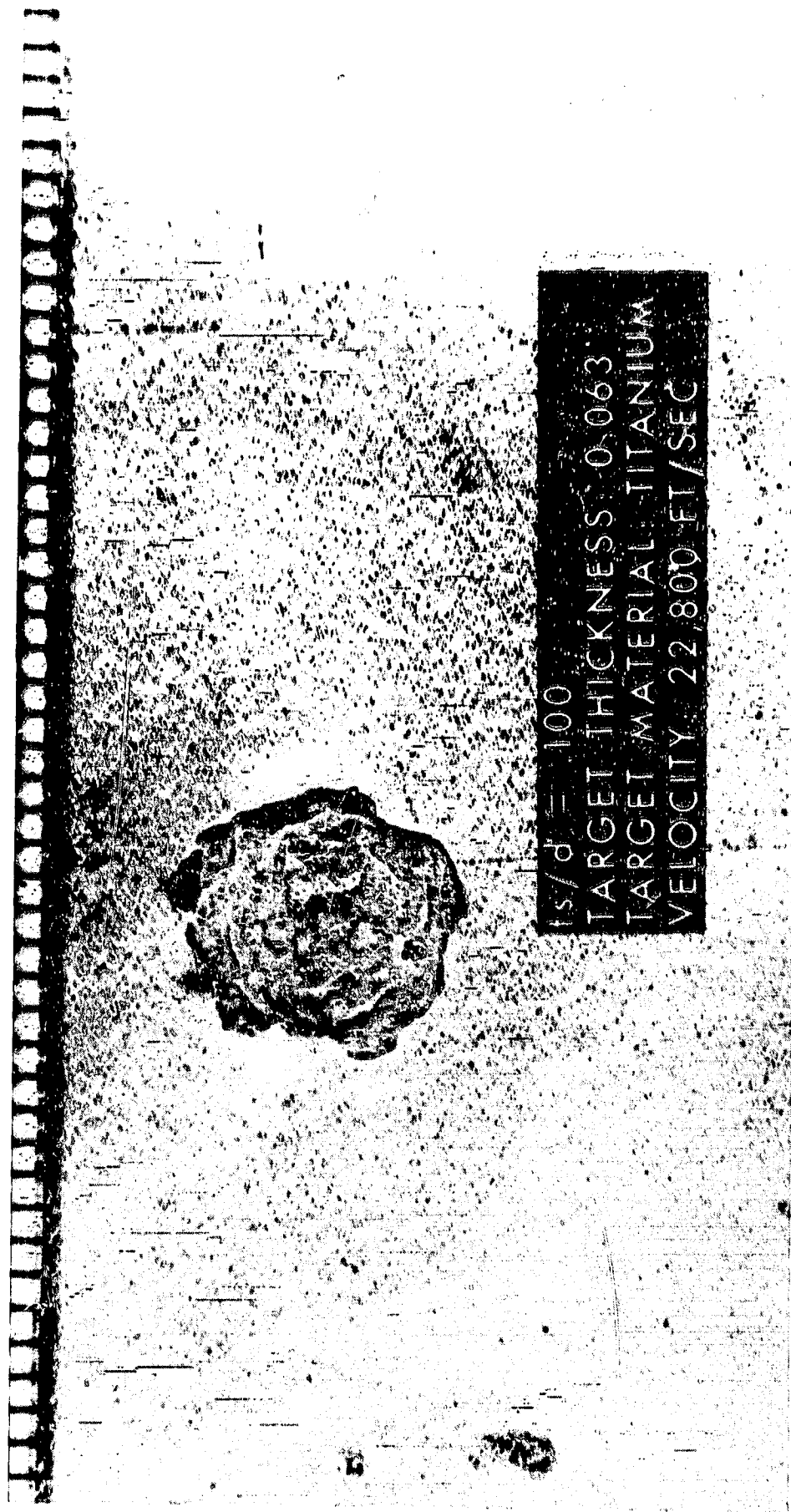


$r/d = 100$
TARGET THICKNESS 0.063
TARGET MATERIAL TITANIUM
VELOCITY 22,800 FT/SEC

FIGURE 19

TARGET DAMAGE - SPALLATION

REAR FACE



$t_s/d = 100$
TARGET THICKNESS 0.063
TARGET MATERIAL TITANIUM
VELOCITY 22 800 FT/SEC

275

ORIGINAL, PAGE 129
OF POOR QUALITY

FIGURE 20



49 18
N 85 - 21207

Solid Particle Environment and Protection
for
The Galileo Orbiter

Andrew J. Beck
Robert Bamford

Outline of Presentation

1. Introduction

- o Galileo Orbiter and Mission
- o Mission Environment
- o Design Requirements
- o Risk Allocation
- o Criteria for Component Failure
- o Shield Design and Implementation
- o 20-Month Earth-Jupiter Interplanetary Exposure
- o At Least 12-Month Inorbit Operation at Jupiter
- o 0.5g/cc Solid Particle Mass Density
- o Constant 1 AU Characteristic Shape for the Mass-Fluence Distribution
- o Interplanetary Fluence from the Time Integration of a Pioneer Modified Flux Model for the Galileo Nominal Trajectory
- o Worst-Case Pioneer-Voyager Jupiter Flux Model

2. Design Requirements

o Solid Particle Integral Fluence

<u>Mass (g)</u>	<u>Interplanetary Fluence (m⁻²)</u>	<u>Inorbit Fluence (m⁻²)</u>	<u>Mission Fluence (m⁻²)</u>
10 ⁻¹²	4.0x10 ³	7.9x10 ³	1.2x10 ⁴
10 ⁻¹⁰	1.6x10 ³	3.2x10 ³	4.8x10 ³
10 ⁻⁸	2.0x10 ²	4.0x10 ²	6.0x10 ²
10 ⁻⁶	8.2	1.6x10 ¹	2.4x10 ¹
10 ⁻⁴	3.1x10 ⁻²	5.9x10 ⁻²	9.0x10 ⁻²
10 ⁻²	1.1x10 ⁻⁴	2.2x10 ⁻⁴	3.3x10 ⁻⁴
10 ⁰	4.3x10 ⁻⁷	8.3x10 ⁻⁷	1.3x10 ⁻⁶

- o Provide Solid Particles Impact Protection for Interplanetary Transfer and at Least 5 Orbit Inorbit Operation
- o 0.95 Probability of No Solid Particle Produced System Failure

3. Component Failure

- o Excludes Acceptable Degradation
- o Penetration of electronics
 - Particle and Shield Debris Subdivide
- o Portions of Tankage and Wiring Dedicated to Protection
- o Penetration Based on Literature

4. Shield Design

- o Double Surface Protection Unless Functionally Impossible
- o Component Protection Weight
 - Proportional to Contribution to System Risk
 - Proportionality Depends on Redundancy and Shape
 - Depends on Preexistence

a Level of Protection

<u>Type</u>	<u>Level</u>
Single Surface	0.155" of 6061 T6 Aluminum
Double Surface (Dedicated)	T ₁ = 0.037" of Aluminum at S = 2.3" from T ₂ = 0.033" of 6061 T6 Aluminum
Double Surface (Second Preexisting)	T ₁ = 0.0061" of Aluminum at S = 2.3" from T ₂ = 0.054" of 6061 T6 Aluminum

These values are multiplied by 0.82 for linear elements, 0.89 for components not mission critical after Jupiter orbit insertion, and 0.60 for science instruments due to redundancy. They can also be sealed for B not equal to zero, not equal one, and not equal one.

Eldon E. Davis
Ray Sperber

ABSTRACT

This paper presents the results of the space debris protection analysis performed under NASA Contract NAS1-16088. The material presented is taken directly from the final report---NASA CR 3536.

In summary, protection against manmade debris and meteoroids was determined for reusable ground and space based orbital transfer vehicles (OTV's). For the mission between LEO-GEO-LEO, both vehicles required a shielding thickness of 0.62mm (24 mils) equivalent aluminum when using a good double wall design and providing a probability of no tank impact of 0.995. The space based OTV would also require an additional 0.43mm (18 mils) of shielding during its on-orbit storage time between flights. The latter requirement, however, was satisfied by placing the OTV in a hangar at the low earth orbit space base thereby eliminating a flight performance penalty.

3.3.6 Space Debris Protection

A major consideration in the development of a reusable system is to ensure its structural integrity including protection against space debris in the form of meteoroids and manmade objects. This section presents pertinent background information, the analysis leading to the required shield thickness, the design concept to be used, and the unresolved issues.

3.3.6.1 Background

Considerable effort was expended in this area in the 1960's and early 1970's. The major focus was on manned habitats associated with space stations and noncyclic pressure tanks. A review of these data

for applicability to the operation of a reusable OTV for the post-1995 time frame indicated the need for further investigation. This conclusion was the result of a combination of the following factors relative to the 1973 MSFC tug studies.

1. Larger vehicle area
2. Longer exposure times
3. Permanent space basing not considered
4. Manmade debris not considered
5. Different viewpoint regarding sensitivity of propellant tanks to space debris damage

The larger vehicle area is the result of the FOTV systems containing approximately 32t of propellant as compared with 23t for the tug. The longest mission time was greater (8 versus 5 days), as was the average duration (5 versus 3 days). An additional factor for the SB OTV was that it was to remain on orbit (permanent space basing) and thus considerably increase its total exposure time. Prior studies concerning space debris protection only considered meteoroids. NORAD data now indicate a considerable number of manmade objects also exist in orbits that may impact an OTV. A different viewpoint is also suggested regarding the sensitivity of propellant tanks to meteoroid/debris damage. This viewpoint is summarized in table 3.3.6-1. In summary, the tank wall thickness should

Table 3.3.6-1 Propellant Tank Debris Protection Philosophy

- NASA CRITERIA FOR TANKS (NASA SP-8042, MAY 1970):
 - ALLOWS PENETRATION UP TO 25% OF WALL THICKNESS (INTENDED FOR TANKS HAVING A NON-CYCLE SERVICE LIFE REQUIREMENT)
- CURRENT BOEING POSITION ON DAMAGE TO TANKS HAVING A CYCLIC SERVICE LIFE REQUIREMENT
 - CONSERVATIVE APPROACH OF ALLOWING NO DAMAGE (NO FLAWS OTHER THAN THOSE KNOWN AT TIME OF ACCEPTANCE TESTING (I.E. PROOF TEST AND LEAK TEST))
 - INSUFFICIENT DATA BASE FOR CORRELATING NON-PENETRATING DEBRIS DAMAGE TO REMAINING SERVICE LIFE VIA FRACTURED MECHANICS APPROACH
 - IF A TANK DESIGNED FOR NO DAMAGE IS DAMAGED, IT MUST BE SUBJECTED TO NEW ACCEPTANCE TESTING DESIGNED TO GUARANTEE (AS A MINIMUM) ITS REQUIRED REMAINING SERVICE LIFE.

not contribute to the required shield thickness. Furthermore, if a tank is damaged, it is strongly suggested that new acceptance testing be conducted to guarantee its required remaining service life.

3.3.6.2 Shielding Analysis

Guidelines and Assumptions—The guidelines and assumptions used to conduct the space debris analyses are presented in table 3.3.6-2. The tank area used was that established by

Table 3.3.6-2 Space Debris Analysis Guidelines and Assumptions

207V70-126

- EXPOSURE AREA: SIDE PROJECTION OF TANKS
GB AND SB OTV = 35 SQ M ▷
 - EXPOSURE TIME:
 - MISSION ONLY (BOTH GB AND SB OTV)
 - TOTAL FLIGHT AVG = 5.3 DAYS (DESIGN POINT)
 - MANNED FLIGHT AND UNMANNED SERVICING AVG = 7.2 DAYS
 - BASING AT LEO BETWEEN MISSIONS
 - GB OTV --- 1 DAY
 - SB OTV --- 21 DAYS
 - ALLOWABLE TANK PENETRATION: ZERO
 - PROBABILITY OF NO TANK IMPACT $P_{(0)}$: 0.995
(REQUIRED TO SATISFY VEHICLE MISSION SUCCESS CRITERIA)
 - KEY EQUATIONS:
 - METEOROIDS: $\bar{T} = 0.162 \left(\frac{(AT)}{(1 - P_{(0)})} \right)^{.271}$ IN MILLIMETERS ALUMINUM
 - MAN MADE: $\bar{T} = 0.089 \left(\frac{(AT)}{(1 - P_{(0)})} \right)^{.431}$ IN MILLIMETERS ALUMINUM
 - DEBRIS MODEL: KESSLER AND COUR-PALAIS, JGR VOL 83 METEOROIDS DOMINATE TRANSFER TRAJECTORY; MAN MADE DEBRIS DOMINATE LEO
- ▷ DESIGN PT. BUT FINAL DESIGN INDICATED SB = 39 SQ M
GB = 38.9 SQ M

side projection rather than wetted. As indicated earlier, the analysis was conducted without the tank wall contributing to the required shield thickness. The criteria are expressed as probability of no tank impact rather than penetration.

The indicated value of $P_{(0)} = 0.995$ is that which, when considered with the predicted subsystem reliability, gives the required mission success goal of 0.97. The shield thickness (\bar{T}) equations have different constants and exponents because meteoroids and manmade debris have different velocities, density, size, and flux. Both equations reflect use of a double-wall design with its general characteristics being one-third of mass in the bumper and the remainder in the back wall. Spacing between walls would be approximately 30 particle diameters. It should be noted that a single-wall shield would have a mass approximately four times greater than that of a double wall.

The debris model used in the analysis is shown in figure 3.3.6-1. The indicated meteoroid flux is essentially the same as that used in the Apollo, Skylab, and Space Shuttle programs. The manmade debris flux is established by NORAD. As of 1980 there were approximately 5000 objects of 10-cm diameter or greater. Approximately 60% of the objects are fragments resulting from explosions, 20% are mission related such as shrouds, rocket stages, etc., and 20% are payloads (either operating or nonoperating). The value used in the analysis was the predicted flux for 1990 which is approximately 8000 objects.

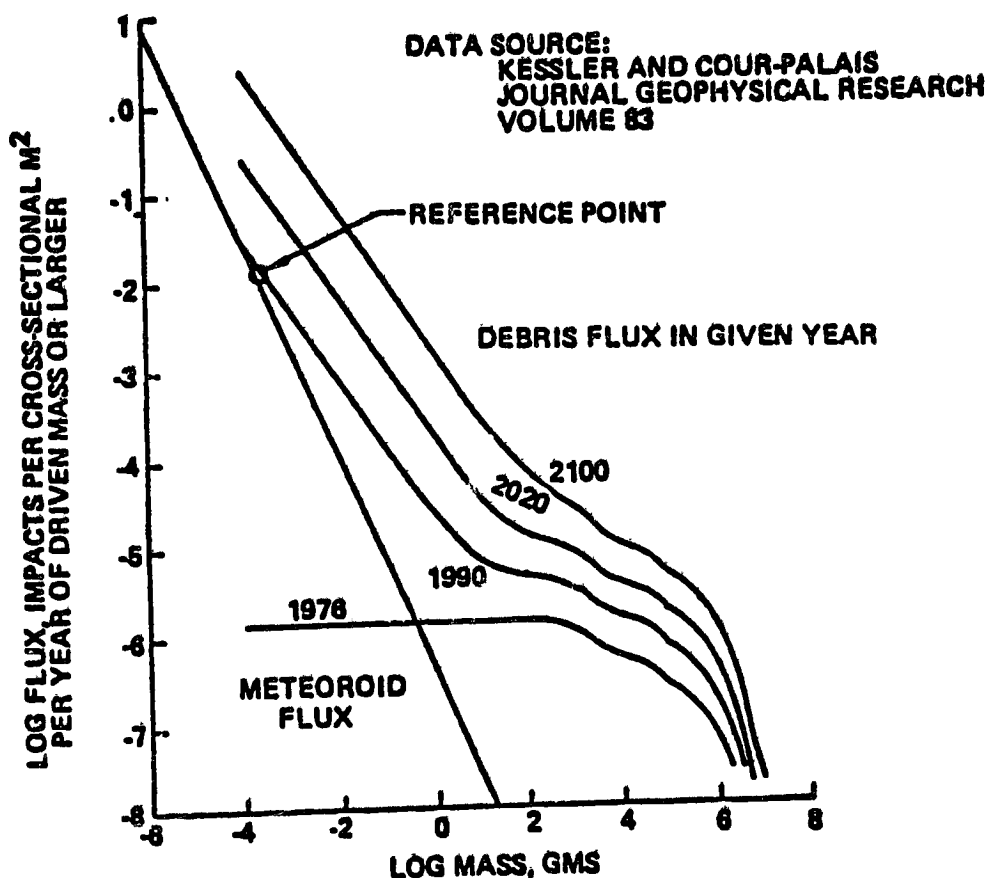


Figure 3.3.6-1 Debris Model

The number of impacts per year expected on an OTV is 10^{-2} with the indicated area and $P_{(0)}$. This also corresponds to protection against objects with a mass of 10^{-3} g.

Shield Thickness Requirement—The amount of protection or shielding required for various combinations of $P_{(0)}$ and vehicle AT (m^2 -years) is shown in figure 3.3.6-2. The shield thickness is defined as \bar{t} expressed in millimeters equivalent of aluminum. For the case of

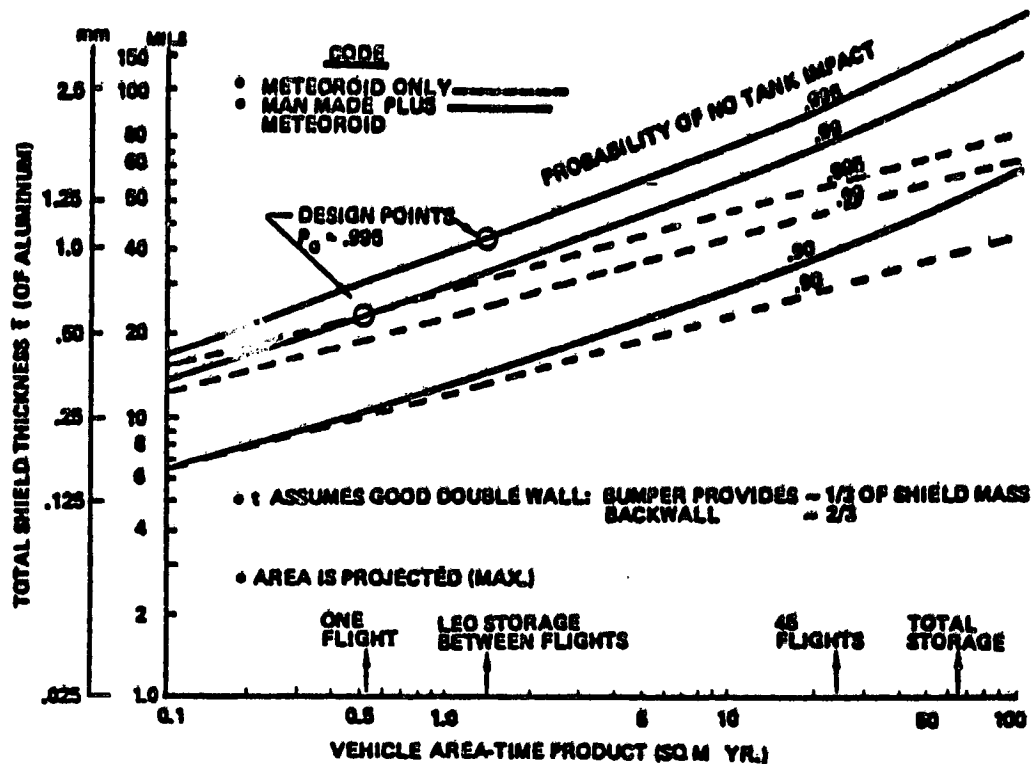


Figure 3.3.6-2 Debris Shield Requirement

a flight between LEO and GEO, meteoroids are the dominating environment. For a single flight and a $P_{(0)} = 0.995$, the resulting \bar{t} is 0.62 mm. For the on-orbit storage period, the dominating environment becomes a combination of manmade and meteoroid debris. Assuming an average of 3 weeks between flights, the required \bar{t} is 1.05 mm.

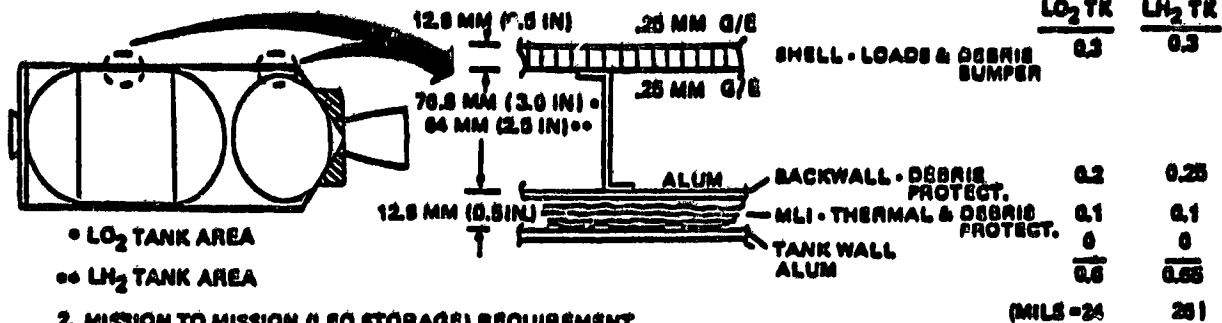
3.3.6.3 Design Approach

The selected design approach for space debris protection is shown in figure 3.3.6-3. The protection incorporated into the vehicle is only that necessary for a single flight since each flight is considered as an independent event. To provide the required protection during on-orbit storage (time between flights), the SB OTV will be placed in a hangar. The \bar{t} provided by the hangar is the difference between the total requirement of 1.05 mm and that provided by the OTV (0.62 mm), or 0.43 mm. Using this approach, the OTV does not have to incur the structural penalty associated with on-orbit storage.

The \bar{t} for the vehicle is provided through a combination of the shell, backwall, and MLI. The backwall was placed between the shell and tank, rather than outside the shell, because of vehicle-diameter constraints. The aluminum equivalent of the shell and MLI

1. MISSION REQUIREMENT

- $\bar{t} = (1.62 \text{ MM}) 24 \text{ MILS FOR } P_{(0)} = .995 \text{ AND ONE LEO-GEO}$
- APPLICATION: GROUND AND SPACE BASED OTV
- DESIGN APPROACH



• LO₂ TANK AREA

•• LH₂ TANK AREA

2. MISSION TO MISSION (LEO STORAGE) REQUIREMENT

- $\bar{t} = (1.68 \text{ MM}) 42 \text{ MILS FOR } P_{(0)} = .995 \text{ AND 18 DAYS AT LEO}$
- APPLICATION: SB OTV ONLY UNLESS GB OTV HAS WAIT TIME GREATER THAN 3 DAYS

3. DESIGN APPROACH

- PROVIDE A HANGAR FOR OTV WHEN IT IS AT SOC.
- HANGAR PROVIDES DIFFERENCE BETWEEN REQUIREMENT AND OTV PROVISION

∴ \bar{t} OF HANGAR = 0.48 MM ALUM EQUIV.

Figure 3.3.6-3 Selected Design Approach

relates to their relative densities. A thicker backwall for the LH₂ tank was necessary since the spacing between walls in that area was not as great $\left[\bar{t} \sim (\text{spacing})^{-1/2} \right]$. Although the resulting design does not have the ideal double wall mass split (1/3-2/3), it is judged to be a reasonable compromise when launch or flight loads as well as debris protection must be considered.

In addition to the selected debris protection design, alternative concepts were also considered such as those indicated in figure 3.3.6-4. These designs relate to concepts which make greater use of MLI rather than "hard" structure for the protection system. For the GB OTV using a structural bumper which also carries the launch loads, approximately 140 layers of MLI would be required to provide the \bar{t} of 0.62 mm. In the case of an SB OTV which only has a minimum of flight loads, consideration can be given to providing all of the protection with MLI, such as indicated in reference 3. To satisfy the FOTV \bar{t} requirement, as many as 300 layers would be a "ballpark" estimate. In summary, use of a very large number of layers of MLI does not appear to provide as straightforward a solution as the hard structure approach indicated with the selected design. The reasons

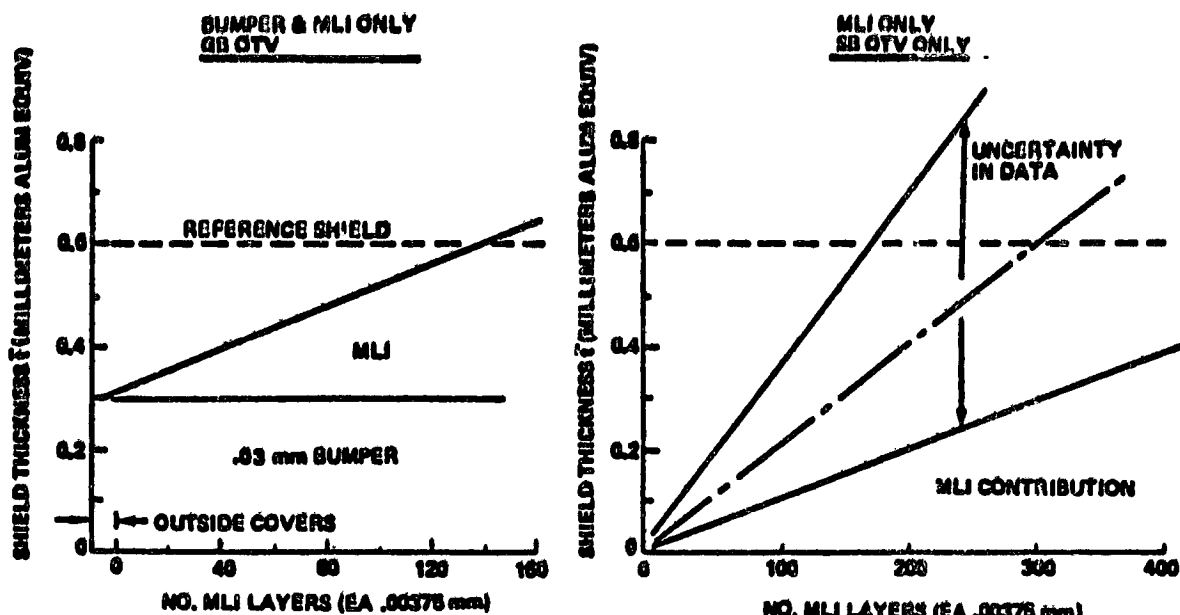


Figure 3.3.6-4 Alternative Debris Shield Designs

are as follows: (1) installation of such a large quantity offers considerable challenges, and (2) in making the literature survey associated with this analysis, very little information was found concerning the real shielding value of a large amount of MLI.

The structural mass impact of providing the indicated debris protection relative to idealistic SB and GB OTV's is shown in figure 3.3.6-5. In the case of the SB OTV, a vehicle that includes provisions for meteoroid protection has nearly a 500 kg penalty over one designed only for flight loads. The majority of the penalty is associated with the provision of the double wall shield. A GB OTV, although having a shell to sustain launch loads and fully loaded tanks, still must be provided with a backwall and results in a 200-kg penalty compared to a concept which does not consider space debris. To put these data into perspective, it must be noted that both of these vehicles are larger (larger propellant loads) and had longer on-orbit times than those which were investigated in the Phase A OTV studies. A ground-based and STS-compatible OTV did not require additional structure beyond that required to carry boost loads.

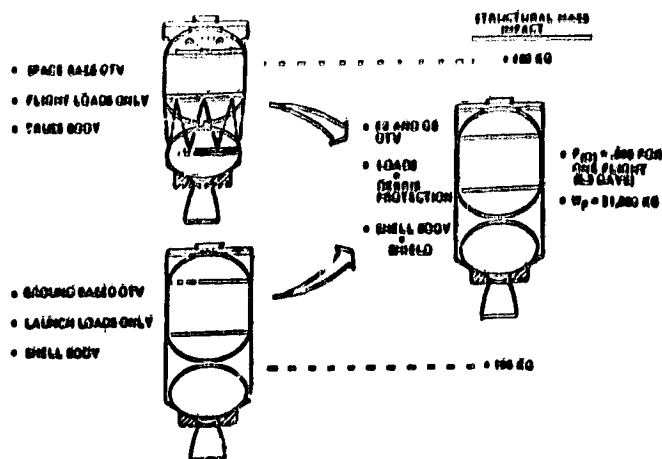


Figure 3.3.8-8 Debris Protection (Meteoroid) Mass Impact

any, test data regarding its debris protection qualities. In the case of MLI only for protection, there is the uncertainty as to whether a multilayer design would actually provide more protection than its mass equivalence. Three-layer (walls) shields have been indicated to improve the protection. Uncertainty also exists in the design criteria for the propellant storage tanks at SOC in terms of debris protection. These tanks have fewer pressure cycles than an OTV; however, their exposure time is longer. Use of a $P_{(0)}$ such as 0.995 would result in a \bar{t} as large as 2.5 mm; however, since each tank is only launched once, the long-term impact may not be too significant.

3.3.6.4 Unresolved Issues

Although a workable design approach has been defined for space debris protection of advanced OTV's, it is recognized that there is considerable work remaining before an optimum design is achieved. Unresolved issues identified at this time are listed below:

1. Value of sandwich or honeycomb shell as bumper
2. Protection characteristics of graphite-epoxy structure
3. Value of three-layer shield
4. True benefit of MLI only for SB OTV
5. Proper viewpoint regarding $P_{(0)}$ and exposure time for propellant storage tanks at SOC

Of foremost importance is the need to establish the shielding characteristics of graphite-epoxy or composite structure as single sheets or in honeycomb or sandwich designs. The importance is indicated by the fact that this material is used extensively throughout the vehicle because it reduces weight; but at this time, there is very little, if

PARAMETRIC ANALYSIS: SOC METEORIOD AND DEBRIS PROTECTION

By: Robert Kowalaki
NASA-Johnson Space Center

It is known that debris and meteoroids in space could be hazardous to space vehicles. This study investigated the meteoroid and man-made space debris environments of an earth-orbital manned SOC (space operations center). Protective shielding thickness and design configurations for providing given levels of no-penetration probability were also calculated.

There are approximately 4,600 tracked objects in LEO (low earth orbit), with sizes greater than 10 cm. Another 15,000 to 20,000 are also estimated to be in LEO, but are too small to be tracked. Approximately 54 percent of the tracked and most of the untracked debris can be attributed to hypergolic rocket stage explosions, or collisions between debris and expended payloads or rocket bodies.

SOC meteoroid/debris protection consists of a radiator/shield thickness (T_s), which is actually an outer skin, separated from the pressure wall, thickness (T_b) by a distance (S). An ideal shield thickness, will, upon impact with a particle, cause both the particle and shield to vaporize, allowing a minimum amount of debris to impact the pressure wall itself. A shield which is too thick will crater on the outside, and release SPALL (small particles of shield) from the inside causing damage to the pressure wall. Inversely, if the shield is too thin, it will afford no protection, and the backup must provide all necessary protection.

Referencing meteoroid/debris flux charts, and the equation $N = FAT$, it is possible to calculate the number of impacts (N) sustained on a surface area (A) during time (T) in a flux field (F), by a particle of mass (M). The probability of no penetration (P_0) is given by $P_0 = 1-N$.

Once a specific particle size (D) and level of no-penetration probability has been decided upon, the optimum shield thickness can be calculated using $T_s = .25 D$. The equation used to relate pressure wall thickness to separation distance is

$$T_b = \frac{.05(\rho_m \cdot \rho_T)^{1/6} M^{1/3} v}{S^{1/2}} \left(\frac{70,000}{\sigma_y} \right)^{1/2}$$

where

M = particle mass, grams

V = impact velocity; 20 km/sec for meteoroids and
10 km/sec for debris

ρ_m = particle density; .5 g/cm³ for meteoroids and
2.7 g/cm³ for debris

ρ_T = pressure wall density; g/cm³

σ_y = pressure wall material yield stress allowable lb/in²

Considering design and weight constraints, it is possible to design for a number of combinations of pressure wall thicknesses and separation distances.

In conclusion, hazards from meteoroids and debris pose a real threat to space vehicles, and protection design must be considered. The SOC employs a double wall concept which is effective in protecting it from particles that may impact its surface.

SOURCES OF INFORMATION

Orbiter Debris Hazard to Space Operations Center
by Siegfried Auer; February 27, 1981

Space Vehicle Meteoroid Shielding Design
by Burton G. Cour-Palais

Meteoroid/Orbital Debris Hazard
by Donald J. Kessler; April 21, 1981

Space Operations Center; Boeing System Analysis, Volume III

SHIELD THICKNESS (CM) MILLS	DIA. LARGEST PART DESTROYED BY SHIELD (CM)	MASS OF PARTICLE (GM)	FLUX PER METRE ² PER YEAR	AVERAGE NUMBER OF IMPACTS	PROBABILITY OF NO PENETRATION ^{P₀}
.0204 10	.102	2.77×10^{-4}	4.0×10^{-2}	2.4	.001
.091 20	.204	2.22×10^{-3}	3.0×10^{-3}	1.0×10^{-1}	.030
.076 30	.304	7.39×10^{-3}	6.4×10^{-4}	3.24×10^{-2}	.908
.102 40	.400	1.77×10^{-2}	9.0×10^{-5}	9.00×10^{-3}	.994
.127 50	.500	3.43×10^{-2}	7.0×10^{-5}	4.2×10^{-3}	.996
.192 60	.600	6.00×10^{-2}	3.0×10^{-5}	2.16×10^{-3}	.999
.176 70	.712	9.99×10^{-2}	1.0×10^{-5}	6.00×10^{-4}	.9994
.203 80	.812	1.40×10^{-1}	0.0×10^{-5}	6.20×10^{-4}	.9996
.229 90	.916	2.01×10^{-1}	7.2×10^{-6}	4.32×10^{-4}	.9996
.254 100	1.016	2.75×10^{-1}	6.6×10^{-6}	3.36×10^{-4}	.9997

METEOROID

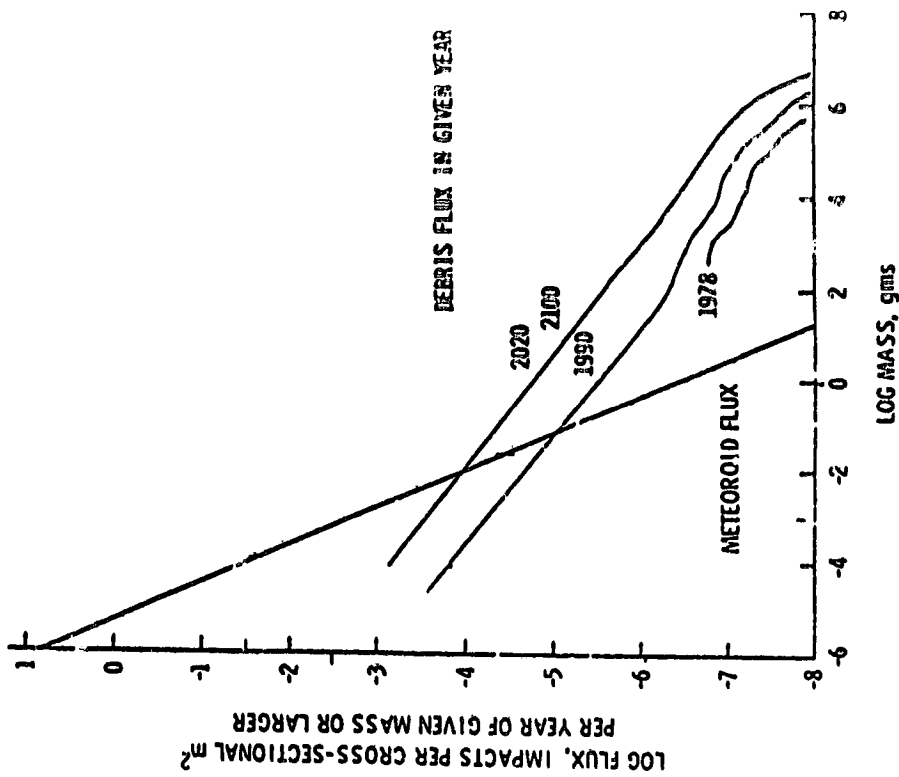
SHIELD THICKNESS (CM) (MILLS)	DIA. LARGEST PART DESTROYED BY SHIELD (CM)	MASS OF PARTICLE (GM)	FLUX IMPACTS PER M ² (1) PER YEAR UP GIVEN MASS OR LARGER		AVERAGE NUMBER OF IMPACTS		P ₀ PROBABILITY OF NO PENETRATION	
			(275 KM)	(400 KM)	275 KM	400 KM	275 KM	400 KM
.0254 10	.102	1.556×10^{-3}	7.5×10^{-7}	7.6×10^{-5}	4.5×10^{-5}	4.56×10^{-3}	.99995	.9955
.051 20	.204	1.245×10^{-2}	6.5×10^{-7}	4.2×10^{-5}	3.9×10^{-5}	2.52×10^{-3}	.99996	.9975
.076 30	.304	4.119×10^{-2}	6.0×10^{-7}	2.0×10^{-5}	3.6×10^{-5}	1.68×10^{-3}	.99996	.9993
.102 40	.400	9.95×10^{-2}	5.5×10^{-7}	9.2×10^{-6}	3.3×10^{-5}	5.52×10^{-4}	.99997	.9994
.127 50	.500	.192	5.1×10^{-7}	6.6×10^{-6}	3.06×10^{-5}	5.16×10^{-4}	.99997	.9995
.152 60	.600	.330	4.8×10^{-7}	7.8×10^{-6}	2.88×10^{-5}	4.68×10^{-4}	.99997	.9995
.176 70	.712	.529	4.7×10^{-7}	7.0×10^{-6}	2.82×10^{-5}	4.2×10^{-4}	.99997	.9996
.203 80	.812	.785	4.6×10^{-7}	6.0×10^{-6}	2.76×10^{-5}	3.6×10^{-4}	.99997	.9996
.229 90	.916	1.127	4.4×10^{-7}	4.8×10^{-6}	2.64×10^{-5}	2.8×10^{-4}	.99997	.9997
.254 100	1.016	1.538	4.3×10^{-7}	4.2×10^{-6}	2.50×10^{-5}	2.52×10^{-4}	.99997	.9997

(1) USING CROSS-SECTION AREA

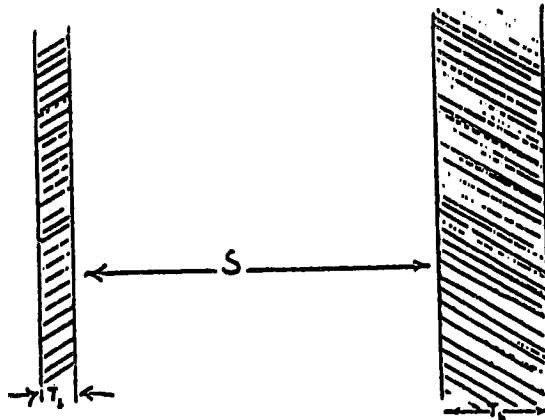
DEBRIS

ASSUMPTIONS AND ANALYSIS

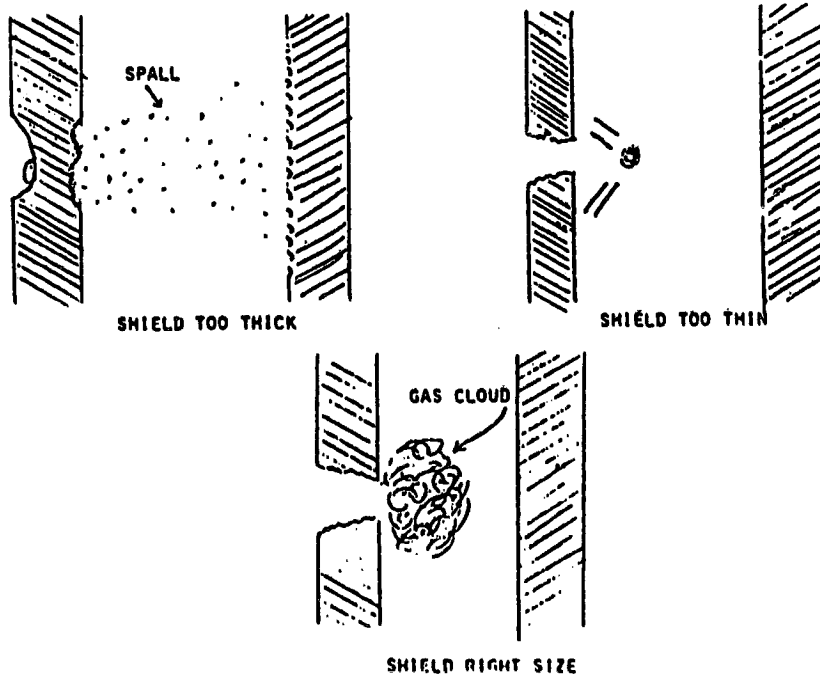
- .999 PROBABILITY OF NO PENETRATION
- ALUMINUM SHIELD AND BACK-UP
- $\frac{T_s}{D} = .25$
- $T_B = \frac{.05 (P_M \cdot P_T)^{1/2}}{S^{1/2}} \cdot \frac{1}{V} \left(\frac{70,000}{\sigma_y} \right)^{1/2}$
- N = FAT
- $P_0 = 1-N$
- D = PARTICLE DIAMETER: CM
- M = PARTICLE MASS: G
- P_0 = PROBABILITY OF NO PENETRATION
- S = SPACING: CM
- T_B = BACK-UP THICKNESS: CM
- T_s = SHIELD THICKNESS: CM
- V = IMPACT VELOCITY: KM/SEC
- P_M = PARTICLE DENSITY: G/CM³
- P_T = BACK-UP MATERIAL DENSITY: G/CM³
- σ_y = BACK-UP MATERIAL YIELD STRESS ALLOWABLE: LB/IN²



AVERAGE FLUX AT 400 KM
 ASSUMES THE NET SATELLITE INPUT RATE CHARGES FROM 510 TO
 ZERO IN THE YEAR 2020



SOC PROTECTION DESIGN



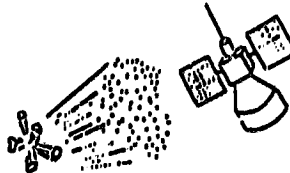
A SINGLE SPACECRAFT CAN BE RESPONSIBLE FOR A MULTITUDE OF HAZARDOUS OBJECTS IN SPACE

HYPERGOLIC ROCKET STAGE EXPLOSIONS

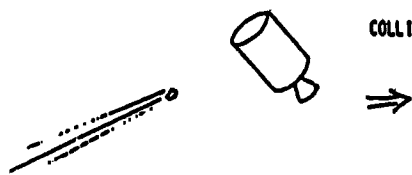


0 42% OF TRACKED POPULATION (2000 OBJECTS)
 0 ESTIMATE 10,000 TO 15,000 OBJECTS LARGER THAN 4cm, MOST NOT TRACKED

INTENTIONAL EXPLOSION OR PARTICLE RELEASE



0 12% OF TRACKED POPULATION (USSR TESTS)
 0 1000 LB PAYLOAD COULD CONTAIN 100 MILLION 1mm PARTICLES

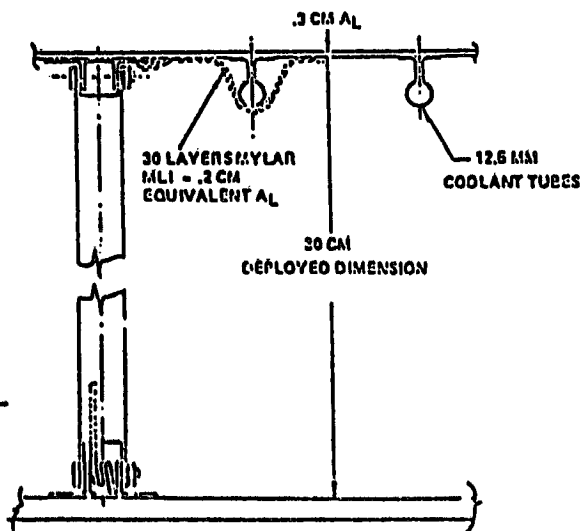
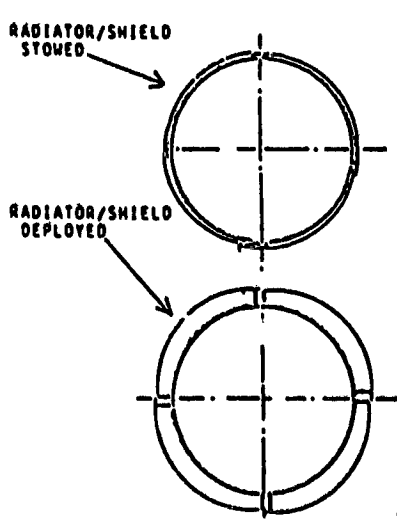


COLLISIONS



AVERAGE COLLISION IS BETWEEN OLD PAYLOAD OR ROCKET BODY AND 5 cm (10lb) EXPLOSION FRAGMENT.

COLLISION PRODUCES 4 MILLION PARTICLES LARGER THAN 1mm, AND 10 THOUSAND PARTICLES LARGER THAN 1cm.



CABIN WALL CONCEPT

OUTLINE

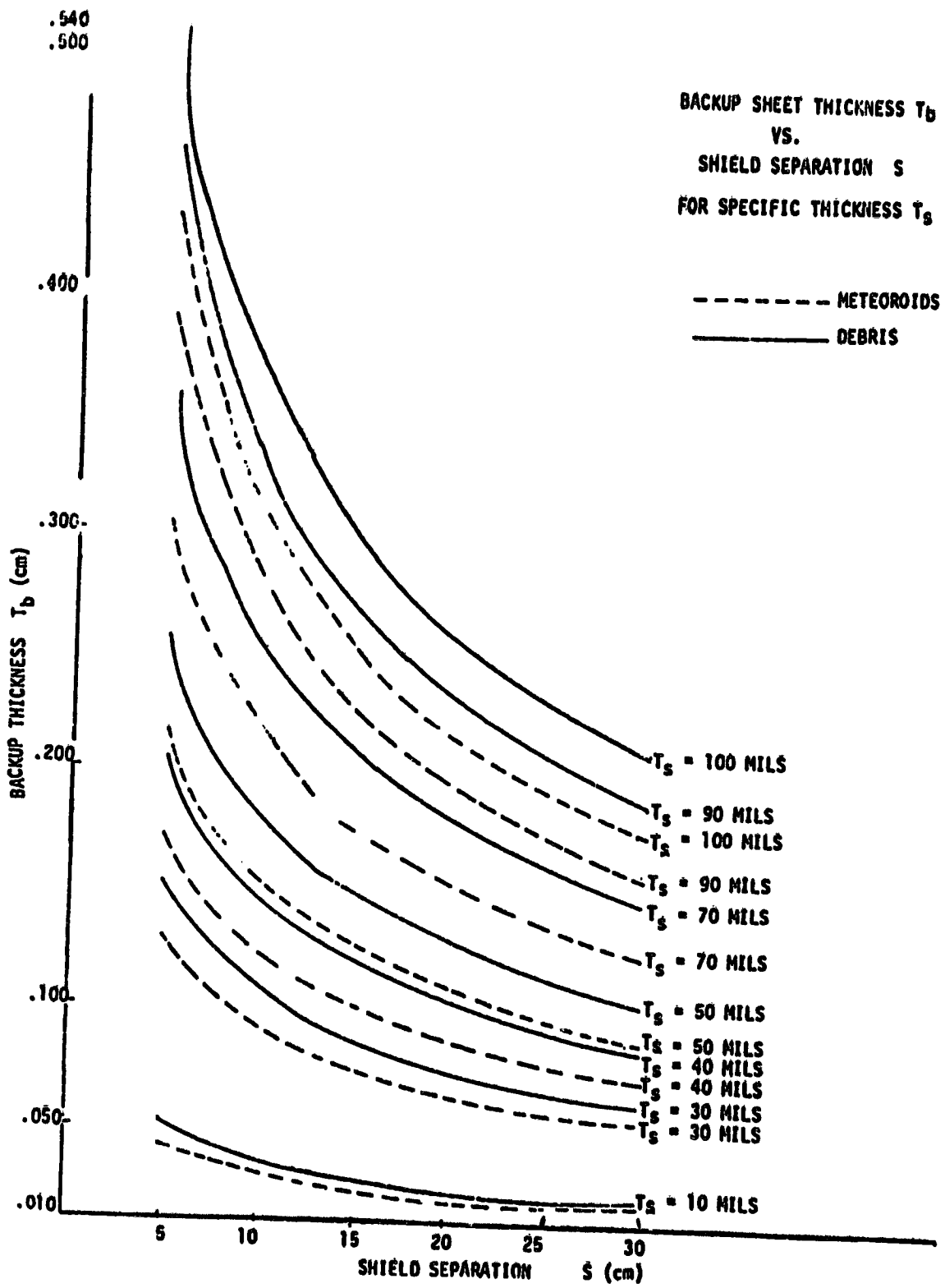
- Introduction
- Meteoroid/Debris Environment
- SOC Protection Design
- Assumptions and Analysis
- Study Results
- Conclusions

INTRODUCTION

THE INVESTIGATION OF METEOROID AND MAN-MADE SPACE DEBRIS ENVIRONMENTS OF AN EARTH-ORBITAL, MANNED SPACE OPERATIONS CENTER AND CALCULATION OF PROTECTIVE SHIELDING THICKNESS AND DESIGN CONFIGURATION FOR PROVIDING GIVEN LEVELS OF NO-PENETRATION PROBABILITY.

METEOROID/DEBRIS ENVIRONMENT:

- 4,600 TRACKED
- $\approx 10,000 - 15,000$ UNTRACKED
- PROJECTED 10^6 BY 1990 VIA COLLISIONS
- METEOROID VELOCITY ≈ 20 KM/SEC
DENSITY $\approx .5$ G/CM³
- DEBRIS VELOCITY ≈ 10 KM/SEC
DENSITY ≈ 2.7 G/CM³



Space Heat Rejection Radiators: Meteoroid/Debris Consideration
by J. Gary Rankin, NASA-Johnson Space Center

INTRODUCTION

This paper addresses (in a qualitative fashion) the effect of the meteoroid/space debris environment on the design and evolution of spacecraft waste heat rejection radiator systems. This discussion applies to "active" radiator systems; i.e. systems in which waste heat is collected from the various heat sources within a spacecraft and delivered to the radiator system by a heat transport loop. The heat is then distributed over the radiator area and thus rejected to space.

PRESENT SYSTEMS

All active radiator systems on manned flight vehicles to date have used pumped fluid radiators for heat rejection. In other words, the heat transport fluid is distributed via a manifold into individual small tubes attached to the radiating surface, as illustrated in Figure 1. The waste heat is transferred to the walls of the individual tubes by convection, through the tube walls and along the radiating surface by conduction, and finally to space by radiation. With this type of design, the puncture of any individual radiator fluid tube would result in the loss of all fluid from the entire heat transport loop. For this and other reliability reasons, multiple transport loops are used to provide either redundant or at least fractional capability if one loop is lost.

No meteoroid/debris punctures of active radiator tubes have been experienced. However, it should be noted that fluid tube wall thicknesses have been driven by structural considerations other than the meteoroid penetration criteria. This has been due to factors such as relatively short life requirements and small exposed fluid areas. Therefore launch vibration and acoustic environments, or other general pressure vessel safety criteria have sized the tube thickness over and above what would be required for meteoroid protection based on current models.

The Shuttle Orbiter radiator panel construction (illustrated in Figure 2) represents the largest (1300 ft²) and most recent example of a pumped fluid radiator design. These panels consist of small aluminum tubes beneath thin aluminum face sheets bonded to a lightweight aluminum honeycomb core material. Although the honeycomb panel design resulted from the structural requirements imposed by the launch environment, it should be noted that it does provide some inherent meteoroid protection to the fluid flow tubes. The honeycomb and the facesheet on the side opposite a tube provide a "bumpering" effect, while immediately above each tube there is an "armoring" effect of the adjacent face sheet.

FUTURE SYSTEMS

Future systems, however, must meet requirements that are quite a bit different from those for current systems. The most important new requirement will be a long lifetime, with space platforms or

Space Stations having a design life of ten years and probably actual life of much longer than that. The next major new requirement will be one of size. We are expecting electrical power levels on the order of several hundred kilowatts, so we would probably have about ten times the radiator area of the Orbiter radiator system. This size, however, is for a fully mature Space Station configuration. For a variety of technical and programmatic reasons, any future Space Station will evolve through a phased approach to its final size. This establishes another unique requirement for future radiator systems: the ability to be "grown" in orbit over a period of months or years from a relatively modest size to a very large size. With these different requirements in mind, our advanced program studies have shown benefits of radiators which incorporate heat pipes rather than individual fluid tubes to distribute heat to the radiating surface itself. Heat will still be collected from various locations around the vehicle with a pumped fluid loop (or some even more advanced designs utilizing a two-phase system) but this central transport loop would not flow through tubes on the radiating area that is exposed to the meteoroid or debris environment.

The heat pipe, illustrated in Figure 3, is a self-contained system that transfers heat by boiling a fluid at one point and condensing it at another; the liquid is transferred back to the boiling area by capillary action through a wick structure. It is the use of the capillary action that is the unique characteristic of the heat pipe. Provided that the pressure gradient in the vapor is kept small, the axial temperature gradient along the heat pipe can be small, resulting in a device of a very high thermal conductivity. The effective thermal conductivity of the device can be more than 1,000 times that of a solid copper rod of similar dimensions.

Most heat pipes proposed for use in spacecraft radiators are made of aluminum, with ammonia as the heat pipe working fluid. In this application, heat would be transferred from the heat transport loop flowing through a central manifold to one end of each heat pipe (the evaporator). Each separate, individually charged and sealed heat pipe would then transport its portion of the heat to its condenser section, which is cooled by the attached radiating fin surface. The internal wicking structure of the pipe would return the condensed liquid to the evaporator section, and the cycle would be repeated as long as the heat load is maintained.

Figure 4 illustrates some of the benefits of the heat pipe radiator over a conventional pumped fluid type. Controls are simpler and pumping requirements are less due to the simpler fluid flow arrangement resulting from the elimination of the individual radiator flow tubes. The biggest single advantage, however, is that a heat pipe system reduces the radiator's sensitivity to the meteoroid/debris environment. As discussed earlier, the puncture of any single tube would cause the loss of all radiator area associated with the same fluid flow system. With the use of heat pipes, the puncture of any single exposed heat pipe would only

cause the loss of that pipe's working fluid charge. With a continuous radiator fin, the reduction in radiator performance would be less than $1/N$, (where N =total number of heat pipes) because the heat pipes adjacent to the damaged one would continue to provide heat to the damaged pipe's fin area. With a longer effective fin length, that area would simply operate at a lower fin efficiency. This response to meteoroid damage has been described as providing "graceful degradation" of radiator performance over a long life.

Heat pipes, with their working fluid charge and wicking material, are heavier than simple tubes. Also, the temperature difference between the bulk transport loop fluid and the radiator fin is greater with a heat pipe radiator than with a pumped fluid radiator. Thus, for a given fluid temperature, a heat pipe radiator will operate at a lower radiating temperature than a pumped fluid radiator and will therefore require more radiator area for a given heat load. Both these factors tend to increase the weight of heat pipe radiators over pumped fluid radiators if meteoroid damage is not considered. Therefore, for short lifetimes or small radiator areas (and thus a minimum exposure to the threat of puncture) the meteoroid design requirement will probably be minimal (as in the previously discussed case of the Orbiter radiator design) and a pumped fluid radiator will be the desired type. However, as radiator size or design lifetimes increase, the threat of puncture also increases, and measures must be taken to protect a pumped fluid system. All these measures, whether armoring, bumping, or providing redundant systems, will cause an increase in radiator system weight. At some point, the initial weight penalty of a heat pipe design is overcome, and a heat pipe system becomes the preferred type of radiator. Figure 5 is an example of the results of an analysis to compare applicable ranges of the two types of systems. This analysis was done considering only the current NASA meteoroid model. In general, if you have a stringent requirement to avoid a puncture, (therefore, a low probability of penetration), then that drives you into the region where you want heat pipes. If you can accept a large probability of penetration, then of course the pumped fluid radiators win out because they are lighter to start with. But as your mission length increases the break point moves down with respect to the vehicle heat load (and therefore, radiator size). For the case where we have a heat rejection load of several hundred kilowatts and a one percent probability of penetration in a five to ten year mission, this analysis indicates that heat pipes are preferred over the pumped fluid system.

Because of the potential benefits of heat pipe radiators discussed above, development of heat pipe radiator technology has been underway at JSC for several years. The most recent concept under development is called a Space Constructable Radiator (SCR) System. The concept, illustrated in Figure 6, utilizes as its primary building block a single "1kw element consisting of a large, high capacity heat pipe with its attached radiating fin. With dimensions of 1-2 feet in width and 50 feet in length, these

single elements can be combined to form the various combinations illustrated in the figure. Full scale prototype elements of the SCR system are scheduled to be tested in a thermal vacuum environment by the end of 1983.

EFFECT OF ORBITAL DEBRIS ON RADIATOR DESIGN

As mentioned in the introduction, the effect of the debris environment on radiator design can only be addressed qualitatively at this time. No analyses have been done to assess the debris impact, so reference must be made to results such as presented in Figure 5 which reflect only the current meteoroid model. Currently, efforts are underway to more accurately define the debris model. If the debris model is found to override the meteoroid model, it should simply shift the tradeoff points where the spacecraft designer would choose heat pipe radiators rather than pumped fluid radiators. In other words, heat pipes would become desirable at even shorter lifetimes or lower heat loads than reflected in the figure.

However, even if the debris model is deemed less severe than the meteoroid model, the meteoroid model alone has provided enough justification for proposing heat pipe radiators as the "baseline" design concept for future large, long-life spacecraft heat rejection systems.

SATELLITE SERVICES AND ORBITAL RETRIEVAL

by

Rudolph J. Adornato**Grumman Aerospace Corporation, Bethpage, N.Y.**

Over the past two years, Grumman Aerospace has been working with NASA/JSC in the development of Satellite Services. Satellite Services is an extension of the Space Transportation System (STS) which will provide on-orbit services and operational capabilities that exploit the uniqueness of the STS (vs. expendable launch vehicles), and the advantages of human presence on-orbit. Within the capabilities of the Space Shuttle Orbiter, a broad range of services can be made available to the satellite user community as summarized in Fig. 1 i.e, payload deployment, close proximity retrieval, and a number of other mission related functions. This presentation will focus on close proximity retrieval and retrieval of payloads in higher energy LEO orbits.

- PAYLOAD DEPLOYMENT
- CLOSE PROXIMITY RETRIEVAL
- ON-ORBIT SERVICING
- BACKUP/CONTINGENCY
- DELIVERY/RETRIEVAL OF HI ENERGY PAYLOADS
(LEO/PROPULSION CLASS)
- EARTH RETURN
- OPTIONAL SERVICES

Fig. 1 Satellite Service Operations

Figure 2 identifies the various satellite classes with which the Orbiter will be required to interface. They include:

- Direct Delivery/Serviceing - those satellites capable of direct delivery to orbit and/or serviceing by the Orbiter
- LEO/Propulsion - those satellites whose LEO operational altitude is above the Orbiter's nominal delivery altitude
- GEO Satellites - those satellites destined for GEO that are deployed in LEO by the Orbiter
- Planetary/Others - Spacecraft destined for planetary missions that are deployed by the Orbiter. Also considered in this class are undefinable satellites/payloads that might be carried as reflight opportunities in the STS manifest
- Sorties/DoD - Sortie missions such as e.g., Spacelab flights and DoD Orbiter flights.

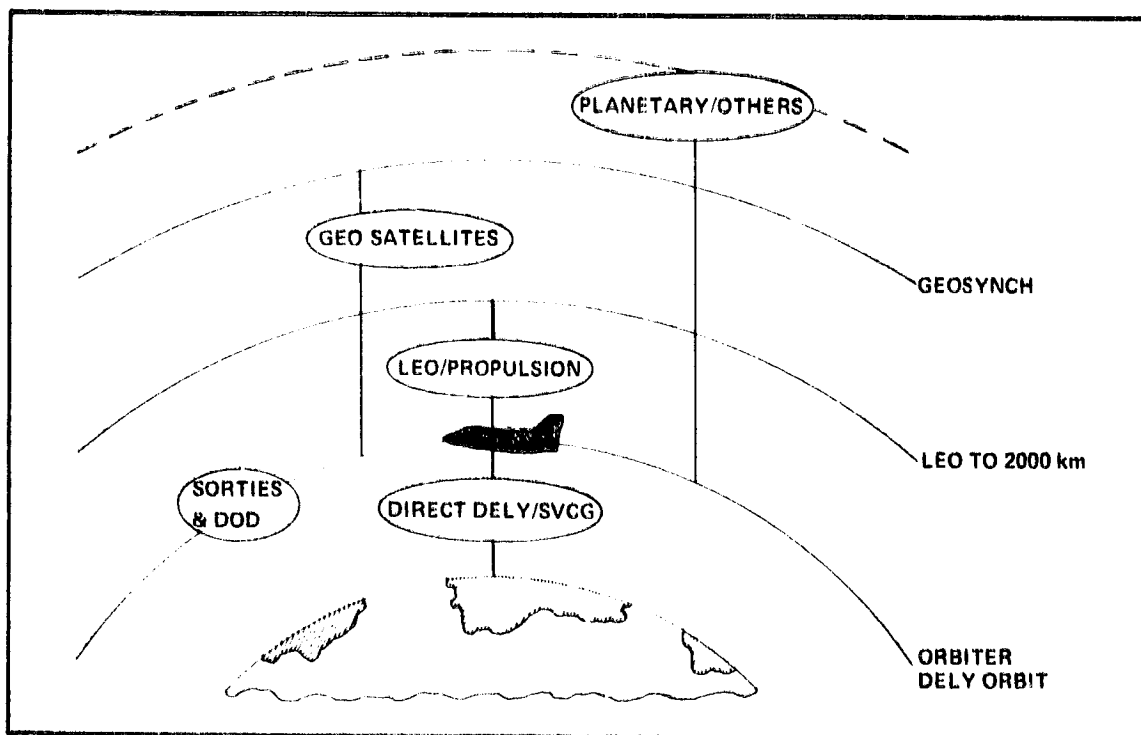


Fig. 2 Satellite Classes

The satellite classes considered for retrieval with the Shuttle Orbiter include Direct Delivery/Serviceing and LEO/Propulsion.

Figure 3 summarizes the satellite retrieval opportunities which may become available in the decade commencing in 1983. These are grouped as a function of the satellite mass because it is an important parameter which relates to retrieval techniques, and the number of opportunities within that grouping are shown. Of importance is the year in which the first opportunity may exist; e.g.; within the satellite mass grouping of up to 1000 kg, there are 12 retrieval opportunities projected, the first occurring in 1986.

SATELLITES DIRECTLY REACHABLE BY ORBITER		
<u>SATELLITE MASS (KG)</u>	<u>NUMBER OF RETRIEVAL EVENTS</u>	<u>EARLIEST TIME FRAME</u>
UP TO 1000 KG	12	1986
1000 - 2500 KG	9	1983
2500 - 5000 KG	18	1985
5000 - 11,000 KG	15	1987
> 11,000 KG	19	1987
SATELLITES WITH LEO PROPULSION		
UP TO 1000 KG	8	1986
1000 - 2500 KG	38	1986
2500 - 5000 KG	33	1984
*APPROVED OR PLANNED SATELLITE PROGRAMS ONLY		

Fig. 3 Satellite Retrieval Opportunity Model (1983-1993)

Also noted, for the satellite mass grouping of 1000 to 2500 kg, the first retrieval opportunity may exist as early as 1983. That date was based on earlier information which first expected Solar Max Mission retrieval and repair in 1983, but which has now been rescheduled for STS Flight 13 in April 1984. All told, opportunities may exist for retrieving more than 150 active satellites through the year 1993, for purposes of on-orbit refurbishment or for their return to the ground for subsequent launchings.

All satellites to be retrieved within these indicated opportunities will be for active satellites launched by the Shuttle and nominally operating. Figure 4 summarizes, however, the types of satellite retrieval conditions which may

be called upon when considering both planned and contingency retrieval situations. Stabilized satellites include both actively and passively stabilized satellites such as gravity gradient stabilized or satellites whose control system has been inhibited so as not to interfere with orbiter retrieval operations. Removal of partially disabled satellites which may be rotating at low rates and retrieval of highly unstabilized inactive satellites and debris may also be required.

- RETRIEVAL OF ACTIVELY STABILIZED SATELLITES
- RETRIEVAL OF PASSIVELY STABILIZED SATELLITES
 - GRAVITY GRADIENT STABILIZED
 - PARTIALLY DISABLED (ROTATING AT LOW RATES)
- RETRIEVAL OF INACTIVE SATELLITES/DEBRIS

Fig. 4 Types of Satellite Retrieval

Figure 5 relates the retrieval modes which are applicable to the Orbiter Direct and LEO Propulsion Class satellites. Satellites directly reachable by the Orbiter can be retrieved by the Orbiter's Remote Manipulator System (RMS) or with the assistance of Proximity Operations Modules (POM). Satellites in the LEO propulsion class are captured and brought back to the Orbiter with a Versatile Service Stage (VSS) also referred to as the Teleoperator Maneuvering System. These retrieval modes will be further explained in subsequent discussions.

- ORBITER DIRECT (SATELLITES REACHABLE BY ORBITER)
 - RETRIEVAL WITH RMS
 - RETRIEVAL WITH ASSISTANCE OF PROXIMITY OPERATIONS MODULE (POM)
- LEO PROPULSION CLASS (SATELLITES NOT DIRECTLY REACHABLE BY ORBITER)
 - RETRIEVAL WITH VERSATILE SERVICE STAGE

Fig. 5 Retrieval Modes

Figure 6 shows a rendering of the Orbiter equipped with an RMS for a baseline retrieval operation. In this sequence, the Orbiter, after completing rendezvous with the satellite to a range of up to a few thousand ft, would then approach the satellite to within the RMS reach of about 35 ft. Figure 6 illustrates the grapple fitting mounted to the satellite and the snare end effector which is attached to the end of the RMS and used to capture the satellite's grapple fitting. This is presently considered to be the nominal retrieval mode for stabilized satellites.

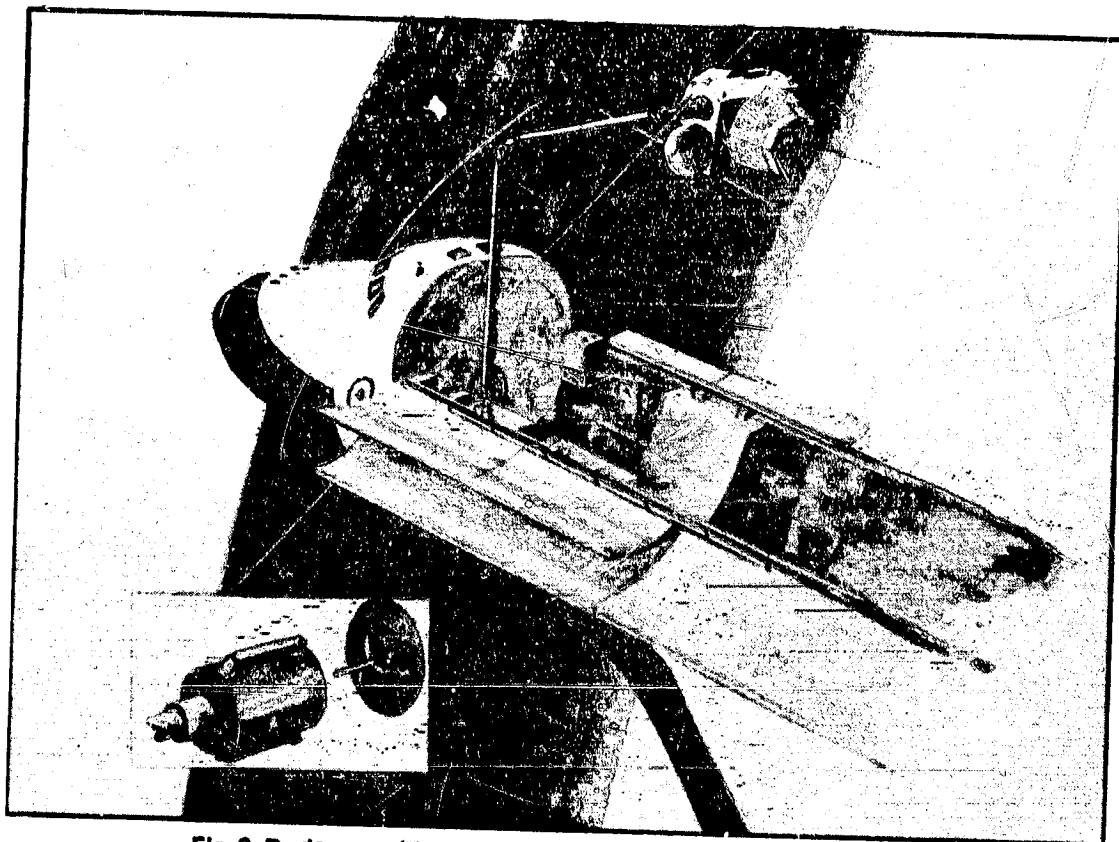


Fig. 6 Deployment/Retrieval with the Remote Manipulator Systems

Figure 7 summarizes the highly stringent requirements and capabilities for RMS retrieval of payloads. Actively stabilized satellites, for example, require an attitude deadband limit to be within ± 0.1 deg/sec about all axes. These limits reflect a grapple point motion of less than ± 3 inches. For the passively stabilized satellites, such as gravity gradient stabilized satellites, the grapple point motion must be contained within ± 15 in. and have attitude rates about all axes to be less than 0.5 in./sec. To employ the RMS retrieval mode the satellite is required to be stabilized to rather tight tolerances throughout the Orbiter/RMS retrieval operations.

- SPIN-STABILIZED PAYLOADS MUST BE DE-SPUN
- PASSIVELY-STABILIZED PAYLOADS MUST HAVE GRAPPLE POINT MOTION LESS THAN ± 16 INCHES AND LESS THAN 0.05 INCHES/SECOND
- ACTIVELY-STABILIZED PAYLOADS MUST HAVE
 - ATTITUDE DEAD-BAND LESS THAN ± 1 DEGREE ABOUT ALL AXES
 - ANGULAR RATE LIMIT LESS THAN 0.1 DEG/SEC ABOUT ALL AXES
 - MAXIMUM GRAPPLE POINT MOTION LESS THAN ± 3 INCHES
- MAXIMUM ALLOWABLE RELATIVE VELOCITY OF PAYLOAD AND ORBITER AT CAPTURE LESS THAN 0.1 FT/SEC
- PAYLOAD SHOULD HAVE SUFFICIENT CONTROL AUTHORITY TO DAMP OUT AND RETURN TO LOCAL VERTICAL/HORIZONTAL (LVLH) ATTITUDE WITHIN 2 MINUTES AFTER DIRECT RCS PLUME IMPINGEMENT AT 35 FEET FROM THRUSTER

Fig. 7 RMS Capabilities for Payload Retrieval

Figure 8 relates other factors which must be considered for Orbiter RMS retrieval, and which in some applications may make it impractical; e.g., the exhaust plume impingement resulting from the Orbiter RCS Z-axis braking maneuvers may cause both attitude and translation disturbances to the satellite which could preclude retrieval using the RMS. Low Z-axis braking maneuvers reduce impingement effects considerably but utilize a significant increase in RCS propellant.

- POTENTIAL ATTITUDE/TRANSLATIONAL DISTURBANCES DUE TO EXHAUST PLUME IMPINGEMENT EFFECTS
- LARGE ORBITER RCS PROPELLANT CONSUMPTION DURING CLOSE PROXIMITY OPERATIONS
- POTENTIAL CONTAMINATION TO SATELLITE/EXPERIMENTS FROM ORBITER RCS EXHAUST PARTICLE DEPOSITION

Fig. 8 RMS Retrieval — Other Considerations

Still another factor to be contended with is the potential contamination to the satellite and/or experiments which result from RCS exhaust particle deposition. This is of particular concern to large optical satellite systems operating in the infra-red and visible light spectrums which are highly sensitive to molecular and particulate deposition. These satellites would then require retrieval using contaminate sensitive retrieval systems.

Illustrated in Fig. 9 is a concept for a contaminate sensitive retrieval system known as the Proximity Operations Vehicle (POV). It consists of a small free flyer vehicle dispatched from the Orbiter payload bay and flown to the satellite which is station-keeping at a range up to 3000 ft. The free flyer is flown using remote commands issued by a crewman in the Orbiter aft flight deck. POV is flown to capture the satellite by its grapple fitting and tow it to within the Orbiter RMS reach distance. It then releases the satellite in a highly stabilized attitude mode for capture with the RMS. A key feature of the POV is its non-contaminating cold gas propulsion system which is used to perform both attitude and translation maneuvers.

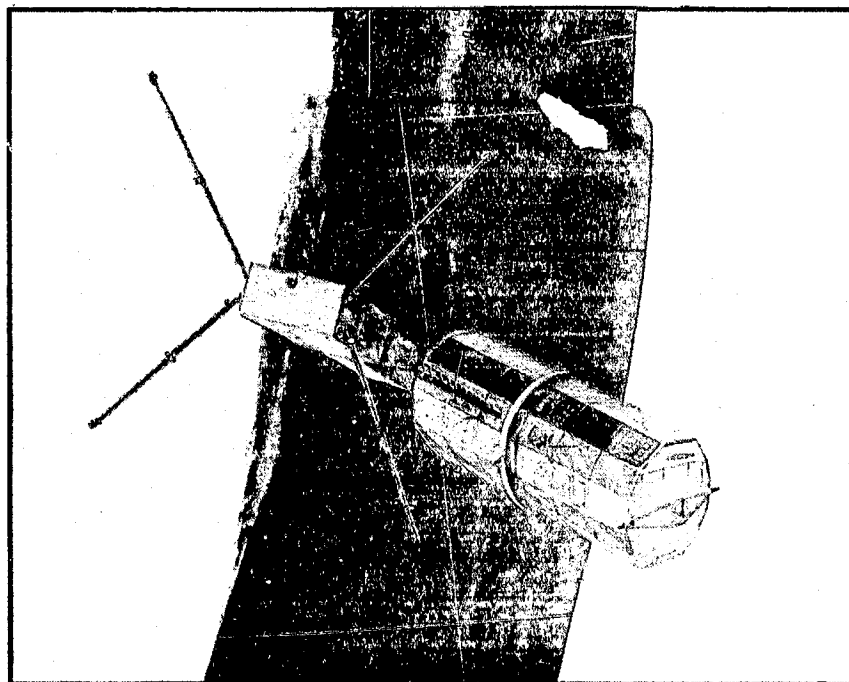


Fig. 9 MTV/Proximity Operations Module -- Satellite Capture

Figure 10 illustrates the flight control concept selected and baselined for maneuvering and controlling the POV to and from a satellite station-keeping within close proximity of the Orbiter. The concept involves a crewman stationed in the Orbiter aft flight deck equipped with hand controllers and displays flying the POM to a satellite by remote attitude and translation commands. The procedure requires the crewman to maintain the POM in inertial attitude hold during approach to the satellite and controlling inertial LOS rates with Y- and Z-axis translational thrust. This flight technique was de-

veloped during the Apollo program for manual terminal rendezvous and docking of LM to the CSM. Man-in-the-loop simulations have shown that near minimum delta-V penalties are incurred when controlling inertial LOS rates to low rates (± 0.2 mrad/sec) during approach. An additional factor which impacts the selection of guidance system components needed to implement this technique is the non-stringent inertial sensor requirements. The impact of gyro drift occurring within approximately 15 minutes of flight time have little effect on the inertial attitude reference accuracy.

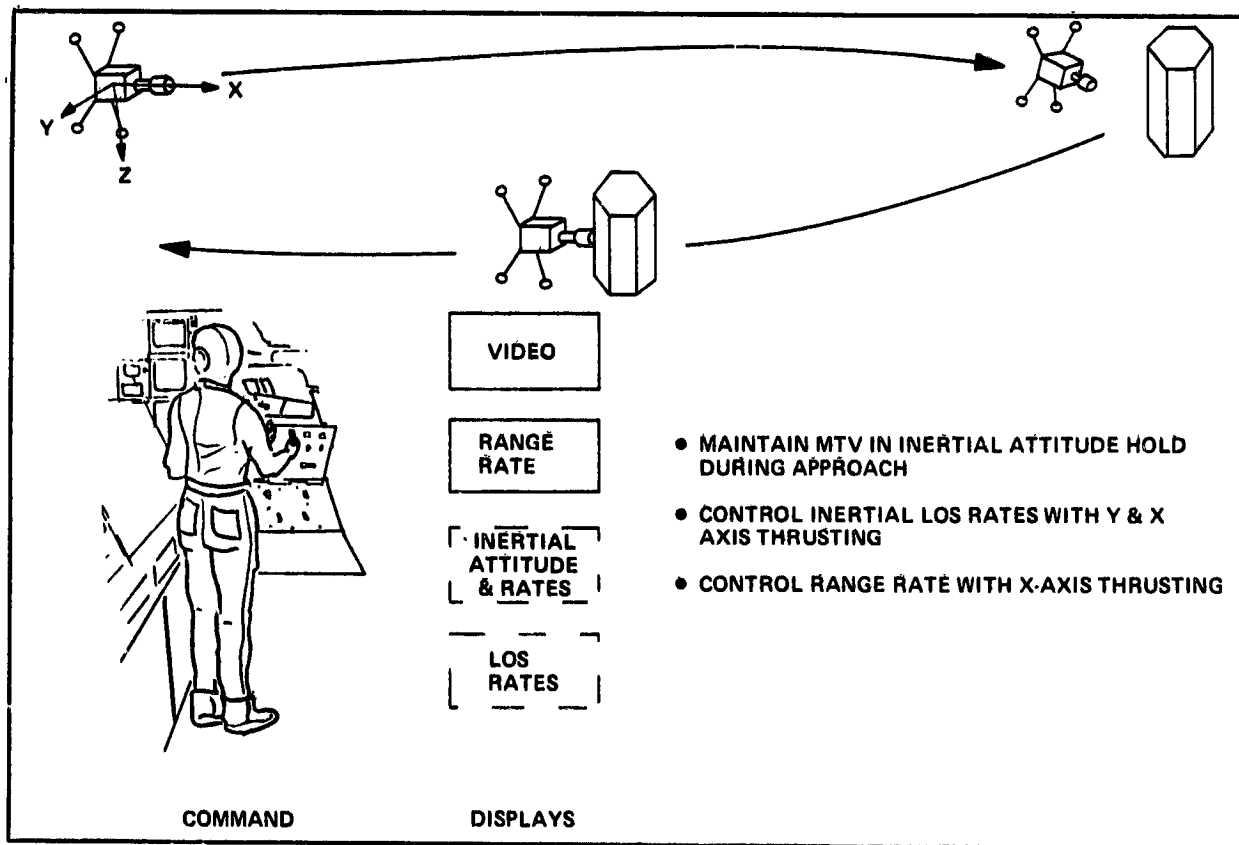


Fig. 10 Flight Control Concept

As can be noted from the illustration, the POV configuration is designed in modular sections, comprised of an aft section containing the propulsion system, propellant and tankage, and a forward section or core module containing the electronic components and all other operating systems.

Figure 11 illustrates the overall design and general equipment arrangement developed for the core module. Major subsystems were organized into

component groupings for ease in maintenance and refurbishment. For example, one side wall contained the power supply and distribution system with an area provided for a second 40 amp-hr battery. The top panel was used to mount the communications system components. The second side wall housed the G&C components. The bottom panel incorporated the passive berthing docking mechanisms while the front face housed the TV system. Additional room was provided for the extendable mast and stow cannister. These components are to be interfaced with the TV system in accordance with prescribed dimensions.

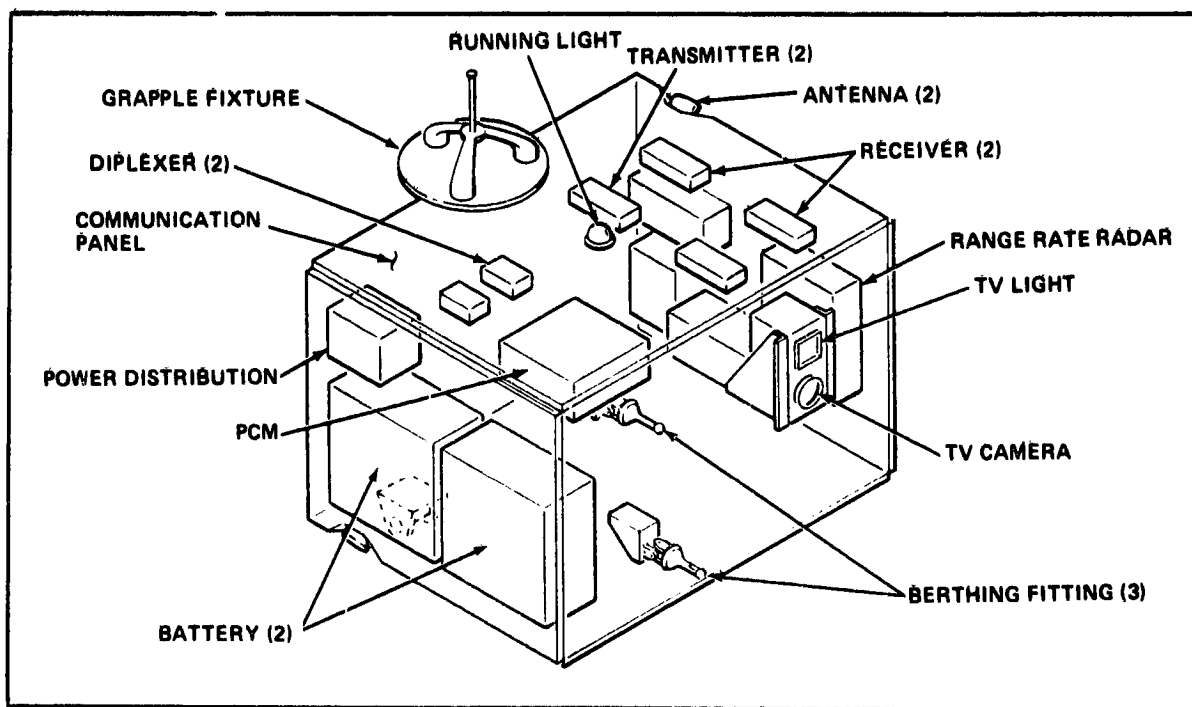


Fig. 11 MTV-Core Module

As illustrated in Fig. 12 the propulsion kit which contains two 28 in. diameter spherical tanks is capable of providing about 175 lb of useable GN_2 propellant. Also contained within the module is an aft facing TV camera used to navigate the POV to the Orbiter when towing the satellite. Four 101 in. deployable thruster booms, each carrying a thruster quad mounted to the end, provide the attitude and translation control authority required for satellite towing. The boom length was sized to minimize thrust loss due to impingement on satellites as large as 15 ft in diameter.

Also incorporated is the snare and effector, which is attached to an extendible boom and used for satellite grappling. Overall size of this configuration measures 76 in. W x 29 in. H x 66 in. L and is estimated at 1110 lb. This configuration is used to retrieve satellites up to 5000 kg at a range of up to 1 km. It could also be used for larger payload sortie missions providing a delta-V of 100 ft/sec for 1000 kg experiment packages.

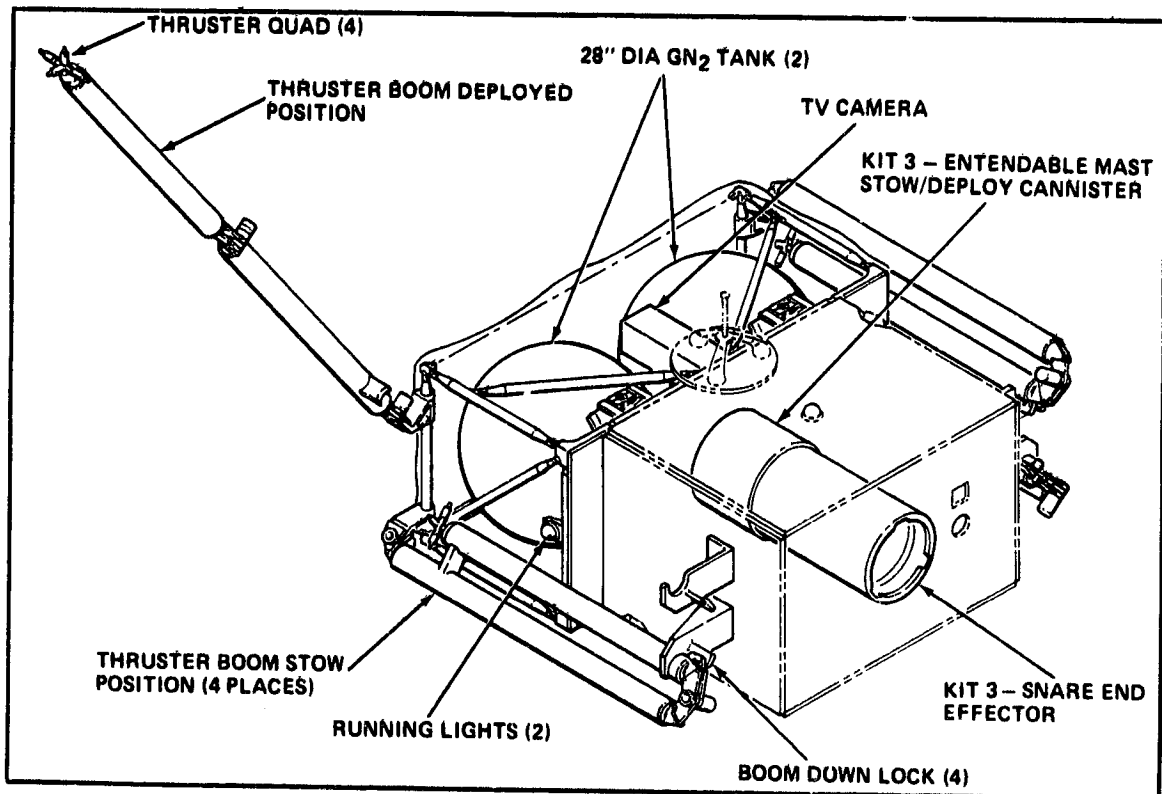


Fig. 12 MTV-POM Kit 2 – Satellite (5000 kg) Retrieval

Figure 13 illustrates how a manipulator system can be integrated with the core and propulsion modules. The manipulator arms, each 5 ft in length are mounted to the front face of the core module, and can be used to capture spinning satellites. The arms store along the core module side panels within the thruster boom stowage envelope. The system also includes a tilt and pan TV system with two additional lights mounted to the front face. The POV is spun-up to match the rotating velocity of a spinning satellite and the manipulator arms are extended to capture the satellite. After capture, the POV is despun to bring the rotational velocity of the satellite to near zero.

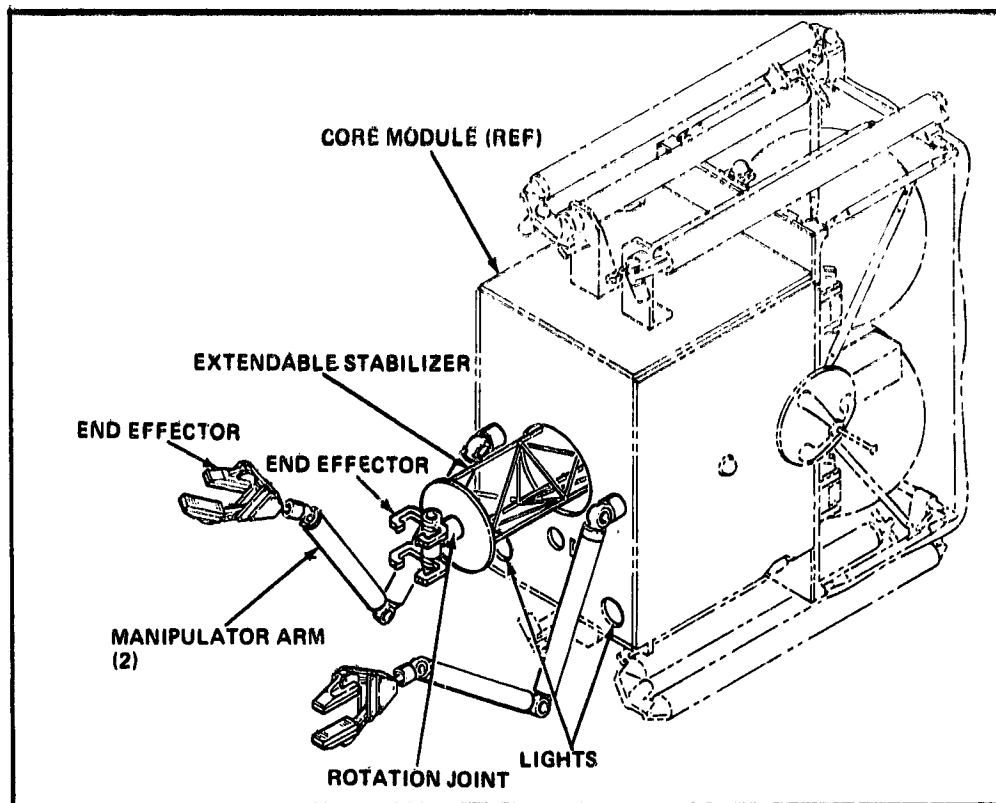


Fig. 13 MTV-POM Kit 4 - Manipulator

Retrieval of satellites within a 100-ft separation distance of the Orbiter can also be accomplished by a manned Proximity Operations Module (POM) as illustrated in Fig. 14 and 15. The POM is an adaptation of the Work Restraint Unit (WRU) and can be used in conjunction with a Manned Maneuvering Unit (MMU) to retrieve moderate-size satellites in the Multimission Modular Spacecraft class (2500 kg).

The POM is equipped with an extendible mast and an RMS end-effector mounted to a support structure to allow the astronaut to fly with the snare end-effector in a forward position during satellite engagement, and in an aft position during satellite towing operations. As astronaut would fly the manned POM to the satellite, capture it via the satellite's RMS-compatible grapple fixture, and tow it to within the reach distance of the RMS.

Figure 14 shows the Manned POM "flying-in" the end effector to engage the satellite's grapple fixture. As illustrated in Fig. 15 the manned Proximity Operations Module (POM) tows a spacecraft to the Orbiter. Via flight control capabilities of the MMU, the astronaut would stabilize/position the satellite

within the reach distance of the Orbiter's RMS arm. The POM would then detach itself from the satellite's grapple fixture and allow the Orbiter RMS to capture the satellite. Following capture, the RMS places the satellite on to a handling and positioning aid or tilt table to enable on-orbit servicing. Since most of the major hardware elements of this concept exist or are in late stages of development, the manned POM could be a more readily available approach to near-term satellite retrieval missions.

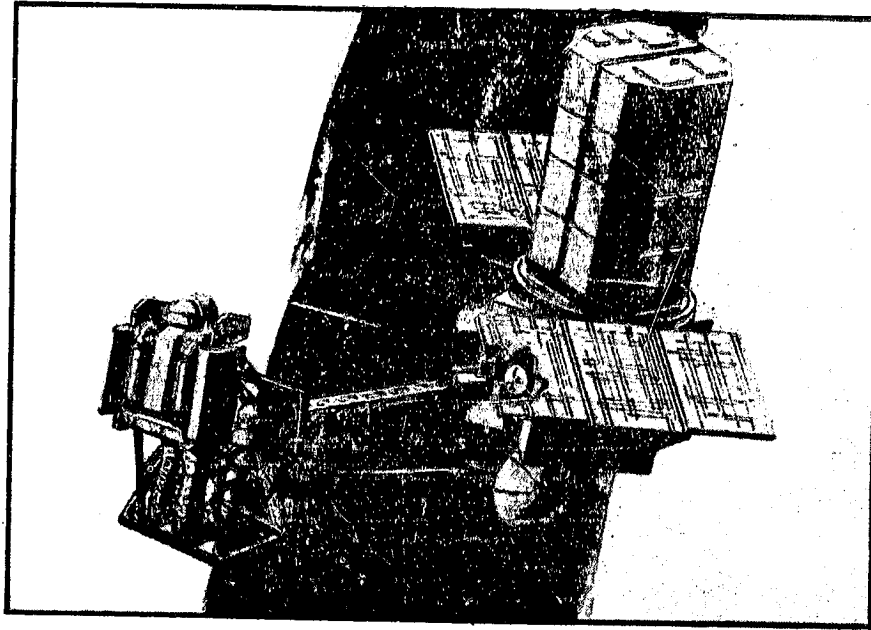


Fig. 14 Manned Proximity Operations Module – Satellite Capture

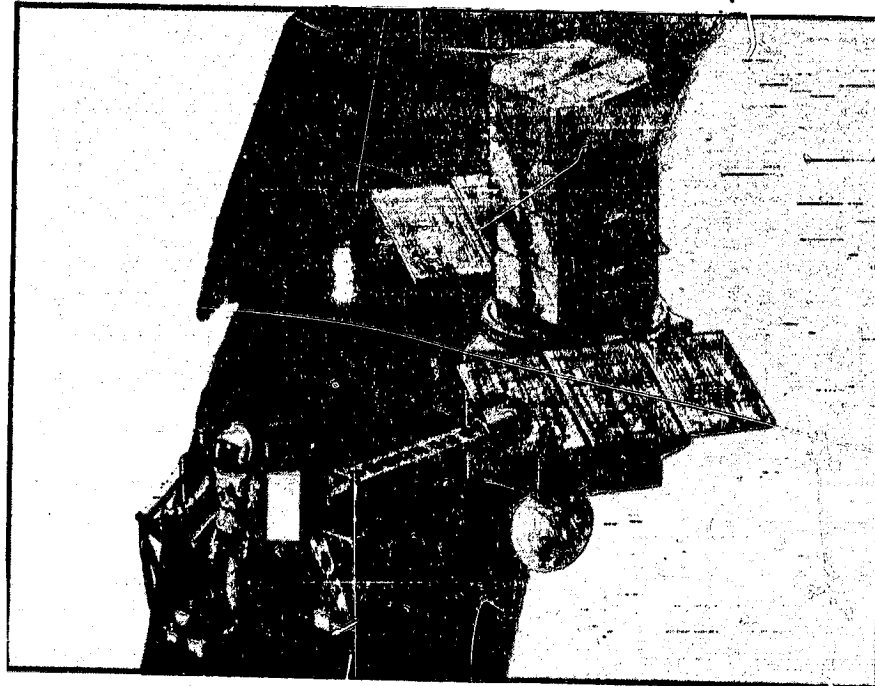


Fig. 15 Manned Proximity Operations Module – Satellite Retrieval

Figure 16 shows a schematic of the baseline work restraint unit or core work station and the additional attachments for satellite retrieval. Included in the figure are the cradle assembly with a snare end effector and a battery powered extendible mast. An additional control panel provides the astronaut with manual control of the extendible mast and a capability to rotate the cradle assembly into position for satellite towing. Without the cradle assembly but with a stabilizer add-on kit the WRU can be used as a work station for repairing satellites or equipments within the Orbiter payload bay. Figure 17 depicts a crewman repairing a satellite appendage hang-up prior to its deployment from the payload bay. After attaching himself to the work site with a stabilizer unit, the crewman releases himself from the MMU and steps into the foot restraint for retention. This design provides the crewman with unobstructed access to the work zone within his immediate surrounding.

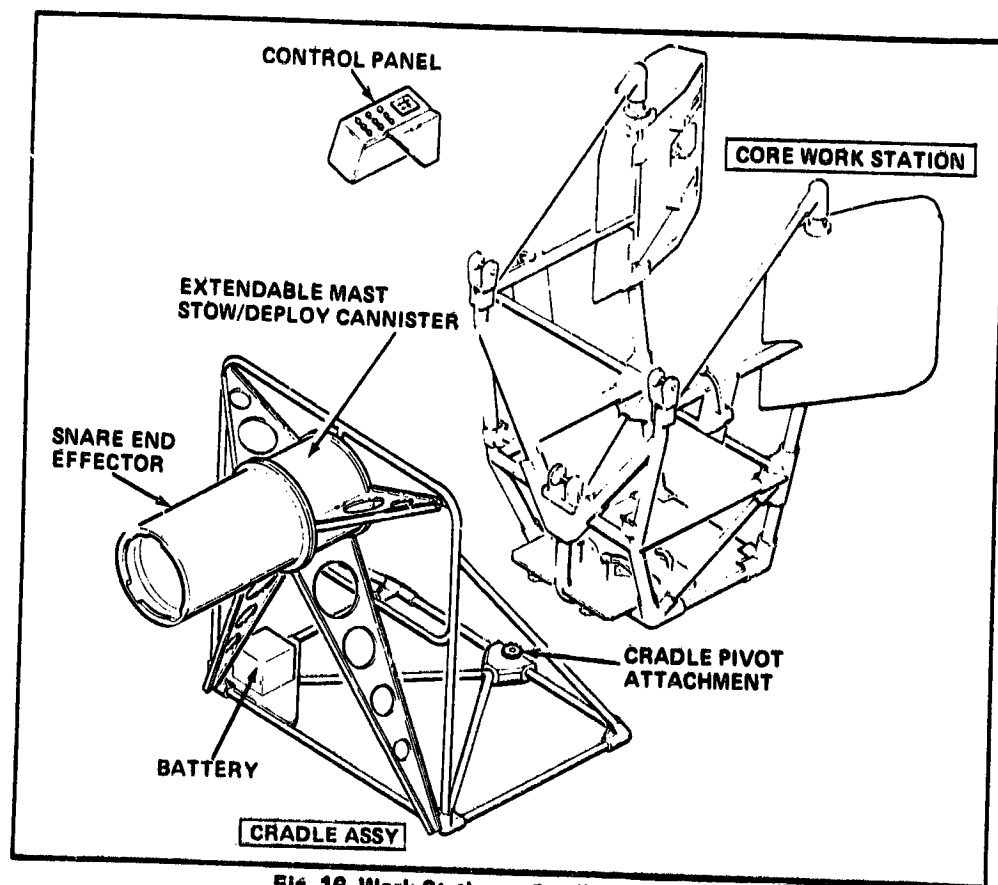


Fig. 16 Work Station - Satellite Retrieval

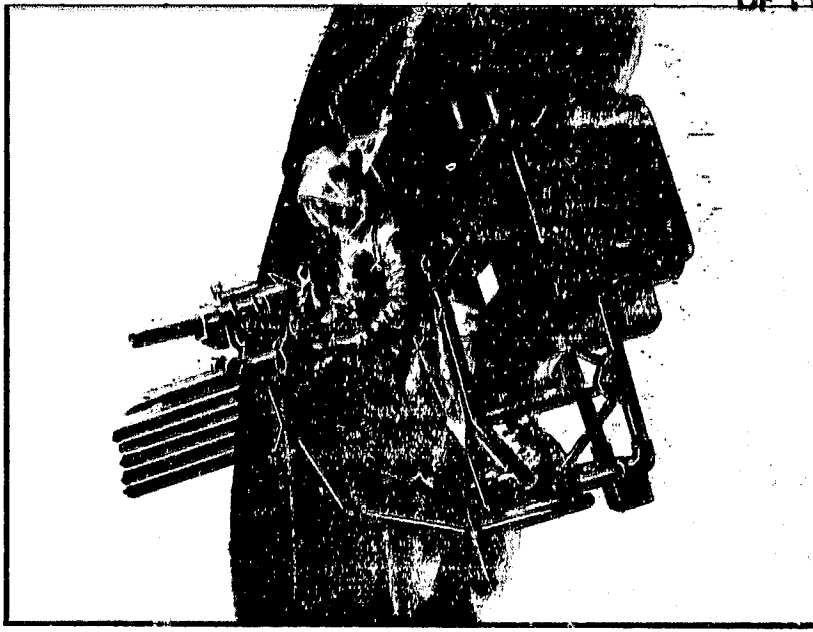


Fig. 17 MMU/Work Station – Backup for Satellite Appendage Hangups

For the LEO/Propulsion satellite class, (satellites in Low earth orbit which cannot be reached directly by the Orbiter) satellite retrieval is accomplished with the use of a Versatile Service Stage (VSS) or Teleoperator Maneuvering System (TMS). As presented in Fig. 18 the VSS is equipped with a snare end effector on an extendible mast as it approaches an uncooperative satellite rotating at low altitude rates. This mechanism is used to capture the satellite and reduce its rotational rates so that a hard docking can be effected to transfer the satellite back to the Orbiter.

Figure 19 illustrates the VSS equipped with dexterous manipulators for retrieving inactive satellites and/or Orbital debris. The illustration depicts the VSS capturing an OAO satellite which is tumbling about one axis at rates up to 10 rpm. Capture is achieved by spinning up the manipulator arms at a rate which is synchronized with the satellite's tumbling rate and then engaging the satellite. After engagement the satellite is despun via a clutch mechanism that transfers the rotational energy to the VSS which in turn dissipates the energy with the VSS reaction control jets. After nulling the satellite's rotational rate, the manipulators are then used to hard dock the satellite to the VSS for transferring the satellite to the Orbiter.

ORIGINAL PARTIAL
OF POOR QUALITY

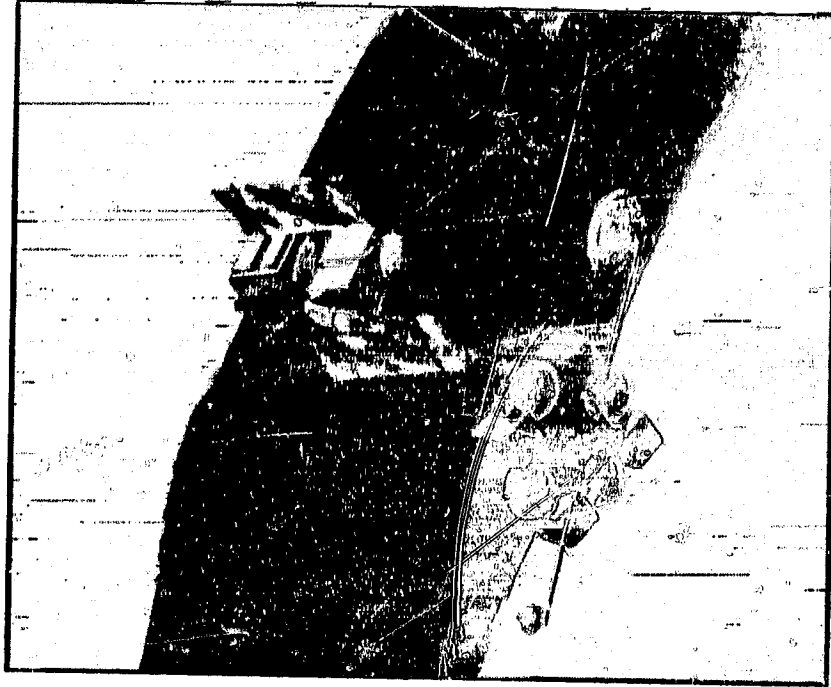


Fig. 18 Versatite Service Stage — Stabilizing Uncooperative Satellite

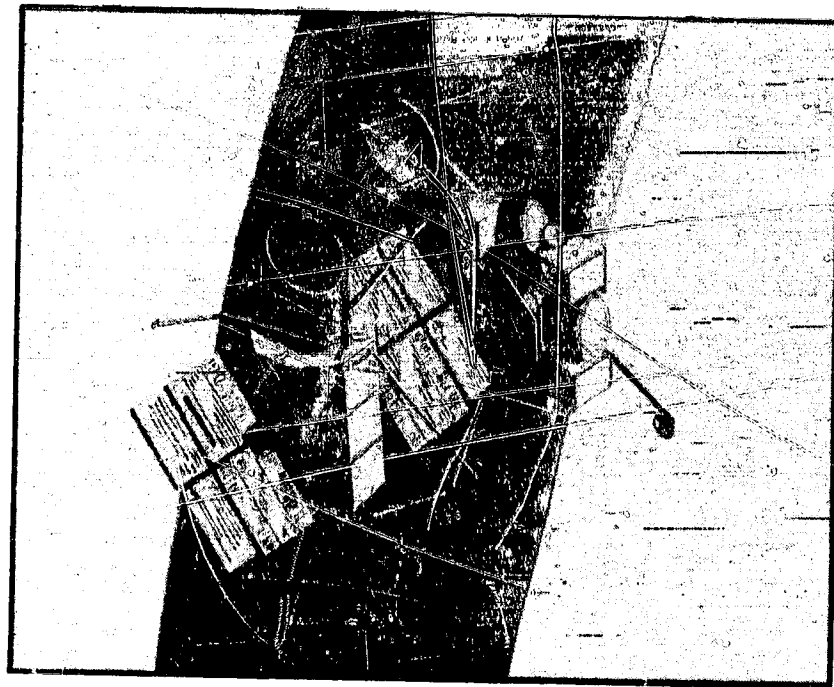
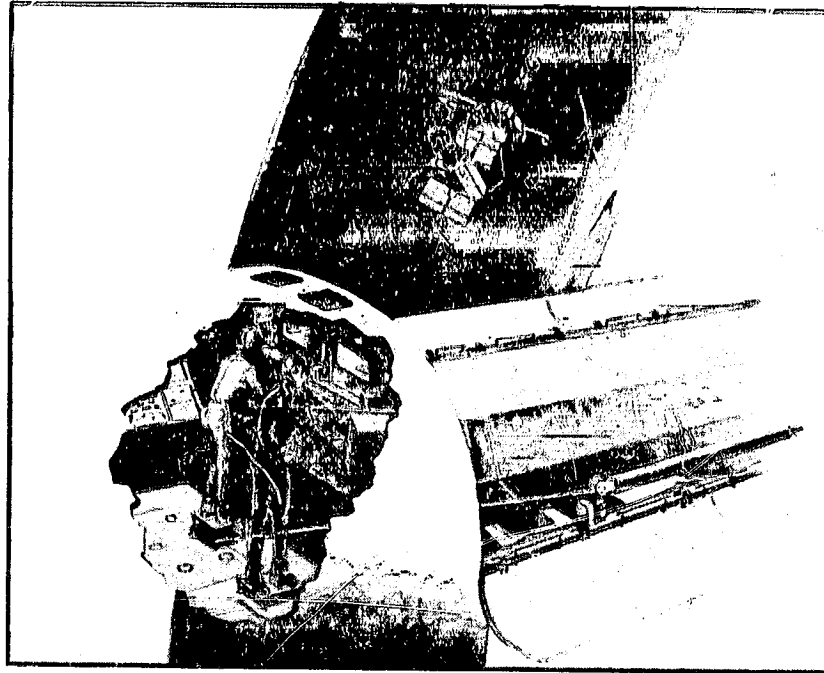


Fig. 19 Versatite Service Stage — Capture of Satellite Debris

Figure 20 shows the crewman in the Orbiter aft flight deck commanding the VSS via remote manual commands to bring the satellite to within Orbiter RMS reach. Manual remote commands are used to fly the VSS when within close proximity of the Orbiter. After the satellite is brought to within Orbiter RMS reach, the Orbiter captures the satellite and places it into the payload bay either for on-orbit repair/refurbishment or for earth return.



ORIGINAL PHOTO
OF POOR QUALITY

Fig. 20 Versatile Service Stage – Close Proximity Flight Control

In conclusion, and as summarized in Fig. 21, the POV has wide use for a number of applications.

- It offers non contaminating retrieval of satellites
- it will minimize Orbiter RCS propellant usage
- it will expand the capture envelope of satellite attitude conditions, and
- can maneuver payloads and experiment packages about the Orbiter.

The manned Proximity Operations Module (MMU/work station) can be used as a work station which will attach to an assortment of work sites. It can be used to transport small payloads to the various work sites, as well as to stabilize/retrieve satellites in close proximity to the Orbiter. It will also serve as back-up to the RMS for satellite deployment.

- **MTV/PROXIMITY OPERATIONS MODULE OFFERS THE FOLLOWING BENEFITS**
 - NON-CONTAMINATING RETRIEVAL
 - MINIMUM ORBITER RCS USAGE FOR CLOS² PROXIMITY OPERATIONS
 - EXPANDS SATELLITE CAPTURE POTENTIAL BEYOND RMS CAPABILITIES
 - SORTIE EXPERIMENT MISSION APPLICATIONS

- **MMU/WORK STATION OFFERS THE FOLLOWING CAPABILITIES FOR NOMINAL AND CONTINGENCY OPERATIONS**
 - WORK STATION ADAPTABLE TO VARIOUS SITES
 - TRANSPORTER OF SMALL PAYLOAD MODULES TO WORK SITES
 - PROXIMITY OPERATIONS MODULE FOR SATELLITE CAPTURE AND RETRIEVAL SATELLITE STABILIZATION
 - RMS BACKUP FOR SATELLITE DEPLOYMENT

- **DEVELOPMENT OF MANNED AND UNMANNED POM'S ARE BOTH TECHNICALLY AND ECONOMICALLY ATTRACTIVE**
 - CAN BE DEVELOPED WITHIN CURRENT TECHNOLOGY BASE USING OFF-THE-SHELF EQUIPMENTS
 - MINIMIZES DEVELOPMENT COSTS
 - OFFERS AFFORDABLE GROWTH

Fig. 21 Conclusions

Considering these applications and the design concepts developed, manned and unmanned POM's are both technically and economically attractive. More importantly they can be developed within the current technology base and at reasonable cost. Because they satisfy many potential mission needs and can be used as a standard mode for satellite retrieval, early system development and flight demonstration is strongly recommended (Fig. 22).

- **BECAUSE RETRIEVAL WITH PROXIMITY OPERATIONS MODULES CAN SATISFY ALL POTENTIAL MISSION NEEDS, IT SHOULD BE CONSIDERED AS A STANDARD MODE FOR SATELLITE RETRIEVAL**

- **EARLY SYSTEM DEVELOPMENT LEADING TO FLIGHT DEMONSTRATION IN 1985 IS RECOMMENDED.**

Fig. 22 Recommendations

24 17
N 85-21212

A REMOTELY CONTROLLED ORBITING RETRIEVER*

Marshall H. Kaplan**
Spacetech, Inc.
State College, PA

Summary

A preliminary design effort was recently carried out to investigate methods of removing a certain class of space objects from Shuttle-type orbits. Specifically, expired satellites, upper stages, and other objects of potential danger to the Shuttle are the targets of this study. The Trash Remover and Satellite Hauler (TRASH-I) design effort was broken into several disciplines: mission analysis, systems engineering, dynamics and control, power, thermal, and propulsion.

A basic requirement is that TRASH-I go up in the Shuttle. It must be reusable and capable of disposing of more than one item per mission for cost effectiveness. These requirements imply TRASH-I should use current technology, be modular in design, and be relatively maneuverable. In order to maximize utility, it should be able to both capture and deorbit objects.

The design was a basic bus with attachable modules which can either capture or deorbit, depending on the module. The bus is divided into two parts, a front section with shelves and thermal control for equipment such as communications, computer control, etc., and a rear section which houses the main kick motor and some of the attitude controls. For communications,

* Work reported here is based on a study carried out at the Pennsylvania State University under the author's direction.

** President

the bus is equipped with a Tracking and Data Relay Satellite System (TDRSS) link package. Also, a remote arm was included to cut any appendages from a spacecraft should it be necessary for capture. Shuttle attachment points are located on the bus. A "strawman" scenario was developed in which the satellite, OSO-6, would be retrieved. In addition, an extensive list of possible retrieval candidates was compiled to assist in developing design criteria.

Spacecraft Requirements and Constraints

The mission is clearly one of maneuvering to, rendezvousing with, docking with, and eliminating objects from future Shuttle orbits. Use of the STS imposes many constraints. The cargo bay limits the diameter to 4.57m (15 ft.) and length to 18.3m (60 ft.). A limiting dry mass of 14,515 kg (32,000 lbs.) is imposed for Earth return. To provide adequate clearance for appendages, a diameter of 3.65m (11.9 ft.) was selected. The length is limited to 6.0m (19.7 ft.). The lift-off mass became 9,525 kg (21,000 lbs.).

TRASH-I must withstand all launch and landing loads. Load factors that the spacecraft was designed for correspond to ultimate g loads encountered during a Return-To-Launch-Site (RTLS) abort and for a hard landing.

A cost-effective approach was vital to the philosophy of a retrieval mission. Thus, TRASH-I is assumed reusable through periodic refurbishment and the use of a modular design. The cost-effective aspects dictated multiple retrievals per mission.

The TRASH-I vehicle is unusual in many respects. It is not designed for a single specific mission, but for a variety of tasks related to collecting space trash. This mission requires that the vehicle be flexible in its maneuverability and attitude control. It is assumed that each mission will involve rendezvous with at least three targets. Normally, each target's orbit will differ in ascending node position, inclination, and semi-major axis. Rendezvous with the first target will be accommodated by the launch vehicle. TRASH-I must then complete this

rendezvous and accomplish at least two others.

Targets will be in orbits which differ by as much as 400 km in radius. This requirement will not place major constraints on the vehicle since radius changes can be accomplished very efficiently. Inclination changes and changes in ascending node position, however, require large velocity increments. The propellant available will probably limit these maneuvers to less than 15 degrees, at least in the case where brute force methods are used. Using the effects of the Earth's oblateness to adjust the ascending node could increase this range. Preliminary calculations indicate that the vehicle should be capable of at least a velocity change of 3.0 km/sec to meet overall requirements. This mission places many constraints on the control system.

Three functions will be necessary:

1. robust attitude control mode,
2. autopilot mode, and
3. articulation control mode.

The robust attitude control mode is needed during rendezvous when the vehicle must be capable of full rotations about pitch, roll, and yaw axes. This is necessary to handle the entire rendezvous since retrieved objects are passive. This capability is applied to point the velocity vector for orbital maneuvers. Orientation accuracy in this mode must be 0.25 degree (3 σ).

The autopilot mode is required during the linear acceleration phases. Any velocity change errors must be sensed during the thruster firing and corrected so that large trajectory errors do not result.

Articulation control is needed to point the high gain antenna and solar panels independently of the main body platform. Solar panels only require control to within 1-5 degrees, but communications via TORSS demand antenna pointing to better than 0.5 degrees. This system must also be able to respond quickly to compensate for commanded body rotations. Overall, the mission requirements for this vehicle specify a high-velocity change capability and a highly maneuverable vehicle with accurate control.

Spacecraft Design

The major design aspects considered here are structural, propulsion, dynamics and control, power, thermal, and communications. To begin, the structural design was divided into several sections. First, there is the bus, the part designed to house the propulsion, communication, computers, and all of the other equipment necessary for a general mission. It is further compartmentalized into a rear section for the main kick thruster and a forward section for all of the equipment. The other structural area is the capture and deorbit modules. These will attach on the front of the bus.

The bus external structure is cylindrical, but the sides are slightly flattened to accommodate the solar panels. Since the beginning, several appendages have been added for various tasks. Figures 1 and 2 show the final design of the TRASH-I spacecraft.

Placed around the external surface of the spacecraft are attitude thrusters. A total of twelve attitude thrusters were chosen to be mounted about the bus. Two thrusters that fire in the positive x direction are canted up 30 degrees. This was done so the exhaust of these two thrusters would not interfere during rendezvous with an object. To provide a pure couple during pitch maneuvers, two thrusters firing in the negative x direction were placed at the other end of the spacecraft.

On the front of the spacecraft is a connecting plate used to supply power to the capture module for its radar, lights, closed circuit TV (CCTV), and other functions pertaining to the capture sequence. The connecting plate will not be used for the deorbit

modules since they have their own internal power source. There are four attachment points on the front of the spacecraft for use in securing the capture/deorbit modules. The attachment points can, on command, release the module, depending on the planned mission.

Connected to one side of the spacecraft is a remote manipulator arm. This arm is 5.5 meters long and six degrees of freedom. On the end of the arm is a cutting tool used to remove any long appendages that would interfere with the capture sequence. Inside the arm is a pressure tank and a valve to vary the amount of pressure applied by the tool so it can grab and hold or cut appendages.

The TDRSS antenna is to be mounted to the rear of the spacecraft so it will not interfere with the capture sequence and to keep it away from thruster exhaust. During launch and reentry, the antenna will fold down, face first, to prevent damage to the reflector. The mast of the antenna was designed to be 3.5 meters (11.5 ft) long so that the spacecraft would not interfere with the transmission and reception of data from the TDRSS satellites.

Mission Analysis

The first task in developing mission profiles for TRASH-I is to identify those objects which present a potential hazard to STS operations. A computer program was developed, using input parameters such as catalog number, a numerical code specifying nationality (i.e. 1 for USA, 2 for USSR, etc.), orbital period in minutes, inclination in degrees, apogee and perigee in kilometers, and node line in degrees. This program was designed to scan each set of input parameters and to calculate the semi-major axis of each orbit, rejecting any satellite with a semi-major axis falling outside the range of the Shuttle operating envelope which is approximately 650 km. Those pieces of debris with semi-major axes falling within this range were further sorted, by inclination, into two arrays. The first array contains information on satellites with inclinations between 28.5° and 57.0° reachable by launching from the Kennedy Space Center. The second array includes those objects that have inclinations between 57.0° and 104.0° and can be reached from Vandenberg Air Force Base. Finally, both of these arrays were generated to provide an up-to-date, comprehensive list of target satellites for each launch site. Final output data include launch site, catalog number, nationality code number, period in minutes, semi-major axis in kilometers, and node line in degrees.

For this report, the 28 February 1981 NASA Satellite Situation Report was used as the data base for the target selection program. As of that date, there were 4539 objects in orbit. Of these, approximately 300 pieces of debris occupied orbits within the STS operating

envelope and, therefore, constituted a potential hazard to Shuttle operations. In addition, there were approximately 50 pieces of debris with orbits crossing the altitude range of 200 to 400 kilometers where the majority of Shuttle missions will take place (see Table 1 for a partial list).

TRASH-I will be capable of performing several types of removal missions. These include retrieval of small objects, deorbit of several small satellites and upper stages, and boosting of nuclear powered satellites. The various mission combinations require independent maneuvering from a low Shuttle orbit to rendezvous with the target followed by return to the Shuttle orbit. It is envisioned that TRASH-I will be capable of performing one capture and one or more deorbits per mission.

The decision to deorbit or capture a particular target depends on its mass, size, and shape. However, there are other factors involved, such as the possibility of a nuclear device on board. To verify the presence of a nuclear device, TRASH-I is equipped with a radiation sensor. If the target is radioactive, it cannot be deorbited or captured; it must be boosted to a higher orbit. This situation is related to the problem of deorbiting or capturing a target owned by a nation other than the United States. For example, the USSR has a large number of objects in the Shuttle operating range which should be removed. Thus, international cooperation will be needed to avoid political repercussions. For this study, missions were selected solely on the basis of position in orbit and size and mass of the objects. The following is a brief description of the various mission

scenarios and associated configurations for TRASH-I.

- (a) The multiple deorbit and single capture mission is designed to remove up to three objects orbiting in very close planes but with different altitudes and periods. The Capture/Containment module is fitted with up to two detachable retro modules, allowing up to two satellites to be deorbited. After rendezvous is completed with a satellite, a retro module is attached. Deorbit of the first satellite clears the Capture/Containment module so the same task can be performed on a second satellite. A third satellite is then captured and returned to the Shuttle for transport back to Earth.
- (b) The large vehicle deorbit/single-capture mission is designed to remove two spacecraft from almost co-planar orbits. The major difference between this mission and (a) is that the Capture/Containment Module contains a single deorbit module which has many characteristics of an Inertial Upper Stage. The reason for this rather sophisticated deorbit module is that large satellites and booster stages will require attitude and stabilization control before deorbit. Further, a larger quantity of propellant will be needed to deorbit such large spacecraft. The capture segment of this mission is the same as in (a).
- (c) To complete the nuclear satellite boost/single-capture mission, the boost module is attached to the radioactive target and is boosted to a higher orbit, using two velocity changes. The capture part of this mission is the same as in (a).

For the example mission to retrieve OSO-6, the Orbiter ascends to a 250 km circular orbit with an inclination of 33 degrees. TRASH-I systems are activated just prior to release and a check is made on all spacecraft systems. The STS crew will use the Remote Manipulator System to deploy TRASH-I at a safe distance before activating it.

The Orbiter is then "backed" away from the spacecraft to avoid interference as it becomes active.

The first step in the power-up sequence is to deploy the TRASH-I solar panels on command from the ground. Once electrical power is assured, the TRASH-I is ready for a systems check independent of the STS. This involves activating the TV cameras, sensors, and propulsion system, and rechecking all other systems to insure a successful mission. The Orbiter may now continue on with deployment of any other payloads, or it may begin preparations for reentry. An interesting aspect of the power-up sequence is that TRASH-I can focus on the STS as an object while checking its floodlights, TV system, and short range sensors.

Since the Orbiter can match both the inclination and node line position of the OSO-6 satellite, the rendezvous maneuvers for TRASH-I breakdown into several simple coplanar transfers. During this mission, TRASH-I will travel in several different orbits to reach OSO-6. The first is the initial circular orbit at 250 km, with a period of 89.50 minutes. It then executes a Hohmann transfer with a half period of 45.39 minutes. The period of the OSO-6 orbit is 92.261 minutes while the period of a circular orbit at 375 km is 92.046 minutes. Because these two periods are nearly equal, relative positions of chase and target vehicles must be specified at each phase of the flight. Accurate navigation and guidance is important. Throughout its approach flight TRASH-I will be gaining on the target due to OSO-6's greater period. A sequence of simple maneuvers brings TRASH-I to the final rendezvous from a station-keeping

position with OSO-6; the final closure and capture sequence can take place at any time. This sequence begins with a re-power-up of the flood light and camera system. After repowering, ground controllers can guide TRASH-1 within a few feet of OSO-6, using sensors and TV feedback and then carefully maneuver it so that it can engulf the arbitrarily spinning OSO-6 and despin and secure it. This is followed by a return to the Shuttle orbit via a standard Hohmann transfer. TRASH-1 may then enter a dormant state for up to three months, awaiting a Shuttle launch for pick up.

Conclusions

To achieve a cost-effective method of retrieving low-orbiting objects, a remotely controlled, modular spacecraft is recommended. Two key aspects of this goal are reuseability and multiple pick-up. The TRASH-1 can be launched on a shared flight and retrieved as part of a return trip for an Orbiter. A unique feature is the ability to attach retro (or boost) packs to objects, avoiding handling by the Shuttle directly and allowing up to three retrieval operations per mission.

Table 1. Partial List of Space Debris Located Within Range of Shuttle Missions

NAME	COUNTRY	PERIOD (min)	INCLN. (deg)	APOGEE (km)	PERIGEE (km)	SIZE (m)	MASS (kg)	SHAPE
?	USSR	90.7	74.0	284	272	?	?	?
OSC-6	US	92.3	33.0	396	375	D=2.31	317	wheel
?	US	90.9	97.4	318	316	?	?	?
Cosmos 582	USSR	89.1	74.0	235	219	?	?	?
?	USSR	92.2	74.0	383	380	?	?	?
Cosmos 610	USSR	89.9	74.0	287	264	?	?	?
?	USSR	91.4	74.0	350	333	?	?	?
Cosmos 631	USSR	90.8	74.0	315	310	L=2? D=1?	500?	cylinder/pedals
Cosmos 631 Booster	USSR	92.0	74.0	378	368	L=7.8 D=2.4	2200?	cylinder
Cosmos 655	USSR	91.9	74.0	372	362	L=4.2? D=1.6?	1250?	minimum's caps
Cosmos 655 Booster	USSR	90.3	74.1	320	312	L=2.0 D=2.0	440	cylinder
Cosmos 661	USSR	91.0	74.0	335	311	?	?	?
Cosmos 696	USSR	92.2	74.0	384	378	L=2? D=1?	500?	cylinder/pedals
Cosmos 698 Booster	USSR	91.6	74.0	356	352	L=7.4 D=2.4	2200?	cylinder
Cosmos 707	USSR	90.6	74.0	312	295	L=2? D=1?	500?	cylinder/pedals

Table 1 (cont.)

NAME	COUNTRY	PERIOD (min)	INCLN. (deg)	APOGEE (km)	PERIGEE (km)	SIZE (m)	MASS (kg)	SHAPE
Cosmos 670	USSR	92.3	74.0	389	387	L=22 D=1?	900?	cylinder/paddles
Cosmos 691	USSR	92.0	65.6	393	356	L=4? D=2?	?	cylinder
Cosmos 699	USSR	91.2	74.0	342	328	L=2? D=1?	900?	cylinder/paddles
Cosmos 699 Booster	USSR	92.1	74.0	386	369	L=7.4 D=2.4	2200?	cylinder
Salyut 6 Booster	USSR	88.9	51.6	227	209	L=12? D=4?	4000?	cylinder
Cosmos 960	USSR	91.3	74.0	342	338	L=2? D=1?	900?	cylinder/paddles
Cosmos 960 Booster	USSR	91.8	74.0	368	359	L=7.4 D=2.4	2200?	cylinder
Interkosmos 19	USSR	89.6	74.0	272	237	?	?	?
?	USSR	88.6	72.8	210	200	?	?	?
Cosmos 1174	USSR	90.3	62.8	311	270	?	?	?
Cosmos 1176	USSR	89.6	65.0	261	247	?	?	?
?	USSR	91.5	72.6	370	329	?	?	?
?	USSR	91.4	72.8	363	318	?	?	?
?	USSR	91.6	72.9	375	331	?	?	?
?	US	88.6	96.4	251	162	?	?	?
Soyuz 37	USSR	91.2	51.6	340	325	?	?	?

Table 1 (cont.)

NAME	COUNTRY	PERIOD (min)	INCLN (deg)	APOGEE (km)	PERIGEE (km)	SIZE (m)	MASS (kg)	SHAPE
Inter-Cosmos 13	USSR	88.5	82.9	236	168	L=1.8? D=1.5?	550?	octagonal/ellipsoid
Cosmos 749	USSR	90.5	74.1	302	293	L=2? D=1?	900?	cylinder/paddles
Cosmos 749 Booster	USSR	92.1	74.2	386	373	L=7.4 D=2.4	2200?	cylinder
Cosmos 752	USSR	92.2	65.8	399	365	L=4? D=2?	?	cylinder
Cosmos 781	USSR	91.9	74.0	370	368	L=2? D=1?	900?	cylinder/paddles
Cosmos 781 Booster	USSR	92.2	74.0	368	371	L=7.4 D=2.4	2200?	cylinder
Cosmos 787	USSR	92.2	74.0	392	373	L=2? D=1?	900?	cylinder/paddles
Cosmos 790	USSR	92.0	74.0	387	361	L=2? D=1?	900?	cylinder/paddles
Cosmos 790 Booster	USSR	92.2	74.0	388	374	L=7.4 D=2.4	2200?	cylinder
Cosmos 812	USSR	91.5	74.0	356	340	L=2? D=1?	900?	cylinder/paddles
Cosmos 812 Booster	USSR	92.2	74.0	392	370	L=7.4 D=2.4	2200?	cylinder
Cosmos 845	USSR	91.8	74.1	365	357	L=2? D=1?	900?	cylinder/paddles

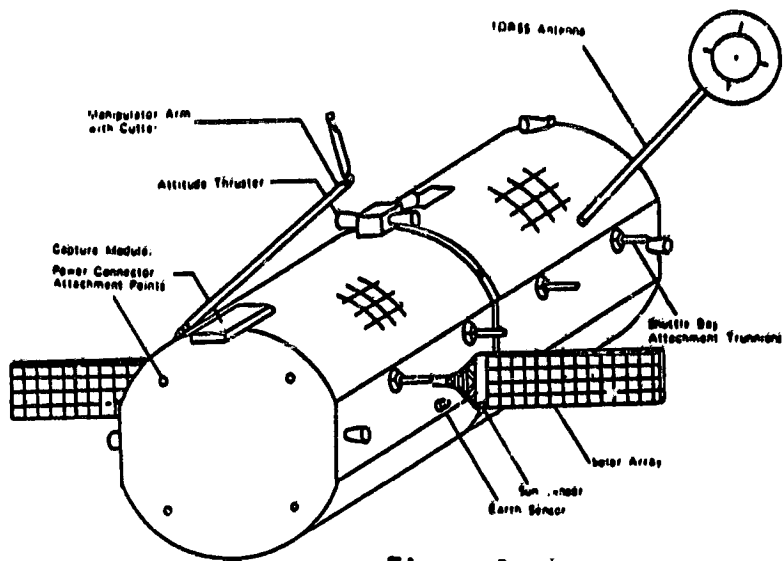


Figure 1. TRASH-1 Design Overview.

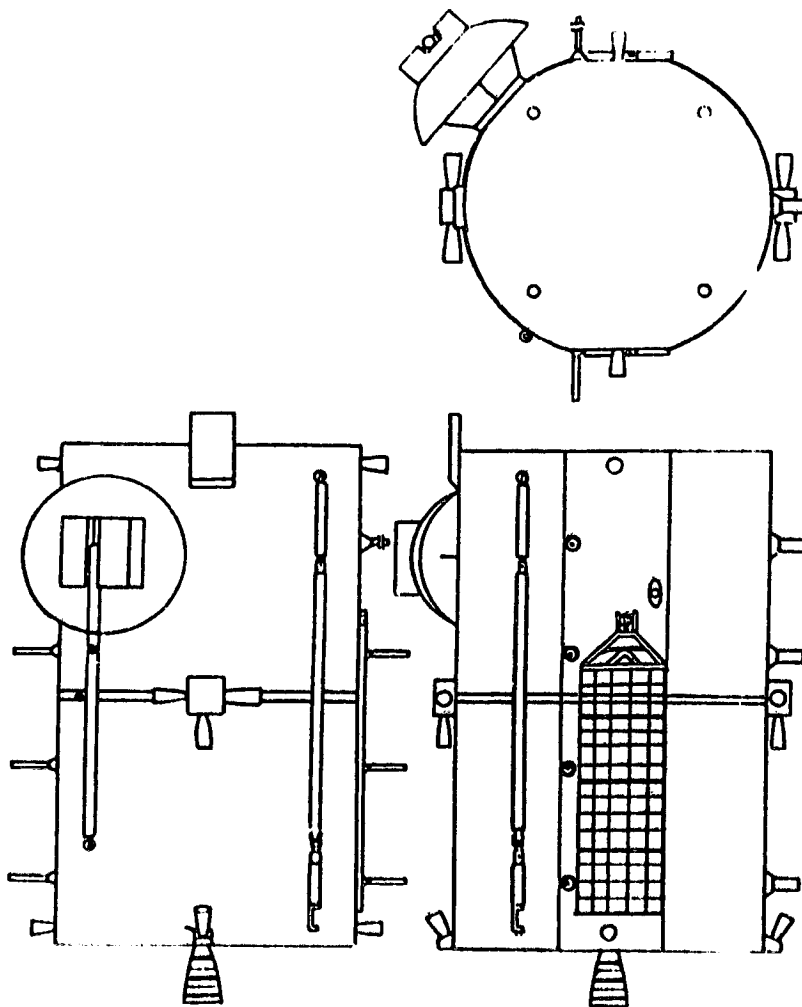


Figure 2. TRASH-1 Three-View

Doc B
N85-21213

The Long Term Behaviour of Earth Orbits
and the Implications for Debris Control

by

Alan C. Mueller

Aerospace & Engineering Mechanics Department
University of Texas at Austin
Austin, Texas

Abstract

The long term dynamics and stability of the geosynchronous orbit (GEO) and its associated transfer orbit have been analyzed. GEO orbits with inclinations which remain less than 45 degrees are very stable. Although the inclination of the orbital plane may vary as much as 15 degrees over a period of about 50 years, the orbit altitude will always remain within a few hundred kilometers of geosynchronous altitude. GEO orbits with inclinations greater than 45 degrees exhibit remarkable instabilities in the eccentricity due to gravitational resonance. Over a period of a century the eccentricity can reach such a large value that re-entry is a possibility.

The combined effects of the sun, moon, and oblate earth play a significant role in determining the lifetime of a GEO transfer orbit. Depending on the initial orientation of the orbital plane with respect to the sun and moon, lifetimes may vary from under 6 months to over several hundred years. Transfer orbits with inclinations over 45 degrees show strong instabilities in the perigee altitude resulting in generally short lifetimes of less than a few years. All transfer orbits can be designed to decay within one year if the initial perigee altitude is less than 231 km. However, there are restrictions on orbit plane placement and time of year of launch.

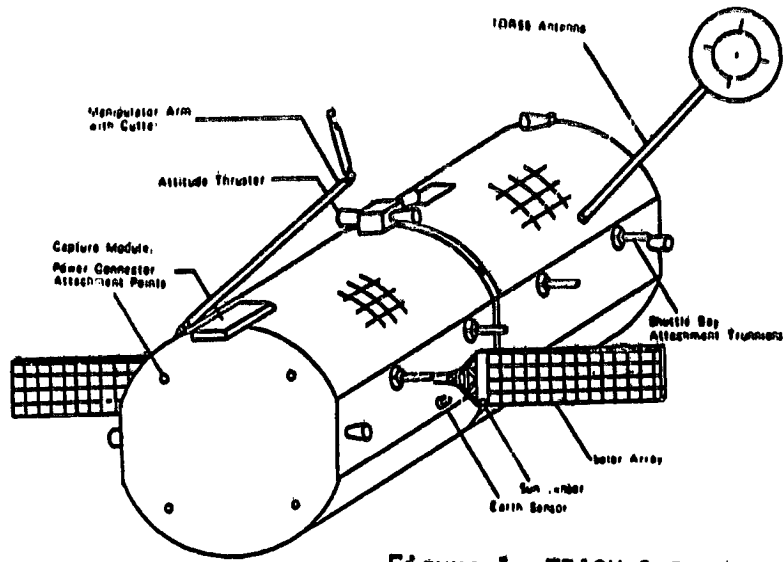


Figure 1. TRASH-1 Design Overview.

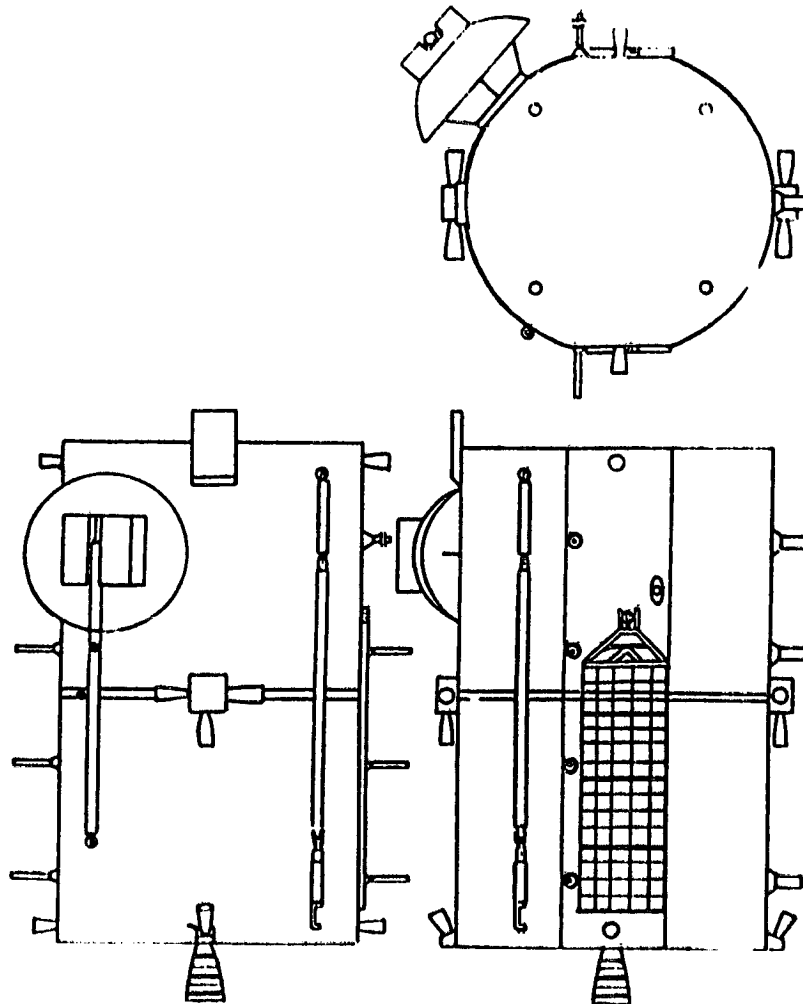


Figure 2. TRASH-1 Three-View

Introduction

The NASA Space Transportation System (STS) offers new economies for placing payloads into orbit. New opportunities are open to organizations for operating their devices in space. There will be a much wider utilization of space as a resource for applications.

At the same time, however, the increasing number of satellites will increase the possibilities of collision in space. In the past, most satellites were in near earth orbit, where air drag eventually removed them from orbit. Now many satellites will be placed into a geosynchronous orbit (GEO) using some upper stage. During the ten year period 1980-1990, there are 164 planned GEO missions using the STS Space Shuttle(1). For each satellite placed into GEO, one or more upper stages will be left in the transfer orbit. As time progresses the GEO satellites also become non-operational and coast freely in GEO space.

The spent upper stages and non-operational GEO satellites become nothing more than hazardous space junk and the question arises as to what should be done about it. Does this junk represent a true collision hazard and if so are there any effective means for its removal. These and other questions may not be answered without a general knowledge of the long term dynamics of the GEO orbit and its transfer orbit.

Two studies, one on the lifetimes of the GEO transfer and the other on the stability of the GEO, have been carried out to more fully understand the long term behaviour. Since it was desirable to define the dynamics over some one hundred years, each study found it necessary to develop computationally efficient semi-analytical techniques to predict the behaviour. The results of the studies may be found in more detail in Graf and Mueller (2) and in Mueller(3). A brief discussion of the results will be presented here.

Lifetimes of the GEO Transfer Orbit

Due to the geometry of the transfer orbit rather small changes in the eccentricity can drastically raise or lower perigee. Although the sun and moon gravitational perturbations are small, they can significantly change the perigee altitude and in so doing have a tremendous effect on the lifetime. Lifetimes range from under six months to several hundred years according to the time of year of the launch (position of sun), the inertial orientation of the orbital plane and the inclination of the orbit. Transfer orbits with inclinations of over 45 degrees show remarkable instabilities. Figure 1 shows the perigee evolution of such an orbit with the initial inclination of 65 degrees. The smooth line is the evolution predicted by DSTROB, the semi-analytical technique, while the triangle and dots are the actual observations from Classy(4). It is the sun and moon, not drag, which actually determines the lifetime. Transfer orbits below 45 degrees do not exhibit such instabilities but variations of over 100 km in perigee altitude is not uncommon.

A series of parameter scans was carried out to determine lifetime as a function of the free parameters of the problem. Initial values of the semi-major axis and the eccentricity are specified by the mission objectives. It will be required that the perigee be near the equator because of delta-v considerations and that the inclination be near 28.6 degrees because of the launch site. The remaining parameters are then the initial longitude of the ascending node and the epoch of the launch. The time of day of launch can be related to the longitude of the node while the time of year of launch can be related to the right ascension of the sun. The parameter scans were done by computing 36 one year trajectories of the GEO transfer

satellite. For each trajectory, the minimum perigee in one year was determined. The angular parameter was incremented by 10 degrees over the 360 degree range. Drag was not considered in these scans but it is assumed that if perigee drops below 100km reentry is expected.

Figure 2 plots the minimum perigee as a function of the initial node for an initial perigee of 278km. Trajectories were initialized at four different times of year. No trajectories fall below the 100km limit although a winter trajectory with initial node of near 200 degrees fell over 140 km. If the initial perigee is dropped to 185km then a large window of opportunities occur for reentry as seen in Figure 3.

The time of the year parameter was taken to be the difference between the sun's right ascension at launch and the initial node. Figure 4 plots the minimum perigee with respect to this parameter, for a given initial node of 180 degrees and initial perigee of 185 km. Opportunities for reentry exist for all times of year for such a initial node placement. With the initial node set to 0 degrees the scan shows that reentry opportunities exist when the sun begins 90 or 270 degrees ahead of the initial node as seen in Figure 5.

The launch strategy for early upper stage reentry would be to select perigee altitude to be moderately low(185-231km). If no strict mission requirements on the transfer orbit initial node exist then select the node to be near 180 degrees and launch can occur any time of the year. If constraints require an initial node other than 180 degrees then select the time of year of launch so that the sun is 90 or 270 degrees ahead of the constrained node.

Stability of the Geosynchronous Orbit

The predominate perturbations on GEO are due to the oblate earth and the gravitational mass of the sun and moon. For satellites with large surface areas relative to their weights, solar radiation pressure can be of equal importance. Although J_{22} is three orders magnitude smaller than J_2 , it too can contribute a significant perturbation if at the exact resonance with the rotating earth. All perturbations are periodic but, in the case of the long period resonances, the periodic variation may become quite large. Since solar pressure does not contribute a long period variation and J_{22} is important only at the exact GEO altitude these terms are neglected in the analysis. The equations of motion have been averaged to eliminate the short period (daily) and intermediate periods of the sun and moon. This allows for much larger step sizes (one year) when numerically integrating the averaged equations. No long period variations occur in the semi-major axis so that any radial instabilities will be due to the variations in the eccentricity. Several numerical experiments over a broad range of GEO initial conditions were conducted. Geostationary (zero inclination) orbits show no radial instabilities as seen in the eccentricity time history of Figure 6a. Figure 6b shows that the inclination can grow to about 15 degrees. With the assumption of small inclination and eccentricity, Graff (5&6) gives a simple analytical solution to the geostationary orbit including solar radiation pressure. One can show that the eccentricity of such an orbit can never grow larger than

$$e < (e_0 + nA/M) \sqrt{A/\mu} + nA/M$$

where

$$\eta = 0.012$$

$$\alpha = 1.1749$$

$$\beta = 1.5569$$

A = Cross-sectional Area in square meters

M = Mass in Kilograms

e_0 = initial mean eccentricity

With $e_0 = 0.001$ and $A/M = 0.05$ one finds

$$e < 0.0024$$

which implies that a non-operational geostationary satellite may be removed from GEO space for all times simply by placing it a few hundred kilometers above or below GEO altitude.

As the initial inclination increases, the variations in the eccentricity become more pronounced. For an initial inclination of 45 degrees and an initial node chosen so that the inclination ranges above 45 degrees, the eccentricity increases markedly as seen in Figure 7a. The inclination history is shown in Figure 7b.

For even higher inclinations the instability becomes quite pronounced suggesting a possible means for disposing such a satellite. With a slight increase in the eccentricity say to $e = 0.05$ and with the proper initial node, the eccentricity can be forced to grow dramatically as seen in Figure 8. In this case reentry is predicted within 100 years. This is not conclusive, however, since the averaging theory breaks down at very high eccentricities.

References

- 1) "NASA STS Mission Model; Payload descriptions and Space Transportation System Cargo Manifests", Johnson Space Center Report JSC-13829, October, 1977.
- 2) Graf, O.F.; Mueller, A.C.: "A Study of the Lifetimes of Geosynchronous Transfer Orbits," AAS/AIAA Paper No. 79-105, Presented at the AAS/AIAA Astrodynamics Specialist Conference, Provincetown Mass., June 25-27, 1979.
- 3) Mueller, A.C.: "Stability of the Geosynchronous Satellite," Orbital Debris Study J.O. 69-067, LEMSCO-17518, Dec., 1981.
- 4) "CLASSY DOCUMENT" - ADCOM REPORT. Regional Computer Center. Aerospace Defence Command.
- 5) Graf, O.F.: "Lunar and Solar Perturbations on the Orbit of a Geosynchronous Satellite," AAS Paper No. 75-023, Presented at the AAS/AIAA Astrodynamics Specialist Conference, Nassau, Bahamas, July, 1975.
- 6) Graf, O.F.: "Orbital Motion of the Solar Power Satellite," ACM Technical Report 105, May, 1977.

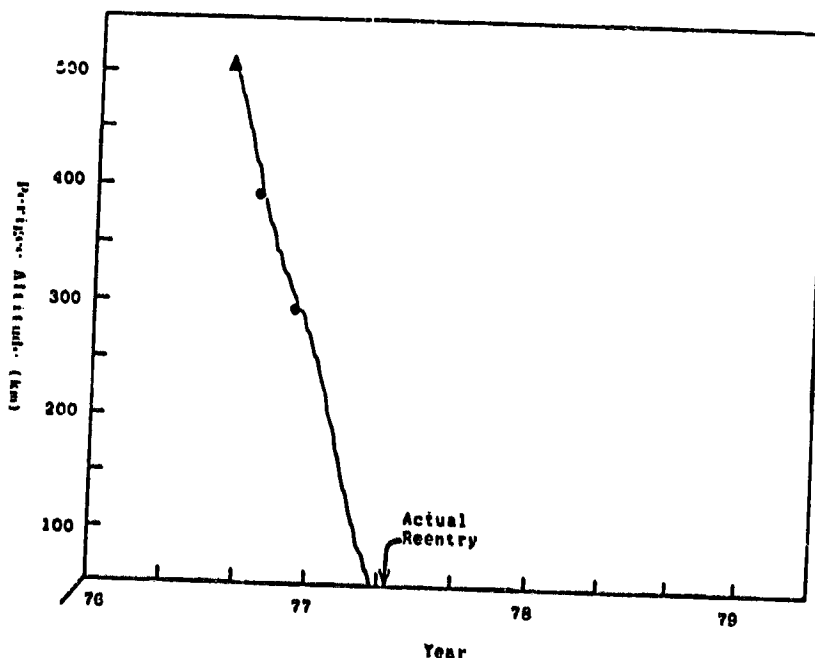
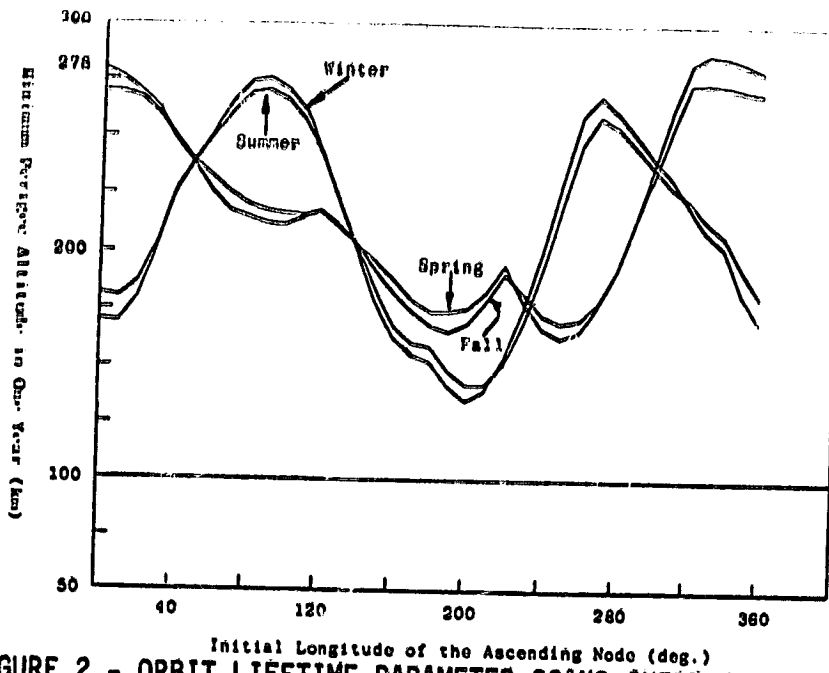
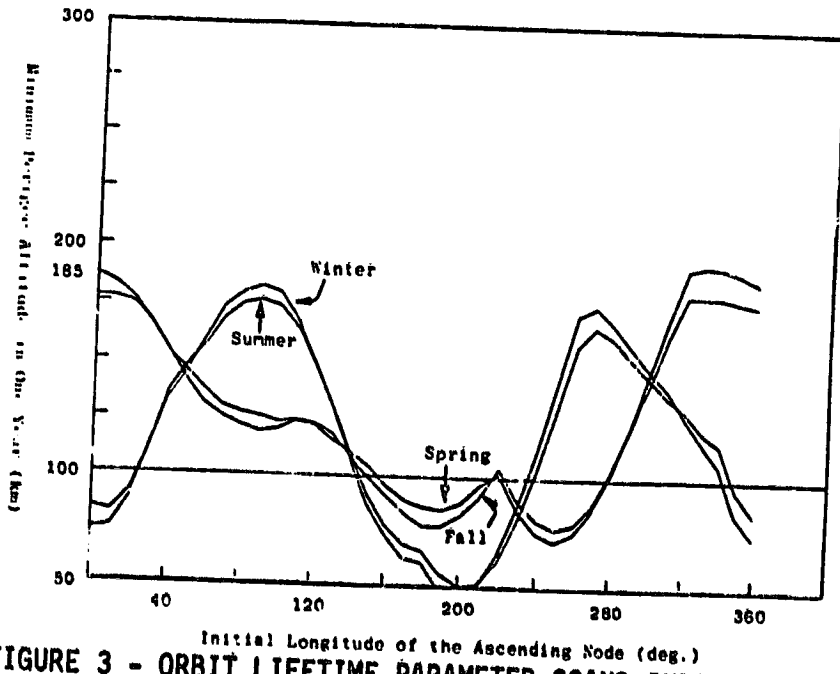


FIGURE 1 - COMPARISON OF DISTROB WITH AIR FORCE TRACKING DATA
 Satellite No. 5713, $i_0 = 85.1^\circ$



Initial Longitude of the Ascending Node (deg.)
FIGURE 2 - ORBIT LIFETIME PARAMETER SCANS INERTIAL PLACEMENT OF ORBITAL PLANE
 $h_{po} = 278 \text{ km} , i_o = 28.6^\circ$



Initial Longitude of the Ascending Node (deg.)
FIGURE 3 - ORBIT LIFETIME PARAMETER SCANS INERTIAL PLACEMENT OF ORBITAL PLANE
 $h_{po} = 185 \text{ km} , i_o = 28.6^\circ$

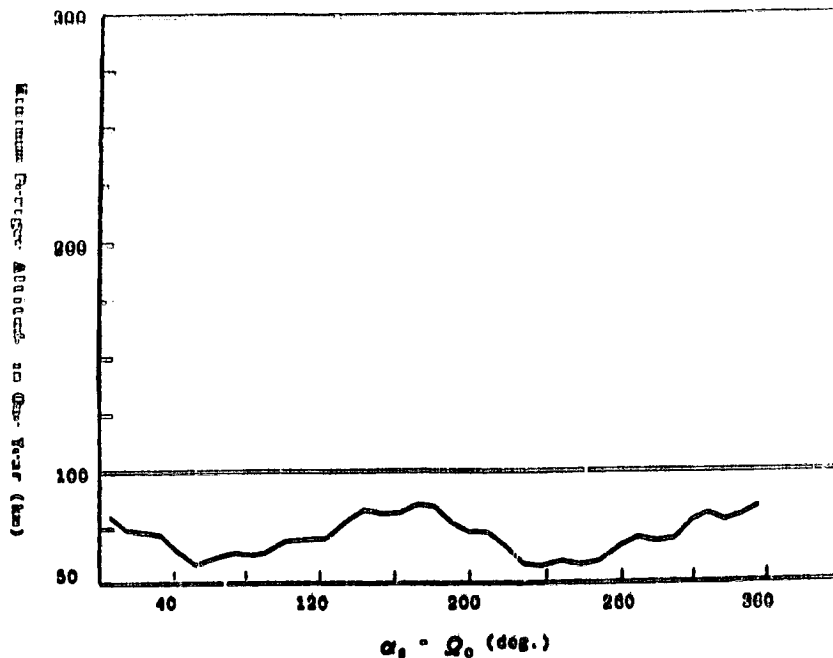


FIGURE 4 - ORBIT LIFETIME PARAMETER SCANS
 Time of Year of Launch
 $h_{p0} = 165 \text{ km}$, $i_0 = 28.6^\circ$, $\Omega = 100^\circ$

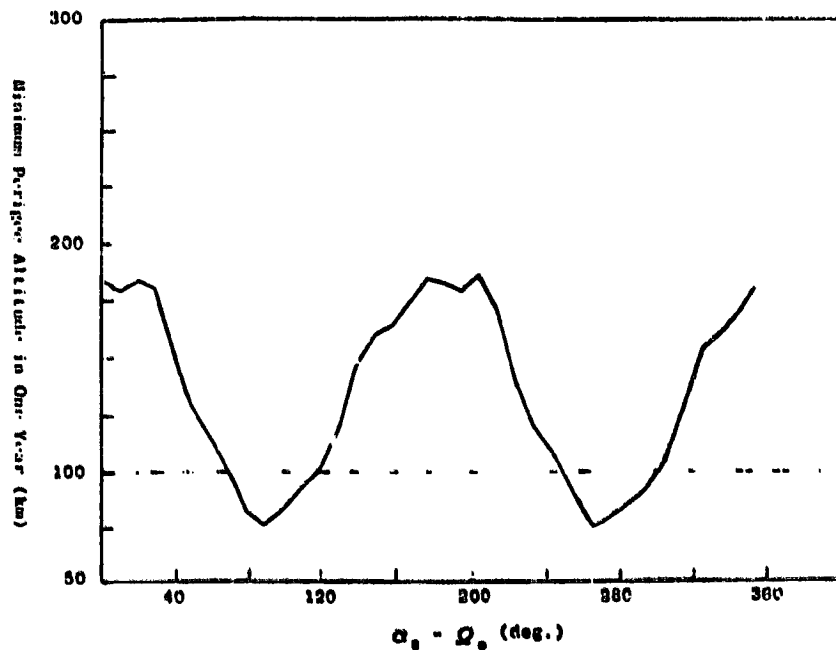


FIGURE 5 - ORBIT LIFETIME PARAMETER SCANS
 Time of Year of Launch
 $h_{p0} = 165 \text{ km}$, $i_0 = 28.6^\circ$, $\Omega_0 = 0$

FIGURE 6b
TEST CASE 1

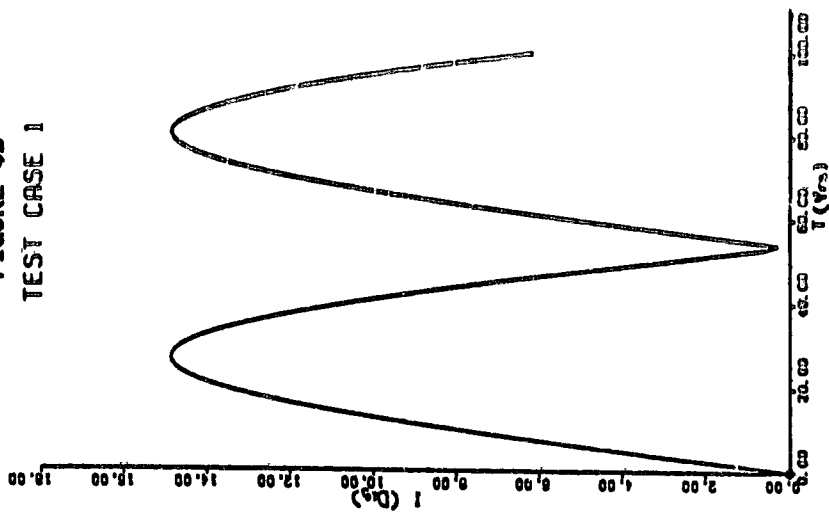


FIGURE 6a
TEST CASE 1

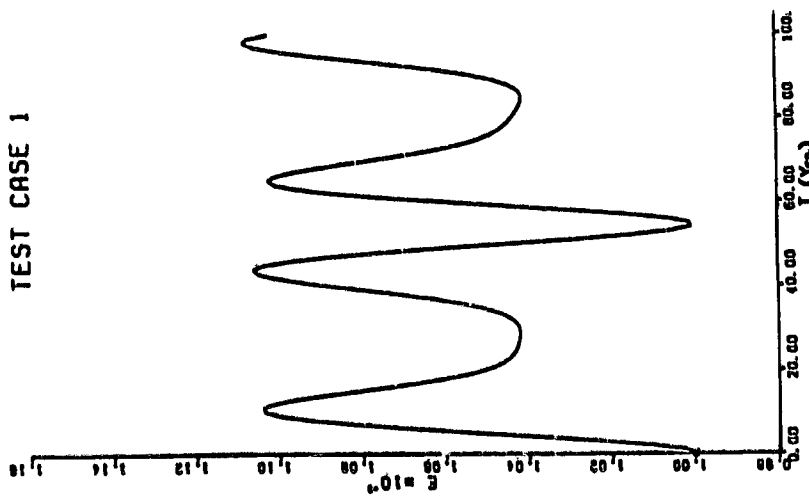


FIGURE 7b
TEST CASE 5

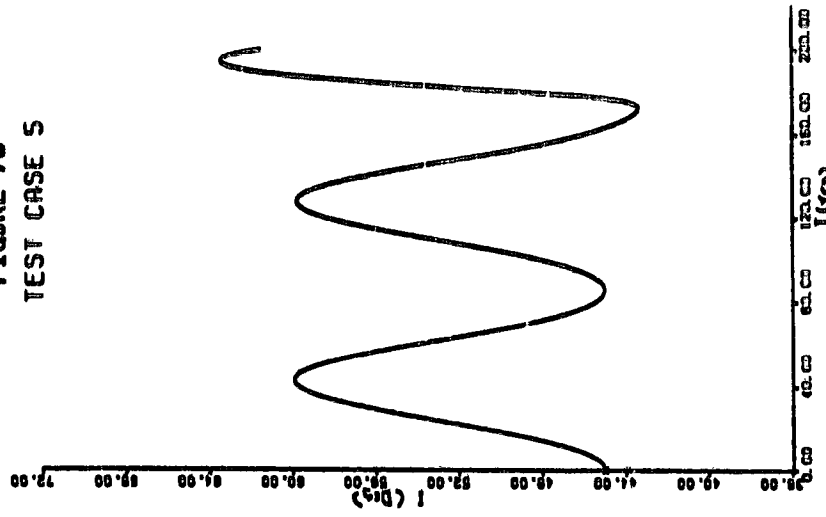
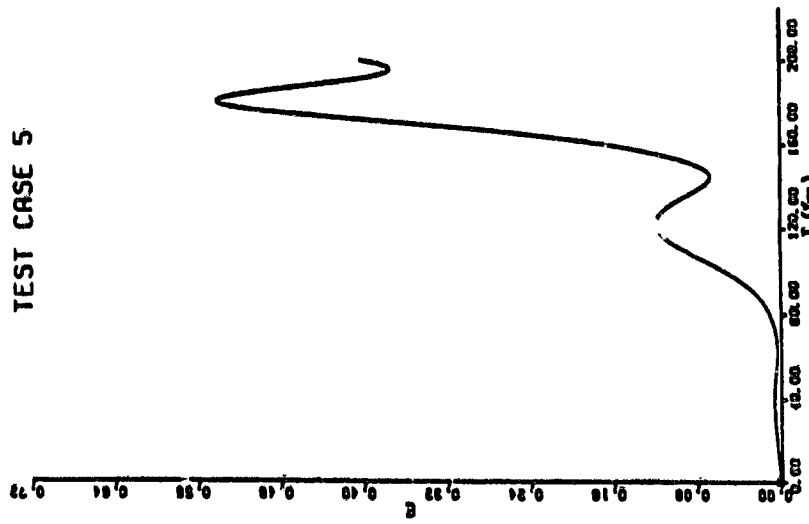
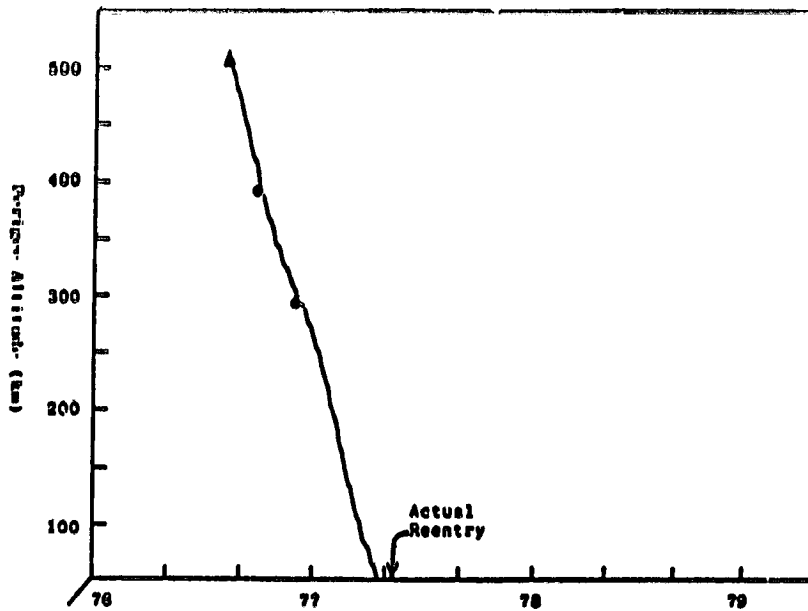


FIGURE 7a
TEST CASE 5





Year
 COMPARISON OF DSTROB WITH
 AIR FORCE TRACKING DATA
 Satellite No. 5713, $i_0 = 65.1^\circ$

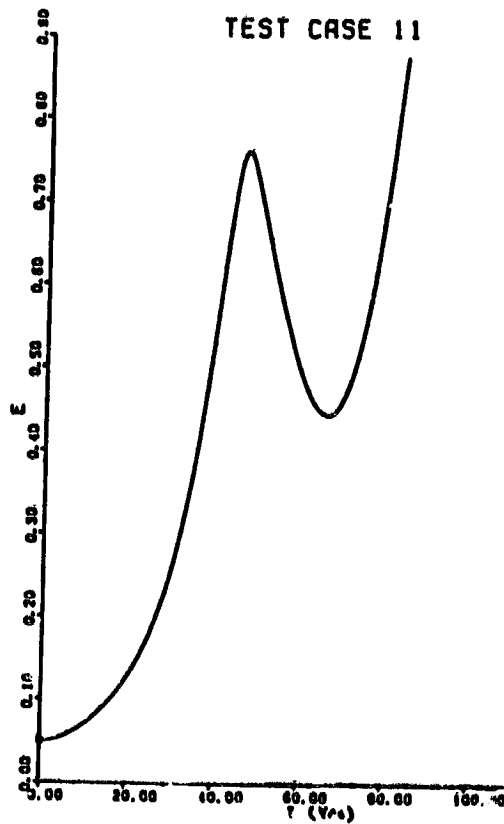


FIGURE 8
 343

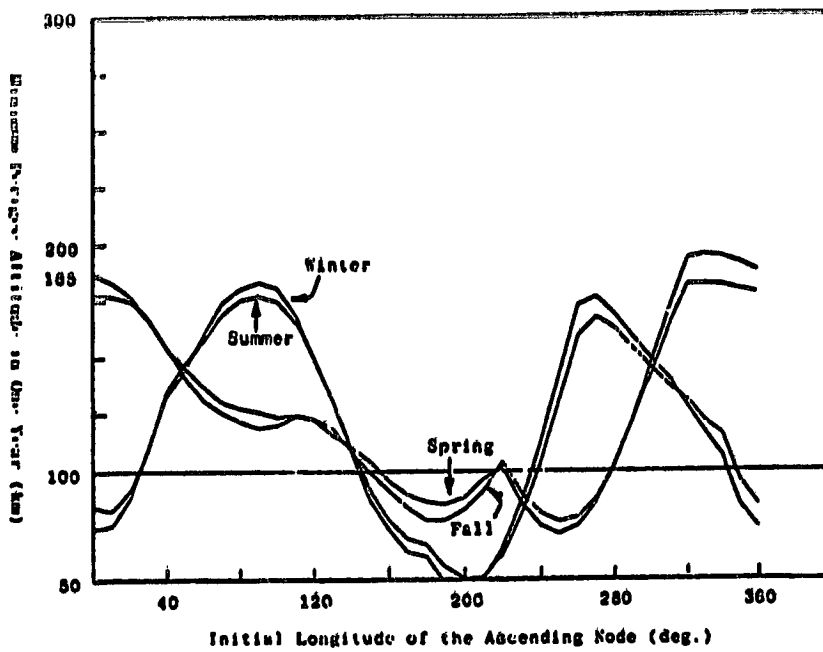


FIGURE 9: ORBIT LIFETIME PARAMETER SCANS
 Inertial Placement of Orbital Plane
 $h_{po} = 185 \text{ km} , I_o = 28.6^\circ$

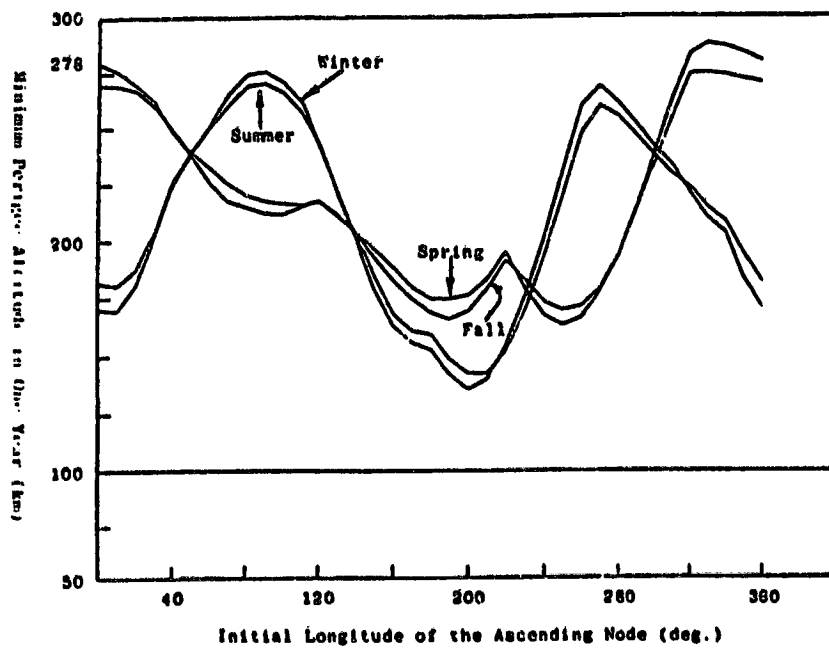


FIGURE 9: ORBIT LIFETIME PARAMETER SCANS
 Inertial Placement of Orbital Plane
 $h_{po} = 278 \text{ km} , I_o = 28.6^\circ$

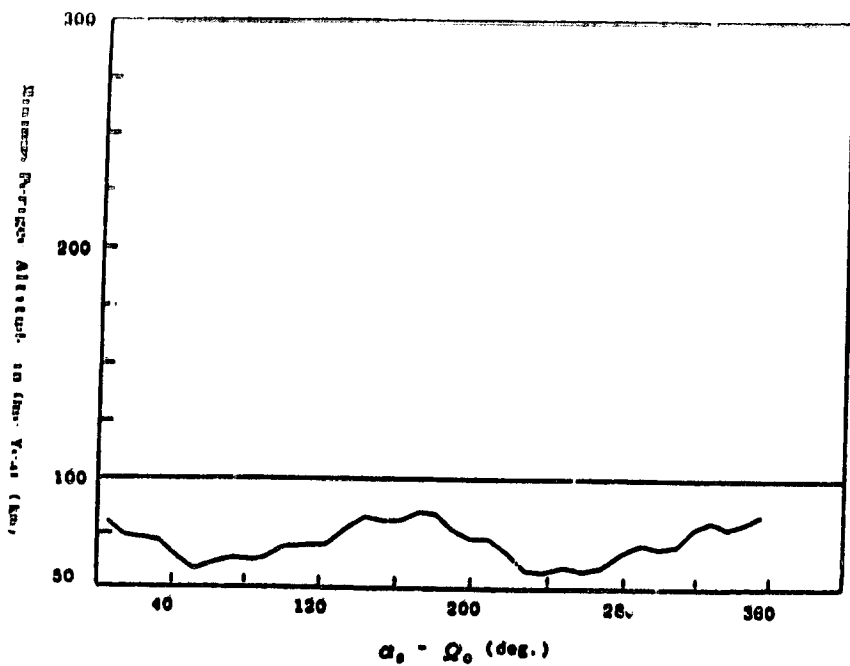


FIGURE 10: ORBIT LIFETIME PARAMETER SCANS

Time of Year of Launch

$$h_{p0} = 185 \text{ km}, i_0 = 28.6^\circ, \Omega_0 = 180^\circ$$

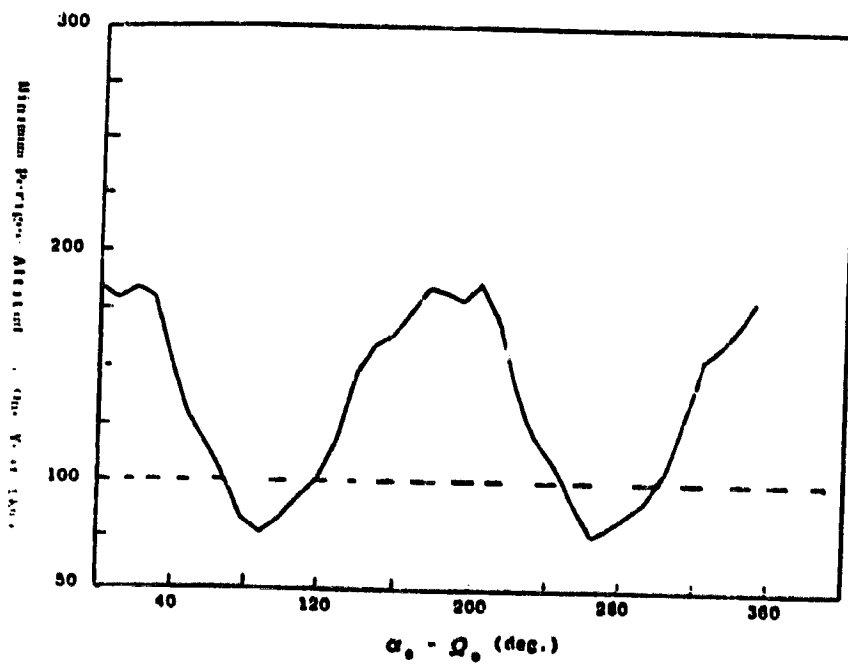
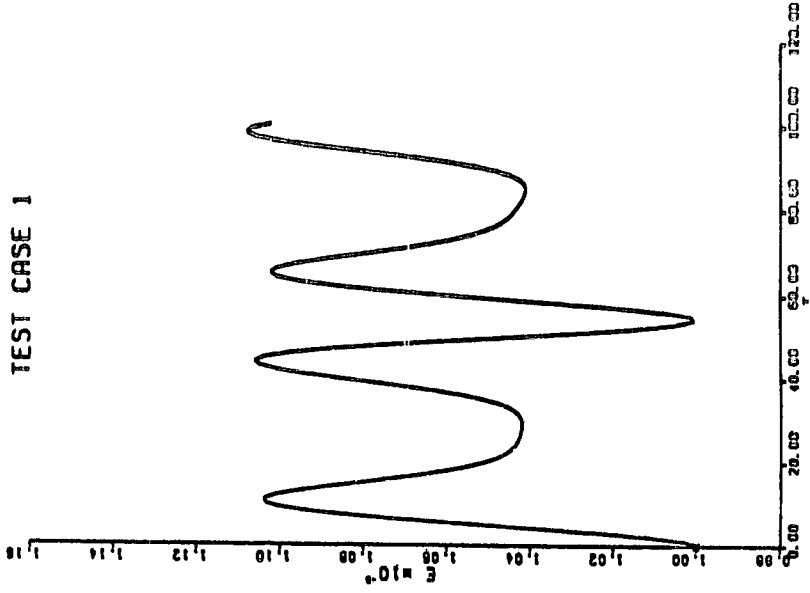


FIGURE 10: ORBIT LIFETIME PARAMETER SCANS

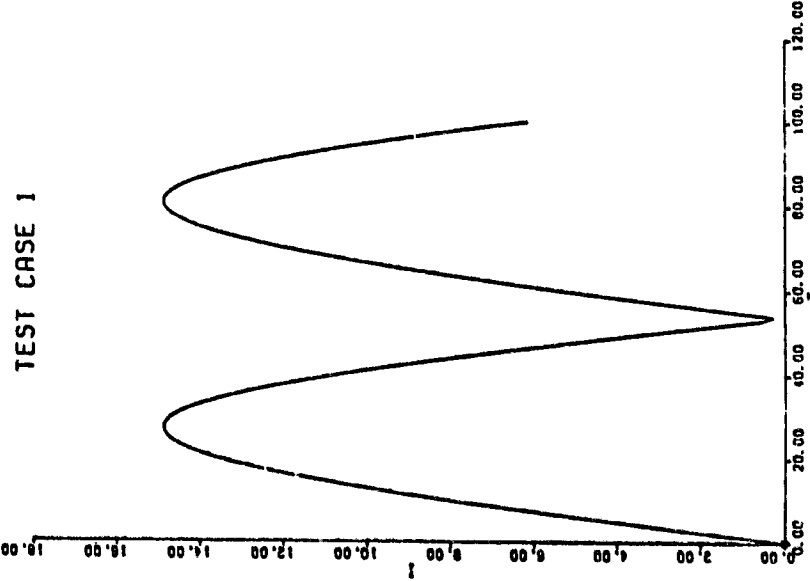
Time of Year of Launch

$$h_{p0} = 185 \text{ km}, i_0 = 28.6^\circ, \Omega_0 = 0$$

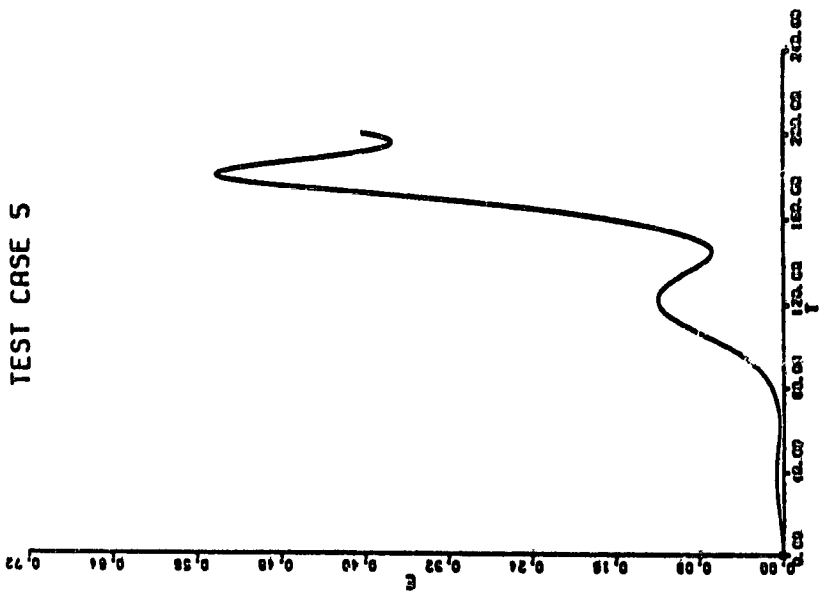
TEST CASE 1



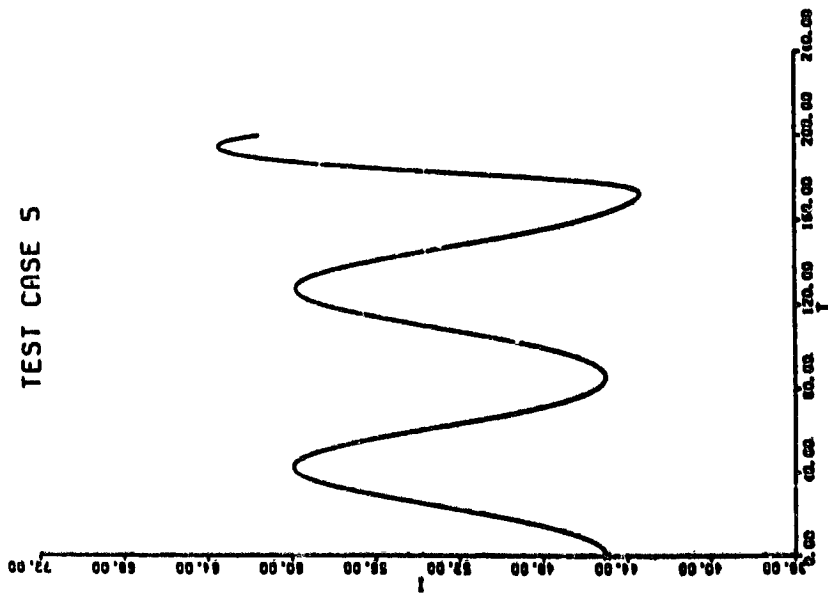
TEST CASE 1



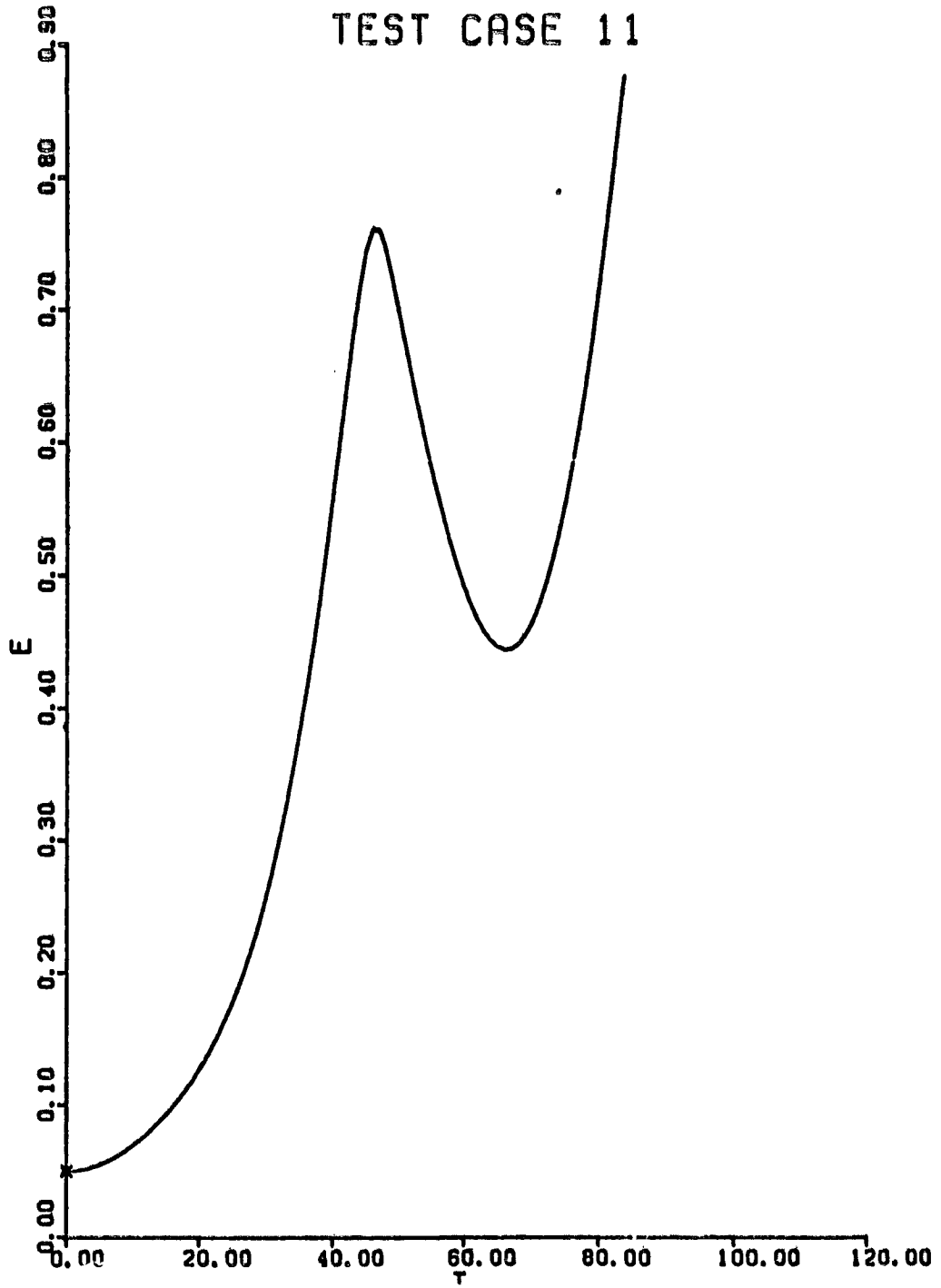
TEST CASE 5



TEST CASE 5



TEST CASE 11



DEBRIS IN THE GEOSTATIONARY ORBIT RING

"THE ENDLESS SHOOTING GALLERY"

THE NECESSITY FOR A DISPOSAL POLICY

DAVID H. SUDDETH

PURPOSE OF PAPER

- o NASA IS CONSIDERING ESTABLISHING A POLICY FOR THE LIMITATION OF THE PHYSICAL CROWDING OF THE GEOSTATIONARY ORBIT. THIS PAPER WAS REQUESTED BY THE DIRECTOR, COMMUNICATION AND DATA SYSTEMS DIVISION, CODE TS, NASA HQ. IT IS TO:
- o DEAL ONLY WITH GEOSTATIONARY ALTITUDES
- o ILLUSTRATE THE UNIQUE VALUE AND USEFULNESS OF THE GEOSTATIONARY ORBIT RING
- o DESCRIBE THE ORBITAL DYNAMICS AS SIMPLY AS POSSIBLE
- o DESCRIBE THE CURRENT SPACECRAFT AND DEBRIS SITUATION
- o BRIEFLY REVIEW CURRENT INDUSTRY AND AGENCY POLICIES
- o PROJECT FUTURE TRENDS OF PHYSICAL CROWDING WITH THE PRESENT NON-POLICY
- o PROPOSE SOLUTIONS THAT CAN BE IMPLEMENTED IN THE NEAR FUTURE
- o USE PREVIOUS WORK AS MUCH AS DESIRABLE

CHARACTERISTICS OF THE GEOSTATIONARY ORBIT RING (FIG. 1)

- o THIS IS A SPECIAL, SINGULAR ONE OF ALL THE GEOSYNCHRONOUS ORBITS.
- o ITS EXACT ALTITUDE ABOVE THE EARTH IS 35,787 KM (19,323 NAUTICAL MILES).
- o IT IS EXACTLY CIRCULAR, OVER EARTH'S EQUATOR.
- o THE ORBITAL PERIOD IS 1,436.2 MINUTES (1 DAY, RELATIVE TO THE STARS).
- o THE VELOCITY OF OBJECTS IN THE ORBIT IS 3,074.8 METERS/SEC (5,977.0 MPH).
- o IT IS PERMANENT. OBJECTS PLACED AT THIS ALTITUDE, ESSENTIALLY STAY THERE. THEY DECAY 1 KILOMETER EVERY THOUSAND YEARS.
- o GRAVITY FORCES OF THE EARTH, MOON AND SUN CONTINUOUSLY ACT TO MODULATE THE MOTION OF UNCONTROLLED OBJECTS IN THE GEOSTATIONARY ORBIT RING.
- o TO STAY IN THE GEOSTATIONARY RING REQUIRES CONTINUAL ROCKET CORRECTION OF SPACECRAFT POSITION IN BOTH THE EAST-WEST AND THE NORTH-SOUTH DIRECTIONS.
- o THE EAST-WEST ROCKET IMPULSE REQUIRED TO MAINTAIN POSITION IS A MAXIMUM OF 2.1 METERS/SEC PER YEAR. THE FUEL MASS NEEDED IS 0.07 % TO 0.1 % OF THE SPACECRAFT MASS, EACH YEAR.
- o THE NORTH-SOUTH ROCKET IMPULSE REQUIRED TO MAINTAIN POSITION AT THE EQUATOR IS ABOUT 53 METERS/SEC PER YEAR. THE FUEL MASS REQUIRED IS ABOUT 1.8 % TO 2.3 % OF THE SPACECRAFT MASS, EACH YEAR.

VALUE AND USEFULNESS OF THE GEOSTATIONARY ORBIT RING

- o SPACECRAFT IN CIRCULAR ORBIT OVER THE EQUATOR, AT THE EXACT ALTITUDE, MOVE AT EXACTLY THE SAME ANGULAR RATE AS THE EARTH BENEATH THEM.
- o WHEN VIEWED FROM EARTH THESE SPACECRAFT HAVE NO APPARENT MOTION.
- o ANTENNAS ON THE GROUND CAN BE NON-MOVING, SMALL, LOW COST AND HIGH-GAIN. THIS ALLOWS MILLIONS OF DIRECT USERS, WHO CAN NOT AFFORD TRACKING ANTENNAS.
- o ANTENNAS ON THE SPACECRAFT CAN BE NEARLY NON-MOVING, SMALL, LIGHT AND EASILY HOLD A TIGHT-FOCUSSED BEAM ON SMALL AREAS OF THE EARTH.
- o THIS ORBIT IS UNIQUE. ONLY THIS PARTICULAR CIRCULAR ALTITUDE OVER THE EQUATOR HAS THESE CHARACTERISTICS.
- o DESPITE THE APPARENT "INFINITY OF SPACE", THE GEOSTATIONARY RING ITSELF IS A STRICTLY LIMITED, VALUABLE TERRITORY ONLY 264,930 KILOMETERS LONG.
- o THE GEOSTATIONARY ORBIT RING, ESPECIALLY AT THE STABLE POINTS AT 107° WEST AND 76° EAST LONGITUDE, IS AN UNIQUELY VALUABLE NATURAL RESOURCE. IT WILL BECOME UTTERLY WORTHLESS AND UNUSABLE IF FURTHER SERIOUSLY LITTERED WITH MOVING TRASH.

OPERATING SPACECRAFT IN THE GEOSTATIONARY RING, 1982 (FIG. 2)

- o 37 COMMERCIAL COMMUNICATION SPACECRAFT
- o 11 WEATHER-WATCHING SPACECRAFT
- o 1 ORBITING ASTRONOMICAL TELESCOPE
- o 46 GOVERNMENT AND MILITARY SPACECRAFT (U. S. AND OTHER)
- o 25 RUSSIAN SPACECRAFT
- o TOTAL, 120 (INCLUDING ECCENTRIC ORBITS)

51 GEOSTATIONARY SPACECRAFT ARE OPERATING IN THE WESTERN HEMISPHERE.

- o CURRENT TRENDS INDICATE THE NUMBER OF OPERATING SPACECRAFT WILL DOUBLE EVERY FIVE YEARS.
- o THE ESSENTIAL VALUE OF THESE SPACECRAFT IS INCREASING RAPIDLY: CORPORATIONS ARE DEPENDING ON THEM FOR PROCESS CONTROL; THE NATION IS DEPENDING ON THEM FOR DEFENSE COMMUNICATION; NASA WILL BE DEPENDING ON THE TDRSS FOR SPACECRAFT CONTROL.

CHARACTERISTICS OF INCLINED GEOSYNCHRONOUS ORBITS

- o AN INFINITE VARIETY OF ORBITS CAN ALL BE GEOSYNCHRONOUS.
- o ALL HAVE ORBITAL PERIOD OF 1436.2 MINUTES (1 DAY, RELATIVE TO THE STARS)
- o ALL HAVE THE SAME AVERAGE ALTITUDE AS THE GEOSTATIONARY RING.
- o THEY MAY HAVE ANY INCLINATION TO EQUATOR, AND MAY NOT BE CIRCULAR.
- o ALL OBJECTS IN THESE INCLINED ORBITS CROSS THE EQUATOR TWICE EACH DAY WITH AN AVERAGE ORBITAL VELOCITY OF 3,075 M/SEC. THEY MAY CROSS AT THE GEOSTATIONARY RING ALTITUDE.
- o THE EQUATORIAL CROSSING POINT OF AN OBJECT WILL SLOWLY DRIFT CYCLICALLY ALONG THE EQUATOR DUE TO UNBALANCED EARTH GRAVITY ATTRACTION.
- o WHEN CORRECTIONAL ROCKET THRUST IS REMOVED FROM ANY SPACECRAFT IN THE GEOSTATIONARY RING, ITS ORBIT WILL IMMEDIATELY BEGIN INCLINING.
- o ALL OBJECTS IN THESE ORBITS ARE AS PERMANENT AS IN THE GEOSTATIONARY RING.
- o ROCKET THRUST IS REQUIRED TO REMOVE OBJECTS FROM THIS ALTITUDE.

DRIFT FORCES, EAST AND WEST (FIG. 3)

- o THE EARTH'S EQUATOR IS ELLIPTIC BY ABOUT 70 METERS. THE HIGH POINTS OF GRAVITY ATTRACTION ARE:

NEAR 107° WEST, OVER THE PACIFIC OCEAN (SOUTH OF DENVER);

AND NEAR 76° EAST, OVER THE INDIAN OCEAN (SOUTH OF BOMBAY).

- o ANY OBJECT THAT CROSSES THE EQUATOR AT THESE STABLE POINTS WITH EXACTLY AVERAGE GEOSTATIONARY VELOCITY, WILL CONTINUE TO CROSS AT THESE POINTS.
- o ANY OBJECT THAT AVERAGES GEOSYNCHRONOUS VELOCITY WHEN CROSSING THE EQUATOR AT A NON-STABLE POINT, TENDS TO BE ATTRACTED BY THE NEAREST STABLE POINT. IT WILL CONTINUE TO MOVE ITS EQUATORIAL CROSSINGS SLOWLY ALONG THE EQUATOR, IN AN EAST-WEST DIRECTION, OSCILLATING CONSTANTLY ACROSS THE STABLE POINT.
- o IT WILL GO ABOUT TWICE AS MANY DEGREES OF LONGITUDE IN EACH CYCLE OF OSCILLATION AS ITS ORIGINAL DISTANCE FROM THE STABLE POINT.
- o THE PERIOD OF EACH OSCILLATION ALONG THE EQUATOR IS 820 DAYS OR MORE.
- o THE OSCILLATION PAST THE STABLE POINT WILL CONTINUE FOREVER, SINCE THERE ARE NO DAMPING FORCES TO SLOW OBJECTS IN THIS EAST-WEST OSCILLATION.

DRIIFT FORCES, NORTH AND SOUTH (FIGURE 4)

- o THE GRAVITATIONAL ATTRACTION OF THE MOON AND SUN CHANGES THE INCLINATION OF ALL GEOSYNCHRONOUS ORBITS.
- o DUE TO THIS ATTRACTION, A SPACECRAFT THAT LOSES ITS ROCKET THRUST, OR ANY OTHER OBJECT ORIGINALLY IN GEOSYNCHRONOUS EQUATORIAL ORBIT, WILL IMMEDIATELY START INCLINATION OF ITS ORBIT AT AN INITIAL RATE OF ABOUT 0.86° PER YEAR.
- o MAXIMUM INCLINATION OF NEARLY 15° WILL BE ACHIEVED IN ABOUT 27 YEARS, THEN INCLINATION WILL DECREASE TO ZERO IN ANOTHER 27 YEARS. A FULL CYCLE IS 54 YEARS.

DEBRIS NOW INTERSECTING GEOSTATIONARY RING TWICE DAILY (FIG. 5)

- o AT LEAST 26 DEAD SPACECRAFT: SYNCOM -1, -2, -3; EARLY BIRD; INTELSAT 2 -F2, -F3, -F4; 1968 81 -A, -B, -C, -D; INTELSAT 3 -F3, -F7; SKYNET A; NATO 1; 1969-13A; NATO 2; 1971-21A; 1973-100A, -100B; MOLNIYA 1S; SMS 1; SYMPHONIE B; 1975-118A; CTS;
- o AT LEAST 25 CENTAUR UPPER STAGES.
- o AT LEAST 10 EJECTED APOGEE KICK MOTORS THAT ARE NOT TRACKED.
- o AT LEAST 15 TRANSTAGE UPPER STAGES, SOME OF WHICH MAY HAVE EXPLODED.

(THE ONLY TRANSTAGE LAUNCHED TO A 700 KM ALTITUDE BLEW UP, PRODUCING 465 TRACKABLE PIECES. VERY FEW OF THE PIECES FROM SUCH AN EXPLOSION AT GEOSYNCHRONOUS ALTITUDE WOULD BE TRACKABLE.)
- o 45 OF THESE MAJOR ITEMS ARE IN THE WESTERN HEMISPHERE.
- o THREE YEARS AGO THERE WERE 200 OBJECTS LARGER THAN 1 METER THAT COULD BE TRACKED. THERE ARE NOW MORE THAN 400 TRACKABLE OBJECTS.
- o THERE ARE ALSO AN ESTIMATED 1600 SMALLER OBJECTS WHICH CANNOT BE TRACKED (BASED ON TESTS AT LOWER ALTITUDE).

THE SCANNING OF DEBRIS ACROSS AND ALONG THE RING (FIGS. 6, 7 AND 8)

- o THE FORCES THAT HAVE BEEN DEFINED CONSTRAIN ALL DEBRIS AT GEOSYNCHRONOUS ALTITUDE TO CONTINUE TO SCAN ACROSS AND ALONG THE GEOSTATIONARY RING; RANDOMLY, FREQUENTLY, AND ENDLESSLY.

- o AN OBJECT IN GEOSYNCHRONOUS ORBIT CROSSES THE EQUATOR TWICE EACH DAY. ITS AVERAGE ORBITAL VELOCITY IS ABOUT 3,075 M/SEC.
THE NORTH-SOUTH COMPONENT OF ITS ORBITAL VELOCITY IS:
 - 107 METERS/SEC, FOR A 2° INCLINATION (208 MILES/HR)
 - 796 METERS/SEC, FOR A 15° INCLINATION (1,547 MILES/HR)
 - 1,467 METERS/SEC, FOR A 28.5° INCLINATION (2,852 MILES/HR)

- o PERTURBATIONS OF THE ORBITS OF GEOSYNCHRONOUS DEBRIS CANCEL, IN THE LONG RUN. EVEN THOUGH ALMOST ALL EQUATORIAL CROSSINGS ARE NOT THROUGH THE GEOSTATIONARY ORBIT RING; THE STATISTICS TEND TO MAXIMIZE EQUATORIAL CROSSINGS AT THAT ALTITUDE.

- o THE EQUATORIAL CROSSING POINTS OF GEOSYNCHRONOUS DEBRIS DRIFT SLOWLY; EAST, WEST, THEN EAST AGAIN, CROSSING AT A DIFFERENT POINT EACH TIME.

- o COLLISION WILL OCCUR IF DEBRIS AND AN OPERATING GEOSTATIONARY SPACECRAFT INTERSECT AT THE SAME ALTITUDE.

- o THE WRECKAGE OF THE COLLISION PRODUCES MANY MORE DEBRIS PARTICLES, WHICH WILL THEN ALSO INTERSECT THE GEOSTATIONARY RING.

- o IN EFFECT, THE DEBRIS MAKES THE ORBIT RING AN ENDLESS SHOOTING GALLERY.

THE CHANCES AND EFFECTS OF COLLISION

SOURCE: DONALD KESSLER OF NASA/JSC

- o RIGHT NOW, THE CHANCES OF COLLISION BETWEEN ANY TWO OBJECTS IN GEOSYNCHRONOUS ORBIT IS CALCULATED TO BE 0.002 % (20 IN A MILLION) PER YEAR.
- o AT THE CURRENT RATE OF INCREASE OF OBJECTS IN GEOSYNCHRONOUS ORBIT, THE CHANCES OF COLLISION THERE ARE ABOUT 4 % IN THE NEXT 10 YEARS. IN THE YEAR 2000 IT WILL BE 5 % PER YEAR.
- o NORAD IS NOT TRACKING SYNCHRONOUS ORBITING OBJECTS SMALLER THAN 1 METER OR PLACED PRIOR TO 1970. THERE ARE 5 OR MORE OBJECTS IN GEOSYNCHRONOUS ORBIT FOR EVERY ONE THAT IS TRACKED.
- o EACH COLLISION WILL PRODUCE DEBRIS THAT WILL ENTER NEW, UNPREDICTABLE ORBITS AND WILL PRODUCE FURTHER COLLISIONS.
- o 3 MILLION PARTICLES LARGER THAN 1 MM AND 14,000 PARTICLES LARGER THAN 1 CM CAN BE PRODUCED BY A COLLISION WITH A MAJOR OBJECT. THESE NEW PARTICLES WILL THEN PRODUCE MORE COLLISIONS.
- o A 1 CM OBJECT IN A 15° INCLINED ORBIT CAN HIT AN OBJECT IN GEOSTATIONARY ORBIT AT 800 METERS PER SECOND (THE SPEED OF A RIFLE BULLET). THIS PRODUCES ENOUGH FORCE TO VAPORIZE A HOLE THROUGH MORE THAN 1 CM OF ALUMINUM OR 1/8 INCH OF STEEL.



REMOVAL POLICIES OF SOME ORGANIZATIONS

- o THE WRITTEN POLICY OF THE INTELSAT BOARD OF GOVERNORS NOW IS:
"DESYNCHRONIZE UNUSABLE SPACECRAFT UPWARD, 40 TO 50 KM."
- o THE WRITTEN POLICY OF NOAA'S NATIONAL ENVIRONMENTAL SATELLITE SERVICE IS:
"DESYNCHRONIZES UPWARD AT LEAST 300 KM."
- o RUSSIA DOES NOT CIRCULARLY DESYNCHRONIZE, BUT HAS FIRED TO PRODUCE LARGE ECCENTRICITY, WHICH REDUCES THE CHANCES OF CROSSING ON THE RING.
- o THE AIR FORCE SPACE COMMAND POLICY IS TO CONSIDER REMOVAL TO SAFE POSITION.
- o SEVERAL GROUPS CONTACTED PREVIOUSLY HAD NOT EVEN CONSIDERED REMOVAL. THEY FELT MERK TURNOFF IS ADEQUATE.
- o THE GEOSYNCHRONOUS EQUATORIAL ORBIT IS "CROWDED" NEAR 107° WEST, AND WILL BECOME MORE SO. SOME GROUPS PLAN TO OPERATE THERE. OTHERS PLAN TO DUMP THEIR UNUSABLE SPACECRAFT THERE.
- o THOSE WITH LEAST OPERATIONAL EXPERIENCE TEND TO TAKE A "WHAT? ME WORRY!" ATTITUDE. THOSE WITH THE MOST EXPERIENCE ARE CONCERNED ABOUT THE COLLISION PROBABILITIES AND HAVE ADOPTED POLICIES TO DESYNCHRONIZE UPWARD.

BASIS FOR RECOMMENDATIONS

- o THERE ARE OVER 400 OBJECTS INTERSECTING THE GEOSTATIONARY RING AND THE NUMBER IS GROWING RAPIDLY.
- o THE GEOSTATIONARY ORBIT RING IS AN UNIQUE, VALUABLE TERRITORY.
- o GEOSYNCHRONOUS ORBIT OCCURS AROUND THE EARTH AT 35,787 KILOMETERS AVERAGE ALTITUDE. A GEOSYNCHRONOUS OBJECT CAN HAVE ANY INCLINATION AND WILL CROSS A PARTICULAR EQUATORIAL POINT TWICE EACH DAY.
- o THIS CROSSING POINT MOVES SLOWLY AND CONTINUOUSLY ALONG THE EQUATORIAL RING, PRODUCING CONCENTRATED COLLISION HAZARD.
- o FOR ANY OBJECT IN INCLINED ORBIT, THE NORTH-SOUTH COMPONENT OF VELOCITY AT EQUATORIAL CROSSING IS HIGH AND DANGEROUS TO GEOSTATIONARY SPACECRAFT
- o SAFE AND ADEQUATE DESYNCHRONIZATION CAN BE DONE BY CHANGING SPACECRAFT ALTITUDE UPWARD 100 KM OR MORE. THIS CAN BE ACHIEVED WITH FUEL EQUAL TO LESS THAN 0.2 % OF SPACECRAFT MASS; A 1-MONTH AMOUNT OF EAST-WEST FUEL.
- o DEORBITING TO EARTH IS NOT REQUIRED. THIS WOULD REQUIRE A FUEL AMOUNT NEARLY 50 PERCENT OF THE REMAINING SPACECRAFT MASS.
- o SINCE COMMERCIAL PRESSURES REQUIRE EACH COMMERCIAL USER TO REMAIN IN GEOSYNCHRONOUS ORBIT AS LONG AS POSSIBLE, TO SQUEEZE THE LAST DROP OF REVENUE OUT OF THE FUEL TANKS, THEY ARE RELUCTANT TO DESYNCHRONIZE, UNLESS A RULE FORCES THEM TO.

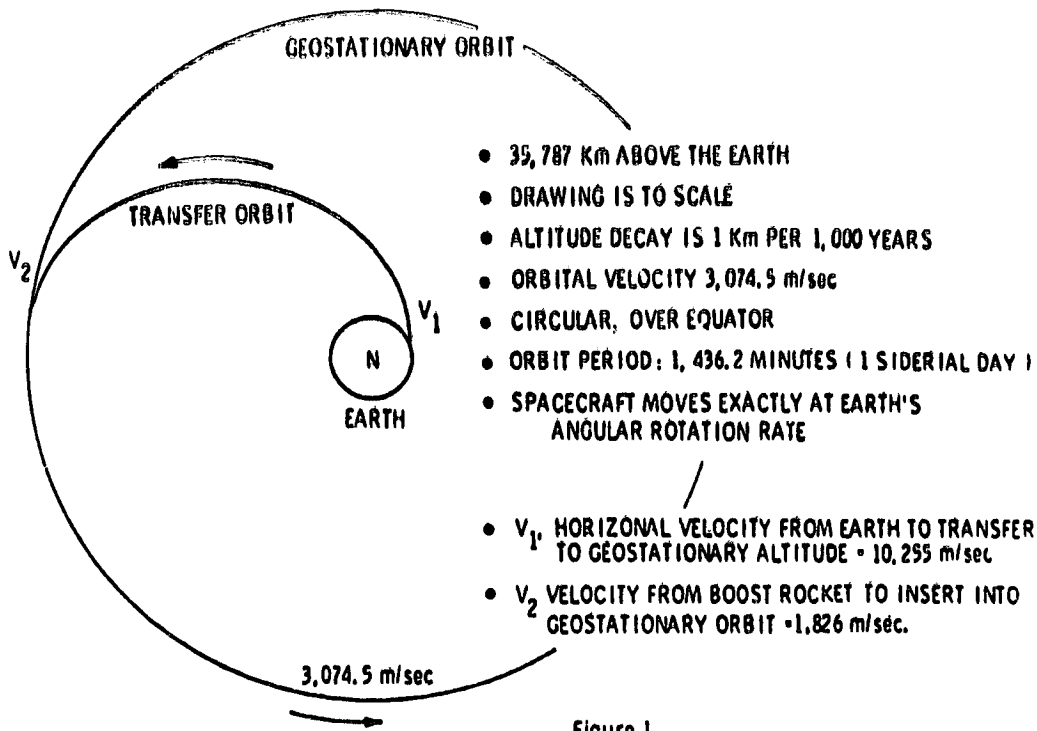
RECOMMENDATIONS FOR ACTION

DUE TO THE COLLISION HAZARD, NASA POLICY SHOULD BE:

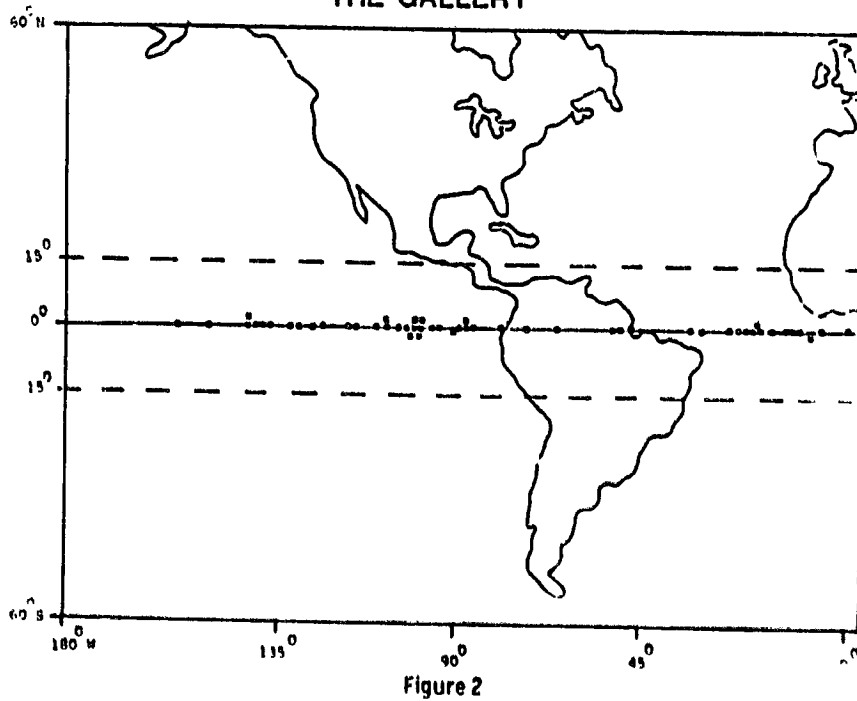
1. THE LAST FIRING, REQUIRED TO INSERT A SPACECRAFT INTO SYNCHRONOUS ORBIT, MUST BE DONE BY A PROPULSION SYSTEM THAT REMAINS ATTACHED TO THE SPACECRAFT.
2. NO OBJECTS SHALL BE RELEASED INTO SYNCHRONOUS ORBIT FROM SPACECRAFT.
3. DESYNCHRONIZE GEOSYNCHRONOUS SPACECRAFT AS FAR AS POSSIBLE AT THE END OF THEIR USEFUL LIFE. FUEL MUST BE RETAINED FOR THIS PURPOSE.
4. MOVEMENT INTO A HIGHER (WESTWARD DRIFTING) ORBIT SHALL BE USED, IF POSSIBLE, TO AVOID COMMUNICATION INTERRUPTION AND IMPEDING LATER ARRIVALS.
5. THERE SHOULD BE GOVERNMENTAL AGREEMENT REQUIRING ALL GEOSYNCHRONOUS ORBIT USERS TO DESYNCHRONIZE BEFORE THEIR FUEL RUNS OUT.
6. NASA AND THE U. S. SHOULD STRIVE TO ESTABLISH A WORLD-WIDE POLICY FOR REMOVAL, BINDING ON ALL USERS OF THE GEOSYNCHRONOUS ORBIT.
7. ULTIMATELY, NASA SHOULD PLAN AND CARRY OUT A PROCEDURE FOR CLEARING DEAD SPACECRAFT AND DEBRIS FROM THE GEOSYNCHRONOUS ORBIT.



GEOSTATIONARY ORBIT RING



51 OPERATING SPACECRAFT, 1982 WESTERN HEMISPHERE POSITIONS "THE GALLERY"



GEOSTATIONARY ORBIT GRAVITY ATTRACTION EQUATORIAL STABLE POINTS

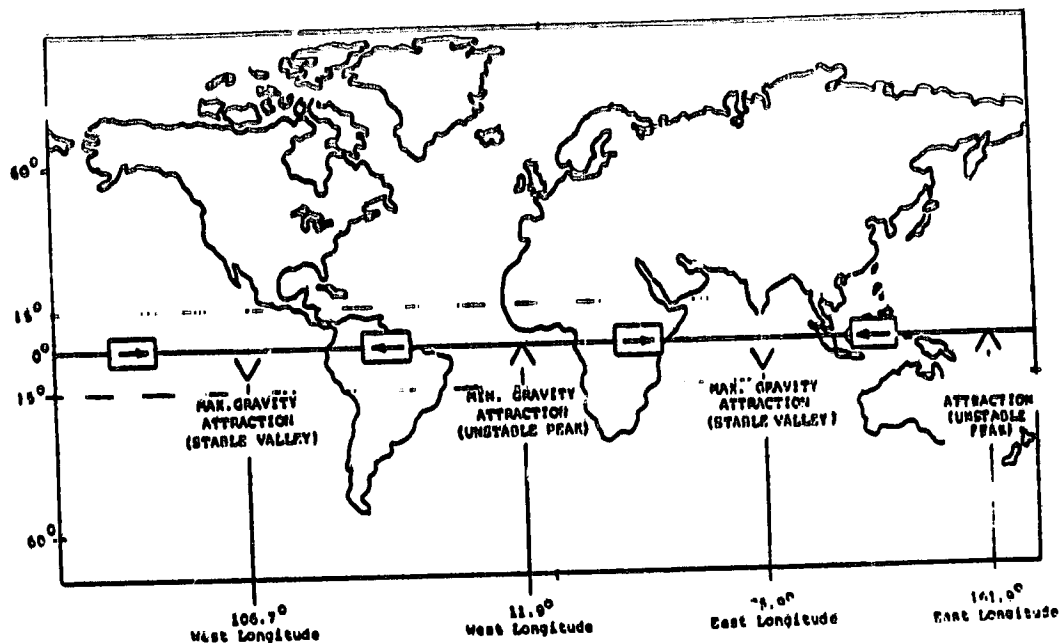


Figure 3

CHANGE OF 24 HR. ORBIT INCLINATION DUE TO GRAVITY OF SUN AND MOON

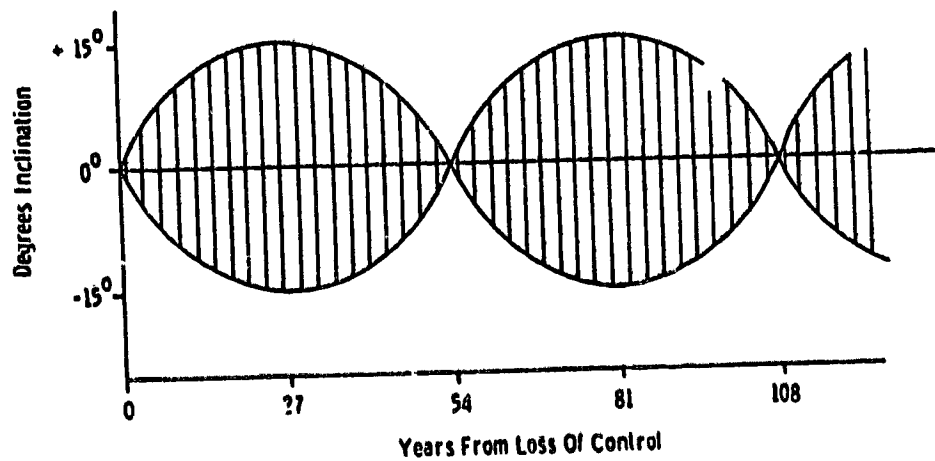


Figure 4

MAJOR OBJECTS IN GEOSTATIONARY RING

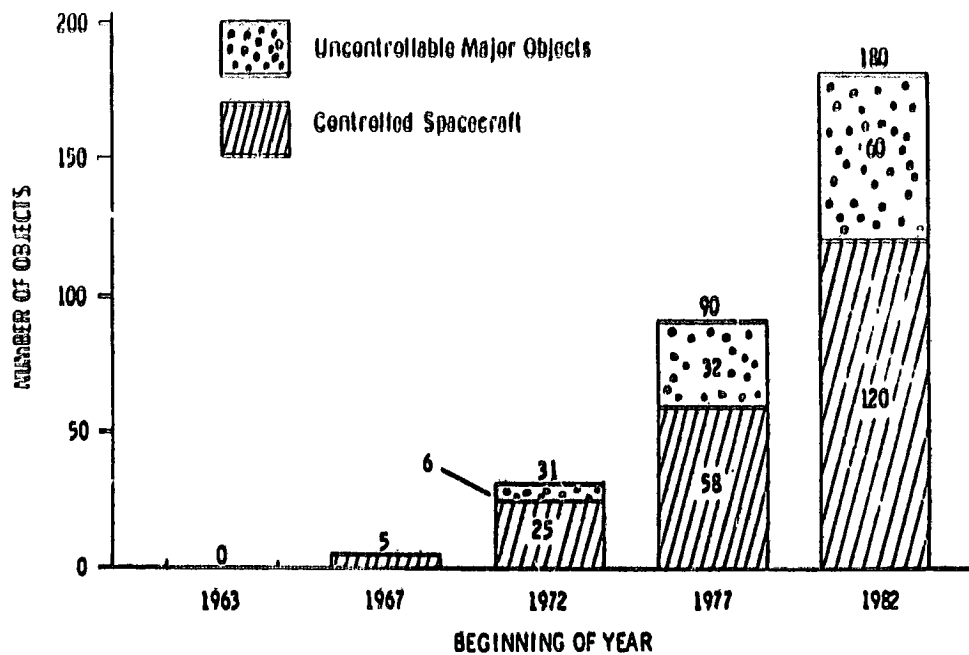


Figure 5

1-YEAR PATH OF EQUATOR CROSSINGS (Schematic) 4 of 45 UNCONTROLLABLE MAJOR OBJECTS (1982) "THE SHOOTERS"

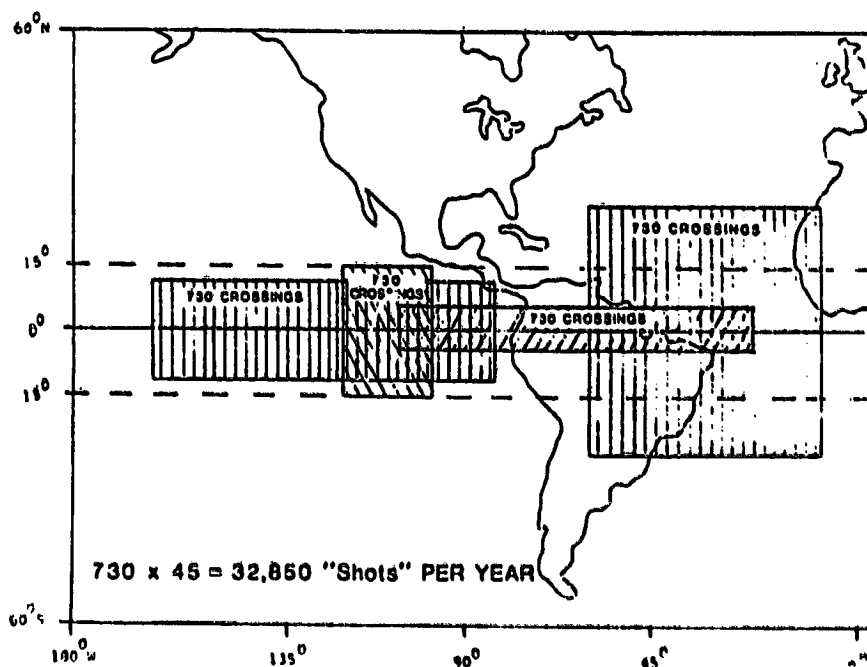


Figure 6

51 OPERATING SPACECRAFT,
1982 WESTERN HEMISPHERE POSITIONS
"THE SHOOTING GALLERY"

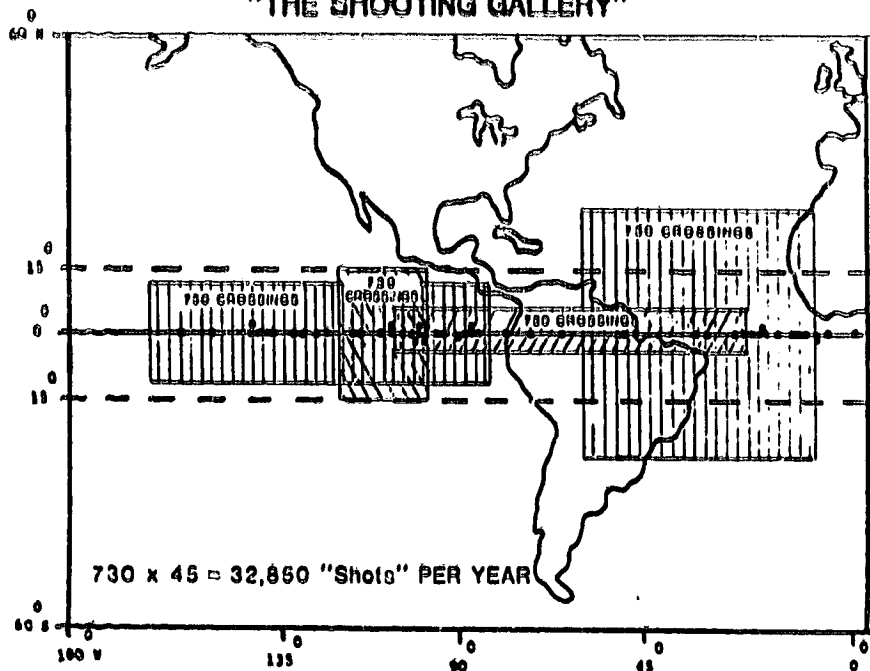


Figure 7

ORBITAL INTERSECTION

- SPACECRAFT AND DEBRIS AT 24 HR ALTITUDE
DEBRIS INCLINATION 15°
- IMPACT VELOCITY 796 m/sec (1,500 Miles per hour)

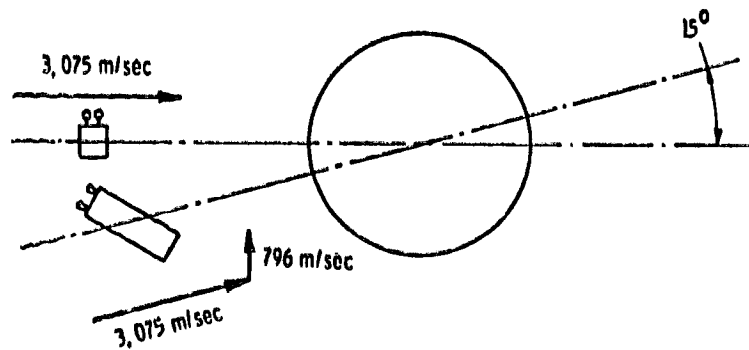


Figure 8

Space Debris

An AIAA Position Paper

MALCOLM G. WOLFE

*Prepared by the
AIAA Technical Committee on Space Systems*

July 1981

SUMMARY

The presence of man-made debris in orbit about the earth presents a hazard to spacecraft operating in that environment. The level of hazard to a given spacecraft depends on the size of the spacecraft, the number and size of debris fragments in its operating environment, and the length of time the spacecraft remains on orbit. Efforts to provide a definitive assessment of this problem have been directed toward analyzing the hazard level presented by particular debris populations and predicting how this hazard level will change with time. Much less effort has been directed toward satellite design and strategies to minimize the short-term and long-term effects of debris deposition.

A key aspect of the on-orbit debris hazard is that it is self-perpetuating. This arises from three factors: (1) a single spacecraft launch can be responsible for a multitude of hazardous objects in space; (2) orbital debris tends to disperse randomly, producing high intersection velocities and making avoidance extremely difficult; and (3) objects accumulate in earth orbit rather than passing through the near earth space in the manner of meteoroids. Impact protection may not be feasible in most cases because of the likelihood of very high approach velocities and the fact that certain protuberances, especially those of relatively large area such as solar arrays and antennae, cannot easily be permanently shielded. Evasive maneuvering techniques may reduce the *present* probability of collision for specific satellites in certain circumstances, but do not provide a practical long-term solution.

The only natural mechanism opposing debris buildup is removal by atmospheric drag. However, this process can take a very long time, especially from high altitudes, and causes debris to migrate from higher to lower altitudes. Another mechanism, collection by a spacecraft ("orbital garbage truck") would be extremely difficult and expensive. Prevention of debris formation is the most effective approach.

At the present time, the collision hazard is real but not severe. However, continuation of present policies and practices ensures that the probability of collision will eventually reach unacceptable levels, perhaps within a decade. Future problems can be forestalled by initiating studies and implementing their results in five major areas: (1) education, (2) technology, (3) satellite and vehicle design, (4) operational procedures and practices, and (5) national and international space policies and treaties.

There is presently no coordinated national or international concern for space use management. The National Aeronautics and Space Administration (NASA), the Department of Defense (DoD), and other organizations using the near-earth space environment should perform a combined and detailed evaluation of debris control, including both design and operations practices and policies. In addition, a dialog should be initiated as soon as possible to involve other countries and the United Nations in developing practical design and operating standards and regulatory policies. The impact of program and policy decisions relevant to the deposition of objects in orbit should be understood by all space users for both immediate and future space operations.

INTRODUCTION

Although the natural meteoroid environment has been considered in the designs of past and existing spacecraft, future satellite designs may have to take account of space debris in addition to the natural environment.

Man-made space debris differs from natural meteoroids because it is in permanent earth orbit during its lifetime and is not transient through the regions of interest. As a consequence, a given mass of material presents a greater problem in the design and operation of spacecraft because of the extended time period over which there is a collision risk.

Past design practices and deliberate and inadvertent explosions in space have created a significant debris population in operationally important orbits. The debris consists of spent spacecraft and rocket stages, separation devices, and explosion products. Much of this debris is resident at altitudes of considerable operational interest. Products larger than 10 cm² in low orbits can be observed directly. The existence of a substantially larger population of small fragments can be inferred from terrestrial tests in which the particle distributions from explosions have been assayed. From these tests it is reasonable to infer small particle numbers, of the order of 10 thousand for each low-intensity explosion and 10 million for high-intensity explosions.

Two types of space debris are of concern: (1) large objects whose population, while small in absolute terms, is large relative to the population of similar masses in the natural flux (by a factor of about 10³); and (2) a larger number of smaller objects whose size distribution approximates natural meteoroids. The interaction of these two classes of objects, combined with their long residual times in orbit, leads to the further concern that inevitably there will be collisions producing additional fragments and causing the total population to grow rapidly.

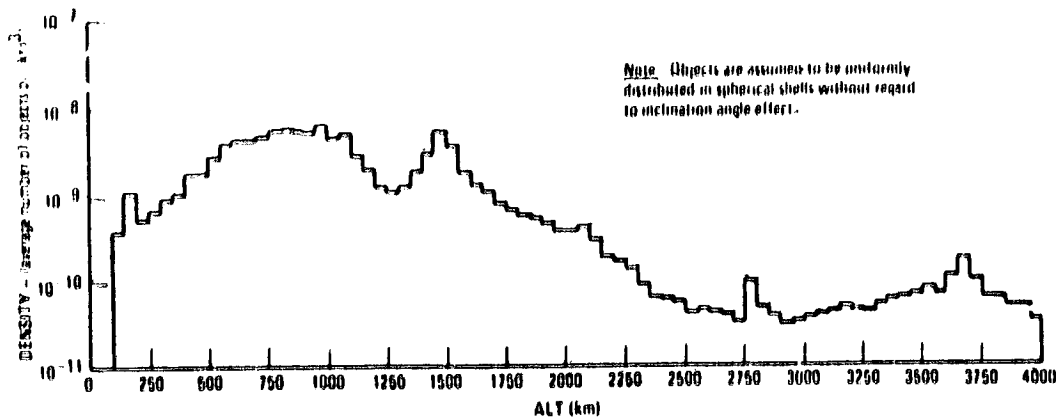
PROBLEM DEFINITION

The space debris population consists mostly of explosion fragments, but also includes operating and expended satellites; mission-related objects such as shrouds, clamps, and separation components; and spent propulsive elements. The larger of these can be tracked by the North American Aerospace Defense Command (NORAD), but the smaller ones cannot. In addition to the problem of future orbit prediction, those objects that can be tracked are difficult to track with the precision required to prevent collisions.

Analysis has identified three areas of concern: (1) the hazard from the tracked population, (2) the hazard from the untracked population, and (3) the hazard from the future population. These are manifested in both low earth orbit (below 2000 km) and geostationary orbit.

Tracked Population

NORAD is presently tracking more than 5000 objects in space. Most appear to be larger than about 10 cm in diameter, are in low earth orbit, and originate from explosions - either U.S. spent Delta stages or USSR anti-satellite tests. Over the last 10 yrs this population has grown at a rate of about 10%



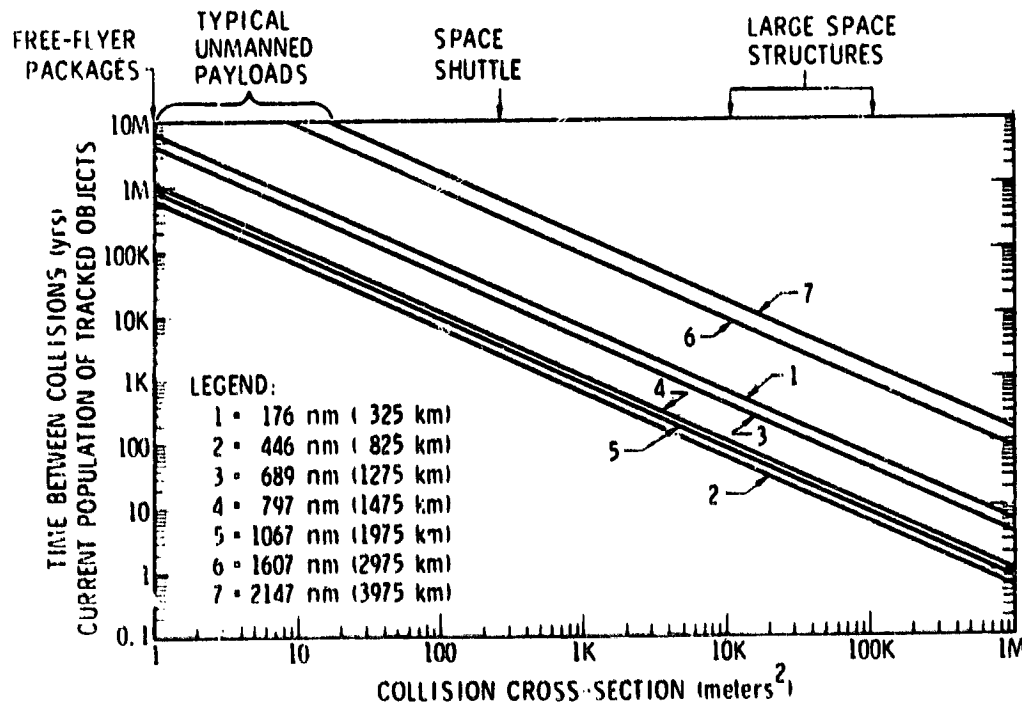
Source: Adapted From: Chobotov, V. A., "Collision Hazard in Space," The Aerospace Corporation Report TR-0081(6790)-1, February 1981

FIG. 1 Observed Space Object Density vs. Altitude

per year. Figure 1 shows how the average number density of objects varies with altitude for the observed (tracked) population of objects. The greatest concentration is between altitudes of 500 km and 1100 km. Maximum density occurs near 850 km. Figure 2 provides a graphical representation of the hazard levels presented by tracked debris for several altitudes. This hazard is characterized by the expected time

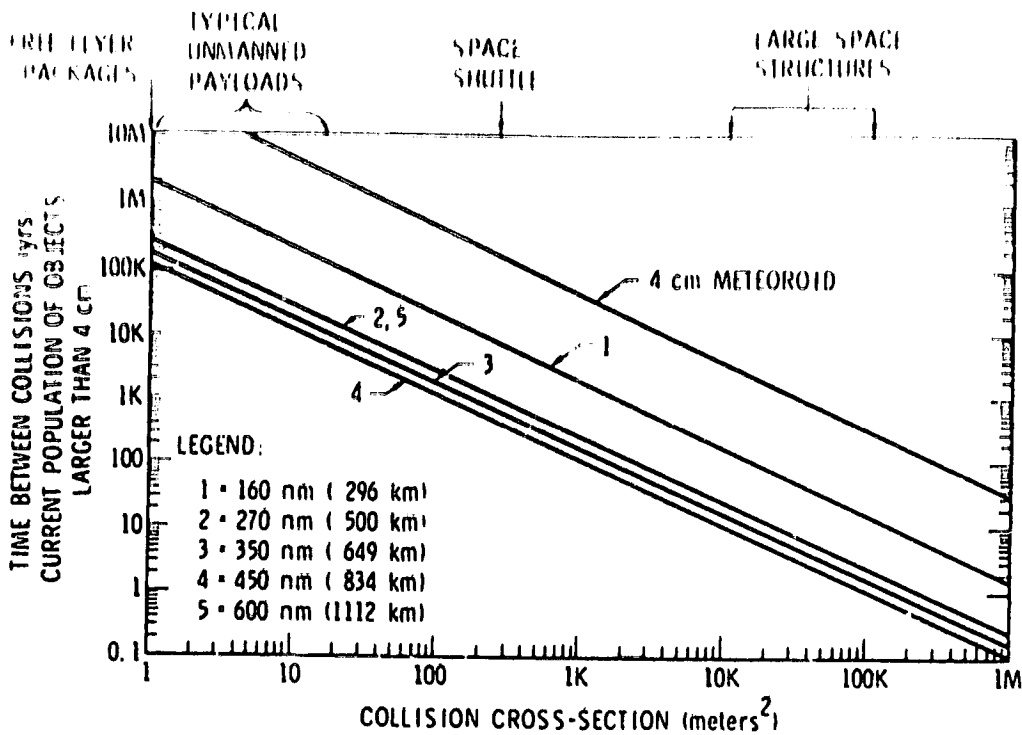
between collisions (ETBC), which is inversely proportional to the spatial density given in Figure 1, and depends on the size of the object and the altitude at which it is operating. The sizes of typical spacecraft, actual as well as projected, are also indicated in Figure 2.

The probability of collision for the space shuttle orbiter is only 4×10^{-6} for a typical 7-day flight. However, the probabil-



Source: Adapted from: Reynolds, Robert C., and Donald S. Edgecombe, "Status of the On-Orbit Debris Problem for Spacecraft in Low Earth Orbit," Battelle Briefing Notes, 13 February 1981

FIG. 2 Time Between Collisions as a Function of Collision Cross-Section and Altitude for the Current Tracked Debris Population



Source: Kessler, D. J., "Sources of Orbital Debris and the Projected Environment for Future Spacecraft," Presented at AIAA International Meeting and Technology Display, AIAA-80-0855, 6-8 May 1980

FIG. 3 Time Between Collisions as a Function of Collision Cross-Section and Altitude for the Current Background Debris Population Larger than 4 cm

ity of collision for a large 50-m diameter spacecraft in one year is about 0.031 at 500 km and 0.003 at 850 km. For geostationary satellites, the probabilities of collision with other tracked objects in one year are between 2×10^{-6} and 2×10^{-5} . However, only objects larger than approximately 1 m diameter are detected at this altitude, and the numbers may actually be greater.

Planned spacecraft cover many orders of magnitude in size; debris densities vary by several orders of magnitude. The results in ETBCs will vary from days to millions of years. Although at present the shuttle orbiter and smaller spacecraft at 850 km and below do not face a significant collision problem, future large-area spacecraft at these altitudes could be seriously endangered.

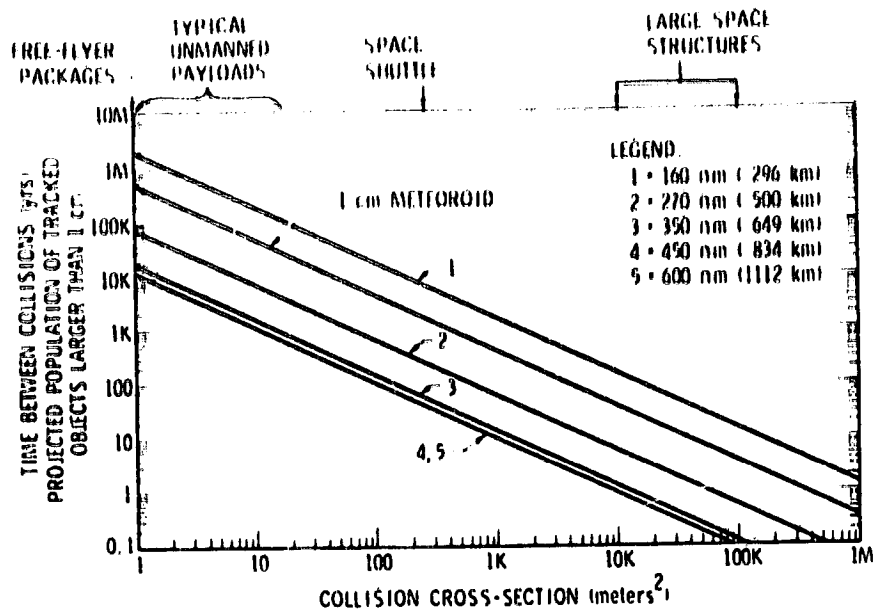
Untracked Population

An untracked population of objects is known to exist because (1) more than 60 explosions have occurred in space, undoubtedly producing many objects too small to be tracked; and (2) objects apparently as small as 4 cm in diameter are frequently detected just prior to reentry. Objects of this size, not detectable at higher altitudes, can be detected when their orbits decay to about 400 km, just before reentry. Based on the observed number of these objects at 400 km and the size distribution characteristics of particles generated in low-intensity explosions on the ground, collision probabilities can

be estimated. The collision probability of a 50-m diameter spacecraft with the 4-cm and larger population in one year is estimated to be 0.007 at 500 km and 0.016 at 850 km. These rates are characterized in Figure 3 by showing the ETBC as a function of spacecraft cross-section. The probabilities of collision are surely higher from fragments smaller than 4 cm, but the data which exist are inadequate to support definitive estimates.

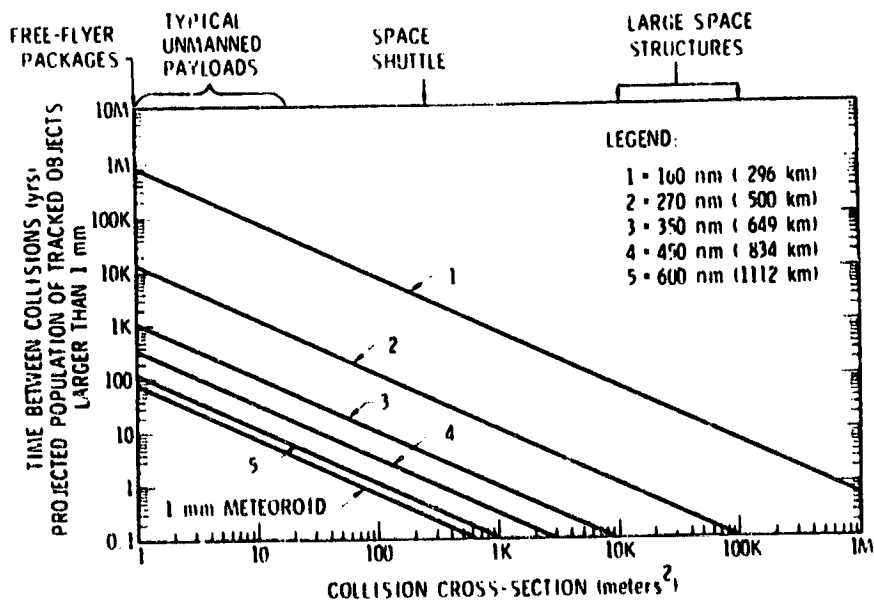
Future Population

If past trends continue, the number of tracked objects in space is predicted to increase by a factor of 2 to 8 (depending on the rate of future explosions) within the next 20 years, significantly increasing the probabilities of collision. Furthermore, there may be sufficient objects in space so that collisions could be expected between non-operational objects in low earth orbit. Just one of these collisions could produce 1.4×10^4 particles larger than 1 cm, and 3.5×10^6 particles larger than 1 mm. A 1-cm object in low earth orbit could penetrate a 5-cm thickness of solid aluminum. The collision frequency between a 50-m diameter spacecraft and the 1-cm population in the year 1995 could be about 0.033/yr at 500 km and 0.25/yr at 850 km. The increased number of small fragments could significantly reduce the reliability of even small structures. In addition, this high frequency of collision will propagate an irreversible growth in fragment population. For



Source: Based on Data From: Kessler, D. J. and B. G. Cour-Palais, "Collision Frequency of Artificial Satellites: The Creation of a Debris Belt," J. Geophysical Res., Vol. 83, No. A6, 1 June 1978, and Kessler, D. J., "Sources of Orbital Debris and the Projected Environment for Future Spacecraft," Presented at AIAA International Meeting and Technology Display, AIAA-80-0855, 6-8 May 1980

FIG. 4 Time Between Collisions as a Function of Collision Cross-Section and Altitude for the Projected Debris Populations Larger than 1 cm in the Year 1995.



Source: Based on Data From: Kessler, D. J. and B. G. Cour-Palais, "Collision Frequency of Artificial Satellites: The Creation of a Debris Belt," J. Geophysical Res., Vol. 83, No. A6, 1 June 1978, and Kessler, D. J., "Sources of Orbital Debris and the Projected Environment for Future Spacecraft," Presented at AIAA International Meeting and Technology Display, AIAA-80-0855, 6-8 May 1980

FIG. 5 Time Between Collisions as a Function of Collision Cross-Section and Altitude for the Projected Debris Populations Larger than 1 mm in the Year 1985.

illustration, the ETBCs from debris equal to or larger than 1 cm and 1 mm in diameter are shown in Figures 4 and 5, respectively, for the year 1995.

Periodically over the course of the solar sunspot eleven-year cycle, the earth's atmosphere is excited and rises significantly above its median altitude. During these periods, drag effects cause particles to migrate to lower altitudes. Eventually such a process is cleansing, but it is extremely slow and is inadequate to deal with past or present rates of debris generation.

WHAT IS BEING DONE?

There is at present no strong national or international concern for space debris management, although individual investigators are studying the problem and operational satellite program offices have expressed concern about the safety of their own satellites. Questions on the subject have been posed by the State Department, the United Nations, the National Aeronautics and Space Administration (NASA), the Office of the Under Secretary of Defense for Research and Engineering, and representatives of a number of foreign countries. However, there is no central organization to coordinate and implement the actions which may be required. In general, reclamation or disposal of space objects is not perceived by the user community as being economical or even important. For this reason, there is a tendency to view the collision problem only as it impacts the economic loss of a specific satellite or in terms of the legal liability of the responsible agency. The issue of space debris control needs to be dealt with not in this parochial fashion, but as a common problem shared by all space users.

Funded work is being carried out by the NASA Johnson Space Center (NASA/JSC), the U.S. Air Force Space Division, The Aerospace Corporation, Battelle Columbus Laboratories, and the European Space Agency. Studies are continuing to better define and predict the threat of collision. Devices to track smaller objects and to improve the accuracy of tracking are being tested. NASA/JSC is attempting to evaluate the magnitude of the problem and the effectiveness of various methods to minimize the propagation of debris. Operational procedures are being modified to reduce the probability of collision, and the probability of collision is being considered in selecting orbital parameters for new satellites. The problem of space debris has already been shown to be controllable to some degree when sound planning decisions are made.

WHAT SHOULD BE DONE?

Before any potential "solutions" become policy, it is extremely important to understand fully the problems generated by orbital debris, the alternatives for debris control, and the effectiveness of the proposed controls. Consequently, it is imperative that the formal and informal interchange of information at all levels (national and international) begin

immediately, with the ultimate goal of forming a central group to coordinate and encourage research and to recommend policy. Some of the fundamental policy and procedural questions that need to be addressed are:

- *Should a policy be adopted that requires all spacecraft to be boosted out of geostationary orbit at the end of useful life?* This would alleviate a specific, very important problem.

- *Should a policy be adopted to regulate which objects may be left in long-life orbits?* The reduction in hazard implied by the adoption of this type of policy will have to be traded off against the penalty in deliverable payload. On-orbit debris modeling will provide a quantitative assessment of such a policy. Unless this question is addressed, certain regions in the near-earth environment may become unusable.

- *If the on-orbit debris hazard becomes significant, will the use of collision avoidance systems relieve the problem?* The velocity of a spacecraft relative to the debris objects will typically be on the order of 10 km/sec. Hence, objects which are quite small (and which will be the most numerous) may cause considerable damage if a collision occurs. The small size of these objects will probably require sophisticated detection equipment on the spacecraft. The added mass for the detection system and propellant needed to perform the evasive maneuvers will reduce useful payload.

- *If the on-orbit debris hazard becomes significant, will the employment of impact protection (bumpers) relieve the problem?* The major considerations in answering this question come from the field of fracture mechanics under hypervelocity impact conditions. Bumpers will have to be able to stop particles moving at velocities on the order of 10 km/sec, while themselves producing a minimum number of debris particles. Although bumpers of any size will reduce the useful payload that can be carried, decisions on the maximum particle size to be protected against and the parts of the spacecraft which are critical and must be protected (and, therefore, on the amount of bumper material required) will be guided by a definitive knowledge of the debris population and its kinematic properties.

- *What are the implications of anti-satellite operations?* There are several military space activities which leave debris in orbit. The consequences of such actions must be understood before they are undertaken, and even if such actions are essential to national security, they should be carried out with a clear understanding of the consequences. An analysis of the debris production will not only provide information on the short-term and long-term effects, but also suggest strategies and procedures for minimizing their impact.

Comprehensive documents should be produced which specify operational and procedural techniques for minimizing debris in critical areas. In the long term, the issue must be faced cooperatively by all space users, and international agreements should be drawn up to ban or restrict to low orbit the explosion of satellites. In the interim, the United States space community should immediately institute a program for evaluating actions to minimize the collision problem for all users. Consideration should be given to:

- *Education*

—Education of the total space-user community on the critical nature of the problem

—Education of space system designers on the need for litter-free systems

• *Technology*

- Advanced ground and space-based detection techniques
- Comprehensive models of the earth-space environment
- Design and operation of a debris monitoring system
- Design and operation of a debris collection system

• *Space Vehicle Design*

- Litter-free systems
- Space system disposal by (1) retrieval, (2) earth reentry, (3) earth escape, and (4) transfer to selected "dump" regions or less-frequented orbits

—Addition of shielding to enhance survival after collisions with small debris

—Rocket designs which limit the likelihood of accidental explosions

—Designs that decentralize or minimize critically sensitive areas

• *Operational Procedures and Practices*

- Safe spacing of satellites
- Avoidance of crowding specific orbit locations
- Limitation of explosions to low altitudes so that fragments reenter quickly

—Planning of launch trajectories for early reentry of spent rocket stages and dead payloads

• *Space Policies and Treaties*

—Identification within each agency of responsible groups for recommending and implementing required actions

—Initiation of conferences at the international level to develop policy and agreements

—Identification of national and international groups responsible for coordinating research, establishing standards and policy, and enforcing agreements

CONCLUSIONS AND RECOMMENDATIONS

The AIAA believes that the space debris issue is real, that action to resolve it is imperative, and that no obvious, simplistic resolution is evident. The AIAA position can be summarized as follows:

- At the present time, the collision hazard posed by space debris is real but not severe. However, continuation of present design and operational practices and procedures ensures that the probability of collision will increase and will eventually reach unacceptable levels, perhaps within a decade.

- The space debris issue should be faced by all space users, and coordinated action should be taken immediately if the future use of space is not to be seriously restricted.

- Design to tolerate debris impact (bumpers) or to provide evasive capability may provide a measure of protection to particular satellites, but the most effective approach is to eliminate the need for such action by constraining the generation of further debris.

- The space debris problem can be forestalled by immediate action in five major areas:

- Education

- Technology

- Space vehicle design

- Operational procedures and practices

- National and international space policies and treaties.

- There is an immediate need for an international dialog to be initiated on the space debris issue, with the goal of forming responsible groups to coordinate research and recommend policy.

- Corrective action must begin now to forestall the development of a serious problem in the future.

AIAA TECHNICAL COMMITTEE ON SPACE SYSTEMS

CHAIRMAN: Mr. Richard L. Kline
Grumman Aerospace Corporation

Mr. Lewis S. Beers
General Electric Co., Space Division

Mr. Ivan Bekey
NASA Hqs.

Mr. James R. Blankenship
RCA Corp., Astro-Electronics

Dr. Robert M. Bowman
General Dynamics / Convair

Mr. Fred E. Bradley
McDonnell Douglas Astronautics Co.

Dr. Darrell Branscome
House Committee on Science &
Technology

Dr. Robert F. Brodsky
TRW Defense and Space
Systems Group

Mr. Morton H. Cohen
Fairchild Space & Electronics Co.

Dr. Kevin C. Daly
Charles Stark Draper
Laboratory, Inc.

Mr. Hubert P. Davis
Eagle Engineering Inc.

Mr. Douglas G. Dwyre
Ford Aerospace
& Communications Corp.

Dr. M. Edmund Ellison
Hughes Aircraft Co.

Mr. John A. Erickson
Honeywell Avionics Div.

Mr. Norman Fischer
Space Systems and Applications
Battelle Columbus Laboratories

Mr. Jerry J. Florey
Rockwell International

Mr. Robert J. Gunkel
McDonnell Douglas Astronautics
Company

Mr. E. Larry Heacock
NOAA / National Environmental
Satellite Service

Mr. William D. Hibbard
NASA Goddard Space Flight Center

Mr. W. Ray Hook
NASA Langley Research Center

Dr. William F. Hubbarth
IBM

Dr. Marshall Kaplan
Dept. of Aerospace Engineering
Pennsylvania State University

Mr. Paul Lane, Jr.
Aerospace Vehicle Branch
Wright-Patterson AFB

Mr. J. Preston Layton
Consultant

Mr. Benn Martin
Jet Propulsion Laboratory

Mr. Ernesto R. Martin
COMSAT General Corporation

Mr. Willfred J. Mellors
European Space Agency

Mr. B. G. Morals
Lockheed Missiles & Space
Company, Inc.

Mr. Steven Myers
Western Laboratories

Mr. David J. Rohrbaugh
Boeing Aerospace Co.

Maj. Stanley G. Rosen
USAF

Maj. Carl C. Schade
United States Air Force Academy

Mr. Peter B. Teets
Martin Marietta Corporation

Dr. Fred Teren
NASA / Lewis Research Center

Mr. H. Robert Warren
Space Applications
Department of Communications
Government of Canada

Mr. Peter G. Wilhelm
Naval Research Lab

Dr. Malcolm G. Wolfe
The Aerospace Corporation

NASA'S PARTICIPATION IN THE ITU

NASA's participation in the ITU is largely focused on the Plenipotentiary Conferences, the World Administrative Radio Conferences (WARC), the International Consultative Committee for Radio (CCIR), and the CCIR Study Groups.

The Plenipotentiary Conference has the authority to amend the guiding document of the ITU. The last conference was in 1973, the next will begin September 28, 1982.

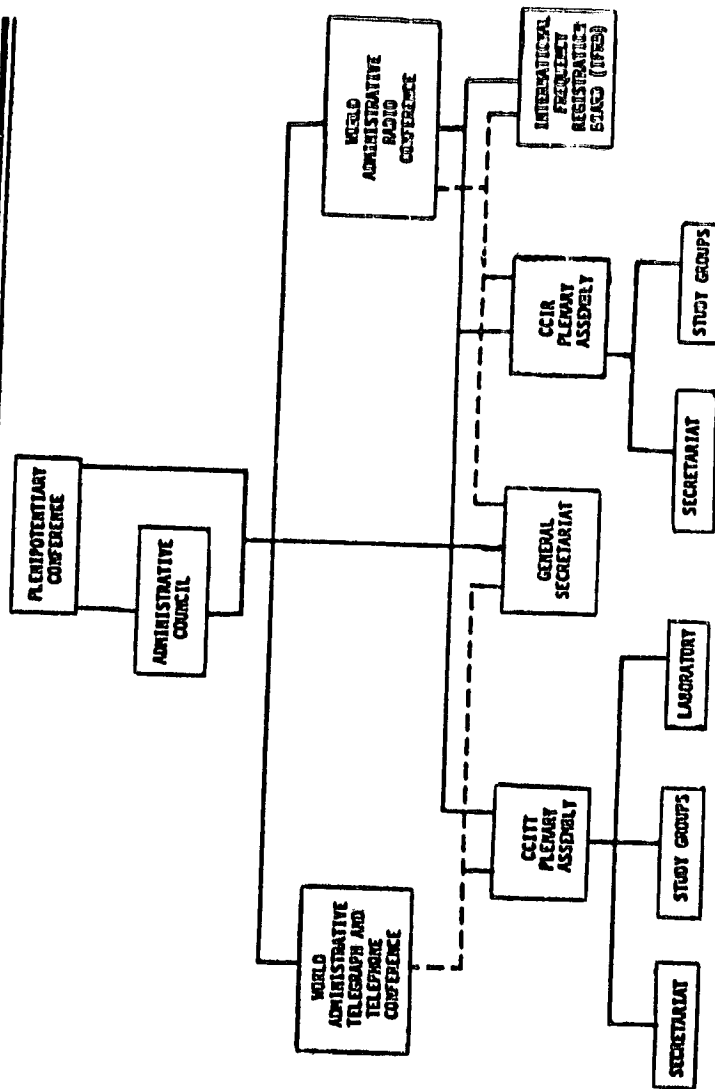
The WARC's have the authority to amend parts or all, depending on the scope of the conference, of the Radio Regulations which contain the allocations of frequencies to the different services. In the two-session 1985-87 Space Services WARC, the ITU will consider the method of allocating the orbit-spectrum resource to the services and countries which utilize the geostationary orbit.

The CCIR and its study groups provide the technical basis for the decisions made in the above mentioned conferences. The U.S. has an organization which parallels the CCIR in structure, and NASA provides strong support including several study group chairmen.

THE ITU WITHIN THE UN SYSTEM

The International Telecommunications Union (ITU) is the autonomous specialized agency within the United Nations system, with the responsibility of promoting international cooperation in the use of telecommunications. With its predecessor dating back to 1865, the ITU is the oldest of the international organizations.

ORGANIZATIONAL CHART OF ITU

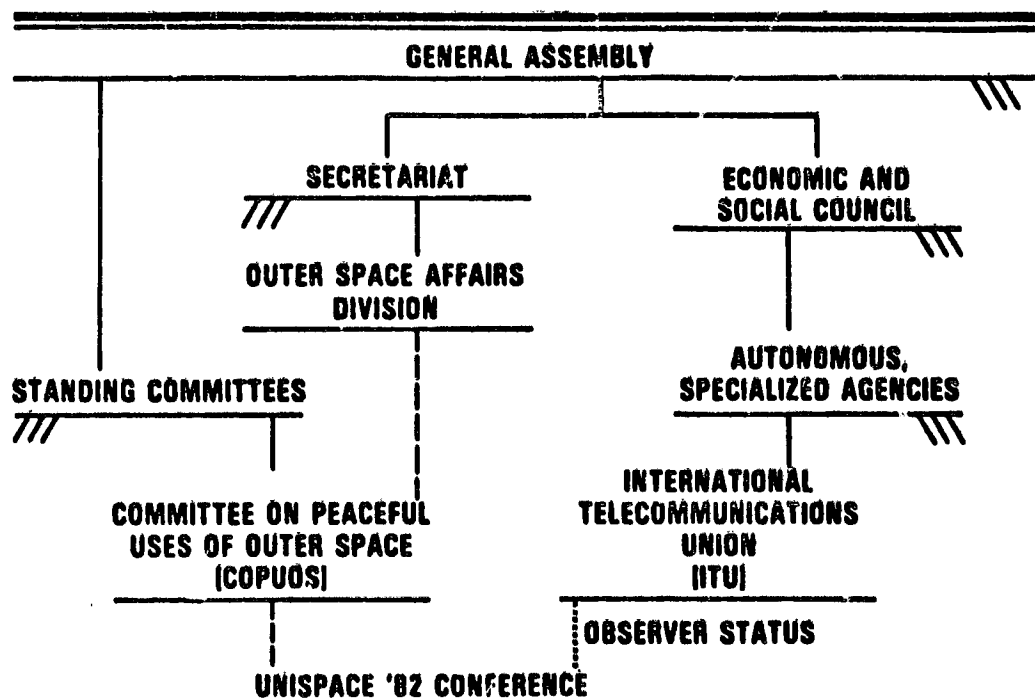


UNISPACE '82 AND THE ITU

The United Nations Conference on the Exploration and Peaceful Use of Outer Space (UNISPACE '82) is the second such conference, the first being in 1968. NASA's Administrator will head the U.S. delegation to the UNISPACE Conference.

The ITU and UNISPACE '82 are formally related within the UN system; however, UNISPACE '82 is much less structured and will be much more political than ITU conferences.

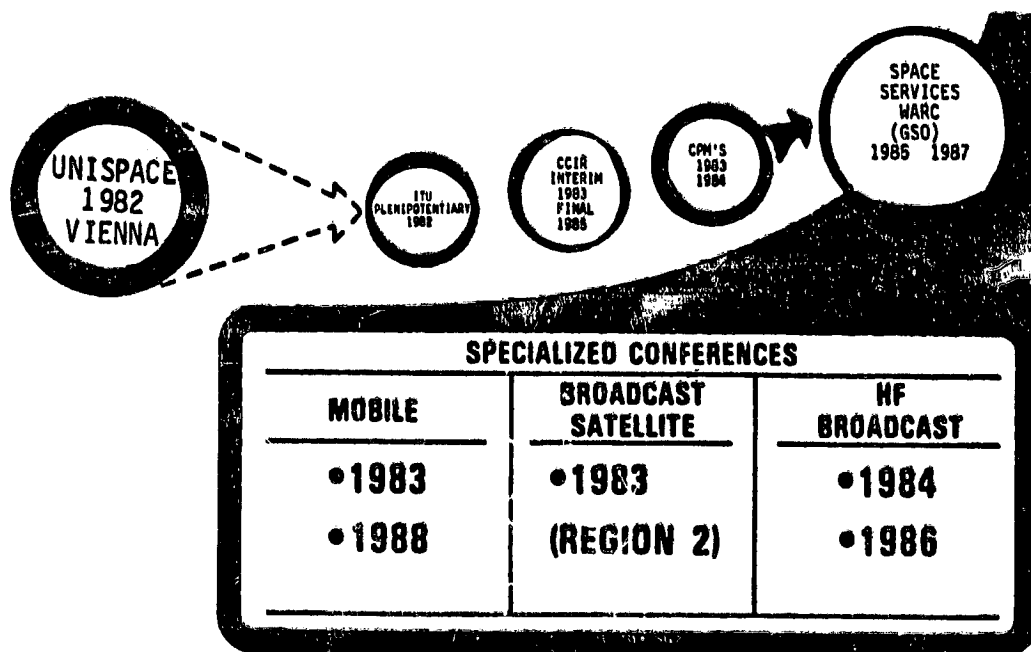
ITU AND UNISPACE RELATIONSHIP



FUTURE RADIO CONFERENCES

UNISPACE '82 will have no formal impact on the ITU, but the activities during, and the outputs of, the Conference will influence the international political environment and may prejudge ITU conferences on several important issues. Many of the participants at the conferences will be the same, and positions that are formed at UNISPACE '82 will carry over to the ITU Plenipotentiary Conference, which will in turn influence the 1985 Space Services WARC.

FUTURE RADIO CONFERENCES



ORBITAL DEBRIS IN THE UNISPACE '82 CONTEXT

The orbital debris issue is likely to arise in discussions regarding the following two topic areas within the UNISPACE '82 context:

A number of lesser developed countries (LDC's) have pushed for language in the UNISPACE '82 document which calls on the "space" utilizing countries to vacate the orbit-spectrum that is used for fixed point-to-point satellite communications (e.g., telephone) or to at least reserve portions for the LDC's future use. There is a perception on the LDC's part that crowding in the preferred orbital locations and frequency bands will preclude their use by LDC's when they are ready. The LDC's claim they have a right to exploit these resources just as the developed countries have done and that developed countries can afford to move into the more expensive technologies (e.g. 30/20 GHz and inclined orbits). Orbital debris will arise in this context because it is seen as another element of the crowding problem, making the use of the preferred orbit-spectrum more difficult.

More directly, concern exists over the possible degradation of the space environment. This includes launch vehicle emissions, experimentation, electromagnetic effects and orbital debris. Though focused on the near earth orbital space, reference is made to the possibility of collisions in the geostationary orbit.

ORBITAL DEBRIS IN THE ITU CONTEXT

It is expected that the orbital debris issue will come up within the ITU context in relation to the orbit-spectrum allocation issue. An example of this relationship is an article in the New Delhi PATRIOT (in English, April 1, 1982, page 4) which states that "India is for making the removal of "spent" satellites from

parking slots mandatory." In the same article it is also put forth that "India is, therefore, seeking revision of the present allocation methodology, making the present and future needs of a country an essential criterion in a new dispensation, rather than the present method which only accounts for a country's ability to occupy a slot in the GSO."

The linkage of these two issues (orbit-spectrum access and orbital debris), though technically not related, is inevitable over the long term as LDC's search for leverage to achieve guaranteed access to the orbit-spectrum resource. This linkage adds a political element to the GSO component of the orbital debris issue which sets it apart from the near-earth orbit considerations.

A U.S. STATEMENT AT UNISPACE '82

Of the 155 countries that are members of the ITU, most are LDC's whose perspectives on the orbit-spectrum access issue do not parallel the U.S.'s perspective. Therefore, given the positive nature of current U.S. action on the orbital debris issue (de-orbiting satellites when practical and funding programs to better understand the problem) the U.S. will make a statement at UNISPACE '82 which underscores U.S. concern for future users of the geostationary orbit. All orbit-spectrum resource crowding problems can be alleviated through the development and application of technology, and taking action to preserve the usability of the geostationary orbit is a concrete example.

FOR THE FUTURE

The geostationary orbital debris issue is receiving growing attention in international fora. Thus, there is a need for the U.S. to continue funding research examining options for dealing with orbital debris and improving the understanding of the implications of implementing those options, so that the U.S. will be ready by the 1985 Space Services WARC to propose positive actions which indicate U.S. consideration for the future users of the geostationary orbit.

TRANSMISSION AND ORBITAL CONSTRAINTS IN SPACE-RELATED PROGRAMS:
BRIEFING SUMMARY

A. L. Hiebert

I. INTRODUCTION

The United States Air Force has a leadership role in the development and operation of space systems for the Department of Defense. Planning for future space-related programs needs to include anticipated growth in number of space systems, including ground networks, large multifunction satellites, increased data-transmission rates, and effects on future requirements for spectrum allocations and orbital positions.

A study project,* sponsored by the Air Force, was initiated to develop a capability for predicting and analyzing the spectrum/orbital geometry requirements of current and projected U.S. and international space-related systems. Essential components of the project include development of a comprehensive space environment data base and computer analysis programs. This capability will provide a resource for evaluating engineering and architectural designs, identifying and analyzing the impact of intentional and unintentional electromagnetic (EM) interference, and predicting probable saturation conditions in spectrum usage and satellite/orbital positions. Assessments of means for accommodating the anticipated growth are also an important part of the study project.

The Directorate of Space Systems and Command, Control, Communications (AF/RDS), Headquarters, United States Air Force is providing support for this project within the Air Force through the

* A. L. Hiebert and A. F. Brewer, Transmission and Orbital Constraints in Space-Related Programs: Project Description, The Rand Corporation, N-1536-AF, August 1980.

Program Management Directive (PMD) of the Advanced Space Communications Program (PE634431F). AF/RDS is the Office of Primary Responsibility (OPR) for the Rand effort and will assist in requesting the support and participation of other DoD organizations, the FCC, NASA, NTIA, and space-related industries. Rand's work will be coordinated with these agencies. The project will be structured for a continuing analysis program that will comply with technical criteria, rules and regulations, and coordination procedures established by the national and international spectrum management agencies. As projected, the analysis program will be designed to be accessible to the space community as operational capabilities are acquired.

II. PROJECT OBJECTIVES

Projected advances in the use of space by the military and other organizations for communications, navigation, surveillance, and other mission capabilities--coupled with the prospect of substantial increases in launch rates by U.S. military, intelligence, and civil agencies, as well as by international agencies--will add substantially to data link traffic and data-processing requirements in ground-to-satellite, satellite-to-satellite, and satellite-to-ground communications and relay systems. Data transmission requirements could expand by several orders of magnitude as new and larger spacecraft are developed; LANDSAT-D, for example, proposed that resolution be increased from 1.2 acres to 0.2 acre (4850 M^2 to 810 M^2) and that the IR data rate be increased from 1000 to 1,000,000 bits/sec. Such expansion could severely tax the data-handling capacities of current equipment and affect the frequency spectrum allocations and orbit assignments of satellite systems. Available spectrum, and the useful orbital positions as defined by today's capabilities, may be inadequate. This could negate the operational advantage of the increased sensing capabilities now being sought in spacecraft, and the increased demand in time of crisis could result in disruption of critical data transmission.

The future growth in both commercial and military space systems will be constrained by technical problems associated with the frequency spectrum, orbital congestion, and costs stemming from proliferated terminals. The seriousness of these constraints is shown in an assessment of the useful areas and coverage of the geostationary

circle;* these areas are essentially full at current assignments with communications satellites at C-band and are expected to reach saturation at X and K_u-bands in the future. The military UHF and SHF frequency bands are also almost saturated because large portions of them are shared with terrestrial links.

Future deep-space-based exploration systems may also be characterized by high-data-rate-mission sensors and thus will create additional problems in the use of the frequency spectrum and in data transmission. The high data rates are based on the demand for timely and accurate sensor information covering wide spatial areas and are generated by fast detectors with high sensitivity and resolution. Deep-space exploration sensors are expected to exhibit data rates that will exceed the data transmission capacity of the currently planned communication links and ground-processing equipment.

This briefing outlines the project objectives and tasks required to develop a continuing program for predicting and analyzing the spectrum and orbital requirements of current and future space-related systems, and for predicting potential saturation conditions.

* The FCC has acknowledged that additional steps must be taken to meet the continued demand for satellite capacity and to provide for new entry. To address this matter, the FCC has issued a "Notice of Inquiry and Proposed Rulemaking," Docket No. 81-704, November 18, 1981, on the "Licensing of Space Stations in the Domestic Fixed-Satellite Service and Related Revisions of Part 25 of the Rules and Regulations." A reduction in the geostationary orbital space from 4 degrees to 2 degrees between satellites operating in the 4/6 GHz bands, and in spacing from 3 degrees to 2 degrees between satellites operating in the 12/14 GHz bands, is proposed. A 3-dB improvement in earth station antenna sidelobe gain standards and a 10-dB cross-polarization isolation standard for small off-axis angles are also proposed. These changes should provide spacing for 37 U.S. satellites in each of the bands listed.

The project objectives are to design and develop a capability for

- o Predicting and analyzing spectrum/orbital requirements of current and projected U.S. and international space-related programs.
- o Evaluating engineering and architectural designs.
- o Identifying and analyzing intentional/unintentional EMI.
- o Predicting saturation in spectrum usage/orbital positions.
- o Assessing means to accommodate growth.
- o Supporting preparations for space services--WARC.

III. TECHNICAL REQUIREMENTS

To accomplish the project objectives, it will be necessary to design and develop a comprehensive Space Environment Data Base and Analysis Codes and Computer Programs.

SPACE ENVIRONMENT DATA BASE

The proposed Space Environment Data Base should consist of a file on electromagnetic and operational characteristics and a file on the deployment status of currently active and projected U.S. and international space systems, related earth segments, and network systems. The Electromagnetic and Operational Characteristics File should include three levels of information:

1. Level 1 - minimum data.
2. Level 2 - nominal and expanded data.
3. Documentation, reports, measured data.

The Deployment Status File should include four time-related information categories:

1. Current and active-deployed systems.
2. Approved-for-launch systems and scheduled dates.
3. Firm and funded development space system programs.
4. Future development plans and schedules.

A proposed data collection format has been designed by Rand and ECAC/IITRI and is intended for use in developing the Electromagnetic and Operational Characteristics File on Level 1.* The data will support preliminary interference analyses and will provide indications of the operational usage of systems. The format applies to communications, navigation, relay, sensor satellites, space transportation systems, their related earth segments, launch operations, and TT C operations. Technical characteristics of the hardware involved and operational characteristics of the system are to be reported. Other types of satellites, such as radar and solar power satellites, require additional data to describe the system adequately. Formats to accommodate these systems are being designed and will be published at a later date.

The data collection format (Appendix A) proposed by Rand and ECAC was designed to accommodate current and active deployed systems. The same format should be used to report known or projected data on systems in other categories of the Deployment Status File. Estimates or projections should be identified as such.

The proposed format is currently being tested and evaluated on Air Force space systems in cooperation with the Air Force Space Division Program Offices and the Communications Electronics Support Office (CSD/DC). It will be reviewed with NTIA, the FCC, Frequency Management Offices of the Department of Defense, and participants in the conference.

* Appendix A: SPACE SYSTEMS DATA RECORD--Electromagnetic Characteristics and Operational Information for Space Systems and Related Earth Segments. Not included in this report.

Design and modification of the Space Environment Data Base should be conducted as a continuing joint effort by The Rand Corporation, the DoD Electromagnetic Compatibility Analysis Center (ECAC), the DoD Frequency Management Agencies, NTIA, FCC, and other participating agencies. Responsibility for constructing and maintaining the Data Base and developing an analysis capability for space-systems planning has been assigned to the ECAC at Annapolis, Maryland.* ECAC already has the necessary computer and data-processing equipment, the trained personnel, and a substantial portion of the required space-environment data and associated analysis codes and programs. Additional facilities may be needed to process highly classified and proprietary data.

ECAC also maintains an extensive and active data base on the electromagnetic and operational characteristics of terrestrial and earth environment equipment that may affect some of the space-related programs.

Preliminary discussions have been initiated with NORAD, ADCOM (SPADOC), and other agencies about the acquisition and processing of needed data on the operational condition and status of space systems. Since these data will be at various levels of security and in some cases will include proprietary information, appropriate means for processing proprietary and classified information will need to be developed and approved by the cognizant agencies. A preliminary list of agencies and contacts was published in the Rand Report mentioned earlier and is being updated as the project develops.

* Memorandum: "Electromagnetic Compatibility Analysis Center Support for Space Systems Planning," 25 June 1981, Office of the Under Secretary of Defense, Research and Engineering, Assistant Deputy Under Secretary (Technical Policy and Operations).

The Data Base should be made available--as needed, and under appropriate security procedures--to Rand space studies, to DoD, and to Government agencies and sponsored contractors conducting analyses in the subject areas.* The Data Base should be updated for satellite launches/decays and changes in space systems development plans to provide a continuing source of information for analyzing current and future space systems.

Prediction and analysis of probability of spacecraft collision and/or physical impact with space objects will not be addressed in this project. However, the Data Base should provide useful information on the ephemerides of current and future satellites, which is essential to such investigations.

ANALYSIS CODES AND COMPUTER PROGRAMS

The objectives are to devise analytic codes and computer programs for interrogating the Space Environment Data Base so that current and projected usage/saturation levels and impact of EM interference can be determined for the spectrum allocation, orbital positions of space systems, and related earth segments.

It may be necessary to develop new analysis techniques and usage/saturation criteria for each type of space communications, navigation relay, or sensor service. Since the results depend on space, time, frequency, message length, and scenario, usage and saturation

* "Accessibility to the Data Base" will be discussed by J. Atkinson of ECAC in a separate briefing, and will be published in The Proceedings of the Conference.

levels will have to be determined for each elemental space volume of the system at various times and frequencies, at mean message lengths, and under different scenarios for different levels of usage. Space, even useful portions of space, is a very large volume. Conditions prevailing in one portion (or elemental volume) tend to be different from those prevailing in another.

For each authorized frequency band and/or channel, completely defined emissions, partially defined emissions (random in space or time), and undefined emissions (random in space and time) will have to be statistically combined and compared with receiver sensitivity, antenna gain, and system losses in order to derive a measure of band usage.

This correlation will provide a basis for projecting future demands on each allocated band in terms of the anticipated increase for users or frequency of use. After "saturation" is defined for each type of service, it should be possible to determine which usage rates are approaching saturation in an assigned frequency band and orbital position and how soon this is likely to occur.

Limits of orbital spacing are based on beamwidths of the earth station/terminal (may include mobile) antennas, electromagnetic interference criteria, and adherence to the ITU Radio Regulations. Hence, intentional and unintentional interference situations and their impact on usage/saturation levels should be assessed. Analysis of system vulnerability to intentional EM interference is an additional and essential requirement for hardened and secure systems.

Once suitable criteria have been determined and analyzed and programs have been developed, they will be applied to the Data Base to answer questions such as

1. What are the usage and saturation rates of existing and planned space communication systems?
2. Can a new system be added to the existing space environment and function as required? What will a new system (assuming it became operational) do to the existing systems?
3. What are intentional/unintentional interference situations, sources, and effects?
4. What will defined jamming situations do to a specified military data link that is already X percent saturated?
5. Which systems are the least conservative of spectrum?
6. Which systems approach orbital congestion?

Answers to questions such as these should make it possible to recommend communication practices, band allocations, and orbital assignments that will permit transmission of essential information within the available finite spectrum.

A list of proposed analysis codes and computer programs have been compiled to provide the capabilities for performing the types of analysis discussed and for meeting the overall project objectives (Table 1).

This list is based on a series of joint Rand/ECAC technical surveys and reviews of existing programs and those recommended for development. It will be augmented as the surveys and project activities continue and as user requirements are identified.

IV. PROJECT STATUS AND FUTURE EFFORTS

During the formative period of the Rand project, and in subsequent Air Force/Rand reviews, we were advised to develop concepts and plans for listing the uses of the analysis programs and for accessing the data base, as required. It was assumed that ECAC would be assigned the responsibility of developing a data base and analysis capability with respect to military space systems for the purpose of improving EMC planning and minimizing the potential intersystem harmful EM interference. Other related space efforts, as listed in the Rand project objectives, may require the development and use of analysis capabilities by other DoD and government agencies and possibly by Air Force aerospace contractors.

Examples of such efforts would include capabilities for

1. EMC intrasystem analysis of space systems.
2. Assessments and analysis of Blue/Grey Forces interference or intentional Red Forces jamming.
3. Analysis of special space systems requiring compartmental data bases and 24-hour operational support.
4. Engineering analysis of architectural formulations of proposed space systems.
5. Determination of the transmission capacity of space systems, their usage rate and efficiency of use, and the predicted saturation of spectrum utilization and orbital positions.
6. Technical preparations space services WARC.

This extended support will require access to the ECAC data base and selected analysis computer programs. A joint conference on Space Systems Data Bases and Analysis Capabilities was organized to assist us and the ECAC in defining the items for inclusion in the data base and its subsequent updating, and in reviewing and evaluating existing and needed analysis programs. Representatives from industry and government agencies were asked to participate. The conference was conducted and hosted by ECAC, on November 17-19, 1981 at Annapolis, MD. ECAC will compile a report on the Proceedings.

Rand will be requesting the assistance of ECAC, the Aerospace Corporation, and other participating agencies in conducting assessments of the data base items and analysis programs required to meet the overall objectives outlined in this briefing. We hope to continue the design and development of analysis programs and to assist in determining the Air Force technical analysis and support requirements.

Among the objectives of the project is that it be timed to provide a usable capability for the technical development of Air Force positions on spectrum usage and orbital location issues for Space Services WARC. Attaining this objective will require the combined effort of and coordination with agencies outside Rand.

Study efforts aimed at assessing means to accommodate the growth of space systems and related proliferated earth terminals have not been discussed in this briefing. However, candidate techniques that may offer ways of accommodating increased proliferation of space data are being monitored and assessed as the project develops. Examples of such techniques include:

- o Current and potential developments in data processing and compression, multibeam antennas, etc..
- o Use of higher frequencies.
- o Added spectrum allocations.
- o More efficient energy dispersal.
- o Improved side lobes of earth station antennas.
- o Satellite data relay systems.

Table 1

Proposed Analysis Codes and Computer Programs

Title	Organization
1. Cull and coordination models: Space and earth segments ITU Radio Regulation Appendix 28, 29--Automation Ground mobile satellite terminals	ECAC ECAC, NTIA ECAC
2. Co-site analysis: space segment	ECAC
3. Co-site analysis: earth stations, fixed/mobile	ECAC
4. Intrasystem EMC Analysis: AF/IAP	RADC
5. Engineering and architectural design analysis: NITRE Interactive Communication Analysis Program (NICAP) Interference Analysis in Satellite Communications	NITRE NITRE
6. Intersystem EMC and vulnerability analysis: Geostationary orbit: Spectrum-Orbit Utilization Program (SOUP) Satellite Link Interference Prediction Nongeostationary orbits and fixed/mobile stations Environmental Analysis Model: frequency planning Deep Space RFI Prediction Program (DSIP-II) MILSATCOM vulnerability analysis	NTIA, NASA, ORI Rand Rand ECAC JPL AF/ESC, Bell
7. Saturation prediction and analysis: System capacity Usage rate/efficiency Orbital positions	Rand

AIR FORCE ORBITAL POSITION MANAGEMENT POLICY
D. HYLAND

-- UNLIKE THE EARLIER SPEAKERS WHO DISCUSSED DATA, STATISTICS, AND TEST RESULTS, I WILL DISCUSS PERCEPTIONS.

-- THESE PERCEPTIONS ARE THOSE OF THE PEOPLE WHO MAKE POLICY DECISIONS WITHIN THE AIR FORCE AND DEPARTMENT OF DEFENSE.

THE FIRST QUESTION ASKED WHENEVER THE SUBJECT OF ORBITAL DEBRIS IS MENTIONED IS "IS THERE A PROBLEM?".

- IT IS NOT CLEAR THAT THERE IS A CURRENT OR NEAR TERM MISSION THREATENING PROBLEM.
- WHILE SPACE DEBRIS DOES POSE A MEASURABLE STATISTICAL PROBLEM TO NATIONAL SECURITY SPACE MISSIONS, IT MUST BE NOTED THAT TO DATE NO MISSIONS HAVE BEEN LOST DUE TO COLLISIONS WITH DEBRIS.
- OF COURSE, WE MUST ALSO RECOGNIZE THAT WITH THE INCREASED PRESENCE OF MAN IN SPACE AND THE VALUE OF A SPACE SHUTTLE, ESPECIALLY IN A LIMITED FLEET, THE FIRST DEBRIS TO DISABLE THE ORBITER WILL PROVE CATASTROPHIC IN MANY ASPECTS INCLUDING NATIONAL SECURITY.
- THE FIRST GOAL OF THIS WORKSHOP MUST BE TO DEFINE THE PROBLEM.

IN DEFINING THE PROBLEM, WE MUST DETERMINE WHEN ORBITAL DEBRIS WILL BECOME MISSION THREATENING.

- WHILE IT APPEARS THAT IT IS NOT A NEAR TERM PROBLEM; IT IS EASY TO SEE THAT WITH MORE AND LARGER SPACECRAFT, ALONG WITH THEIR ASSOCIATED DEBRIS, BEING LAUNCHED THAT ORBITAL DEBRIS WILL BE A PROBLEM IN THE FUTURE.

- BASED ON DATA WE HAVE SEEN AND PROJECTIONS ON LAUNCH RATES, ORBITAL DEBRIS MAY BECOME A PROBLEM TO THE DEPARTMENT OF DEFENSE IN THE 1990s; BUT MORE LIKELY WILL NOT BECOME MISSION THREATENING TILL AFTER THE YEAR 2000.
- ON THE OTHER HAND, ORBITAL DEBRIS MAY BE, EVEN NOW, A PROBLEM FOR VERY LARGE SPACECRAFT IN MEDIUM ALTITUDE, SUCH AS SPACE STATIONS, BUT CURRENT AND PLANNED DOD SPACECRAFT DO NOT FALL INTO THIS CATEGORY.
- THE MAJOR UNKNOWN THAT MUST BE DEALT WITH IS HOW MUCH AND WHERE IS THE DEBRIS THAT WE DO NOT KNOW ABOUT? THIS MAY BE OUR BIGGEST HURDLE IF WE WANT TO CONVINCE PEOPLE THAT A PROBLEM DOES EXIST.
- AS WE START TO ANALYSIS THE ORBITAL DEBRIS PROBLEM WE NEED TO DETERMINE WHERE THE PROBLEM IS.
 - SPACE DEBRIS TENDS TO BE CONCENTRATED IN ALTITUDE AND PERHAPS INCLINATION. PROBABILITIES OF COLLISION WHICH DO NOT ADDRESS THIS FACT ARE NOT PARTICULARLY ENLIGHTENING.
 - MOST DEBRIS PROBABLY RESIDES IN HEAVILY USED, MODERATE TO HIGH ALTITUDE BANDS.
 - THE DEBRIS IN LOWER ORBITS DECAYS RAPIDLY BECAUSE OF ITS POOR BALLISTIC PROPERTIES.
 - WHILE DEBRIS FROM TRANSFER ORBITS TENDS TO CIRCULARIZE ITS ORBIT ABOUT THE PERIGEE ALTITUDE, THEN DECAY.
 - ONCE THE PROBABILITY OF COLLISION IS CHARACTERIZED MORE PRECISELY BY ORBITAL PARAMETER, THEN OPERATIONAL PROCEDURES OR MISSION PLANNING MIGHT REDUCE PROBABILITY OF MISSION -THREATENING COLLISION TO ACCEPTABLE LEVELS.

- TO CHARACTERIZE THE ORBITAL PARAMETERS OF DEBRIS, WE MAY NEED TO FACE THE ISSUE OF ADDITIONAL TRACKING CAPABILITIES.
 - NORAD IS THE SINGLE FOCAL POINT WITHIN THE DEPARTMENT OF DEFENSE FOR THE SATELLITE CATALOG AND ITS ASSOCIATED ORBITAL DATA PRODUCTS.
 - THE MISSION OF NORAD SENSORS IS TO PROVIDE WARNING OF MISSILE ATTACK AND SPACE SURVEILLANCE.
 - MOST TRACKERS ARE MISSILE WARNING RADARS. THEY WERE DESIGNED TO TRACK DEBRIS LARGE ENOUGH TO ALARM WARNING RADARS. THEREFORE, PARTICLES TYPICALLY SMALLER THAN ONE SQUARE METER, AT UHF, NEED NOT BE ROUTINELY TRACKED TO FULFILL THE NORAD WARNING MISSION.
 - CURRENT THRESHOLDS ARE BASED ON THESE MISSION REQUIREMENTS AND CANNOT BE ARBITRARILY CHANGED.
 - EVEN IF THE RADARS WERE IMPROVED ENOUGH TO ALLOW TRACKING OF SMALL DEBRIS (CURRENTLY, THERE ARE NO PLANS TO IMPROVE THESE RADARS), CHANGING THEIR TASKING COULD ADVERSELY IMPACT THE PRIME NORAD MISSION.
 - BESIDES THE INCREASED RADAR TASKING, THE TRACKING OF SMALL DEBRIS WILL OVERLOAD OUR CURRENT COMPUTATIONAL AND DATA COLLECTION CAPABILITY.
- IN ADDITION TO WHERE, IT IS IMPORTANT TO CONSIDER HOW ORBITAL DEBRIS THREATENS A SPACECRAFT.
 - WE KNOW THAT SPACECRAFT HAVE BEEN HIT BY SMALL PARTICLES WITHOUT HAVING THEIR MISSIONS DEGRADED. SOME SPACECRAFT HAVE BEEN DESIGNED TO BE HIT BY PARTICLES AND CONTINUE TO FUNCTION IN ORDER TO REPORT THE INFORMATION

- FOR SCIENTIFIC PURPOSES.
- IMPACT DAMAGE TESTS MUST BE REALISTICALLY DONE; SIMPLE HYPERVELOCITY IMPACT AGAINST A TARGET MASS IS INSUFFICIENT.
 - SPACECRAFT COMPONENTS MUST BE SIMULATED IN THEIR OPERATING STATE, THEN STRUCK BY HYPERVELOCITY PARTICLES.
 - SPECIFICALLY, SHUTTLE ORBITER COMPONENTS NEED TO BE INCLUDED IN THIS PROGRAM.
 - THE RESULTS SHOULD TELL US HOW TO BUILD OUR SPACECRAFT SO THAT THE CHANCES OF A COLLISION BEING MISSION THREATENING IS MINIMIZED. ALSO, WE SHOULD DESIGN TO PREVENT SPACECRAFT BREAKUP DUE TO COLLISION.
 - BEFORE A PLAN TO SOLVE AN ORBITAL DEBRIS PROBLEM CAN BE DEVELOPED A SET OF CRITERIA MUST BE ESTABLISHED.
 - THE FIRST AND FOREMOST CRITERIA IS THAT THE SOLUTION MUST BE COST EFFECTIVE.
 - THIS MEANS THAT WE CAN NOT SPEND A BILLION DOLLARS TO REMOVE DEBRIS THAT THREATENS A HUNDRED MILLION DOLLAR SPACECRAFT.
 - PLANS TO REMOVE DEBRIS FROM ORBIT AS CURRENTLY ENVISIONED WOULD APPEAR TOO COSTLY. THESE PLANS FORESEE USING THE SPACE SHUTTLE OR A SPECIALLY DESIGNED SPACECRAFT TO COLLECT DEBRIS.
 - A BETTER START SHOULD BE TO PREVENT UNNECESSARY DEBRIS FROM GETTING INTO SPACE.
 - THIS LEADS TO A SECOND OBSERVATION, THAT SPACE

DEBRIS IS NOT A PROBLEM THE UNITED STATES CAN SOLVE ALONE.

- THE SPACE DEBRIS PROBLEM IS AN INTERNATIONAL PROBLEM.
 - SOVIET PAYLOADS AND ROCKET BODIES COMMONLY BREAKUP IN ORBIT, SOME MAY BE COMMANDED TO DO SO.
 - CHINA, EUROPE, AND THE "THIRD WORLD" COUNTRIES ARE JUST ENTERING THE "SPACE AGE" AND WE SHOULD EXPECT THEM TO DUMP THEIR SHARE OF DEBRIS IN SPACE IN GAINING TECHNOLOGICAL KNOWLEDGE.
 - ANOTHER USER OF SPACE THAT MUST NOT BE FORGOTTEN IS THE COMMERCIAL SECTOR. THEY WILL OWN AN EVER INCREASING NUMBER OF SPACECRAFT. THIS SECTOR WILL BECOME EVEN MORE IMPORTANT IF SOME PORTIONS OF THE NATIONAL SPACE LAUNCH CAPABILITY COMES UNDER COMMERCIAL CONTROL.
 - WE MUST REALIZE THAT WE HAVE NO SOLUTION UNLESS ALL THESE PARTIES ARE IN AGREEMENT.
- WHAT IS THE AIR FORCE DOING IN THE AREA OF ORBITAL POSITION MANAGEMENT?
 - OUR MAIN EFFORTS HAVE BEEN IN THE GEOSYNCHRONOUS BELT.
 - FIRST, WE ARE TRYING TO KEEP DEBRIS OUT OF GEOSYNCHRONOUS ORBIT. THIS BEING DONE BY LEAVING ROCKET BODY IN LOWER ORBIT.
 - SECOND, WE ARE MAKING EFFORTS TO INSURE ADEQUATE SPACING BETWEEN OUR SPACECRAFT.
 - THIRD, WE ARE WORKING ON DETERMINING PROPER COLLISION AVOIDANCE PROCEDURES.

- THESE EFFORTS HAVE BEEN DISCUSSED ELSEWHERE IN THIS WORKSHOP.
- WE HOPE THAT THE LESSONS LEARNED FROM THESE GEOSYNCHRONOUS ORBIT EFFORTS CAN EVENTUALLY BE APPLIED TO ALL ORBITS, OR AT LEAST THOSE REQUIRING SOME CONTROL.
- THE SUBJECT OF REMOVING SPACECRAFT FROM GEOSYNCHRONOUS ORBIT AT THE END OF THEIR USEFUL LIFE IS CURRENTLY BEING DISCUSSED WITHIN THE AIR FORCE.
 - THE AIR FORCE BASICALLY SUPPORTS THE IDEA OF REMOVING SPACECRAFT FROM GEOSYNCHRONOUS ORBIT AT THE END OF THEIR USEFUL LIFE.
 - WE ARE DOING THIS BECAUSE OUR SPACECRAFT ARE IN EXCELLENT ORBITAL POSITIONS TO SUPPORT THEIR MISSIONS AND WE WANT TO PUT THEIR REPLACEMENT SPACECRAFT IN THE SAME ORBITAL POSITION WITHOUT HAVING TO CONCERN OURSELVES ABOUT INTERFERENCE FROM THE OLD SPACECRAFT.
 - WE DO NOT SEE THIS IDEA REDUCING THE NUMBER OF GEOSYNCHRONOUS SPACECRAFT. WE SEE IT AS A WAY OF KEEPING THE FAVORABLE POSITIONS WE NOW HAVE.
- IN SUMMARY, WHAT SHOULD BE OUR NEAR-TERM GOAL?
 - WE MUST DEFINE THE PROBLEM AND SHOW THAT WE DO HAVE A PROBLEM.
 - WE MUST SHOW THAT THE PROBLEM IS MISSION-THREATING TO A SPACECRAFT.
 - WE MUST DEFINE THE PROBLEM IN LAYMAN'S TERMS SO THAT OUR POLICY-MAKERS WILL UNDERSTAND IT.
 - WE MUST MAKE THE COMMERCIAL AND INTERNATIONAL COMMUNITIES AWARE OF THIS PROBLEM, BECAUSE WITHOUT THEM WE HAVE NO SOLUTION.

N 85 - 21217

Air Force Satellite Position Management

Captain R. Davis
Space Division
Los Angeles, CA

1. Introduction

My intent this afternoon is to describe the plans and procedures the Air Force uses for satellite position management. I will review briefly the major Air Force organizations that are involved with satellite position management, describe our approach and general planning procedures, and address some of our concerns in this realm.

2. Air Force Agencies

As you know the Space Act of 1958 identified the Department of Defense as responsible for conducting military operations in space. Subsequently, the United States Air Force was assigned to act as the DOD's executive agent for space. In addition, the Air Force is responsible for acquisition and launch of DOD space systems. Within the Air Force, space related roles and activities have been delegated to several subordinate organizations and agencies.

With regard to satellite position management, tasks are divided as shown in Figure 1. The roles and responsibilities of all these agencies are still evolving. The Air Force has designated the Air Force System Command's Space Division as its office of primary responsibility for satellite position management. Spacecraft program offices at Space Division are required by regulation to include position management planning in both pre-launch and orbital phases of spacecraft development and operation.

However, position management activities also focus on the Air Force Satellite Control Facility (AFSCF), which is subordinate to Space Division, and the Aerospace Defense Center in Colorado Springs. The tracking facility at Sunnyvale controls or operates around twenty Air Force spacecraft and is responsive primarily to the users. They also have a current responsibility for identifying possible orbital collisions and notifying affected parties as early as possible. ADC is responsible for tracking, monitoring, and cataloging some 4700 space objects, including both space debris and active satellites.

At Headquarters, Air Force, the Directorate of Operational Requirements, under the Deputy Chief of Staff for Research, Development, and Acquisition (AF/RDQ), is the action office for managing the Air Force Survivability Program. As such it determines proper spacecraft hardening criteria and advises spacecraft program offices on appropriate requirements for spacecraft system survivability. Also at the Air Staff, the Deputy Chief of Staff for Operations Plans (AF/XO) and Requirements is responsible for resolving positioning conflicts with agencies outside the Air Force. Finally, frequency assignments for spacecraft systems are obtained by using Air Force Frequency Management Center channels as an interface with the International Telecommunications Union (ITU).

3. Air Force Approach to Position Management

The Air Force approach to position management itself is divided into three broad categories: the avoidance of collateral damage, radio frequency management, and physical positioning and collision avoidance.

The collateral damage question, which involves that damage resulting from an attack on another spacecraft or space object, is of special concern to the military. We in the Air Force are charged with a responsibility for national security and for insuring the survivability and viability of our national space systems. Developing, launching, and operating our space systems requires us to consider overall mission requirements, the potential threat against our space systems, and the hardening of spacecraft against the effects of nuclear detonations. This latter consideration follows the guidelines published by the Joint Chiefs of Staff and the criteria established by the Nuclear Criteria Group. This office interfaces with the Directorate of Operational Requirements under the Air Force Survivability Program.

Radio frequency management involves reducing the potential for electro-magnetic interference among both space and terrestrial systems. To do this we coordinate through our Frequency Management Center channels to obtain international registration and frequency assignment from the International Telecommunications Union. This includes both radio band selection and, within the geosynchronous belt, orbital spacing.

Finally, in an effort to preclude physical damage from orbital collisions, as well as to consolidate guidance for frequency management and for hardening and design, the Air Force has established responsibilities and procedures to coordinate our spacecraft positioning well prior to actual launch. These procedures and responsibilities are given in Space Division Regulation 55-1 and in a draft Air Force regulation to be published this Fall. These two regulations address the relationship of all Air Force agencies directly concerned with satellite position management and apply to all Air Force agencies and organizations using space systems.

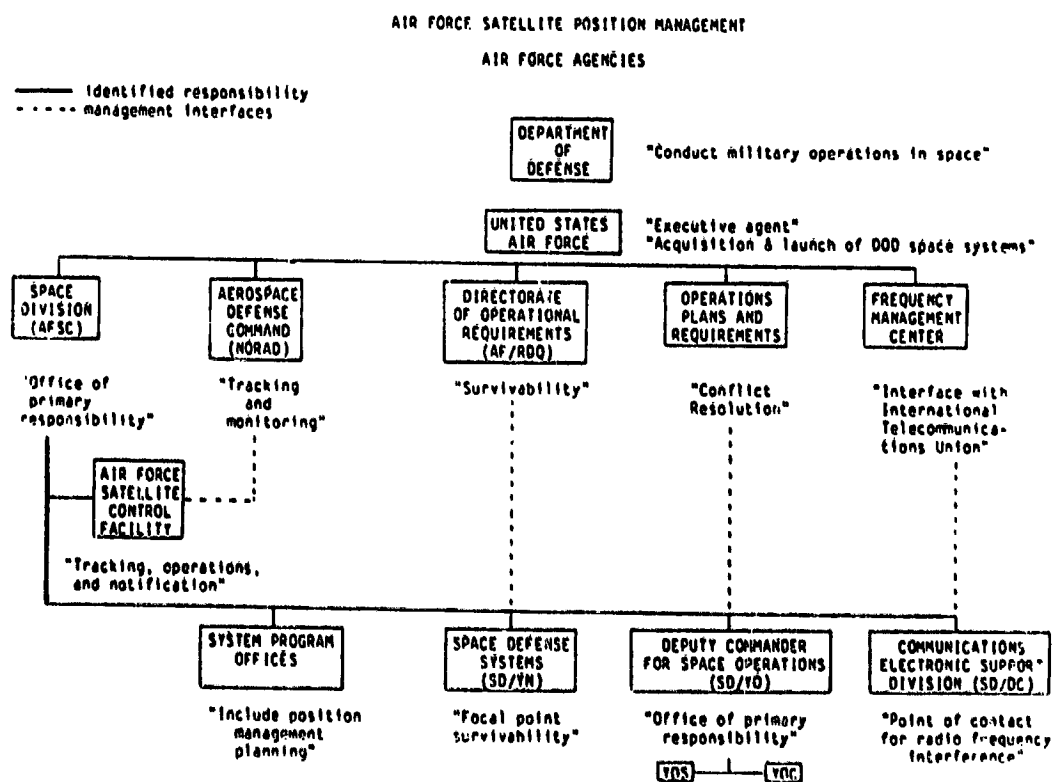
4. Management Roles

The purpose of these regulations is to describe procedures for establishing our spacecraft orbital positions and to provide a mechanism for resolving orbital conflicts. In the spacecraft development phase the spacecraft system program office is required by regulation to coordinate with appropriate agencies to obtain proper frequency assignment, to incorporate effective survivability design, and to plan for proper orbital placement and spacing. Just prior to launch, the program office will coordinate directly with both the Satellite Control Facility and the Aerospace Defense Center to confirm trajectory and final orbit compatibility with all objects known to be in orbit. In the event that a spacecraft is repositioned, such as at geosynchronous orbit, similar procedures are followed, except that positioning review is initiated by the Air Force unit exercising spacecraft mission control, whether the SCF or a user.

This entire process is coordinated throughout by Space Division's Deputy Commander for Space Operations (DCS), who acts as Space Division's OPR for

satellite position management. The intent is to establish positioning and to resolve any positioning conflicts at the lowest possible organizational level. If conflicts cannot be resolved within the jurisdiction of Space Division, the DCSO may refer the issue to the Deputy Chief of Staff for Operations Plans and Requirements (AF/XO). AF/XO would, in turn, resolve the conflict coordinating with the Air Force Space Operations Steering Committee or the Director, Joint Staff, depending on the nature of the problem.

A word about the new Space Command: the role and responsibilities of this organization are still evolving. Clearly, we look on SPACECOM as a means of enhancing the management and operation of space systems, and SPACECOM will have a definite interest in--if not ultimately be responsible for--the policies the Air Force will develop concerning satellite position management.



ORBITAL DEBRIS POLICY ISSUES
BATTELLE INVOLVEMENT AND SOME PERSONAL OBSERVATIONS

N 85-21218

Dr. Donald S. Edgcombe
Manager, Space Systems and Applications
Battelle Columbus Laboratories
Columbus, Ohio 43201

July 28, 1982

INTRODUCTION

This paper discusses a number of topics pertinent to orbital debris policy. Most of the discussion focuses on aspects of orbital debris policy development in which Battelle has been involved over the last decade and a half. The final part of the paper presents some personal observations regarding orbital debris policy status and approaches.

BACKGROUND

The possible hazards presented by orbital debris have been a matter of concern since the early 1960s.^{(1)*} The area of initial concern was the potential hazard to the Earth from reentering debris. In the very early days of the space program, it was believed that only specially protected objects would survive reentry. Subsequent events showed this to be incorrect. A chunk of Sputnik IV landed at an intersection in Manitowoc, Wisconsin. Pieces of the skin of John Glenn's Atlas booster were recovered in Africa, with inspectors' hand-stamps still readable. Intact spherical highpressure gas bottles were recovered from Australia and Saudi Arabia.

The recognition of this unexpected hazard gave rise to a wide range of policy issues. The debate on these issues continued for a number of years, culminating in such actions as the signing of the United Nations Treaty on Liability for Operations in Outer Space, and the positive actions taken to reduce the impact hazard in the Skylab program.

The recognition of the potential hazard of orbital debris to orbiting objects did not occur until the late 1970s. Concern over this potential hazard has increased, and has also given rise to a number of policy issues. These issues are, at present, largely unresolved.

Characteristics of the Debris Hazard to Earth

To understand the policy issues that were generated by reentering orbital debris, some basic facts regarding the hazard they presented must be understood. First, objects placed in very low-Earth orbit (e.g., circular orbits of less than 300 n.mi. altitude) will undergo orbital decay and reenter the Earth's atmosphere,

*Superscript numbers refer to References shown at the end of this paper.

usually within a few months to a few years. The time between orbital placement and eventual Earth impact is a function of the initial orbital altitude, the size and mass of the object and other factors such as the upper atmospheric density, which is strongly influenced by the solar sunspot cycle. The exact time of reentry is difficult to predict in advance. Therefore, until a short time before reentry the location of the eventual impact point must be treated as random within the latitude bands set by the orbital inclination. Since most low-Earth orbital spacecraft have orbits with inclinations of at least 28.5 degrees, with Soviet spacecraft operating at higher inclinations and polar or near-polar orbits used for Landaat, Ticon, and various scientific spacecraft, the reentry of debris represents a worldwide potential hazard.

The masses of recovered reentering objects ranged from very small (less than an ounce) to hundreds of pounds.⁽¹⁾ It was predicted that even larger objects might survive (e.g., the film vaults from the Skylab).⁽²⁾ Because of the aerodynamic drag experienced during reentry, these objects were predicted to impact with relatively low terminal velocities, ranging from a few feet per second for lighter, flat objects (e.g., solar cell cover glasses, small portions of external skin) to a few hundred feet per second for large, dense objects.

Taken in total, the impact of these objects represented an obvious potential hazard to human life. The larger objects posed a risk of fatalities or injuries through direct impact on individuals or through the generation of secondary debris upon impact. Even the smaller objects were considered capable of causing injury if undetected (e.g., injuries from solar cell cover glasses lying in vegetation or in the soil). A less likely, but more difficult to assess, possibility was that of a catastrophic accident (e.g., debris striking a crowd, a fully-loaded jet airliner, etc.).

Hazard to Earth--Policy Issues

The initial and most persuasive issue faced in developing policy for impacting debris was the characterization of the risk, i.e., did it represent a severe, moderate, or possibly even a negligible risk? This is, of course, the problem of assessing the acceptability of the risk, a problem not unique to this situation, but one faced continually in such areas as public health and safety, public and private transportation, and environmental protection. It is a subjective judgment, and influences the entire range of responses and actions subsequently taken.

A second issue of major concern was the definition of the liability for damage due to debris impacts, particularly the means for establishing the liable party and providing indemnity for losses. Here again, the type of procedures established would depend in part on whether such cases were likely to be frequent or relatively rare.

A third issue, with many facets, concerned the types of measures that could or should be mandated to either reduce or at least document the risk associated with specific space operations. A number of steps were proposed and examined.⁽¹⁾ One called for the preparation of detailed risk assessments for each individual mission, including an engineering analysis of the likely surviving pieces, their distribution relative to each other at impact (their "footprint"), the potential areas of impact, and the likely hazard in terms of probability of causing an injury or fatality. This analysis would be used to document that the specific risk for each mission had been considered and, presumably, been found acceptable.

A specific proposal from France would have required the registration and labeling of all components in a spacecraft prior to launch. Each component would be given a unique identification number so that it could be unambiguously identified when found.

The obvious step for reducing the hazard would be to deliberately reenter the debris at a preselected location for ocean impact. This would require the provision of some form of propulsion to initiate reentry at the desired time and location, as well as active communications to transmit the command for each separate system or piece to be reentered.

Two additional proposals were advanced for reducing the hazard. One proposed that larger objects be exploded in orbit prior to reentry, reducing the size of reentering objects. The other proposed that space systems designs be altered to maximize burnup during reentry. This was proposed to be done through more extensive use of low melting point materials, and designing for early breakup during reentry to expose all internal components to the full reentry environment.

All of the above proposals and issues were debated vigorously over the decade from the mid-1960s to the mid-1970s. Eventually, a satisfactory approach has evolved.

Hazard to Earth--Resolution

The key factor in resolving the issues regarding reentry debris was the eventual characterization of the hazard. A major contribution to this characterization was a study conducted by Battelle. This study reached two major conclusions. First, it was concluded that the analyses of reentry hazards being conducted by various organizations in the U.S. appeared to be technically credible and formed a basis for a reasonable estimate of the hazard associated with reentering debris. These analyses indicated a probability of injury for reentering systems generally ranging from 10^{-4} to 10^{-3} ,⁽¹⁾ with some very large systems such as Skylab as high as approximately 6×10^{-2} ⁽²⁾ (approximately a one in one-hundred and fifty chance of injury, worldwide). Second, the relative hazard posed by these reentries was low and, specifically, was lower than the background hazard due to reentering meteorites. Since there were no verified deaths and only a few verified injuries due to meteorites over the last two-hundred years, it was concluded that injury or significant damage due to reentering space debris should be a relatively rare event. Therefore, extreme measures did not appear to be justified.

The characterization of the debris risk as low helped to resolve a number of the policy issues discussed previously. Since such cases were not likely to be widespread, special procedures for handling liability did not appear necessary, and the general provisions of the United Nations treaty on the Liability for Space Operations, which was being negotiated during this time period, were held to apply. This treaty defines the country of launch as responsible for any damage caused by its operations. Since damage cases were expected to be relatively rare, the French proposal for registration and labeling of all components was not adopted, the conclusion being that the country of origin could be established with reasonable confidence without registration and labeling, and that the proposed system was unacceptably burdensome in view of the relative infrequency of expected incidents.

Some selected hazard reduction or documentation steps were taken, where feasible, particularly for large systems. First, NASA developed a net of hazard analyses

for some specific flight systems (e.g., HEAO, Centaur) that could be considered representative of most medium-to-large space systems that were either in orbit or likely to be launched in the near future. These generic analyses, plus those already conducted for systems like Skylab, served as the basis for future inquiries and assessments concerning the surviving debris and associated hazard levels. Second, wherever feasible, large orbiting objects would be deliberately reentered into remote areas to reduce their hazard. This was done for the SIVB stages used in the Skylab program, with the residual hydrogen being cold-flow vented through the J-2 engines to provide the required Delta-V for reentry. In the case of Skylab itself, where reentry was not originally expected, a degree of control over the reentry location was achieved by deliberately initiating the final tumble during reentry, using the remaining attitude control propellants. This crude form of control did move the projected reentry point more towards ocean areas.

Some proposed steps for hazard reduction were not taken. The proposal for deliberate reentry of all objects was considered impractical and unnecessary in view of the low hazard estimates. The proposal to fragment systems prior to reentry was also not taken up. In this case, the overall hazard, including that to workers handling the explosives at launch and processing facilities, might have been increased significantly by the proposed action.

ORBITAL HAZARD--CHARACTERISTICS

As mentioned in the Background section, the potential hazard of orbital debris to orbiting objects is a more recent concern than the hazard of reentering debris to Earth. The origin of current concern was a 1978 paper by Kessler and Cour-Palais of the NASA Johnson Space Center.⁽³⁾ That paper first identified the existence of a possibly serious threat, analyzed the magnitude of the hazard presented by known orbital objects, and speculated about both the hazard from unobservable objects (too small for detection by current ground-based instrumentation), and the possible growth in the hazard in the near term.

Battelle became active in the orbital hazard area in 1979. The original emphasis was on producing an independent assessment of the on-orbit hazard. The basic result of this evaluation was a corroboration of the hazard mechanism and overall hazard magnitudes projected by Kessler and Cour-Palais.⁽⁴⁾ Since that time, Battelle has worked on general policy issues, the specific hazards due to expendable launch vehicle operations,⁽⁵⁾ and the development of dynamic models to study debris population evolution.⁽⁶⁾ Only the first item will be discussed here.

Orbital debris possesses certain characteristics which define the nature of the hazard it presents and which, in turn, give rise to many current policy issues. The debris of greatest concern is that located in low Earth orbit between altitudes of roughly 300 n.mi. to 1200 n.mi. Within that orbital region, the existing debris is highly randomized, particularly regarding the orientation of the orbital plane (line of nodes). Many of the objects are in near-polar or high-inclination orbits. Because of these orbital characteristics, encounters of an orbiting object with a piece of debris are likely to occur with large encounter angles and, therefore, very high relative velocities (average relative velocities are estimated to be of the order of 25,000 ft/sec).⁽³⁾ At these high encounter velocities, significant damage is possible even from very small objects (of the order of a few grams).

A major characteristic of this debris is the absence of any effective mechanism for debris removal. Above approximately 300 n.mi., the upper atmosphere is so tenuous that decay times are very long, and atmospheric drag is usually not an effective scrubbing mechanism. In addition, because of the random orientation of the debris orbital planes previously discussed, the propulsion requirements to collect multiple pieces of debris on a given flight is prohibitively high. Therefore, the sometimes mentioned concept of collecting the debris with an orbital "vacuum cleaner" is not practical. Because of these two factors, low Earth orbital debris, once deposited, tends to remain in place, so that the buildup is cumulative and not easily reversed or reduced.

Given this persistence of the debris, there is concern that a level of hazard inadvertently could buildup which could inhibit or prevent certain future uses of low Earth orbit. This is particularly true for large systems with long orbital residence time, such as the proposed space station. There is general agreement on the hazard presented by observable debris currently on orbit, which does not seem to present a major threat. However, there is no such agreement concerning the possible additional hazard due to unobservable debris, and the likely rate of growth of both the observable and unobservable debris. These are areas of significant uncertainty.

A final area of uncertainty is the possibility of a runaway buildup of debris. As indicated, collisions with orbital debris would be expected to occur at high velocities. Such collisions could produce multiple or even numerous pieces of secondary debris. If collisions begin to occur, this secondary debris could cause a dramatic increase in the number of objects in orbit, further increasing the rate of collisions and generating additional secondary debris. A cascade or runaway type of buildup could occur. At present, however, the dynamics of this situation have not been analyzed in the depth required, and so it remains a speculative possibility.

ORBITAL HAZARD--POLICY ISSUES

As in the previous case with reentry debris, a key factor in developing effective policy for orbital debris is the characterization of the risk. In the case of orbital debris, this has been a relatively difficult task. Unlike reentry debris, orbital debris hazards are not negligible compared to the natural background. At the present time, the hazard due to observed manmade objects is of the same order as the natural background due to meteorites, and may increase beyond the background level in the future. Therefore, the hazard cannot be dismissed through comparison with background levels. Adding to this problem is the previously mentioned uncertainties regarding the amount of unobserved debris and the likely rate of growth of both observed and unobserved debris. With these uncertainties, it is difficult to characterize the overall hazard. What probably can be said is that the hazard does not appear to be serious for current systems and operations, but could be very serious for future systems or operations. This type of situation makes it difficult to decide whether there is a need for immediate action, with the result that many courses of actions, ranging from near-total inaction to immediate policy promulgation, have been urged.

If policy for orbital debris is to be developed, several specific issues will need to be examined carefully. One is the degree of which design or operational changes designed to reduce the generation of orbital debris can or should be mandated for operational or R&D programs. A number of such approaches are possible, including:

- Minimization of the number of objects released in the use of separation mechanisms
- Provision of propulsion systems to assure prompt reentry of large items of debris (which are potential sources of large numbers of secondary debris objects)
- Positive venting of residual propellants to prevent subsequent on-orbit explosions
- Restriction of ASAT tests to low altitudes where aerodynamic scrubbing is effective.

These steps are similar in program and cost impact to the types of steps that were proposed for reentry debris hazard reduction. The decision regarding whether they should be implemented will depend upon the way that the orbital debris risk is eventually categorized and on the magnitude of the cost (including cost impacts) and risk associated with each option. At present, these are all largely undetermined.

A second major issue concerning orbital debris is the degree and timing of national and international cooperative efforts. It is clear that the orbital debris problem extends beyond the operations and responsibilities of any one organization or nation. Both the Soviet Union and NASA have been major sources of current debris, while other nations now beginning to become active in low Earth orbit (e.g., France through the SPOT program) are potential future sources. An effective debris policy would require the cooperation of all potential generators. However, the time may not be appropriate for serious international negotiations on this issue. Perhaps some single agency, such as NASA, should assume a leadership role by developing policy for its own operations, making these known to other debris contributors, and inviting dialogue and similar initiatives.

A third area of major concern is the potential military implications of orbital debris. Tests of ASAT systems could become a major source of orbital debris. As mentioned before, debris growth would be reduced if future ASAT tests were restricted to very low Earth orbit where the debris would be removed relatively rapidly. However, this restriction could compromise the effectiveness of the ASAT tests, a tradeoff that the DoD would need to weigh carefully. As a part of this tradeoff, the possible detrimental effects of this debris on other DoD programs (e.g., surveillance) would need to be considered.

A further military concern is the possible use of debris as a weapon. It is conceivable that one nation might decide that certain regions of space are more valuable to their enemies than themselves, so that they would be willing to deny its use to anyone. This might be affected by depositing sufficient quantities of debris in selected altitude zones to generate a high-risk situation, possibly through runaway generation of secondary debris. Nondiscriminatory use of debris in this way would be similar to the use of mines in land and naval warfare, and is a possibility that needs to be examined.

All of the above policy issues are currently unresolved, certainly on a national or international scale. It is not the purpose of this paper to recommend specific solutions to each of these various issues. However, there are some specific personal comments and suggestions that are offered for consideration.

PERSONAL OBSERVATIONS ON ORBITAL DEBRIS POLICY ISSUES

The first observation is that the existing data based on orbital debris is inadequate to support any definitive policy actions. It is not possible to answer certain critical questions at this time--questions such as what is the likely rate of growth of debris, is a runaway buildup of debris possible and even likely, and what are the specific results of collision with debris material at velocities of 25,000 ft/sec or greater on spacecraft structure and materials. Until such questions can be answered more definitively, policy decisions on orbital debris cannot be made on a solid basis of defensible fact or logic. Therefore, studies designed to develop understanding of the basic phenomena of orbital debris and debris collisions should be pursued with vigor.

At the same time that basic studies are proceeding, efforts need to be made to increase the general awareness of this potential problem. This should not be done in an alarmist manner, but with full admission of the uncertainties present in our current knowledge. This type of effort is needed because the hazard from debris is a counterintuitive phenomena--at first consideration, it usually is concluded that the risk must be very small because of the large volume of space involved as compared to the value of debris, and because the high average encounter velocities are not considered. Experience with Skylab reentry also indicates that physical phenomena with statistical or probabilistic aspects are not quickly grasped by the public, press, or even some decision makers. Therefore, it will likely take time to develop a proper understanding of this problem among wider segments of the population. The AIAA position paper on orbital debris hazards is one good example of such information dissemination.(7)

Efforts to increase informal dialogue at the working level both within the United States and internationally need to be increased. This current meeting is an excellent example of such dialogue, as were the previous year's presentations at the IAF meeting in Rome. As indicated earlier, eventual effective action on orbital debris control would have to involve all agencies and nations contributing to the generation of debris. Informal discussions among the appropriate groups can provide a basis for higher-level negotiations at a later date.

Because the hazard from observed debris is probably small for conventional military space systems, there may be a temptation to defer or downgrade any serious consideration of this potential problem in favor of more immediate military needs. This could be a serious error, since there could be major impacts on future military plans and operations if the orbital debris buildup continues without control, particularly if ASAT testing increases dramatically or if debris is deliberately introduced. The military implications of orbital debris deserve a hard look.

As a final personal observation, thought needs to be given to the form and purpose of any space debris policy. In particular, care should be taken to define policy in terms of broad objectives and principles. Developing effective policy in this area will probably require extensive negotiations at high levels of authority. The policy should be stated in terms of general guidance that will not need to be renegotiated as more is learned about the specifics of debris hazards. Specific steps to reduce the hazard should be suggested and eventually implemented by the personnel at the operational and design level, with the approval of higher-level decision makers. For those cases where it is considered essential to mandate certain rules or procedures to operational personnel, these should be contained in a set of implementing instructions which supplement the

basic policy, and which can be more easily modified than the basic policy as time progresses. Formulation of the policy in this manner can avoid much time-consuming renegotiations of base policy while still providing senior decision makers with the degree of detailed control that they feel necessary.

FINAL REMARKS

This paper has discussed the general problem of developing effective policy for orbital debris. The experience with reentering debris hazard policies does provide some insight for policy development for orbital hazards. The possibility that many useful regions of low Earth orbit could be inadvertently or even deliberately made extremely hazardous for space operations should be sufficient motivation for vigorous pursuit of basic understanding and viable and prudent policy courses. It is hoped that some of the suggestions offered in this paper would, if adopted, aid in this objective.

References

- (1) Drago, V. J., and Edgecombe, D. S., "A Review of NASA Orbital Decay Reentry Hazard", Battelle Columbus Laboratories, Columbus, Ohio, Report No. BMI-NLVP-TM-74-1, March 7, 1974.
- (2) Edgecombe, D. S., "Skylab Special Analyses", Battelle Columbus Laboratories, Columbus, Ohio, Report No. BMI-NLVP-LR-78-1, April 25, 1978.
- (3) Kessler, D. J., and Cour-Palais, B. G., "Collision Frequency of Artificial Satellites: The Creation of a Debris Belt". Journal of Geophysical Research, Vol. 83, June 1, 1978, pp. 2637-2646.
- (4) Reynolds, R. C., and Fischer, N. H., "The Hazard Presented to the Shuttle by Other Satellites in Its Operating Equipment", Proceedings of the 1980 JANNAF Safety and Environmental Protection Session, March, 1980, CPIA Publication Number 313.
- (5) Weber, W. P., "Orbital Debris Resulting from the Explosion of Delta Launch Vehicle Second Stages", Battelle Columbus Laboratories, Columbus, Ohio, Report No. BMI-NLVP-ICM-81-20, April 29, 1981.
- (6) Reynolds, R. C., "A Review of the Modeling Efforts for the Man-Made Orbital Debris Hazard", Battelle Columbus Laboratories, Columbus, Ohio, Presented at the NASA/Johnson Space Center Orbital Debris Workshop, July 27, 1981.
- (7) Space Debris, An AIAA Position Paper, AIAA Space Systems Technical Committee, Presented at the 22nd IAF Congress, Rome, Italy, September, 1981.

D31-12
N 85-21219

CONSIDERATIONS FOR POLICY ON MAN-MADE DEBRIS PROPAGATION CONTROL

D. FIELDER

PREMISE

The present rates of man-made, space object propagation are such that there is a real probability of self propagation which, if uncontrolled can lead to a serious limitation to future uses of spacecraft for beneficial purposes.

Effective control over the debris issue requires adoption and adherence to policy at a world wide level (any one nation's unknowing, selfish or deliberately adverse action can conceivably jeopardize other useful applications of space satellites for years into the future).

The near-term environment may not seriously jeopardize the near-term missions. However, absence of control and/or nonadherence to a control policy in the near-term can result in a debris environment that can severely limit long-term mission opportunities.

The data upon which these observations are based continues to be investigated. These investigations tend to validate the preceding observations and emphasize the need for near-term action to establish responsible control policy and implementation actions.

POLICY STATEMENT ON SPACE DEBRIS

(Note: - This statement is intended to be specific enough to focus upon the issue but general enough to allow flexibility in its implementation such that as the issue becomes better understood so can the levels of implementation be adjusted. The policy statement would have longevity as a national objective and should support the development of related policy applicable at the international level. The implementing instructions would be changed in accord with the development of the related knowledge of the debris issue and that technology which bears upon the abatement or control over debris propagation.)

Policy on unnecessary propagation of space debris:

In that earth orbital space is an international domain and, by the nature of its international use, can be defined as a resource of limited capacity, it shall be U.S. policy to adopt all practical means to preserve the capacity of earth orbital space for useful space satellite applications.

In that placement or propagation of useless and or residual man-made objects in space can jeopardize the capabilities of future space missions. It shall be immediate U.S. policy to avoid all unnecessary increases in the population of man-made space objects.

In addition it shall be immediate U.S. policy to initiate international proceedings to establish a world-wide policy to avoid unnecessary increases in the population of man-made objects.

In addition it shall be continuing U.S. policy to develop spacecraft launch and operational techniques such that the man-made population of space debris and useful spacecraft, together with the natural background, does not exceed, or portend to exceed an acceptable combined flux level (a level to be determined from ongoing investigations).

(Note: If "NASA" is substituted for "U.S." in the above it must be contingent upon NASA having the authority to act in a national and international capacity on behalf of the U.S.)

DEFINITIONS:

The following typical definitions must be developed as they are applicable to the policy statement:

Earth Orbital Space -

The term "earth orbital space" refers to that volume surrounding the earth encompassed by a sphere of radius equal to geosynchronous orbit apogee. For circular or near circular geosynchronous orbits this spherical radius is approximately 42,000 kilometers. For geosynchronous orbits with eccentricities up to 0.5 (as may be considered for future applications), this radius can be up to 60,000 kilometers.

Of particular interest are those orbits associated with domestic applications satellites (approx. 36,000 kilometers, circular altitude, 0-5 degree inclination).

Debris -

The term "debris" refers to all man-made objects remaining in space that serve no useful purpose and applies to the following typical objects:

- a. spent, depleted, or otherwise non-operational payloads.
- b. spent, depleted, or otherwise non-operational launch stages, payload shrouds, interface hardware, pyrotechnic separation by-products, etc.
- c. fragments generated by accidental or deliberate explosions.
- d. fragments generated by collisions between any of the above.
- e. particles and other combustion by-products from rocket engines.

Natural Background -

The term "natural background" refers to the flux of natural objects occupying the volume of interest. These objects are primarily of cometary origin. The motion of these objects is well defined. The natural background has been and continues to be an environmental consideration in the design of spacecraft to provide protection against the statistical probability of impact.

Note: The natural background constitutes the galactic environment through which the earth passes; space debris is in earth orbital domain and emanates from earth based, man-made origins.

GENERAL DISCUSSION

Man-made debris contributes an extra dimension to the natural background. This extra dimension includes a relatively small number of large objects and a relatively large number of small objects. Being man-made, these objects do not follow the natural distribution and result in a higher statistical hazard probability for their relatively small population. These higher probabilities occur at altitudes of operational interest (STS and geostationary) and, in part, are further increased by the formation of secondary debris products from impact between and amongst man-made objects and the resultant change in flux and flux density. It is theoretically possible that, through mutual collisions, man-made debris can become self-propagating.

As nations explore and then exploit the use of objects in space to their benefit, they must necessarily place objects into space and thereby extend the natural flux. Although the net population (natural plus man made) is increased, there is no meaningful increase in the overall hazard probability due to the useful objects. However, the attendant increase in the population of useless man-made objects can increase exponentially, with the increased probability of impact with useful objects (and the equivalent reduction of impact with useful objects (and the equivalent reduction in their mission capability). Because there is no physical means presently available to remove, or otherwise dispose of man-made debris, it behooves all nations to take appropriate action to exercise some form of control over any unnecessary increases in the overall population of man-made objects. Until means of physical disposal are developed, it would be expected that NASA and other international, space related institutions would jointly pursue actions which:

- reduce unnecessary space object propagation,
- develop a better understanding of the natural background and its dynamics,
- develop a better understanding of the potential hazard from future propagation of man-made objects,
- develop a better understanding of the mission effects of operating spacecraft within the combined natural and man-made object populations, and
- develop a better understanding of means for physical removal (or other disposition) of man-made objects.

POLICY IMPLEMENTATION

To be implementable, a policy should have the following properties:

- a valid purpose,
- practical objectives,
- institutional representation,
- delegated institutional authority and responsibility,
- defined control parameters, and
- means of enforcement.

The purpose, or need for a debris related policy is embodied in the recognition that, if uncontrolled, man-made debris can become a prime factor in limiting, or even inhibiting the future use of spacecraft.

Note that immediate future space program missions need not be compromised. However, it is in this same immediate future period that the seeding can take place which could result in long-term deterioration of future mission opportunities. It is therefore prudent and timely to adopt obvious and sensible practices which avoid those totally unnecessary and most flagrant forms of debris propagation. This approach may alone provide time for the research and development necessary to bring the problem under control and yield continued growth in the virtually unlimited opportunities for the beneficial uses of space.

Practical policy objectives require an extensive iteration with the user communities. It must be agreed that the objectives are not only possible, but that they serve community interests and that they will not incur costs or other impediments that would jeopardize the ability of the community to meet their objectives, further, the objectives must support practical means of enforcement.

To become effective, the implementation mechanisms must be appropriately embodied within the institutional structure. Given the international character of the policy objectives, it follows that the institutional structure can be profound and complex. Without attempting to orchestrate this structure, it must nonetheless contain the following basic elements:

- an upper management hierarchy to administer the policy,
- a service operation that "measures" the current debris population and assesses planned mission collision probabilities,
- a technical operation that assesses collision and incurred damage, the resultant mission degradation, and/or any secondary debris propagation and its affects,
- a program management operation that assesses the acceptability of degradation and or secondary debris propagation, and implements the resulting decisions.

POLICY CONTROL PARAMETERS

It is postulated that there is some allowable limit to the population level and altitude distribution of man-made objects in space. At any point in time, this population would include the projected number of currently operational spacecraft plus that distribution of debris which does not reduce the mission success probability for each operational spacecraft below an acceptable level. In the absence of debris, the number of concurrently operational spacecraft could be virtually unlimited (being under constant control and, at the present time, being the much smaller portion of the total man-made population). In the presence of debris, it is conjectured that there is some limiting level of debris distribution where the statistical probability of collision with each operational object (and the related probability of mission degradation for that object) is such that the probability of mission success for any operational object could fall below an acceptable level. Such a limiting value could be developed and established as a specific objective to be met and maintained through debris policy implementation.

From the presently available data base it is estimated that the likelihood of arriving at a limiting condition is several years into the future. This limiting condition has been dramatically aggravated by the occurrence of untoward explosions and fragment propagation, a practice which should be avoided if at all possible in the future.

The debris population at any point in time is a function of the following typical parameters:

- a. the current population of operational satellites, the projected population of new satellites, and their respective operational lifetimes (after which they become units of debris).
- b. the current debris population, the projected debris added during the deployment of new satellites, the occurrence of any self propagation due to mutual collision, all subsequent secondary debris products, and the rate at which units of debris may reenter due to orbital decay.

The probability of degradation of any operational satellite beyond a useful level of capability is a function of the following typical parameters:

- a. the probability of mutual collision or collision with debris.
- b. the probability that the operational satellite(s) may incur physical damage and the extent to which such damage may contribute to the debris population.
- c. the probability that the damage incurred to the operational satellite(s) will result in degradation of mission performance below an acceptable level.
- d. the determination of an acceptable, degraded level of performance for any one satellite.

POLICY CONTROL PARAMETERS (continued)

The acceptable level of degraded performance for each satellite can be used to determine an acceptable gross population for man-made debris. This, in turn can be compared with the projected debris population in the same time period. Theoretically, if the projected debris population exceeds the acceptable population then, at the associated point in time some physical corrective measures would be required. Such conceivable measures could include the following:

- a. "hardening" of the vulnerable satellite(s), if they are yet to be launched.
- b. delaying the launch of the vulnerable satellite(s) until the projected debris population abates to an acceptable level.
- c. reducing any tendency for the satellite to generate secondary debris particles.
- d. physically changing the projected debris population before the projected launch of the vulnerable satellite(s).

Note: Collisions occur at a statistical average of 10 km/sec. At these hypervelocities, a .01 gm particle, at the moment of impact has a kinetic energy of approximately 50 kg. meter (or 350 ft.lb). The subsequent impact involves a complex energy transfer and can cause considerable primary damage, depending upon the characteristics of the spacecraft material and structure. Some of the energy is transferred in the form of secondary debris products (ejecta). These high temperature, high velocity particles can, in turn, add to the net population or, if the primary structure is penetrated, cause subsequent damage to secondary structure. Successive penetrations can have a cascading effect and the area of secondary damage can be much larger than the area of primary damage.

POLICY IMPLEMENTATION ACTIONS

The following list of statements present an array of typical actions required to implement the preceding statement of policy:

1. Inhibit (outlaw) all deliberate, planned explosions (offensive or defensive weapons, disposition of spent space systems, etc.)
2. Inhibit (outlaw) the deployment of payloads which, in turn would deploy very large numbers of long-lived, independent elements (shrapnel, wire shredding, chaff, etc.).
3. Prevent and protect against the possibility of accidental explosion or detonation of any space system employing potentially explosive elements to perform its mission (rocket stages, propulsion systems, hypergolic fuel systems, combustible gas mixes, high pressure fluid storage systems, etc.)
4. Avoid, minimize, or otherwise reduce to the absolute minimum, the number of elements of a space system that must be released into space in the process of deploying and initiating that system (marmon clamps, retention bolts, shrouds, covers, panels, etc.).
5. Avoid, minimize, or otherwise reduce the release of solid particles during the period of operation of a space system (solid propellant combustion products, pyrotechnic devices, waste dumping, fluid bypass or overflows, etc.).
6. Tether, articulate, or otherwise retain all equipment to be used in an EVA operation or in robotic association with spacecraft servicing (service systems, tools, cameras, test gear, and other devices).
7. Design for and provide positive means for the debris free disposition of spent space systems:
 - self reentering
 - self maneuvering to a predetermined disposition area (dump or spent system cluster)
 - interface compatibility with an available propulsion stage capable of performing the above mission maneuvers
 - planned reuse of spent systems in other, committed to space programs.
8. Continue to explore and investigate new, innovative or other unique methods of increasing the effective capacity of earth orbital space:
 - multifunctional space systems (platform concepts, space operations centers, serviceable satellites, etc.).
 - unused orbital domains (circular, inclined, and or elliptical, inclined geosynchronous orbits).
9. Establish means to measure and predict the man-made debris population:
 - dedicated tracking and data acquisition systems
 - in-flight (space) measurement systems
 - statistical modeling and prediction systems

POLICY IMPLEMENTATION ACTIONS (continued)

10. Establish means to assess and predict the compatibility of projected future space systems with the correlating prediction for the net population of man-made objects:
 - determine collision probabilities
 - determine spacecraft/system damage probability
 - assess spacecraft/system performance degradation
 - assess acceptability of performance degradation
 - implement any related program changes
11. Continue and improve the means for assessing and predicting the compatibility of projected future space systems with the correlating prediction for the natural background.
12. Assess the interplay, if any, between the total population of space objects (natural and man-made) and the earth's natural environment as regulated by the environmental protection agency.
13. Establish ways and means to arrive at a practical implementation of space utilization policy on a world-wide basis:
 - adoption and enforcement throughout NASA (all program and project offices, field installations, etc.).
 - adoption and enforcement throughout other U.S. space using organizations (DOD, NOAA, etc.).
 - Adoption and enforcement over international customers provided space services by the U.S.
 - Adoption and enforcement by other countries and international organizations with independent means of implementing spaceflight operations (USSR, ESA, France, Germany, Japan, China, etc.).
 - Adoption and enforcement by countries who develop space systems and are dependent upon nations other than the U.S. for space launch services or other space services (world-wide national potential).

Note: Some of the above actions (1-6) may be beyond NASA's jurisdiction in which case they might be regarded as initial positions for subsequent negotiation.

ENVIRONMENT DEFINITION, LARGE PARTICLES

DON KESSLER

The orbital debris environment of objects larger than 1 sq. met. in Low Earth Orbit (LEO) is fairly well defined. Objects of this size and altitude are tracked by NORAD with sufficient accuracy that collisions can be avoided by maneuvering a spacecraft away from regions of close approach. However for sizes smaller and at the higher geosynchronous altitudes, the environment is not so well defined, and must be approached statistically.

In LEO, there is some knowledge of the number of objects down to about 0.1 sq. met. However, for smaller sizes, the uncertainty in the number of objects increases. Below 0.001 sq. met, the environment is totally unmeasured. Because of the history of past explosions in space, there is reason to believe that there is currently a significant source of debris between sizes 1cm in diameter and radar cross section 0.001 sq. met. By the 1990's, there is a possibility of a significant source of smaller particles. Depending on the nature of the spacecraft system being impacted, particles as small as 0.1 mm (100 μ) could cause significant damage.

In order to determine if a significant number of these particles exist, or can be realistically produced, to cause a problem, a combination of modeling and data gathering is required.

Perhaps the most direct technique of obtaining some measure of the current population, while at the same time understanding the significance of the environment, is to examine the history of spacecraft failures and breakups. It is generally believed that no spacecraft have failed as a result of collisions. If so, then an analysis of what constitutes a failure, combined with some environmental modeling would provide an upper limit to the current environment. However, it may not be obvious that the failure of some spacecraft component was due to penetration by a small particle (e.g., the failure of the Voyager camera control as Voyager flew through Saturn's rings cannot be proven to have been caused by a particle impact). Therefore, it may be appropriate to reexamine some spacecraft failures for the possibility of failure due to penetration. This could lead to a more realistic estimate of the current environment.

In addition, hypervelocity fragmentation data should be researched and modeled to predict what a "collision signature" should look like from the ground. The fragments orbital characteristics and sizes may have unique characteristics when they originate from a collision. The existing data of satellite breakups and anonymous events could then be examined for those characteristics, leading to another possible determination of the existing environment. However, depending on satellite failures and breakups to warn us of an impending problem could be very short sighted. (like a swimmer who refuses to look for sharks, but waits to be bitten, the situation can get much worse very fast.) For this reason, other data are required. This data should be modeled to project future population trends. Model assumptions should be tested by further experiments.

As future breakups occur, there will be an increasing need to analyze the data generated by these events. A procedure needs to be set up with NORAD so that the paper data is delivered to those responsible for analyzing the data, which could be either NORAD, NASA, or DOD. However, there should be an interagency sharing of data available from NORAD.

NORAD should perform routine tests on a non-interfering basis. Some radar or optical systems could be designated to take "snapshots" or statistically sample the smaller population. Or the analysis and data reduction of smaller objects detected by NORAD could be performed by other interested agencies. Existing data at NORAD could also be analysed by these agencies. This could alleviate some of the problems which NORAD has in cataloging small objects, objects in highly elliptical orbits, and objects at high altitudes, while providing the other agencies with the information they require. More dialogue with NORAD would be required to fully explore these possibilities.

In LEO, the critical need is to have more data. Some untaped data sources may exist in the classified world, and should be explored.

In GEO, the critical needs are for both more data and more modeling. Neither of these two areas have progressed to the point that we believe that we understand the environment in GEO. As the GEODSS system becomes operational, more data will become available.

D. 3. 12

N 85-21221

Modeling

Herb Zook

A prediction of the future population of satellites, satellite fragments, and assorted spacecraft debris in earth orbit can be reliably made only after three conditions have been satisfied: (1) the size and spatial distributions of these earth-orbiting objects are established at some present-day time, (2) the processes of orbital evolution, explosions, hypervelocity impact fragmentation, and atmospheric drag are understood, and (3) a reasonable "traffic model" for the future launch rate of earth-orbiting objects is assumed. The theoretician will then take these three quantities as "input data" and will carry through the necessary mathematical and numerical analyses to project the present-day orbital population into the future.

The input data can be put into two categories: (1) known, or measured; and (2) unknown. The known data include: (1) the spacecraft and fragment population detected and tracked by NORAD, (2) something of the orbital characteristics of fragments resulting from explosions in space (from the work of John Gabbard), (3) the distribution of fragment sizes resulting from Delta launch vehicle explosions on or near the ground, (4) limited data on the distribution of fragment sizes resulting from hypervelocity impact tests on simulated spacecraft shapes, (5) the sampling of the near-earth penetration environment by the Explorer 46 satellite (including Kessler's interpretation that many of the penetrations are due not to meteoroid impacts but to debris impacts), (6) the historical launch rate of spacecraft, and (7) the fact of the USSR conducted ASAT tests. There are undoubtedly other "knowns" not listed here.

The "unknowns" must be assumed by the theoretician as part of his "model" before he can proceed with his calculations. What are they? We don't know what would result, in detail, from an in-space collision. We don't know the size distribution of fragments very well, and we have to extrapolate from our ground-based impact tests at low impact velocities. We probably need to look some more into the orbital distribution of fragments resulting from explosions. We do not know the current number of small, 1 mm to 10 cm diameter, fragments in space. There are sources for these: there are pieces that come off the spacecraft during launch, there have been explosive fragmentations, and there have been ASAT tests. In geosynchronous orbit we know practically nothing about the fragment population. If there have been explosions at geosynchronous orbit, we wouldn't know about it. They even loose entire spacecraft out there and are unable to find them. We don't know what the future traffic model is but must make an assumption about what it will be. That is going to have to remain as an assumption. We don't know what the size distribution of particles resulting from ASAT tests are, but I believe we can make an assumption and proceed ahead.

What needs to be accomplished then? These are some items that our working group came up with, although we didn't really assign priorities to them at

the time. Therefore I have prioritized them from one through ten here using my sense of what I thought the group felt were proper priorities. These may, of course, be rearranged.

1. We were all concerned about our lack of knowledge of the current earth orbit population of small particles. We extended that concern down to 100 um particles diameters, but we are particularly interested in the 1mm to 10cm range. We would like to have that knowledge as inputs into our modeling, but also, to some degree, to test our modeling. That is, we have obtained a small particle population as an output from modeling previous inputs and we would like to do some testing of this modeling.
2. What differences, if any, exist between fragments determined to be derived from internal explosions and those derived from in-space collisions? Can we somehow recognize in the NORAD data - especially the one prepared by John Gabbard - that there is some unique signature that can tell us that one population of particles is due to collision and another population is due to some internal energy process? Right now we don't know of any unique signature.
3. Continue and expand special analyses such as John Gabbard has done of the NORAD radar data.
4. Do additional in-space object detection tests with a ground-based radar to better characterize small objects.
5. Do additional parametrics studies. What assumptions give rise to worst case space object hazards? We need to find out what kind of assumptions regarding size distribution, or what type of activities, such as ASAT tests, really give rise to the worst case. This may mean that we will want to gather more data about processes leading to worst case results, perhaps on high priority basis.
6. Project far into the future to 200 or 1000 years from now. Do the modeling and see if we get any unpleasant surprises. Are we getting ourselves into some kind of severe and irreversible problem? We need to take a look at that. For example, how important are cascade processes? We not only have spacecraft colliding with spacecraft, fragments colliding with spacecraft, but fragments colliding with fragments, and so on down to granddaughters. How important is the traffic model in this larger projection?
7. Examine hazards to a specific space mission. For example, can we safely build a solar power station in low earth orbit and then move it up to geosynchronous orbit?

8. Examine the interaction between orbital transfer vehicles and objects in geosynchronous orbit, and with objects in low earth orbit.
9. Look for more efficient numerical techniques to accomplish the modeling so we can quickly investigate a wider variety of parametric variations.
10. This is kind of a political one. We believe that there is enough work to be accomplished so that not only should all the current activity be continued, but that additional people should be energetically involved in extending and increasing the analyses. Different groups typically looked at different problems. They may look at the same problems with different techniques. A tremendous advantage with more people is that once one group gets a new result it can be quickly confirmed by another group. The confidence of the rest of the space community in the results obtained will, therefore, be much enhanced.

#34-12
N 85-21222 1

Measurements

Andrew E. Potter ✓

Concerning the measurements required for a better definition of the debris environment, the panel chose to divide the debris population into large and small regimes. Large debris includes 10 centimeters. The source of data for this size range are the existing NORAD optical and radar systems. The regime of small debris objects is chosen to be the range from about 1mm to 10cm. We currently have no source of data for this size range. Direct measurements of the small debris population from ground based systems and satellite based systems are concernable. Indirect measurements could also give information about this size range. These are laboratory measurements designed to give some reality to models which estimate the number of particles produced from an explosion or an impact.

As mentioned, NORAD is the source of data in the size range above 10cm. It was brought out in the panel discussion that not all of the NORAD data is analyzed. That is interesting from the point of view of establishing a complete census of all the debris that can be detected by NORAD. NORAD discards uncorrelated or uncataloged data after a period of time, simply because these are particles that are too small to be of significance relative to their mission. Analysis of this data would expand our catalog of objects in the 10cm and longer range. Who would do this analysis is not the subject of this meeting. It might be that another agency would have to take on the job of saving the uncataloged data, and carrying the analysis a step further in order to expand our knowledge. A significant point in the panel discussion was that NORAD might not continue to analyze breakups in the same way as they have in the past. If this analysis doesn't continue, we will lose important evidence for explosions and collisions. It may start up again in the future, 1987, when SPADOC becomes operational, but in the meantime, there is a possibility of a gap. We should pay attention to this possibility, and not let it happen.

The last topic relative to NORAD is the PARCS tests. These have been extremely useful in giving us statistical data on the population at the small end of the NORAD capability. The group felt that these tests were important, and that they should be continued, perhaps on an annual basis to see what trends develop. They are very useful tests and the group highly endorsed continuing them.

For small (<10cm) debris particles the lower limit size of interest was a matter of debate within the panel. Everyone could agree that 1cm was certainly a dangerous particle size. Impact by a 1cm particle would be a definite problem. Below 1cm, the lower limit was questionable. The impact of a 1mm particle might or might not be significant, depending on the relative velocity and the position of impact on the spacecraft. So at any rate, the lower limit is certainly at least 1cm, and perhaps is as low as 1mm. Insofar as ground-based measurements of small debris, it appears that there is a possibility that the GEODSS system may be capable of collecting new data in this size range. One of the actions that came out of the panel was to study the GEODSS system and determine its capabilities. We might be able to collect data with that system on a noninterference basis, to

support the census of the small debris population. There was a paper in this session on optical systems optimized for small debris particles. An optimum system should be able to collect data on sizes down to about 1cm. Perhaps the GEODSS system is already optimized, and has the capability to get the data we need. Satellite-based measurements offer the best possibility for measuring debris in size ranges down to 1mm. The Shuttle platform is attractive from the view of costs and availability. It is not the best place to do the measurement, simply because the Shuttle is constrained to relatively low orbits. This means your instrument doesn't fly among the particles it is looking at, but has to reach out and sense them from a distance. This makes a difficult experiment. The group felt that the possibility of a Shuttle experiment should be looked into carefully. Free-flying satellites are the best way of measuring small debris particles, but suffer from the problem of cost. It is more expensive to build and fly spacecraft in the right kind of orbit for this measurement. A piggy-back instrument, to be flown as a passenger on various spacecraft seems the most economical choice.

Indirect measurements are those which do not measure particles directly in orbit, but are laboratory measurements which support and extend the model. What we are interested in in these measurements are the particle size and the velocity distribution that result from explosions and high velocity impacts, particularly high velocity impacts on spacecraft structures. These results can then be fed into models of the debris population. One point brought out by the panel was that some work has been done in this area, but is reported only in the classified literature. We need to review that literature very carefully before we proceed with future measurements.

235-12
N 85-21223 |

ENVIRONMENT DEFINITION, SMALL PARTICLES, DIAMETER \leq 1 MM

MEMBERS:

Barney Roberts/ET4, Chairman
Uel Clanton/SN6
Jack Hartung/NASA Headquarters, EL-4
Eberhard Grün/MPI-Für Kern Physics

WHY IS ENVIRONMENT IMPORTANT?

The collection of particles of diameters one millimeter and less far outnumber the larger particle distribution in orbit. These small particles cannot be tracked from ground based radar as can the larger debris, therefore, there is greater uncertainty in their properties. The population is growing from contributions due to collisions of larger debris, explosions, and aluminum oxide particles from solid rocket motors. The solid rocket motor contribution is the prominent growth parameter, and the input from Space Shuttle deployed upper stages will range between 50,000 and 100,000 pounds per year.

The environment is important because of the different design problems that will be posed to the engineer and scientist. For the engineer the emphasis shifts from catastrophe design, probability versus exposure time, and tracking-avoidance, to a continuous degradation problem. Penetrations will occur in the upper sizes of this population (\sim 1MM), however, the major problem will be erosion of surfaces. This will alter the ratio of radiant energy absorption to emittance and subsequently impact thermal control. Glass surfaces such as windows, lenses, and mirrors are much more sensitive to this environment since they can quickly, with very little erosion, lose a significant amount of their optical quality. That is, not only is transmittance and reflectivity affected, but visual quality is reduced and instrument "noise" increased due to light scattering and diffraction from the microscopic damage sites.

support the census of the small debris population. There was a paper in this session on optical systems optimized for small debris particles. An optimum system should be able to collect data on sizes down to about 1cm. Perhaps the GEODSS system is already optimized, and has the capability to get the data we need. Satellite-based measurements offer the best possibility for measuring debris in size ranges down to 1mm. The Shuttle platform is attractive from the view of costs and availability. It is not the best place to do the measurement, simply because the Shuttle is constrained to relatively low orbits. This means your instrument doesn't fly among the particles it is looking at, but has to reach out and sense them from a distance. This makes a difficult experiment. The group felt that the possibility of a Shuttle experiment should be looked into carefully. Free-flying satellites are the best way of measuring small debris particles, but suffer from the problem of cost. It is more expensive to build and fly spacecraft in the right kind of orbit for this measurement. A piggy-back instrument, to be flown as a passenger on various spacecraft seems the most economical choice.

Indirect measurements are those which do not measure particles directly in orbit, but are laboratory measurements which support and extend the model. What we are interested in in these measurements are the particle size and the velocity distribution that result from explosions and high velocity impacts, particularly high velocity impacts on spacecraft structures. These results can then be fed into models of the debris population. One point brought out by the panel was that some work has been done in this area, but is reported only in the classified literature. We need to review that literature very carefully before we proceed with future measurements.

For the experimenter, this environment represents background "noise" which may compromise his experimental objectives. These particles, of course, generate an electromagnetic environment due to their reflection and radiation properties, and many experiments are specifically designed to measure electromagnetic radiation, therefore, the experimenter is immediately faced with a problem of "cluttering" in his optical path. For the experimenter who wishes to observe the natural particulate environment of cosmic origin, the manmade contribution to this population will compromise his measurements as well.

In summary, for short lifetime, low earth orbit (LEO) types of spacecraft, this environment, in most cases, will be negligible. However, with the advent of the Space Shuttle, space stations, and reusable orbit transfer vehicles, the planned stay-time in LEO will be increasing as well as the number density of particles.

These two factors combined yield the conclusion that this environment is now a significant design problem.

HOW WELL IS ENVIRONMENT KNOWN?

As mentioned earlier, this environment cannot be observed from ground based instruments. A space based instrument is absolutely necessary for accurate measurements, and, to date, only very limited data is available. Stratospheric collection by high altitude aircraft has yielded substantial data on this environment. Unfortunately, however, the size selectivity of atmospheric dispersion upon entry of these particles, the different initial conditions of manmade debris versus those of cosmic origin, and the selectivity of the collection technique all combine to negate the possibility of determination of relative size distribution and relative composition of the orbital population. Stratospheric collection does offer an excellent opportunity to

return representatives of this population to the laboratory for chemical and physical property determinations of individual particles.

Another factor which will make this environment difficult to quantify is the as yet undetermined time dependance of the population caused by the burning of solid rocket motors and the fragmentation of larger debris. Of the two, fragmentation is probably best known and could be easily improved upon by performing some experiments; however, it is believed that the largest contributor to the time dependance will be the solid rocket exhaust particles and not the fragmentation problem.

There are two effects expected from the burning of solid rocket motors in orbit. One is a long term buildup by that portion of the exhaust particles that happen to be ejected into long lifetime orbits; the other is a short time increase caused by those particles injected into orbits with perigees low enough to enter the earth's atmosphere and, over a short period of time, be removed from the orbital population.

Inability to ground track, lack of orbital measurements, and the time dependance make this environment less well known than the large debris environment ($\geq 1\text{MM}$). It was estimated that the physical properties of this environment were known only within an order of magnitude. The critical area of uncertainty is the manmade portion of this environment: the production and reduction rates and the physical characteristics of the current population.

TESTING REQUIRED

GROUND BASED - Fragmentation tests, both collision and explosion are required unless it can be shown that this contribution is much less than the solid rocket motor contribution.

SPACE BASED - As mentioned earlier, only a space based experiment can be expected to yield the data required. The working group considers such experiments mandatory in order to define the environment. These measurements should be designed to measure the short term effects from an upper stage as well as the steady state environment. It would also be beneficial to examine any spacecraft returned from orbit. Procedures should be established to accomplish this inspection and make other organizations aware of our desires.

RECOMMENDATIONS

- o Upgrade current models
- o Perform additional stratospheric cosmic dust collections with larger collector (~ \$140K for collector)
- o Support NASA/FRG experiment (~ \$4.8M) to measure short term environment (Approval still tenuous)
- o Establish interagency working group
 - o To coordinate and disseminate
 - o To serve as co-principal investigators on experiments
 - o To share funding/eliminate duplication
 - o To build broad base of support
 - o To publish findings
- o Perform fragmentation/collision experiments

Members:	Ralph Chen	Jet Propulsion Laboratory
	Eldon Davis	Boeing, Seattle
	Harvey Ebersole	Battelle, Columbus
	Don Humes	NASA, Langley
	Karen Morrison	NASA, Johnson
	Jim Rand	Southwest Research Institute
Chairman:	Burton Cour-Palais	NASA, Johnson

1.0 DISCUSSIONS

1.1 The panel considered the elements related to Hazard Assessment shown in Figure 6 of the proposed JSC 10-yr Space Debris Assessment Plan, i.e., Systems Damage Criteria; Impact Damage Assessment; and Mission Success Assessment Algorithms.

1.2 Section 2 of the 10-yr plan schedule (Figures 5-2 and 5-3) was reviewed for validity of the research elements; accuracy of the proposed effort and cost; duration of the task element; and interaction with the other elements of the plan. There was no specific discussion of whether NASA, DOD, or industry should perform the proposed tasks.

2.0 BACKGROUND

Before getting into the comments, it is important to reiterate the purpose of the 10-yr Debris Assessment Plan.

The plan was requested by NASA Headquarters as a pre-requisite to a decision on whether to formalize an Agency space debris policy or not. The existence of concentrations of space objects in low earth orbits, 4cm in diameter and larger, is incontestable. The extrapolation to related populations of sizes to 1mm diameter, and even smaller, was viewed as not based on firm evidence. Also, given the existence of a debris environment in low earth orbit, it's significance to proposed space activities was not clear. The mere calculation of an impact probability is not synonymous with catastrophic failure. Thus there was, and is a need to answer several questions in relation to the space debris issue, before any agency action/policy can be formally adopted. The encouragement to produce the 10-yr plan, the funding levels already authorized by two Headquarter's program offices, and the high level support given to the Orbital Debris Workshop is evidence of a de-facto recognition of the subject in NASA, as well as the DOD.

Figure 6 of the 10-yr plan document lays out the building blocks leading to space debris decisions at the various National & International levels ultimately involved. The Mission Success Assessment Algorithms combine the current environment definition (flux vs size; velocity distributions at various inclinations; flux vs altitude and inclination), with penetration equations relating to the various spacecraft systems exposed to impact, their impact

failure modes, and mission vulnerability/survivability specifications. It should be understood that for the objective of the 10 yr plan, spacecraft & system design criteria are generic in nature. The process of determining the success or failure of a proposed real mission would be dealing with a specific spacecraft design and possibly unique system elements.

3.0 COMMENTS

3.1 Impact Testing

There will always be a need for impact tests on specific vehicle components, both low velocity and hypervelocity. Generalizations with regard to typical components are not possible, although some spacecraft, i.e., the Multimission Spacecraft and its basic components can be considered "generic". Also, there are new systems, new operational procedures, longer life requirements, repeatable duty cycles, etc. Although we may need a new "breed" of tests, it is not necessary to re-do everything we have done so far. It was generally agreed that hypervelocity impact penetration equations are required for new materials being used in space structures, specifically the composites. An interesting opinion was that the need for testing depends upon the "end-item". Penetration equations relating to generic shielding concepts and systems are required for paper studies, i.e., preliminary investigations for program management decisions. However, the survivability assessment of an actual space vehicle will most probably require impact tests of actual system elements.

3.2 Systems Damage Criteria

System damage criteria will have to be re-established for the new breed of space vehicles because reusability, recycling and refurbishment have affected the designs. A prime example is that the Apollo fuel tanks were allowed to sustain wall damage from meteoroid impacts up to a 25% reduction in thickness. The Orbital Transfer Vehicle Study by Boeing, with a requirement for repeated missions with a tank set, could not permit any wall thickness damage by meteoroid or orbital debris. System damage criteria are established by safety and reliability failure modes, and as such, are usually outside the domain of the mission success analyst. For preliminary studies, these criteria can be obtained from generic impact related system failure data. When it comes to assessing actual space vehicle survival probabilities for the meteoroid/debris environment, specific system damage criteria will have to be obtained either by impact test, as mentioned previously, or by minimum system performance requirements imposed by other disciplines.

3.3 Mission Success Assessment Algorithms

Although it was generally agreed that mission success assessment algorithms, based on environment data, impact equations, and systems damage allowables were possible, it was pointed out that overall mission success was more than just an orbital debris number. Also, within this limited framework, the definition of "success" levels or survivability classes, must be clarified. There are several interpretations of a successful mission and specific criteria must be established for use in the algorithms, to allow program managers the flexibility to decide what they can afford. Again, the Apollo/Skylab era single mission criteria for survivability may not be applicable. It is generally agreed that the "building blocks" leading to mission success assessment was acceptable, as each element was a necessary sub-set.

3.4 Literature Survey

The need for a literature survey was brought out by those who are currently having to calculate space vehicle or platform hazard assessments for the meteoroid/orbital debris environment. It was stated that low velocity equations are readily available from such sources as the Ballistic Research Laboratory (BRL), Battelle, and any organization working in the area of personnel armor research. In the field of hypervelocity data, there is a strong requirement to catalog both the classified and unclassified research done up to the present. The DOD has made a start on this and Southwest Research Institute has completed a classified literature survey. A bibliography of reports dealing with the research completed between 1962 to 1970 will be provided in the report of the Orbital Debris Workshop.

3.5 Section 2.0 of the 10-yr Space Debris Assessment Plan

The panel was asked to review the 10-yr plan and to provide a marked up copy to the Workshop chairman. There was not enough time for a very critical review of the document, however, section 2.0 of the schedule was discussed. It was the general opinion of the panel that Section 2.0, taken together with Figure 6 (the building blocks), made sense. Specific changes were marked up and are attached to this report.

4.0 RECOMMENDATIONS

4.1 Obtain hypervelocity impact test data and derive expressions for hazard assessment of spacecraft elements using "new" materials, specifically metallic and non-metallic composites.

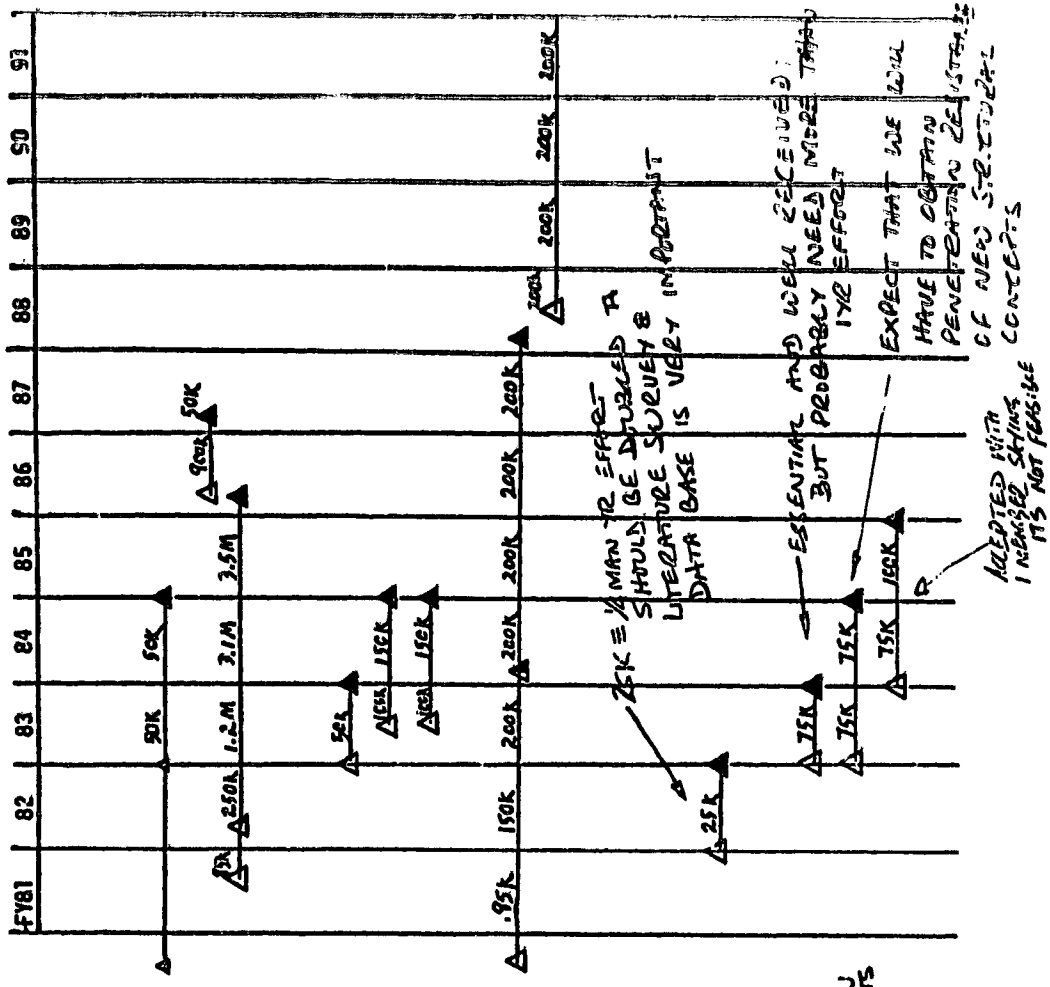
4.2 Take another look at allowable damage criteria derived during the Apollo/Skylab era, as they may not be applicable to current technology and operating modes.

4.3 A literature survey and data base for all applicable hypervelocity impact data is a very important asset for future hazard assessment. The existing level of effort in the 10-yr plan is equivalent to 1/4 man year and should be at least doubled.

4.4 Survivability classifications corresponding to various levels of mission success should be identified for civilian operations, as they are for the military, e.g. "class B" kill for military aircraft & helicopters corresponds to the pilot still alive, aircraft flyable, and a return to base possible.

4.5 Clarify that "mission success" in the 10-yr plan refers only to the meteoroid/orbital debris issue.

4.6 Hazard analyses should attempt to use existing, typical, i.e., generic, hypervelocity impact equations, and systems impact damage data whenever possible. Testing the actual spacecraft element for survivability in a simulated debris/meteoroid impact should be the second choice.



- 1.0 DEBRIS ENVIRONMENT DEFINITION
 - 1.1 DATA GATHERING
 - 1.1.1 GROUND BASED OBS.
 - 1.1.2 SPACE BASED OBS.
 - o INST. DDT&E
 - 1.1.3 EXPERIMENTAL FRAG. DISTRIBUTIONS
 - o TEST DEFINITION
 - o EXPLOSIONS
 - o COLLISIONS
 - 1.2 DATA ANALYSIS
 - 1.2.1 MODELLING
 - 1.3 DEBRIS ENV. MONITORING
- 2.0 DEBRIS HAZARD ASSESSMENT
 - 2.1 IMPACT DAMAGE
 - 2.1.1 LITERATURE SURVEY FOR APPLICABLE DATA
 - 2.1.2 EXPERIMENTAL IMPACT DATA
 - 2.1.2.1 NEW MATERIALS
 - 2.1.2.2 NEW DESIGN CONCEPTS
 - 2.1.2.3 GENERATE DAMAGE ASSESSMENT ALGORITHMS

25K ≡ 1/2 MAN YR EFFORT SHOULD BE SURGED A LITERATURE SURVEY & DATA BASE IS VERY IMPORTANT

ESSENTIAL AND WELL RECEIVED BUT PROBABLY NEED MORE THAN 1YR EFFORT

EXPECT THAT WE WILL HAVE TO OBTAIN PENETRATION RESISTANCE OF NEW SUBSTITUTED CONCEPTS

ACCEPTED WITH IMPROVED SKIN IS NOT FEASIBLE

FIGURE 5-2 - SCHEDULED ELEMENTS FOR ORBITAL DEBRIS ASSESSMENT

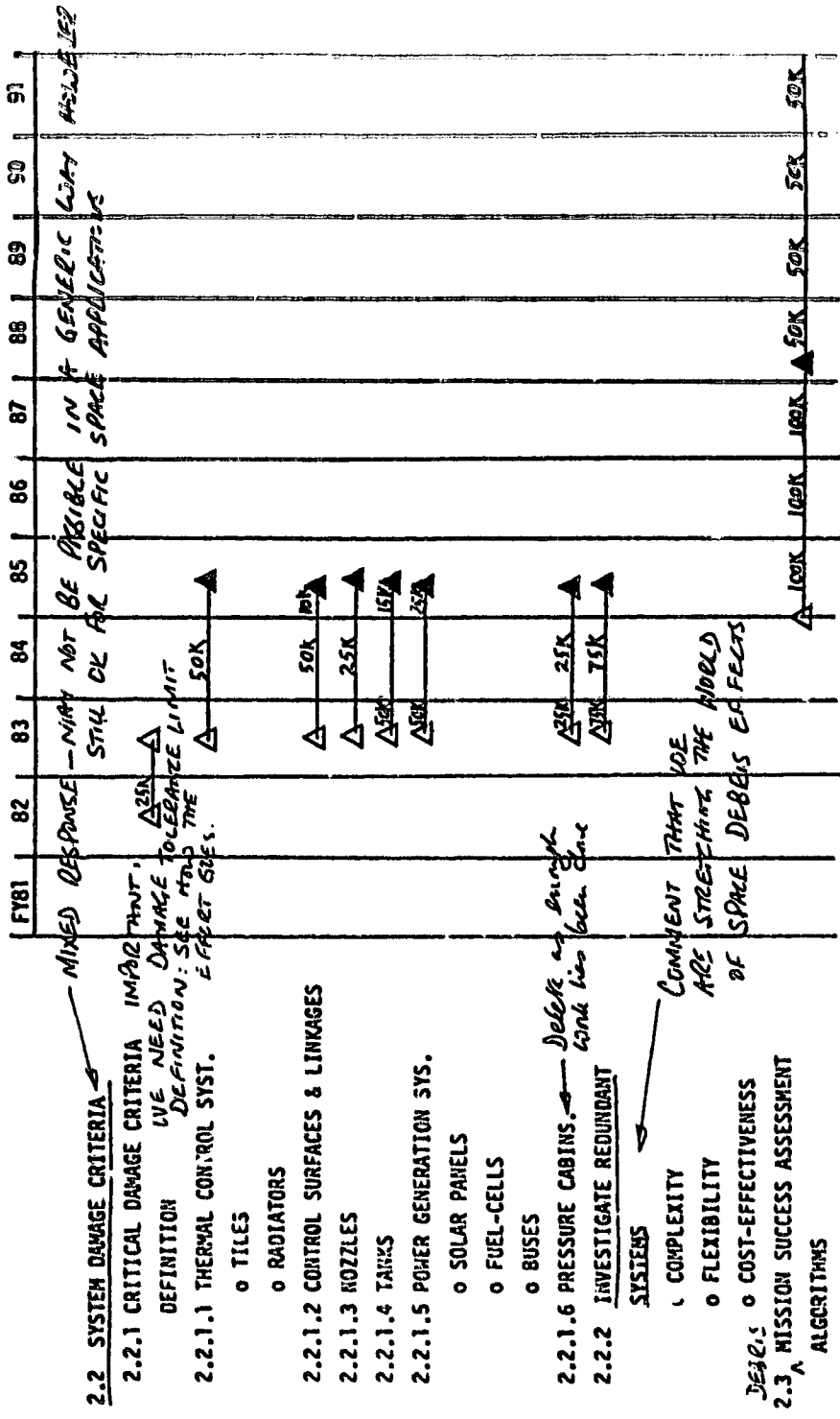


FIGURE 5-3 - SCHEDULED ELEMENTS FOR ORBITAL DEBRIS ASSESSMENT

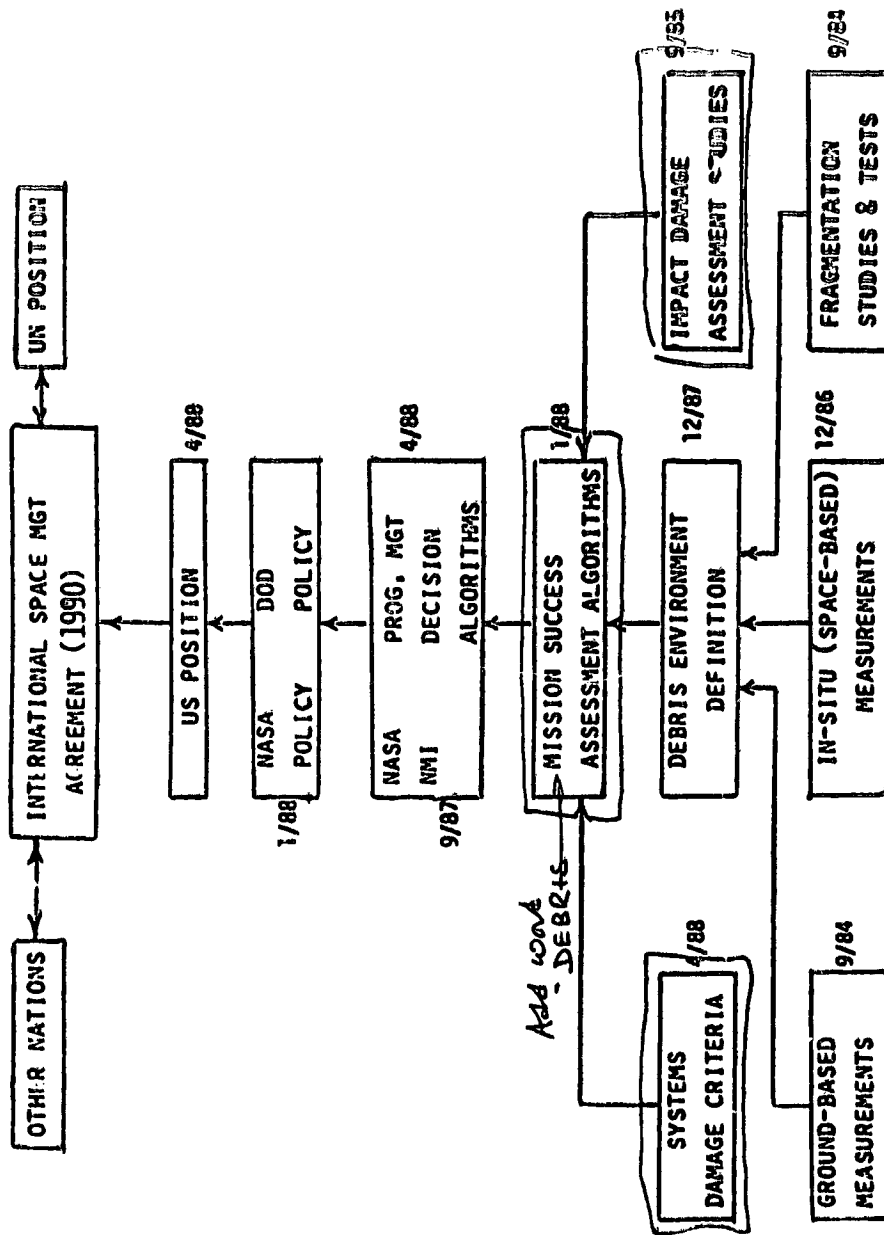


FIG. 6-1 PROGRAM ELEMENTS AND MILESTONES

Disposition Techniques
J. P. Basu

Disposition techniques for controlling the space environment are not well defined. Emphasis should be on management of space environment, which involves policy making on how much debris can be tolerated, what constraints should be imposed on spacecraft design to make it immune to some amount of impact, how orbits should be established to minimize collision risk. In the course of discussion the following suggestions were made.

I. Space Environment Control

- a. Minimize debris associated with launch by imposing design and operation constraints on spacecrafts.
- b. Allow passive decay
- c. Develop active disposal techniques comprising retrieval devices and techniques effecting direct reentry through propulsion stages.
- d. Develop passive trajectory shaping techniques including boosting geosync. satellites to different (higher/lower) orbit.

II. Establish Priorities

- a. Need cost and risk trade off studies.
- b. Identify problems and objectives.

III. Low Orbit vs. GEO

- a. Passive decay will be suitable for LEO and orbit shaping for geosync.

Participants:

J. P. Basu, NASA JSC
Lou Barbieri, NOAA
Marshall Kaplan, Spacotech
John Martin, COMSAT
Rudy Adornato, Grumman Aerospace
Alan Mueller, Self

POLICY CONSIDERATIONS

DENNIS FIELDER

We, as the largest working group, operated as a small 3-ring circus. I have attempted to consolidate all the developed wisdom and knowledge.

If we can have the first chart please. One of the things the group did was to compile a list of existing policy. The list encompasses both policy with a capital "P" such as presidential directives, and policy which is accountable by internal NASA and (probably) internal Air Force regulations and policies. The thought being that perhaps within the context of these policies, and perhaps others, there is already room to address aspects of debris. Perhaps in the long term context we may not be seeking a specific capital "P" policy on space debris, but perhaps appendixes to existing policy. I should address perhaps items 7 and 8 because they relate to present policies under which this whole activity has taken place. The list of NASA internal action assignments are essentially structured by a letter from the associate administrator requesting Mr. Weiss, Code O; and Mr. Smylie, Code T; at headquarters to address the subject of space debris.

Code O was to focus upon low earth orbit and code T was to focus upon geosynchronous orbits. That is the institutional arrangement under which all the activities have taken place to date to my knowledge.

By observation, Code O no longer exists. It has been absorbed into Code M and therefore, the existing letter which is over 2 years old is no longer accurate in terms of establishing a continuing action activity. Further reflected in the internal commitment, which again is a form of policy, are the three sources of funding which we have enjoyed and hope to continue to enjoy: the development of a data base and the collision statistics by the code M, the database and statistics relating to geosynchronous work by code T, and work which is just starting into the materials in the hypervelocity impact research by Code R. So that perhaps the question is the status of the internal operations which NASA has enjoyed and whether that needs to be reinforced with more current letters of assignment, or perhaps some form of NMI which establishes the subject. Going to the next chart. I am afraid there are some apples and oranges here in terms of what might be policy and what might be procedure. But in terms of policy or policy development a point has been made that the requirement for any commitment to domestic or international policy pertaining to debris is going to be dependent on the development of the information on the debris population, the collision probability, the propagation probability, and the collision hazard. These are some pivotal data which determine the need for, and the form of future debris policy. This is characterized by noting that the present catalog of orbiting objects (4500) does not support the short term demand for a debris related policy directive because the risk isn't

apparent to that extent. The requirement for a specific debris related policy in the long term seems to relate to the knowledge we get on the unknown factors of the population. The degree of credibility associated with policy requirements is whether the population remains a constant population or whether it has exponential growth. Mission related considerations, in terms of establishing debris related risks, involve specific spacecraft design assessment in terms of the debris effects. This may be difficult to arrive at because we won't have the system designs in hand at the time we are trying to assess the implications of collision damage. Somehow we have to address the difference between determining things that are statistically assessable and determining things which are dependant on system design.

Another consideration is the difference between geostationary orbit and low earth orbit. Operational procedures are being considered and implemented towards physical disposal from the geostationary orbit. However, the thrust behind implementing these dispositions is much more influenced by the user community. The economic significance of the geostationary orbit has probably given that subject much more attention in terms of RF spacing than in physical crowding. Nonetheless, there has been the move to put policy into effect there; and that is not bad. However, early policy decisions with respect to the geostationary orbit should not set any precedent for what we believe to be the disposition requirements in low earth orbit. Any low earth orbit policy should not be established by the precedent of whatever is going on in geostationary orbit.

There was a consensus, or I think it was a consensus because I didn't get involved in the total discussion that there should be a lead center, or a lead agency to focus and coordinate all the types of investigations that relate to debris including; the information exchange, the general activity planning and the coordination and development of the civil policy approaches, and that NASA was the appropriate lead agency to do that. This all remains to be seen.

The timing in the emergence of any policy is critical, especially in the emergence of issue and policy debate, until the technical information needs are well established. We have to understand all of the technical issues associated with debris before we should start moving into international arenas with any proposal for policy and we should certainly try to get our internal dispositions established first. In the mean time we should continue to encourage the adoption and use of low cost measures that lessen problems relating to debris propagation. These types of things, which don't incur unnecessary costs and are perhaps fairly easy to live with include: to reduce incidents of unplanned explosions such as the Delta has experienced in the past is relatively easy to address in terms of policy practice, the use of short-lived trajectories for trans-stages (it may have some contingency associated with it but it seems to be a good idea) minimize the jettison paraphernalia associated with mission

sequences seems to be a good idea, the use of reentering trajectories associated with ASAT tests seems to be a good approach, and the adoption of general anti-litter design practices seem to be good things to do. One could spread this word through several forums without necessarily establishing it as a foregone policy. There are good things to do, there are good ideas and they could be well adopted, if the messages get distributed through the appropriate forums. Proceed with low level policy ground work, identify the resources that are required, and plan to acquire them. Identify who the participants are. Promote the appropriate coordinative and exploratory discussions (interagency, domestic and international levels) to support these things.

Establish working procedures keyed to the 10-year planning objective and revisions and changes thereto. It seems proper to have a device that tends to connect all the institutional elements together. The 10-year plan that was distributed and reviewed was intended, at that time, to serve that cause. We really didn't have time, in our own discussions, for a detailed review of that plan, although most of the people plan to take a good hard look at it. But there is a suggestion, if not a proposition; that the 10-year plan can serve as a central device for connecting our independent thoughts and approaches. There is also a consensus that there should be a focal working group that is the continuum of what we have had today.

I don't think we have been bold enough to suggest just exactly what that forum should be or how it should work but that there should be one.

In the continuity of looking at policy implications, this is a list that Malcom Wolfe had in his presentation. It is what we believe is representative of the kinds of questions that ought to be considered in the course of thinking about policy. There are other types of issues one could add to that list, but they do constitute the type of data that needs to be digested by people concerned with policy formulation or policy adaptation as it relates to debris activity.

I had mentioned the 10-year plan. There had been several constructive comments received in the course of our discussions yesterday particularly as the plan itself relates to policy. We will make those comments available.

The thought here has been that to some extent this has been a very gentlemanly approach to debris investigation. There has been a lot of personal relationships as opposed to institutional relationships. In many cases the personal relationships have sustained but in some cases the personal relationships have changed because their institutional association changed. What committees, working groups, other management operational structures are in effect that may or may not serve as forums for interchange on debris and debris related matters? We will compile a list of the institutional elements involved and make it available for you.

Chart 1

Existing Policies

Not necessarily in order of significance as they may relate to space debris, or the development of space debris policy.

1. Presidential Directive No. 9, July 4, 1982.
2. Peaceful Uses of Outer Space Treaty, 1967.
3. DOD Policy on Free Access to Space, Date.
4. DOD Directive 5/60.32., Date.
5. Air Force Regulation on Satellite Position Management 55-XY (Draft).
6. USAF Space Division Regulation on Satellite Position Management 55-1, Mar 6, 1981.
7. NASA Internal Action Assignment Date:
Low Earth Orbit, Code O, Weiss.
GEO. Earth Orbit, Code T, Smylie.
8. NASA Resource Commitments
Code M; Debris Population Data Base and Collision Statistics for LEO.
Code T; Data Base and Statistics for GEO.
Code R; Materials and Hypervelocity Impact Research.
9. U.S. Unispace Statement of Principle, Date.
10. Intelsat Policy Directive on Disposal of Spent Satellites In/From Geostationary Orbit, Date.
11. NOAA Policy Directive on Disposal of Spent Satellites In/From Geostationary Orbit, Date.
12. United Nations Convention on Liability, Date.
13. European Space Agency Consideration on Disposal of Spent Satellites In/From Geostationary Orbit, Date.
14. India Statement on Disposal of Spent Satellites In/From Geostationary Orbit, Date.
15. National Space Act, 1968 and as Amended.

Chart 2

Major Policy Considerations

- I. The requirement for any commitment to domestic or international policy pertaining to debris will be dependent upon the development of further information on the debris population, space object collision probability, debris propagation probability, and collision hazard.
 - A. The present catalog of orbiting objects does not evidence a short term demand for a debris related policy directive.
 - B. The "known" unknown population can have a pivotal effect upon the timely need for a related policy directive:
 1. On the basis of population increase factor,
 2. On the basis of population growth factor.
- II. The argument for a debris policy may be much more difficult to establish if it is to be based upon mission related considerations; for example:
 - A. Spacecraft's ability to perform its mission in the event of collision damage is a spacecraft unique issue and can only be assessed in the presence of that spacecraft design.
- III. The circumstances surrounding debris and its effects in low earth orbit are different from those in geostationary orbit. It is not evident that the momentum toward physical disposal from the geostationary orbit stems from the same issues as are being developed for the lower earth orbit. Early policy decisions with respect to geostationary orbit disposition should not set any precedent for disposition requirements in lower earth orbit.

Chart 2 (continued)

IV. Short term activity recommendations

1. Establish NASA as a lead agency to focus and coordinate debris related investigations, information exchange and general activity planning, and coordinate the development and formulation of prospective civil policy approaches.

2. Continue to encourage the adoption and use of low cost measures that lessen the accentuation of a problem (relating to debris propagation), e.g.:

Reduce incidence of unplanned explosions,
Use short-lived trajectories for trans stages,
Minimize jettisoned paraphernalia,
Use reentry trajectories for ASAT tests,
Adopt anti-litter design habits, etc.

3. Proceed with low level policy ground work

Identify resources, participants, etc.,
Promote appropriate coordinative and exploratory discussions (interagency, domestic, international), etc.

4. Establish working meeting procedures keyed to the 10-year planning objectives and revisions and changes thereto, i.e., expand the plan to involve other involved agencies as appropriate.

5. Establish a focal work group whose structure can be reviewed and revised to include appropriately interested parties.

6. Within the context of the preceding short term plan, continue to consider and explore the implications of potentially major policy issues.

MAJOR POLICY ISSUES

IS IT GENERALLY ACCEPTED THAT US SPACE SYSTEMS
ARE (OR WILL BE) AT RISK

IF SO

- SHOULD THE US TAKE A LEADING ROLE IN DEVELOPING POLICY
- SHOULD THE US COMMIT TO UNILATERAL ACTION
- SHOULD THE US PUBLISH A POLICY STATEMENT
- WHAT US AGENCY SHOULD BE CHARGED WITH COORDINATING POLICY
- IF THE US DECIDES TO TAKE A POSITION, WHAT IS THE FIRST STEP

AND

WHAT IMPACT COULD A PUBLISHED US POLICY
HAVE ON THE MILITARY POSTURE OF THE US

Chart 4

10-Year Plan Review

Several constructive comments have been developed against the space debris assessment 10-year program plan, particularly as the plan itself relates to policy.

The comments address both the relationship of debris issues to existing policy and the prospect of formulating policy as a function of debris assessment.

Specific comments are not documented here but should be addressed in a specific overall review of the plan.

Operations

A continuing action to identify the formal institutional elements involved and likely to become involved has been initiated but is incomplete at this time. Data is intended to include both formal and informal mechanisms as may exist to provide coordination, information exchange, concurrences and mutual agreements amongst the institutions and elements involved.